

**Modelling melanoma control by immunotherapy
and tissue-resident memory T cells
using CRISPR/Cas9-based approaches**

Maïke Effern

ORCID ID:

0000-0002-1766-9881

from Unna, Germany

Submitted in total fulfilment of the requirements of the joint degree of

Doctor of Philosophy (PhD)

of

The Medical Faculty

The Rheinische Friedrich-Wilhelms-Universität Bonn

and

The Department of Microbiology and Immunology

The University of Melbourne

Bonn/Melbourne, 2020

Performed and approved by The Medical Faculty of The Rheinische Friedrich-Wilhelms-Universität Bonn and The University of Melbourne

1. Supervisor: Prof. Dr. med. Michael Hölzel
2. Supervisor: A/Prof. Dr. med. Thomas Gebhardt

Date of submission: September 2019

Date of oral examination: January 2020

Institute of Experimental Oncology (University Hospital Bonn),
Director: Prof. Dr. med. Michael Hölzel

Table of contents

Table of contents	I
List of abbreviations	VIII
List of tables	XVIII
List of figures	XIX
Abstract	XXIV
Declaration	XXVI
Preface	XXVII
Dedication	XXVIII
Acknowledgements	XXIX
List of publications	XXXI
Chapter 1: Literature review	2
1.1. Melanoma	2
1.1.1. An introduction.....	2
1.1.1. Incidence	2
1.1.2. UV radiation.....	4
1.1.3. Mutations	5
1.1.4. Pigmentation.....	6
1.1.5. MITF and its effects on the tumour microenvironment.....	6
1.2. Adoptive cell transfer therapy.....	8
1.2.1. CD8 ⁺ T lymphocytes and their anti-tumour function.....	8
1.2.2. A brief history of T cell therapy	9
1.2.3. Adoptive cell therapy using tumour-infiltrating lymphocytes as effective immunotherapy for patients with advanced melanoma ..	10
1.2.4. What are tumour antigens?	13

1.2.5.	Products of tumour-associated antigens and tumour mutations are recognised by melanoma tumour-infiltrating lymphocytes	16
1.2.6.	Genetic engineering of lymphocytes for adoptive cell therapy	19
1.2.7.	Targeting antigens shared by normal and tumour-tissue (on target off-tumour toxicity)	20
1.2.8.	The future of adoptive cell therapy.....	21
1.3.	Primary, adaptive and acquired resistance to cancer immunotherapy	22
1.3.1.	Tumour cell-intrinsic resistance mechanisms	23
1.3.2.	Tumour cell-extrinsic resistance mechanisms	26
1.3.3.	Acquired resistance mechanisms	29
1.3.4.	Antigen presentation and immune regulation in the tumour.....	34
1.4.	Tissue-resident memory CD8 ⁺ T cells.....	36
1.4.1.	Effector and memory CD8 ⁺ T cells.....	36
1.4.2.	Phenotype and ontogeny of tissue-resident memory CD8 ⁺ T cells	38
1.4.3.	Function and protective mechanisms of tissue-resident memory CD8 ⁺ T cells.....	40
1.4.4.	Tissue-resident memory T cells and their anti-tumour immunity...	41
1.5.	Thesis aims	44
Chapter 2: Material and methods		47
2.1.	Materials.....	47
2.1.1.	Antibodies.....	47
2.1.2.	Bacteria and virus strains	51
2.1.3.	Experimental models	51
2.1.4.	Cell culture media and supplements.....	59
2.1.5.	Chemicals and reagents	60
2.1.6.	Commercially available buffers and reagents	61

2.1.7.	Commercially available kits	63
2.1.8.	Enzymes	63
2.1.9.	General consumables	64
2.1.10.	General laboratory equipment	65
2.1.11.	Oligonucleotides	66
2.1.12.	Peptides and recombinant proteins	70
2.1.13.	Software and algorithms	71
2.1.14.	Vectors and plasmids	72
2.2.	Methods	75
2.2.1.	Molecular cloning techniques	75
2.2.1.1.	Polymerase chain reaction	75
2.2.1.2.	Oligonucleotide annealing	76
2.2.1.3.	Restriction enzyme digest	76
2.2.1.4.	Ligation	76
2.2.1.5.	Agarose gel electrophoresis	77
2.2.1.6.	Transformation	77
2.2.1.7.	Plasmid DNA preparation from <i>Escherichia coli</i> cultures	77
2.2.2.	Tissue culture	78
2.2.3.	Generation of CRISPR/Cas9-engineered melanoma cells	79
2.2.3.1.	Generation of sgRNA/Cas9-expressing plasmids	79
2.2.3.2.	Generation of homology constructs	79
2.2.3.3.	Generation of CRISPR target selectors and universal donor plasmids	79
2.2.3.4.	Transfections of CRISPR/Cas9 knockout and knockin constructs	83
2.2.3.5.	Validation of knockin by homology-directed repair using next	

generation sequencing	83
2.2.3.6. Generation of SWITCHitope target selectors and universal donor plasmids	85
2.2.4. Immunoblotting	86
2.2.5. Epifluorescence microscopy	86
2.2.6. Flow cytometry.....	87
2.2.6.1. Cell sorting	87
2.2.6.2. Cell surface immunostainings and intracellular immunostainings	87
2.2.7. Mice	88
2.2.8. T cell activation	88
2.2.9. <i>In vitro</i> T cell activation assay	89
2.2.10. Intracutaneous tumour transplantation experiments.....	90
2.2.11. Adoptive cell transfer immunotherapy	90
2.2.12. Tissue digestion and processing	91
2.2.13. <i>Ex vivo</i> cultures	92
2.2.14. PCR analysis of recurrent melanoma	92
2.2.15. Melanoma cell dedifferentiation assay <i>in vitro</i>	93
2.2.16. 3'mRNA-Seq analysis of melanoma	93
2.2.17. Gene set enrichment analysis	95
2.2.18. Data resources	95
2.2.19. Salvage immune checkpoint inhibition therapy.....	95
2.2.20. IFN γ response assay of recurrent melanoma after salvage immune checkpoint therapy	96
2.2.21. Histology.....	96
2.2.22. Production of retroviral particles and transduction of melanoma cells	98

2.2.23.	Treatment of melanoma cells with 4-hydroxytamoxifen.....	99
2.2.24.	PCR analysis of SWITCHitope-engineered melanoma cells	99
2.2.25.	CD8 ⁺ T cell enrichment.....	99
2.2.26.	Subcutaneous tumour transplantation experiments	100
2.2.27.	Epicutaneous inoculation of T cells	100
2.2.28.	Epicutaneous tumour transplantation experiments.....	101
2.2.29.	Treatment of mice with tamoxifen.....	102
2.2.30.	Quantification and statistical analysis	102
Chapter 3: Generation of a CRISPR/Cas9-based knockin strategy to fuse model CD8 ⁺ T cell epitopes to endogenous gene products in melanoma cells.....		
3.1.	Introduction	105
3.2.	Results	109
3.2.1.	CRISPR-assisted insertion of epitopes – 1 st generation	109
3.2.1.1.	Harnessing homology-directed repair to generate endogenously tagged melanoma cells	109
3.2.1.2.	Genetic and functional validation of endogenously tagged melanoma cells	111
3.2.2.	CRISPR-assisted insertion of epitopes (CRISPiTope) – 2 nd generation.....	119
3.2.2.2.	Generation of HC.PmelKO melanoma cells using CRISPR/Cas9	122
3.2.2.3.	TYRP1 and CDK4 ^{R24C} as model melanosomal and oncogenic T cell targets.....	124
3.2.2.4.	Activation and induction of effector function of pmel-1 TCRtg T cells by CRISPiTope-modified melanoma cells <i>in vitro</i>	129
3.2.2.5.	Modularity of the CRISPiTope approach	135
3.3.	Discussion.....	144

Chapter 4: Investigation of how the choice of the targeted gene product of ACT immunotherapy impacts on therapy outcome and resistance mechanisms ...	151
4.1. Introduction	151
4.2. Results	153
4.2.1. TYRP1 and CDK4 ^{R24C} as model melanosomal and oncogenic targets for adoptive cell transfer immunotherapy	153
4.2.2. Antigen status in recurrent melanoma treated with adoptive cell transfer immunotherapy	159
4.2.3. Diverse mechanisms of antigen loss in adoptive cell transfer recurrent melanoma.....	161
4.2.4. Adoptive cell transfer targeting of the melanosomal protein TYRP1 enforces melanoma phenotype switching	167
4.2.5. Target antigen status defines immune contexture of recurrent melanoma.....	175
4.2.6. Responsiveness of recurrent melanoma to anti-PD-L1 salvage immunotherapy	182
4.2.7. Long-term tumour control by systemic immunity.....	187
4.3. Discussion.....	192
Chapter 5: Investigating the requirement of antigen persistence on tumour surveillance by T _{RM} cells.....	199
5.1. Introduction	199
5.2. Results	202
5.2.1. Histological characterisation of epicutaneous melanoma model	202
5.2.2. Generation of SWITCHitope tagging plasmid	207
5.2.3. Generation of B16 melanoma cells with inducible antigen depletion	210
5.2.4. Cre-ERT2 plasmid #22776 has less spontaneous activity than #59701.....	215

5.2.5.	The target γ -actin shows a more robust switch upon 4-hydroxytamoxifen treatment than the target β -actin.....	223
5.2.6.	SWITCHitope-engineered melanoma cells can activate T cells .	227
5.2.7.	Generation of gBT-I tissue-resident memory T cells <i>in vivo</i>	234
5.2.8.	SWITCHitope-engineered melanoma cells have lower tumour incidence than wildtype B16 melanoma cells	236
5.2.9.	SWITCHitope-engineered melanoma cells prime naïve gBT-I T cells and recruit them into the skin.....	240
5.2.10.	HSV-1 gB antigen can be depleted in a tamoxifen-inducible fashion	246
5.2.11.	SWITCHitope-engineered melanoma cells have higher penetrance in immunodeficient mice	254
5.3.	Discussion.....	258
Chapter 6: Concluding remarks.....		264
6.1.	General discussion.....	264
6.2.	Key findings of the study	265
6.2.1.	Chapter 3.....	265
6.2.2.	Chapter 4.....	265
6.2.3.	Chapter 5.....	266
6.3.	Relevance	267
6.4.	Limitations of the study.....	272
Bibliography.....		277
Curriculum vitae		326
Appendix		329

List of abbreviations***Special characters***

%	Percent
#	Number
°C	Degree Celsius
µg	Microgram
µl	Microlitre
µM	Micromolar
α	alpha
β	beta
γ	gamma
ε	epsilon
ζ	zeta

Numbers

4-OHT	4-Hydroxytramoxifen
-------	---------------------

A

α-CTLA-4	Anti-Cytotoxic T-lymphocyte-associated protein 4
α-MSH	Alpha-melanocyte-stimulating hormone
α-PD-1	Anti-Programmed cell death protein 1
A2A	Adenosine A2a receptor
ACT	Adoptive cell transfer
Ad-gp100	Adenovirus expressing human gp100
AKT	AKT Serine/Threonine kinase
AMP	Adenosine monophosphate
APC	Antigen presenting cell
ATP	Adenosine triphosphate

B

B2M	Beta-2-microglobulin
-----	----------------------

B7-H4	B7 family member, H4
BCG	Bacillus Calmette-Guérin
BFA	Brefeldin A
BiP	Binding Protein
BlastR	Blasticidin resistance cassette
Blimp1	PR domain zing finger protein 1
BRAF	B-Raf proto-oncogene

C

CAD	Carbamoyl-Phosphate Synthetase 2
cAMP	Cyclic adenosine monophosphate
CAR	Chimeric antigen receptor
CCL2	C-C motif chemokine ligand 2
CCL3	C-C motif chemokine ligand 3
CCL4	C-C motif chemokine ligand 4
CCL4	C-C motif chemokine ligand 4
CCL5	C-C motif chemokine ligand 5
CCR5	C-C motif chemokine receptor 5
CCR7	C-C motif chemokine receptor 7
CD	Cluster of differentiation
CD3	CD3 molecule
CD3 ϵ	CD3 epsilon molecule
CD3 ζ	CD3 zeta molecule
CD4	CD4 molecule
CD8	CD8 molecule
CD28	CD28 molecule
CD44	CD44 molecule
CD49 α	Molecule CD49 alpha; also known as VLA-1 (Very late activation protein 1)
CD62L	CD62L molecule
CD69	CD69 molecule
CD73	5'- Nucleotidase ecto

CD80	CD80 molecule
CD86	CD86 molecule
CD103	CD103 molecule
CD122	CD122 molecule consisting of IL-2/IL-15R beta chain)
CD127	CD127 molecule; also known as IL-7R alpha
CDK4 ^{R24C}	Cyclin-dependent kinase 4 (amino acid substitution at position 24; Arginine to Cysteine)
CDK5	Cyclin-dependent kinase 5
CDKN2A	Cyclin dependent kinase inhibitor 2A
CEACAM1	Carcinoembryonic antigen cell adhesion molecule-1
c-Jun	Jun proto-oncogene
c-Met	Met receptor tyrosine kinase
CNX	Calnexin
CO ₂	Carbon dioxide
Cre-ERT2	Tamoxifen-inducible Cre-recombinase
CRISPR	Clustered Regularly Interspaced Short Palindromic Repeats
CRT	Calreticulin
CTL	Cytolytic T lymphocyte
CTLA-4	Cytotoxic T-lymphocyte-associated protein 4
CXCL10	C-X-C motif chemokine ligand 10
CXCL9	C-X-C chemokine ligand 9
CXCR3	C-X-C motif chemokine receptor 3

D

DAB	3,3'Diaminobenzidine
DC	Dendritic cell
DCT	Dopachrome tautomerase
DNA	Deoxyribonucleic acid
DNFB	1-Fluoro-2,4-dinitrobenzene
dNTPs	Deoxynucleotides
DSB	Double strand break

E

e.c.	Epicutaneously
EGFR	Epidermal growth factor receptor
EMT	Epithelial-to-mesenchymal transition
Eomes	Eomesodermin
ER	Endoplasmic reticulum
ERAP1	Endoplasmic reticulum aminopeptidase 1
ERAP2	Endoplasmic reticulum aminopeptidase 2
ERBB2IP	ErbB2 interacting protein
ERp57	Endoplasmic reticulum resident protein 57

F

FACS	Fluorescence-activated cell sorting
FCS	Fetal calf serum
FDR	false discovery rate
FoxP3	Forkead box P3

G

g	Gram
gB ₄₉₈₋₅₀₅	HSV-1 glycoprotein B epitope; amino acids: 498-505 (SSIEFARL)
gBT-I	TCRtg T cells recognising HSV-1 gB ₄₉₈₋₅₀₅
gDNA	genomic DNA
cDNA	complementary DNA
GFP	Green fluorescent protein
gp100	Glycoprotein 100
GPNMB	Glycoprotein NMB
GSEA	Gene set enrichment analysis

H

h	Hour
H&E	Haematoxylin and eosin
H2-Db	H-2 class I histocompatibility antigen, D-B alpha chain

H2-Kb	H-2 class I histocompatibility antigen, K-B alpha chain
HDR	Homology-directed repair
hgp100 ₂₅₋₃₃	Human gp100 epitope; amino acids: 25-33 (KVPRNQDWL)
HLA	Human leukocyte antigen
Hobit	Homolog of Blimp-1 in T cells
HRP	Horseradish peroxidase
HSV-1	Herpes simplex virus 1

I

i.c.	Intracutaneously
i.p.	Intraperitoneally
i.v.	Intravenously
IDO	Indolamine-2,3-deoxygenase
IFNGR1/2	Interferon gamma receptor 1 and 2
IFN γ	Interferon gamma
IHC	Immunohistochemistry
IL-2R	Interleukin 2 receptor
IL-6	Interleukin 6
IL-7	Interleukin 7
IL-8	Interleukin 8
IL-10	Interleukin 10
IL-12	Interleukin 12
IL-15	Interleukin 15
IL-21	Interleukin 21
IL-33	Interleukin 33
IRF1	Interferon regulatory factor 1
ITGA1	Integrin subunit alpha 1
ITGAV	Integrin subunit alpha V

J

JAK1	Janus kinase 1
JAK 2	Janus kinase 2

K

kb	Kilobase
kg	Kilogram
KLF2	Krüppel-like Factor 2
KLRG1	Killer cell lectin like receptor G1
KRAS	KRAS proto-oncogene

L

L	Litre
LAG-3	Lymphocyte activation gene 3
Lck	Lymphocyte cell-specific protein-tyrosine kinase
LMP10	Proteasome subunit β 10
LMP2	Proteasome subunit β 9
LMP7	Proteasome subunit β 8
LN	Lymph node
LPS	Lipopolysaccharide
Ly5.1	Molecule CD45.1

M

mAB	Monoclonal antibody
MAPK	Mitogen-activated protein kinase
MART-1	Melanoma antigen recognised by T cells 1
MC1R	Melanocortin-1 receptor
MDA	Melanocyte differentiation antigen
MDSC	Myeloid derived suppressor cell
MFI	Mean fluorescence intensity
mg	Milligram
mgp100 ₂₅₋₃₃	Murine gp100 epitope; amino acids: 25-33 (EGSRNQDWL)
MHC	Major histocompatibility complex
min	Minute
MITF	Microphthalmia-associated transcription factor
ml	Millilitre

mm	Millimetre
mM	Millimolar
mm ²	Cubic millimetre
mRNA	Messenger RNA
MYC	MYC proto-oncogene

N

NF1	Neurofibromin 1
NFgB	CRISPiotope tag: mNeon-FLAG-HSV-1 gB epitope
NFhgp100	CRISPiotope tag: mNeon-FLAG-human gp100 epitope
ng	Nanogram
NGFR	Nerve Growth Factor Receptor
NGS	Next Generation Sequencing
NHEJ	Non-homologous end-joining
NK cells	Natural killer cells
nm	nanometer
nM	Nanomolar
NMD	Non-sense mediated mRNA decay
NRAS	NRAS proto-oncogene
ns	Not significant
NT	Non-treated
NY-ESO1	New York esophageal squamous cell carcinoma-1

O

ORF	Open reading frame
OT-I	TCRtg T cells recognising Ova ₂₅₇₋₂₆₄
Ova ₂₅₇₋₂₆₄	Ovalbumin epitope; amino acids: 257-264 (SIINFEKL)

P

PAM	Protospacer adjacent motif
PBS	Phosphate-buffered saline
PCR	Polymerase chain reaction

PD-1	Programmed cell death protein 1
PES1	Pescadillo 1
PI3K	Phosphoinositide 3-kinase
Pmel	Other name for gp100
Pmel-1	TCRtg T cells recognising hgp100 ₂₅₋₃₃ and mgp100 ₂₅₋₃₃
pMHC	Peptide-MHC
PTEN	Phosphatase and tensin homolog
PuroR	Puromycin resistance cassette

R

Rab38	Ras-related protein Rab38
RAC1	Rac family small GTPase 1
RGS2	Regulator of G protein signalling 2
RNA	Ribonucleic acid
RP10	Complete RPMI1640 media supplemented with 10 % FCS
RPL28	60S ribosomal protein L28
rpm	Rounds per minute
RT	Room temperature

S

s	Second
s.c.	Subcutaneously
S1P	Shingosine-1-phosphate
S1PR1	Sphingosine-1-phosphate receptor-1
SD	Standard deviation
SFgB	CRISPitope tag: mScarlet-FLAG-HSV-1 gB epitope
SFhgp100	CRISPitope tag: mScarlet-FLAG-human gp100 epitope
SFmgp100	CRISPitope tag: mScarlet-FLAG-murine gp100 epitope
sgRNA	single-guide RNA
sgRNA	single-guided RNA
sICI	Salvage immune checkpoint inhibitor
SLO	Secondary lymphoid organ

SOX10	SRY-Box 10
STAT	Signal transducer and activator of transcription protein family

T

TAP	Transporter associated with antigen processing
TAE	Tris-Acetate-EDTA
T-bet	T-cell-specific T-box transcription factor
T _{CM}	Central memory T cell
TCM	T cell conditioned media
TCR	T cell receptor
TCRtg	TCR transgenic
T _{EFF}	Effector T cell
T _{EM}	Effector memory T cells
TGFβ	Transforming growth factor beta
Thy1.1	Molecule CD90.1
TIL	Tumour-infiltrating lymphocyte
TIM-3	T-cell immunoglobulin and mucin-domain containing-3
TME	Tumour microenvironment
TNFα	Tumour necrosis factor alpha
TP53	Tumour protein p53
TPN	Tapasin
TREG	Regulatory T cell
T _{RM}	Tissue-resident memory T cell
Tyr	Tyrosinase
TYRP1	Tyrosinase related protein 1; also known as TRP1

U

U	Unit
UD	Universal donor
UTR	Untranslated region
UV	Ultraviolet

V

V	Volt
VACV-OVA	Vaccinia virus expressing full-length ovalbumin
VCAM-1	Vascular cell adhesion molecule 1
VEGF	Vascular endothelial growth factor

W

WNT	Wingless
-----	----------

Z

ζ	Zeta
---------	------

List of tables

Table 2.1: Overview of the antibodies used in this study	47
Table 2.2: Overview of the bacteria and virus strains used in this study	51
Table 2.3: Overview of the experimental cell lines used in this study	51
Table 2.4: Overview of the experimental organisms and strains used in this study	58
Table 2.5: Overview of the cell culture media and supplements used in this study	59
Table 2.6: Overview of chemicals and reagents used in this study	60
Table 2.7: Overview of commercially available buffers and reagents used in this study.....	61
Table 2.8: Overview of commercially available kits used in this study.....	63
Table 2.9: Overview of enzymes used in this study.....	63
Table 2.10: Overview of general consumables used in this study	64
Table 2.11: Overview of general laboratory equipment used in this study	65
Table 2.12: Overview of oligonucleotides used in this study	66
Table 2.13: Overview of peptides and recombinant proteins used in this study	70
Table 2.14: Overview of software and algorithms used in this study	71
Table 2.15: Overview of vectors and plasmids used in this study	72
Table 2.16: Overview of the universal donor plasmids generated for the CRISPytope system	81
Table 2.17: Staining protocol for H&E slides	96

List of figures

Figure 1.1: Adoptive cell transfer protocol using naturally occurring autologous tumour-infiltrating lymphocytes.....	12
Figure 1.2: Cell-intrinsic mechanisms of resistance to cancer immunotherapy	25
Figure 1.3: Cell-extrinsic mechanisms of resistance to cancer immunotherapy	28
Figure 3.1: Model antigens can be recognised by single TCRtg CD8 ⁺ T cell species	108
Figure 3.2: Schematic overview of endogenous knockin strategy via homology directed repair	110
Figure 3.3: Validation of B16.gp100-FgB melanoma cells.....	112
Figure 3.4: Validation of B16.PES1-FgB melanoma cells	115
Figure 3.5: <i>In vitro</i> gBT-I T cell functionality assay	116
Figure 3.6: CRISPR/Cas9-modified B16 melanoma cells can induce effector cytokine expression in gBT-I T cells	117
Figure 3.7: CRISPR/Cas9-modified B16 melanoma cells can induce effector cytokine expression in gBT-I T cells (continued)	118
Figure 3.8: CRISPRitope toolbox to fuse model CD8 ⁺ immunodominant T cell epitopes to endogenous gene products	121
Figure 3.9: Generation of HC.PmelKO melanoma cells using CRISPR/Cas9	123
Figure 3.10: Genomic structure of CRISPRitope-engineered TYRP1 and CDK4 ^{R24C}	125
Figure 3.11: TYRP1 and CDK4 ^{R24C} as model melanosomal and oncogenic T cell targets.....	127
Figure 3.12: Expression of CRISPRitope-modified proteins corresponds with mRNA expression of genes.....	128
Figure 3.13: <i>In vitro</i> T cell activation assay using naïve TCRtg pmel-1 T cells	131
Figure 3.14: Activation of pmel-1 T cells by CRISPRitope-modified melanoma cells	132
Figure 3.15: <i>In vitro</i> pmel-1 T cell functionality assay	133
Figure 3.16: pmel-1 TCRtg T cells produce intracellular IFN γ and TNF α after co-	

culture with melanoma cells expressing the hgp100 epitope	134
Figure 3.17: Tagging of various melanosomal target genes with hgp100 leads to activation of pmel-1 T cells	136
Figure 3.18: Epitope-MHC affinity determines the extent of T cell activation .	139
Figure 3.19: <i>In vitro</i> gBT-I T cell functionality assay	141
Figure 3.20: gBT-I TCRtg T cells produce intracellular IFN γ and TNF α after co-culture with melanoma cells expressing the gB epitope	143
Figure 4.1: Pmel (gp100)-deficient HC.PmelKO. melanomas do not respond to ACT immunotherapy using pmel-1 TCRtg T cells	154
Figure 4.2: ACT immunotherapy targeting endogenous TYRP1 or CDK4 ^{R24C} in C57BL/6 mice.....	156
Figure 4.3: Response of TYRP1 or CDK4 ^{R24C} tumours to ACT immunotherapy in C57BL/6 mice	157
Figure 4.4: Circulating pmel-1 T cells after ACT immunotherapy in the two CRISPytope models	158
Figure 4.5: Frequencies of antigen loss in HC.PmelKO.TYRP1-NFhgp100 and HC.PmelKO.CDK4 ^{R24C} -NFhgp100 ACT-recurrent melanomas	160
Figure 4.6: Diverse genetic and epigenetic mechanisms of antigen loss in HC.PmelKO.TYRP1-NFhgp100 ACT recurrent melanomas	162
Figure 4.7: Diverse genetic and epigenetic mechanisms of antigen loss in HC.PmelKO.TYRP1-NFhgp100 ACT recurrent melanomas (continued).....	164
Figure 4.8: Genetic mechanism of antigen loss in HC.PmelKO.CDK4 ^{R24C} -NFhgp100 ACT recurrent melanoma	166
Figure 4.9: ACT targeting melanosomal TYRP1 induces reversible inflammation-induced dedifferentiation	168
Figure 4.10: ACT targeting melanosomal TYRP1 enforces melanoma phenotype switching.....	170
Figure 4.11: ACT targeting melanosomal TYRP1 enforces melanoma phenotype switching (continued).....	171
Figure 4.12: ACT immunotherapy approach to analyse tumour early during treatment by 3'mRNA-Seq.....	173

Figure 4.13: Melanoma dedifferentiation more pronounced in HC.PmelKO.TYRP1-NFhgp100 early during treatment.....	174
Figure 4.14: Antigen persistence is associated with an IFN-rich inflamed tumour microenvironment.....	176
Figure 4.15: Antigen persistence is associated with an IFN-rich inflamed tumour microenvironment (continued).....	177
Figure 4.16: An IFN-rich inflamed tumour microenvironment is associated with an increased T cell signature	179
Figure 4.17: An IFN-rich inflamed tumour microenvironment is associated with an immune checkpoint signature.....	180
Figure 4.18: ACT-treated recurrent melanomas can process and present antigen	181
Figure 4.19: Salvage immune checkpoint inhibitor (sICI) therapy of ACT-recurrent melanomas.....	183
Figure 4.20: sICI melanomas have different abilities to activate TCRtg pmel-1 T cells <i>in vitro</i>	185
Figure 4.21: sICI melanomas respond differently to IFN γ stimulation	186
Figure 4.22: Tumour-free mice have significantly higher frequencies of pmel-1 T cells in secondary lymphoid organs.....	188
Figure 4.23: Long-term tumour control is influenced by systemic immunity ...	189
Figure 4.24: pmel-1 T cells in spleen and in blood do not correlate in ACT-treated recurrent mice	190
Figure 4.25: Long-term tumour control is influenced by systemic immunity ...	191
Figure 5.1: Histological analysis of epicutaneous B16.gB melanoma in C57BL/6 mice (tumour margin)	203
Figure 5.2: Histological analysis of epicutaneous B16.gB melanoma in C57BL/6 mice (tumour centre)	204
Figure 5.3: Histological analysis of skin-draining brachial lymph node metastasis of epicutaneous B16.gB melanoma in C57BL/6 mice	206
Figure 5.4: SWITCHitope universal donor plasmid to fuse a floxed model CD8 ⁺ T cell epitope to endogenous gene products.....	208

Figure 5.5: Cre-recombinase excises floxed HSV-1 gB epitope which can be monitored by a colour switch	209
Figure 5.6: Generation of B16.TyrKO melanoma cells using CRISPR/Cas9..	211
Figure 5.7: B16.TyrKO melanoma cells express Cre-ERT2 after retroviral transduction.....	213
Figure 5.8: The housekeeping proteins β -Actin and γ -Actin were targeted by the SWITCHitope approach	214
Figure 5.9: Plasmid #22776 shows little spontaneous Cre-ERT2 activity.....	216
Figure 5.10: Plasmid #59701 has higher spontaneous Cre-ERT2 activity than plasmid #22776	217
Figure 5.11: 4-OHT induces mNeon expression in B16.TyrKO.ACTB-SWITCHgB-#22776.....	220
Figure 5.12: 4-OHT induces mNeon expression in B16.TyrKO.ACTB-SWITCHgB-#59701.....	222
Figure 5.13: Extended treatment with 4-OHT induces robust mNeon expression in B16.TyrKO.ACTB-SWITCHgB-#22776	224
Figure 5.14: SWITCHitope-targeted ACGT1 induces a more robust mNeon expression upon 4-OHT treatment than ACTB.....	225
Figure 5.15: Monoclonal B16.TyrKO.ACTG1-SWITCHgB cell lines robustly induce mNeon expression upon 4-OHT treatment	226
Figure 5.16: Monoclonal B16.TyrKO.ACTG1-SWITCHgB cell lines upregulate H2-Kb expression upon IFN γ stimulation	228
Figure 5.17: 4-OHT treatment of monoclonal 1G9 reduces gBT-I T cell activation	230
Figure 5.18: 4-OHT treatment of monoclonal 1H9 reduces gBT-I T cell activation	231
Figure 5.19: 4-OHT treatment of monoclonal 2C3 reduces gBT-I T cell activation	232
Figure 5.20: gBT-I T cells co-cultured with B16.TyrKO.ACTG1-SWITCHgB 1H9 treated with 4-OHT have the most reduced fold change in intracellular cytokine production.....	233
Figure 5.21: Generation of tissue-resident memory gBT-I T cells in the skin .	235

Figure 5. 22: 1H9 melanoma cells have low penetrance in C57BL/6 mice.....	238
Figure 5. 23: Influence of <i>in vivo</i> Tamoxifen treatment on tumour penetrance and growth kinetics.....	239
Figure 5.24: Tumour penetrance does not increase when melanoma cells lose antigen in the presence of gBT-I T cells in C57BL/6 mice.....	241
Figure 5.25: SWITCHitope-engineered melanoma cells that are not mScarlet ⁺ might form tumours	242
Figure 5.26: <i>Ex vivo</i> 1H9 cells that lost mScarlet expression cannot induce gBT-I T cell activation.....	244
Figure 5.27: SWITCHitope-engineered melanoma cells can prime naïve gBT-I T cells and recruit them into the skin	245
Figure 5.28: Tamoxifen treatment of C57BL/6 mice with gBT-I T _{RM} cells in the skin does not lead to tumour growth.....	247
Figure 5.29: <i>In vivo</i> Tamoxifen treatment induces a colour switch	248
Figure 5.30: gBT-I T _{RM} cells do no correlate with melanoma cell epitope status	249
Figure 5.31: <i>In vivo</i> switched cells can no longer activate gBT-I T cell <i>in vitro</i>	251
Figure 5.32: Different time points in Tamoxifen treatment does not induce significant differences in frequency and number of gBT-I T cells in different organs	252
Figure 5.33: gBT-I T cells in the different organs do not correlate with HSV-1 gB epitope status.....	253
Figure 5.34: 1H9 melanoma cells have higher penetrance in immunodeficient mice.....	255
Figure 5.35: <i>In vivo</i> treatment of Rag1 ^{-/-} mice with Tamoxifen does not lead to tumour escape from T _{RM} control.....	256
Figure 5.36: Tamoxifen treatment of Rag1 ^{-/-} mice that were e.c. inoculated with activated gBT-I and 1H9 cells does not lead to significant differences of gBT-I T cells in different organs	257

Abstract

In recent years, immunotherapy has demonstrated remarkable efficacy in the treatment of metastatic melanoma due to the development of T cell-based therapies such as checkpoint inhibitors or adoptive T cell transfer therapy (ACT) directed against defined antigens. However, tumours frequently relapse from therapy by diverse acquired resistance mechanisms. Currently, it is not well understood how the choice of target antigen influences resistance mechanisms to antigen-specific immunotherapies. A better understanding of tumour recognition by the immune system is of utmost importance to further improve currently used immunotherapies.

Therefore, we established CRISPR-assisted insertion of epitopes (CRISPEpitope), a technique that fuses a model CD8⁺ T cell epitope, human gp100, to endogenous gene products. We applied CRISPEpitope to murine melanoma cells to tag the endogenous melanosomal protein, TYRP1, and the oncogenic protein, CDK4^{R24C}, with the same model epitope, rendering them targetable by the same TCR-transgenic T cells. This defined experimental setting enabled us to investigate how the choice of the targeted gene product impacts on therapy outcome and immune evasion mechanisms.

Using experimental mouse models, we could identify different escape mechanisms to gp100-specific immunotherapy in TYRP1 versus CDK4^{R24C} melanomas. Resistance to ACT targeting TYRP1 was mainly caused by permanent antigen loss, accompanied by a non-inflamed microenvironment, or reversible downregulation of the antigen associated with melanoma phenotype switching. In contrast, CDK4^{R24C} melanomas escaping ACT displayed antigen persistence and were associated with an IFN-rich inflamed tumour microenvironment. In CDK4^{R24C} melanomas IFN-driven feedback inhibition by negative immune-checkpoint molecules promoted resistance to ACT despite persistent antigen expression.

Applying CRISPEpitope to syngeneic mouse models, we could show that target antigen choice can influence ACT resistance mechanisms, phenotype and immune contexture of melanomas in response to antigen-specific

immunotherapies. Thus, our work could help to better understand acquired resistance and optimise personalised cancer immunotherapy.

Furthermore, we aimed to apply this platform to a model of melanoma immune surveillance by T_{RM} cells in order to understand the importance of cognate antigen expression and presentation for long-term tumour control by $CD8^+$ tissue-resident memory T cells (T_{RM}).

To address this question, we used a modified CRISPiTope-approach, called SWITCHiTope, to generate melanoma cell lines that express a floxed model antigen under the control of an endogenous promoter and a Tamoxifen-inducible Cre-recombinase.

We could confirm successful Tamoxifen-inducible depletion of the model antigen in melanoma cells *in vitro* and *in vivo*. Moreover, we showed that antigen-depleted melanoma cells have significantly reduced potential to activate TCR-transgenic T cells *in vitro*. Using a transplantable epicutaneous melanoma inoculation technique, we could demonstrate that SWITCHiTope-engineered melanoma cells can prime naïve T cells, recruit them into the skin and induce T cell differentiation towards a T_{RM} phenotype.

Our approach enables us to investigate the importance of antigen expression and presentation for T_{RM} melanoma control. This work will help to better understand the interplay between tumour cells and T_{RM} cells and thereby advance clinical translation.

Declaration

The work that is presented in this thesis was conducted at the University of Bonn in the laboratory of Prof. Dr. med. Michael Hölzel and at the University of Melbourne in the laboratory of A/Prof. Dr. med. Thomas Gebhardt. This work was supported by the Deutsche Forschungsgemeinschaft (DFG, German Research Council) within GRK 2168, the Medical Faculty of the Rheinische Friedrich-Wilhelms-Universität Bonn and by the Deutsche Forschungsgemeinschaft under Germany's Excellence Strategy (EXC2151-390873048). Maïke Efferen was supported by the Deutsche Forschungsgemeinschaft, the Medical Faculty of the Rheinische Friedrich-Wilhelms-Universität Bonn and the Melbourne International Research Scholarship.

This is to certify that,

- (i) the thesis only comprises my original work towards the PhD except where indicated
- (ii) due acknowledgement has been made in the text to all other material used
- (iii) the thesis is less than 100,000 words in length, exclusive of tables, maps, bibliographies and appendices.

Bonn, 15th September 2019

Maike Efferen

Preface

(i) Contribution

My contribution to the experiments within each chapter was as follows:

Chapter 3: 85 %

Chapter 4: 65 %

Chapter 5: 85 %

I acknowledge the important contributions of others to the experiments presented herein:

Chapter 3: Emma Bawden, Debby van den Boorn-Konijnenberg, Daniel Hinze, Jana Liebing

Chapter 4: Dr. rer. nat. Tobias Bald, Dr. rer. nat. Nicole Glodde

Chapter 5: Biomedical Histology Facility – University of Melbourne, Debby van den Boorn-Konijnenberg, Emma Bawden, Teagan Wagner

Dedication

This dissertation is dedicated to Kirsten Plaß.

Acknowledgements

Firstly, I would like to express my sincere gratitude to my two PhD supervisors Prof. Dr. med. Michael Hölzel and A/Prof. Dr. med Thomas Gebhardt for giving me the opportunity to conduct the research for my PhD thesis in their labs. Thank you for the continuous support and motivation from near and far, encouragement and the great mentorship.

Besides my supervisors, I would like to thank Prof. Ian van Driel and Prof. Dr. med. Christian Kurts for being part of my Melbourne and Bonn PhD committee.

A very special thanks goes to Dr. rer. nat. Nicole Glodde, my dear colleague and friend, without whom this work would not have been possible. Thanks for the moral support especially during writing, indispensable help in the lab and all the fun we had along the way.

I would also like to thank my two lab groups in Bonn and Melbourne for the very good working atmosphere and the support throughout the entire time. Thank you for all the helpful words of advice and wonderful time. It was a great pleasure working in such a supportive environment. Thank you to all the past and present members of my Bonn lab: Debby van den Boorn-Konijnenberg, Jana Liebing, Pia Aymans, Daniel Hinze, Julia Reinhardt, Johanna Seier, Helena Boll, Michelle Yong, Freya Kretzmer and Susana Ramirez Valladolid.

Thank you to all the past and present members of the SB-TG lab: Katharina Hochheiser, Nathan McBain, Simone Park, Annabell Bachem, Marie Greyer, Paul Whitney, Elise Gressier and Sabrina Dähling. Thank you Sammy Bedoui for all your insightful comments.

A special thanks goes out to my IRTG2168 sister Emma Bawden who helped me adapt to the Australian language and cuisine. Thanks for proof-reading my thesis, all your helpful comments and the good times we had.

XXX

Another special thanks goes out to Teagan Wagner who continued my work when I had to leave Australia. Although we only worked together for a short time, we had so much fun.

I would like to thank the Bonn and Melbourne IRTG2168 coordination offices for putting such a remarkable program together and their continuous support throughout the past years.

I would also like to thank my fellow IRTG2168 students for all the great trips, encouragement and friendship.

Finally, I would like to thank my family, especially my parents, who always supported me. Thank you for your support throughout the entire time of my studies and always letting me go my own way, make my own mistakes and experiences. I am grateful to my friends, who have provided moral and emotional support along the way.

List of publications**Adoptive T cell therapy targeting different gene products reveals diverse and context-dependent immune evasion in melanoma***Immunity, under revision*

Effern M*, Glodde N*, Liebing J, Braun M, Bawden E, Yong M, Boll H, Hinze D, van den Boorn-Konijnenberg D, Aymans P, Landsberg J, Smyth M, Tüting T, Bald T, Gebhardt T, Hölzel M

* These authors contributed equally.

Tumor CD155 drives resistance to immunotherapy by downregulating the activating receptor CD226 in CD8⁺ T cells*Immunity, submitted*

Braun M, Das I, Roman Aguilera A, Sundarrajan A, Corvino D, Kelly G, Vari F, Lepetier A, Pearson S, Madore J, Krumeich S, Jacquelin S, **Effern M**, Casey M, Nakamura K, Seo E, Veillette A, Hoelzel M, Taheri T, Long G, Scoyler R, Batstone M, Dougall W, Johnston R, Martinet L, Smyth M, Bald T

Targeting CD39 in cancer reveals an extracellular ATP and driven inflammasome driven tumor immunity*Cancer Discov. 2019 Nov 7, DOI: 10.1158/2159-8290.CD-19-0541*

Li XY, Moesta A, Xiao C, Nakamura K, Casey M, Zhang H, Madore J, Lepletier A, Roman Aguilera A, Sundarrajan A, Jacobberger-Foissac C, Wong C, dela Cruz T, Welch M, Lerner A, Spatola B, Soros V, Corbin J, Anderson A, **Effern M**, Holzel M, Robson S, Johnston R, Waddell N, Smith C, Bald T, Geetha N, Beers C, Teng M, Smyth M

Tissue-resident memory CD8⁺ T cells promote melanoma-immune equilibrium in skin*Nature 2019 Jan;565(7739):366-371. DOI: 10.1038/s41586-018-0812-9.*

Park SL, Buzzai A, Rautela J, Hor JL, Hochheiser K, **Effern M**, McBain N, Wagner T, Edwards J, McConville R, Wilmott JS, Scolyer RA, Tüting T, Palendira

U, Gyorki D, Mueller SN, Huntington ND, Bedoui S, Hölzel M, Mackay LK, Waithman J, Gebhardt T.

Amplification of N-Myc is associated with a T-cell-poor microenvironment in metastatic neuroblastoma restraining interferon pathway activity and chemokine expression

Oncolmmunology 2017 Apr; Vol. 6, Iss. 6, 2017;

DOI:10.1080/2162402X.2017.1320626

Layer JP, Kronmüller MT, Quast T, van den Boorn-Konijnenberg D, **Effern M**, Hinze D, Althoff K, Schramm A, Westermann F, Peifer M, Hartmann G, Tüting T, Kolanus W, Fischer M, Schulte J, Hölzel M

Translational reprogramming is an evolutionarily conserved driver of phenotypic plasticity and therapeutic resistance in melanoma

Genes Dev. 2017 Jan 17; 31:18-33. DOI: 10.1101/gad.290940.116

Falleta P, Sanchez-del-Campo L, Chauhan J, **Effern M**, Kenyon A, Kershaw CJ, Siddaway R, Lisle R, Freter R, Daniels MJ, Lu X, Tüting T, Middleton M, Buffa FM, Willis AE, Pavitt G, Ronai ZA, Sauka-Spengler T, Hölzel M, Goding CR

The experimental power of FR900359 to study Gq-regulated biological processes

Nat Commun. 2015 Dec 14; 6:10156. DOI: 10.1038/ncomms10156

Schrage R, Schmitz AL, Gaffal E, Annala S, Kehraus S, Wenzel D, Büllsbach KM, Bald T, Inoue A, Shinjo Y, Galandrin S, Shrinidhar N, Hesse M, Grundmann M, Merten N, Charpentier TH, Martz M, Butcher AJ, Slodczyk T, Ammando S, **Effern M**, Namkung Y, Jenkins L, Horn V, Stößel A, Dargatz H, Tietze D, Imhof D, Galés C, Drewke C, Müller CE, Hölzel M, Milligan G, Tobin AB, Gomeza J, Dohlman HG, Sondak J, Harden TK, Bouvier M, Lapotte SA, Aoki J, Fleischmann BK, Mohr K, König GM, Tüting T, Kostenis E

Chapter 1: Literature review

Chapter 1: Literature review

1.1. Melanoma

1.1.1. An introduction

Melanoma is one of the most aggressive and therapy-resistant cancers. It arises from the uncontrolled proliferation of pigment-producing cells – melanocytes – that reside within the basal layer of the epidermis (Abdel-Malek et al., 1999, 1995; Lerner and Mcguire, 1964; Tsatmali et al., 2002). The majority of melanomas develop in the skin, however they can also arise in the eye (uvea) and mucosal surfaces. Malignant melanoma is the most lethal form of skin cancers and melanoma incidence has risen in the past 50 years (Erdei and Torres, 2010; Guy et al., 2015; Kosary et al., 2014; Linos et al., 2009; Rigel and Carucci, 2000). Although it represents less than 5 % of all cutaneous malignancies, melanoma causes the majority of skin-cancer related deaths (Linus et al., 2009).

If the disease is diagnosed early enough, resection of the lesion is often curative and associated with favourable survival rates. But melanoma is highly aggressive and often metastasises early (Califano and Nance, 2009; Erdei and Torres, 2010). As soon as the melanoma is considered advanced stage, other treatment options are needed (Califano and Nance, 2009; Erdei and Torres, 2010; Filippi et al., 2016; Goodson and Grossman, 2009). There has been an enormous development in new treatments for metastatic melanoma during the past couple of years. More recently tested combination immunotherapies have proven to be effective and increase survival. Overall survival at three years was 58 % during combination therapy using nivolumab (α -PD-1 monoclonal antibody; PD-1: programmed cell death protein 1) and ipilimumab (α -CTLA-4 monoclonal antibody; CTLA-4: cytotoxic T-lymphocyte-associated protein 4) in patients with advanced melanoma compared to 52 % and 34 % in the nivolumab or ipilimumab monotherapy group, respectively (Wolchok et al., 2017).

1.1.1. Incidence

Global melanoma incidence has increased over the last five decades and yearly incidence in mostly fair-skinned populations in Northern Europe, Australian, New

Zealand and Northern America has risen as rapidly as 4 – 6 % (Coory et al., 2006; Erdmann et al., 2013; Guy et al., 2015; Jemal et al., 2001; Kosary et al., 2014; Lasithiotakis et al., 2006; Linos et al., 2009; Lipsker et al., 2007; MacKie et al., 2002; Marrett et al., 2001; Nikolaou and Stratigos, 2014; Stang et al., 2006; Vries et al., 2003; Whiteman et al., 2016). However, incidence rates vary across populations of different geographical locations and ethnicities, and within populations across gender and age (Apalla et al., 2017; Erdei and Torres, 2010; Olsen et al., 2015; Whiteman et al., 2016). Melanoma is most often reported among fair-skinned Caucasian populations, which can be attributed to decreased photoprotection from reduced skin pigmentation by melanin (Brenner and Hearing, 2008; Chao et al., 2017; Padovese et al., 2018).

UV (ultraviolet) radiation is the main risk factor for melanoma and can induce malignant cell transformation and cell death (Li et al., 2016; Moan et al., 2015; Seebode et al., 2016; S. Wu et al., 2014). UV radiation is influenced by factors such as latitude, cloud cover, atmospheric absorption and season, and therefore differences in geography affect melanoma incidence. Along with the first report from 1956, studies show that melanoma mortality rates increase with increasing proximity to the equator; a phenomenon called the “latitude gradient” (Elwood et al., 1974; Lancaster, 1956).

Australia has the second highest age-standardised annual melanoma incidence (34.9 : 100,000 cases per year) after New Zealand (35.8 : 100,000 cases per year) (IARC Cancer Base, 2013). In the northern parts of Australia (Queensland) higher melanoma rates are observed than in the more southern parts (New South Wales) of Australia.

However, in Europe we observe an inverse latitude gradient which is partly attributable to different pigmentation characteristics predominating the populations of the different regions. In Scandinavia, the majority of the population is fair-skinned whereas southern Europe is predominantly inhabited by people with darker olive-coloured skin who have therefore better UV photoprotection. In European populations, such as those in Germany, France or Austria, age-standardised annual melanoma incidence are in the range of 9.9 -14.6 : 100,000 cases per year (IARC Cancer Base, 2013).

In general, melanoma is a cancer of the elderly people and incidence in Australia and in Northern Europe peaks at around 70 – 80 years of age (Coory et al., 2006; Mackie et al., 2002; Sneyd and Cox, 2013; Stang et al., 2006). Although melanoma incidence is low among people under 40 years of age, it is among the most common malignancies diagnosed in young adults or even adolescents (Ballantine et al., 2017; Garbe and Leiter, 2009; Watson et al., 2016). Young women are more often diagnosed with melanoma than young men (Garbe and Leiter, 2009; Watson et al., 2016; Weir et al., 2011). Among Caucasian women, melanoma is more often diagnosed on the lower limbs whereas it is more frequently reported on the shoulders and back in men (Cho et al., 2005). As these body sites are associated with lower UV exposure, these findings support the intermittent UV exposure theory which postulates that intermittent and intense sun, i.e. UV radiation, exposure leads to an increased risk of melanoma (Stierner et al., 1992). In Australia however, women and men are more frequently diagnosed with melanoma on high sun-exposed body sites such as their head and neck (Green et al., 1993).

For the past five decades, melanoma incidence has increased and is predicted to continue to increase over the next years, resulting in the need for a better understanding and treatment of melanoma. There is a diverging trend between melanoma incidence and mortality bringing into question whether there is a true melanoma epidemic or whether increased incidence is associated with more diagnoses due to better screening techniques (Erdmann et al., 2013; Guy et al., 2015; Kosary et al., 2014; Linos et al., 2009; Whiteman et al., 2016).

1.1.2. UV radiation

The majority of melanomas are thought to be caused by UV irradiation (Koh et al., 1996). UVA (315-400 nm) and UVB (280-315 nm) are the two main types of UV radiation that are primarily responsible for skin carcinogenesis. UVA can penetrate more deeply into the dermal layer of the skin but it is less genotoxic than UVB radiation (de Gruijl, 2002). Research suggests that UVA causes damage to the skin and tumourigenesis by oxidative stress-induced DNA damage whereas UVB can cause direct DNA damage by photoproducts (de Gruijl, 2002).

UVA-induced DNA damage is repaired by the base excision repair whereas the photoproduct damage by UVB radiation is repaired by nucleotide excision repair (Dahle et al., 2008; Shah and He, 2015).

1.1.3. Mutations

Specific familial and somatic mutations are associated with the risk of melanomagenesis. Familial predisposition accounts for 3-15 % of melanomas. In these cases, UV-independent mutations play a major role (Dębniak, 2004). Germline mutations in the *CDK4* (Cyclin-dependent kinase 4) or *CDKN2A* (Cyclin dependent kinase inhibitor 2A) loci are rare but they correlate with the development of melanomas (Borg et al., 2000; Soufir et al., 1998; Zuo et al., 1996).

Lawrence and colleagues showed that melanoma is the cancer type with the highest rate of somatic mutations (Lawrence et al., 2013). Other key somatic mutations such as BRAF^{V600E} (B-Raf proto-oncogene) and mutated NRAS (NRAS proto-oncogene) are UV-independent but are found in 60 % and 15-20 % of melanomas, respectively (Ellerhorst et al., 2011). BRAF^{V600E} is often insufficient to drive tumourigenesis of melanocytes and additional acquired UV-induced somatic mutations are required to drive malignant transformation (Michaloglou et al., 2005). In mouse models that harbour BRAF^{V600E} mutation, UV exposure accelerates tumourigenesis and resulting tumours often exhibit a UV-signature mutation in the *TP53* (tumour protein p53) gene encoding the tumour suppressor p53 (Viros et al., 2014). This was also observed in 20 % of melanoma patients that have BRAF^{V600E} mutant melanoma (Hodis et al., 2012; Viros et al., 2014; Xia et al., 2014). Recent studies show that UV-signature driver mutations in *CDKN2A*, *TP53*, *PTEN* (phosphatase and tensin homolog), *RAC1* (Rac family small GTPase 1) and *NF1* (Neurofibromin 1) accumulate in melanocytic nevi when they transform into melanoma (Melamed et al., 2017; Viros et al., 2014). Mutations, either inherited or acquired through environmental risk factors, play a critical role during the process of melanomagenesis.

1.1.4. Pigmentation

Melanocytes produce eumelanin and pheomelanin. When α -melanocyte-stimulating hormone (α -MSH) binds to melanocortin-1 receptor (MC1R), eumelanin is synthesised. Eumelanin is more prevalent in dark hair and dark skin. Individuals with freckles and red hair have mutations in the MC1R causing its inactivation. Therefore, eumelanin cannot be produced and pheomelanin accumulates (Nasti and Timares, 2015). Pheomelanin may induce free radical formation and may therefore contribute to UV-induced DNA damage, whereas eumelanin reduces the accumulation of photoproducts (Raimondi et al., 2008). UVB radiation induces the expression of α -MSH and MC1R in melanocytes (Choi et al., 2010). cAMP (cyclic adenosine monophosphate) signalling acts downstream of MC1R and activates the transcription factor MITF (Microphthalmia-associated transcription factor) (Gilchrist, 2011). MITF is a lineage-specific transcription factor and master regulator of melanocyte differentiation (Garraway et al., 2005; Hsiao and Fisher, 2014; Levy et al., 2006). MITF not only controls the pigmentation programme of melanocytes but also cell proliferation and DNA repair (Giuliano et al., 2010; Strub et al., 2011).

1.1.5. MITF and its effects on the tumour microenvironment

It was previously shown that dysregulation of MITF can alter drug or immunotherapy responsiveness (Konieczkowski et al., 2014; Müller et al., 2014). Melanoma cells can appear in distinct cell states termed 'proliferative' and 'invasive' (Hoek et al., 2008; Hoek and Goding, 2010). In the centre of this 'phenotype switching model' lies MITF and opposing epithelial-to-mesenchymal-like and hypoxia-related programmes (Cheli et al., 2012; Cheng et al., 2015; Eichhoff et al., 2011; Feige et al., 2011; Javelaud et al., 2011; O'Connell et al., 2013; Webster et al., 2015; Widmer et al., 2013).

Pro-inflammatory cytokines, such as TNF α (Tumour necrosis factor α) that are produced by T cells during cancer immunotherapy, lead to a suppression of MITF by the transcription factor c-Jun (Jun proto-oncogene). Low MITF expression levels are linked to the so-called 'invasive' phenotype which is characterised by epithelial-to-mesenchymal-like transition of melanoma cells and reciprocal

activation of inflammatory pathways.

Inflammatory MITF^{low}/c-Jun^{high} melanomas recruit myeloid immune cells via the expression of Ccl2 (C-C motif chemokine ligand 2), Ccl5 (C-C motif chemokine ligand 5) and Cxcl10 (C-X-C motif chemokine ligand 10) into the tumour microenvironment (TME) (Riesenberg et al., 2015).

It was also shown that aberrant MAPK (mitogen-activated protein kinase) signalling and inflammation in the TME can lead to MITF downregulation and potential immunotherapy failure. Pro-inflammatory cytokines, such as TNF α , and activating MAPK mutations cooperate through the transcription factor complex c-Jun/AP1 to activate CD73 expression as an adaptive resistance mechanism. CD73 (NT5E; 5'- Nucleotidase ecto) is a 5'-ectonucleotidase that produces immunosuppressive adenosine and can thereby lead to immunotherapy failure by generating an immunosuppressive TME (Reinhardt et al., 2017; Young et al., 2017). Furthermore, it was demonstrated that pro-inflammatory cytokines produced by T cells during cancer immunotherapy can induce phenotype switching through the MITF/c-Jun antagonism (Reinhardt et al., 2017).

MITF antagonism causes a concomitant downregulation of pigmentation genes. Therefore, if immunotherapy such as ACT (adoptive cell transfer) uses T cells that target a pigmentation protein therapy might fail as the target can be lost due to therapy-induced immune responses. This was demonstrated by Landsberg and colleagues who showed that ACT therapy using pmel-1 T cells that target the murine gp100 (glycoprotein 100) protein can resist therapy through inflammation-induced reversible dedifferentiation. Inflammation-induced reversible dedifferentiation is a phenotype switch from a differentiated (melanocyte lineage program high) to a dedifferentiated (neural crest / mesenchymal progenitor program) state largely driven by pro-inflammatory cytokines such as TNF α (Landsberg et al., 2012).

In conclusion, melanoma phenotype switching changes the TME. Phenotype switching from MITF^{high}/c-Jun^{low} ('proliferative') to MITF^{low}/c-Jun^{high} ('invasive') leads to the acquisition of immunosuppressive properties of the TME and potential failure of cancer immunotherapy (Landsberg et al., 2012; Reinhardt et al., 2017; Riesenberg et al., 2015; Verfaillie et al., 2015).

1.2. Adoptive cell transfer therapy

ACT therapy is a personalised cancer treatment option for patients suffering from advanced malignant melanoma (Benlalam et al., 2007; Chodon et al., 2014; Rosenberg et al., 2011). It is based on the fact that melanoma is often infiltrated by tumour-reactive lymphocytes, so-called tumour-infiltrating lymphocytes (TILs). It has been shown that naturally occurring tumour-reactive T cells used for ACT can mediate durable and complete regressions with acceptable toxicities.

1.2.1. CD8⁺ T lymphocytes and their anti-tumour function

In the late 19th century, William Coley suggested a role for the immune system in cancer regression. In patients who had acute bacterial infections he sporadically observed spontaneous remission of tumours. Following these observations, he mixed different bacterial toxins to activate a cancer patient's immune system and reported that this mixture of toxins was effective and even curative in some patients (Coley, 1893). However, with the advent of radio- and chemotherapy this method was no longer used. One other important example from history shows that a broad immune response induced by bacteria can be used as effective immunotherapy to treat cancer. *Bacillus Calmette-Guérin* (BCG), which is a live attenuated vaccine originally produced from *Mycobacterium bovis* to prevent tuberculosis, was reported to have positive effects on cancer rates in animal studies in the 1950s. In 1976, Morales and colleagues published the use of intravesical BCG in patients for the treatment of non-muscle invasive bladder cancer. To date, BCG is still used to treat bladder cancer as it has not been surpassed by any other treatment in terms of its ability to reduce progression and recurrence. Although, its potential to cause side effects and severe toxicities is a limitation (Fuge et al., 2015; Morales et al., 1976; Pearl, 1929). In the late 20th century it was firmly established that the immune system can control tumour growth. Studies in immunodeficient mice showed that CD8⁺ T cells and NK (natural killer) cells decrease the incidence and severity of tumour development in spontaneous and chemically induced mouse cancer models (Kaplan et al., 1998; Shankaran et al., 2001; Smyth et al., 2001, 2000).

Once it was established that the immune system had a potent role in controlling

tumours it also became obvious that immune pressure can edit tumours. Immune pressure can drive individual tumour clones with mutations favourable to survival, such as those that cause loss of antigen expression, to expand. This editing process ultimately leads to loss of control by the immune system and tumour outgrowth. Additionally, other immune cells that can suppress anti-tumour immunity and contribute to tumour outgrowth such as CD4⁺ FoxP3⁺ regulatory T (T_{REG}) cells and several myeloid cell types have been identified (Coussens et al., 2000; De Palma et al., 2005; Lin et al., 2001; Turk et al., 2004; Yang et al., 2004). Nonetheless, correlative studies of patients with various tumour types, including melanoma, showed that the presence of TILs was associated with longer survival (Clark et al., 1989; Lauder and Aherne, 1972; Palma et al., 1978).

1.2.2. A brief history of T cell therapy

Already in the 1980s, a study showed that the injection of lymphocytes that were expanded using Interleukin 2 (IL-2) could lead to responses in a few patients with metastatic lymphoma. Administration of IL-2 after lymphocyte transfer enhanced the therapeutic effect of the transferred T cells in mice (Donohue et al., 1984; Eberlein et al., 1982). Treatment of a few individual patients suffering from metastatic melanoma that were administered IL-2 showed complete durable tumour regression which ultimately led to the identification of tumour-reactive T cells and their cognate antigens (Rosenberg et al., 1985).

Around the same time, Rosenberg and colleagues identified that murine tumour-infiltrating lymphocytes were able to recognise the tumour cells *ex vivo*. Additionally, they showed that the transfer of these syngeneic TILs, in combination with the chemotherapeutic drug cyclophosphamide, could mediate regression of metastatic hepatic and pulmonary tumours (Rosenberg et al., 1986). *In vitro* studies analysing TILs from surgically removed melanomas showed that isolated lymphocytes were able to specifically recognise autologous melanoma cells. This discovery led to the first objective regression of a tumour after a patient with metastatic melanoma had been treated with autologous TILs (Muul et al., 1987; Rosenberg et al., 1988). Although it was shown that TILs can mediate cancer regression and that they play a major role in human cancer

immunotherapy, responses were often short lived and transferred lymphocytes were rarely found in the blood just days after injection. In 2002, however, a study showed that non-myeloablative chemotherapy immediately before the transfer of the lymphocytes led to regression of metastatic melanoma and that the transferred tumour-reactive lymphocytes repopulated the patient (Dudley et al., 2002).

The idea to apply ACT to treat cancer led to studies in mice that manipulated lymphocytes by genetically engineering them to express T cell receptors (TCR) recognising specific tumour antigens. In 2006, humans were treated for the first time with lymphocytes that were transduced with a retrovirus encoding a TCR recognising the melanocyte differentiation antigen (MDA) MART-1 (melanoma antigen recognised by T cells 1; also known as Melan-A) and tumour regression was observed in two out of 17 patients (Morgan et al., 2006). Shortly after, patients suffering from advanced B cell lymphoma were treated with lymphocytes engineered to express a chimeric antigen receptor (CAR) against the B cell antigen CD19 and anti-tumour responses were observed. The discoveries that either naturally occurring tumour-reactive lymphocytes or genetically engineered lymphocytes could mediate tumour regression was the foundation for research into ACT for the treatment of cancer (Kochenderfer et al., 2010).

1.2.3. Adoptive cell therapy using tumour-infiltrating lymphocytes as effective immunotherapy for patients with advanced melanoma

Overall response rates to TIL immunotherapy range between 34 % and 55 % and are independent of the site of the metastases or the bulk of the disease. ACT has shown to be effective in some patients who failed standard treatments. Ten to 25 % of the patients who respond achieve durable complete responses. The majority of these patients remain disease-free years after TIL immunotherapy. (Dudley et al., 2002; Pilon-Thomas et al., 2012; Radvanyi et al., 2012; Rosenberg et al., 1988, 2011; Besser et al., 2013).

In order to treat patients suffering from advanced melanoma with autologous TILs these cells need to be isolated from the melanoma tissue and expanded *in vitro*. This involves the surgical removal of tumour tissue which is digested into a single

cell suspension or multiple smaller tumour fragments. These cultures are then grown in IL-2 whereby lymphocytes will expand and destroy the tumour cells within two to three weeks. The pure lymphocyte cultures can then be assessed for their reactivity against tumour cells. Single cultures are then expanded using an antibody targeting CD3 ϵ , IL-2 and irradiated feeder cells. Five to six weeks after tumour resection, lymphocytes (up to 10^{11}) are ready for the infusion into the patient (Figure 1.1) (Rosenberg and Restifo, 2015).

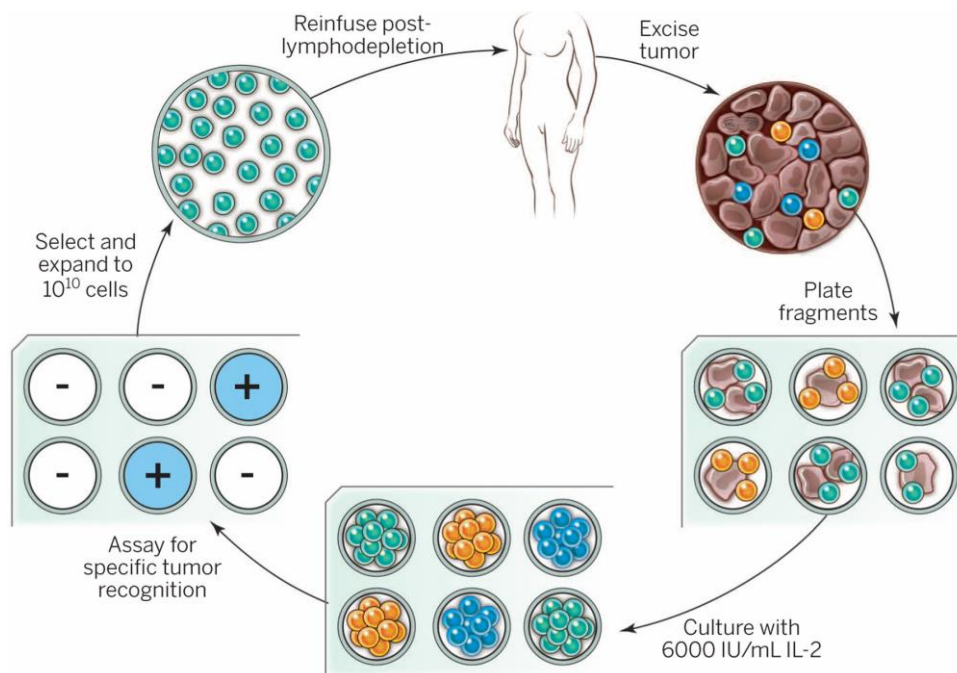


Figure 1.1: Adoptive cell transfer protocol using naturally occurring autologous tumour-infiltrating lymphocytes

Resected melanoma tissue is digested into a single-cell suspension or the tumour is divided into multiple smaller tumour fragments that are grown in IL-2 containing tissue culture media. The lymphocytes overgrow and destroy the tumour cells within two to three weeks. This leads to the generation of a pure lymphocyte culture. These lymphocytes can then be tested for their reactivity against tumour cells in co-culture assay. Tumour-reactive lymphocytes are then expanded using IL-2, OKT3 and irradiated feeder cells. Five to six weeks after tumour resection 10^{11} lymphocytes can be obtained and infused into the patient (Restifo and Rosenberg, 2015).

Patients usually receive a lympho-depleting preparative regimen consisting of the chemotherapeutics cyclophosphamide and fludarabine immediately before the transfer of the lymphocytes. It was shown that lymphodepletion leads to a substantial increase in persistence of transferred lymphocytes and an increase in duration of clinical responses. The link between lymphodepletion and improved clinical response to ACT is not fully understood. Chemotherapeutic preconditioning of the patients leads to reduced myeloid cells and lymphocytes in the circulation (Yao et al., 2012). In preclinical mouse models, it was shown that myeloid-derived suppressor cells (MDSCs) and T_{REG} cells can exist in high abundance in the tumour microenvironment and repress anti-tumour T cell responses (Bronte et al., 1998). In addition to generating a niche for the transferred T cells, lymphodepletion leads to the induction of homeostatic cytokines, such as IL-7 and IL-15, promoting T cell proliferation and survival in mice (Becker et al., 2002; Dudley et al., 2008; Gattinoni et al., 2005a; Goldrath et al., 2002; Judge et al., 2002; Schluns et al., 2000; Tan et al., 2002). In mice, lymphodepletion was also shown to enhance translocation of commensal bacteria across mucosal barriers which can activate antigen-presenting cells (APCs) by stimulating Toll-like receptors and therefore increase efficiency of ACT (Paulos et al., 2007).

TILs can mediate durable and complete responses in patients suffering from advanced malignant melanoma which raised the interest to also treat other cancer entities with this therapeutic approach. TILs can be isolated and grown from almost all tumour types but in the past identification of tumour-reactive T cells has been largely limited to melanoma. Promising new preclinical studies have now also successfully isolated tumour-reactive T cells from ovarian cancer which led to the initiation of a clinical trial (NCT02482090) (Westergaard et al., 2019).

1.2.4. What are tumour antigens?

Tumour antigens can broadly be divided into two classes: self/shared antigens or non-self/neoantigens. Self-antigens can be further subdivided into three categories.

(1) Cancer germline antigens, also known as cancer-testis antigens, are proteins that are expressed during foetal development, have limited expression in adult tissue, but can be re-expressed in a variety of cancer cells. One example of such antigen is NY-ESO1 (New York esophageal squamous cell carcinoma-1) which has been successfully targeted by T lymphocytes engineered to express a TCR specifically recognising this protein. NY-ESO1 is expressed in approximately 25 % of melanomas and 70-80 % of synovial cell sarcomas. Eleven of 20 patients with NY-ESO1⁺ melanomas and 11 out of 18 patients with NY-ESO1⁺ synovial cell sarcomas demonstrated objective clinical responses when treated with ACT immunotherapy. The broader application of this therapeutic approach is however limited as only very few cancers homogenously express the epigenetically controlled NY-ESO1 protein (Robbins et al., 2015).

(2) The second class of tumour antigens is overexpressed antigens; an example of these antigens is the carcinoembryonic antigen, which is a glycoprotein of the immunoglobulin superfamily and a tumour-associated antigen overexpressed in a variety of epithelial cancers. These overexpressed antigens have higher expression levels in cancer cells but they are still expressed at lower levels in normal tissue cells. ACT using genetically engineered T lymphocytes that expressed a high-avidity murine TCR against human carcinoembryonic antigen were administered to patients suffering from metastatic colorectal cancer. One out of three patients had an objective response but severe colitis developed in all three patients (Parkhurst et al., 2011).

(3) Differentiation antigens are the third category of self-antigens that can be targeted by ACT. Differentiation antigens are specific for a certain type of tissue and are expressed in healthy cells and tumour cells of the same origin. Normal cells that express these antigens are at risk of an attack by the transferred T cells specific for the differentiation antigen. ACT using genetically engineered T lymphocytes that expressed a high-avidity TCR against either of the melanocyte differentiation antigens gp100 or MART-1 induced a transient melanoma response but also led to severe toxicities in other organs that expressed these antigens. Approximately 42 % of the patients suffered from uveitis and/or ototoxicity (Johnson et al., 2009).

Non-self-antigens, or neoantigens, include protein products originating from viral gene products or derived from non-synonymous DNA mutations that arise during the process of tumourigenesis. Therefore, their expression is restricted to cancer cells and targeting these antigens by immunotherapy should be more effective and safe as there will be less off-target effects.

Each class of tumour-associated antigen has their advantages and disadvantages. Public antigens such as cancer-testis antigens or differentiation antigens can be shared by multiple patients and multiple cancer entities making it a therapeutic option for many patients (Anichini et al., 1993). Due to better feasibility, targeted immunotherapies have mostly focused on public antigens. These antigens have often high expression levels in the tumour tissue. However, these antigens are often only tumour-associated and not tumour-specific as they can be expressed by normal tissues. This can result in on-target off-tumour reactivity. TCRs recognising public antigens have low-affinity for the targets due to central tolerance. Attempts in the past to increase TCR affinity has led to adverse effects ranging from manageable morbidities to severe adverse events including death (Chodon et al., 2014; Johnson et al., 2009; Linette et al., 2013; Morgan et al., 2013; Rapoport et al., 2015; van den Berg et al., 2015).

Due to the afore mentioned challenges with public antigens and the advent of new sequencing technologies, there has been an interest in targeting neoantigens which are tumour-specific and therefore patient-specific (Gubin et al., 2015). These private mutations only occur in the tumour tissue which means that they do not induce central tolerance. Hence, TCRs recognising neoantigens may have higher affinity towards their antigen and be more specific compared to TCRs targeting public antigens. This leads to less toxicity and severe adverse events as there is less on-target off-tumour reactivity. However, therapeutic approaches targeting private neoantigens is highly personalised and only individual patients benefit from such a therapeutic approach. Moreover, additional time for neoantigen discovery is required potentially delaying treatment onset.

1.2.5. Products of tumour-associated antigens and tumour mutations are recognised by melanoma tumour-infiltrating lymphocytes

Early studies identified two non-mutated MDAs, MART-1 and gp100, that were frequently recognised by TILs in melanoma patients. Although not only melanoma cells but also melanocytes in the skin, ear or eye express these proteins, on-target off-tumour toxicities were rarely seen in patients who underwent complete regression treated with TILs targeting these proteins (Kawakami et al., 1994a, 1994b). However, when a high-affinity TCR recognising either MART-1 or gp100 was transduced into autologous peripheral lymphocytes, that were subsequently used for ACT, severe skin, ear and eye toxicities, but limited anti-tumour activity, were observed (Johnson et al., 2009). These results suggested that the reactivity against MDAs was not the critical target that resulted in anti-tumour activity using naturally occurring TILs or that tumour editing had already occurred.

A study by Lawrence and colleagues analysing somatic mutation rates showed that the frequency of non-synonymous mutations, a nucleotide mutation that alters the amino acid sequence of a protein, varies more than 1000-fold across different cancer entities. Paediatric cancers exhibit the lowest mutation frequencies (0.1 mutations/Megabase), whereas melanoma and lung cancer, which are often induced by environmental factors or carcinogens, can have more than 100 mutations/Megabase (Lawrence et al., 2013).

An early study from 1995 suggested that mutations might be critical targets of immune cells infiltrating the TME. The first neoantigen to be reported was mutated CDK4 that was identified in a human melanoma and recognised by autologous cytolytic T lymphocytes (CTLs) (Wolfel et al., 1995). Melanoma responsiveness to a variety of immunotherapeutic treatment options such as IL-2, ACT or checkpoint inhibitors suggested that peptide epitopes that are encoded by mutations might be the target of TIL therapy in melanoma (Gubin et al., 2014). Clinical trials showed that α -PD-1 or α -CTLA-4 checkpoint therapy can mediate an overall response in melanoma, lung cancer and bladder cancer patients, as well as cancer patients with DNA-mismatch-repair-deficiencies (Hugo et al.,

2016; Le et al., 2015; Powles et al., 2014; Naiyer A Rizvi et al., 2015; Naiyer A. Rizvi et al., 2015a; Snyder et al., 2014a; Topalian et al., 2012a; Van Allen et al., 2015; van Rooij et al., 2013); the tumour entities that have highest mutation frequencies after melanoma (Lawrence et al., 2013; Topalian et al., 2012a). A study by Brown and colleagues found that somatic missense mutations, leading to the formation of neoantigens, correlate with CTL tumour infiltration and patient survival (Brown et al., 2014). Such studies provide evidence of an association between mutational burden and survival. Additionally, they suggest that in principle directing the immune system at neoantigens can lead to cancer regression.

New whole-exome sequencing approaches identified missense cancer mutations that were recognised by autologous TILs from melanoma patients and led to complete regression (Lu et al., 2014; Robbins et al., 2013). Although melanoma has a very high mutation frequency, not every mutated protein can be recognised by T lymphocytes. Proteins that harbour the mutations must be properly processed into short peptides (~9 amino acids) for major histocompatibility complex (MHC) class I or (~13-25 amino acids) for MHC class II. The processed peptides can then be loaded onto MHC and presented on the cell surface.

One way of identifying immunogenic mutations are peptide-MHC binding algorithms. Polypeptides (21 – 25 amino acids) that have a mutated amino acid in the centre of their structure can be scanned to identify peptides that have a high binding affinity to the MHC molecules of individual patients. The top hits are then synthesised and assessed for recognition in co-culture assays with TILs from the patient. This method is dependent on the prediction of the peptide-MHC (pMHC) algorithms, which can be less reliable when it comes to less abundant human MHC molecules (Robbins et al., 2013).

An alternative screening method that does not rely on *in silico* predicted pMHC interactions involves so-called minigenes. Instead of polypeptides, minigenes are constructed that code for all mutated amino acids (flanked by 10 – 12 amino acids) in a patient. Six to 20 minigenes are linked together into tandem minigenes, cloned into expression plasmids, *in vitro*-transcribed into RNA and then electroporated into the patient's antigen-presenting cells. The APCs present the

mutated processed peptides on either MHC class I or class II. By co-culturing electroporated APCs with autologous TILs, tandem minigenes that code for individual mutations leading to tumour recognition can be identified (Lu et al., 2014). The minigene screening approach analysed TILs from 21 melanoma patients and identified a total of 45 mutated proteins. Each mutation was from a different protein and not shared among melanomas from individual patients. These findings suggest that melanoma TILs mediate anti-tumour responses by the recognition of random somatic mutations. It might explain why patients treated with TILs can experience tumour responses without auto-immune toxicity as TILs only target cancer cells expressing the mutations but not healthy cells (Klebanoff et al., 2011; Rosenberg et al., 2004).

Therapeutic cancer vaccines often cause the expansion of T cells with low-affinity TCRs against self-proteins that escaped negative selection in the thymus. This suggests that cancer vaccines that target individual mutated antigens might be more effective. In 2017, two groups demonstrated that highly personalised vaccine approaches can lead to tumour regression. Sahin and colleagues showed that a personalised RNA mutanome vaccine can induce therapeutic immunity against melanoma. They identified a patient's individual mutations to predict neoantigens and designed and manufactured a vaccine for the individual patient. The vaccine induced T cell infiltration into the tumour and killing of autologous cancer cells in the patients (Sahin et al., 2017). Ott and colleagues showed that vaccination with neoantigens of melanoma patients can induce an anti-tumour response. They generated a vaccine that targeted up to 20 predicted personal tumour neoantigens which led to the expansion of poly-functional CD4⁺ and CD8⁺ T cells. Four out of six melanoma patients had no recurrence two years after treatment and two patients were additionally treated with α -PD-1 antibody which led to further expansion of the neoantigen-specific T lymphocytes (Ott et al., 2017). If, however, mutated immunogenic epitopes are the key to success of ACT, it presents a hurdle for a broadly applicable "off-the-shelf" therapy.

Although melanoma is the prime example when it comes to immunotherapy, a study from 2014 showed that, although less abundant in other epithelial cancers, mutated immunogenic epitopes recognised by TIL can lead to an anti-tumour

immune response. Exome sequencing of a patient suffering from metastatic cholangiocarcinoma showed 26 non-synonymous mutations. Using the tandem minigene approach described above, a mutated protein, ERBB2IP (ErbB2 interacting protein), presented on MHC class II was capable of inducing an anti-tumour response. The patient was treated with bulk autologous TILs which did not lead to a clinical response, however, when infused with TILs that were more than 95 % ERBB2IP-mutation reactive, regression of lung and liver metastases was observed (Tran et al., 2014). This shows that other epithelial cancers may also be treatable with ACT as long as mutations that produce immunogenic epitopes are identified.

Techniques, such as the minigene approach, led to the identification of 75 neoantigens that were recognised by autologous TILs or peripheral blood lymphocytes in 29 out of 31 patients suffering from melanoma. These antigens were presented on a wide variety of MHC class I or class II molecules (Cohen et al., 2015; Gros et al., 2016; Huang et al., 2004; Lu et al., 2014, 2013; Parkhurst et al., 2017, p. 137; Robbins et al., 2013; Tran et al., 2014, p. 137; Zhou et al., 2005). Each of the individual antigens identified was unique and not shared among different patients. The antigens were derived from various expressed genes and there was no single pathway that was overrepresented.

1.2.6. Genetic engineering of lymphocytes for adoptive cell therapy

By genetically engineering T lymphocytes researchers hoped to broaden the application of ACT. T cells were redirected by either introducing a conventional $\alpha\beta$ -TCR or chimeric antigen receptor.

CARs were developed in the late 1980s (Gross et al., 1989). Variable regions of an antibody's light and heavy chain were linked to intracellular signalling chains (e.g. CD3 ζ) and additional co-stimulatory signalling domains such as CD28 or CD137 to achieve full activation of the T lymphocyte (Maher et al., 2002; Song et al., 2011). One major advantage of CAR T cells is that they recognise proteins in an MHC-independent manner. However, CAR T cells can only recognise cell surface components which also limits their application to proteins or mutated proteins being naturally expressed on the cell surface.

The phenotype and the functional status of the transferred lymphocytes influences efficiency of ACT. One important aspect of genetically engineering T cells for ACT is the determination of the ideal T cell subpopulation. Pre-clinical studies in mice showed that T lymphocytes in early differentiation states such as naïve or central memory T cells have improved anti-tumour characteristics (Klebanoff et al., 2005). This was supported by a study performed in monkeys that showed that persistence of transferred central memory T (T_{CM}) cells *in vivo* was better than effector memory T (T_{EM}) cells (Berger et al., 2008). Several studies have shown that the differentiation state of $CD8^+$ T lymphocytes is related to their capacity to be activated, to proliferate and to survive *in vivo* (Buchholz et al., 2013; Gattinoni et al., 2005b; Gerlach et al., 2013). In general, it was shown that cells early in their differentiation pathway led to a better persistence of the T cells in the circulation and therefore targeting these cells in immunotherapies is more likely to be associated with partial or complete clinical responses (Rosenberg et al., 2011).

1.2.7. Targeting antigens shared by normal and tumour-tissue (on target off-tumour toxicity)

The fact that T cells can recognise very small amounts of antigen expressed and presented on a normal body cell can lead to severe on-target off-tumour toxicities when normal, non-mutated proteins such as melanocyte differentiation antigens are targeted. Ideally, only antigens that are not essential for the patient's survival or even better, exclusively expressed on the tumour cells, are targeted. In 2006, Morgan and colleagues successfully engineered autologous T cells from patients suffering from metastatic melanoma to express a low-avidity TCR specific for MART-1 melanocyte differentiation antigen (Morgan et al., 2006). Two patients out of 17 treated experienced objective partial response. The study was then expanded and patients received T lymphocytes that were transduced with high-avidity TCRs that recognised either of the melanocyte differentiation antigens, gp100 or MART-1 (Johnson et al., 2009). The objective response rate was higher than in the previous study, 19 % and 30 %, respectively, however patients suffered from severe on-target off-tumour toxicities in organs that also express

the MDAs such as the skin, ears (hearing loss) and eyes (uveitis) (Johnson et al., 2009). Similar on-target off-tumour toxicities even to the degree of life-threatening adverse effects have been observed in other studies where high-affinity TCRs have been used or where previously unknown cross-reactivities caused severe side effects (Lamers et al., 2013; Morgan et al., 2013; Palmer et al., 2008; Parkhurst et al., 2011).

1.2.8. The future of adoptive cell therapy

Improvement of ACT and other immunotherapeutic treatment approaches, such as cancer vaccines or checkpoint blockade, is vastly dependent on the identification and in-depth understanding of the biology of suitable immunogenic target epitopes and the insight into the function of our immune system.

Mutations that are involved in oncogenesis and are shared not only among patients but also across different tumour entities would be excellent targets for ACT using conventional $\alpha\beta$ -TCRs. Mutated BRAF and NRAS are the most common oncogenic mutations in melanoma. Mutated NRAS or KRAS (KRAS proto-oncogene) can also be found in other cancers such as colorectal cancer, pancreatic cancer and non-small cell lung cancer (Ferrer et al., 2018; Jo et al., 2016; Lanfredini et al., 2019). Nevertheless, immunogenic epitopes that can be recognised by T cells have only been recently identified for mutated KRAS, but not for mutated BRAF or NRAS. Wang and colleagues generated two TCRs that recognise the two most common mutated variants of KRAS. In a preclinical mouse model, peripheral blood lymphocytes transduced with either of these TCRs could recognise multiple tumour cell lines expressing mutated KRAS. Adoptive transfer of these T cells led to a significantly reduced growth of pancreatic tumours (Wang *et al.*, 2016). Clinical data from colorectal cancer patients showed that the infusion of CD8⁺ T cells that target mutated KRAS can mediate an effective anti-tumour response (Tran et al., 2016).

Random somatic mutations or oncogenic driver mutations that lead to the generation of immunogenic epitopes may be ideal targets for ACT. Technological advances such as whole exome sequencing in combination with HLA (human leukocyte antigen) peptidome mass spectrometry or nano-ultra-performance

liquid chromatography coupled to high-resolution mass spectrometry (nUPLC-MS/MS) may be cheaper and faster approaches for the identification of immunogenic neoantigens of individual cancer patients than the more currently used methods described previously (Kalaora et al., 2016; Purcell et al., 2019). Among efforts to improve ACT are studies that investigate how to expand T cells *in vitro* in conditions that promote proliferation without differentiation by using IL-21 or AKT-inhibitors (AKT Serine/Threonine kinase). Moreover, improved lymphodepleting regimens are being evaluated. Furthermore, it is being tested whether the introduction of a transgene in addition to the TCR into T lymphocytes can actively alter the tumour microenvironment, for instance by the expression of IL-12 (Crompton et al., 2015; Gros et al., 2014; Kerkar et al., 2011; Li et al., 2005). It was shown that constitutive expression of IL-12 by engineered T cells can result in improved tumour protection in mice but also carries the risk of IL-12-mediated toxicity as seen in patients. Alsaieedi and colleagues showed that inducible IL-12 expression in melanoma-specific T cells leads to inhibition of B16F10 tumours in mice without causing systemic toxicity (Alsaieedi et al., 2019; Chmielewski et al., 2011; Kerkar et al., 2011; van Herpen et al., 2005). However, these improvements of ACT only focus on immune cells. It is also of critical importance to understand the biology of tumour cells. In the context of antigen-directed immunotherapy, a better understanding of how proteins that generate immunogenic epitopes are regulated can be used to improve therapy and prevent relapse by acquired resistance mechanisms.

1.3. Primary, adaptive and acquired resistance to cancer immunotherapy

It has become evident that products of random somatic mutations or oncogenic driver mutations are attractive targets for ACT. However, we need to understand why some patients do not respond to this line of therapy despite the approach being highly personalised.

Although cancer immunotherapies, such as ACT or checkpoint blockade, can induce long lasting immunity in patients suffering from metastatic disease, there is still a rather high percentage of patients which do not respond to immunotherapy at all (primary resistance) or initially respond and then relapse

(acquired resistance). A further subtype of resistance is adaptive immune resistance. In this situation the tumour is recognised by immune cells but it protects itself by adaptation. As the interactions between tumour and immune cells are highly dynamic and constantly evolving, this can either present as a primary resistance, a mixed response or acquired resistance.

1.3.1. Tumour cell-intrinsic resistance mechanisms

The easiest explanation for why a tumour does not respond to immunotherapy is the absence of tumour antigens that can be recognised by T lymphocytes (Gubin et al., 2014). Alterations in the tumour cells in the antigen presentation and processing machinery can lead to the tumour-associated antigen not being presented on MHC molecules on the cell surface and therefore no recognition of the tumour cell by immune cells. Downregulation or mutations of proteasome subunits or transporters that are important for antigen processing, beta-2-microglobulin (B2M) or MHC can prevent tumour antigen presentation on the cell surface (Figure 1.2) (Marincola et al., 2000; Sucker et al., 2014).

Other cell-intrinsic mechanisms that prevent successful cancer immunotherapy include expression or repression of genes or even entire pathways that can inhibit immune cell infiltration into the tumour tissue or modulate the microenvironment in such a way that it inhibits immune cell function (Figure 1.2).

Many tumours have overactive oncogenic signalling through MAPK pathways that can result in the production of IL-8 and VEGF (vascular endothelial growth factor) which are both described as having inhibitory effects on T lymphocyte recruitment and function (Liu et al., 2013). The loss of PTEN which is found in 30% of melanomas, but is also common in other tumour entities, enhances PI3K (phosphoinositide 3-kinase) signalling. PTEN loss in tumour cells has been associated with resistance to cancer immunotherapy. Loss of PTEN leads to the expression of immunosuppressive factors such as CCL2, IL-6, IL-10 and VEGF (Dong et al., 2014; Peng et al., 2016). In PTEN^{low} tumours significantly reduced protein expression of Lck (Lymphocyte cell-specific protein-tyrosine kinase), predominantly expressed by T cells, and the effector molecules granzyme B and IFN γ (Interferon γ) was observed (Peng et al., 2016). Moreover, it was shown that

PD-L1 (CD274; Programmed cell death 1 ligand 1) is repressed by PTEN expression leading to enhanced anti-tumour immunity by tumour-reactive T cells and targeted killing of melanoma cells (Dong et al., 2014).

Another oncogenic signalling pathway involved in T cell exclusion from tumour tissue is the WNT (wingless) signalling pathway. Stabilisation of β -catenin leads to constitutive WNT signalling (Spranger et al., 2015). In a murine melanoma model, tumours with increased β -catenin levels also showed decreased CCL4 levels which in turn led to reduced infiltration with CD103⁺ DCs. This in turn leads to an altered CXCR3-CXCL9/10 chemokine axis and defective migration of effector CD8⁺ T cells into the tumour (Spranger et al., 2017).

Tumour cells that constitutively express the negative checkpoint ligand PD-L1 can actively inhibit T cell function via the interaction with PD-1 on the T cell surface. PTEN deletions, PI3K and AKT mutations, EGFR (epidermal growth factor receptor) mutations, CDK5 (cyclin-dependent kinase 5) disruption, MYC (MYC proto-oncogene) overexpression or an increase in PD-L1 transcripts that are stabilised by the truncation of the 3'UTR (untranslated region) can all lead to constitutive PD-L1 expression on the tumour cells surface (Akbay et al., 2013; Casey et al., 2016; Dorand et al., 2016; Kataoka et al., 2016; Lastwika et al., 2016; Parsa et al., 2007). The IFN γ signalling pathway has been described as a critical player in different types of resistance to cancer immunotherapy (Gao et al., 2016; Pardoll, 2012; Ribas, 2015; Shin et al., 2017; Zaretsky et al., 2016b). IFN γ is a double-edged sword; it has both a positive and negative effect on the anti-tumour immune response (Figure 1.2). Tumour-infiltrating T lymphocytes that have recognised their cognate antigen on APCs or tumour cells are a major source of IFN γ in the TME. It has several positive effects on the anti-tumour response. Firstly, IFN γ enhances antigen processing and presentation by inducing increased expression of proteins involved in antigen presentation, such as MHC molecules. Secondly, through the induction of chemokine expression, it leads to the recruitment of other immune cells into the TME. And lastly, it has a direct pro-apoptotic and anti-proliferative effect on cancer cells (Platanias, 2005). Nevertheless, continuous IFN γ exposure can result in immune escape by immunoediting of tumour cells (Shankaran *et al.*, 2001; Benci *et al.*, 2016).

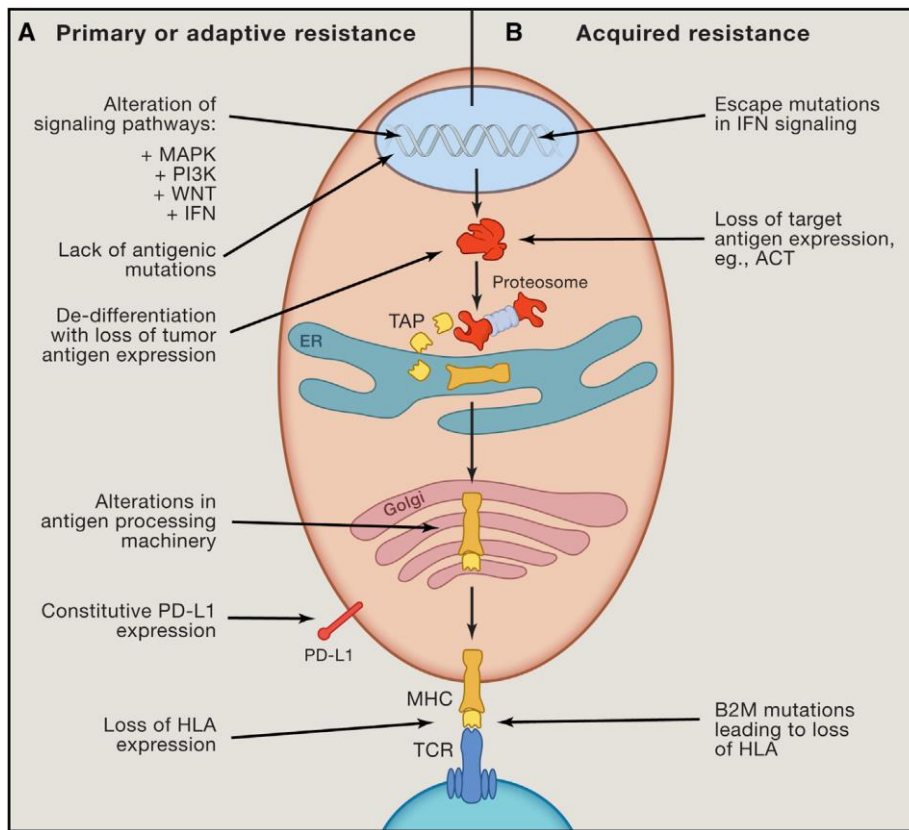


Figure 1.2: Cell-intrinsic mechanisms of resistance to cancer immunotherapy

(A) Cell-intrinsic factors that lead to primary or adaptive resistance include alterations of signalling pathways, lack of antigenic mutations, de-differentiation, alterations in the antigen processing machinery, constitutive PD-L1 expression and loss of MHC. (B) Cell-intrinsic factors that are associated with acquired resistance are escape mutations in the IFN γ signalling pathway, loss of target antigen expression or B2M mutations leading to the loss of MHC (Sharam et al., 2017).

Tumour cells can escape the effects of IFN γ by either mutating or downregulating proteins involved in the IFN γ signalling pathway. These molecules can be part of the IFN γ receptor, JAK 1/2 (Janus kinase 1/2) or STATs (signal transducer and activator of transcription protein family) which are transcriptional activators critical for this pathway (Darnell et al., 1994). Analyses of cell lines and animal models revealed that mutations or transcriptional silencing of proteins involved in the IFN γ signalling pathway in the tumour cells results in the loss of the anti-tumour effect of IFN γ (Dunn et al., 2005; Kaplan et al., 1998). Recently, it was shown that patients suffering from metastatic melanoma who did not respond to checkpoint therapy have an increased frequency of mutations in genes involved in the IFN γ signalling pathway such as JAK2, IRF1 (interferon regulatory factor 1) or IFNGR1/2 (interferon gamma receptor 1 and 2) (Gao et al., 2016).

It was also shown that epigenetic modifications of the DNA in tumour cells can change gene expression of immune related genes which can in turn have an impact on antigen presentation and immune evasion. Combination therapies using immunotherapy and epigenetic modifiers, such as demethylating agents, can induce re-expression of immune related genes and thereby positively influence cancer immunotherapy. In a murine melanoma model, ACT in combination with histone deacetylase inhibitors resulted in a significant improvement of anti-tumour activity of transferred T cells as the expression of MHC molecules and tumour antigens was increased (Vo et al., 2009).

1.3.2. Tumour cell-extrinsic resistance mechanisms

Tumour-extrinsic mechanisms that counteract successful cancer immunotherapy can involve many cell types within the tumour microenvironment. These include neutrophils, MDSCs, macrophages, T_{REG} cells or other suppressive immune cells (Figure 1.3).

It was previously shown that a certain subset of neutrophils that infiltrate the TME can limit the efficacy of ACT immunotherapy. The c-Met⁺ (Met receptor tyrosine kinase) neutrophils that are in part recruited by cytokines and chemokines produced by melanoma cells express inhibitory ligands such as PD-L1 on their cell surface and thereby repress T cell proliferation and function (Glodde et al.,

2017; Riesenberger et al., 2015).

MDSCs can promote tumour cell invasion, metastases and angiogenesis (Figure 1.3) (Yang et al., 2008, 2004). Breast and colorectal cancers infiltrated with MDSCs have been correlated with reduced survival of the patients (Solito et al., 2011). Overall, the presence of MDSCs has been correlated with decreased efficiencies of various cancer immunotherapies including ACT and checkpoint therapy (Kodumudi et al., 2012; Laborde et al., 2014; Meyer et al., 2014). PI3K γ is a critical player that regulates the function of these immune cells. The absence of PI3K γ , induced by an inhibitor or in genetically-engineered mouse models, is associated with decreased suppressive immune signature in the tumours and therefore increased survival (De Henau et al., 2016; Kaneda et al., 2016).

Tumour-associated macrophages can be classed into two distinct subpopulations based on their anti-tumourigenic or pro-tumourigenic properties (Figure 1.3) (Chanmee et al., 2014). The two subpopulations differ by the differential expression of transcription factors, surface molecules, cytokine profile and metabolism (Biswas and Mantovani, 2010; Hu et al., 2016). Higher frequencies of tumour-associated macrophages are associated with a poorer prognosis in human cancer (Hu et al., 2016). Several studies suggest that these macrophages express negative checkpoint surface molecules such as PD-L1 and B7-H4 (B7 family member, H4) that directly suppress T cell function in different tumour models (Kryczek et al., 2006; Kuang et al., 2009).

The immune response in the TME is highly dynamic and initial activation of T cells and anti-tumour immune responses also induce expression of inhibitory genes and signalling cascades in the T cells themselves that in turn can lead to therapy failure. These mechanisms are tightly regulated and are critical to prevent auto-immunity. T cell activation via the TCR and the co-stimulatory molecule CD28 leads to the expression of CTLA-4, a negative immune checkpoint molecule. Similarly, effector T cells produce and secrete IFN γ which, on the one hand, induces antigen presentation but, on the other hand, induces expression of PD-L1 on several cell types, such as macrophages and tumour cells (Figure 1.2 and 1.3) (Chen, 2004; Dong et al., 2002).

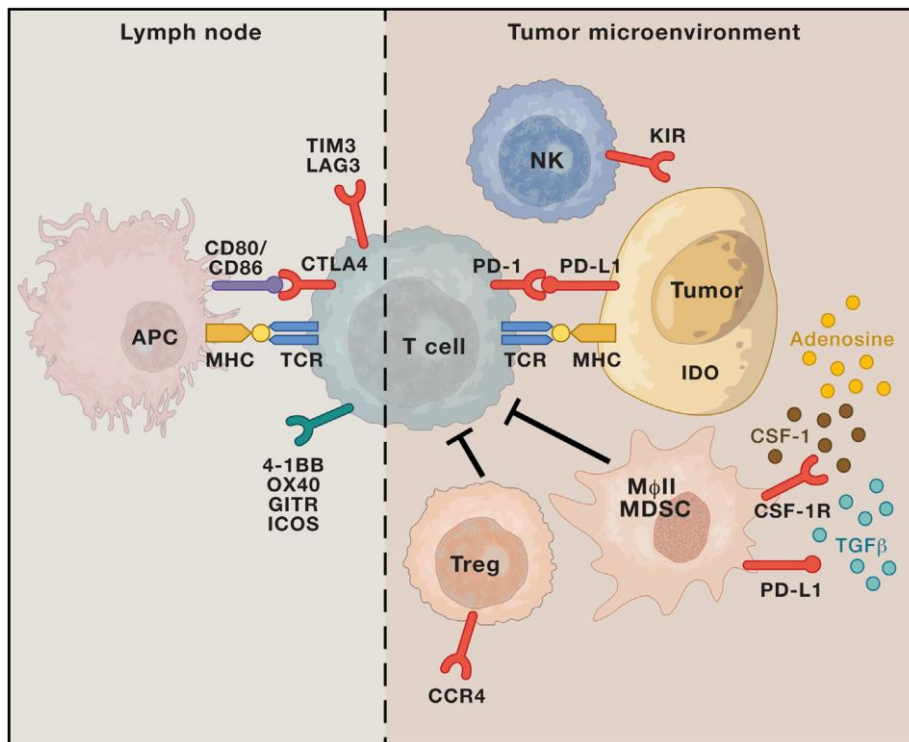


Figure 1.3: Cell-extrinsic mechanisms of resistance to cancer immunotherapy

These mechanisms include other immune cells that mediate resistance to cancer immunotherapy. Immune suppressive cell populations are T_{REG} cells, MDSCs and macrophages. Other mechanisms are the upregulation of negative immune checkpoint molecules such as PD-1 or CTLA-4 on anti-tumour T lymphocytes or corresponding ligands of other immune cell populations or tumour cells themselves. Additionally, cytokines and metabolites released into the tumour microenvironment can mediate resistance (Sharam et al., 2017).

IFN γ can also induce expression of immunosuppressive molecules such as IDO (indolamine-2,3-deoxygenase), a metabolic enzyme that can have a negative effect on T cell effector function by contributing to peripheral tolerance (Gajewski et al., 2013). Other molecules that exert inhibitory functions on T cells such as CEACAM1 (carcinoembryonic antigen cell adhesion molecule-1) and TIM-3 (T-cell immunoglobulin and mucin-domain containing-3) have been identified as possible therapeutic targets for combination therapy (Gray-Owen and Blumberg, 2006; Ortenberg et al., 2012). The cytokine TGF β (transforming growth factor β) plays an important role in immunosuppression by stimulating T_{REG} cells which in turn can suppress effector T cell function (Lebrun, 2012). Increased TGF β levels are associated with poor prognosis in various tumour entities (Lin and Zhao, 2015; Massagué, 2008).

The enzyme CD73 expressed on various cancer cells catalyses the dephosphorylation of AMP (adenosine monophosphate) to adenosine which has an immunosuppressive function (Stagg et al., 2010). Adenosine inhibits proliferation and cytotoxic effector function of CD8⁺ T cells via the receptor A2A (Adenosine A2a receptor) on the T cell surface (Zhang et al., 2004). It was previously demonstrated that CD73 is linked to melanoma phenotype switching. Growth factor signalling and activating MAPK mutations drive CD73 expression on the tumour cells and mark a mesenchymal-like melanoma cell state program. The pro-inflammatory cytokine TNF α produced by activated T cells cooperates with MAPK signalling inducing the expression of CD73 on the melanoma cells (Reinhardt et al., 2017).

1.3.3. Acquired resistance mechanisms

Patients who respond to immunotherapy for a period of time can acquire resistance leading to disease relapse. One fourth to one third of patients with advanced melanoma who have objective response to checkpoint therapy using α -PD-1 or α -CTLA-4 blocking antibodies relapse even under continued immunotherapy (Schachter et al., 2017). Acquired resistance mechanisms include escape mutations in the tumour cell, lack of T cell recognition by inadequate antigen processing and presentation, or loss of T cell function.

Studies showed that each of these mechanisms can lead to acquired resistance to either ACT or checkpoint blockade therapy.

Acquired resistance to ACT using TCR-engineered T cells is common. Initial response to treatment is good but is followed by a high frequency of patients that relapse within months. Studies investigating the phenotype and functionality of engineered T cells used for ACT showed that, although T cells are cytolytic at the time of transfer, they can have lost cytolytic function at the time of recurrence (Ma et al., 2013, 2011).

Endogenous antigens are constantly presented to T cells on MHC class I molecules on the surface of every nucleated cell. The presentation of peptide-MHC class I complex provides a snapshot of the intracellular status (healthy vs. cancerous/infected) of the cell to circulating CD8⁺ T cells. T cells are activated by foreign antigens, such as antigens derived from bacteria or viruses, which results in the killing of the infected cell. However, tumour antigens can also activate T cells which enables killing of the malignantly transformed cells. One resistance mechanism of tumour cells to escape immunotherapy is an alteration in the antigen processing and presentation pathway (Figure 1.2) (Leone et al., 2013). Several studies have shown that the downregulation or loss of pMHC I on the tumour cell surface from different tumour entities is associated with progression of disease and reduced survival of the patients (Angell et al., 2014; Cabrera et al., 2003; Kaneko et al., 2011; Mandic et al., 2004; Mehta et al., 2008; Meissner et al., 2005; Ogino et al., 2006; Rolland et al., 2007; Ward et al., 2014). Surface pMHC I expression can be reduced by gene deletions or mutations or by reduction or loss of transcription. These alterations may directly influence the MHC class I genes or can lead to defects in peptide generation, peptide transport or loading of peptides into MHC class I molecules (Seliger *et al.*, 1997; Delp *et al.*, 2000; Seliger *et al.*, 2001; Mandic *et al.*, 2004; Atkins *et al.*, 2004; Meissner *et al.*, 2005; Mehta *et al.*, 2008; Seliger *et al.*, 2010; Hasim *et al.*, 2012; Leone *et al.*, 2013).

B2M is a protein essential for folding and transport of HLA class I molecules to the cell surface and therefore is critical for CD8⁺ T cell recognition. It was shown in the 1990s, that some cancer patients treated with ACT or IL-2 immunotherapy

developed acquired resistance by loss of B2M resulting in the absence of HLA class I surface expression on the tumour cells (D'Urso et al., 1991; Restifo et al., 1996). A more recent study using PD-1 blocking antibodies showed that a patient relapsed from therapy because resistant tumour cells acquired a homozygous truncating mutation in the B2M gene that resulted in the absence of HLA class I on the surface of the tumour cells (Zaretsky et al., 2016a). In the same study, two additional patients were identified that had copy number neutral loss-of-function mutations in the JAK1 or JAK2 gene in addition to a loss of heterozygosity as the wildtype allele was lost. The mutations in the JAK genes allowed the tumour cells to evade the anti-proliferative effect of IFN γ (Zaretsky et al., 2016a). An additional study in which a patient with metastatic colorectal carcinoma was treated with TIL ACT identified additional evidence for loss of the antigen presentation machinery. The administered TILs recognised mutated KRAS which was presented on HLA-C*08:02. The transfer of the TILs led to an objective response but one of the metastases relapsed as it had specifically lost a part of chromosome 6 that encodes HLA-C*08:02. Although KRAS mutations are common across different cancer entities such as gastrointestinal cancers, HLA-restriction limits the numbers of patients that could benefit from this line of treatment to around 10 % of the population. Cancer vaccination approaches seem to be more feasible as restricting HLA alleles are a major drawback of these therapeutic interventions (June, 2016; Tran et al., 2016).

The peptides presented by MHC class I on the cell surface originate from a broad variety of proteins. These can either be functional proteins involved in various cellular processes or proteins from defective protein synthesis. Peptides are processed into 8-11 amino acids to ensure high-affinity binding into the peptide-binding groove of MHC class I. The small peptides have specific amino acid properties at position 2/5 and the C-terminal amino acid, the so-called anchor residues. Two key processing events ensure optimal peptide binding. The cytosolic proteasome/immunoproteasome degrades larger protein fragments into smaller peptides by a process called peptide proteolysis. This process is responsible for the generation of the C-terminal amino acid residue that binds to MHC class I. The next processing step by the proteins ERAP1/2 (Endoplasmic

reticulum aminopeptidase 1/2) in the endoplasmic reticulum (ER) is responsible for processing the N-terminal region of the peptide. Although both processing steps are independent of each other, defect in either or both results in the cell not being able to produce stable pMHC I that reaches the surface and to activate CD8⁺ T cells.

The proteasome is a multi-catalytic enzyme complex that resides within the cytosol. It regulates protein homeostasis and generates antigens for the presentation on MHC class I on the cell surface (Goldberg et al., 2002; Pagano et al., 1995; Wang and Maldonado, 2006). The three catalytic subunits, $\beta 1$, $\beta 2$ and $\beta 5$, that reside within the 20S subunit core of the proteasome are responsible for the proteolytic activity. Inflammatory cytokines, such as IFN γ , induce the upregulation of the catalytic subunits LMP2 (Proteasome subunit $\beta 9$), LMP7 (Proteasome subunit $\beta 8$) and LMP10 (Proteasome subunit $\beta 10$) that can replace the $\beta 1$, $\beta 2$ and $\beta 5$ subunits and produce an immunoproteasome (Glynne et al., 1991; Kelly et al., 1991; Ortiz-Navarrete et al., 1991). The immunoproteasome results in the enhanced generation of antigenic peptides. The reduction, loss or even a single nucleotide polymorphism in either of the immunoproteasome subunits can lead to immune evasion (Hasim et al., 2012; Mehta et al., 2007; Rock et al., 1994; Schwarz et al., 2000).

The protein TAP (transporter associated with antigen processing) transports peptides (11-14 amino acids) that were generated in the cytosol by the proteasome/immunoproteasome into the ER. ERAP1 and ERAP2 process the N-terminal extensions of the imported peptides with optimal length and affinity for MHC class I loading (Evnouchidou et al., 2014; Saric et al., 2002; York et al., 2006, 2002). Studies have reported that ERAP1 can be regulated at the transcriptional and post-transcriptional levels and that even single nucleotide polymorphisms in ERAP1 can influence the quality and quantity of pMHC I surface expression (Hammer et al., 2007, 2006; Kamphausen et al., 2010; Mehta et al., 2009; Reeves et al., 2014). Functionality of ERAP1 is coupled to the ability to generate tumour antigens and properly present them on MHC class I molecules and thereby may influence anti-tumour T cells response and tumour control.

Successful antigen presentation of processed high-affinity antigens involves peptide transport, folding and loading onto MHC class I molecules. The first step is peptide transport from the cytosol to the ER via the TAP heterodimer where peptides are further processed and eventually loaded onto MHC class I molecules. In the ER lumen the chaperone proteins CNX (calnexin), CRT (calreticulin) and BiP (Binding Protein) orchestrate the association of the immature heavy chain and β_2 microglobulin. This is required for stable folding of the MHC class I heavy chain before the formation of the peptide loading complex consisting of TAP, ERp57 (Endoplasmic reticulum resident protein 57), TPN (tapasin) and MHC class I. TPN protein selects and edits optimal peptides and thereby ensures that stable pMHC I complex is formed. This ultimately results in the dissociation from the peptide loading complex and transport to the cell surface via the golgi apparatus.

The TAP heterodimer (TAP1 and TAP2) consists of two ATP-hydrolysing (adenosine triphosphate) subunits which transport peptides from the cytosol into the ER. It forms part of the peptide loading complex and facilitates peptide loading onto MHC class I molecules (Neefjes et al., 1993). Down-regulation or loss of either or both TAP1 or TAP2 correlate with a reduction of pMHC I surface expression and loss of these proteins has been observed in a variety of cancer cell lines and primary tumours (Bukur et al., 2012; Cromme et al., 1994). TAP function and expression in cancerous cells impacts pMHC I expression as they play a critical function in importing potential tumour antigens from the cytosol into the ER (Kaklamanis et al., 1994).

The chaperon proteins that reside within the ER help folding the MHC class I immature heavy chain and β_2 microglobulin before the mature MHC class I molecules associate with other proteins that together form the protein loading complex. Altered expression levels of the chaperons CNX and CRT has been linked to a variety of tumour types. These chaperons help in basic cellular functions such as cell migration and adhesion, cell cycle regulation and ER stress responses (Delom et al., 2007; Leone et al., 2013; Lu et al., 2015). The reduced expression of the chaperone ERp57, which is responsible for the formation of disulphide bonds to form the mature peptide loading complex, has been shown

to be a predictor of survival in cervical carcinoma and the loss or reduction of the thiol oxidoreductase involved in the same process is correlated with the progression of gastric cancer (Chung et al., 2013; Leys et al., 2007).

The protein TPN is essential for the formation of a stable pMHC I complex as it enables optimal slow off-rate peptides to bind the MHC class I molecule and form a stable pMHC I complex by facilitating the release of sub-optimal fast off-rate peptides (Hateren et al., 2010). TPN levels directly correlate with pMHC I expression and TPN deficiency results in fewer stable pMHC I on the cell surface suggesting that TPN may contribute to immune escape of several tumour types (Seliger *et al.*, 2001; Williams *et al.*, 2002; Hateren *et al.*, 2010; Leone *et al.*, 2013). There is a wide variety of evidence that demonstrates that alteration in the antigen processing and presentation pathway has major impact on response to cancer immunotherapies.

In summary, acquired resistance to cancer immunotherapy, either ACT or checkpoint blockade, can be mediated by a genetic loss or mutation of genes encoding the antigen presentation machinery or IFN γ signalling. Tumour-reactive T cells specifically recognise tumour cells that express the cognate antigen. Tumours may mutate or decrease expression of these antigens and thereby become resistant to cancer immunotherapy. T cells that are reinvigorated by checkpoint therapy predominantly recognise antigens derived from mutated proteins (Schumacher and Schreiber, 2015; van Rooij et al., 2013). Hence, epigenetic silencing, mutations or genetic deletions leading to the loss of expression of the mutated proteins, recognised as cognate antigens by the tumour-reactive T cells, would result in therapy failure.

1.3.4. Antigen presentation and immune regulation in the tumour

Immunosurveillance mechanisms, of the innate and adaptive immune system, control and prevent tumour growth. But an immunosuppressive TME can alter the immune response and malignant cells may survive despite the presence of the immune cells in the TME (Vesely and Schreiber, 2013).

Dendritic cells (DCs) and macrophages are crucial for the orchestration of innate and adaptive immune response to the tumour. DCs are professional antigen

presenting cells that present antigens on MHC class II or via cross-presentation of internalised antigens on MHC class I. DCs are required for the activation of naïve tumour-reactive T cells in the tumour-draining lymph nodes. DCs and macrophages are abundant in the TME and tumour-draining lymph nodes. Immature DCs that infiltrate the tumour tissue are unable to efficiently activate T cells as they usually express low levels of MHC class I, MHC class II and co-stimulatory molecules. However, once they encounter tumour antigen, these DCs mature and upregulate these molecules. The mature DCs then migrate to the lymph nodes and present the encountered tumour antigens to either CD4⁺ or CD8⁺ T cells through classical antigen presentation or cross-presentation, respectively. DC maturation is often suppressed by the immunosuppressive nature of the TME which results in the infiltration of functionally impaired or immature DCs. These DCs have reduced endocytic activity which leads to a reduction of internalising proteins and therefore a reduced activation of CD8⁺ T cells by cross-presentation in the lymph nodes (Gerner and Mescher, 2009). In order to mount a peripheral T cell response, maturation of DCs to efficiently present tumour antigen is critical. DC infiltration in primary tumours is associated with reduced incidence of metastases and better survival in several cancer types (Ma et al., 2012).

Macrophages are a second class of antigen presenting cells in the TME. Macrophages are phagocytic cells that can adapt their phenotype in response to the surrounding microenvironment as part of an immune evasion mechanism.

The anti-tumourigenic macrophages express high levels of MHC class I and class II and have the ability to efficiently process and present tumour antigens. These macrophages interact with T helper cells and NK cells to contribute to the elimination of cancer cells early during tumourigenesis.

Conversely, the pro-tumourigenic macrophages cannot present tumour antigen efficiently as they have reduced expression levels of MHC class I and class II (Quatromoni and Eruslanov, 2012). The phenotype of the macrophages can change during the course of tumourigenesis from being anti-tumourigenic to pro-tumourigenic.

1.4. Tissue-resident memory CD8⁺ T cells

Lymphocytes were classically viewed as continuously circulating through the blood and lymphoid organs. However, during the past decade, studies showed that lymphocytes can also establish residency in non-lymphoid tissues such as the skin. Most prominently they can be found at barrier sites. These tissue-resident lymphocytes can originate from innate lymphocytes, unconventional T cells and T lymphocytes (Artis and Spits, 2015; Clark, 2015; Godfrey et al., 2015; Schenkel and Masopust, 2014). One important shared function of all these different resident lymphocytes is protection of tissue function and integrity during infection but also homeostasis.

1.4.1. Effector and memory CD8⁺ T cells

Adaptive immune responses are initiated by APCs that migrate from the site of infection to the draining lymph node where they present antigen to naïve T cells. Clonal expansion of T cells is initiated when a naïve T cell encounters its cognate antigen. APCs present antigens on MHC class I molecules. Additionally, they express co-stimulatory molecules, such as CD80 or CD86, and effector cytokines, which trigger a proliferation and differentiation programme of T cells. This leads to clonally expanded effector cells. Effector T cells migrate to the site of the primary infection and help clear the pathogen, whereas circulating memory T cells persist long-term and can mount a rapid immune response upon re-infection.

The effector T cell population consists of short-lived effector cells and a smaller population of memory precursor effector cells (Cui and Kaech, 2010; Kaech and Cui, 2012). Whether a CD8⁺ T cell adopts an effector or memory phenotype is determined early after activation and this process is influenced by several parameters. These parameters include exposure to inflammatory or regulatory cytokines, the extent of co-stimulation by APCs and TCR signalling strength. These input signals regulate the expression of transcription factors, the metabolic program, chromatin accessibility and the expression of cytokine and chemokine receptors which all together define the different T cell phenotypes and their function (Gray et al., 2014).

Effector CD8⁺ T cells (T_{EFF}) have high expression levels of the transcription factor T-bet (T-cell-specific T-box transcription factor T-bet). T-bet promotes the expression of granzyme B, perforin and IFN γ (Cruz-Guilloty et al., 2009; Joshi et al., 2007). Additionally, the transcription factor Eomes (Eomesodermin) cooperates with T-bet (Banerjee et al., 2010; Intlekofer et al., 2008; Joshi et al., 2007; Pearce et al., 2003; Rao et al., 2010). During T cell activation, signalling through the IL-2R (Interleukin 2 receptor) upregulates Blimp1 (PR domain zing finger protein 1) which thereby promotes short-lived effector cell differentiation and represses autologous IL-2 expression (Gong and Malek, 2007; Kallies et al., 2009; Martins et al., 2008; Rutishauser et al., 2009). T_{EFF} cells also gain the ability to egress from secondary lymphoid tissues in order to enter non-lymphoid tissues and contribute to pathogen clearance (Bachmann et al., 1999; Hamann et al., 2000; Sharma et al., 2015). After the contraction of the short-lived effector cells, remaining memory T cell precursors develop into long-lived memory cells. These memory T cells have a different functional, phenotypical and transcriptional profile to naïve T cells and T_{EFF} cells (Chang et al., 2014; Kaech and Cui, 2012). The transcription factor T-bet is downregulated whereas Eomes expression is increased (Joshi et al., 2011; Zhou et al., 2010). The cooperation of both transcription factors leads to the upregulation of CD122 (IL-2/IL-15R β chain) which supports homeostatic IL-15 signalling important for proliferation and survival (Banerjee et al., 2010; Intlekofer et al., 2005; Pipkin et al., 2010).

When memory CD8⁺ T cells re-encounter their cognate antigen they can respond rapidly. They expand and/or secrete effector cytokines and/or cytotoxic granules immediately to control infection. IL-15- and IL-7-mediated homeostatic turnover and survival signals maintain stable levels of memory CD8⁺ T cells even in the absence of cognate antigen (Becker et al., 2002; D'Souza et al., 2002; Goldrath et al., 2002; Kaech et al., 2003).

Memory CD8⁺ T cells are a heterogeneous population of cells. Based on effector functions, proliferative capacities, migration ability, expression of surface markers and anatomical localisation several subsets of memory CD8⁺ T cells have been defined (Bachmann et al., 2005; Gebhardt et al., 2009; Hawke et al., 1998; Jameson and Masopust, 2009; Jiang et al., 2012; Masopust et al., 2001). Central

memory T cells express the surface markers CD62L, CCR7 and CD127 (IL-7R α). T_{CM} cells reside in secondary lymphoid organs such as lymph nodes and spleen but also in the blood. They have a high proliferative capacity and express more IL-2 compared to other memory T cell subpopulations (Sallusto et al., 2004, 1999; Wherry et al., 2003). Effector memory T cells do not express the lymphoid tissue homing receptor CD62L and CCR7 and localise to peripheral organs and the blood (Masopust et al., 2004, 2001; Sallusto et al., 2004, 1999). T_{EM} cells express high levels of CD127 and sustain a higher cytolytic activity through expression of perforin and granzyme B. Upon TCR engagement they additionally express the effector cytokines TNF α and IFN γ . But in contrast to T_{CM} cells, T_{EM} cells have a rather poor proliferative capacity (Sallusto et al., 2004).

In the last decade a new subset of memory T cells, tissue-resident memory T cells (T_{RM}), has been described. This subset is disconnected from the circulation and resides long-term in different non-lymphoid tissues (Casey et al., 2012; Gebhardt et al., 2009; Wakim et al., 2010; T. Wu et al., 2014). Studies have shown that long-lived, pathogen-specific T_{RM} cells can be found in the intestinal and vaginal mucosa, brain, liver, salivary glands and skin (Gebhardt et al., 2011; Hofmann et al., 2013; Hofmann and Pircher, 2011; Jiang et al., 2012; Masopust et al., 2006; Pallett et al., 2017; Posavad et al., 2017; Sathaliyawala et al., 2013; Smith et al., 2015; Thom et al., 2015; Wakim et al., 2008; Woodberry et al., 2005). T_{RM} cells do not recirculate and only migrate locally within the tissue they reside in. These T cells can provide immediate control of localised infections such as herpesvirus infection (Gebhardt et al., 2011; Teijaro et al., 2011; Thom et al., 2015; Wakim et al., 2008; Zens et al., 2016). Recently, not only pathogen-specific, but also tumour-specific, T_{RM} cells have been described (Bösmüller et al., 2016; Webb et al., 2015; Edwards et al., 2018; Egelston et al., 2017; Murray et al., 2016).

1.4.2. Phenotype and ontogeny of tissue-resident memory CD8⁺ T cells

Like all memory T cells, T_{RM} cells have differentiated from naïve T cells and express CD44, a marker for antigen experience (Budd et al., 1987).

T_{RM} cells can lodge in non-lymphoid tissues in response to local inflammation but they may also form without inflammation. T_{RM} cells do not express the lymph node homing molecules CD62L and CCR7. A molecule that is commonly used to identify T_{RM} cells is CD103 although not all T_{RM} cell populations express CD103. CD103 is the α -chain of the integrin $\alpha E\beta 7$ which binds to E-cadherin. E-cadherin is an adhesion molecule that is found on epithelial cells and thereby contributes to the retention of CD103⁺ T_{RM} cells in the peripheral tissues (Ariotti et al., 2012b; Bevan, 2011; Lefrançois et al., 1999; Schön et al., 1999; Sheridan and Lefrançois, 2011). Human and murine T_{RM} cells express CD69, a T cell activation marker. Expression of CD69 antagonises expression of the sphingosine-1-phosphate receptor-1 (S1PR1), a molecule which is important for tissue egress, and thus additionally promotes residency (Bankovich et al., 2010). S1PR1 is a G-protein coupled receptor and its signalling promotes trafficking toward S1P (sphingosine-1-phosphate). S1P is a lipid ligand that is highly abundant in the lymph and blood. Therefore, downregulation of S1PR1 prevents egress from the tissue as the T_{RM} cells can no longer migrate towards the S1P gradient (Hla et al., 2008). Not all T_{RM} cells in different peripheral tissues can be described by the expression of CD69 and CD103 however, both surface molecules are crucial for the generation of T_{RM} cells in the epidermis (Mackay et al., 2013). In addition to CD69 and CD103, T_{RM} cells in the skin typically express CD49a (VLA-1) which promotes tissue retention through binding to collagen type IV (Richter and Topham, 2007).

T_{RM} cells express high levels of granzyme B, TNF α and IFN γ (Hombrink et al., 2016). Additionally, it was described that T cells express high levels of co-inhibitory receptors such as PD-1 and CTLA-4 (Fan and Rudensky, 2016; Wakim et al., 2008). The unique T_{RM} phenotype is coordinated by the expression of various transcription factors. The transcription factors Blimp-1 and Hobit (Homolog of Blimp-1 in T cells) seem to operate in a synergistic manner in mice to form T_{RM} cells (Mackay et al., 2016). Downregulation of the transcription factors Krüppel-like Factor 2 (KLF2), Eomes and T-bet is important for T_{RM} cell formation. KLF2 regulates the expression of the *S1pr1* gene and thus KLF2 downregulation promotes tissue retention.

TGF β and the T-box transcription factors Eomes and T-bet operate in a feed-forward loop. TGF β is important for the downregulation of Eomes and T-bet which in turn leads to increased signalling via the TGF β receptor (Mackay et al., 2015). T_{RM} cells express several chemokine receptor including CXCR3, CCR5 and CCR6 and produce chemokines such as CCL3, CCL4 and CCL5 (Djenidi et al., 2015; Hombrink et al., 2016).

Effector T cells can enter peripheral non-lymphoid tissues by downregulating molecules important for lymphoid homing and upregulate cell adhesion molecules. The current concept of T_{RM} ontogeny is that early effector KLRG1^{low} (Killer cell lectin like receptor G1) CD8⁺ T cells, that are not terminally differentiated, give rise to T_{RM} cells (Mackay et al., 2013). Once the early effector T cells enter the peripheral tissues, local cues are important for the formation of T_{RM} cells. The cytokine TGF β that is secreted by various epithelial and mucosal cells promotes T_{RM} cell differentiation as it induces the expression of CD103 (Mueller and Mackay, 2016). Other cytokines such as TNF α and IL-33 have also been shown to induce T_{RM} cell formation as they lead to the downregulation of transcription factor KLF2 (Skon et al., 2013). In the majority of tissues, T_{RM} cells can even form in the absence of their cognate antigen (Mackay et al., 2012; Thom et al., 2015).

1.4.3. Function and protective mechanisms of tissue-resident memory CD8⁺ T cells

When T_{RM} cells encounter their cognate antigen upon re-infection, they are activated immediately and provide local protection against infections such as herpesvirus or influenza virus infection (Gebhardt et al., 2011; Teijaro et al., 2011; Thom et al., 2015; Wakim et al., 2008; Zens et al., 2016). T_{RM} cells do not recirculate but it was shown that T_{RM} cells constantly patrol the skin in a skin infection mouse model (Ariotti et al., 2012a). Upon local activation, T_{RM} cells can secrete pro-inflammatory IFN γ , TNF α and cytotoxic effector proteins such as granzyme B (Djenidi et al., 2015; Ganesan et al., 2017; Hombrink et al., 2016; Masopust et al., 2001; Webb et al., 2015). While it is difficult to investigate the direct cytotoxic capacity of T_{RM} cells in peripheral tissues, it is likely that T_{RM} cells

have direct targeting and killing ability of infected cells as they express high levels of granzyme B. Masopust and colleagues showed in an *ex vivo* chromium release assay that virus-specific CD8⁺ memory T cells isolated from peripheral tissues, but not from lymphoid tissues, are constitutively cytolytic (Masopust et al., 2001; Rosato et al., 2017).

Additionally, T_{RM} cells can provide protection via indirect mechanisms. T_{RM} cells secrete IFN γ which induces an anti-viral state in the surrounding tissue (Ariotti et al., 2014). IFN γ signalling on vascular endothelial cells induces the upregulation of VCAM-1 (Vascular cell adhesion molecule 1), an adhesion molecule, and the production of CXCL9 that allows memory B and T cells to enter the inflamed peripheral tissue (Glennie et al., 2015; Schenkel et al., 2014, 2013). T_{RM} cells also express other retention and adhesion-molecules such as RGS2 (Regulator of G protein signalling 2), ITGA1 (Integrin subunit alpha 1) and ITGAV (Integrin subunit alpha V) (Djenidi et al., 2015; Hombrink et al., 2016). Additionally, cytokines that are secreted by T_{RM} cells enhance DC maturation and activation of NK cells (Schenkel et al., 2014).

1.4.4. Tissue-resident memory T cells and their anti-tumour immunity

T_{RM} cells have largely been defined and characterised in the context of immunity to infection but research now shows that they are also a critical component in the host immune response to cancer.

It is well established that CD8⁺ T cells have a major anti-tumour effect. The majority of cancer immunotherapies aim to increase the numbers or functionality of tumour-reactive CTLs. Many studies performed using human samples or experimental mouse models show an important role for CD8⁺ T cells in controlling tumour growth. (Bruggen et al., 1991; Darrow et al., 1996; Echchakir et al., 2000; Pagès et al., 2009). However, the role of T_{RM} cells in immune responses against tumours is only beginning to be explored and understood.

T_{RM} cells have been mainly described during infections in non-lymphoid tissues but they can also be found in various tumours including melanoma and ovarian cancer (Bösmüller et al., 2016; Edwards et al., 2018; Egelston et al., 2017; Murray et al., 2016). Lung tumours with a high frequency of CD8⁺ TILs also show an

enrichment for CD103⁺ cells (Ganesan et al., 2017). CD103⁺ CD8⁺ T cells within human tumours are linked to improved prognosis (Djenidi et al., 2015; Komdeur et al., 2017; Vasquez et al., 2017; Wang Bo et al., 2015; Z.-Q. Wang et al., 2016; Webb et al., 2014; Workel et al., 2016).

For a long time, there were only correlative associations between improved patient survival and T_{RM} cells. Only very recently did experimental mouse studies definitively demonstrate that T_{RM} cells can mediate cancer immunity.

Nizard and colleagues showed that intranasal vaccination generates antigen-specific T_{RM} cells in the lung tissues that are protective against E7-expressing TC1 head and neck tumours as opposed to intramuscular vaccination (Nizard et al., 2017).

Another study by Enamorado and colleagues showed that infection of mice with VACV-OVA (vaccinia virus expressing full length ovalbumin) through different infection routes showed different patterns of antigen-specific memory T cells in the peripheral tissues and circulation. In their experiments they showed that either circulating or resident memory T cells can protect against B16-OVA melanoma in the skin. The study showed that T_{RM} cells delayed tumour occurrence and reduced tumour growth (Enamorado et al., 2017).

Furthermore, Malik et al. showed that T cells in the skin can mediate long-lived protection in the skin against B16 melanoma. In order to address residency, they used a skin transplantation model which showed that tumour-specific T_{RM} cells persist in the skin several months after grafting skin onto T cell deficient mice and that these T cells do not migrate to the draining lymph node (Malik et al., 2017).

By using a new mouse model of transplantable epicutaneous melanoma inoculation, we could show that CD8⁺ T_{RM} cells mediate durable melanoma-immune equilibrium restricted to the epidermis of the skin. A large proportion of mice that were transplanted with melanoma cells never developed macroscopic tumour lesions and generation of tumour-reactive epidermal T_{RM} cells correlated with spontaneous tumour control. In the mice where there were no macroscopic tumours visible, intravital imaging showed that there were still melanoma cells present in the epidermis. These melanoma cells were in close contact with antigen-specific T_{RM} cells. In addition, mice deficient in T_{RM} formation were more

susceptible to tumour development (Park et al., 2019).

T_{RM} cells in the skin are characterised by the surface expression of CD103. Concomitant signalling from the TCR and TGF β receptor, triggered by MHC class I/tumour antigen and TGF β , respectively, leads to induction of CD103 signalling (Floc'h et al., 2007; Franciszkiewicz et al., 2009; Mokrani et al., 2014). Only a very small fraction of circulating T cells express CD103 implying that the tumour-reactive T cell needs to encounter its cognate antigen in an TGF β -rich (tumour)microenvironment in order to become a T_{RM} cell (Mami-Chouaib et al., 2018) .

CD103 is not only important for retention in the epithelial peripheral tissue via its interaction with E-cadherin but is also required for polarised exocytosis of lytic granules. During formation of an immune synapse between T cell and tumour cell, CD103 is recruited at the synapse and its interaction with E-cadherin leads to polarised exocytosis of granules that mediate target cell lysis and the secretion of cytokines important for an anti-tumour cytotoxic T cell response (Franciszkiewicz et al., 2013).

E-cadherin is often lost on epithelial cells during tumorigenesis when cells undergo epithelial-to-mesenchymal transition (Higgins et al., 1998). Studies have shown that there are unknown binding partners of CD103 in the peripheral tissue and one could speculate that these unknown partners may engage CD103 on the T cells in E-cadherin negative tumours (Brown et al., 1999; Jenkinson et al., 2011).

The role of cognate antigen in the priming process of the T_{RM} cells is still not fully elucidated. In the lung and brain the T cell needs to encounter its cognate antigen to form a T_{RM} cell (Takamura et al., 2016; Wakim et al., 2010). However, in the skin or the genital tract the topical application of the irritant DNFB (1-Fluoro-2,4-dinitrobenzene) or the local application of cytokines after systemic priming is sufficient for the local formation or recruitment of T_{RM} cells, respectively (Park et al., 2018; Shin and Iwasaki, 2012).

1.5. Thesis aims

In the recent years, there has been tremendous progress in the development and improvement of personalised cancer immunotherapies. Different therapeutic strategies such as cancer vaccines or the transfer of T cells, which target tumours in an epitope-specific manner, are currently evaluated in clinical studies. ACT targeting shared tumour antigens, such as differentiation antigens, has emerged as a promising treatment option especially in patients with metastatic melanoma. However, with the better understanding of tumour biology and the results from previous clinical studies, neoantigens that arise from somatic mutations represent another class of target antigens for ACT immunotherapy. A major challenge to these therapy approaches is the selection of the right target antigen(s). Targeting shared differentiation antigens is applicable to many patients, because this class of antigen is usually highly and broadly expressed. However, expression in non-tumour tissues may cause severe toxicities. Targeting tumour-specific neoantigens is expected to produce less immune-related adverse effects, but mutation frequencies and HLA-context require highly personalised ACT approaches. In general, our knowledge of how the regulation and function of epitope-encoding gene products (antigens) influence T cell therapies and how antigen selection contributes to resistance mechanisms remains limited. Therefore, we aimed to generate an experimental platform that allows us to target different endogenous gene products with the same epitope-specific TCRtg (TCR transgenic) T cells in mouse melanomas and study the respective immune evasion mechanisms. Furthermore, we aimed to apply this platform to a model of melanoma immune surveillance by T_{RM} cells in order to understand the importance of cognate antigen expression and presentation for T_{RM} tumour control.

In summary, the experiments contained within this dissertation address the following aims:

- (1) Generation of a CRISPR/Cas9-based knockin strategy to fuse model CD8⁺ T cell epitopes to endogenous gene products in melanoma cells (Chapter 3)
- (2) Investigation of how the choice of the targeted gene product of ACT immunotherapy impacts on therapy outcome and resistance mechanisms (Chapter 4)
- (3) Investigating the requirement of antigen persistence on tumour surveillance by T_{RM} cells (Chapter 5)

Chapter 2: Materials and methods

Chapter 2: Material and methods

2.1. Materials

2.1.1. Antibodies

Table 2.1: Overview of the antibodies used in this study

The table shows the antibody name, clone, dilution, application and company.

Antibodies	Application	Company
Anti-mouse CD3 ϵ (145-2C11)	<i>In vitro</i> T cell activation	Tonbo Biosciences
Anti-mouse CD28 (37.51)	<i>In vitro</i> T cell activation	Tonbo Biosciences
β -Actin (C4, 1:2,000)	WB (primary AB)	Santa Cruz Biotechnologies
CDK4 (DCS-35, 1:100)	WB (primary AB)	Santa Cruz Biotechnologies
FLAG (L5, 1:250)	WB (primary AB)	Novus Biologicals
gp100 (PMEL17/SILV, 1:1,000)	WB (primary AB)	Novus Biologicals
MITF (HPA003259, 1:250)	WB (primary AB)	Atlas Antibodies by Sigma-Aldrich
Pescadillo (H10, 1:200)	WB (primary AB)	Santa Cruz Biotechnologies
TRP1 (G-9, 1:100).	WB (primary AB)	Santa Cruz Biotechnologies
IRDye [®] 800CW donkey anti-goat IgG (H + L) (1:15,000)	WB (secondary AB)	LI-COR Biosciences
IRDye [®] 680LT donkey anti-mouse (1:15,000)	WB (secondary AB)	LI-COR Biosciences
IRDye [®] 800CW donkey anti-rabbit (1:15,000)	WB (secondary AB)	LI-COR Biosciences
IRDye [®] 800CW donkey	WB (secondary AB)	LI-COR Biosciences

anti-rat (1:15,000)		
Anti-mouse CD16/CD32 (Clone 93; 1:200)	FC	Biolegend
Anti-mouse CD16/CD32 (Clone 2.4G2; 1:200)	FC	BD Biosciences
Anti-mouse CD3 ϵ Alexa Fluor 700 (Clone eBio500A2; 1:100)	FC (primary AB)	eBioscience
Anti-mouse CD3 ϵ Brilliant Ultraviolet 395 (Clone145- 2C11; 1:100)	FC (primary AB)	BD Biosciences
Anti-mouse CD8 α Brilliant Violet 605 (Clone 53-6.7; 1:200)	FC (primary AB)	Biolegend
Anti-mouse CD8 α Brilliant Violet 711 (Clone 53-6.7; 1:200)	FC (primary AB)	Biolegend
Anti-mouse CD8 α Brilliant Violet 785 (Clone 53-6.7; 1:200)	FC (primary AB)	Biolegend
Anti-mouse CD8 α PE (Clone 53-6.7)	FC (primary AB)	BD Biosciences
Anti-mouse CD44 Alexa Fluor 700 (Clone 1M7; 1:200)	FC (primary AB)	Invitrogen by Thermo Fisher Scientific
Anti-mouse CD44 Brilliant Ultraviolet 395 (Clone 1M7; 1:100)	FC (primary AB)	BD Biosciences
Anti-mouse CD44 PerCP- Cy5.5 (Clone 1M7; 1:200)	FC (primary AB)	Invitrogen by Thermo Fisher Scientific
Anti-mouse CD45.1 APC	FC (primary AB)	eBioscience

(Clone A20; 1:100)		
Anti-mouse CD45.1 Brilliant Violet 785 (Clone A20; 1:100)	FC (primary AB)	Biolegend
Anti-mouse CD45.2 APC (Clone 104; 1:100)	FC (primary AB)	Invitrogen by Thermo Fisher Scientific
Anti-mouse CD45.2 APC- Cy7 (Clone 104; 1:100)	FC (primary AB)	Biolegend
Anti-mouse CD45.2 Brilliant Violet 786 (Clone 104; 1:100)	FC (primary AB)	BD Bioscience
Anti-mouse CD62L PE- Cy7 (Clone MEL-14; 1:200)	FC (primary AB)	Invitrogen by Thermo Fisher Scientific
Anti-mouse CD69 Brilliant Violet 605 (Clone H1.2F3; 1:200)	FC (primary AB)	Biolegend
Anti-mouse CD90.1 APC (Clone HIS51; 1:200)	FC (primary AB)	eBioscience
Anti-mouse CD90.1 PerCP (Clone OX-7)	FC (primary AB)	BD Biosciences
Anti-mouse CD103 APC (Clone 2E7; 1:200)	FC (primary AB)	Biolegend
Anti-mouse CD103 PerCP-Cy5.5 8Clone 2E7; 1:200)	FC (primary AB)	Biolegend
Anti-mouse TCR β Brilliant Violet 510 (Clone H57- 597; 1:200)	FC (primary AB)	Biolegend
Anti-mouse V α 2 TCR Brilliant Violet 421 (Clone	FC (primary AB)	BD Biosciences

20.1; 1:200)		
Anti-mouse V α 2 TCR PE (Clone B20.1; 1:200)	FC (primary AB)	eBioscience
Anti-Mouse V β 13 TCR FITC (Clone MR12-3)	FC (primary AB)	BD Biosciences
Anti-mouse H-2K ^b APC (AF6-88.5.5.3; 1:100)	FC (primary AB)	eBioscience
Anti-mouse IFN γ PE-Cy7 (Clone XMG1.2; 1:100)	FC (primary AB)	BD Biosciences
Anti-Mouse TNF APC (Clone MP6-XT22; 1:100)	FC (primary AB)	BD Biosciences
Anti-mouse H-2D ^b Biotin (Clone KH95)	FC (primary AB)	BD Biosciences
Anti-mouse H-2K ^b Biotin (Clones AF6-88.5)	FC (primary AB)	BD Biosciences
Streptavidin APC	FC (secondary AB)	BD Biosciences
Anti-mouse CD8 α (Clone EPR20305; 1:500)	IHC	Abcam
Anti-mouse CD103 (Clone 2E7; xxx)	IHC	Biolegend
Anti-mouse gp100 (Clone EP4863(2); 1:200)	IHC	Abcam
Anti-mouse PD-L1 (B7- H1) (Clone 10F.9G2)	<i>In vivo</i> checkpoint immunotherapy	Hölzel Biotech
Ter119 (1:12.5)	CD8 enrichment cocktail	The Walter and Eliza Hall Institute – Antibody Facility
M5/114 (1:25)	CD8 enrichment cocktail	The Walter and Eliza Hall Institute – Antibody Facility
GK1.5 (1:50)	CD8 enrichment	The Walter and Eliza

	cocktail	Hall Institute – Antibody Facility
RB6-8C5 (1:100)	CD8 enrichment cocktail	The Walter and Eliza Hall Institute – Antibody Facility
M1/70 (1:50)	CD8 enrichment cocktail	The Walter and Eliza Hall Institute – Antibody Facility
F4/80 (1:50)	CD8 enrichment cocktail	The Walter and Eliza Hall Institute – Antibody Facility

2.1.2. Bacteria and virus strains

Table 2.2: Overview of the bacteria and virus strains used in this study

The table shows the bacteria and virus strains and the origin/source.

Bacteria and virus strains	Origin / Source
Chemically competent Escherichia coli DH10 β	Originally obtained from the laboratory of Veit Hornung, University Hospital Bonn
Recombinant adenoviral vector Ad-gp100	(Kohlmeyer et al., 2009)

2.1.3. Experimental models

Table 2.3: Overview of the experimental cell lines used in this study

The table shows the experimental cell lines and the origin/source.

Cell lines	Origin / Source
Mouse: HCmel12	Established in the laboratory of Thomas Tüting (Bald et al., 2014) <i>Differentiated melanoma cell line</i>

	<i>(‘proliferative’ phenotype) that has a mutation leading to a clinically relevant oncogene (CDK4^{R24C}).</i>
Mouse: HC.PmelKO	HCmel12 Pmel knockout clone 17 (generated by Debby van den Boorn-Konijnenberg) <i>Melanoma cell line that has above mentioned characteristics and a genetic ablation of the gene gp100; therefore, murine gp100 (low affinity epitope) can be substituted with human gp100 (high affinity epitope).</i>
Mouse: HC.PmelKO.TYRP1-mNeon	Generated during this study <i>Melanoma cell line that has above mentioned characteristics. Endogenous TYRP1 protein (example of a MDA) was tagged with mNeon (control cell line).</i>
Mouse: HC.PmelKO.TYRP1-NFhgp100	Generated during this study <i>Melanoma cell line that has above mentioned characteristics. Endogenous TYRP1 protein (example of a MDA) was tagged with mNeon plus human gp100. This allowed targeting of TYRP1 by epitope-standardised ACT protocol in vivo.</i>
Mouse: HC.PmelKO.CDK4 ^{R24C} -mNeon	Generated during this study <i>Melanoma cell line that has above mentioned characteristics. Endogenous CDK4^{R24C} protein (example of an oncogene) was tagged with mNeon (control cell line).</i>

<p>Mouse: HC.PmelKO.CDK4^{R24C}_NFhgp100</p>	<p>Generated during this study <i>Melanoma cell line that has above mentioned characteristics.</i> <i>Endogenous CDK4^{R24C} protein (example of an oncogene) was tagged with mNeon plus human gp100. This allowed targeting of CDK4^{R24C} by epitope-standardised ACT protocol in vivo.</i></p>
<p>Mouse: HC.PmelKO.DCT-mNeon</p>	<p>Generated during this study <i>Melanoma cell line that has above mentioned characteristics.</i> <i>Endogenous DCT protein (example of a MDA) was tagged with mNeon (control cell line).</i></p>
<p>Mouse: HC.PmelKO.DCT-NFhgp100</p>	<p>Generated during this study <i>Melanoma cell line that has above mentioned characteristics.</i> <i>Endogenous DCT protein (example of a MDA) was tagged with mNeon plus human gp100. This allowed targeting of DCT by TCRtg T cells during in vitro proof-of-principle experiments.</i></p>
<p>Mouse: HC.PmelKO.GPNMB-mNeon</p>	<p>Generated during this study <i>Melanoma cell line that has above mentioned characteristics.</i> <i>Endogenous GPNMB protein (example of a MDA) was tagged with mNeon (control cell line).</i></p>
<p>Mouse: HC.PmelKO.GPNMB-NFhgp100</p>	<p>Generated during this study <i>Melanoma cell line that has above mentioned characteristics.</i></p>

	<p><i>Endogenous GPNMB protein (example of a MDA) was tagged with mNeon plus human gp100. This allowed targeting of GPNMB by TCRtg T cells during in vitro proof-of-principle experiments.</i></p>
<p>Mouse: HC.PmelKO.SOX10-mNeon</p>	<p>Generated during this study <i>Melanoma cell line that has above mentioned characteristics. Endogenous SOX10 protein (example of a transcription) was tagged with mNeon (control cell line).</i></p>
<p>Mouse: HC.PmelKO.SOX10-NFhgp100</p>	<p>Generated during this study <i>Melanoma cell line that has above mentioned characteristics. Endogenous SOX10 protein (example of a transcription) was tagged with mNeon plus human gp100. This allowed targeting of SOX10 by TCRtg T cells during in vitro proof-of-principle experiments.</i></p>
<p>Mouse: HC.PmelKO.TYRP1-mScarlet</p>	<p>Generated during this study <i>Melanoma cell line that has above mentioned characteristics. Endogenous TYRP1 protein (example of a MDA) was tagged with mScarlet (control cell line).</i></p>
<p>Mouse: HC.PmelKO.TYRP1-SFmgrp100</p>	<p>Generated during this study <i>Melanoma cell line that has above mentioned characteristics. Endogenous TYRP1 protein (example of a MDA) was tagged with mScarlet</i></p>

	<i>plus murine gp100. This allowed targeting of TYRP1 by TCRtg T cells during in vitro proof-of-principle experiments that compared the impact of epitope affinity on T cell activation.</i>
Mouse: HC.PmelKO.TYRP1-SFhgp100	Generated during this study <i>Melanoma cell line that has above mentioned characteristics. Endogenous TYRP1 protein (example of a MDA) was tagged with mScarlet plus murine gp100. This allowed targeting of TYRP1 by TCRtg T cells during in vitro proof-of-principle experiments that compared the impact of epitope affinity on T cell activation.</i>
Mouse: B16-F1 (B16)	ATCC (CRL-6323) <i>Differentiated melanoma cell line regularly used for in vivo melanoma mouse studies.</i>
Mouse: B16.gB	Generated in the laboratory of Jason Waithman (Park et al., 2019) <i>B16-F1 expressing full length HSV-1 glycoprotein B. This cell line was in vivo to generate tumour that were analysed via histological methods.</i>
Mouse: B16.TyrKO	B16-F1 Tyrosinase knockout clone D8 (generated by Debby van den Boorn-Konijnenberg) <i>Melanoma cell line that has a genetic ablation of the gene tyrosinase. This cell line does not produce pigment and is suitable for intravital imaging</i>

	<i>studies.</i>
Mouse: B16.ACTB-mNeon	Generated during this study <i>B16.TyrKO melanoma cell line in which endogenous ACTB protein (housekeeping gene) was tagged with mNeon (control cell line).</i>
Mouse: B16.ACTB-NFgB	Generated during this study <i>B16.TyrKO melanoma cell line in which endogenous ACTB protein (housekeeping gene) was tagged with mNeon plus HSV-1 gB. This allowed targeting of the cell line by TCRtg T cells during in vitro proof-of-principle experiments.</i>
Mouse: B16.ACTB-mScarlet	Generated during this study <i>B16.TyrKO melanoma cell line in which endogenous ACTB protein (housekeeping gene) was tagged with mScarlet (control cell line).</i>
Mouse: B16.ACTB-SFgB	Generated during this study <i>B16.TyrKO melanoma cell line in which endogenous ACTB protein (housekeeping gene) was tagged with mNeon plus HSV-1 gB. This allowed targeting of the cell line by TCRtg T cells during in vitro proof-of-principle experiments.</i>
Mouse: B16.ACTG1-mNeon	Generated during this study <i>B16.TyrKO melanoma cell line in which endogenous ACTG1 protein (housekeeping gene) was tagged with mNeon (control cell line).</i>

<p>Mouse: B16.ACTG1-NFgB</p>	<p>Generated during this study <i>B16.TyrKO melanoma cell line in which endogenous ACTG1 protein (housekeeping gene) was tagged with mNeon plus HSV-1 gB. This allowed targeting of the cell line by TCRtg T cells during in vitro proof-of-principle experiments.</i></p>
<p>Mouse: B16.SWITCHgB Clone 1G9</p>	<p>Generated during this study <i>Monoclonal B16.TyrKO melanoma cell line in which endogenous ACTG1 protein (housekeeping gene) was tagged with mNeon plus HSV-1 gB. This allowed targeting of the cell line by TCRtg T cells during in vitro proof-of-principle experiments.</i></p>
<p>Mouse: B16.SWITCHgB Clone 1H9</p>	<p>Generated during this study <i>Monoclonal B16.TyrKO melanoma cell line in which endogenous ACTG1 protein (housekeeping gene) was tagged with mNeon plus HSV-1 gB. This allowed targeting of the cell line by TCRtg T cells during in vitro proof-of-principle experiments and in vivo studies.</i></p>
<p>Mouse: B16.SWITCHgB Clone 2C3</p>	<p>Generated during this study <i>Monoclonal B16.TyrKO melanoma cell line in which endogenous ACTG1 protein (housekeeping gene) was tagged with mNeon plus HSV-1 gB. This allowed targeting of the cell line by TCRtg T cells during in vitro proof-</i></p>

	<i>of-principle experiments.</i>
Human: HEK293T	ATCC (CRL-3216) <i>Human embryonic kidney cells used for the generation of retroviral particles for transduction.</i>

Table 2.4: Overview of the experimental organisms and strains used in this study

The table shows the experimental organisms/strains and the origin/source.

Organisms / Strains	Origin / Source
Mouse: C57BL/6J (H2-Db)	Janvier LABS
Mouse: C57BL/6J (H2-Db)	Charles River
Mouse: C57BL/6J (H2-Db)	The Peter Doherty Institute for Infection and Immunity
Mouse: pmel-1 TCRtg / Thy1.1	Jackson Laboratory
Mouse: gBT-I TCRtg / Ly5.1	The Peter Doherty Institute for Infection and Immunity
Mouse: OT-I TCRtg / Ly5.1	The Peter Doherty Institute for Infection and Immunity
Mouse: Rag1 ^{-/-}	The Peter Doherty Institute for Infection and Immunity
Mouse: Rag2 ^{-/-} ; IL2rg ^{-/-}	The Peter Doherty Institute for Infection and Immunity

2.1.4. Cell culture media and supplements

Table 2.5: Overview of the cell culture media and supplements used in this study

The table shows cell culture media, supplements and company.

Cell culture media and supplements	Company
DMEM	Media preparation Unit – The Peter Doherty Institute for Infection and Immunity
DPBS (Dulbecco's Phosphate Buffered Saline)	Gibco – Life Technologies
Fetal Bovine Serum	Gibco – Life Technologies
HEPES	Gibco – Life Technologies
L-Glutamine	Gibco – Life Technologies
Penicillin – Streptomycin	Gibco – Life Technologies
RPMI1640	Gibco – Life Technologies
RPMI1640	Media preparation Unit – The Peter Doherty Institute for Infection and Immunity
Trypsin-EDTA	Gibco – Life Technologies
Trypsin-EDTA	Sigma-Aldrich
Opti-MEM® I, reduced serum medium, no phenol red	Gibco – Life Technologies
HBSS (Hanks' buffered salt solution)	Media preparation Unit – The Peter Doherty Institute for Infection and Immunity
PBS (Phosphate buffered saline)	Media preparation Unit – The Peter Doherty Institute for Infection and Immunity
EDTA BSS	Media preparation Unit – The Peter Doherty Institute for Infection and Immunity

2.1.5. Chemicals and reagents

Table 2.6: Overview of chemicals and reagents used in this study

The table shows chemicals, reagents and company.

Chemicals and reagents	Company
Acetic acid	Carl Roth
Agar agar	Carl Roth
Agarose	Carl Roth
Ammonium chloride	Carl Roth
Ammonium persulfate	Carl Roth
Ampicillin	Carl Roth
Aqueous eosin (1 %)	Australian Biostain
Baxter water for irrigation	Superior Healthcare
Bromophenol blue	Carl Roth
Denatured ethanol	Hurst Scientific
Dimethyl sulfoxide	Carl Roth or Sigma-Aldrich
Disodium hydrogen phosphate heptahydrate	Carl Roth
Disodium-EDTA	Carl Roth
Dithiothreitol	Carl Roth
Ethanol	Carl Roth
Ethidumbromide	Carl Roth
Ethylenediaminetetraacetic acid	Carl Roth
GelGreen Nucleic Acid Stain	Life Research Pty Ltd
Glycerol	Carl Roth
Glycine	Carl Roth
Guanidine hydrochloride	Carl Roth
H ₂ O Ampuwa	Fresenius
Haematoxylin	Australian Biostain
Hydrochloric acid, 32 %	Carl Roth
Isopropyl alcohol	Carl Roth

Methanol	Carl Roth
p-formaldehyde, 37%	Carl Roth
Potassium acetate	Carl Roth
Potassium bicarbonate	Carl Roth
Potassium chloride	Carl Roth
Potassium phosphate	Carl Roth
Rotiphorese Gel 30 (37.5:1)	Carl Roth
Scott's tap water	Amber Scientific
Sodium azide	Carl Roth
Sodium chloride	Carl Roth
Sodium dodecyl sulfate	Carl Roth
Sodium hydroxide	Carl Roth
Tetramethylethylenediamine	Carl Roth
Tris	Carl Roth
Triton X-100	Sigma-Aldrich
Trypan blue	Sigma-Aldrich
Tween-20	Carl Roth
Xylene	Hurst Scientific

2.1.6. Commercially available buffers and reagents

Table 2.7: Overview of commercially available buffers and reagents used in this study

The table shows commercially available buffers and reagents and company.

Commercially available buffers and reagents	Company
(Z)-4-Hydroxytamoxifen (≥98 %)	Sigma-Aldrich
10x Zinc-fixative (formalin free)	BD Biosciences
All-in-One cDNA SuperMix	Bioutil
BioMag goat anti-rat IgG	Qiagen
Blasticidine S hydrochloride	Sigma-Aldrich
Bovine serum albumin fraction V	Carl Roth

Brefeldin A	Sigma-Aldrich
Broad Range Markers	Santa Cruz Biotechnologies
Cyclophosphamide	Endoxan, Baxter
Cytofix/Cytoperm™ Fixation/Permeabilization Solution Kit	BD Biosciences
DAPI	Thermo Fisher Scientific
dNTPs	Thermo Fisher Scientific
dNTPs	Qiagen
Fluoroshield mounting medium	Sigma-Aldrich
FuGENE® HD transfection reagent	Promega
Ilium Xylazil-20 (20 mg/ml xylazine in hydrochloride)	Troy Laboratories
Ketavet (100 mg/ml ketamine in hydrochloride)	Parnell Laboratories
LB-Medium (Lennox)	Carl Roth
LIVE/DEAD™ Fixable Near-IR Dead Cell Stain Kit for 633 or 635 nm excitation	Thermo Fisher Scientific
LPS	Sigma-Aldrich
Matrigel® Matrix	Corning®
Oligo dT primer	Promega
PolyI:C (HMW)	Invivogen
Propidium iodide	Sigma-Aldrich
Puromycin	Sigma-Aldrich
Red Blood Cell Lysing Buffer Hybri-Max™	Sigma-Aldrich
RLT buffer	Qiagen
RW1 buffer	Qiagen
Sunflower seed oil from Helianthus annuus	Sigma-Aldrich
Tamoxifen	Cayman Chemical Company
TRIzol™	Thermo Fisher Scientific
Ultrapure DNase and RNase-free distilled water	Invitrogen

Zombie Aqua™ Fixable Viability Dye	Biolegend
Zymo RNA wash buffer	Zymo Research

2.1.7. Commercially available kits

Table 2.8: Overview of commercially available kits used in this study

The table shows commercially available kits and company.

Commercially available kits	Company
DNeasy® Blood & Tissue Kit	Qiagen
MEGAquick-spin™ Plus Total Fragment DNA Purification Kit	iNtRON Biotechnology
NucleoSpin® RNA kit	Macherey-Nagel
NucleoSpin® Tissue kit	Macherey-Nagel
PureLink™ HiPure Plasmid Midiprep Kit	Life Technologies
QuantSeq 3'mRNA-Seq Library Prep Kit FWD for Illumina	Lexogen
REAL Detection System, Peroxidase/DAB+	Dako
RNeasy® Plus Mini Kit	Qiagen
Wizard® SV Gel and PCR Clean-Up System	Promega

2.1.8. Enzymes

Table 2.9: Overview of enzymes used in this study

The table shows enzymes and company.

Enzymes	Company
Antarctic Phosphatase	New England Biolabs
Collagenase D	Sigma
Collagenase Type 3	Worthington Biochemical
DNaseI	Roche or Sigma-Aldrich

DreamTaq DNA Polymerase	Thermo Fisher Scientific
Liberase TL Research Grade	Sigma-Aldrich
Omniscript reverse transcriptase	Qiagen
Phusion High Fidelity DNA Polymerase	New England Biolabs
Proteinase K	Qiagen
PureLink™ RNase A	Invitrogen
Q5® High-Fidelity DNA Polymerase	New England Biolabs
Restriction enzymes (AvrII, BsrGI, DpnI, DraIII, EcoNI, NheI,)	New England Biolabs
RNase A	Life Technologies
T4 DNA Ligase	New England Biolabs
T4 Polynucleotide Kinase	New England Biolabs

2.1.9. General consumables

Table 2.10: Overview of general consumables used in this study

The table shows the consumables and company.

Consumables	Company
Cell strainer, 70 µm	Falcon
DNA spin columns	Centic Biotec
Lacri-Lube® lubricating eye ointment	Allergen Australia
MACS® SmartStrainers, 30 µm	MACS-Miltenyi Biotec
MACS® SmartStrainers, 70 µm	MACS-Miltenyi Biotec
Micropore™ tape	3M Health Care
Nitrocellulose membrane (pore size: 0.2 µm)	GE Healthcare
Nylon mesh, 30 µm	Clear Edge Filtration Pty Ltd
Nylon mesh, 75 µm	Clear Edge Filtration Pty Ltd
OpSite Flexigrid® (6 cm x 7 cm)	Smith & Nephew
Stericup® Vacuum Filter 0.22 µm (funnel and bottle; 250 ml and 500 ml)	Merck Millipore

Transpore™ tape	3M Health Care
Veet hair removal cream – sensitive skin	Reckitt Benckiser
Zymo Spin III C columns	Zymo Research

2.1.10. General laboratory equipment

Table 2.11: Overview of general laboratory equipment used in this study

The table shows general laboratory equipment and company.

General laboratory equipment	Company
AutoStain XL	Leica
AxioVert A1 Microscope	Carl Zeiss
CV5030 Coverslipper	Leica
D1000 high sensitivity tape station	Agilent
Dremel® Stylus 7.2v cordless rotary tool with a 3.2 mm grindstone attachment	Dremel
FACS ARIA III	BD Biosciences
FACSCanto II	BD Biosciences
HiSeq2500 platform	Illumina®
Infinite 200 PRO multimode plate reader	TECAN
LSRFortessa	BD Biosciences
Mini Trans-Blot® Cell	Bio-Rad
Mini-PROTEAN® Tetra Cell Systems	Bio-Rad
NanoDrop™ 2000	Thermo Fisher Scientific
Observer Z1 Microscope	Carl Zeiss
Odyssey® Sa Imaging system	LI-COR Biosciences
Panoramic SCAN II	3D HISTECH
PowerPac™ Basic Power Supply	Bio-Rad
SubCell® GT Cell	Bio-Rad

T100™ Thermal Cycler	Bio-Rad
Wahl super cordless clipper	Savhoo Hair & Beauty

2.1.11. Oligonucleotides

Table 2.12: Overview of oligonucleotides used in this study

The table shows oligonucleotide names, sequences and company.

Oligonucleotides	Company
CPG Oligo 1826; 5'- T*C*C*A*T*G*A*C*G*T*T*C*C*T*G*A*C*G*T*T-3'	Biomers
P1/P2_forward CAAGAATGAAGCCAACCAGCC	Microsynth
P1/P3_reverse CGCTTGCCATTTCCAGTGG	Microsynth
P2_reverse GTTAGCAGACTTCCTCTGCCC	Microsynth
P3_forward GAATCTCTGCCTTCCGAGCC	Microsynth
Actb_forward CCAGTTGGTAACAATGCCATGT	Microsynth
Actb_reverse GGCTGTATTCCCCTCCATCG	Microsynth
PmeI_TS CACCGCTTGTGCTGAGTGCTCTGC	Microsynth
PmeI_BS AAACGCAGAGCACTCAGCACAAGC	Microsynth
Tyrp1_TS CACCGGCAGGCGGCTATCAGACCA	Microsynth
Tyrp1_BS AAACTGGTCTGATAGCCGCCTGCC	Microsynth
Cdk4_TS CACCGCACTCCTACCTGCACAAGG	Microsynth

Cdk4_BS AAACCCTTGTGCAGGTAGGAGTGC	Microsynth
Dct_TS CACCGCAGCAGCAAGAGATACACGG	Microsynth
Dct_BS AAACCCGTGTATCTCTTGCTGCTGC	Microsynth
Gpmb_TS CACCGCCAAAGACTTAGAGTGTCCT	Microsynth
Gpmb_BS AAACAGGACACTCTAAGTCTTTGGC	Microsynth
Sox10_TS CACCGACTCTATCCCGACCTTAGAG	Microsynth
Sox10_BS AAACCTCTAAGGTCGGGATAGAGTC	Microsynth
Actb_TS CACCGCACCGCAAGTGCTTCTAGG	Microsynth
Actb_BS AAACCCTAGAAGCACTTGCGGTGC	Microsynth
Actg1_TS CACCGCCACCGCAAATGCTTCTAGA	Microsynth
Actg1_BS AAACTCTAGAAGCATTGCGGTGGC	Microsynth
BlastR_EcoNI_forward GATCCCTGGCCCAGGGAAGACCTTCAACATCT CTCAGC	Microsynth
BlastR_S_DraIII_reverse GATCCACCAGGTGTTAGTTCCTGGTGTACTTG AGG	Microsynth
mScarlet_1st_forward GGGTCTGGTGGCAGTGGAGGGGGATCCGTGA GCAAGGGCGAGGCAG	Microsynth

mScarlet_2nd_forward GATCGCTAGCGGGCCAGTACCCAAAAAGCGG GGGGTCTGGTGGCAGTGGAG	Microsynth
mScarlet_long_reverse CTTGTACAGCTCGTCCATGCCGCCGGTGGAG	Microsynth
CP_PuroR(M1G)_forward GGAGAATCCTGGCCCAGGGACCGAGTACAAG CCCAC	Microsynth
CP_PuroR_(M1G)_reverse GTGGGCTTGTACTCGGTCCCTGGGCCAGGATT CTCC	Microsynth
Mgp100_mut_forward CGATCGGGGCCTAGGCTGGAAGGGTCGCGCA ACCAGGATTGGCTG	Microsynth
Mgp100_mut_reverse CAGCCAATCCTGGTTGCGCGACCCTTCCAGCC TAGGCCCCGATCG	Microsynth
FLAG-Ova-BsrGI_forward GATCTGTACAAGGGCAGCGGCGACTACAAGG A	Microsynth
SIINFEKL_BsrGI_reverse GATCTGTACACCAGCTTCTCGAAGTTGATGA	Microsynth
FLAG-HSV-BsrGI_forward GATCTGTACAAGAGCGGCTCCGCCGATTACAA	Microsynth
SSIEFARL_BsrGI_reverse GATCTGTACACCAGTCTGGCGAACTCGATGC	Microsynth
FLAG-hgp100_TS GTACAAGAGCGGCTCCGCCGATTACAAGGATG ACGACGACAAACGATCGGGGCCTAGGCTGAA AGTGCCGCGCAACCAGGATTGGCTGGT	Microsynth
FLAG-hgp100_BS	Microsynth

GTACACCAGCCAATCCTGGTTGCGCGGCACTT TCAGCCTAGGCCCGATCGTTTGTGTCGTGTC TCCTTGTAATCGGCGGAGCCGCTCTT	
UTP_Pes1_Ct_forward AGCCCATGATGATGCTGTGAGGTCTGAGAAAA AGGCCAAGAGGACAAGGCCCGTGAGCGGCTC CGCCGATTA	Microsynth
Pes1_UTP_SSIEFARL_reverse CTAGCTTGCTTCTGCCAAGTCCAAATCTCAGTG AGGGACAACCTGGAGCTCACAGTCTGGCGAACT CG	Microsynth
Pes1_MiS_Ct_forward ACACTCTTTCCCTACACGACGCTCTTCCGATCT CCCAGCCTGAGATCCTCTTTCC	Microsynth
Pes1_MiS_Ct_rerverse TGA CTGGAGTTCAGACGTGTGCTCTTCCGATC TCTGGGGCTAGCCACATAACCAC	Microsynth
Pes1 Ctx RTgen forward CCCAGCCTGAGATCCTCTTTCC	Microsynth
UTP_Pmel_forward GCCCGCGGCCTTGGAGAAAACAGCCCGCTCC TCAGTGGACAGCAGGTCTGGAGCGGCTCCGC CGATTA	Microsynth
UTP_SSIEFARL_Pmel_reverse TGCAGAAAACACAGGCACTGCTGTCAACCCCA GGAAATCCACGGTGCCTTACAGTCTGGCGAAC TCG	Microsynth
gp100 CtKI gen fw GTGGGGCGTGGAGAAATGTA	Microsynth
gp100 CtKI gen rv CCACCTCACTGCTCCCATAC	Microsynth

gp100-Ct-Miseq-fw ACACTCTTTCCCTACACGACGCTCTTCCGATCT AGACTTAAGAAGCAGGGCTCA	Microsynth
gp100-Ct-Miseq-rv TGACTGGAGTTCAGACGTGTGCTCTTCCGATC TGGTAGTCTCGAAGGGAAGAC	Microsynth
Tubb_forward GGGAGGTCATCAGTGATGAGC	Integrated DNA technologies
Tubb_reverse CAAATACAAAGTTGTCTGGCCG	Integrated DNA technologies
Cre_seq_forward_1 GACCGTACACCAAATTTGCC	Microsynth
ERT2_reverse CTGTGGCAGGGAAACCCTC	Integrated DNA technologies

2.1.12. Peptides and recombinant proteins

Table 2.13: Overview of peptides and recombinant proteins used in this study

The table shows peptide names and amino acid sequences, recombinant proteins and company.

Peptides and recombinant proteins	Company
H2-Db binding peptide KVPRNQDWL (hgp100 ₂₅₋₃₃)	JPT
H2-Kb binding protein SSIEFARL (HSV gB ₄₉₈₋₅₀₅)	GenScript
Recombinant human IL-2	Peprtech
Recombinant human IL-2 (Aldesleukin)	Novartis Pharma
Recombinant murine IFN γ	Peprtech

2.1.13. Software and algorithms

Table 2.14: Overview of software and algorithms used in this study

The table shows software and algorithms and company/source.

Software and algorithms	Company / Source
Bioconductor – R-based computing platform	Bioconductor developer team
CaseViewer 2.3 (64-bit version) for Windows	3D HISTECH
edgeR – Bioconductor package	(Robinson et al., 2010) DOI: 10.18129/B9.bioc.edgeR
Fiji package	ImageJ
FlowJo v10	Tree Star, Inc.
GSEA (gene set enrichment analysis)	GSEA Subramanian, Tamayo, et al. (2005, PNAS 102, 15545-15550) and Mootha, Lindgren, et al. (2003, Nat Genet 34, 267-273) http://software.broadinstitute.org/gsea/index.jsp
Heatmap.3 – An Improved Heatmap Package. R package.	Package authors: Zhao, S., Guo, Y., Sheng, Q., Shyr, Y. https://www.rdocumentation.org/packages/GMD/versions/0.3.3/topics/heatmap.3
limma	R-package author: Aron Eklund http://CRAN.Rproject.org/package=beeswarm
Org.Mm.eg.db – Bioconductor package; Genome wide annotation for Mouse. R package version 3.4.1	Package author: Carlson, M. DOI: 10.18129/B9.bioc.org.Mm.eg.db
Outknocker	www.outknocker.org (Schmid-Burgk et al., 2014)

Prism v8	GraphPad
RNA-seq algorithm	As described by Shi et al., Bioinformatics Division, WEHI, Melbourne, Australia http://bioinf.wehi.edu.au/RNAseqCaseStudy/
Rstudio	Rstudio
Rsubread – Bioconductor package	(Liao et al., 2013) DOI: 10.18129/B9.bioc.edgeR
Voom – algorithm (implemented in limma)	(Law et al., 2014) DOI: 10.18129/B9.bioc.limma014
Zen Software	Carl Zeiss

2.1.14. Vectors and plasmids

Table 2.15: Overview of vectors and plasmids used in this study

The table shows vectors and plasmids and origin/source.

Vectors and plasmids	Origin / Source
pCAS9-mCherry-Frame +1	Addgene plasmid #66939
pCAS9-mCherry-Frame +2	Addgene plasmid #66940
pCAS9-mCherry-Frame +3	Addgene plasmid #66941
pCRISPaint-mNeon-PuroR	Gift from Veit Hornung (Schmid-Burgk et al., 2016)
pCRISPaint-mNeon-PuroR [M1G]	Generated by Daniel Hinze
pCRISPaint-mNeon-F-hgp100-PuroR [M1G]	Generated during this study
pCRISPaint-mNeon-F-mgp100-PuroR [M1G]	Generated by Jana Liebing
pCRISPaint-mNeon-F-gB-PuroR [M1G]	Generated during this study
pCRISPaint-mNeon-F-Ova-PuroR [M1G]	Generated during this study
pCRISPaint-mNeon-BlastR [M1G]	Generated during this study

pCRISPaint-mNeon-F-hgp100-BlastR [M1G]	Generated during this study
pCRISPaint-mNeon-F-mgp100-BlastR [M1G]	Generated by Jana Liebing
pCRISPaint-mNeon-F-gB-BlastR [M1G]	Generated during this study
pCRISPaint-mNeon-F-Ova-BlastR [M1G]	Generated during this study
pCRISPaint-mScarlet-PuroR [M1G]	Generated during this study
pCRISPaint-mScarlet-F-hgp100-PuroR [M1G]	Generated during this study
pCRISPaint-mScarlet-F-mgp100-PuroR [M1G]	Generated by Jana Liebing
pCRISPaint-mScarlet-F-gB-PuroR [M1G]	Generated during this study
pCRISPaint-mScarlet-F-Ova-PuroR [M1G]	Generated during this study
pCRISPaint-mScarlet-BlastR [M1G]	Generated during this study
pCRISPaint-mScarlet-F-hgp100-BlastR [M1G]	Generated during this study
pCRISPaint-mScarlet-F-mgp100-BlastR [M1G]	Generated by Jana Liebing
pCRISPaint-mScarlet-F-gB-BlastR [M1G]	Generated during this study
pCRISPaint-mScarlet-F-Ova-BlastR [M1G]	Generated during this study
pmScarlet_C1	Addgene plasmid #85042 (Bindels et al., 2017)
px330-U6-Chimeric_BB-CBh-hSPCas9	Addgene plasmid #42230 (Cong et al., 2013)
px330_PmeIKO	Generated by Debby van den Boorn-

	Konijnenberg
px330-Tyrp1-Ct	Generated during this study
px330-Cdk4-Ct	Generated during this study
px330-Actg1-Ct	Generated during this study
px330-Gpnmb-Ct	Generated during this study
px330-Sox10-Ct	Generated during this study
px330-Dct-Ct	Generated during this study
px330-Actb-Ct	Generated during this study
pUC57-loxP-gB	BioCat
pCRISPaint-mScarlet-loxP-F-gB- BlastR-loxP-mNeon (SWITCH.gB)	Generated during this study
pRP-GFP	Gift from Eicke Latz
gag-pol	Gift from Eicke Latz
VSV-G	Gift from Eicke Latz
MSCV CreERT2 puro	Addgene plasmid #22776
pMIR-EGFP-hMITF-M	Generated by Stefanie Riesenber
pEGFP-FLAG-Ova	Generated by Stefan Holtin
UTP-HSV-L-SSIEFARL (5.1)	Generated by Lennart Tegethoff
px458_Pes1_Ct	Generated by Stefan Holtin
px458_Pmel_Ct	Generated by Stefan Holtin

2.2. Methods

2.2.1. Molecular cloning techniques

2.2.1.1. Polymerase chain reaction

For the amplification of inserts that were used for the generation of new plasmids or the generation of amplicons Q5 polymerase was used. A 50 μ l PCR reaction contained the following components:

10 μ l	5x Q5 [®] reaction buffer
1 μ l	dNTPs (10 mM each)
2.5 μ l	Forward primer (10 μ M)
2.5 μ l	Reverse primer (10 μ M)
1 μ l	Template DNA
0.5 μ l	Q5 [®] High-Fidelity DNA Polymerase
10 μ l	5x Q5 [®] High GC enhancer (optional)
ad 10 μ l	ultrapure H ₂ O

Mass of template DNA differed between experiments. If the template DNA was plasmid DNA, 1 ng was used, however if the template DNA was gDNA or cDNA 1 ng – 1 μ g was used. Therefore, 1 ng of plasmid DNA or 1 ng -1 μ g of gDNA or cDNA were used for amplification.

The PCR reactions were incubated in a PCR thermocycler using the recommended thermocycling conditions for the Q5 polymerase as follows:

Initial denaturation	98	°C	30 s	
Denaturation	98	°C	10 s	30x
Annealing	50 - 72	°C	30 s	
Extension	72	°C	30 s/kb	
Final extension	72	°C	2 min	
Hold	12	°C	∞	

The annealing temperature was 3 °C above the T_m of the lower T_m primer.

2.2.1.2. Oligonucleotide annealing

Oligonucleotides were reconstituted to a final concentration of 100 μ M and 1 μ l of the top- and bottom-strand oligonucleotide were annealed in a total volume of 50 μ l annealing buffer (100 mM NaCl, 50 mM HEPES in ultrapure water; pH 7.4). Oligonucleotides were annealed in a thermocycler using the following programme:

90 °C 4 min
70 °C 10 min
69 °C 1 min (decrease 1 °C / 60 s until RT is reached)
20 °C ∞

2.2.1.3. Restriction enzyme digest

For molecular cloning, purified PCR products or 10 μ g of plasmid were incubated with 10 U of a restriction enzyme and the corresponding buffer in a reaction volume of 50 μ l. Purified PCR products or plasmids were incubated for 2 h or 4 h at 37 °C, respectively. After restriction digest, PCR products and plasmids were purified using the MEGAquick-spin Plus Total Fragment DNA Purification Kit or the Wizard[®] SV Gel and PCR Clean-Up System.

2.2.1.4. Ligation

Insert DNA mass was calculated according to the following formula:

Required mass insert (g) = desired insert/vector molar ratio x mass of vector (g)
x ratio of insert to vector length

50 ng of plasmid and the calculated mass of insert were incubated with 1 μ l T4 DNA ligase and the corresponding buffer in a 10 μ l reaction for 10 min to 24 h at room temperature.

For the ligation of annealed oligonucleotides, 100 ng of BbsI-digested plasmid DNA (px330 or px458) and 1 μ l of the annealed oligonucleotides were incubated with 1 μ l T4 DNA ligase and the corresponding buffer in a 10 μ l reaction for 10

min to 24 h at room temperature.

2.2.1.5. Agarose gel electrophoresis

DNA resulting from PCR reactions or restriction digests was size separated using agarose gel electrophoresis. Agarose gels (0.8 % - 2 %) were prepared using 1 x TAE buffer (1 mM EDTA Na₂, 40 mM TRIS, 20 mM acetic acid) and Ethidium bromide or Gel Green nucleic acid stain. Gels were run at 140 V for 30 min. DNA was visualised using UV light.

2.2.1.6. Transformation

50 µl of chemically-competent *Escherichia coli* DH10β were thawed on ice and 5 µl of ligation mixture was added to the bacteria. The bacteria were incubated on ice for 10 min and then subjected to a heat shock at 42°C for 45 s. After another 2 min on ice, the bacteria were streaked on LB agar plates containing 100 mg/ml ampicillin. The agar plates were incubated upside down overnight at 37°C.

2.2.1.7. Plasmid DNA preparation from *Escherichia coli* cultures

For small-scale or medium-scale plasmid preparations, 1.5 ml or 100 ml LB broth containing 100 mg/ml ampicillin were inoculated with a single *E. coli* colony, respectively. Cultures were incubated overnight at 37 °C shaking (180 rpm).

For small-scale plasmid preparations, the bacteria were pelleted in a table-top centrifuge at 6,000 x g for 10 min and were resuspended in 180 µl resuspension buffer P1 containing RNase A. Following resuspension, 180 µl lysis buffer P2 was added and the solution was mixed by inverting the tube six times. Then, 250 µl of neutralisation buffer N3 was added and the solution was again mixed by inverting the tube six times. The solution was centrifuged in a table-top centrifuge at full speed for 10 minutes and the supernatant was transferred to a spin column for DNA isolation. The spin column was centrifuged at 10,000 rpm in a table-top centrifuge and the plasmid DNA bound to the membrane was washed twice with 750 µl PE washing buffer. After a dry spin at highest speed, plasmid DNA was eluted in 40 µl ultrapure H₂O.

Resuspension buffer P1:	50 mM Tris-HCl (pH 8.0), 10 mM EDTA, 50 µg/ml RNaseA
Lysis buffer P2:	200 mM NaOH, 1% SDS
Neutralisation buffer N3:	4.2 M Guanidine hydrochloride, 0.9 mM potassium acetate; pH 4.8
Wash buffer PE:	10 mM Tris-HCl (pH 7.5), 80% Ethanol

Medium-scale plasmid preparations were processed using the PureLink® HiPure Plasmid Midiprep Kit according to the manufacturer's instructions. Plasmid DNA was reconstituted in 100 µl ultrapure H₂O.

DNA concentration of small or medium- scale plasmid preparations were measured using the spectrophotometer NanoDrop 2000.

2.2.2. Tissue culture

All melanoma cell lines were routinely cultured in RPMI1640 supplemented with 10 % FCS, 2 mM L-glutamine, 10 mM non-essential amino acids, 1 mM HEPES, 20 µM β-Mercaptoethanol, 100 U/ml penicillin and 100 µg/ml streptomycin (RP10). HEK293T cells were routinely cultured in DMEM supplemented with 10 % FCS, 2 mM L-Glutamine and 100 U/ml penicillin and 100 µg/ml streptomycin (DMEM10). All cells were cultured in a humidified incubator with 5% CO₂ at 37°C. All cell lines used in this study were routinely tested for Mycoplasma contamination by PCR.

The cell line HCmel12 was established from a primary melanoma in the Hgf-CDK4^{R24C} mouse melanoma model by serial transplantation as previously described (Bald et al., 2014). The *Pmel* gene was knocked out using the CRISPR/Cas9 technology to generate the HCmel12 Pmel KO (HC.PmelKO) melanoma cell line. The melanoma cell line B16 was originally obtained from ATCC. The *Tyrosinase* gene was knocked out using the CRISPR/Cas9 technology to generate the B16 Tyr KO (B16.TyrKO) melanoma cell line.

2.2.3. Generation of CRISPR/Cas9-engineered melanoma cells

2.2.3.1. Generation of sgRNA/Cas9-expressing plasmids

In order to generate sgRNA/Cas9-expressing plasmids that target a genomic region leading to either a gene knockout or a knockin, single stranded DNA oligonucleotides were annealed. This generated a double stranded DNA oligonucleotide with 5' overhangs compatible to a BbsI restriction site. The plasmid px330-U6-Chimeric_BB-CBh-hSPCas9 (short: px330) or pSPCas9(BB)-2A-GFP (short: px458) were digested with BbsI and gel purified using the MEGAquick-spin Plus Total Fragment DNA Purification Kit. A double-stranded DNA oligonucleotide was cloned into either px330 or px458 using T4 DNA ligase. px330-U6-Chimeric_BB-CBh-hSPCas9 and pSPCas9(BB)-2A-GFP were a gift from Feng Zhang (Addgene plasmid #42230 and 48138).

2.2.3.2. Generation of homology constructs

The basis for the generation of the homology constructs was the plasmid UTP-HSV-L-SSIEFARL (5.1), which was generated by Lennart Tegethoff (a former student in the Hölzel laboratory) and encodes FLAG tag followed by the HSV-1 gB₄₉₈₋₅₀₅ epitope (FLAG-gB). Primers with long 5' overhangs that were compatible to either the *Pmel* or *Pes1* endogenous locus were designed and used to amplify the FLAG-gB coding sequence by PCR. The PCR reaction was digested with 2 U DpnI to remove the template plasmid and then purified using the MEGAquick-spin™ Plus Total Fragment DNA Purification Kit.

2.2.3.3. Generation of CRISPR target selectors and universal donor plasmids

The plasmid px330 was used as target selector and digested with BbsI as described above. A double-stranded DNA oligonucleotide targeting the C-terminus of the desired target gene was cloned into the BbsI-digested px330. Frame selectors pCAS9-mCherry-Frame +0, pCAS9-mCherry-Frame +1 and pCAS9-mCherry-Frame +2 were a gift from Veit Hornung (Addgene plasmids #66939, #66940 and #66941).

Universal donor plasmids used in this study were cloned based on the

pCRISPaint-mNeon-PuroR plasmid described by Schmid-Burgk and colleagues (Schmid-Burgk et al., 2016). The universal donor pCRISPaint-mNeon-PuroR was a gift from Veit Hornung. Using molecular cloning approaches, the pCRISPaint-mNeon-PuroR plasmid was further modified by:

(1) Exchanging the Puromycin resistance cassette by a Blastocidin resistance cassette. The vector backbone was digested using EcoNI and DraIII. The Blastocidin resistance cassette coding sequence was amplified by PCR from the vector pMIR-EGFP-hMITF-M using primers that generate 5' overhangs compatible to EcoNI and DraIII. The PCR-purified and digested Blastocidin resistance cassette insert was then ligated into the new vector backbone using T4 DNA ligase.

(2) Exchanging the Methionine start codon (ATG) of the resistance cassettes by a Glycine (GGG) using a site-directed mutagenesis approach to prevent transcription from random genomic integrations [this was performed by Daniel Hinze, a member of the Hölzel laboratory].

(3) Exchanging the mNeon fluorescent protein by the mScarlet fluorescent protein (Bindels et al., 2017; Shaner et al., 2013). The vector backbone was digested using NheI and BsrGI. The mScarlet-coding sequence was amplified by a 2-step PCR from the vector pmScarlet_C1 using primers that generate 5' overhangs compatible to NheI and BsrGI. The PCR-purified and digested mScarlet insert was then ligated into the new vector backbone using T4 DNA ligase. The plasmid pmScarlet_C1 was a gift from Dorus Gadella (Addgene plasmid #85042).

(4) The addition of a FLAG-tag and one of four immunodominant CD8⁺ T cell epitopes [hgp100₂₅₋₃₃ (KVPRNQDWL), mgp100₂₅₋₃₃ (EGSRNQDWL), HSV-1 gB₄₉₈₋₅₀₅ (SSIEFARL) or Ova₂₅₇₋₂₆₄ (SIINFEKL)] to the C-terminus of the fluorescent protein (Hogquist et al., 1994; Mueller et al., 2002; Overwijk et al., 1998). The vector backbone was digested using BsrGI and was treated with Antarctic phosphatase to prevent re-ligation. A double-stranded annealed and phosphorylated DNA oligonucleotide encoding FLAG-hgp100 and 5' overhangs compatible to the BsrGI restriction site was ligated using T4 DNA ligase into the vector backbone. The human gp100 epitope was exchanged with the murine

gp100 epitope using a site-directed mutagenesis approach [this was performed by Jana Liebing, a member of the Hölzel laboratory]. The FLAG-Ova and FLAG-gB inserts were amplified by PCR from the plasmids GFP-FLAG-Ova and UTP-HSV-L-SSIEFARL (5.1), respectively, digested with BsrGI and ligated into the digested vector backbone using T4 DNA ligase.

Table 2.16: Overview of the universal donor plasmids generated for the CRISPitope system

The table shows the plasmid name, the encoded fluorescent protein, the tag and selection marker.

Plasmid name	Fluorescent protein	Tag		Selection marker
pCRISPaint-mNeon-PuroR [M1G]	mNeon			Puromycin
pCRISPaint-mNeon-F-hgp100-PuroR [M1G]	mNeon	FLAG	KVPRNQDWL [hgp100 ₂₅₋₃₃]	Puromycin
pCRISPaint-mNeon-F-mgp100-PuroR [M1G]	mNeon	FLAG	EGSRNQDWL [mgp100 ₂₅₋₃₃]	Puromycin
pCRISPaint-mNeon-F-gB-PuroR [M1G]	mNeon	FLAG	SSIEFARL [HSV-1 gB ₄₉₈₋₅₀₅]	Puromycin
pCRISPaint-mNeon-F-Ova-PuroR [M1G]	mNeon	FLAG	SIINFEKL [Ova ₂₅₇₋₂₆₄]	Puromycin
pCRISPaint-mNeon-BlastR [M1G]	mNeon			Blasticidin
pCRISPaint-mNeon-F-hgp100- BlastR [M1G]	mNeon	FLAG	KVPRNQDWL [hgp100 ₂₅₋₃₃]	Blasticidin
pCRISPaint-mNeon-F-mgp100- BlastR [M1G]	mNeon	FLAG	EGSRNQDWL [mgp100 ₂₅₋₃₃]	Blasticidin
pCRISPaint-mNeon-F-gB- BlastR [M1G]	mNeon	FLAG	SSIEFARL [HSV-1 gB ₄₉₈₋₅₀₅]	Blasticidin

pCRISPaint-mNeon-F-Ova-BlastR [M1G]	mNeon	FLAG	SIINFEKL [Ova 257-264]	Blasticidin
pCRISPaint- mScarlet-PuroR [M1G]	mScarlet			Puromycin
pCRISPaint- mScarlet-F-hgp100-PuroR [M1G]	mScarlet	FLAG	KVPRNQDWL [hgp100 25-33]	Puromycin
pCRISPaint- mScarlet-F-mgp100-PuroR [M1G]	mScarlet	FLAG	EGSRNQDWL [mgp100 ₂₅₋₃₃]	Puromycin
pCRISPaint- mScarlet-F-gB-PuroR [M1G]	mScarlet	FLAG	SSIEFARL [HSV-1 gB 498-505]	Puromycin
pCRISPaint- mScarlet-F-Ova-PuroR [M1G]	mScarlet	FLAG	SIINFEKL [Ova 257-264]	Puromycin
pCRISPaint- mScarlet-BlastR [M1G]	mScarlet			Blasticidin
pCRISPaint- mScarlet-F-hgp100- BlastR [M1G]	mScarlet	FLAG	KVPRNQDWL [hgp100 25-33]	Blasticidin
pCRISPaint- mScarlet-F-mgp100- BlastR [M1G]	mScarlet	FLAG	EGSRNQDWL [mgp100 ₂₅₋₃₃]	Blasticidin
pCRISPaint- mScarlet-F-gB- BlastR [M1G]	mScarlet	FLAG	SSIEFARL [HSV-1 gB 498-505]	Blasticidin
pCRISPaint- mScarlet-F-Ova- BlastR [M1G]	mScarlet	FLAG	SIINFEKL [Ova 257-264]	Blasticidin

2.2.3.4. Transfections of CRISPR/Cas9 knockout and knockin constructs

For transfections of the px458_Pmel_Ct or px458_Pes1_Ct in combination with the corresponding homology construct, 3×10^5 B16 melanoma cells were seeded in a 12-well plate. After adherence was established, the cells were transfected with 1 μg of the px458 plasmid and 1 μg of the homology construct in OptiMEM® using 6 μl FuGENE® HD transfection reagent according to the manufacturer's instructions.

For transfections of the px458 knockout plasmids to generate either Pmel or Tyrosinase-deficient melanoma cells lines, 5×10^4 to 1×10^5 melanoma cells were seeded in a 96-well plate. After adherence was established, the cells were transfected with 200 ng of the px458 knockout plasmid DNA in OptiMEM® using 0.6 μl of FuGENE® HD transfection reagent according to the manufacturer's instructions.

For CRISPitope and SWITCHitope plasmid transfections, 5×10^4 to 1×10^5 melanoma cells were seeded in a 96-well plate. After adherence was established, the cells were transfected with 200 ng of DNA (50 ng target selector, 50 ng frame selector and 100 ng universal donor) in OptiMEM® using 0.6 μl of FuGENE® HD transfection reagent according to the manufacturer's instructions.

2.2.3.5. Validation of knockin by homology-directed repair using next generation sequencing

After establishing monoclonal cultures of CRISPR/Cas9-modified melanoma cells via homology directed repair (HDR), monoclones were screened for successful homozygous or heterozygous knockin of the FLAG-gB insert into the *Pmel* or *Pes1* locus using PCR. After identifying clones with potential homo- or heterozygous knockins by knockin independent PCRs and agarose gel electrophoresis, these were analysed by Next Generation Sequencing (NGS) using the Illumina MiSeq platform. MiSeq PCRs were performed that amplify the region of interest in a first step and add barcodes to the amplicon in a second step. MiSeq PCRs were performed according to the following protocol:

1st MiSeq PCR

2.5	μl	5 x Phusion buffer HF
0.25	μl	dNTPs (10 mM each)
0.625	μl	Forward primer and reverse primer for target region (5 μM each)
1	μl	Template gDNA
0.125	μl	Phusion High-Fidelity DNA Polymerase
8	μl	ultrapure H ₂ O

The PCR reaction was incubated in a PCR thermocycler using the following thermocycling conditions:

Initial denaturation	98	°C	30 s	
Denaturation	98	°C	10 s	18x
Annealing	57	°C	15 s	
Extension	72	°C	30 s	
Final extension	72	°C	3 min	
Hold	12	°C	∞	

2nd MiSeq PCR

5	μl	5 x Phusion buffer HF
0.5	μl	dNTPs (10 mM each)
2.5	μl	Forward primer and reverse barcode primer (5 μM each)
2	μl	DNA product from 1 st MiSeq PCR
0.25	μl	Phusion High-Fidelity DNA Polymerase
14.75	μl	ultrapure H ₂ O

The PCR reaction was incubated in a PCR thermocycler using the following thermocycling conditions:

Initial denaturation	98	°C	30 s	
Denaturation	98	°C	10 s	18x
Annealing	57	°C	15 s	
Extension	72	°C	30 s	
Final extension	72	°C	3 min	
Hold	12	°C	∞	

The 2nd MiSeq PCR product was analysed by gel electrophoresis. Samples were pooled and analysed using NGS by the Next Generation Sequencing Core Facility of the Medical Faculty of the University of Bonn. The results were analysed using the web tool OutKnocker (Schmid-Burgk et al., 2014). OutKnocker is a deep-sequencing and evaluation tool allowing reliable, convenient and cost-effective identification of knockout cell lines. The tool aligns an amplicon to a reference sequence, detects mismatches and determines indel size.

2.2.3.6. Generation of SWITCHitope target selectors and universal donor plasmids

The plasmid px330 was used as target selector and was digested with BbsI as described above. A double-stranded DNA oligonucleotide targeting the C-terminus of the desired target gene was cloned into the BbsI-digested px330.

Frame selectors pCAS9-mCherry-Frame +0, pCAS9-mCherry-Frame +1 and pCAS9-mCherry-Frame +2 were a gift from Veit Hornung (Addgene plasmids #66939, #66940 and #66941).

A customised DNA insert was ordered from the company BioCat which encodes the desired DNA sequence and individually chosen restriction sites to facilitate molecular cloning into the CRISPitope universal donor backbone. The desired DNA insert was cut out of the BioCat backbone (pUC57) using AvrII and DraIII, gel purified and ligated into digested pCRISPaint-mScarlet-F-hgp100-BlastR[M1G] using T4 DNA ligase.

2.2.4. Immunoblotting

Total cell lysates were prepared by lysing cultured melanoma cells in 1xLaemmli buffer and incubation at 95 °C for 5 min. Cell lysates were separated using 10 % SDS-PAGE and proteins were transferred to a nitrocellulose membrane (pore size: 0.2 µm) by wet blotting. After 1 h of blocking with 5 % bovine serum albumin (BSA) in Tris-buffered saline (TBS) with 0.5 % Tween-20, membranes were incubated with primary antibodies overnight at 4 °C. The proteins were detected using corresponding secondary antibodies and the Odyssey Sa Imaging system (LI-COR Biosciences). Primary antibodies: β-Actin (C4, Santa Cruz, 1:2,000), CDK4 (DCS-35, Santa Cruz, 1:100), FLAG (L5, Novus Biologicals, 1:500), gp100 (PMEL17/SILV, Novus Biologicals, 1:1,000), MITF (HPA003259, Atlas Antibodies, Sigma-Aldrich, 1:250), Pescadillo (H10, Santa Cruz, 1:200) and TRP1 (G-9, Santa Cruz, 1:100. Secondary antibodies: donkey anti-mouse IRDye 680 LT, donkey anti-rabbit IRDye 800 CW, donkey anti-rat IRDye 800 CW and donkey anti-goat IRDye 800 CW (all by LI-COR Biosciences, 1:15,000). Ladder: Broad Range Markers (Santa Cruz).

Laemmli buffer: 4 % SDS, 20 % Glycerol, 120 mM Tris-HCl (pH 6.8), 0.02 % bromophenol blue, 20 mM Dithiothreitol
 Running buffer: 25 mM Tris, 192 mM glycine, 0.1 % SDS
 Blotting buffer: 25 mM Tris, 192 mM glycine, 20 % methanol
 TBS: 50 mM Tris (pH 7.6), 150 mM NaCl

2.2.5. Epifluorescence microscopy

Melanoma cells were seeded on coverslips overnight. Fixation was performed using 4 % p-formaldehyde in PBS for 4 minutes at room temperature followed by three short washes with PBS. Cells were then permeabilised using 0.04 % Triton X-100 in PBS for 5 min at room temperature followed by three short washes with PBS. Fixed cells were incubated with 0.5 µg/ml DAPI (4,6-diamindino-2-phenylindole) in PBS for 1 min followed by a final wash with PBS. Cells were mounted on objective slides using Fluoroshield mounting medium. Epifluorescence microscopy was performed using Carl Zeiss Oberserver Z1 (40 x oil-immersion objective). Data processing was performed using Carl Zeiss Zen

software and ImageJ (Fiji package).

2.2.6. Flow cytometry

2.2.6.1. Cell sorting

Cell sorting was performed when only a proportion of melanoma cells with specific properties were needed. Melanoma cells were harvested according to standard protocols using Trypsin and resuspended in RP10 before cell sorting.

For the generation of the B16.PMEL-FgB and the B16.PES1-FgB melanoma cells, a polyclonal culture that was transfected with px458 encoding a Cas9 and a sgRNA that leads to a knockin of a co-transfected homology construct was sorted. px458 encodes GFP and therefore cells that were GFP-positive were sorted and single cells were directly sorted into 96-wells to generate monoclonal cultures.

For the generation of the HC.PmelKO and the B16.TyrKO cells, a polyclonal culture that was transfected with px458 encoding a Cas9 and a sgRNA that leads to a knockout of the respective gene was sorted. px458 encodes GFP and therefore successfully transfected cells that were GFP-positive. These cells were sorted and single cells were directly sorted into 96-wells to generate monoclonal cultures.

For the generation of the CRISPitope-modified melanoma cells, polyclonal cultures that were transfected with the three CRISPitope plasmids were sorted. Successfully transfected cells were mNeon or mScarlet-positive after transfection and sorted accordingly. Sorted cells were plated as polyclonal cultures.

For the generation of the SWITCHitope-modified melanoma cells, polyclonal cultures that were transfected with the three SWITCHitope plasmids were sorted. Melanoma cells that were mScarlet-positive after successful transfection were sorted accordingly. Sorted cells were plated as polyclonal and monoclonal cultures.

2.2.6.2. Cell surface immunostainings and intracellular immunostainings

Cell surface immunostainings were performed according to standard protocols.

Single cell suspensions of tissues harvested from mice were stained with fixable live-dead dyes in PBS before or with DNA-intercalating live-dead dyes after cell surface immunostainings were performed. Cells were stained with fluorophore-conjugated antibodies or in two steps with a primary antibody followed by a secondary fluorophore-conjugated antibody in FACS buffer (50 mM EDTA, 1 % BSA in PBS) for 30 min on ice in the dark. Melanoma cell lines or *ex vivo* established melanoma cells were stained as described above. Melanoma cells were additionally analysed for endogenous mNeon and/or mScarlet expression. For intracellular cytokine stainings, cells were fixed and permeabilised using the Cytofix/Cytoperm kit according to the manufacturer's instructions.

All data were recorded on a FACS Cantoll or LSR Fortessa flow cytometer. Flow cytometry analyses were performed using FlowJo v10 software for Windows. Quantifications and statistical analyses were performed using Microsoft Excel and GraphPad Prism 8.

2.2.7. Mice

C57BL/6 were either purchased from Janvier LABS or Charles River or were bred in the Bioresource facility of the Peter Doherty Institute for Infection and Immunity. TCR-transgenic pmel-1 mice were purchased from Jackson Laboratory. TCR-transgenic gBT-I mice, Rag1^{-/-} and Rag2^{-/-}; IL2rg^{-/-} were bred in the Bioresource facility of the Peter Doherty Institute for Infection and Immunity.

All animal experiments were approved by the local government authorities (LANUV, NRW, Germany and The University of Melbourne Animal Ethics Committee) and were performed in adherence to the national and institutional guidelines for the care and use of laboratory animals.

2.2.8. T cell activation

In order to activate pmel-1 TCRtg T cells for in vitro T cell functional assays, a spleen from a naïve TCRtg mouse was harvested and a single cell suspension was prepared by meshing the spleen through a 70 µm cell strainer and washing with PBS. After centrifugation (1600 rpm, 5min, 4 °C), the splenocytes were resuspended in 50 ml PBS and counted using Trypan blue and analysed by flow

cytometry using the cell surface markers CD45, CD8, CD90.1 and V β 13 to determine the frequency of pmel-1 T cells. After another centrifugation step, pmel-1 TCRtg T cells were resuspended in complete RPMI at a concentration of 1×10^6 cells/ml. Additionally, 100 U/ml recombinant human IL-2 and 1 μ g/ml hgp100 peptide were added to the tissue culture media. On days two, three and four, cells were split 1:2 and fresh RPMI media and recombinant human IL-2 were added. Experiments were performed 5 days after cell culturing.

In order to activate T cells used for epicutaneous inoculations or *in vitro* T cell functional assays, a spleen from a TCRtg mouse (gBT-I or OT-I mouse) was harvested and a single cell suspension was prepared by meshing the spleen through a 70 μ m cell strainer and washing with Hanks' Balanced Salt Solution (HBSS). After centrifugation (1600 rpm, 5min, 4 °C) the splenocytes were resuspended in 4 ml HBSS and the splenocyte solution was halved. Half of the splenocytes were peptide-pulsed with 0.1 μ g/ml gB₄₉₈₋₅₀₅ or Ova₂₅₇₋₂₆₄ peptide for 45 min at 37 °C. Afterwards, the cells were washed three times with HBSS and resuspended in 5 ml RP10 containing 6 μ g of LPS. The other half of the splenocytes was centrifuged and the splenocytes were resuspended in 35 ml of RP10 media. The peptide-pulsed and the naïve splenocytes were then both transferred to a single T75 tissue culture flask and incubated upright in a tissue culture incubator. On days two, three and four, cells were split 1:2 and 20 ml of fresh RP10 and recombinant human IL-2 was added (final concentration 12.5 U/ml). Experiments were performed 5 days after cell culturing.

2.2.9. *In vitro* T cell activation assay

T cell activation assays were performed in order to assess whether CRISPR/Cas9-engineered melanoma cells could activate and be recognised by T cells *in vitro*.

T cells were isolated from spleens of TCRtg mice (pmel-1, gBT-I or OT-I). Spleens were harvested and single cell suspensions were prepared. T cells were either used naïve or activated for different assays.

For an *in vitro* T cell assay with naïve cells, melanoma cells were plated in multi-well plates and treated for 3 days with 1000 U/ml murine recombinant IFN γ . After

IFN γ pre-treatment, MHC class I surface expression of melanoma cells was analysed by flow cytometry and TCRtg T cells from naïve mice were added at a ratio of 1:1.5 (melanoma cell: T cell). After 18h of co-culture, the supernatants and the T cells were harvested. The supernatant was analysed for IFN γ concentration using an ELISA. T cell activation by CD69 surface expression was analysed by flow cytometry.

For an *in vitro* T cell assay with activated T cells, melanoma cells were plated in multi-well plates and treated for 18 hours with 0.1 ng/ml murine recombinant IFN γ . After IFN γ pre-treatment, MHC class I surface expression of melanoma cells was analysed by flow cytometry and activated TCRtg T were added at a ratio of 1:0.5 (melanoma cell: T cell). Melanoma cells and T cells were co-cultured in media containing Brefeldin A (10 μ g/ml). After 5h of co-culture, T cells were harvested and analysed by flow cytometry for intracellular IFN γ and TNF α cytokine expression.

2.2.10. Intracutaneous tumour transplantation experiments

Melanoma cells were harvested using Trypsin and washed twice with PBS. Melanoma cells were then resuspended in PBS at a density of 2×10^6 cells/ml. Cohorts of syngeneic C57BL/6 mice were injected intracutaneously (i.c.) with either 2×10^5 HC.PmelKO.TYRP1-NFhgp100 or HC.PmelKO.CDK4^{R24C}-NFhgp100 melanoma cells (in 100 μ l PBS) on the right flank. Tumour size was measured twice weekly and recorded as mean tumour diameter in millimeter. Tumour area was calculated by using the following equation: $A = \text{width} \times \text{length}$ [mm^2]. Mice were sacrificed when tumours reached 100 mm^2 or when signs of illness were observed.

2.2.11. Adoptive cell transfer immunotherapy

Adoptive cell transfer immunotherapy was performed as previously described (Landsberg et al., 2012). When transplanted CRISPRitope-modified HC.PmelKO melanoma cells reached a size of 4 – 5 mm in diameter mice were treated with the established ACT immunotherapy. Mice were pre-treated for ACT by a single intraperitoneal (i.p.) injection of 2 mg cyclophosphamide (in 100 μ l PBS; 100

mg/kg) one day prior to intravenous injection of 2×10^6 naïve gp100-specific CD8⁺ CD90.1⁺ pmel-1 TCRtg T cells (in 200 µl PBS) isolated from spleens of pmel-1 TCR transgenic mice. The transferred T cells were *in vivo* activated by a single i.p. injection of 5×10^8 PFU of a recombinant adenoviral vector Ad-gp100 (in 100 µl PBS). On day 3, 6 and 9 after adoptive pmel-1 T cell transfer, 50 µg of CpG 1826 and 50 µg of poly(I:C) (polyinosinic:polycytidylic acid) in 100 µl distilled water were injected intratumorally (i.t.).

2.2.12. Tissue digestion and processing

Draining lymph nodes (LN), spleens, tumour tissues and skins were harvested from mice.

LNs and spleens were dissociated mechanically by meshing the organs through a 75 µm cell strainer or a metal mesh followed by filtration through a 75 µm nylon mesh. Additionally, spleen single cell suspensions were treated with red blood cell lysis buffer. Tissues were either washed with PBS or FACS buffer.

Tumour tissue was incubated in 5 ml collagenase-containing tissue digestion buffer (1 mg/ml Collagenase D, 1 mg/ml DNase I, 5 % FCS in PBS) for 30 min at 37 °C. After incubation the tissue was meshed through a 75 µm cell strainer and red blood cell lysis was performed if tissue appeared bloody. Tissue was washed with PBS or FACS buffer.

Another method used during this study to generate single cell suspension from tumour tissue was as follows: Tumour tissue was harvested and cut into small pieces followed by 90 min of incubation at 37 °C in 1 ml collagenase-containing tissue digestion buffer (3 mg/ml collagenase III, 5 µg/ml DNase I, 2 % FCS in RPMI1640). After the incubation, the tissue was transferred to RP10 and vigorously pipetted using a disposable transfer pipette. Afterwards, the tissue was filtered through a 75 µm nylon mesh and red blood cell lysis was performed if tissue appeared bloody. Tissue was washed with PBS or FACS buffer.

Skin (1 mm²) was incubated in 1ml liberase-containing tissue digestion buffer for 30 min at 37 °C. The skin was removed from the buffer and curved forceps were run up and down the skin to separate the epidermis from dermis. Both epidermal and dermal layer were transferred back into the liberase-containing tissue-

digestion buffer, finely cut using scissors and incubated for another 60 min at 37 °C. Next, the tissue was transferred to RP10 and vigorously pipetted using a disposable transfer pipette. Afterwards, the cells were filtered through a 75 µm nylon mesh and washed with PBS or FACS buffer.

For the analysis of circulating immune cells in the blood, submandibular bleeding was performed using blood lancet needles or 23 G needles. Approximately, 75 µl of blood was obtained during weekly bleeds. Blood was treated with red blood cell lysis buffer and washed with PBS or FACS buffer.

2.2.13. Ex vivo cultures

Ex vivo cell cultures were established from all transplanted non-treated and ACT recurrent melanomas. Tumour tissue was harvested and incubated in 5 ml collagenase-containing tissue digestion buffer (1 mg/ml Collagenase D, 1 mg/ml DNase I, 5 % FCS in PBS) for 30 min at 37 °C. After incubation, the tissue was meshed through a 75 µm cell strainer and red blood cell lysis was performed if tissue appeared bloody. After washing, single tumour cell suspensions were cultured in RP10 medium in a humidified incubator with 5 % CO₂ at 37 °C. CRISPitope-modified melanoma cells were analysed for endogenous mNeon expression by flow cytometry immediately after isolation and two weeks after *ex vivo* culturing. SWITCHitope-modified melanoma cells were analysed for endogenous mScarlet and mNeon expression immediately after isolation.

2.2.14. PCR analysis of recurrent melanoma

Genomic DNA (gDNA) from *ex vivo* cultured melanoma cells was extracted using the NucleoSpin[®] tissue kit according to the manufacturer's instructions.

For RNA isolation, melanoma cells were lysed in 350 µl RLT lysis buffer. The lysate was mixed with equal volume of 70 % ethanol and loaded onto Zymo Spin IIIC columns. The spin columns were centrifuged and the membrane-bounded RNA was washed with 700 µl RW1 buffer followed by 350 µl Zymo RNA wash buffer. After a dry spin at highest speed, total RNA was eluted from the column using 20 µl of Ampuwa H₂O. For cDNA generation, reverse transcription of total RNA (750 ng) in 10 µl volume was performed using the All-in-One cDNA

Synthesis SuperMix according to the manufacturer's protocol. The reaction was incubated for 10 min at 25 °C, followed by 30 min at 42 °C, and a final inactivation step for 5 min at 85 °C. After synthesis, the cDNA was diluted 1:5 with ultrapure H₂O.

gDNA and cDNA were used as template for the amplification of the desired target region by PCR using Q5 High-Fidelity DNA polymerase.

PCR amplicons were visualised by agarose gel electrophoresis and analysed by Sanger sequencing (Microsynth).

2.2.15. Melanoma cell dedifferentiation assay *in vitro*

For the generation of T cell conditioned media (TCM), splenocytes of naïve C57BL/6 mice were activated by anti-mouse CD3ε/CD28 stimulation.

Therefore, multi-well plates were coated with 10 µg/ml anti-mouse CD3ε antibody in 50 µl PBS overnight at 4 °C and washed twice with PBS before adding splenocytes. On the day of the assay, spleens from C57BL/6 mice were harvested and single cell suspensions were prepared. Splenocytes were resuspended in RP10 and seeded into wells at a density of 1x10⁶ cells/ml. The cells were stimulated with 2 µg/ml anti-mouse CD28 and 30 U/ml recombinant IL-2 for 60 hours. CRISPiTope-modified melanoma cells were treated with the supernatant for 3 days and analysed by flow cytometry for endogenous mNeon expression. All data were recorded on a FACSCantoII or LSRFortessa flow cytometer and analysed using FlowJo v10 software for Windows.

2.2.16. 3'mRNA-Seq analysis of melanoma

Total RNA from homogenised melanoma tissue was extracted using TRIzol reagent and the Nucleospin RNA kit according to the manufacturer's recommendations. RNA concentrations were determined using a NanoDrop spectrophotometer. 3'mRNA-Seq library preparation was performed using the forward QuantSeq 3'mRNA-Seq Library Prep Kit for Illumina according to the manufacturer's protocol by the NGS Core Facility at the University Hospital Bonn. Size distribution and yield of the library after the PCR step was determined by the D1000 high sensitivity tape station prior to pooling of the barcoded libraries. The

pooled libraries were loaded in the Illumina HiSeq2500 platform and analysed by 50 cycles high-output run. Computational analyses were performed using the R-based Bioconductor computing environment. Bioinformatic analyses were jointly performed with Prof. Dr. Michael Hölzel. FASTQ files were aligned to the mm10 mouse reference genome using the RSubread aligner package (Liao et al., 2013). This R software package allows easy and fast alignment for quantification of RNA sequencing reads (principle of subread alignment). It performs high performance alignment and read counting of RNA-seq reads. It can quantify expression at the level of either exons, exon junctions or genes. To adjust the alignment procedure to 3' mRNA-Seq data, the RSubread align function was executed without trimming but allowing for mismatches in the initial cycles. Only reads with at least 45 bases in length were included in the analysis. Initial mapping with the RSubread algorithm ('align') was done with a relaxed setting allowing for ambiguous mapping (maximum two genomic sites to allow for junction reads), but gene level summary with the 'featureCounts' methods was set to unique mapping. The voom method of the limma package was used for normalisation and linear modelling (Law et al., 2014). The voom method is a linear modelling strategy that estimates the mean-variance relationship of the log-counts generating a precision weight for all individual observations. These are entered into the limma empirical Bayes analysis pipeline. The mRNA expression values were transformed to log₂ values of read counts per million (log₂ cpm). Differential expression analyses were done using the limma functions 'lmFit', 'eBayes' (eBayes moderated t-test statistics) and 'topTable'. The 'lmFit' function of the limma package fits a linear model for each gene given a series of arrays. The 'eBayes' step estimates the 'average' variability over all genes and adjust low variability genes up and high variability genes down. The 'topTable' function of the limma packages gives as an output a list containing a linear model fit produced by 'lmFit'. The contrast design is outlined in the respective figure panels, legends and main text. Other Bioconductor and R packages used for the analyses and data visualisation include: edgeR, org.Mm.eg.db, heatmap.3 (with modifications) and beeswarm. 'edgeR' was used for differential expression analysis of RNA-seq expression profiles with biological replication. The package

implements a range of statistical methods for multigroup experiments including empirical Bayes methods that allow the estimation of gene-specific biological variation. 'org.Mm.eg.db' was used for genome wide annotation of Mouse genes. 'heatmap.3' is an R package that allows enhanced heatmap representation. The 'beeswarm' package generates bee swarm plot, which is a one-dimensional scatter plot with closely-packed, non-overlapping points.

2.2.17. Gene set enrichment analysis

The java-based stand-alone version of the Broad Institute GSEA software was obtained from <http://software.broadinstitute.org/gsea/index.jsp> (Broad Institute, Inc., 2018). GSEA determines whether a pre-defined set of genes shows statistically significant, concordant differences between two biological states. For the analysis, the t-test statistics values (eBayes moderated t-test statistics) were used as ranked metrics for the pre-ranked gene list algorithm of the GSEA algorithm with 1000 perturbations (Subramanian et al., 2005). The hallmark gene set collection of the Molecular Signature database (MSigDb) was used and complemented with melanoma phenotype signatures ('invasive', 'proliferative') (Liberzon et al., 2015a; Verfaillie et al., 2015).

2.2.18. Data resources

Raw 3'mRNA-Seq data is deposited in EBI ENA under the study accession PRJEB30997 (<http://www.ebi.ac.uk/ena/data/view/PRJEB30997>).

2.2.19. Salvage immune checkpoint inhibition therapy

When ACT immunotherapy recurrent HC.PmelKO.CDK4^{R24C}-NFhgp100 melanomas reached a size of ≥ 4 mm in diameter, α -PD-L1 salvage therapy was initiated. Therefore, mice received four doses of 250 μ g (in 100 μ l PBS) per i.p. injection over the course of two weeks. Tumour size was measured twice weekly and recorded as mean tumour diameter in millimetre. Tumour area was calculated by using the following equation: $A = \text{width} \times \text{length}$ [mm^2]. Mice were sacrificed when tumours reached 100 mm^2 or when signs of illness were observed.

2.2.20. IFN γ response assay of recurrent melanoma after salvage immune checkpoint therapy

Ex vivo generated cell cultures established from recurrent melanoma after salvage immune checkpoint inhibition therapy were analysed for their responsiveness toward IFN γ treatment. Therefore, melanoma cells were treated for three days with increasing amounts of recombinant murine IFN γ (10 U/ml – 1000 U/ml) and then analysed by flow cytometry for H2-Db surface expression.

2.2.21. Histology

Tumour tissue and control skin was harvested from mice fixed for 24 h in 1 x zinc-fixative. Tissue processing was performed by the Histology Facility at the School of Biomedical Sciences at the University of Melbourne. The fixed tissue was paraffin embedded and the tissue was cut into 4 μ m sections. Various sections were stained by standard H&E (Haematoxylin and Eosin) procedures in addition to antibody-specific stains using immunohistochemistry (IHC).

For standard H&E stains the following procedure was used:

All samples were stained using Haematoxylin and Eosin stain using an autostainer (Leica AutoStainer XL) as listed in the table below and then transferred to a coverslipper (Leica CV5030 Coverslipper).

Table 2.17: Staining protocol for H&E slides

The table shows the indicated staining or washing solution and incubation times.

Staining solution	Time
<i>Deparaffinise and rehydrate sections</i>	
Xylene	4 minutes
Xylene	2 minutes
Xylene	2 minutes
100 % Ethanol	1 minute
100 % Ethanol	2 minutes
90 % Ethanol	2 minutes
70 % Ethanol	2 minutes
Wash in running tap water	1 minute or more (not critical)

Stain	
Stain nuclei with Harris haematoxylin	4 minutes
Wash in running tap water	2 minutes
Blue nuclei in Scott's tap water	1 minute
Wash in running tap water	3 minutes
Stain with 1 % eosin	4 minutes
Wash in running tap water	1 minute
Dehydrate, clear and mount	
100 % Ethanol	1 minute
100 % Ethanol	30 seconds
100 % Ethanol	30 seconds
100 % Ethanol	30 seconds
100 % Ethanol	30 seconds
Xylene	2 minutes
Xylene	2 minutes
Xylene	2 minutes

For IHC the following procedure was used:

After sectioning, the tissue was washed in deionised water. Then the sections were washed three times with xylene (3 min each) and then 2 min in three alcohol solutions with decreasing percentages of ethanol (100 %, 90 %, 70 %) followed by a final wash in deionised water. Antigen retrieval was performed using sodium citrate buffer (10 Mm sodium citrate; pH 6) before the tissue sections were stained with specific primary antibodies. Therefore, sections were microwaved in the buffer for 15 min at 90 % power in a heat proof container followed by two washes with deionised water (5 min each) and three washes with PBS (5 min each). Following antigen retrieval, endogenous peroxidases were blocked. Sections were treated with 3 % hydrogen peroxide solution for 5 min at room temperature followed by one wash with deionised water and three washes (each 5 min) with PBS. Next, a protein block was applied by using 20 % blocking serum (swine or FCS) for 30 min at room temperature. Afterwards, sections were immediately stained with a primary antibody. A solution containing the primary antibody in 20

% blocking serum was added to the tissue section and the antibodies were incubated for 1 h at room temperature. The sections were washed three times with PBS (5 min each) and incubated with a secondary antibody conjugated with horseradish peroxidase for 15 min at room temperature followed by two washes with PBS (5 min each). Next, the sections were incubated with a buffered solution containing hydrogen peroxide for 15 min at room temperature followed by two washes with PBS (5 min each). Then the sections were treated with the chromogen 3,3'-Diaminobenzidine for 5 – 10 min and washed with PBS and tap water. The tissue was counterstained with haematoxylin for 30 s, washed in water, dehydrated using three washes with 100 % ethanol (30 s each) and cleared using three washes with xylene (2 min each). Finally, the sections were mounted on coverslips using mounting medium.

Following processing, tissue sections were scanned using the slide scanner Panoramic SCAN II provided by the APN Mouse Histopathology and Digital Slide Service Facility at the School of Biomedical Sciences at the University of Melbourne.

2.2.22. Production of retroviral particles and transduction of melanoma cells

In order to overexpress certain proteins in cells, melanoma cells can be transduced with retroviral overexpression constructs. For this purpose, viral particles need to be produced in HEK293T cells. On day 1, 1.8×10^6 HEK293T cells were plated in a 6-well in DMEM10. Six hours later, the HEK293T cells were transfected using the calcium phosphate method. Therefore, 200 μ l 1x HBS (25 mM HEPES, 140 mM NaCl, 0.71 mM $\text{Na}_2\text{HPO}_4 \times 7\text{H}_2\text{O}$; pH 7) were mixed with 2 μ g gag-pol plasmid, 220 ng VSV-G plasmid, 2 μ g of the desired retroviral overexpression plasmid and 10 μ l CaCl_2 (2.5 M). This mixture was incubated for 20 min and added to the adherent HEK293T cells. On day 2, the media of the HEK293T cells was changed twice and the target cells were plated in a 6-well plate. On day 3, the supernatant of the HEK293T cells was harvested and filtered (0.45 μ m). The media of the target cells was exchanged with the filtered supernatant containing the viral particles. On day 4, the media of the target cells

was either changed or the cells were split if confluent. On day 5, antibiotic selection with either Puromycin (2 µg/ml; approx. 3 days) or Blasticidin (5 µg/ml – 10 µg/ml; approx. 7 days) was started.

2.2.23. Treatment of melanoma cells with 4-hydroxytamoxifen

4-Hydroxytamoxifen (4-OHT) is the active metabolite of Tamoxifen and was used for *in vitro* assays. 4-OHT was reconstituted in ethanol and melanoma cells were treated with varying concentrations (100 ng/ml – 2µg/ml) for up to five days. Control cells were treated with ethanol only.

2.2.24. PCR analysis of SWITCHitope-engineered melanoma cells

Genomic DNA and total RNA were extracted using the DNeasy® Blood & Tissue Kit or RNeasy® Plus Mini Kit, respectively.

For the generation of cDNA, reverse transcription of total RNA (2000 ng) was performed according to the following protocol:

- 2 µl Omniscrypt Reverse Transcriptase
- 2 µl 10x Omniscrypt buffer
- 1 µl dNTPs (5mM each)
- 2 µl Oligo dT primer
- 1 µl RNase OUT
- 2 µl Ultrapure H₂O

The reaction was incubated at 37 °C for 90 min. After synthesis, cDNA was diluted 1:5 with ultrapure H₂O.

gDNA and cDNA were used as template for the amplification of the desired target region by PCR using Q5 High-Fidelity DNA polymerase.

PCR amplicons were visualised by agarose gel electrophoresis.

2.2.25. CD8⁺ T cell enrichment

Lymph nodes and spleens were harvested from naïve mice and single cell suspensions were established by meshing the organs through a 75 µl cell strainer. Red blood cell lysis was performed on the spleens. The cells were

washed in EDTA-BSS supplemented with 2.5 % FCS (wash buffer). After centrifugation, either all cells isolated from the LNs or all splenocytes were resuspended in 1 ml antibody cocktail (Ter119, M5/114, GK1.5, RB6-8C5, M1/70, F4/80; see table Antibodies for dilutions) and incubated for 30 min at 4 °C. After the incubation, the cells were washed with the wash buffer and each organ was resuspended in 2 ml of the wash buffer. 1 ml of this sample was then added to 2 mg of washed BioMag goat-anti rat IgG magnetic beads and incubated for 20 min at 4 °C under constant rotation. After the incubation, the samples were put in a magnetic rack. The supernatant was collected (negative selection) and the cells were counted using a hemocytometer and trypan blue.

2.2.26. Subcutaneous tumour transplantation experiments

Melanoma cells were harvested using Trypsin and washed three times with PBS. Melanoma cells were then resuspended in PBS at a density of 1×10^6 cells/ml. Cohorts of syngeneic C57BL/6 mice were anaesthetised using inhalation anaesthesia with isoflurane; the anaesthetic machine generates an isoflurane/oxygen mixture (3 -4 % at 0.8 – 1 L/min for induction; 1 – 2.5 % for maintenance). Once anaesthetised, mice were injected subcutaneously (s.c.) with 1×10^5 B16.SWITCHgB cells (in 100 μ l PBS) into the left flank. Tumour size was measured twice weekly and recorded as mean tumour diameter in millimeter. Tumour area was calculated by using the following equation: $A = \text{width} \times \text{length}$ [mm^2]. Mice were sacrificed when tumours reached approximately 50 - 100 mm^2 or when signs of illness were observed.

2.2.27. Epicutaneous inoculation of T cells

Activated T cells were harvested and washed three times with HBSS. T cells were then resuspended in matrigel on ice at a density of 1×10^8 cells/ml.

Cohorts of C57BL/6, Rag1^{-/-} or Rag2^{-/-}; IL2rg^{-/-} mice were anaesthetised by intraperitoneal injections of a mixture of xylazine (15 mg/kg bodyweight) and ketamine (100 mg/kg bodyweight). To prevent eyes from drying out, a small amount of eye gel was applied to cover each eye. The left flank was clipped with electrical clippers and then depilated using Veet hair removal cream applied for

not longer than 2 minutes. All traces of Veet were removed by wiping the skin with wet tissues. Four small patches of skin ($4 \times 2 \text{ mm}^2$) surrounding the desired tumour inoculation site were lightly abraded for 15 sec using a small abrasive tip on a hobby power-tool. This procedure removes the keratin and epithelial layers generating a contained inoculation site. 1×10^6 T cells resuspended in 10 matrigel were applied to each of the four abraded skin areas. The matrigel was allowed to set before the area was covered with a piece of Op-Site Flexigrid (a flexible, plastic "second skin") to contain the T cells at the site. The Op-Site Flexigrid is an adhesive, waterproof dressing which is bacteria-proof and provides a moist wound environment. The torso of the mouse was wrapped with micropore and transpore tape to hold the second skin in place. Four days later the second skin and bandages were removed from the mice. After epicutaneous T cell inoculation, mice were subjected to epicutaneous tumour inoculation.

2.2.28. Epicutaneous tumour transplantation experiments

Melanoma cells were harvested using Trypsin and washed three times with HBSS. Melanoma cells were then resuspended in matrigel on ice at a density of 1×10^7 cells/ml or 1×10^8 cells/ml.

Cohorts of syngeneic C57BL/6, Rag1^{-/-} or Rag2^{-/-}; IL2rg^{-/-} mice were anaesthetised by intraperitoneal injections of a mixture of xylazine (15 mg/kg bodyweight) and ketamine (100 mg/kg bodyweight). To prevent eyes from drying out, a small amount of eye gel was applied to cover each eye. The left flank was clipped with electrical clippers and then depilated using Veet hair removal cream applied for not no longer than 2 minutes. All traces of Veet were removed by wiping the skin with wet tissues. A small patch of skin (2 mm^2) was lightly abraded for 15 sec using a small abrasive tip on a hobby power-tool. Up to 1×10^6 (in most experiments 1×10^5) tumour cells (model antigen expressing variants of B16), resuspended in 10 μl matrigel were applied to the abraded skin and the matrigel was allowed to set before the area was covered with a piece of Op-Site Flexigrid Flexigrid (a flexible, plastic "second skin") to contain the cells at the site. The Op-Site Flexigrid is an adhesive, waterproof dressing which is bacteria-proof and provides a moist wound environment. The torso of the mouse was wrapped with micropore

and transpore tape to hold the second skin in place. Four days later the second skin and bandages were removed from the mice. In order to monitor tumour growth, the fur was removed bi-weekly or weekly. The mice were anaesthetised using isoflurane as described above. Fur on the flank was clipped with an electric hair clipper and then depilated using Veet hair removal cream applied for not no longer than 2 minutes. All traces of Veet were removed by wiping the skin with wet tissues. Tumour size was measured twice weekly and recorded as mean tumour diameter in millimetre. Tumour area was calculated by using the following equation: $A = \text{width} \times \text{length} [\text{mm}^2]$. Mice were sacrificed when tumours reached approximately 25 mm² or when signs of illness were observed.

2.2.29. Treatment of mice with tamoxifen

In order to modulate protein expression *in vivo*, mice were treated with Tamoxifen. Tamoxifen was reconstituted in ethanol at a concentration of 50 mg/ml and diluted (1:10) in sunflower seed oil immediately before injection. Mice were i.p. injected with 1 mg Tamoxifen in oil (200 µl) for five consecutive days. Control animals were injected with 200 µl oil only.

2.2.30. Quantification and statistical analysis

Statistical significance of experimental results was evaluated with GraphPad Prism 7 and 8 software using the parametric unpaired two-tailed student's t-test, non-parametric Mann-Whitney-U test and log-rank test depending on the type of source data. P-values less than 0.05 were considered statistically significant. Raw p-values were corrected for multiple comparisons if required using the Benjamini & Hochberg (B&H) methods (false discovery rate, FDR).

Tumour area was considered as normally distributed values with similar variances. Parametric test (t-test) were used for significance analysis in these cases. Frequencies of cell populations (percentages) determined by flow cytometry were compared with non-parametric Mann-Whitney-U test as well as parametric T-tests after reciprocal transformation. 3' mRNA-Seq gene expression data was considered as normally distributed after Voom normalization and linear modeling allowing for parametric statistical tests and other methods requiring

normal distribution of data (Law et al., 2014). Survival probabilities with 95 %-CI were calculated according to Kaplan-Meier and compared with log-rank-statistics. The statistical tests were performed using GraphPad Prism 7 or 8 software or the R computing platform.

**Chapter 3:
Generation of a CRISPR/Cas9-based
knockin strategy to fuse model CD8⁺
T cell epitopes to endogenous gene
products in melanoma cells**

Chapter 3: Generation of a CRISPR/Cas9-based knockin strategy to fuse model CD8⁺ T cell epitopes to endogenous gene products in melanoma cells

3.1. Introduction

Malignant melanoma is a highly aggressive form of skin cancer that arises from neoplasms of the melanocytic lineage. In the recent years, therapy outcome of patients suffering from malignant melanoma has significantly increased due to the development of new treatment approaches. ACT immunotherapy using autologous tumour derived T cells targeting tumour antigens has emerged as an effective treatment approach in melanoma patients (Chodon et al., 2014; Goff et al., 2016; Rosenberg and Restifo, 2015). Although this approach has shown promising results, there are still patients who do not respond to the therapy or relapse due to acquired resistance after initial therapy response. Selection of optimal target epitopes and understanding how they impact resistance mechanisms still remains an unresolved challenge. Improved prediction algorithms have facilitated target epitope choice. However, they largely focus on the characteristics of the epitope such as binding affinity to MHC molecules (Stranzl et al., 2010). How the biology, and the endogenous regulation, of the epitope-encoding gene product (antigen) influences resistance mechanisms to ACT immunotherapy has not been elucidated.

Melanocyte differentiation antigens which are not essential for cell growth and survival, such as gp100 or MART-1, have been targeted by ACT immunotherapy in the past (Johnson et al., 2009). Pro-inflammatory cytokines, such as TNF α produced by activated T cells in the TME, affect expression of the transcription factor MITF which in turn controls expression of MDAs (Landsberg et al., 2012; Riesenberber et al., 2015). In 2018, Mehta and colleagues showed that ACT therapy targeting a MDA can lead to inflammation-induced dedifferentiation and therefore to the loss of target MDA in a melanoma patient. (Mehta et al., 2018). Cancer cells, however, contain multiple genetic abnormalities which can result in the translation of oncogenic proteins. By a phenomenon called 'oncogene addiction', inactivation of a single oncogene can impair cell growth and survival

making oncogene expression essential (Weinstein and Joe, 2008). Other non-oncogenic proteins which are essential for cell survival can also harbour mutations that can be recognised by tumour-reactive T cells. Landsberg and colleagues showed, by using tumour-specific CTL clones, that recognition of mutated essential proteins which are not oncogenes is not reduced by pro-inflammatory cytokines such as TNF α (Landsberg et al., 2012).

We know that many variables impact T cell responses to tumours. For instance, targeting different endogenous gene products is associated with different peptide-MHC binding affinities. This is a confounding factor for experimental studies when comparing T cell responses towards different target antigens. However, the rapid advancement of the CRISPR/Cas9 (Clustered Regularly Interspaced Short Palindromic Repeats) technology enabled us to develop a strategy to circumvent this confounding factor and focus on the biology of the epitope-encoding gene product.

Advances in the CRISPR/Cas9 genome engineering technology enables researchers to interrogate functions of the mammalian genome in a simple way compared to techniques that were used in the past. The CRISPR-associated RNA-guided endonuclease, Cas9, can be targeted to specific locations in the mammalian genome by a single-guided RNA (sgRNA). This system makes it possible to modulate or edit almost any desired gene or genomic region. The applications of the CRISPR/Cas9 technology are very diverse. It can be used for simple applications such as the knockout of a single protein-encoding gene or the knockin of large heterologous DNA cassettes, as demonstrated by Schmid-Burgk and colleagues (Schmid-Burgk et al., 2016). This knockin approach was termed CRISPaint (CRISPR-assisted insertion tagging) and leads to a site-specific insertion of a large heterologous DNA cassette into the mammalian genome. The CRISPaint technique is a modular system which relies on a three-plasmid system ultimately leading to the insertion of a linearized piece of double-stranded DNA at the 3'-end of the protein-coding DNA region.

Plasmid #1 is the target selector. It encodes a Cas9 protein and a sgRNA targeting the 3'end of a protein-coding region of a desired gene. Plasmid #2 is the frame selector. It encodes a Cas9 protein and a sgRNA that targets the third

plasmid. There are three different frame selectors (T_0 , T_1 and T_2) which cut plasmid #3 at different nucleotide sequences. The frame selector is chosen depending on the location of the DSB introduced by plasmid #1 so that the resulting knockin is in frame with the C-terminus of the protein-coding sequence. Plasmid #3 is the universal donor (UD). The UD encodes a target site that is cut by the frame selector and a molecular tag. Molecular tags include a FLAG-tag or fluorescent proteins. Additionally, this approach integrates an antibiotic selection cassette into the desired locus. Using the CRISPaint technique, a C-terminal fusion protein of a murine or human gene product with a desired molecular tag is generated.

The CRISPR/Cas9 technology has given researchers the opportunity to edit genomes of normal cells and also cancer cells with relative ease. These flexible genetic manipulations make it possible to model cancer and study genes that are involved in this disease. In the future, the CRISPR/Cas9 technology will enable the improvement of personalised cancer therapies by identifying resistance mechanisms, thereby helping to develop new treatment strategies.

The aim of the following chapter was to generate a CRISPR/Cas9-based toolbox to facilitate endogenous gene tagging with a defined $CD8^+$ T cell epitope that can be recognised by TCRtg T cell species and thereby create a platform that enables us to investigate how the biology of an epitope-encoding gene product impacts resistance mechanisms in the context of ACT immunotherapy. We expect that knowledge gained from implementing this technique in experimental models will help to improve criteria for target epitope selection for ACT or vaccine approaches (Figure 3.1).

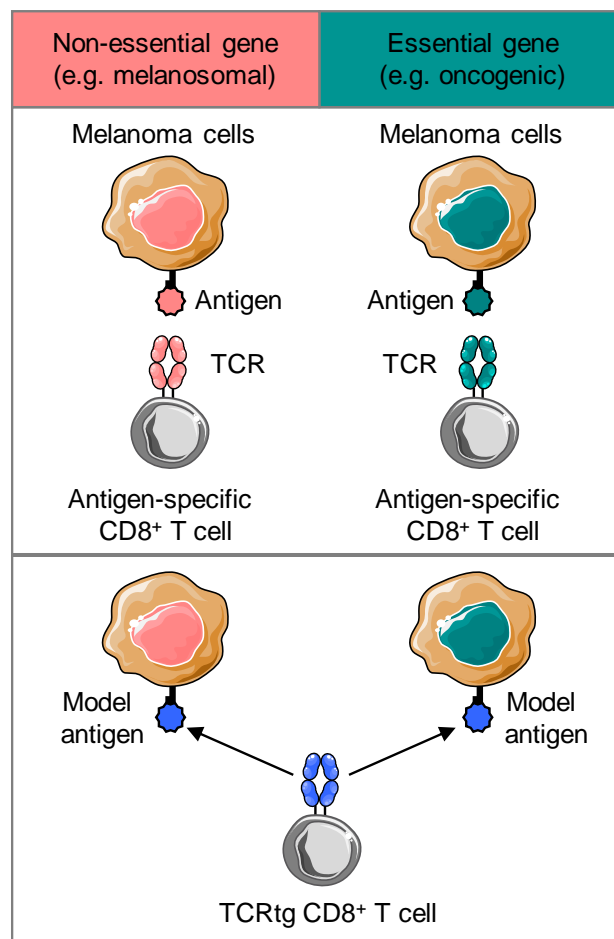


Figure 3.1: Model antigens can be recognised by single TCRtg CD8⁺ T cell species

Antigen-specific CD8⁺ T cells can recognise their cognate antigen (top panel). If however, a model antigen fused to an endogenous gene product that can be recognised by a single TCRtg CD8⁺ T cell species is used, it eliminates the need for individual antigen-specific CD8⁺ T cells.

3.2. Results

3.2.1. CRISPR-assisted insertion of epitopes – 1st generation

3.2.1.1. Harnessing homology-directed repair to generate endogenously tagged melanoma cells

The Cas9 protein is an RNA-guided DNA endonuclease that is able to introduce targeted DNA double strand breaks (DSB) into the genome. Cas9 protein will only bind and cleave a target DNA sequence that is followed by a protospacer adjacent motif (PAM) which itself is a 2-6 base pair DNA sequence.

Here, the murine pre-melanosome protein gp100 (gene name: *Pmel*) and the murine ribosomal biogenesis factor Pescadillo 1 (gene name: *Pes1*) were targeted by CRISPR/Cas9 at the 3' end of the protein coding region (C-terminus). *Pes1* is an essential gene involved in ribosome biogenesis highly expressed in cancer cells (Hölzel et al., 2005, p. 12). By introducing a DSB at this specific site and simultaneously providing a homology construct (repair template), the cell can repair itself via homology directed repair. The homology construct consists of two main parts: the homology arms and the insert that encodes a FLAG-tag and an immunological epitope tag, gB [HSV-1 glycoprotein B (aa: 498-505; SSIEFARL)]. Additionally, the homology construct codes for two short linker sequences that ensures proper folding of the final protein. After successful targeting, the endogenous protein has a C-terminal fusion with a FLAG-tag and an immunological epitope tag. The H2-Kb-restricted gB epitope will be presented on the cell surface and can be recognised by gBT-I TCR transgenic (TCRtg) T cells whereas the FLAG-tag can be used for antibody-dependent detection approaches such as immunoblotting or immunocytochemistry (Figure 3.2).

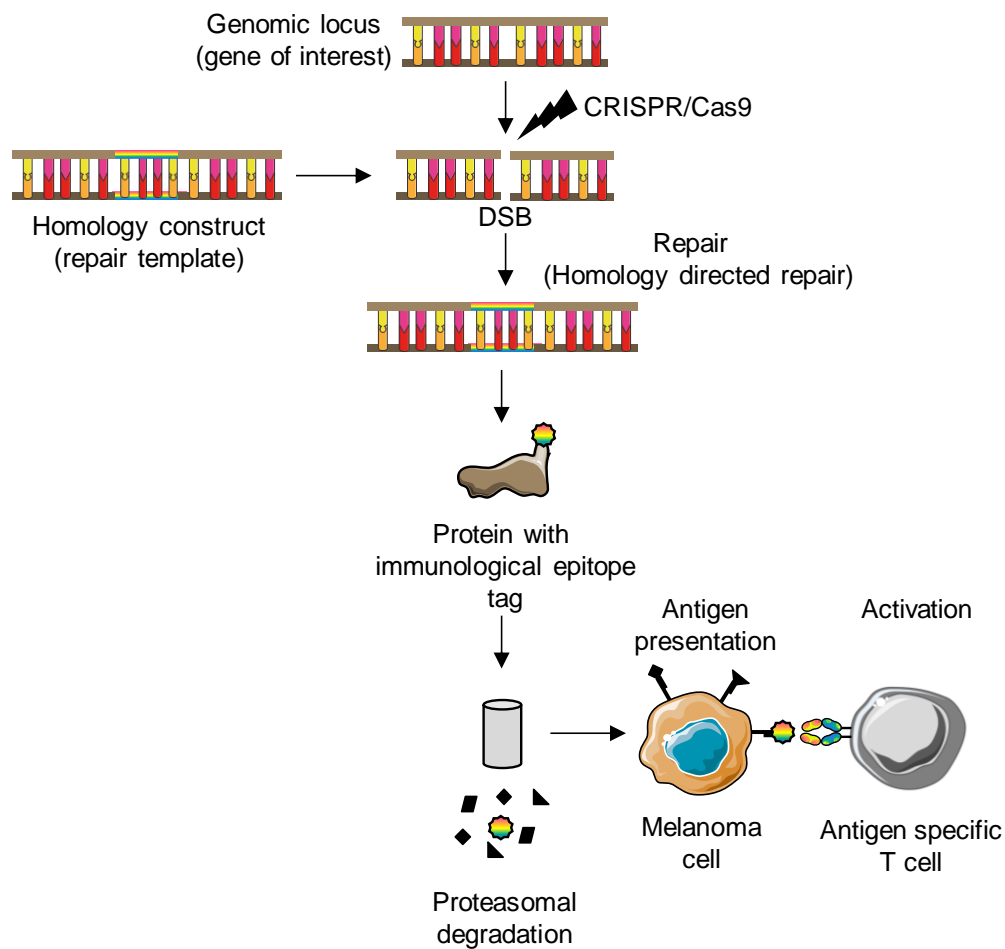


Figure 3.2: Schematic overview of endogenous knockin strategy via homology directed repair

Using CRISPR/Cas9 a DSB at the 3' end of a protein-coding gene is introduced. This lesion will be repaired by homology directed repair when a homology construct (repair template) is provided. The repair template encodes homology arms and an additional insert that codes for a FLAG-tag and a CD8⁺ immunodominant epitope tag. The CRISPR/Cas9-induced DSB will be repaired leading to an insertion of the FLAG-tag and the CD8⁺ immunodominant epitope tag (rainbow colours). If the MHC class I-restricted epitope is presented on the melanoma cell surface, T cells with the appropriate specificity will be able to recognise the melanoma cell and become activated.

3.2.1.2. Genetic and functional validation of endogenously tagged melanoma cells

To target the *Pmel* and *Pes1* genes with the previously described CRISPR/Cas9-based knockin strategy, B16 melanoma cells were transfected with a plasmid called px458 that codes for the Cas9 protein and the gene-specific single-guide RNA (sgRNA), as well as the corresponding homology construct. The plasmid additionally encodes a green fluorescent protein (GFP) to monitor successful transfection. Cells that were GFP positive 48 hours after transfection were enriched by flow cytometry-based cell sorting and single cells were plated in 96-well plates to generate monoclonal cultures. Monoclonal cultures have the advantage that they arise from an individual cell and therefore every cell in such a culture has an identical modification of the genome. For monoclonal cultures in which knockin was successful, the *Pmel* and *Pes1* genes have an in-frame fusion with a FLAG-tag and the earlier described CD8⁺ immunodominant epitope tag. These cell lines were called B16.gp100-FgB and B16.PES1-FgB, respectively (Figures 3.3A and 3.4A). The monoclonal cultures were validated using different techniques. The monoclonal cultures were sequenced using the Illumina MiSeq system and analysis was performed using the *Outknocker 1.2* alignment tool (Schmid-Burgk et al., 2014). MiSeq analysis identified four monoclonal cultures that had the successful genomic integration of the tag in the *Pmel* locus. The NGS (Next Generation Sequencing) data was aligned against the predicted sequence that was generated using information where the Cas9 cut (3 bp upstream of the PAM) and the sequence of the repair template. Grey areas in the pie charts resulting from analysis with the *Outknocker 1.2* alignment tool indicate no indel (insertion – deletion) therefore successful knockin of FLAG-gB tag. Clones 2G6, 3B3, 3F10 and 4A11 had a heterozygous integration of the tag (Figure 3.3B). These monoclonal cell lines were chosen for further analysis due to growth characteristics comparable to wildtype B16 cells. MiSeq analysis also showed that there were four monoclonal cultures that had the successful genomic integration of the tag in the *Pes1* locus, whereas one monoclonal culture had a homozygous knockin (2A6) and three monoclonal cultures had a heterozygous knockin (2E5, 3G4, 4B6) (Figure 3.4B).

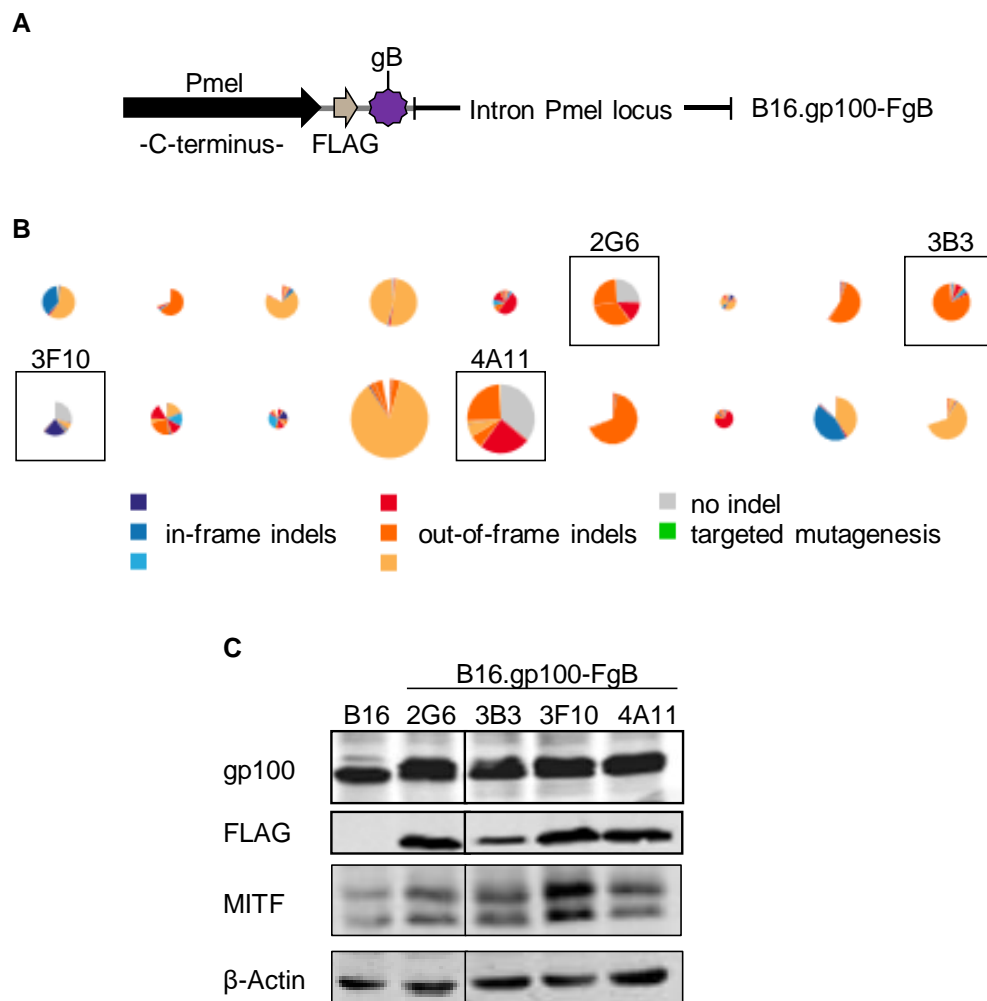


Figure 3.3: Validation of B16.gp100-FgB melanoma cells

(A) Schematic overview of the *Pmel* 3' end of the protein-coding region. The illustration shows an in-frame knockin of a FLAG-gB (HSV-1 gB₄₉₈₋₅₀₅) sequence at 3' end of the protein-coding region of the *Pmel* gene. (B) MiSeq analysis using the *Outknocker 1.2* alignment tool. The NGS data were aligned against the sequence from Figure 2A. Grey areas show no indel (insertion-deletion) indicating successful knockin of the insert. Clones 2G6, 3B3, 3F10 and 4A11 were chosen due to growth characteristics comparable to B16 wildtype cells. (C) Immunoblot analysis for successfully tagged monoclonal cells. Analysis was performed for gp100, FLAG, MITF and β -Actin.

Immunoblot analysis using antibodies against the target protein and FLAG was performed to validate the monoclones. In both cases, the target protein shifted to a higher molecular weight compared to the parental B16 control which coincided with a positive FLAG signal. Additionally, immunoblot analysis was performed for the master regulator of the melanocytic lineage, MITF

, and the housekeeping protein, β -Actin, to check for lineage identity and equal protein loading, respectively (Figures 3.3C and 3.4C). The majority of monoclonal B16.gp100-FgB and B16-PES1-FgB cell lines showed comparable MITF protein expression to wildtype B16, whereas B16.gp100-FgB 3F10 had slightly increased MITF protein expression.

To test whether the CRISPR/Cas9-modified melanoma cell lines could activate TCRtg T cells, an *in vitro* T cell activation assay was performed (Figure 3.5A). The following experiments were performed by Emma Bawden. B16.gp100-FgB and B16.PES1-FgB melanoma cells were stimulated with IFN γ for 18 hours, which leads to upregulation of the antigen processing and presentation machinery and MHC class I surface expression. After stimulation with IFN γ , melanoma cells were stained for H2-Kb surface expression and analysed by flow cytometry. In general, H2-Kb upregulation showed high inter-experimental heterogeneity after IFN γ stimulation of either parental B16 cell or CRISPR/Cas9-engineered B16 cells (Figures 3.6A and 3.6B). B16.gp100-FgB monoclonal cell lines had higher upregulation of H2-Kb surface expression compared to wildtype B16 cells whereas B16.PES1-FgB had lower H2-Kb surface expression. On the day of the assay, pre-activated splenocytes from gBT-I.Ly5.1 mice and IFN γ -stimulated melanoma cells were co-cultured (ratio 1:1). After five hours of co-culture, T cells were stained for intracellular IFN γ and TNF α and analysed by flow cytometry (Figure 3.5B). In general, B16.gp100-FgB (Figures 3.6C, 3.6E and 3.7) and B16.PES1-FgB (Figures 3.6D, 3.6E and 3.7) monoclonal melanoma cell lines were able to induce IFN γ and TNF α expression in gBT-I T cells whereas parental B16 cells were not able to induce IFN γ and TNF α expression in gBT-I T cells. These results confirmed that the cognate antigen was successfully presented on the surface of the melanoma cell lines and able to directly stimulate the antigen specific gBT-I T cells. Generally speaking, we observed more IFN γ - and TNF α -

producing gBT-I.Ly5.1 T cells when co-cultured with B16.gp100-FgB monoclonal melanoma cell lines compared to B16.PES1-FgB cell lines. Intracellular cytokine expression of the gBT-I T cells was entirely dependent on IFN γ pre-stimulation of the melanoma cells. H2-Kb surface expression on the melanoma cells did not correlate with intracellular cytokine expression levels. In conclusion, melanoma cell lines that have been modified by CRISPR/Cas9 to express a defined T cell epitope can be recognised by their respective TCRtg T cell.

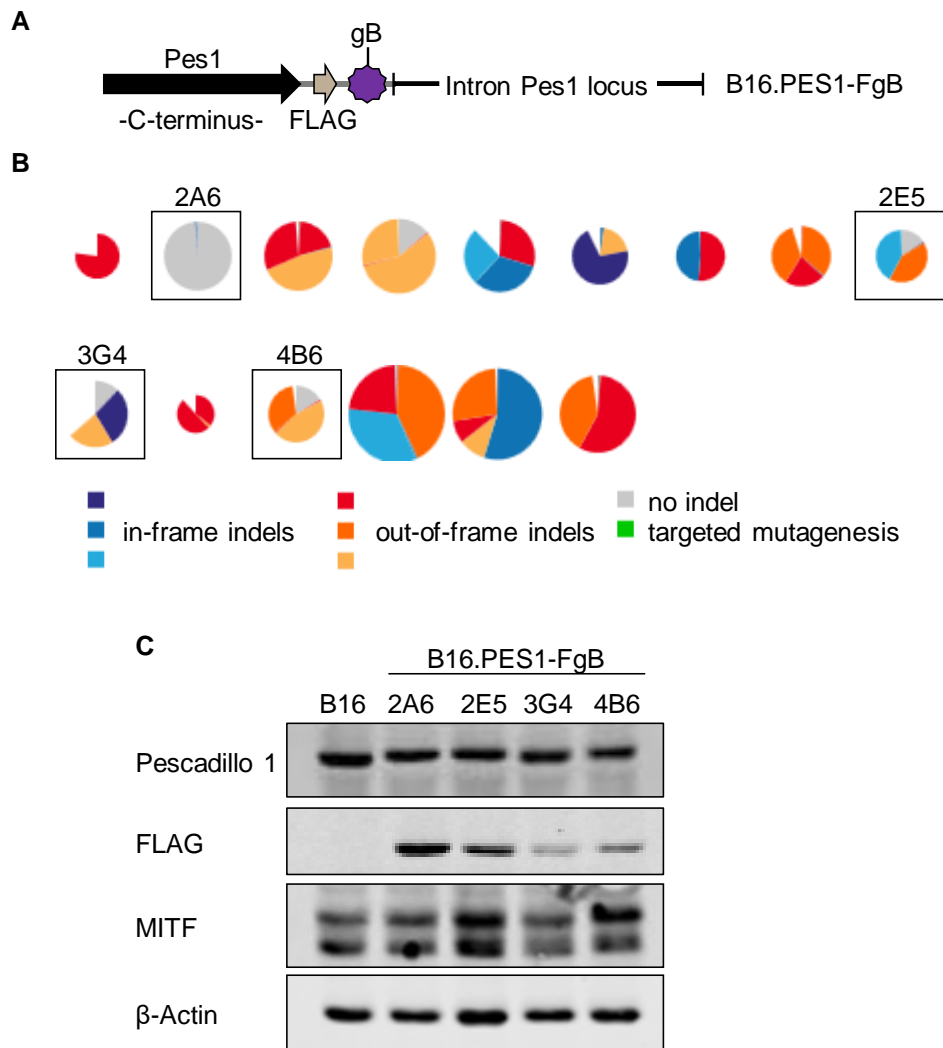


Figure 3.4: Validation of B16.PES1-FgB melanoma cells

(A) Schematic overview of the *Pes1* 3' end of the protein-coding region. The illustration shows an in-frame knockin of a FLAG-gB (HSV-1 gB₄₉₈₋₅₀₅) sequence at 3' end of the protein-coding region of the *Pes1* gene. (B) MiSeq analysis using the *Outknocker 1.2* alignment tool. The NGS data were aligned against the sequence from Figure 3A. Grey areas show no indel indicating successful knockin of the insert. Clones 2A6, 2E5, 3G4 and 4B6 were chosen due to growth characteristics comparable to B16 wildtype cells. (C) Immunoblot analysis for the successfully tagged monoclonal cells. Analysis was performed for PES1, FLAG, MITF and β -Actin.

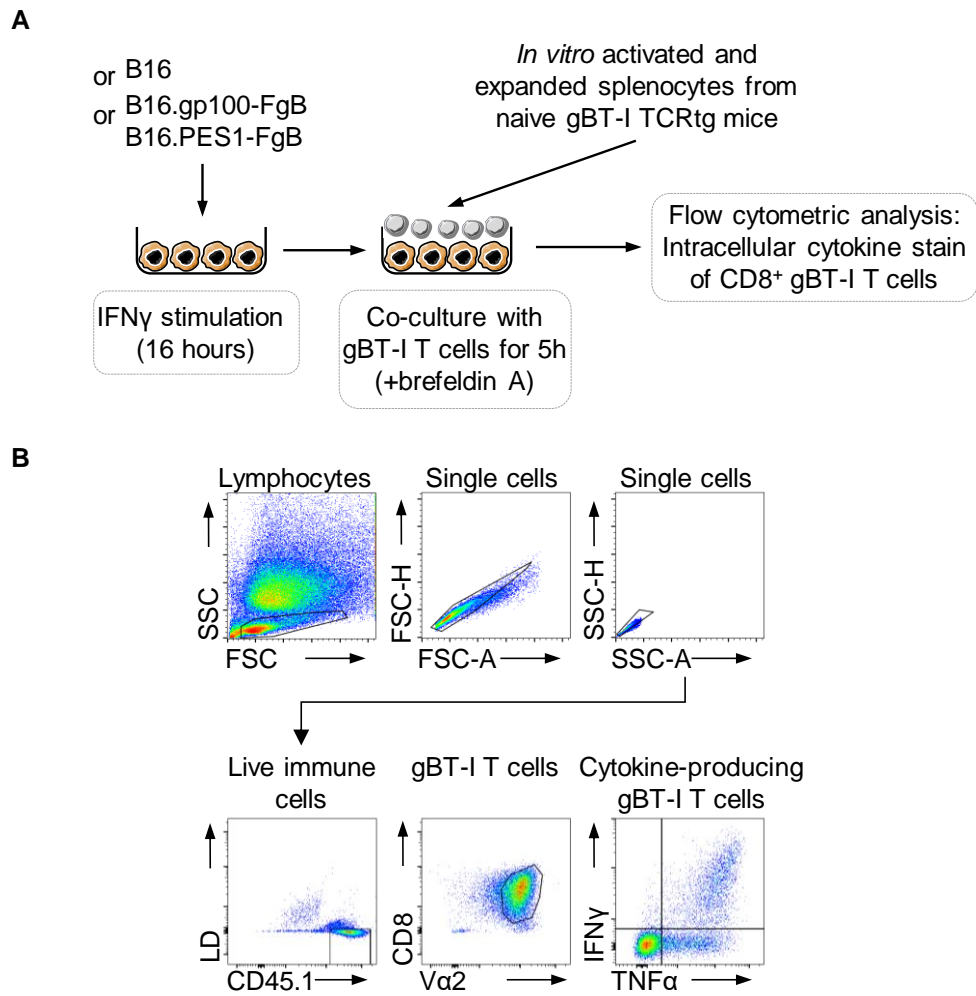


Figure 3.5: *In vitro* gBT-I T cell functionality assay

Experimental outline (A) and gating strategy (B) of a co-culture assay to assess intracellular cytokine production of gBT-I T cells incubated with indicated melanoma cell lines. This experiment was performed by Emma Bawden.

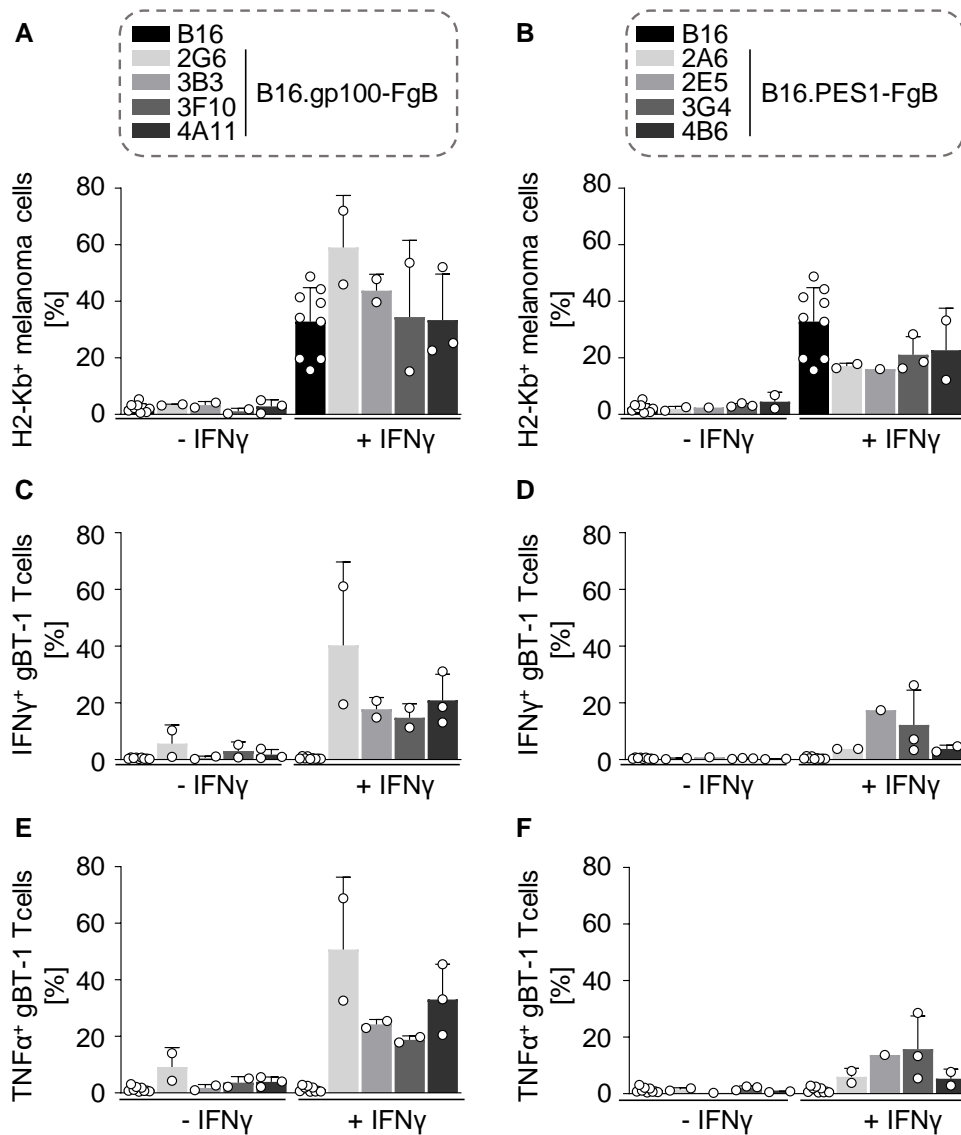


Figure 3.6: CRISPR/Cas9-modified B16 melanoma cells can induce effector cytokine expression in gBT-I T cells

(A) Quantification of H2-Kb surface expression of indicated B16.gp100-FgB and (B) B16.PES1-FgB cells treated with IFN γ (0.1 ng/ml) for 18 hours ($n \geq 1$; mean \pm SD). (C,D) Quantification of intracellular IFN γ expression of CD45.1⁺ CD8⁺ V α 2⁺ gBT-I T cells after 5 hours of co-culture with the indicated B16.gp100-FgB (C) and B16.PES1-FgB cells (D) ($n \geq 1$; mean \pm SD). (E,F) Quantification of intracellular TNF α expression of CD45.1⁺ CD8⁺ V α 2⁺ gBT-I T cells after 5 hours of co-culture with the indicated B16.gp100-FgB (E) and (F) B16.PES1-FgB cells (F) ($n \geq 1$; mean \pm SD). This experiment was performed by Emma Bawden.

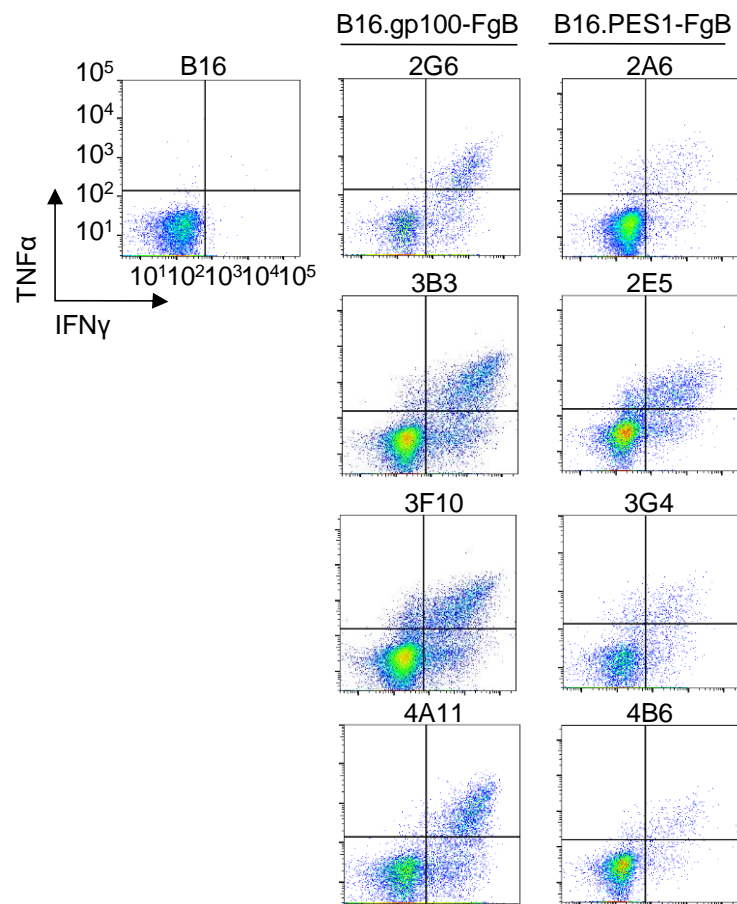


Figure 3.7: CRISPR/Cas9-modified B16 melanoma cells can induce effector cytokine expression in gBT-I T cells (continued)

Representative flow cytometry plots showing expression of intracellular IFN γ and TNF α in gBT-I TCRtg T cells after co-culture with indicated B16 melanoma cells. This experiment was performed by Emma Bawden.

3.2.2. CRISPR-assisted insertion of epitopes (CRISPitope) – 2nd generation

3.2.2.1. Generation of CRISPitope toolbox

The CRISPR/Cas9-based knockin approach described in the previous chapter is rather inefficient, time-consuming, labour-intensive and only generates monoclonal cultures. Although monoclonal cultures have the advantage of being genetically identical, these monoclonal cultures can differ from the parental cell line which is usually a polyclonal culture. These polyclonal cultures display some degrees of heterogeneity despite being an established cell line. Monoclonal cell lines can differ from the parental cell line with regard to mRNA and protein expression profiles, growth characteristics and morphology. In the past, we have experienced that monoclonal cultures show higher variability, in particular in the *in vivo* setting. These variabilities included tumour growth onset, tumour kinetics and tumour penetrance. Therefore, a polyclonal culture is more desirable particularly for *in vivo* studies. By modifying the CRISPaint system published by Schmid-Burgk and colleagues (Schmid-Burgk et al., 2016), we developed an easy and efficient polyclonal approach to endogenously tag any desired protein with a fluorescent protein, a FLAG-tag, a CD8⁺ immunodominant epitope and a selection marker. This CRISPR/Cas9-based tagging approach was termed CRISPitope which is short for CRISPR-assisted insertion of epitopes. The CRISPitope system relies on three different plasmids. Plasmid #1 is the target selector. It encodes a Cas9 protein and a sgRNA targeting the 3' end of a protein-coding region of a desired gene. Plasmid #2 is the frame selector. It encodes a Cas9 protein and a sgRNA that targets the third plasmid. There are three different frame selectors (T₀, T₁ and T₂) which cut plasmid #3 at different nucleotide sequences. The frame selector is chosen depending on the location of the DSB introduced by plasmid #1 so that the resulting knockin is in frame with the C-terminus of the protein-coding sequence. Plasmid #3 is the universal donor (UD). The UD encodes a target site that is cut by the frame selector, a fluorescent protein, a FLAG-tag, a CD8⁺ immunodominant epitope, a T2A site and a selection marker (Figure 3.8A). The UD is integrated into the mammalian genome via non-homologous end-joining (NHEJ) at the DSB induced by the target selector. We

generated a CRISPiTope toolbox that gives us flexibility regarding the choice of fluorescent marker, CD8⁺ T cell epitope sequence and selection marker. The UD encodes either mNeon (green) or mScarlet (red) fluorescent protein, a FLAG-tag and an epitope sequence. Either hgp100₂₅₋₃₃ [KVPRNQDWL; (H2-Db)] or mgp100₂₅₋₃₃ [EGSRNQDWL; (H2-Db)] which are both recognised by pmel-1 TCRtg T cells or HSV-1 gB₄₉₈₋₅₀₅ [SSIEFARL; (H2-Kb)] recognised by gBT-I T cells or Ova₂₅₇₋₂₆₄ [SIINFEKL; (H2-Kb)] recognised by OT-I T cells (Bindels et al., 2017; Hogquist et al., 1994; Mueller et al., 2002; Overwijk et al., 2003; Shaner et al., 2013). Additionally, the UDs either encode a puromycin or blasticidin selection marker (Figure 3.8B). The design of the UDs allows for visualisation by flow cytometry or microscopy, cell sorting, detection by immunoblotting, recognition by specific TCRtg T cells and selection by antibiotics. The CRISPiTope approach is easier and faster compared to the approach described in the previous paragraph. It provides experimental flexibility with regard to MHC class I-restriction (H2-Kb / H2-Db), peptide MHC-affinities (hgp100 / mgp100), the usage of TCRtg T cells (pmel-1 / gBT-I / OT-I TCRtg T cells) and the combination with other coloured cell population (mNeon / mScarlet) or other molecular biology tools (puromycin / blasticidin selection marker).

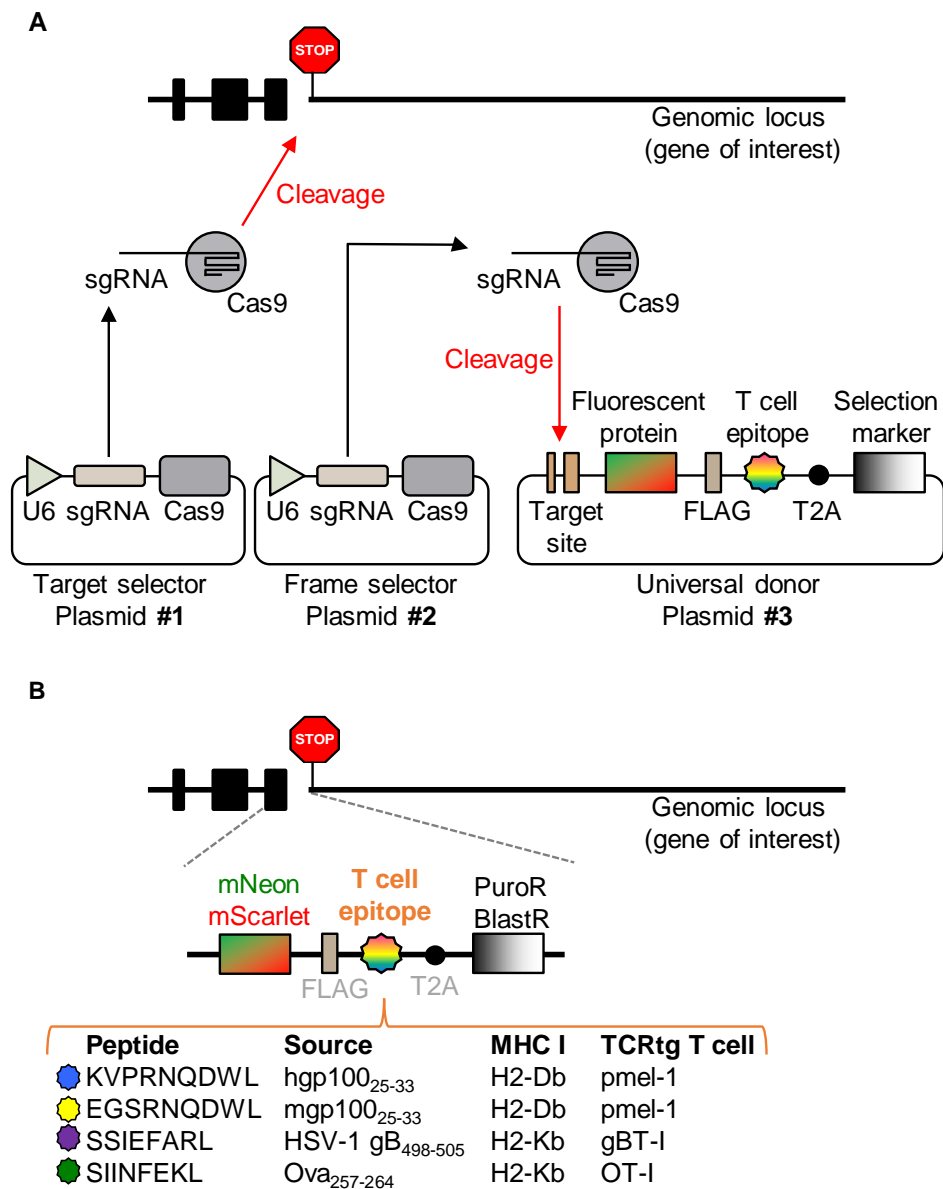


Figure 3.8: CRISPRtope toolbox to fuse model CD8⁺ immunodominant T cell epitopes to endogenous gene products

(A) Graphical depiction of the CRISPRtope method using a three plasmid system (target selector, frame selector and universal donor). (B) Graphical depiction of the different universal donor elements and table indicating peptide sequence, source, MHC class I restriction and corresponding TCRtg T cells for CD8⁺ T cell model epitopes.

3.2.2.2. Generation of HC.PmelKO melanoma cells using CRISPR/Cas9

For this study, we used the HCmel12 murine melanoma cell line. This cell line was derived from a serial transplant of a primary melanoma originating from a *Hgf-Cdk4^{R24C}* mouse (Bald et al., 2014). The cell lines harbour a homozygous single base pair mutation (c.70 C>T) that leads to a clinically relevant missense mutation in the protein cyclin dependent kinase 4 (*Cdk4^{R24C}*; p.R24C) (Tormo et al., 2006b). We knocked-out the pre-melanosomal protein Pmel (also called gp100) using a CRISPR/Cas-9 knockout plasmid that targets exon 1 (Figure 3.9A). The ablation of the murine gp100 gene generated a cell line that does no longer expresses the endogenous epitope that is recognised by pmel-1 TCRtg T cells. The following experiments were performed by Debby van den Boorn-Konijnenberg, a former member of the Hölzel laboratory. HCmel12 melanoma cells were transfected with a plasmid expressing a Cas9, a sgRNA targeting the first exon of the *Pmel* gene and GFP. Forty-eight hours after transfection, GFP-positive cells were sorted and plated as monoclonal cells. After establishing monoclonal cultures, cells were analysed using NGS. The data was analysed using the Outknocker 1.2 web tool showing a homozygous knockout of the *Pmel* gene when aligned against the wildtype sequence in exon 1 in one of the monoclonal cultures (Figure 3.9B) (Schmid-Burgk et al., 2014). We also performed immunoblot analysis to validate this HC.PmelKO monoclonal. Wildtype, mock-transfected and knockout (KO) melanoma cells were treated with Capmatinib, a c-Met inhibitor (1000 nM, 3 days), which causes growth arrest of HCmel cells stimulating gp100 protein expression for easier detection. The KO melanoma cells have lost the ability to express gp100 whereas the WT and the mock-transfected cells still express gp100 after Capmatinib treatment (Figure 3.9C). The HC.PmelKO cell line established in these experiment was used as the parental cell line for the following experiments.

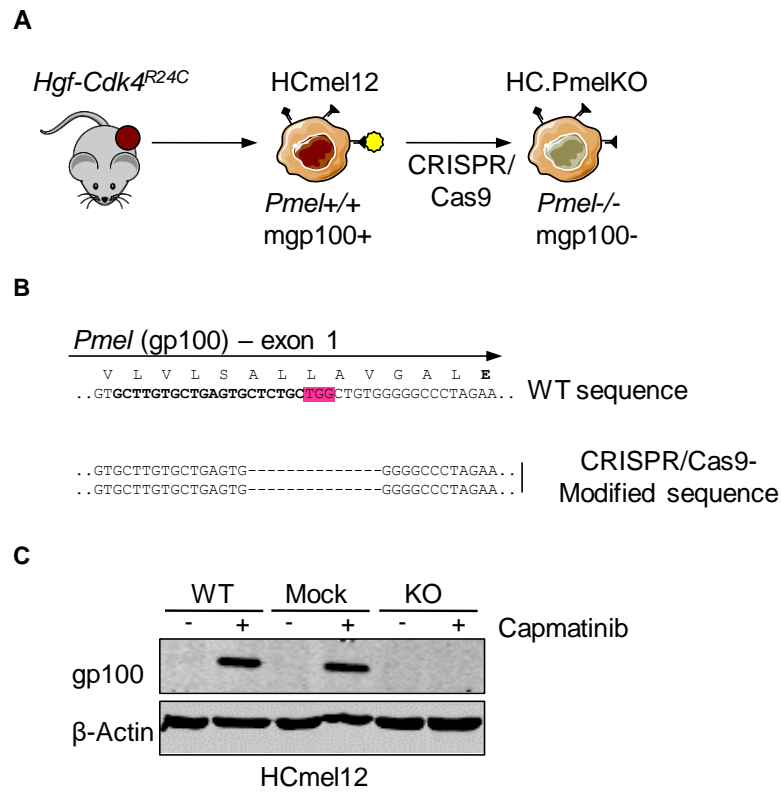


Figure 3.9: Generation of HC.PmelKO melanoma cells using CRISPR/Cas9

(A) Graphical depiction of the generation of *Pmel* (gp100)-deficient HCmel12 cells (HC.PmelKO) (B) Genomic validation of HC.PmelKO cells; pink: PAM. (C) Immunoblot analysis of gp100 expression in CRISPR/Cas9-modified HCmel12 melanoma cells after Capmatinib treatment (1000 nM, 3 days); WT: wildtype, Mock: mock-transfected, KO: knockout. These experiments were performed by Debby van den Boorn-Konijnenberg.

3.2.2.3. TYRP1 and CDK4^{R24C} as model melanosomal and oncogenic T cell targets

Using the CRISPiTope-approach, we tagged endogenous Tyrosinase-related protein 1 (TYRP1) as model MDA (Kawakami et al., 1994b) with mNeon fluorescent protein (N), a FLAG tag (F), human gp100 epitope (hgp100) and a puromycin resistance cassette. The mNeon fluorescent protein serves as surrogate marker for hgp100 expression. The puromycin resistance cassette is connected to the other components of the integrated universal donor plasmid by a T2A cleavage site. A T2A site is a “self-cleaving” peptide site that is derived from the thossea asigna virus 2A and generates two individual proteins after translation (Szymczak and Vignali, 2005). After puromycin selection, we additionally purified successfully tagged melanoma cells by stringent selection of mNeon⁺ melanoma cells by FACS. We named the resulting polyclonal culture HC.PmelKO.TYRP1-NFhgp100 (Figure 3.10A). As a model oncogene, we chose CDK4^{R24C} protein and tagged it using CRISPiTope in the same way as described above for the TYRP1 protein. The resulting cell line was called HC.PmelKO.CDK4^{R24C}-NFhgp100 (Figure 3.10B). Additionally, we generated control cell lines called HC.PmelKO.TYRP1-mNeon and HC.PmelKO.CDK4^{R24C}-mNeon that harbour a mNeon-only tag (no epitope).

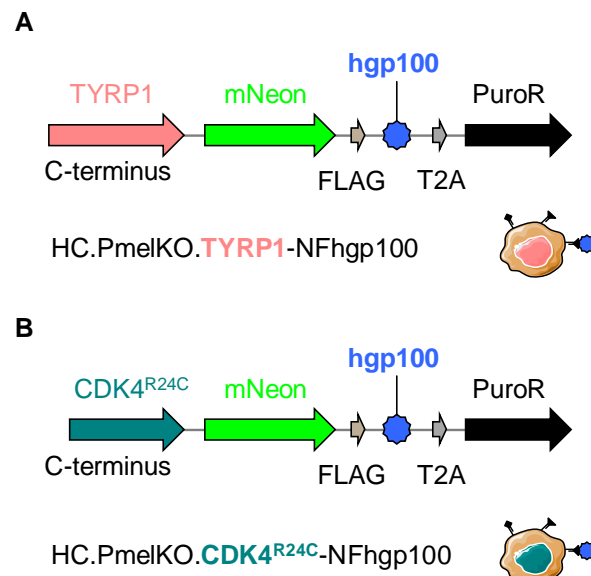


Figure 3.10: Genomic structure of CRISPitope-engineered TYRP1 and CDK4^{R24C}

Graphical depiction of CRISPitope-modified endogenous (A) TYRP1 and (B) CDK4^{R24C} gene fusion products with mNeon-FLAG-hgp100 (NFhgp100).

We analysed the CRISPitope-engineered melanoma cells by immunoblot analysis, epifluorescence microscopy and flow cytometry. Immunoblot analysis showed a molecular weight shift of either TYRP1 or CDK4 of approximately 30 kDa in the indicated cell lines corresponding to the *in silico* predicted molecular weight change after successful tagging. We observed protein with increased molecular weight in addition to wildtype protein, indicating heterozygous tagging of protein (Figure 3.11A). Epifluorescence microscopy showed expected subcellular localisation of the protein. TYRP1-NFhgp100 localised to the cytoplasm whereas CDK4^{R24C}-NFhgp100 localised to the nucleus (Figure 3.11B). Finally, the CRISPitope-modified melanoma cells were analysed by flow cytometry for mNeon expression in comparison to untagged HC.PmelKO cells. HC.PmelKO.TYRP1-NFhgp100 melanoma cells had higher expression levels of the tagged protein compared to HC.PmelKO.CDK4^{R24C}-NFhgp100 (Figure 3.12A). This was consistent with gene expression data (3'mRNA-Seq) from parental Hcmel12 melanoma cells showing significantly higher expression of *Tyrp1* mRNA than *CDK4^{R24C}* mRNA (Figure 3.12B). In summary, we generated and validated CRISPitope-modified melanoma cells that can model expression of clinically relevant melanoma antigens (Bassani-Sternberg et al., 2016).

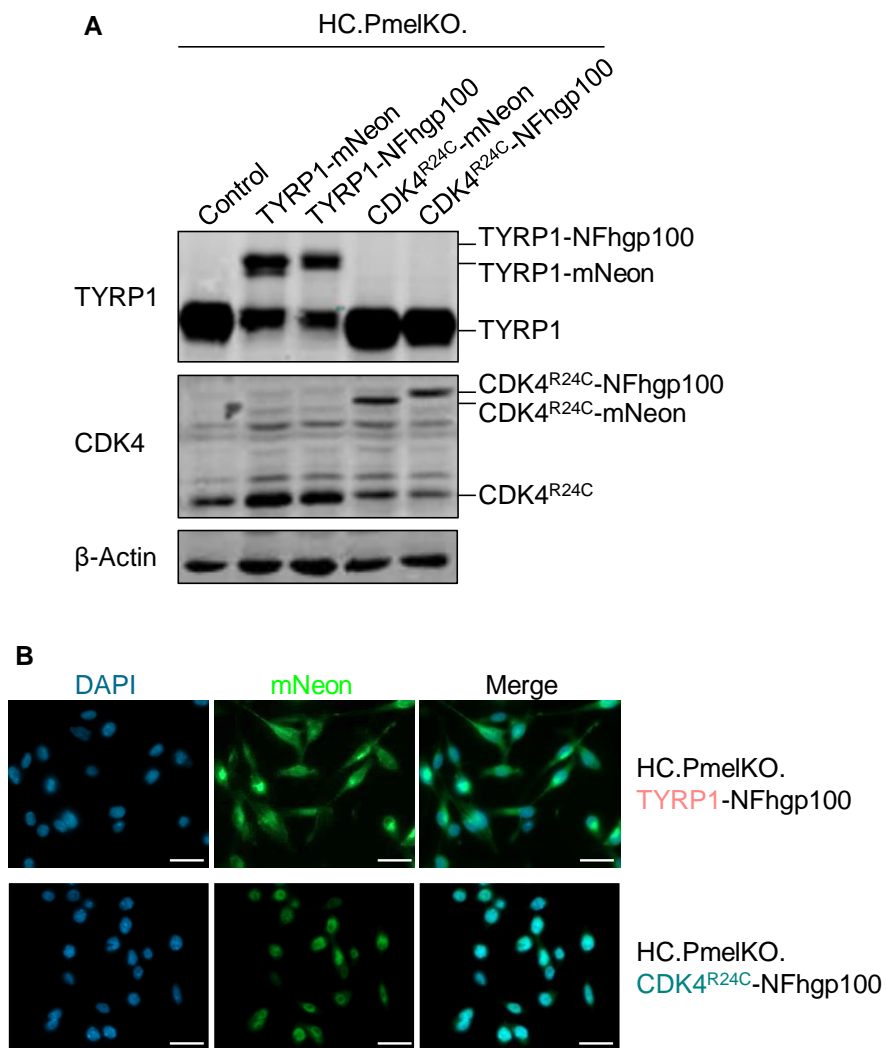


Figure 3.11: TYRP1 and CDK4^{R24C} as model melanosomal and oncogenic T cell targets

(A) Immunoblot analysis of TYRP1 and CDK4^{R24C} protein expression in CRISPRitope-modified melanoma cells. (B) Representative epifluorescence microscopy images showing subcellular localisation of TYRP1-NFhgp100 (upper panel) and CDK4^{R24C}-NFhgp100 (lower panel); left: DAPI, middle: mNeon, right: merge. The universal donor plasmid pCRISPaint-mNeon-PuroR[M1G] used to generate the control cell lines was generated by Daniel Hinze.

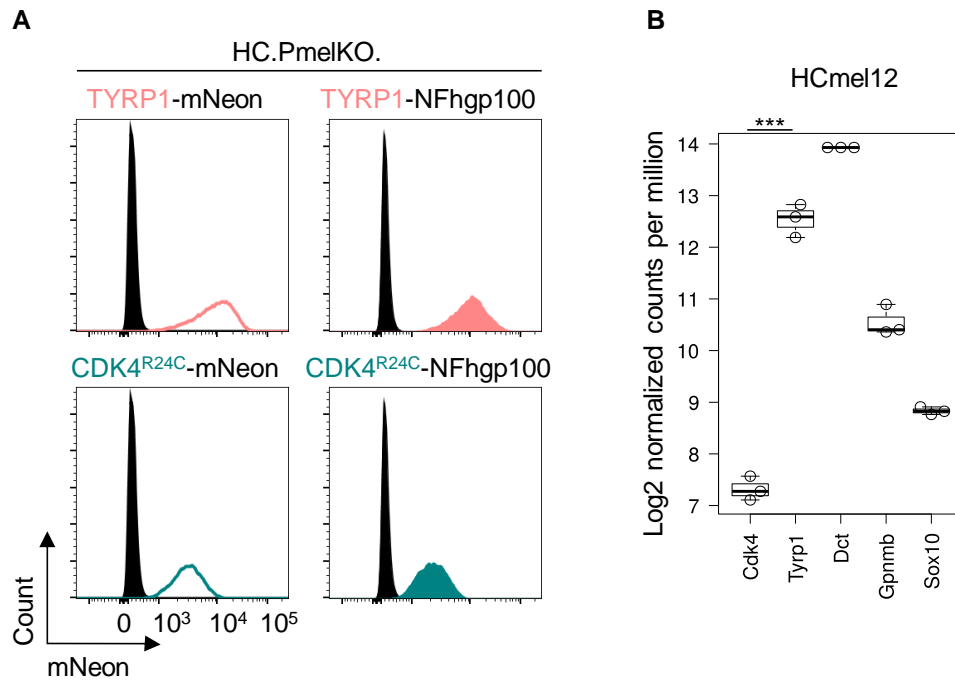


Figure 3.12: Expression of CRISPIlope-modified proteins corresponds with mRNA expression of genes

(A) Representative histograms comparing mNeon protein expression by flow cytometry in HC.PmelKO.TYRP1-NFhgp100 and HC.PmelKO-CDK4^{R24C}-NFhgp100 melanoma cells and corresponding controls cells with mNeon-only tags (HC.PmelKO.TYRP1-mNeon and HC.PmelKO.CDK4^{R24C}-mNeon). Black histograms: untagged HC.PmelKO cells. (B) mRNA expression of indicated genes in HCmel12 cells determined by 3'mRNA-Seq (log₂ read counts per million, cpm). Statistics: ***p<0.001, unpaired two sided t-test.

3.2.2.4. Activation and induction of effector function of pmel-1 TCRtg T cells by CRISPytope-modified melanoma cells *in vitro*

Next, we wanted to verify whether the CRISPytope-modified melanoma cells can activate pmel-1 TCRtg T cell *in vitro*. Prior to co-culture, we stimulated HC.PmelKO.TYRP1-NFhgp100 or HC.PmelKO.CDK4^{R24C}-NFhgp100 with IFN γ for three days so that the melanoma cells upregulate antigen processing and presentation machinery. We then co-cultured the indicated melanoma cells with splenocytes isolated from naïve pmel-1 TCRtg mice for 16 hours. Next, we analysed CD69 surface expression on the T cells as an early activation marker by flow cytometry (Figure 3.13). HC.PmelKO.TYRP1-NFhgp100 and HC.PmelKO.CDK4^{R24C}-NFhgp100, but not the negative control cells only expressing mNeon fluorescent protein, activated pmel-1 TCRtg T cells (Figure 3.14A). The activation of pmel-1 T cells by the CRISPytope-modified melanoma cells was dependent on IFN γ pre-stimulation and upregulation of MHC class I (H2-Db) on the melanoma cells (Figures 3.14B and 3.14C). Co-culture with HC.PmelKO.TYRP1-NFhgp100 induced higher CD69 surface expression on the pmel-1 T cells compared to HC.PmelKO.CDK4^{R24C}-NFhgp100 correlating with higher expression levels of TYRP1-NFhgp100 (Figures 3.12A and 3.14B). Thus, epitope expression by CRISPytope-modified melanoma cells can induce T cell activation in an MHC class I-dependent manner.

Moreover, we wanted to verify whether the CRISPytope-modified melanoma cells can induce effector cytokine production in pmel-1 TCRtg T cell *in vitro*. Prior to co-culture, we stimulated the melanoma cells with IFN γ for three days so. We then co-cultured the indicated melanoma cells with pre-activated pmel-1 T cells for five hours in the presence of brefeldin A, and analysed the T cells by flow cytometry. The pmel-1 T cells were *in vitro* activated and expanded for five days. Afterwards, we analysed intracellular IFN γ and TNF α in the T cells as markers for effector function by flow cytometry (Figure 3.15). HC.PmelKO.TYRP1-NFhgp100 and HC.PmelKO.CDK4^{R24C}-NFhgp100, but not the negative control cells only expressing mNeon fluorescent protein, induced effector cytokine expression in pmel-1 TCRtg T cells (Figure 3.16). The expression of IFN γ and/or

TNF α of pmel-1 T cells induced by the CRISPitope-modified melanoma cells was dependent on IFN γ pre-stimulation and upregulation of MHC class I (H2-Db) on the melanoma cells (data not shown). Co-culture with HC.PmelKO.TYRP1-NFhgp100 induced higher expression of effector cytokines in the pmel-1 T cells compared to HC.PmelKO.CDK4^{R24C}-NFhgp100 correlating with higher expression levels of TYRP1-NFhgp100 (Figures 3.12A and 3.14B). Thus, epitope expression by CRISPitope-modified melanoma cells can induce T cell effector functions in an MHC class I-dependent manner.

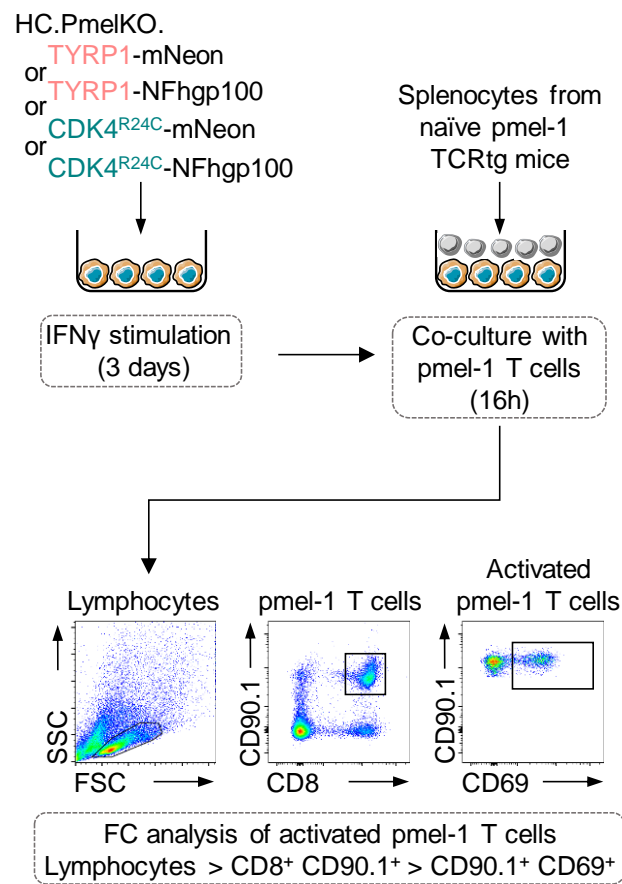


Figure 3.13: *In vitro* T cell activation assay using naïve TCRtg pmel-1 T cells
 Experimental outline and gating strategy for *in vitro* pmel-1 T cell activation assay using indicated melanoma cell lines.

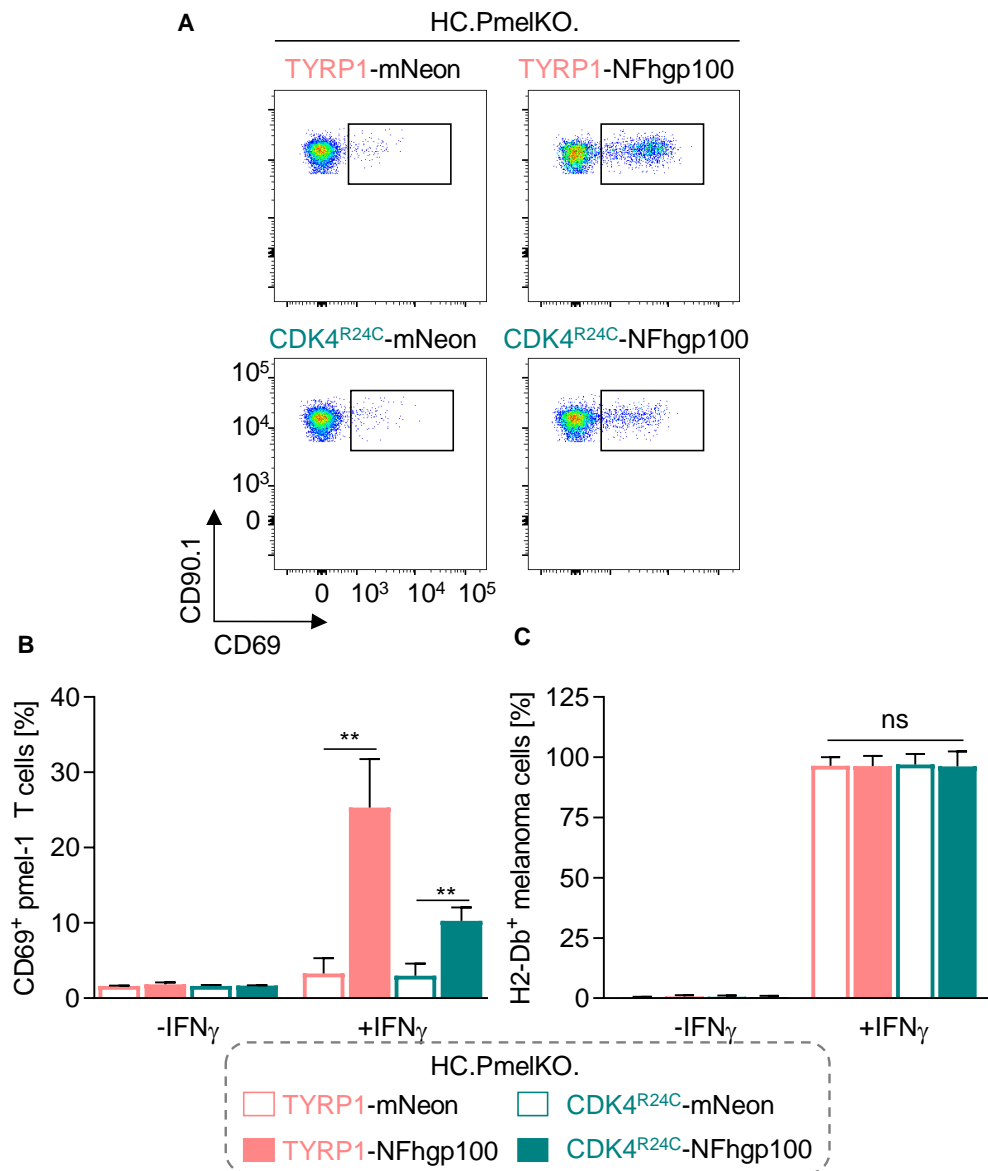


Figure 3.14: Activation of pmel-1 T cells by CRISPRitope-modified melanoma cells

(A) Representative flow cytometry plots and (B) quantification of CD69 surface expression on pmel-1 TCRtg T cells 16h after co-culture with indicated CRISPRitope-modified melanoma cell lines ($n \geq 3$; mean \pm SD). (C) Quantification of H2-Db surface expression on indicated melanoma cells stimulated with IFN γ (1000 U/ml) for 72 hours ($n \geq 3$; mean \pm SD). Statistics: ** $p < 0.01$, ns-not significant, unpaired two-sided t-test and Mann-Whitney-U test.

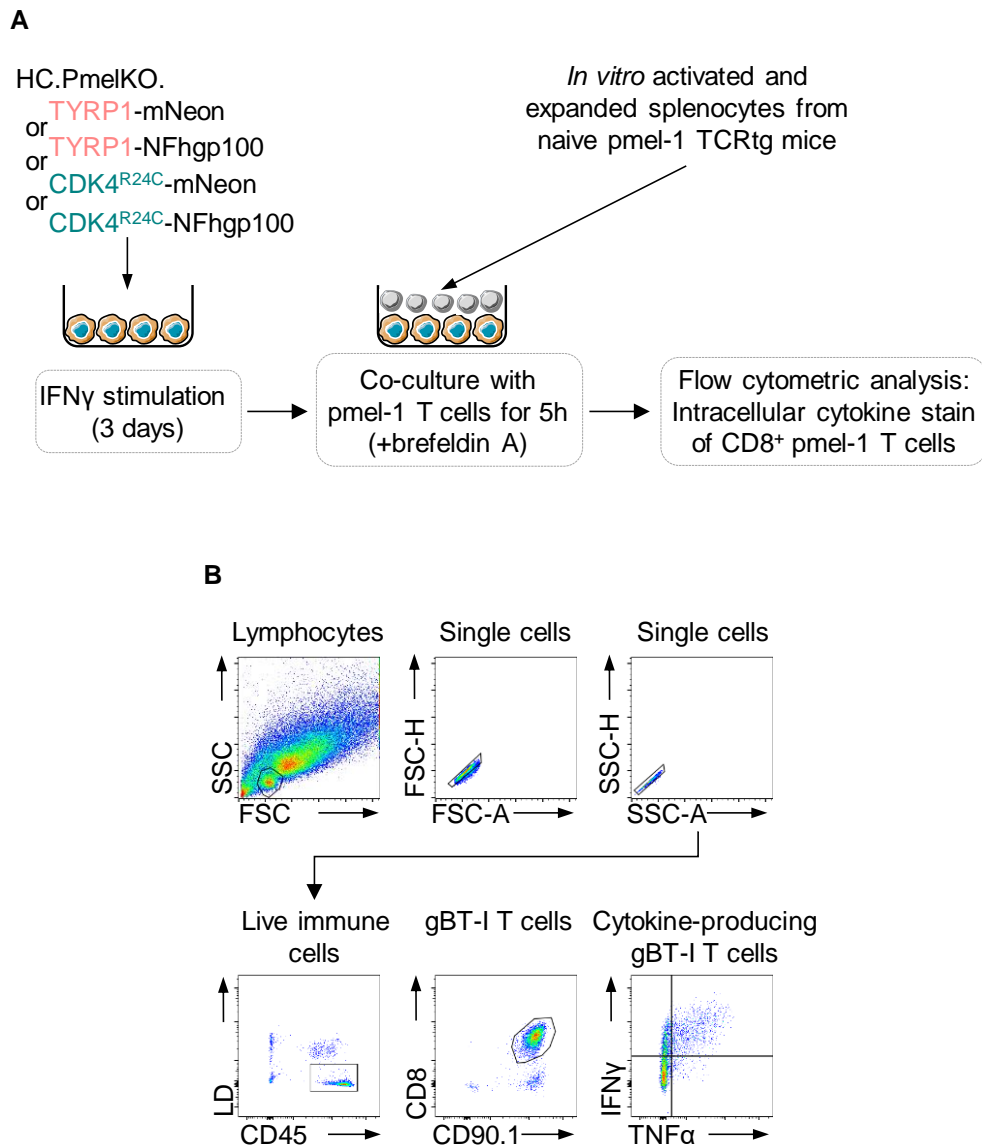


Figure 3.15: *In vitro* pmel-1 T cell functionality assay

Experimental outline (A) and gating strategy (B) of a co-culture assay to assess intracellular cytokine production of pmel-1 T cells incubated with indicated melanoma cell lines.

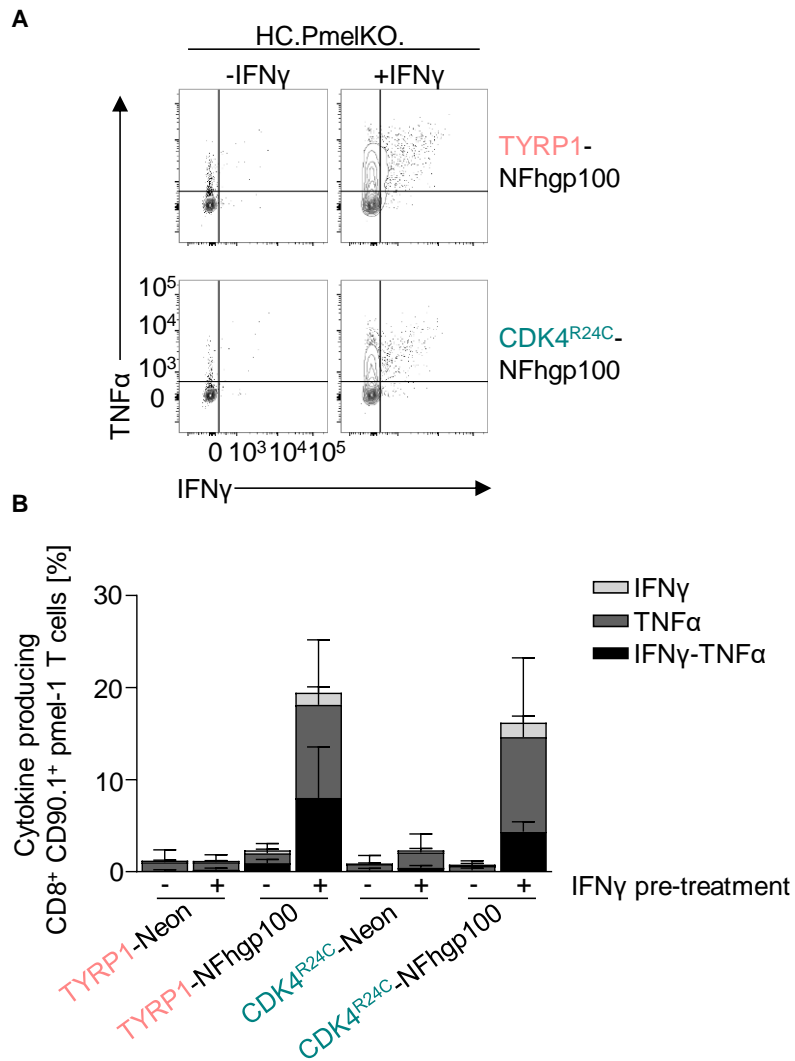


Figure 3.16: pmel-1 TCRtg T cells produce intracellular IFN γ and TNF α after co-culture with melanoma cells expressing the hgp100 epitope

(A) Representative flow cytometry plots showing expression of intracellular IFN γ and TNF α pmel-1 TCRtg T cells co-cultured with indicated melanoma cells. (B) Quantification of intracellular IFN γ and TNF α expression of pmel-1 T cells after co-culture with indicated melanoma cells (n \geq 2; mean \pm SD).

3.2.2.5. Modularity of the CRISPitope approach

In order to show the flexibility and modularity of the CRISPitope approach, we generated more variants of melanoma cell lines using this method.

Firstly, we chose different target proteins to tag including the melanosomal proteins DCT (dopachrome tautomerase) and GPNMB (glycoprotein NMB) and the transcription factor SOX10 (SRY-Box 10) which is important for melanocyte development and is associated with cancerous transformation. We tagged these proteins with the NFhgp100 tag in HC.PmelKO cells (Nonaka et al., 2008; Yamaguchi and Hearing, 2009)(Figure 3.17A). When naïve pmel-1 T cells were co-cultured with the engineered melanoma cell lines, as described above, they upregulated CD69 surface expression indicating T cell activation (Figures 3.17B and 3.17C).

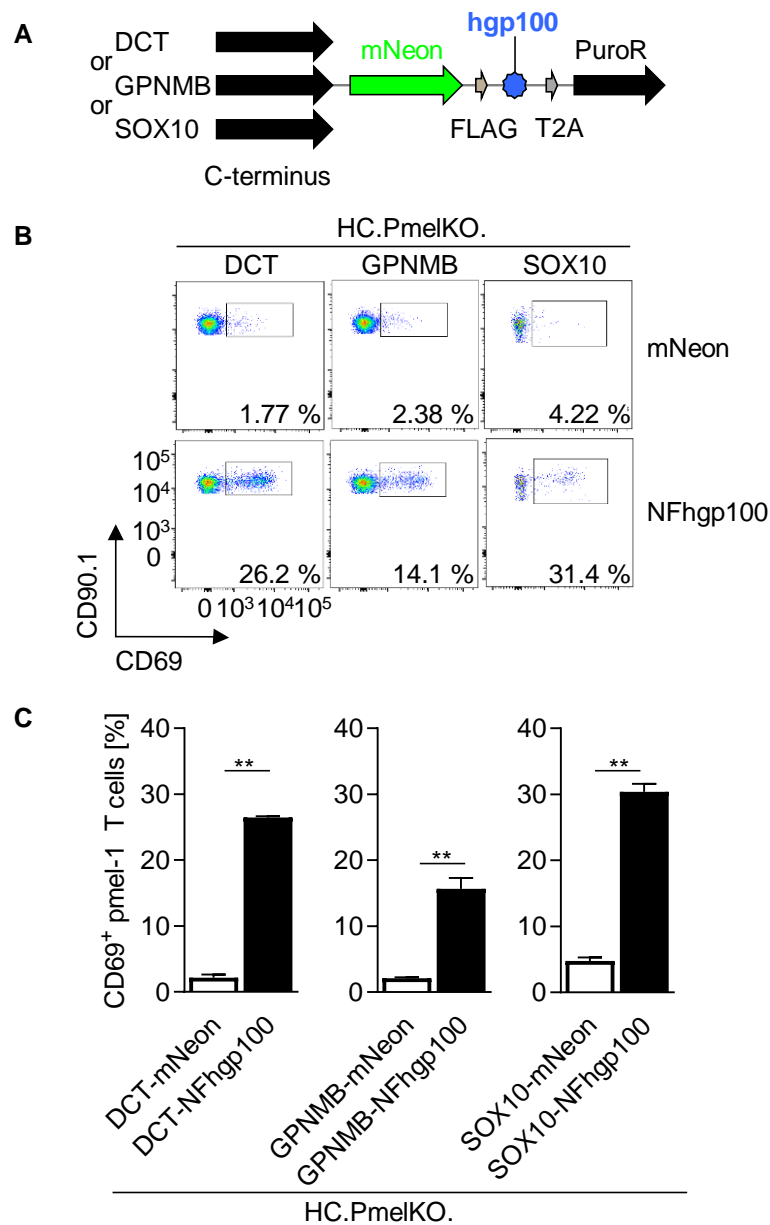


Figure 3.17: Tagging of various melanosomal target genes with hgp100 leads to activation of pmel-1 T cells

(A) Graphical depiction of CRISPR/Cas9-mediated endogenous DCT, GPNMB and SOX10 gene fusion products with mNeon-FLAG-hgp100 (NFhgp100). Representative flow cytometry plots (B) and quantification (C) of CD69 surface expression by flow cytometry of CD8⁺ CD90.1⁺ pmel-1 TCRtg T cells after co-culture (16 h) with indicated IFN γ stimulated melanoma cells (n = 3; mean \pm SD). Statistics: **p < 0.01, unpaired two-sided t-test and Mann-Whitney-U test.

Secondly, we chose two antigens, murine gp100 (mgp100) and human gp100 (hgp100), that are recognised by the same TCRtg T cell species to demonstrate the influence that epitope-MHC affinity has on the activation of T cells. Murine gp100 is a low affinity epitope (peptide-MHC affinity IC_{50} : 23 μ M) compared to the high-affinity hgp100 (peptide-MHC affinity IC_{50} : 186 nM) (Engels et al., 2013). The following experiments were performed by Jana Liebing, a member of the Hölzel laboratory. We tagged TYRP1 protein in HC.PmelKO cells with either mScarlet, mScarlet-mgp100 or mScarlet-hgp100 (Figure 3.18A). In all three cell lines, at least 97 % of the cells have been tagged successfully using the CRISPiotope approach (Figure 3.18B). In order to compare the influence of epitope affinity to MHC molecules, we validated the cell lines in an *in vitro* T cell activation assay as described above. Whereas mgp100 led to only a minor induction of CD69 surface expression, hgp100 led to a major upregulation of CD69 on the pmel-1 TCRtg T cells (Figures 3.18C and 3.18D).

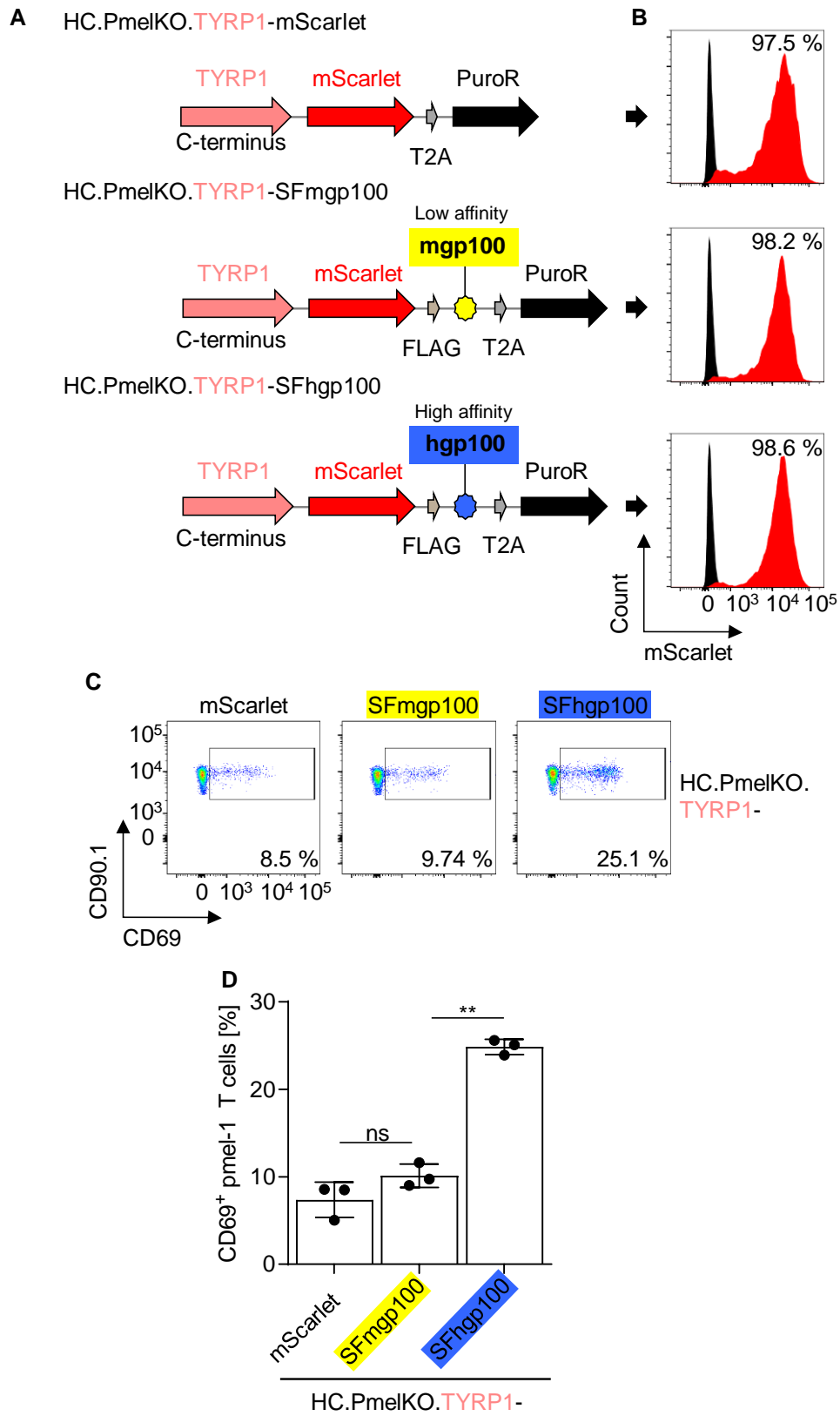


Figure 3.18: Epitope-MHC affinity determines the extent of T cell activation

(A) Graphical depiction of CRISPRitope-modified endogenous TYRP1 gene fusion products with mScarlet, mScarlet-FLAG-mgp100 (SFmgp100) or mScarlet-FLAG-hgp100 (SFhgp100). (B) Representative histograms showing mScarlet expression as surrogate marker for either mgp100 or hgp100 epitope expression. Representative flow cytometry plots (C) and quantification (D) of CD69 surface expression by flow cytometry of CD8⁺ CD90.1⁺ pmel-1 TCRtg T cells after co-culture (16 h) with indicated IFN γ stimulated melanoma cells (n = 3; mean \pm SD). Statistics: **p<0.01, ns-not significant; unpaired two-sided t-test. These experiments were performed by Jana Liebing.

Thirdly, to further demonstrate the flexibility of the CRISPiTope method, we used a different parental cell line, different target genes, a different epitope tag for recognition by different TCRtg T cells, as well as a different antibiotic resistance cassette. The housekeeping genes β -Actin (ACTB) and γ -Actin (ACTG1) were tagged with the gB epitope recognised by gBT-I TCRtg T cells and a blasticidin resistance cassette in the melanoma cell lines B16 (Figure 3.19A). In this case, we chose a different readout for the activation of the T cells by measuring intracellular cytokine expression of IFN γ and TNF α as markers for effector cell function (Figure 3.19B). We stimulated the indicated CRISPiTope-modified melanoma cells with IFN γ for 18 hours and measured H2-Kb surface expression on the melanoma cells. We co-cultured the indicated melanoma cells with activated gBT-I T cells for five hours, in the presence of brefeldin A, and analysed the T cells by flow cytometry measuring intracellular IFN γ and TNF α . gBT-I T cells that were co-cultured with IFN γ pre-stimulated gB-tagged melanoma cells produced IFN γ and TNF α (Figures 3.20A, 3.20C and 3.20D). gBT-I T cells that were co-cultured with melanoma cells that were only tagged with a fluorescent protein but not the gB epitope did not produce IFN γ and TNF α (Figures 3.20A, 3.20C and 3.20D). All CRISPiTope-modified melanoma cells upregulated H2-Kb although with some variability (Figure 3.20B). Intracellular cytokine expression depended on expression of the epitope and IFN γ pre-stimulation.

In conclusion, we generated a system that is rapid, highly flexible and modular. It takes between one and two weeks from the transfection of the cell line with the CRISPiTope plasmids to a selected and expanded new cell line. We can use the CRISPiTope-approach in different murine melanoma cell lines to tag proteins of various functional categories with different fluorescent proteins, different antigens recognised by varying species of CD8⁺ TCRtg T cells and select for successful tagging by selection with different antibiotics. Additionally, we could show that we can measure successful T cell activation by either the upregulation of the early activation marker CD69 on the T cell surface or intracellular expression of the effector cytokines IFN γ and TNF α .

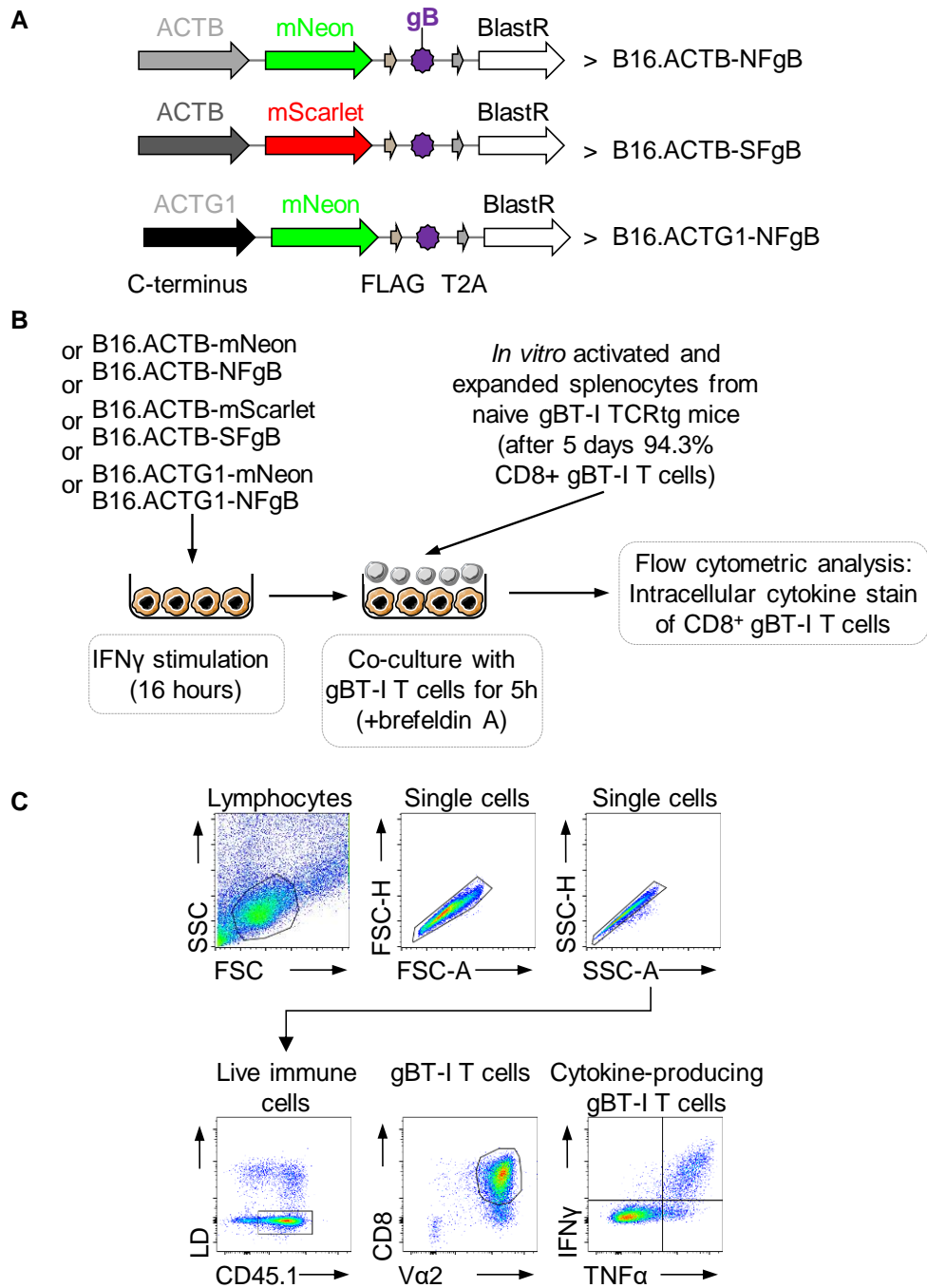


Figure 3.19: *In vitro* gBT-I T cell functionality assay

(A) Graphical depiction of modified endogenous gene fusion products with different fluorescent proteins and the gB epitope in B16 melanoma cells. Experimental outline (B) and gating strategy (C) of a co-culture assay to assess intracellular cytokine production of gBT-I T cells incubated with the indicated melanoma cell lines.

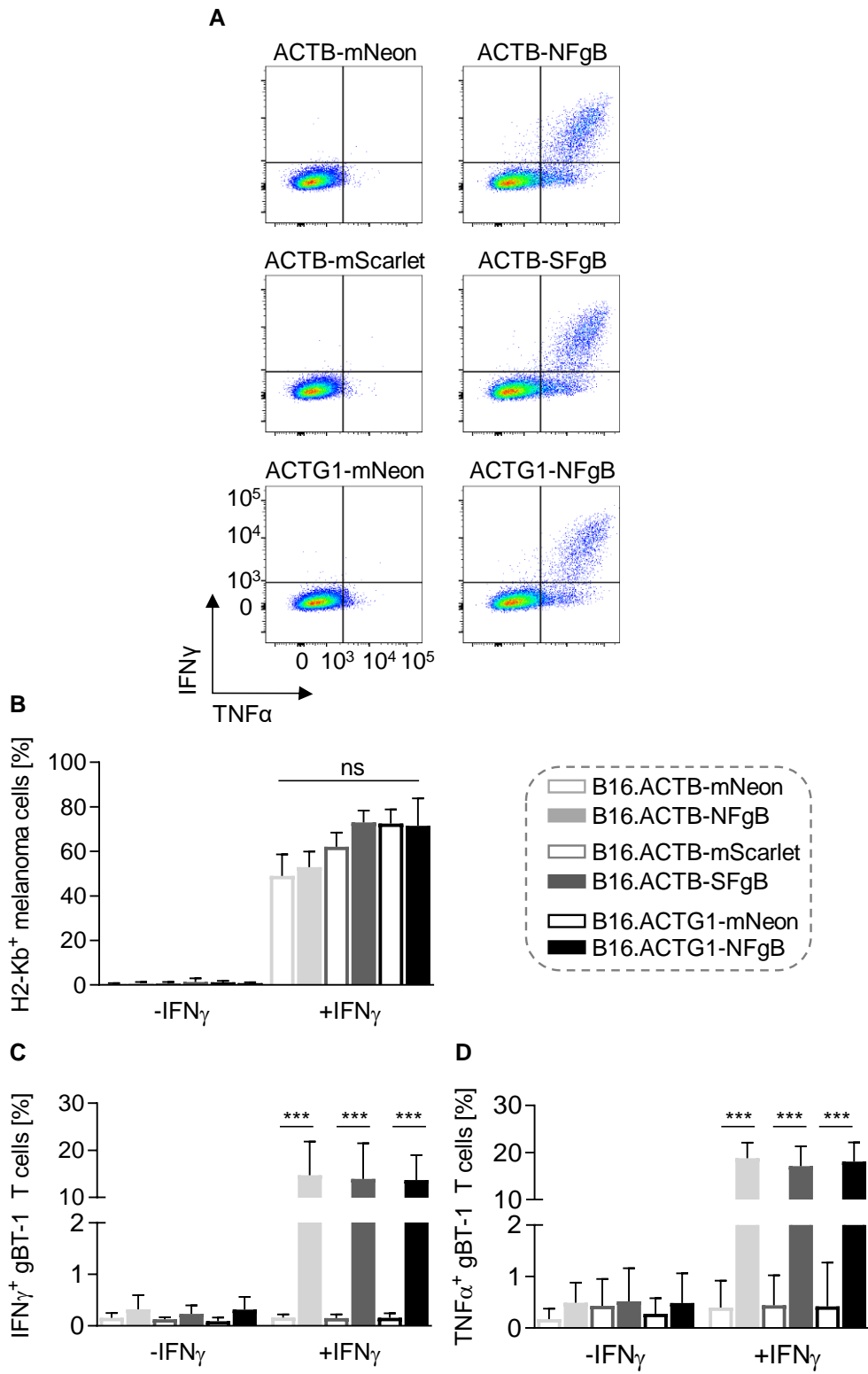


Figure 3.20: gBT-I TCRtg T cells produce intracellular IFN γ and TNF α after co-culture with melanoma cells expressing the gB epitope

(A) Representative flow cytometry plots showing expression of intracellular IFN γ and TNF α in gBT-I TCRtg T cells. (B) Quantification of H2-Kb surface expression after IFN γ stimulation of CRISPRitope-modified B16 cells (n = 3; mean \pm SD). (C and D) Quantification of intracellular IFN γ (C) and TNF α (D) expression of gBT-I T cells after co-culture with indicated B16 melanoma cells (n = 6; mean \pm SD). Statistics: ***p<0.001, ns-not significant, multiple t-tests.

3.3. Discussion

In recent years, T cell-based immunotherapies have demonstrated notable efficacy in the treatment of melanoma. Nevertheless, this treatment approach has limitations as patients can develop resistance toward this therapy. A detailed understanding of tumour recognition by the immune system is of critical importance to further improve these promising therapeutic options.

Work in this chapter aimed at establishing a CRISPR/Cas9-based experimental approach to eventually study the diversity of melanoma resistance and immune evasion mechanisms.

A previous study showed that melanomas can escape T cell therapy targeting melanocyte differentiation antigens by inflammation-induced dedifferentiation. Inflammation-induced dedifferentiation causes the downregulation of MDAs including the one targeted by the adoptively transferred T lymphocytes (Landsberg et al., 2012). However, the same study showed, in an *in vitro* assay, that other targets such as oncogenic proteins are not affected by the inflammation-induced dedifferentiation and can still be recognised by antigen-specific T lymphocytes. In order to investigate whether tumour immune evasion mechanisms would differ if epitope-specific T cells targeted different types of tumour antigens, we developed a CRISPR/Cas9-based approach as adequate *in vivo* models were not available.

Here, we present two CRISPR/Cas9-based knockin approaches that harness different mechanisms of the mammalian cell DNA repair machinery. Both approaches were successfully implemented to generate cell lines used to investigate the importance of the biology of tumour antigens. The proteins studied in this chapter have different cellular locations, different cellular functions and are regulated by different mechanisms.

Using homology directed repair we targeted the essential protein PES1 and the non-essential melanosomal protein gp100 (also known as Pmel). PES1 is an essential ribosomal biogenesis factor located in the nucleolus. Pre-melanosome protein gp100 underlies the control of the master regulator of melanocyte development and melanoma oncogene MITF. The gp100 protein belongs to the group of melanocytic tumour-antigen coding proteins (Van den Eynde and van

der Bruggen, 1997). These proteins are only expressed in melanocytes or melanomas and have been successfully targeted by ACT therapy in the past (Benlalam et al., 2007; Besser et al., 2013; Dudley et al., 2002; Pilon-Thomas et al., 2012; Radvanyi et al., 2012; Rosenberg et al., 2011, 1988).

The second approach (CRISPitope) described in this work is based on the CRISPaint approach published by Schmid-Burgk and colleagues and relies on non-homologous end joining as DNA repair mechanism as opposed to homology directed repair (Schmid-Burgk et al., 2016). The CRISPaint, and our adapted CRISPitope, approach is a polyclonal tagging technique that generates endogenously tagged mammalian cells with relative ease. During polyclonal tagging a few thousand cells are modified simultaneously which in the end give rise to a new cell line that is derived from a polyclonal culture rather than from an individual modified cell. As this system allows the modification of a cell line by three individual plasmids it is a highly flexible approach. Any desired protein can be tagged C-terminally by cloning only one sgRNA into a plasmid that already codes for a Cas9 protein. By creating a CRISPitope toolbox we can generate C-terminal endogenous fusion proteins with a fluorescent protein, a FLAG-tag, an immunological epitope tag and an antibiotic resistance cassette. Successful engineering of melanoma cells using the CRISPitope technique can be validated by flow cytometry, microscopy or immunoblotting. Additionally, this technique allows us to select for cells harbouring the in-frame fusion of the target protein and the universal donor plasmid by using antibiotics. More importantly however, the CRISPitope-modified melanoma cells can be used for immunological assays such as T cell activation assays and *in vivo* experiments to answer questions regarding resistance towards cancer immunotherapy. The majority of the CRISPitope experiments were performed in HC.PmelKO melanoma cells that were generated by Debby van den Boorn-Konijnenberg. These cells lack the murine gp100 protein which was subsequently replaced with the high affinity human gp100 epitope recognised by pmel-1 TCRtg T cells. The greater number of CRISPitope experiments presented in this chapter involved the melanosomal protein TYRP1 and the oncogenic protein CDK4^{R24C}.

TYRP1 is like gp100, a melanosomal protein controlled by the transcription factor

MITF, and is thereby equally affected by inflammation-induced dedifferentiation (Van den Eynde and van der Bruggen, 1997). Cyclin-dependent kinase 4 (CDK4) has gained importance in melanoma research after it became evident that a germline mutation in the *Cdk4* locus predisposes for melanoma development. The mutation results in an amino acid substitution at position 24 of arginine with cysteine (R24C) and results in impaired cell cycle control by p16^{Ink4a} (Chawla et al., 2010). CDK4^{R24C} is considered a tumour antigen which can be recognised by infiltrating T cells. The HcMel12 murine melanoma cell line used in this study originates from a primary melanoma of transgenic Hgf x *Cdk4*^{R24C} mice. It is a genetically engineered mouse model in which melanoma formation is driven by transgenic overexpression of HGF (hepatocyte growth factor) leading to deregulated tyrosinase kinase signalling and an oncogenic CDK4^{R24C} germline mutation (Wölfel et al., 1995; Tormo, Ferrer, Bosch, et al., 2006; Landsberg et al., 2010a).

It was previously shown that a pro-inflammatory tumour microenvironment generated by infiltrating immune cells drives downregulation of MITF expression which leads to the loss of the melanocytic signature. MDAs are downregulated during melanoma cell phenotype switching also known as melanoma cell dedifferentiation (Landsberg et al., 2012; Riesenberger et al., 2015). ACT immunotherapy used for the treatment of melanoma often targets melanocytic antigens. If, however, the melanocytic signature is downregulated due to inflammatory stimuli, melanoma-specific T cells can no longer recognise and efficiently eradicate the tumour cells. Landsberg and colleagues showed that T cell-driven inflammation causes reversible melanoma dedifferentiation of murine and human melanoma cells. Melanoma cells that have been exposed to the inflammatory cytokine TNF α are poorly recognised by T cells specific for melanocytic antigens such as gp100 and Melan-A, whereas the melanoma cell recognition by T cells specific for non-melanocytic antigens such as SNRPD1^{mut} and CDK4^{mut} was unaffected (Landsberg et al., 2012).

We could demonstrate that by using either CRISPR/Cas9 approach we can specifically tag our target protein with either just a model epitope, using homology-directed repair, or with a fluorescent protein, a FLAG-tag, a CD8⁺ T

cell epitope and a selection marker, using the CRISPitope approach. We validated specific tagging by various approaches such as immunoblotting, NGS and microscopy. An *in vitro* T cell assay, performed by Emma Bawden, showed that melanoma cells modified using the CRISPR/Cas9-based approach that relies on HDR can induce expression of the effector molecules IFN γ and TNF α in epitope-specific TCRtg gBT-I T cells. Preliminary results showed that melanoma cells in which the model antigen was conjugated to the melanocytic protein gp100 induced higher effector cytokine expression in gBT-I T cells compared to the antigen being conjugated to the essential nucleolar protein PES1. However, due to inter-experimental heterogeneity of MHC Class I upregulation upon IFN γ stimulation a final conclusion cannot be drawn. Higher induction of effector cytokines by B16.gp100-FgB cells in gBT-I T cells could be either due to higher MHC Class I surface expression or different subcellular localisation compared to B16.PES1-FgB cells.

The CRISPR/Cas9-based knock-in approach using homology directed repair is very inefficient, time-consuming, labour-intensive and only generates monoclonal cultures. These monoclonal cultures can differ from the parental cell line with regard to mRNA and protein expression profiles, growth characteristics and morphology. Therefore, a polyclonal culture as generated by using the CRISPitope approach is more desirable, in particular for downstream *in vivo* experiments. The CRISPitope toolbox gives us flexibility with regards to fluorescent protein, antibiotic selection markers, model antigen and therefore TCRtg T cell species.

Proteins tagged in this study originate from different cellular localisations, have different cellular functions and control mechanism. All proteins tagged in this study, served as model tumour antigens in order to investigate the biology of tumour antigens using the same epitope-specific TCRtg T cells. In a study described by Lu and colleagues, it was shown that TILs from 21 melanoma patients could recognise a total of 45 mutated proteins. Each mutation was from a different expressed protein originating from different subcellular localisations and not shared among melanomas from other patients (Lu et al., 2014) .It is difficult to directly compare antigen-specific immunotherapies targeting different-

antigen encoding genes as many variables impact on anti-tumoural T cell response. One major variable that influences T cell activation and function is peptide-MHC binding affinity which therefore confounds direct comparability of T cell responses to different antigens. This confounding factor is however eliminated by applying the CRISPiotope technique.

We validated that the CRISPiotope-engineered melanoma cells were able to activate and induce effector cytokine production in TCRtg T cells. The focus of this chapter was on generating and validating HC.PmelKO.TYRP1-NFhgp100 and HC.PmelKO.CDK4^{R24C}-NFhgp100 for in vivo studies presented in Chapter 4 but also on demonstrating the flexibility of the CRISPiotope approach by exploiting the modularity of this technique.

In general, we observed higher activation of T cells when a melanocytic protein was tagged with the cognate epitope compared to when the non-melanocytic protein was tagged. This correlated with higher mRNA and protein expression levels of the melanocytic proteins. However, we do not know whether the subcellular localisation of the tagged protein might also play a role in the presentation of the antigen on MHC class I on the melanoma cell surface. The melanocytic proteins gp100, TYRP1, DCT and GPNMB that were chosen in this study are involved in melanosome formation and are also part of the secreted melanosomes. On the other hand, PES1, CDK4 and SOX10 are located in the nucleus. SOX10, however, represent a special case as it is highly expressed, part of the melanocyte transcription programme and partially involved in the regulating the activity of MITF (Tudrej et al., 2017). Zeelenberg and colleagues showed that antigen localisation influences T cell-mediated tumour immunity. They compared T cell responses to antigens located at different cellular localisations and found that tumour-secreted vesicle-bound (exosome) antigens elicit a better CD8⁺ T cells response compared to secreted soluble proteins or non-secreted cell-associated proteins (Zeelenberg et al., 2011).

Furthermore, we showed that, with the CRISPiotope toolbox, we can compare T cell activation by low and high affinity epitopes. The availability of corresponding low and high affinity epitope gives us the opportunity to create a situation observed in cancer patients. Immunogenic neoepitopes have higher peptide-

MHC affinity compared to their corresponding wildtype epitopes (Łuksza et al., 2017). We could show that the hgp100 epitope, representing a neoepitope, has a higher ability to activate T cells than the mgp100, representing a wildtype epitope.

Moreover, we demonstrated that various proteins that have different cellular localisations can be targeted by the CRISPEpitope approach. The nature of the targeted protein and therefore intracellular antigen localisation is important and can affect T cell mediated tumour immunity as demonstrated by Zeelenberg and colleagues (Zeelenberg et al., 2011). We could only validate that proteins from different subcellular locations with different cellular functions have the ability to activate T cells in an *in vitro* T cell activation assay. However, an investigation of the mechanism why proteins have different capabilities of activating T cells was beyond the scope of this thesis. A screen investigating the potential of antigens originating from different subcellular compartments to activate T cells could help elucidate the impact of the localisation of an antigen-producing protein on the efficacy of ACT immunotherapy.

Furthermore, we established the CRISPEpitope technique in different murine melanoma cell lines, H1mel12 and B16. Nevertheless, it is still to be proven whether the CRISPEpitope technique is also applicable to human melanoma cell lines or other tumour cell lines. Of note, we have successfully targeted the housekeeping genes ACTB, ACTG1 and TUBB in HEK283T cells.

In summary, we present a CRISPR/Cas9-based approach allowing the investigation of expression, presentation and recognition of tumour antigens. We created a platform that offers the opportunity to efficiently tag any desired protein with various MHC class I-restricted immunogenic epitopes that can be recognised by various TCRtg T cell species. This technique enables us to investigate the biology of tumour antigens using single transgenic T cell species as we eliminate the confounding factor that different epitopes have varying affinities for their corresponding T cell receptors.

Chapter 4:
Investigation of how the choice of
the targeted gene product of ACT
immunotherapy impacts on therapy
outcome and resistance
mechanisms

Chapter 4: Investigation of how the choice of the targeted gene product of ACT immunotherapy impacts on therapy outcome and resistance mechanisms

4.1. Introduction

Adoptive cell therapy is a personalised treatment approach for patients suffering from advanced melanoma. In the past, it has been shown that transfer of isolated and expanded tumour-reactive T cells can mediate durable and complete tumour regression with acceptable toxicities.

In early studies, non-mutated melanocyte-derived antigens, MART-1 and gp100, were identified to be often recognised by TILs. However, when peripheral lymphocytes were transduced with a high-affinity TCR recognising MDAs, patients suffered from severe on-target off-tumour toxicities as opposed to low-affinity naturally occurring TCRs (Kawakami *et al.*, 1994; Johnson *et al.*, 2009).

By 1995, Wölfel and colleagues identified T lymphocytes that are reactive to mutated CDK4 in human melanoma suggesting that somatic mutations may be attractive target antigens for ACT and vaccines. Current clinical studies that test the efficacy of checkpoint inhibitors showed that this line of therapy works best in cancer types with high somatic mutation frequencies such as melanoma, lung cancer, bladder cancer and tumours with DNA-mismatch-repair-deficiencies (Topalian *et al.*, 2012b; van Rooij *et al.*, 2013; Powles *et al.*, 2014; Snyder *et al.*, 2014a; Rizvi *et al.*, 2015; Rizvi *et al.*, 2015b; Le *et al.*, 2015; Van Allen *et al.*, 2015a; Hugo *et al.*, 2016). This indicates that checkpoint therapy reinvigorates TILs that recognise somatic mutations.

In 2012, Landsberg and colleagues established an ACT protocol in a mouse model that closely recapitulates tumour regression, remission and recurrence observed in melanoma patients. They found that when melanomas were treated with ACT targeting a MDA they escaped by a process called reversible inflammation-induced dedifferentiation (Landsberg *et al.*, 2012). Pro-inflammatory cytokines such as TNF α secreted by activated tumour-reactive T cells induced a dedifferentiation programme in the melanoma cells. This inflammation-induced dedifferentiation, also known as phenotype switching, is

regulated by the transcription factor MITF that controls the expression of melanocytic genes (Landsberg et al., 2012; Riesenberger et al., 2015). Landsberg and colleagues compared how TNF α influences the recognition of either a melanocyte-derived antigen or mutated oncogenic antigen by autologous antigen-specific T cells. They found that recognition of the melanocyte-derived antigen is largely abrogated while recognition of the mutated oncogenic antigen remains intact (Landsberg et al., 2012). These experiments were performed *in vitro* using human melanoma cell lines and corresponding autologous T cells.

A study from 2018 reported for the first time that a patient who was treated with ACT immunotherapy directed against the MDA MART-1 underwent melanoma dedifferentiation as an acquired resistance mechanism. Initially, the patient's melanoma regressed but the patient relapsed. The recurrent tumours lacked the MDAs, MART-1 and gp100, but they expressed the inflammation-induced neural crest marker NGFR. Corresponding *in vitro* studies showed that with withdrawal of the inflammatory stimuli the phenotype is reversible as observed in our mouse model (Mehta et al., 2018).

The aim of this study was to compare resistance mechanisms of melanomas when either a non-essential melanocyte-derived antigen or an essential oncogenic antigen is targeted by an epitope-standardised ACT immunotherapy approach that uses the same TCRtg T cells.

We hypothesised that targeting a melanocyte-derived antigen, such as TYRP1, would result in therapy escape by different mechanisms such as inflammation-induced dedifferentiation as described by Landsberg and colleagues but also by common mechanisms such as antigen loss. Whereas ACT targeting an oncogene-derived antigen, such as mutated CDK4, would induce complete responses and mice would not experience tumour recurrence.

4.2. Results

4.2.1. TYRP1 and CDK4^{R24C} as model melanosomal and oncogenic targets for adoptive cell transfer immunotherapy

Before comparing our two newly generated CRISPRi cell lines that model ACT immunotherapy, targeting either a melanosomal non-essential protein or an oncogenic essential protein, *in vivo* we verified that the parental cell line HC.PmelKO used for all experiments does not respond to our ACT immunotherapy approach. For this purpose, we transplanted HC.PmelKO melanoma cells intracutaneously into the right flank of wildtype C57BL/6 mice. Fifteen days after tumour transplantation, we started with our immunotherapy approach as previously described (Kohlmeyer et al., 2009; Landsberg et al., 2012). The mice were pre-conditioned with a single dose of the chemotherapeutic cyclophosphamide (Cy) one day prior to the adoptive T cell transfer. On the day of the T cell transfer, mice were intravenously injected with splenocytes isolated from naïve pmel-1 TCRtg mice and additionally injected intraperitoneally with an adenoviral vector expressing hgp100 (Ad-hgp100) to activate dendritic cells (DCs) *in vivo*. On days 3, 6 and 9 after adoptive T cell transfer, mice were additionally injected intratumourally with CpG/Poly(I:C) to stimulate the innate immune system (Figure 4.1A). We compared growth characteristics between non-treated and ACT-treated melanomas and found no considerable difference regarding growth kinetics. However, mice that were treated with ACT immunotherapy had to be sacrificed one week later than non-treated mice. The ACT-treated mice experienced a marginal response induced by the administration of CpG/Poly(I:C) which activates the innate immune system but did not experience tumour regression (Figures 4.1B, 4.1C and 4.1D).

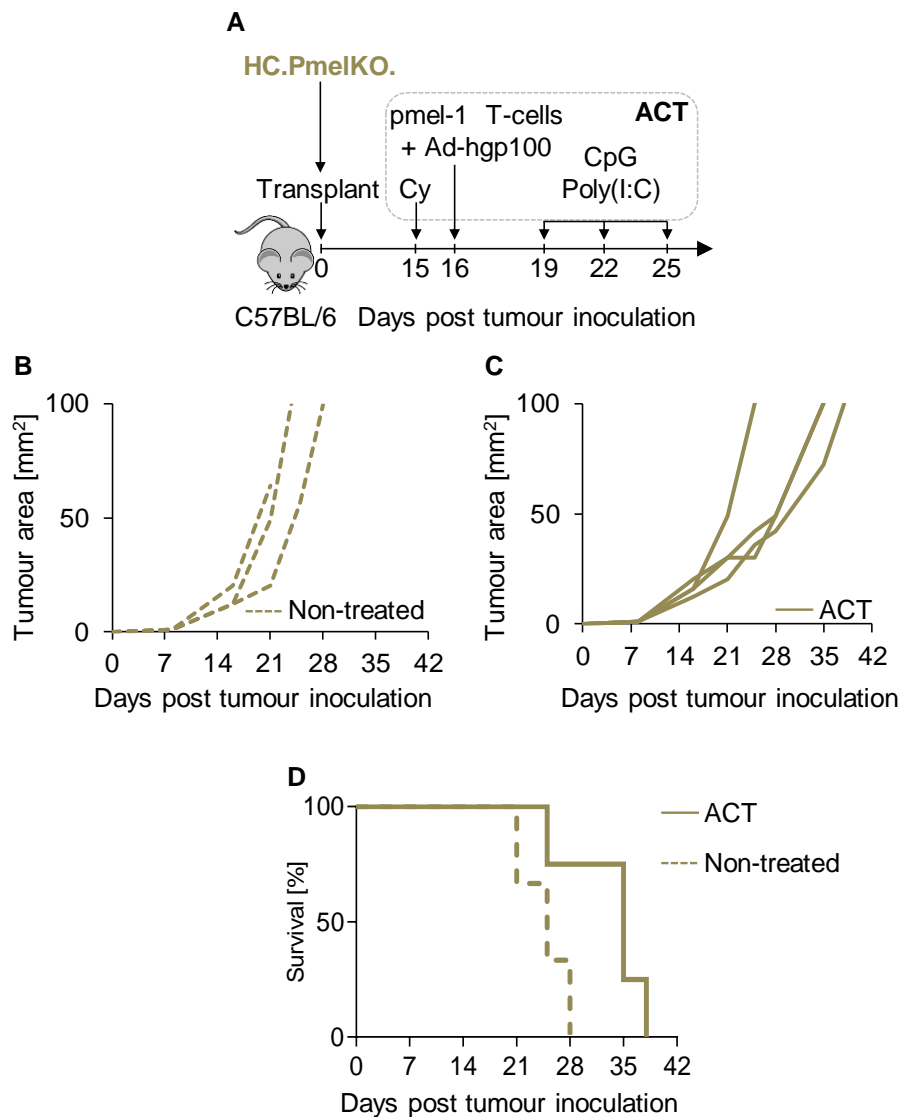


Figure 4.1: Pmel (gp100)-deficient HC.PmelKO. melanomas do not respond to ACT immunotherapy using pmel-1 TCRtg T cells

(A) Experimental setup of pmel-1 ACT in C57BL/6 mice bearing HC.PmelKO. melanomas. Cy: cyclophosphamide, Ad-hgp100: hgp100-expressing adenovirus, CpG/Poly(I:C): innate immune ligands. (B and C) Individual tumour growth curves (tumour area in mm²) of non-treated (B) and ACT-treated (C) HC.PmelKO. melanomas (n ≥ 3). (D) Kaplan-Meier survival plots of indicated tumour cohorts of either non-treated (dashed line; n = 3) or ACT-treated (solid line; n = 4) mice. These experiments were performed by Nicole Glodde and Tobias Bald.

After verifying that HC.PmelKO cells do not respond to our ACT immunotherapy protocol, we aimed at comparing therapies targeting either melanosomal TYRP1 or oncogenic CDK4^{R24C}. We transplanted HC.PmelKO.TYRP1-NFhgp100 or HC.PmelKO.CDK4^{R24C}-NFhgp100 into C57BL/6 mice and treated them with pmel-1 ACT immunotherapy as previously described (Figures 4.2A and 4.2B). In both cohorts, over half of the mice survived long-term (TYRP1: 68%, CDK4^{R24C}: 52%) and tumours went into complete regression (Figures 4.2C and 4.2D). All mice inoculated with either cell line that were not treated with ACT developed tumours that reached the volumetric tumour endpoint within 28 days post-inoculation (Figures 4.3A and 4.3B). In the case of HC.PmelKO.TYRP1-NFhgp100 bearing mice that received ACT, 17/25 mice survived and were tumour-free after ACT immunotherapy and 8/25 mice initially responded to therapy but later relapsed (Figure 4.3C). In case of HC.PmelKO.CDK4^{R24C}-NFhgp100 bearing mice that received ACT, 12/23 mice survived and were tumour-free after immunotherapy and 11/23 initially responded but then relapsed (4.3D).

Additionally, we analysed circulating pmel-1 T cells in the blood of the two different mouse cohorts 7, 14 and 21 days after adoptive T cell transfer (Figures 4.4A and 4.4B). There was no significant difference in frequency of circulating CD8⁺ CD90.1⁺ pmel-1 T cells at any time point after T cell transfer in either the HC.PmelKO.TYRP1-NFhgp100 or HC.PmelKO.CDK4^{R24C}-NFhgp100-bearing mice (Figure 4.4B).

From these results, we concluded that therapy efficacy did not significantly differ between the two CRISPR tumour models with regard to survival, growth kinetics and expansion of circulating pmel-1 T cells.

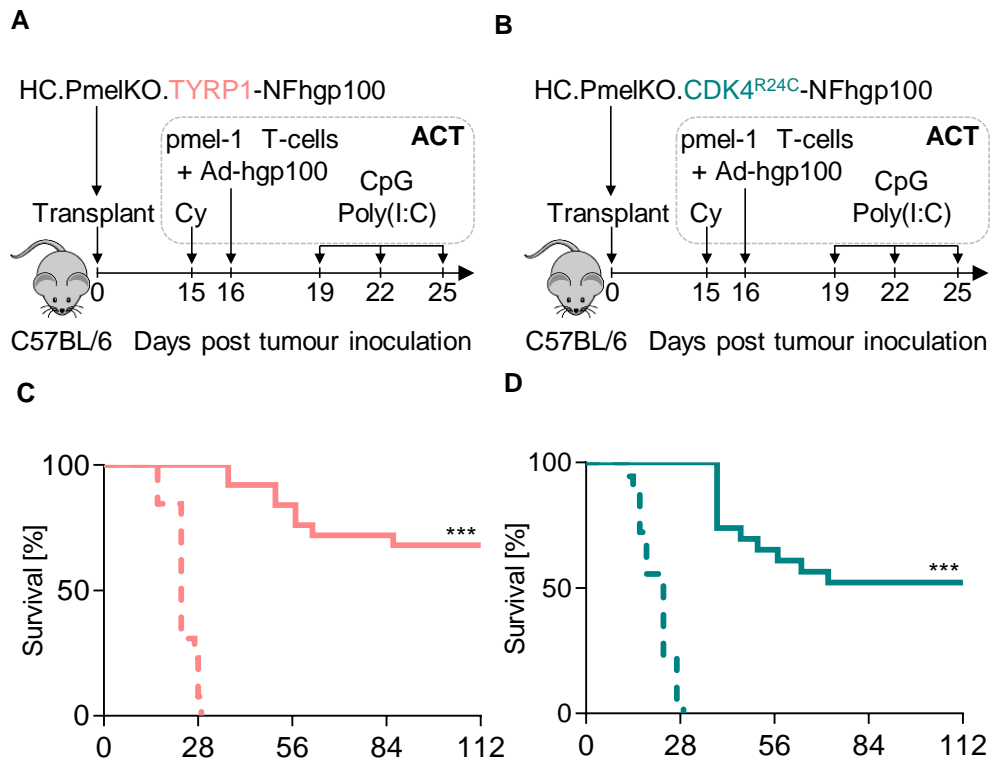


Figure 4.2: ACT immunotherapy targeting endogenous TYRP1 or CDK4^{R24C} in C57BL/6 mice

(A and B) Experimental setup of pmel-1 ACT in C57BL/6 mice bearing HC.PmelKO.TYRP1-NFhgp100 (A; pink) or HC.PmelKO.CDK4^{R24C}-NFhgp100 (B; green) melanomas. Cy: cyclophosphamide, Ad-hgp100: hgp100-expressing adenovirus, CpG/Poly(I:C): innate immune ligands. (C and D) Kaplan-Meier survival plots of indicated tumour cohorts of either non-treated (dashed line; n ≥ 13) or ACT-treated (solid line; n ≥ 23) mice. Statistics: ***p<0.001, log-rank test.

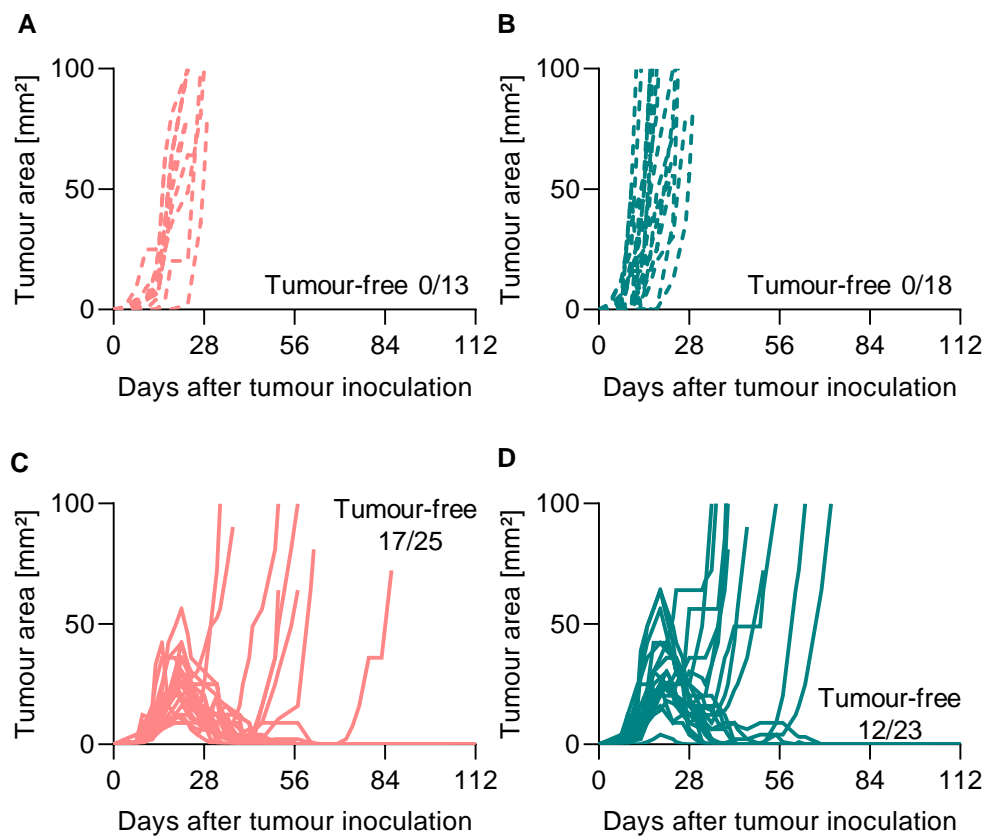


Figure 4.3: Response of TYRP1 or CDK4^{R24C} tumours to ACT immunotherapy in C57BL/6 mice

(A and B) Individual tumour growth curves (tumour in mm²) of non-treated HC.PmelKO.TYRP1-NFhgp100 (A) and HC.PmelKO.CDK4^{R24C}-NFhgp100 (B) melanomas (n ≥ 13). (C and D) Individual tumour growth curves (tumour in mm²) of ACT-treatedd HC.PmelKO.TYRP1-NFhgp100 (C) and HC.PmelKO.CDK4^{R24C}-NFhgp100 (D) melanomas (n ≥ 23).

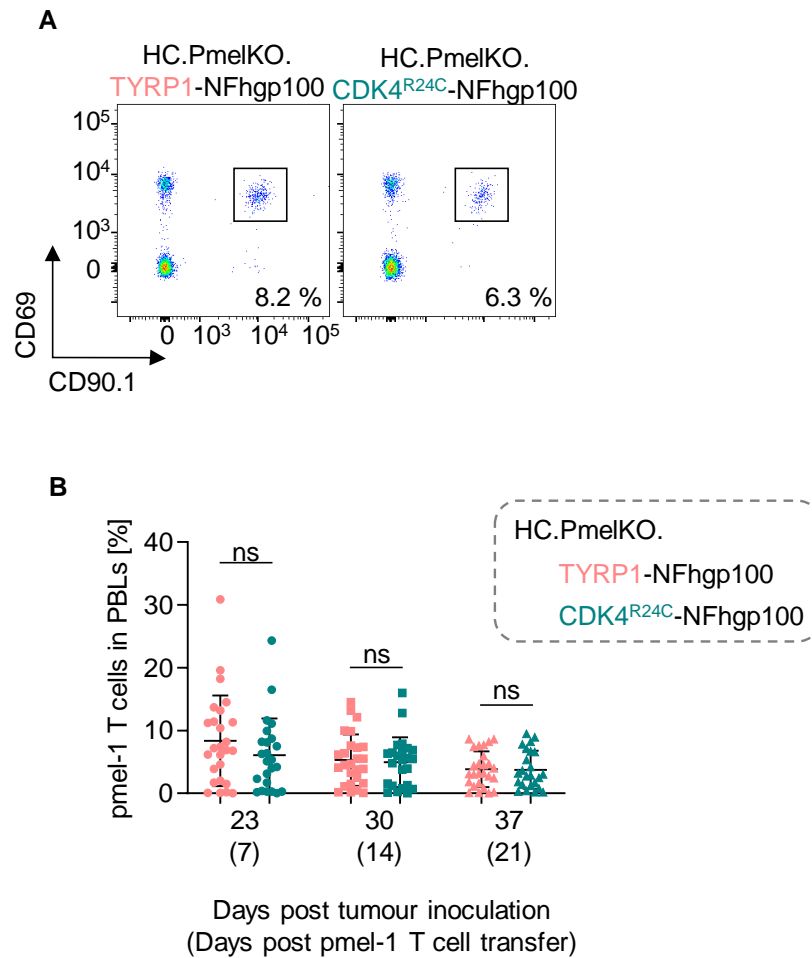


Figure 4.4: Circulating pmel-1 T cells after ACT immunotherapy in the two CRISPiotope models

(A) Representative flow cytometry plots showing CD8⁺ CD90.1⁺ pmel-1 TCRtg T cells 7 days after adoptive T cell transfer in the peripheral blood of tumour bearing mice as indicated. (B) Quantification of CD8⁺ CD90.1⁺ pmel-1 TCRtg T cells 7, 14 and 21 days after adoptive T cell transfer in the peripheral blood in individual tumour bearing mice as indicated. In parentheses: days post tumour inoculation. (HC.PmelKO.TYRP1-NFhgp100: n = 25, HC.PmelKO.CDK4^{R24C}-NFhgp100: n = 23). Statistics: ns-not significant, unpaired two-sided t-test and Mann-Whitney-U test.

4.2.2. Antigen status in recurrent melanoma treated with adoptive cell transfer immunotherapy

Next, we were interested whether the resistance mechanisms between the two CRISPiTope tumour groups differed.

When tumours reached volumetric endpoints, we harvested the tissue and established *ex vivo* cell lines from all non-treated and recurrent ACT-treated melanomas. In addition, we isolated RNA from the tumour tissue for 3'mRNA-Seq analysis. We analysed mRNA expression of the NFhgp100 tag and mNeon protein expression by flow cytometry which served as a surrogate maker for the level of hgp100 epitope expression by the cells. We found that the majority of HC.PmelKO.TYRP1-NFhgp100 tumours had either reduced or lost mRNA and protein expression of NFhgp100 compared to HC.PmelKO.CDK4^{R24C}-NFhgp100 and untreated melanomas. In the HC.PmelKO.CDK4^{R24C} tumour cohort, we only found one melanoma that had lost mRNA and protein expression of NFhgp100 (Figures 4.5A and 4.5B).

When correlating mNeon protein expression and NFhgp100 mRNA expression in HC.PmelKO.TYRP1-NFhgp100 tumours, we could identify three individual clusters. Cluster 1 consists of the non-treated HC.PmelKO.TYRP1NFhgp100 tumours that are mNeon positive and have high protein and mRNA expression levels of the NFhgp100 tag. Cluster 2 was made up of the mNeon positive ACT-treated recurrent melanomas that had intermediate expression levels of the NFhgp100 tag protein and mRNA. Finally, cluster 3 consisted of mNeon negative ACT-treated recurrent melanomas. The majority of the tumours had low to no NFhgp100 tag protein and mRNA expression. The one exception was melanoma R3 which had no mNeon protein expression despite having intermediate mRNA expression of the NFhgp100 tag (Figure 4.5C).

In conclusion, antigen loss was a cause of escape from pmel-1 ACT immunotherapy, however it was mostly observed in the HC.PmelKO.TYRP1-NFhgp100 tumour models (TYRP1-NFhgp100: 5/8, CDK4^{R24C}-NFhgp100: 1/11).

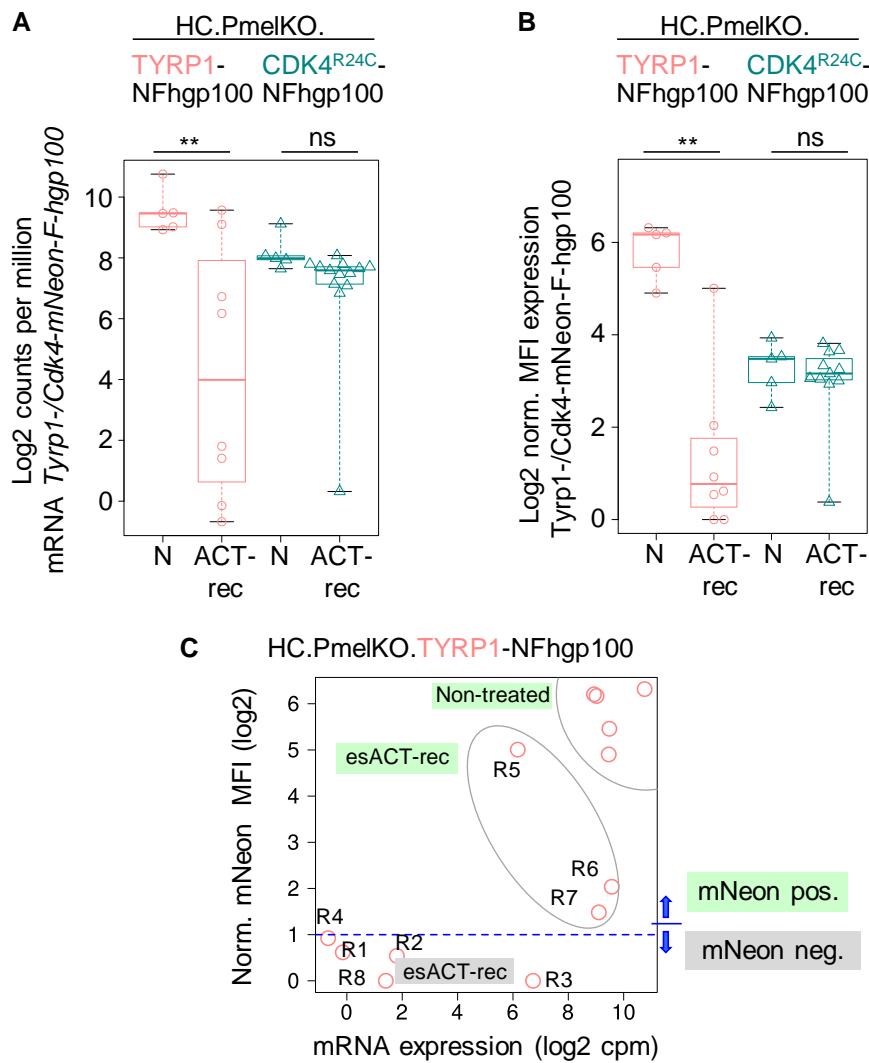


Figure 4.5: Frequencies of antigen loss in HC.PmelKO.TYRP1-NFhgp100 and HC.PmelKO.CDK4^{R24C}-NFhgp100 ACT-recurrent melanomas

(A) *Tyrp1*-*NFhgp100* and *Cdk4*^{R24C}-*NFhgp100* mRNA expression by RNA-Seq (log₂ read counts per million, cpm) in indicated non-treated (NT) and ACT-treated recurrent (ACT-rec) melanomas. (B) mNeon protein expression measured by flow cytometry of indicated non-treated (N) and ACT-treated recurrent (ACT-rec) melanomas (log₂-normalised mean fluorescence intensity (MFI)). (C) Scatter plot correlating TYRP1-NFhgp100 mRNA and protein expression. Individual ACT-treated recurrent melanomas are identified by numbers. Statistics: **p<0.01, unpaired two-sided t-test.

4.2.3. Diverse mechanisms of antigen loss in adoptive cell transfer recurrent melanoma

In order to further elucidate the resistance mechanisms that led to melanoma recurrence we employed various strategies. As previously discussed, we analysed all *ex vivo* cultures by flow cytometry for mNeon expression as surrogate marker for hgp100 epitope expression. Flow cytometry analysis was performed as soon as the melanoma cells had established adherence on a tissue culture dish.

All tumour cells isolated from a non-treated HC.PmelKO.TYRP1-NFhgp100 tumour (NT) were mNeon positive and therefore considered hgp100 epitope positive (Figure 4.6A, top panel). mNeon expression levels are comparable to the HC.PmelKO.TYRP1-NFhgp100 cell line that was originally transplanted (Chapter 3; Figure 3.10A). However, five out of eight recurrent HC.PmelKO.TYRP1-NFhgp100 melanomas were mNeon negative after therapy and therefore considered hgp100 epitope negative (Figure 4.6A, bottom panel).

We chose a tiling PCR-and Sanger sequencing based-approach to characterize the mechanisms of epitope loss in the HC.PmelKO.TYRP1-NFhgp100 recurrent melanomas. Using two different primer pairs we found that three recurrent melanomas (R) lacked the NFhgp100 tag on the genomic DNA (gDNA) level (R1, R4 and R8) (Figure 4.6B, top panel). As expected, the absence of the tag on a gDNA level correlated with missing *Tyrp1-NFhgp100* mRNA transcript in matching complementary DNA (cDNA) (Figure 4.6B, bottom panel). Additionally, we identified one recurrent melanoma (R2) that expressed the gDNA but lacked the *Tyrp1-NFhgp100* mRNA transcript which is suggestive of a transcriptional silencing mechanism (Figure 4.6B, bottom panel).

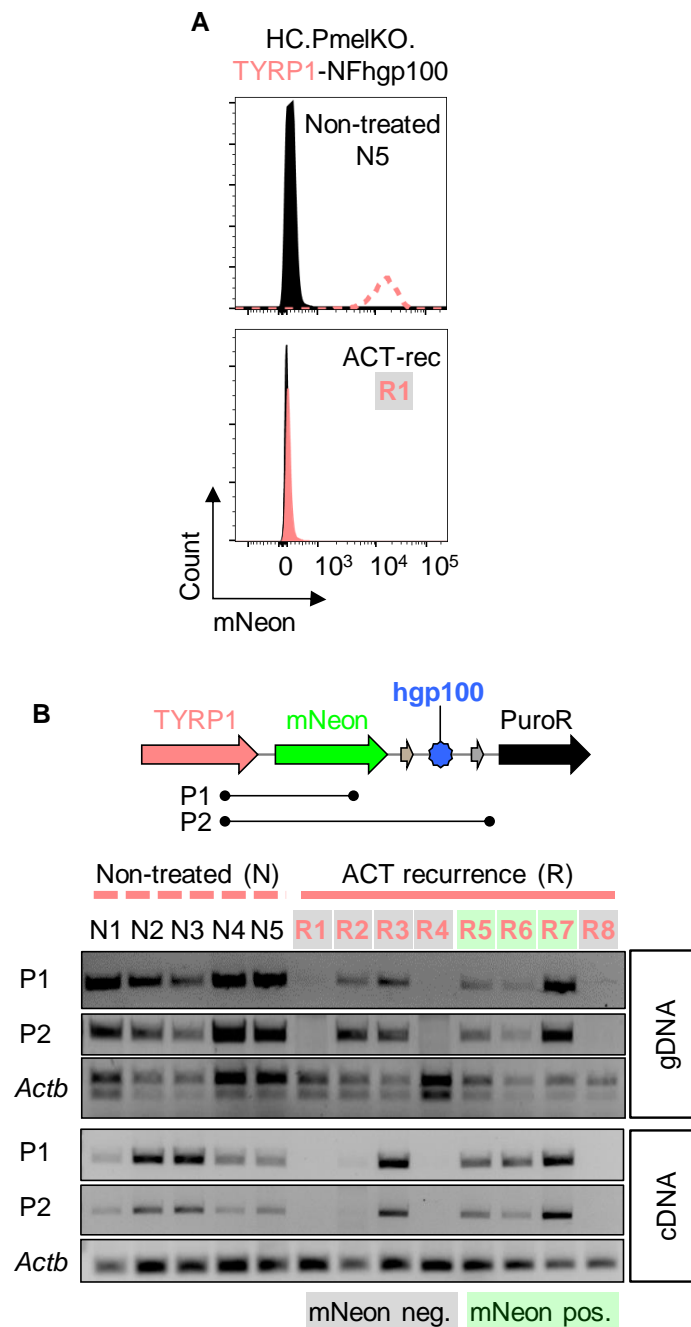


Figure 4.6: Diverse genetic and epigenetic mechanisms of antigen loss in HC.PmelKO.TYRP1-NFhgp100 ACT recurrent melanomas

(A) Exemplary histograms showing mNeon protein expression by flow cytometry in non-treated (N5) and ACT recurrent melanoma (R1). (B) Detection of NFhgp100 tag by PCR analysis of genomic DNA (top panel) and cDNA (bottom panel) from non-treated (N) and ACT recurrent melanomas (R). Amplified regions and primer pairs are depicted. *Actb* served as loading control. Numbers are matched with Figure 4C. Grey: NFhgp100 negative, green: NFhgp100 positive.

Furthermore, we identified one recurrent melanoma (R3) that was mNeon negative on protein level although it still had the NFhgp100 tag on gDNA and cDNA levels. We analysed the PCR amplicons by Sanger sequencing and identified a point mutation in the mNeon coding sequence of HC.PmelKO.TYRP1-NFhgp100 melanoma R3 that leads to a premature stop codon (TAC > TAA; Tyr > STOP) and therefore to truncation of the mNeon protein and the hgp100 epitope (Figure 4.7A). Moreover, we analysed all mNeon negative recurrent melanomas (R1, R2, R3, R4 and R8) by immunoblotting (Figure 4.7B). All NT tumours show two TYRP1 protein bands whereas the upper band corresponds to the modified TYRP1-NFhgp100 protein and the lower band with the wildtype TYRP1 protein. In the five mNeon negative recurrent melanomas, we only observed the wildtype TYRP1 protein but not the modified TYRP1-NFhgp100 protein. Additionally, we analysed the cells for FLAG protein expression as FLAG is also a component of the NFhgp100 tag. All ACT-treated recurrent melanomas analysed were FLAG negative. Melanomas were also analysed for MITF protein expression and two recurrent melanomas (R1 and R2) show downregulated MITF protein expression in comparison to NT tumours. To conclude, we identified three different mechanism of hardwired antigen loss: genomic loss of the antigen, transcriptional silencing of the antigen-encoding allele and premature stop codon. Our analysis also showed that the melanomas selectively lost the TYRP1 allele that was targeted by our CRISPiotope approach and harboured the hgp100 epitope. Thereby the target of the pmel-1 ACT immunotherapy was lost and the melanoma cells escaped from therapy.

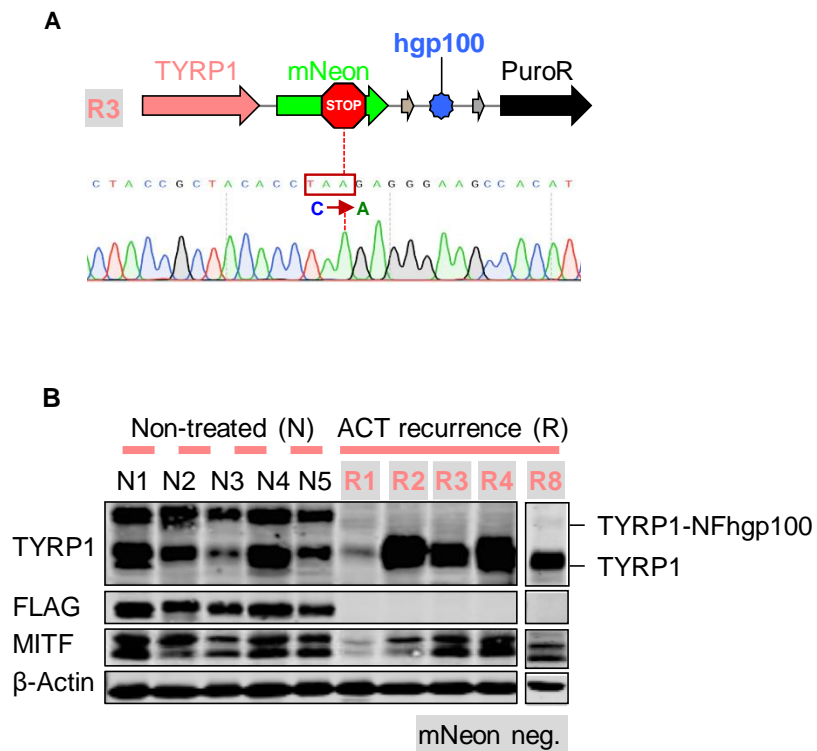


Figure 4.7: Diverse genetic and epigenetic mechanisms of antigen loss in HC.PmelKO.TYRP1-NFhgp100 ACT recurrent melanomas (continued)

(A) Truncating mutation in mNeon open-reading-frame from HC.PmelKO.TYRP1-NFhgp100 ACT recurrent melanoma R3 identified by Sanger sequencing. (B) Immunoblot analysis of TYRP1, FLAG, MITF and β -Actin from non-treated (N) and ACT-recurrent (R) melanomas with antigen loss (R1-R4, R8).

In case of the HC.PmelKO.CDK4^{R24C}-NFhgp100 recurrent melanomas we identified only one (R10) out of eleven tumours that was mNeon negative and therefore hgp100-epitope negative (Figure 4.8A and 4.8B). All HC.PmelKO.CDK4^{R24C}-NFhgp100 NT melanomas and ten of the ACT-treated recurrent melanomas were mNeon positive (Figure 4.8A). mNeon expression levels were comparable to the HC.PmelKO.CDK4^{R24C}-NFhgp100 cell line that was originally transplanted (Chapter 3; Figure 3.10A). We analysed all HC.PmelKO.CDK4^{R24C}-NFhgp100 recurrent melanoma using a PCR-based approach and identified tumour R10 as lacking the NFhgp100 tag on the genomic level. Therefore, for HC.PmelKO.CDK4^{R24C}-NFhgp100 recurrent melanomas we only found a genomic hardwired event for one recurrent melanoma whereas the others remained elusive.

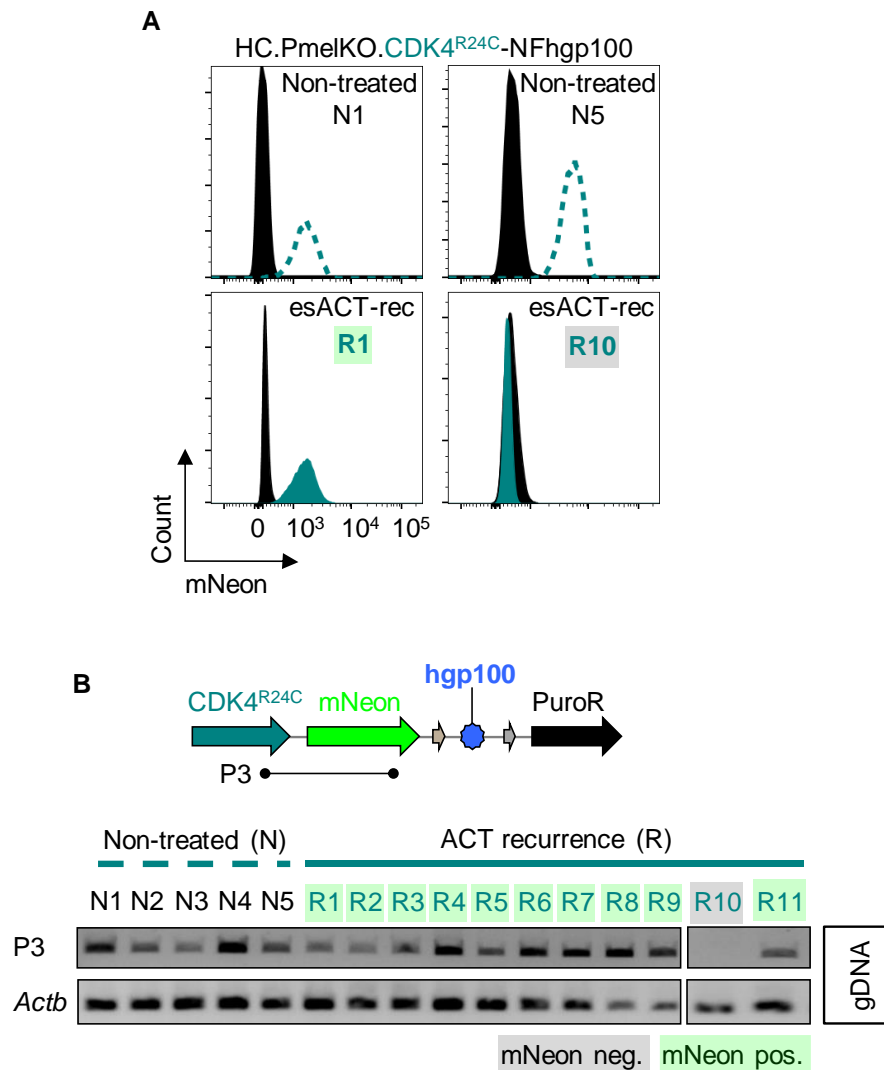


Figure 4.8: Genetic mechanism of antigen loss in HC.PmelKO.CDK4^{R24C}-NFhgp100 ACT recurrent melanoma

(A) Exemplary histograms showing mNeon protein expression by flow cytometry in non-treated (N1 and N5) and ACT-treated recurrent melanoma (R1 and R10). (B) Detection of NFhgp100 tag by PCR analysis of genomic DNA from non-treated (N) and ACT recurrent melanomas (R). Amplified regions and primer pair are depicted. *Actb* served as loading control. Grey: NFhgp100 negative, green: NFhgp100 positive.

4.2.4. Adoptive cell transfer targeting of the melanosomal protein TYRP1 enforces melanoma phenotype switching

In the previous experiments, we identified five out of eight HC.PmelKO.TYRP1-NFhgp100 tumours that escaped ACT immunotherapy by hardwired antigen loss by either genetic or epigenetic mechanisms. In the remaining three out of eight HC.PmelKO.TYRP1-NFhgp100 ACT recurrent melanomas (R5, R6 and R7), we noticed reduced mNeon expression compared to NT tumours shown in Figure 4.6A (Figure 4.9A, top panel). These *ex vivo* cell lines were cultured under non-inflammatory conditions *in vitro* for two weeks and re-analysed by flow cytometry. The melanoma cells regained mNeon and therefore hgp100 epitope expression in culture (Figures 4.9A, bottom panel, and 4.9B). This suggests that the repective tumours had undergone reversible inflammation-induced dedifferentiation; a mechanism whereby melanocyte differentiation antigens are downregulated as previously described by our group (Landsberg et al., 2012; Riesenbergr et al., 2015). Activated T cells infiltrating the tumour microenvironment during ACT immunotherapy are an important source of pro-inflammatory cytokines such as TNF α and IFN γ (Glodde et al., 2017). To recapitulate this phenomenon *in vitro*, we exposed the CRISPiotope-modified HC.PmelKO.TYRP1-NFhgp100 and the HC.PmelKO.CDK4^{R24C}-NFhgp100 melanoma cells to T cell conditioned media (Figure 4.9C). T cell conditioned media was generated by the activation of C57BL/6 splenocytes *in vitro* using CD3 ϵ and CD28 antibodies for 60 h. Exposure of HC.PmelKO.TYRP1-NFhgp100 to T cell conditioned media led to significantly reduced mNeon expression levels compared to HC.PmelKO.CDK4^{R24C}-NFhgp100. Results of this experiment mimicked our *in vivo* observations and is consistent with a previous study that showed exposure of human melanoma cells *in vitro* to TNF α does not lead to reduced activation of T cells recognising CDK4^{R24C} but reduced activation of T cells recognising a melanocyte differentiation antigen (Landsberg et al., 2012).

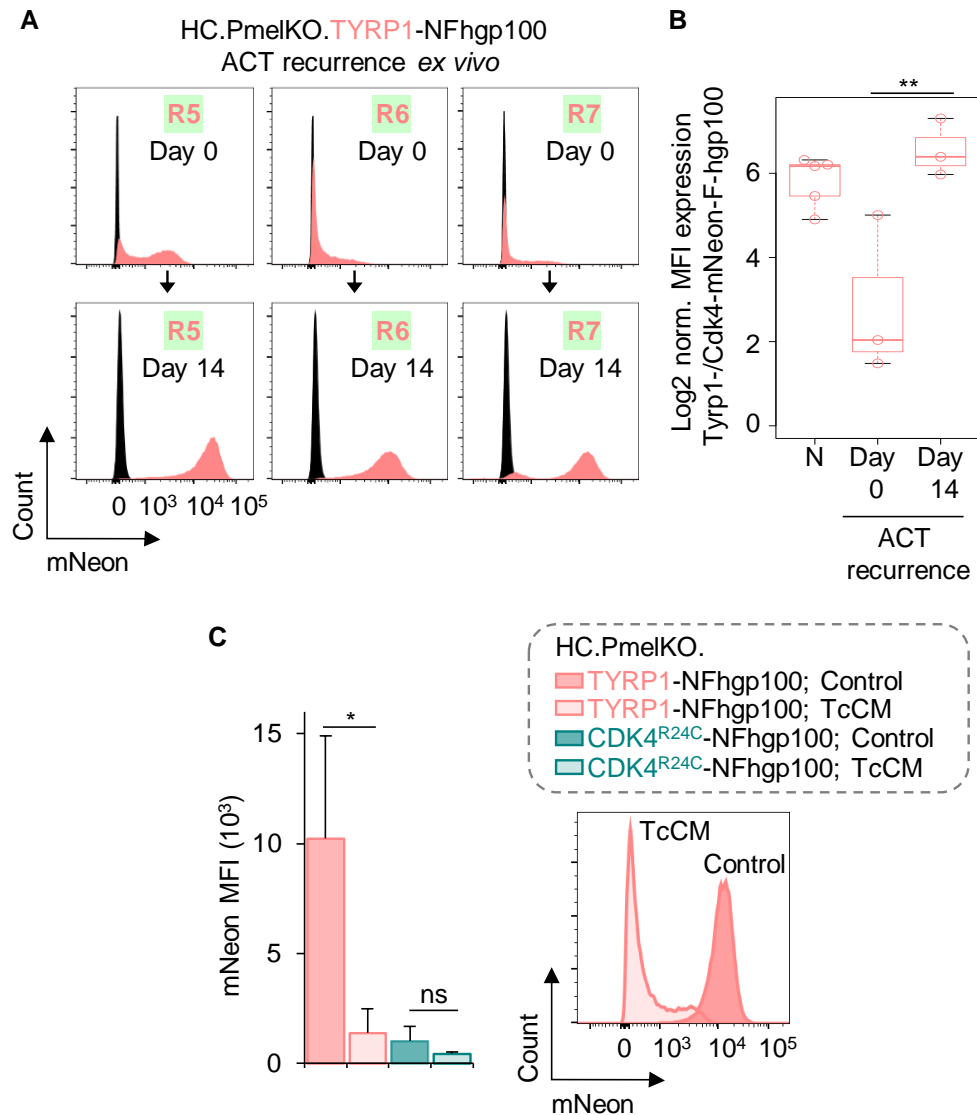


Figure 4.9: ACT targeting melanosomal TYRP1 induces reversible inflammation-induced dedifferentiation

(A) Representative histograms showing mNeon expression by flow cytometry of indicated HC.PmelKO.TYRP1-NFhgp100 melanomas on day 0 and d 14 of ex vivo culture. (B) Quantification of mNeon mean fluorescence intensity (MFI) of non-treated (N) and indicated ACT-treated recurrent melanomas on day 0 and day 14 of ex vivo culture (log₂ normalised). ***p*<0.01, Mann-Whitney-U test. (C) Quantification of mNeon MFI and representative histograms of indicated HC.PmelKO. Melanoma cells treated with T cell conditioned media (TcCM) for 72 hours. Statistics: ***p*< 0.01, **p*<0.05, ns-not significant, unpaired two-sided t-test.

Next, we wanted to investigate whether differential regulation of TYRP1-NFhgp100 and CDK4^{R24C}-NFhgp100 in response to inflammation influences escape mechanisms of recurrent melanomas with persistent (albeit in some cases reduced) antigen expression (HC.PmelKO.TYRP1-NFhgp100: R5 – R7, HC.PmelKO.CDK4^{R24C}-NFhgp100: R1 – R9, R11). Using 3'mRNA-Seq data and the MSigDB hallmark gene set collection complemented with melanoma phenotype signatures, we compared the two groups by gene set enrichment analysis (GSEA) (Liberzon et al., 2015b; Subramanian et al., 2005; Verfaillie et al., 2015). The gene signatures 'Hallmark Epithelial Mesenchymal Transition (EMT)' and 'Verfaillie invasive' were enriched in the HC.PmelKO.TYRP1-NFhgp100 ACT-recurrent melanomas that showed reversible inflammation-induced dedifferentiation (Figures 4.10A and 4.10B). These results indicated that ACT immunotherapy has a stronger effect regarding mesenchymal-like melanoma phenotype switching when targeting melanosomal TYRP1 compared to oncogenic CDK4^{R24C}. RNA-Seq analysis also showed that the 'Melanoma invasive' signature was only enriched in HC.PmelKO.TYRP1-NFhgp100 cells that underwent phenotype switching but not in the HC.Pmel.TYRP1-NFhgp100 with hardwired antigen loss or any of the HC.PmelKO.CDK4^{R24C}-NFhgp100 tumours (Figures 4.11A and 4.11B).

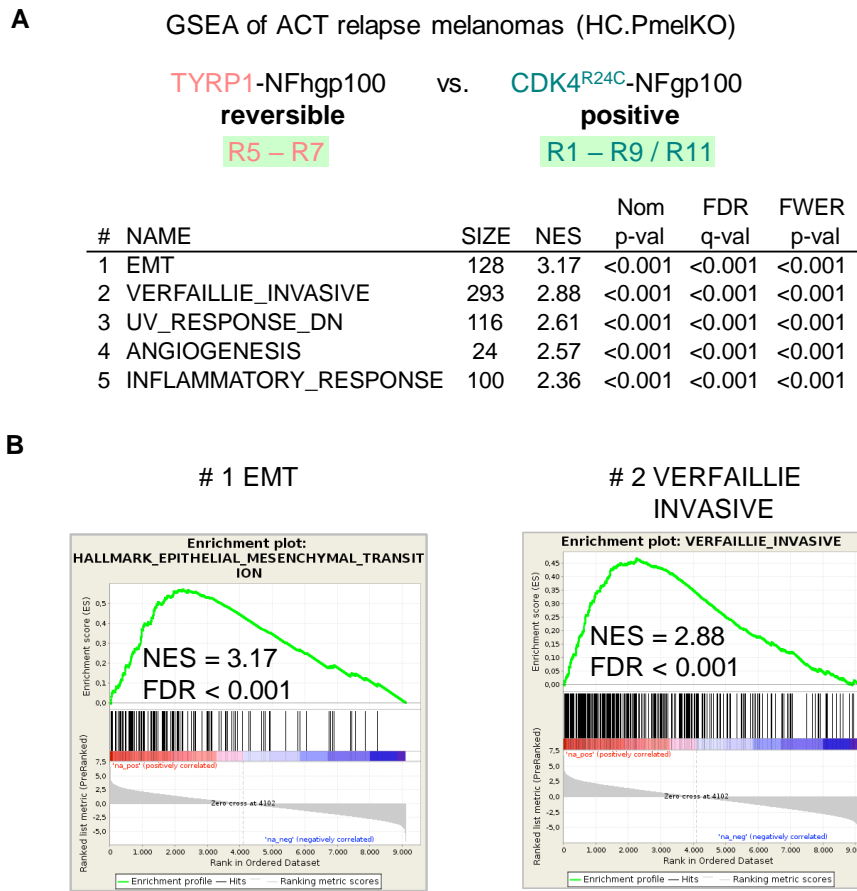


Figure 4.10: ACT targeting melanosomal TYRP1 enforces melanoma phenotype switching

(A) Top five enriched gene sets from GSEA comparing indicated ACT-treated recurrent melanomas with persistent antigen expression. NES: normalised enrichment score, FDR: false discovery rate, FWER: family-wise error rate. (B) GSEA plots for top two enriched gene sets.

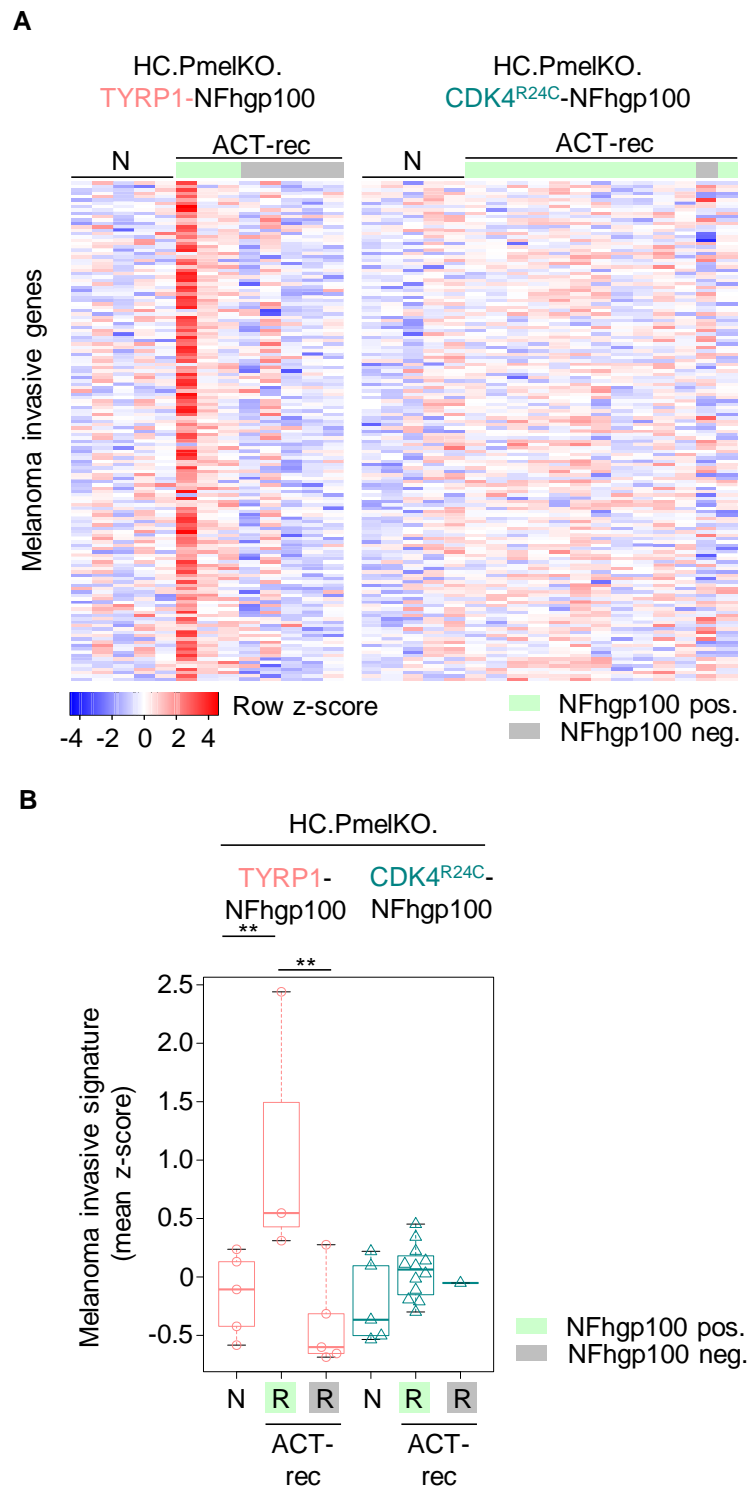


Figure 4.11: ACT targeting melanosomal TYRP1 enforces melanoma phenotype switching (continued)

(A) Heatmap visualisation and (B) quantification of expression of melanoma invasive genes of indicated conditions. N: non-treated, R: recurrent; grey: antigen negative, green: antigen positive. Statistics: ** $p < 0.01$, unpaired two-sided t-test. See Appendix 1 for annotation of the genes shown in (A).

To validate the previous findings, we analysed HC.PmelKO.TYRP1-NFhgp100 and HC.PmelKO.CDK4^{R24C}-NFhgp100 melanomas shortly after receiving ACT immunotherapy (day 10 post cyclophosphamide) by 3'mRNA-Seq (Figure 4.12A). In both HC.PmelKO.TYRP1-NFhgp100 and HC.PmelKO.CDK4^{R24C}-NFhgp100 melanomas the pigmentation signatures were significantly decreased upon ACT immunotherapy (Figure 4.12A). However, this signature indicative of melanoma phenotype switching was decreased to a significantly greater extent in HC.PmelKO.TYRP1-NFhgp100 melanomas (Figure 4.13B). In line with these findings, we also found a stronger downregulation of the 'Verfaillie proliferative' signature (Figure 4.13C). In conclusion, the data suggest that when ACT immunotherapy is targeting a melanocyte lineage gene product such as TYRP1 melanoma phenotype switching is more pronounced in contrast to targeting constitutively expressed oncogenic gene products such as CDK4^{R24C}.

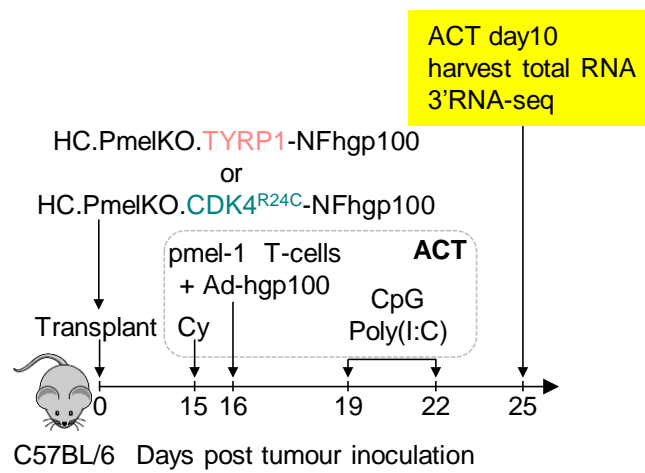


Figure 4.12: ACT immunotherapy approach to analyse tumour early during treatment by 3'mRNA-Seq

Experimental setup for early-during treatment analysis. This experiment was performed by Nicole Glodde.

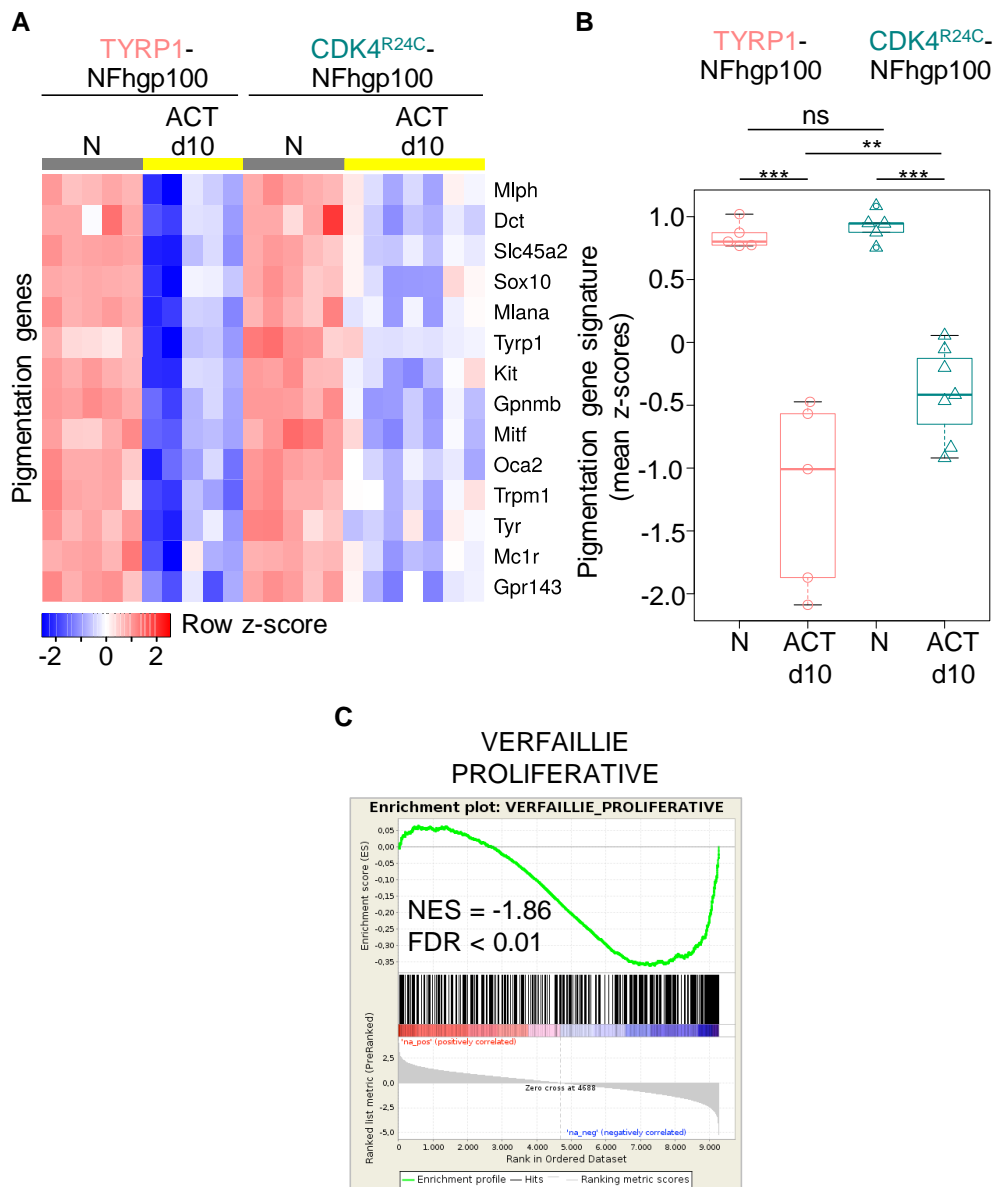


Figure 4.13: Melanoma dedifferentiation more pronounced in HC.PmelKO.TYRP1-NFhgp100 early during treatment

(A and B) Heatmap visualisation (A) and quantification (B) of expression of melanocyte differentiation genes in indicated conditions. N: non-treated, d10: day 10 after start of ACT treatment (C) GSEA plot for Verfaillie_proliferative signature comparing ACT-treated (day 10) HC.PmelKO.TYRP1-NFhgp100 and HC.PmelKO.CDK4^{R24C}-NFhgp100 melanomas. NES: normalised enrichment score, FDR: false discovery rate. Statistics: . **p<0.01, ***p<0.001, ns-not significant, unpaired two sided t-test corrected for multiple testing (B&H). This experiment was performed by Nicole Glodde.

4.2.5. Target antigen status defines immune contexture of recurrent melanoma

In order to investigate how the target antigen status (NFhgp100 positive versus NFhgp100 negative) influences the immune contexture in ACT-recurrent melanomas, we analysed non-treated and recurrent melanomas by 3'mRNA-Seq. In the case of HC.PmelKO.TYRP1-NFhgp100 tumours, we classified tumours being antigen positive for the reversible dedifferentiation group, and antigen negative for the tumours with hardwired antigen loss. The HC.PmelKO.CDK4^{R24C}-NFhgp100 tumours were either truly antigen positive (no reversible downregulation) or antigen negative (genomic loss of antigen).

When comparing antigen positive and antigen negative tumours by GSEA, among the top five enriched signatures were 'Interferon gamma/alpha response' and 'Inflammatory response' in the antigen positive tumours (Figure 4.14). Expression of IFN γ response genes was significantly increased in NFhgp100 positive melanomas compared to non-treated or NFhgp100 negative melanomas (Figure 4.15A and 4.15B). Antigen persistence is associated with an IFN-rich inflamed tumour microenvironment (TME). Benci and colleagues recently showed that sustained chronic interferon signalling induces a multigenic tumour resistance programme including the upregulation of T cell inhibitory ligands such as PD-L1 (Benci *et al.*, 2016).

#	NAME	SIZE	NES	Nom p-val	FDR q-val	FWER p-val
1	INTERFERON_GAMMA_RESPONSE	143	3.13	<0.001	<0.001	<0.001
2	INTERFERON_ALPHA_RESPONSE	72	2.93	<0.001	<0.001	<0.001
3	ALLOGRAFT_REJECTION	109	2.34	<0.001	<0.001	<0.001
4	INFLAMMATORY_RESPONSE	100	2.04	<0.001	<0.001	0.001
5	IL2_STAT5_SIGNALING	133	2.01	<0.001	<0.001	0.001

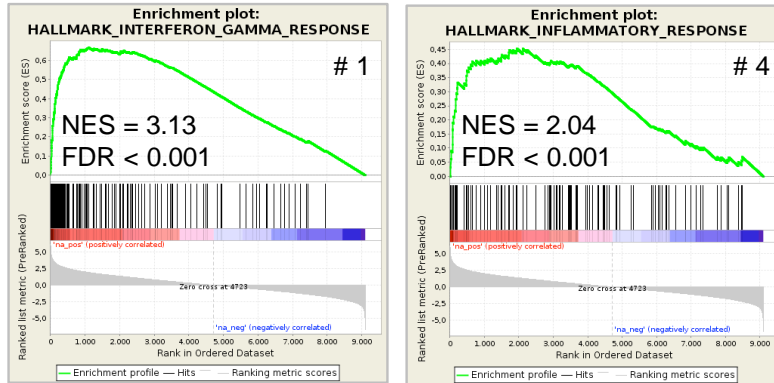


Figure 4.14: Antigen persistence is associated with an IFN-rich inflamed tumour microenvironment

(A) GSEA comparing ACT recurrent melanomas with persistent antigen (HC.PmelKO.TYRP1-NFhgp100 and HC.PmelKO.CDK4R24C-NFhgp100) expression versus antigen loss. Top panel: Top five enriched gene sets. Bottom panels: GSEA plots. NES: normalised enrichment score, FDR: false discovery rate, FWER: family-wise error rate.

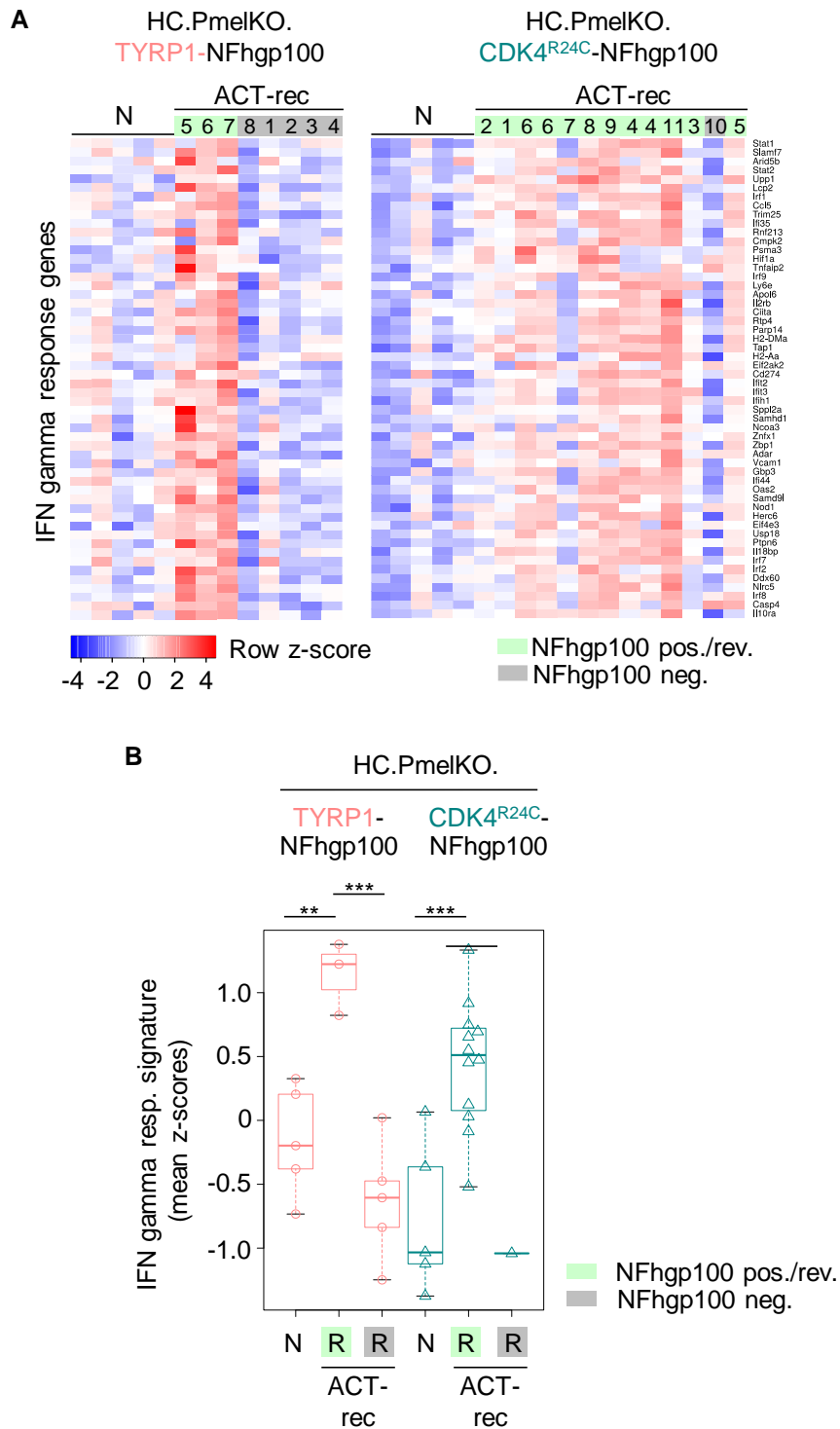


Figure 4.15: Antigen persistence is associated with an IFN-rich inflamed tumour microenvironment (continued)

(A and B) Heatmap visualisation (A) and quantification (B) of IFN gamma response genes in indicated non-treated (N) and ACT recurrent (ACT-rec - R) melanomas. Numbers of ACT-rec are matched with previous figures. Grey: antigen loss, green: antigen persistence. Statistics: ** $p < 0.01$, *** $p < 0.001$, unpaired two-sided t-test.

Consistent with these data, we found increased transcript levels of T cell markers such as Cd8 α or Cd3 ϵ and immune checkpoint genes such as Ctl4 or Pdcd1 in the bulk tumour mass (Figures 4.16A and 4.16B, 4.17A and 4.17B). This suggested that an inflamed IFN γ -rich TME leads to the upregulation of negative immune checkpoint molecules on immune cells and promotes escape from ACT immunotherapy despite antigen persistence.

To validate that the HC.PmelKO.TYRP1-NFhgp100 and HC.PmelKO.CDK4^{R24C}-NFhgp100 tumours were still capable of activating T cells, we performed an *in vitro* T cell activation assay with the *ex vivo* cell lines established from each ACT-treated recurrent tumour. Firstly, we stimulated the melanoma cells to verify that they were all capable of upregulating MHC class I (H2-Db) upon IFN γ treatment. All melanoma cells upregulated H2-Db surface expression upon IFN γ stimulation (Figures 4.18A and 4.18B). Some of the *ex vivo* cell lines had a higher baseline surface expression of H2-Db than the originally transplanted HC.PmelKO.TYRP1-NFhgp100 and HC.PmelKO.CDK4^{R24C}-NFhgp100 cell lines (Chapter 3; Figure 3.12C). Secondly, we co-cultured stimulated melanoma cells with splenocytes from naïve pmel-1 TCRtg mice as described previously (Chapter 3; Figure 3.11) and analysed CD69 surface expression on the T cells. All melanoma cells that retained antigen expression induced CD69 surface expression on the pmel-1 T cells to a greater extent than the originally transplanted CRISPiotope-modified cell lines, whereas melanoma cells that lost the antigen were not able to induce CD69 surface expression on the T cells (Figures 4.18C and 4.18D). Antigen processing and presentation seemed to be unaffected in the ACT-treated recurrent melanomas. *Ex vivo* generated melanoma cell lines that were mNeon, and therefore hgp100-epitope, positive retained the capability to activate T cells.

In conclusion, we found that target antigen status (antigen persistence vs. antigen loss) defines the immune landscape and shapes the TME (inflamed vs. non-inflamed).

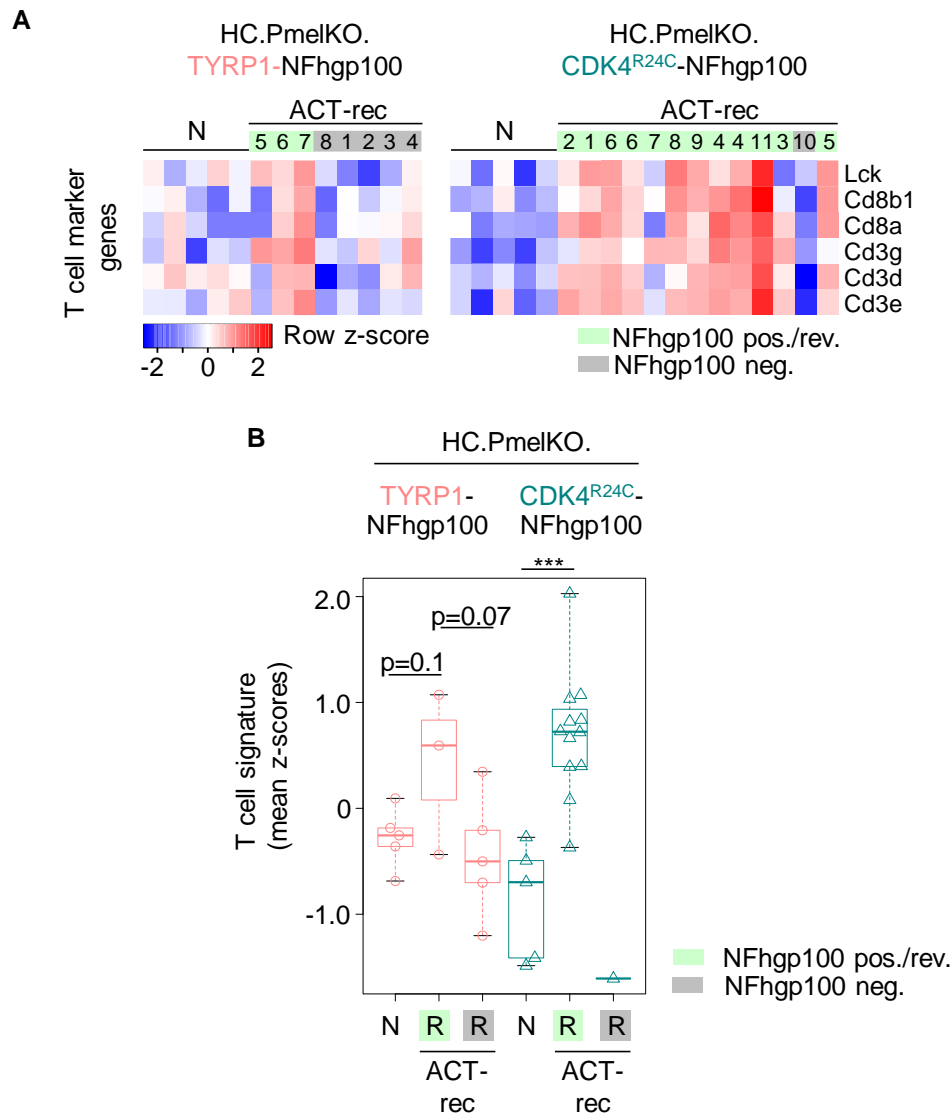


Figure 4.16: An IFN-rich inflamed tumour microenvironment is associated with an increased T cell signature

(A) Heatmap visualisation of T cell marker genes in indicated non-treated (N) and ACT recurrent (ACT-rec - R) melanomas. Numbers of ACT-rec are matched with previous figures. Grey: antigen loss, green: antigen persistence. (B) Quantification of T cell signature in indicated non-treated (N) and ACT recurrent (ACT-rec - R) melanomas. Numbers of ACT-rec are matched with previous figures. Grey: antigen loss, green: antigen persistence. Statistics: *** $p < 0.001$, unpaired two-sided t-test.

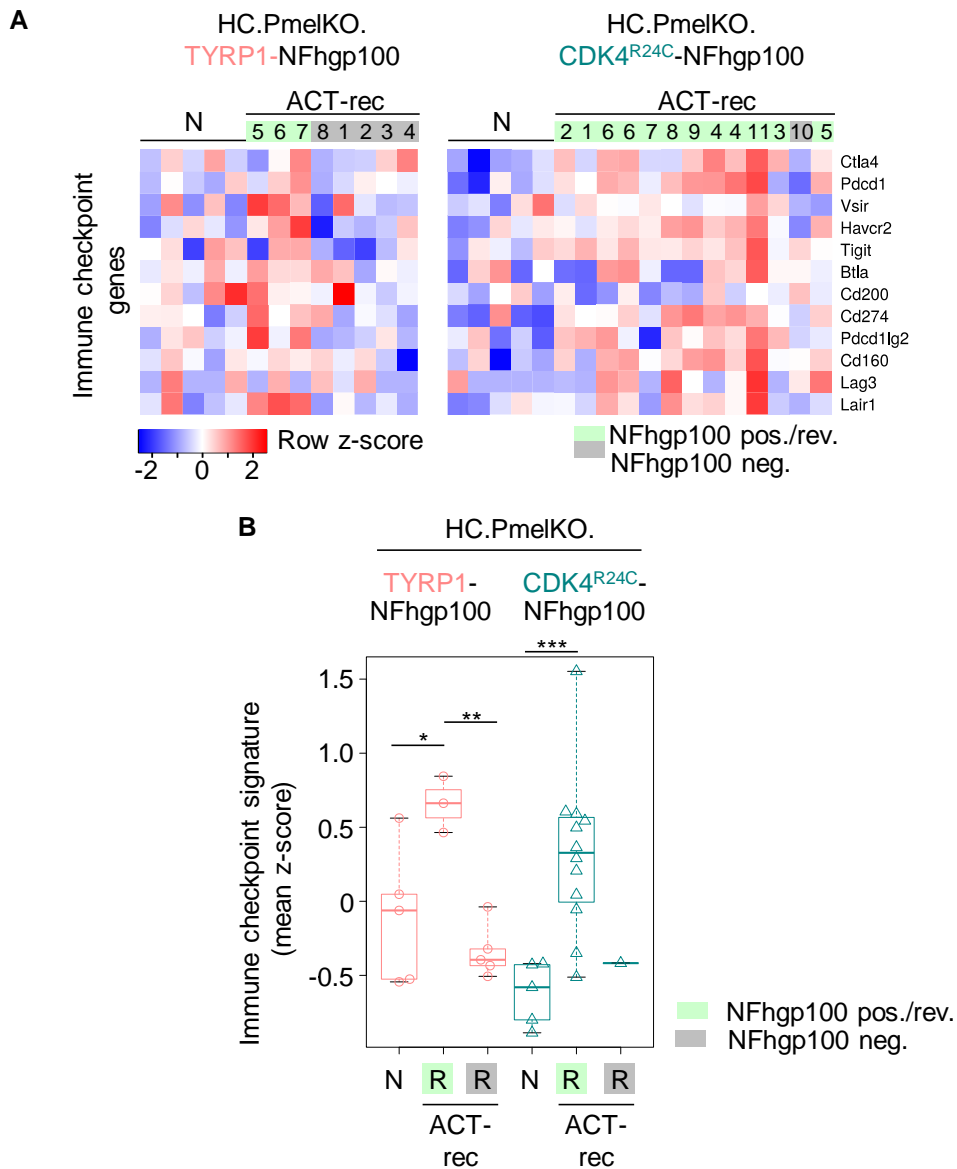


Figure 4.17: An IFN-rich inflamed tumour microenvironment is associated with an immune checkpoint signature

(A) Heatmap visualisation of immune checkpoint genes in indicated non-treated (N) and ACT recurrent (ACT-rec - R) melanomas. Numbers of ACT-rec are matched with previous figures. Grey: antigen loss, green: antigen persistence. (B) Quantification of immune checkpoint signature (D) in indicated non-treated (NT) and ACT recurrent (ACT-rec - R) melanomas. Numbers of ACT-rec are matched with previous figures. Grey: antigen loss, green: antigen persistence. Statistics: * $p < 0.05$, ** $p < 0.01$, *** $p < 0.001$, unpaired two-sided t-test.

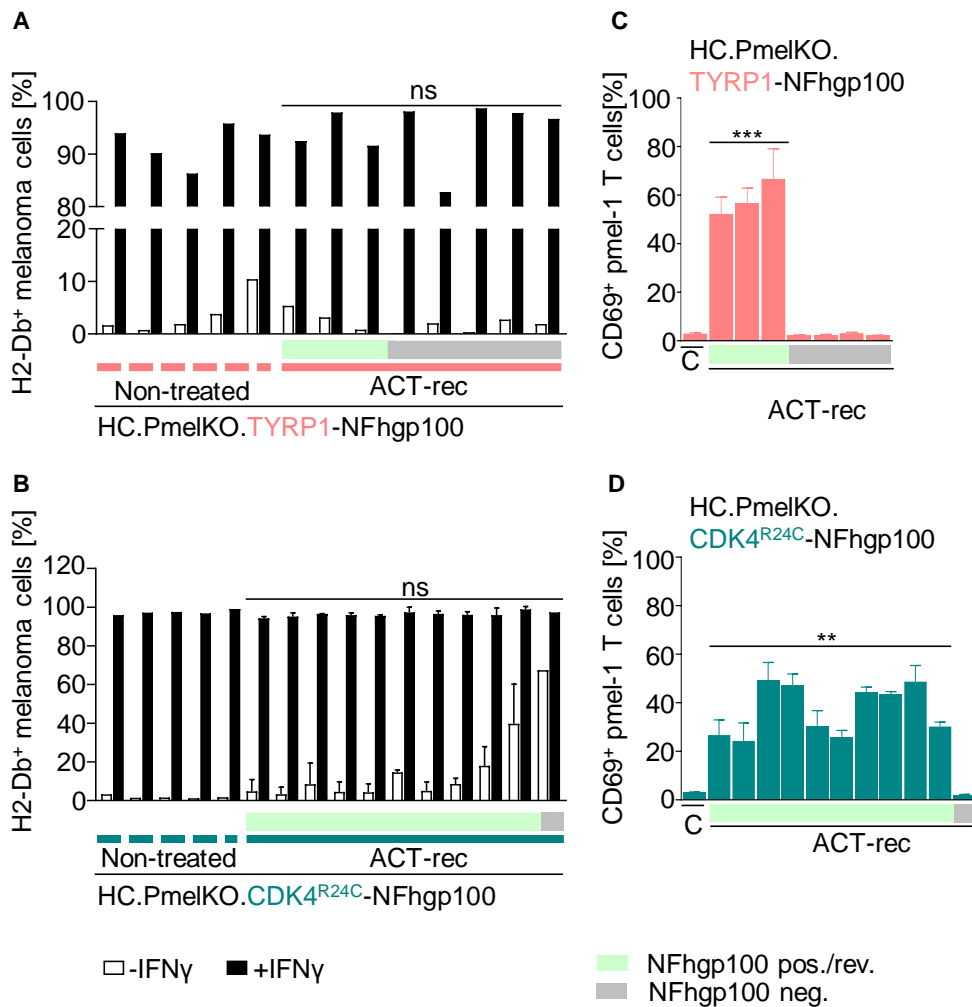


Figure 4.18: ACT-treated recurrent melanomas can process and present antigen

(A and B) Flow cytometric quantification of H2-Db surface expression on non-treated and ACT-treated recurrent HC.PmelKO.TYRP1-NFhgp100 (A) and HC.PmelKO.CDK4^{R24C}-NFhgp100 (B) melanoma after IFN γ stimulation for 72 hours (HC.PmelKO.TYRP1-NFhgp100: n = 1; HC.PmelKO.CDK4^{R24C}-NFhgp100: n \geq 1, mean \pm SD). (C and D) Flow cytometric quantification of CD69 surface expression on CD8⁺ CD90.1 pmel-1 T cells co-cultures (16 h) with ACT-treated recurrent HC.PmelKO.TYRP1-NFhgp100 (C) and HC.PmelKO.CDK4^{R24C}-NFhgp100 (D) melanomas (n = 3, mean \pm SD). Statistics: **p<0.01, *** p<0.001, ns-not significant, unpaired two-sided t-test and Mann-Whitney-U test.

4.2.6. Responsiveness of recurrent melanoma to anti-PD-L1 salvage immunotherapy

Previous publications have shown that PD-L1 expression and a T cell inflamed TME positively correlates with responsiveness to immune checkpoint therapy (Cristescu et al., 2018; Gajewski et al., 2017). As we identified upregulation of inhibitory immune checkpoint molecules as the dominant resistance mechanism in the HC.PmelKO.CDK4^{R24C}-NFhgp100 tumour model, we wondered whether salvage immunotherapy targeting the PD-1:PD-L1 axis would be effective in antigen positive recurrent melanomas. The following experiments were performed by Dr. Nicole Glodde, a member of the Hölzel laboratory.

We transplanted HC.PmelKO.CDK4^{R24C}-NFhgp100 tumours into C57BL/6 mice and treated the mice with our ACT immunotherapy approach as described above (Figure 4.2). When the mice relapsed from ACT immunotherapy (5/10) we started treatment with α -PD-L1 monoclonal antibody as salvage immune checkpoint inhibitor (sICI) (Figure 4.19A). Two out of five mice (sICI-1 and sICI-2) responded poorly to ACT and sICI therapy and will not be discussed in the following section (Figure 4.19A). One melanoma, sICI-3, responded moderately well to ACT and partially regressed upon sICI immunotherapy until resuming tumour growth (Figure 4.19B, left panel). Analysis of isolated melanoma cells from the tumour showed a mixture of antigen positive (40%) and antigen negative (60%) melanomas cells (Figure 4.19C, left panel). We considered sICI-3 melanoma as antigen positive after ACT and it is likely that enforced immune selection by α -PD-L1 lead to the outgrowth of antigen negative melanoma cells. The two remaining tumours, sICI-4 and sICI-5, responded well to ACT immunotherapy and went into complete regression before tumours started growing again (Figure 4.19B, middle and right panel). However, recurrent tumours did not respond to α -PD-L1 salvage therapy. As expected, flow cytometric analysis of isolated melanoma cells showed that sICI-4 was mNeon and therefore hgp100 negative. However, counter-intuitively sICI-5 showed normal mNeon and therefore hgp100 antigen expression as observed previously in antigen positive ACT-treated recurrent HC.PmelKO.CDK4^{R24C}-NFhgp100 melanomas (Figure 4.19C, middle and right panel).

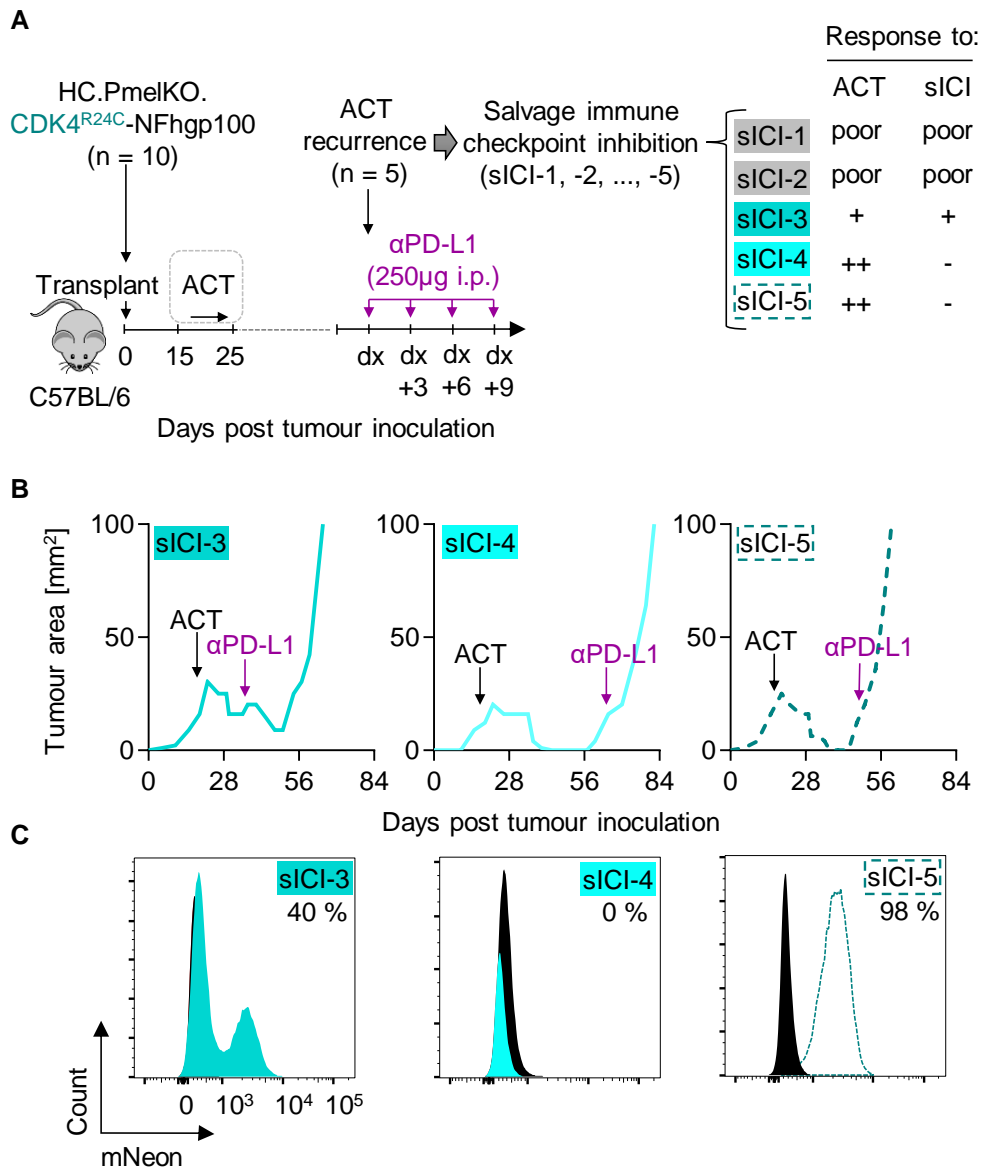


Figure 4.19: Salvage immune checkpoint inhibitor (sICI) therapy of ACT-recurrent melanomas

(A) Experimental setup of ACT and salvage ICI therapy (α -PD-L1 monoclonal antibody) of C57BL/6 mice bearing HC.PmelKO.CDK4^{R24C}-NFhgp100 melanomas (n=10). Of ACT recurrence rate (5/10 \rightarrow sICI-1, ..., -5) and responses to ACT and sICI are indicated. (B) Individual tumour growth curves (tumour area in mm²) of selected cases (sICI-3, -4, -5). (C) Histograms showing mNeon (CDK4^{R24C}-NFhgp100) expression by flow cytometry of melanoma cells isolated from sICI-3, -4 and -5 melanomas compared to mNeon-negative control cells (black). This experiment was performed by Nicole Glodde.

Sanger sequencing of the NFhgp100 tag excluded any mutations downstream of the mNeon open-reading-frame leading to selectively abrogating hgp100 epitope translation (data not shown). We wanted to test whether sICI-5 was still able to activate pmel-1 T cells *in vitro* as these cells are still NFhgp100 positive. We performed an *in vitro* T cell activation assay by measuring CD69 surface expression on CD8⁺ T cells isolated from naïve pmel-1 TCRtg mice as described previously. Before starting the co-culture, we stimulated the melanoma cells with increasing concentrations of IFN γ (0, 10 and 1000 U/ml) for three days. As expected, sICI-3 induced moderate upregulation of CD69 surface expression on the pmel-1 T cells, whereas sICI-4 did not activate the pmel-1 T cells (Figure 4.20). Surprisingly, sICI-5 could not activate T cells despite being NFhgp100 positive and therefore presumably expressing the antigen. We wondered whether these melanoma cells were defective in antigen presentation. We compared MHC class I (H2-Db) upregulation of the three salvage therapy recurrent melanomas in comparison to the HC.PmelKO.CDK4^{R24C}-NFhgp100 cell line that was originally transplanted. sICI-5 did not upregulate MHC class I molecules to the same extent as the control cell line or the other salvage therapy recurrent melanomas indicating defective antigen presentation (Figures 4.21A and 4.21B). However, upregulation of PD-L1 which is also induced by IFN γ stimulation was not affected (data not shown) arguing that impaired antigen presentation prevented response to salvage therapy in ACT recurrent melanoma sICI-5.

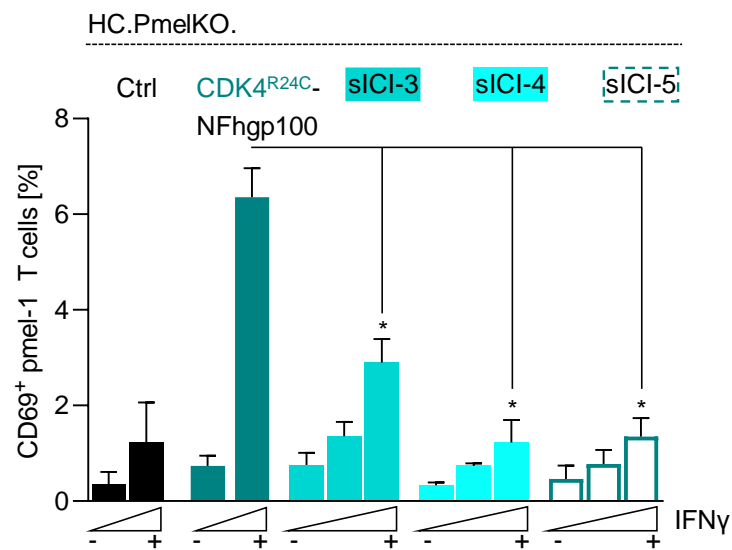


Figure 4.20: sICI melanomas have different abilities to activate TCRtg pmel-1 T cells *in vitro*

Quantification of CD69 surface expression on CD8⁺ CD90.1⁺ pmel-1 T cells co-cultured with indicated melanomas cells (16 h) pre-stimulated with increasing concentrations of IFN γ (0, 10 and 1000 U/ml) for 72 hours. (n \geq 3; mean \pm SD). Statistics: *p<0.05, Mann-Whitney-U test. This experiment was performed by Nicole Glodde.

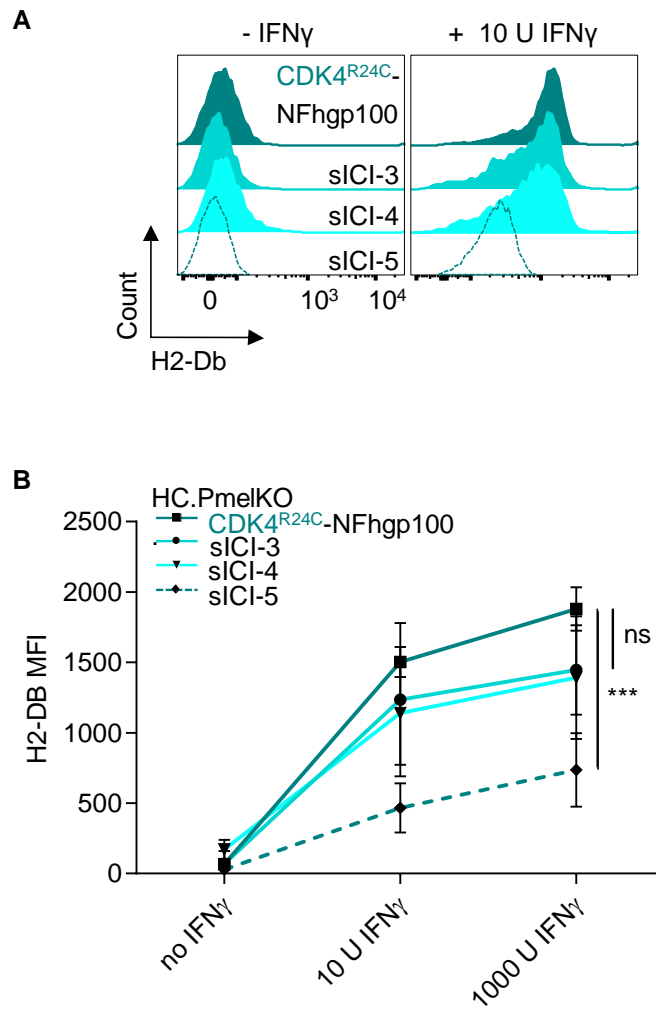


Figure 4.21: sICI melanomas respond differently to IFN γ stimulation

(A) Representative histograms showing the induction of H2-Db surface expression by flow cytometry on indicated melanomas cells treated with IFN γ (10 U/ml) for 72 hours. (B) Quantification of H2-Db surface expression on indicated melanoma cells treated with increasing concentrations of IFN γ (0, 10 and 1000 U/ml) for 72 hours shown as mean fluorescence intensity (MFI). (n = 3, mean \pm SD). Statistics: ***p<0.001, ns-not significant, Mann-Whitney-U-test. This experiment was performed by Nicole Glodde.

4.2.7. Long-term tumour control by systemic immunity

As we observed over 50 % of the mice being cured of either HC.PmelKO.TYRP1-NFhgp100 or CDK4^{R24C}-NFhgp100 melanomas by our ACT immunotherapy approach, we wanted to see what actually determined long-term tumour control and eradication. Almost five months after tumour inoculation, the ACT-treated tumour-free mice were sacrificed and we analysed the secondary lymphoid organs for the presence of pmel-1 T cells by flow cytometry. We found that tumour-free mice that went into complete tumour regression had significantly higher frequencies of pmel-1 T cells in the inguinal tumour-draining lymph node and the spleen compared to mice that relapsed from ACT immunotherapy (Figures 4.22A and 4.22B). Additionally, we observed a positive correlation between the frequency of pmel-1 T cells in the tumour-draining lymph node or the spleen with the frequency of pmel-1 T cells in the blood 14 days after adoptive T cell transfer in the ACT-treated tumour-free mice (Figures 4.23A and 4.23B). On the other hand, we did not observe such a correlation in the ACT-treated recurrent mice (Figures 4.24A and 4.24B). Furthermore, we noted higher frequencies of pmel-1 T cells in the peripheral blood 14 days after adoptive T cell transfer in the ACT-treated recurrent melanomas that turned out to be antigen negative (Figure 4.25). All these observations are independent of the tumour type (HC.PmelKO.TYRP1-NFhgp100 vs. HC.PmelKO. CDK4^{R24C}-NFhgp100). In conclusion, tumour eradication was associated with elevated T cell responses and the generation of long-lived memory T cells.

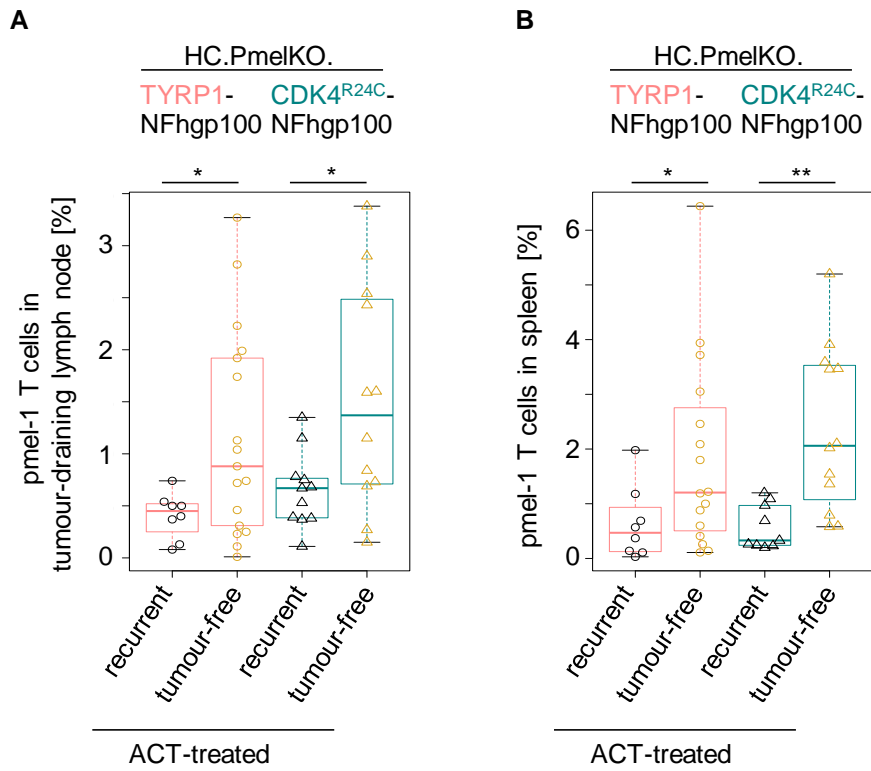


Figure 4.22: Tumour-free mice have significantly higher frequencies of pmel-1 T cells in secondary lymphoid organs

(A and B) Box plots of pmel-1 T cells [frequency %] of all CD45⁺ CD8⁺ T cells in tumour-draining (inguinal) lymph node (A) and spleen (B) of indicated recurrent and tumour-free ACT-treated tumour groups. Statistics: * $p < 0.05$, ** $p < 0.01$, unpaired two-sided Wilcox test.

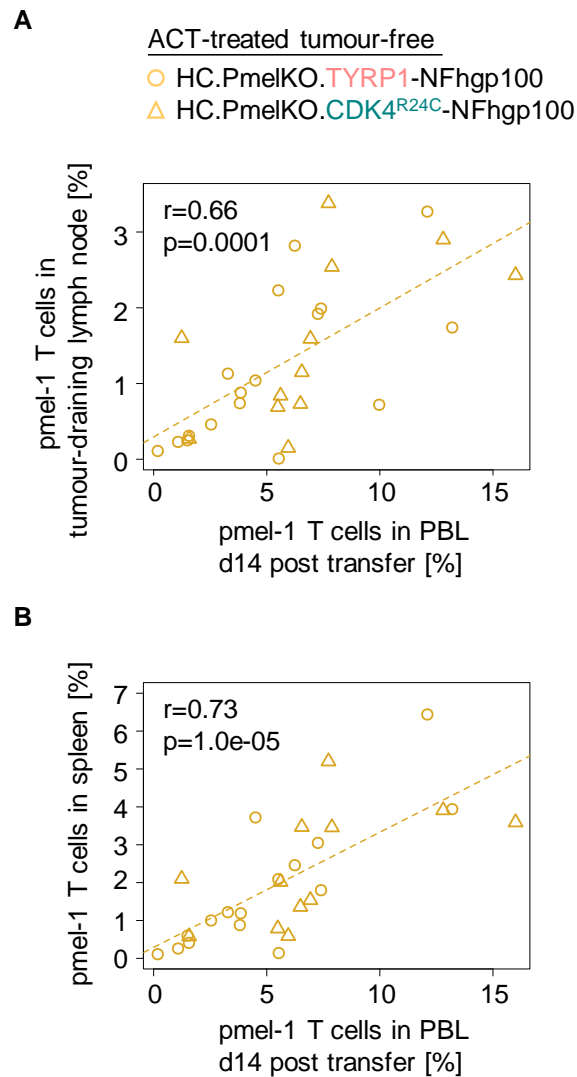


Figure 4.23: Long-term tumour control is influenced by systemic immunity
 (A and B) Correlation between pmel-1 T cells in tumour-draining lymph node (A) or pmel-1 T cells in spleen (B) with pmel-1 T cells in the peripheral blood 14 days post transfer [frequency of CD45⁺ CD8⁺ T cells, %] of indicated melanomas in ACT-treated tumour-free mice. Pearson correlation test.

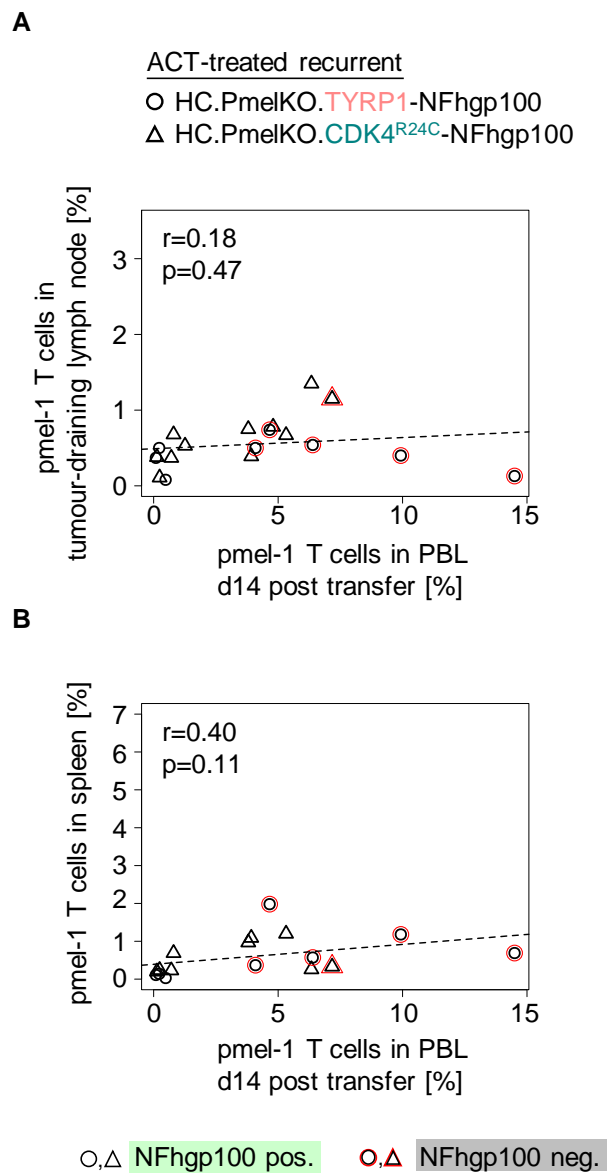


Figure 4.24: pmel-1 T cells in spleen and in blood do not correlate in ACT-treated recurrent mice

(A and B) Correlation between pmel-1 T cells in tumour-draining lymph node (A) or pmel-1 T cells in spleen (B) with pmel-1 T cells in the peripheral blood 14 days post transfer [frequency of CD45⁺ CD8⁺ T cells, %] of indicated melanomas in ACT-treated recurrent mice. Pearson correlation test.

ACT-treated recurrent

○ HC.PmelKO.TYRP1-NFhgp100

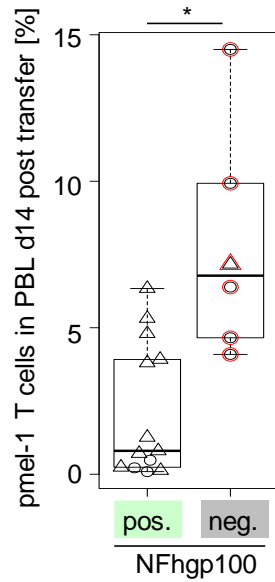
△ HC.PmelKO.CDK4^{R24C}-NFhgp100

Figure 4.25: Long-term tumour control is influenced by systemic immunity
Quantification of pmel-1 T cells [frequency of CD45⁺ CD8⁺ T cells, %] in the peripheral blood 14 days after transfer in indicated ACT-treated recurrent melanomas. Statistics: *p<0.05, unpaired two-sided Wilcox test.

4.3. Discussion

Work in this chapter investigated how ACT immunotherapy either targeting a melanosomal non-essential or an oncogenic essential protein influences melanoma responses and resistance mechanisms using a novel CRISPR/Cas9-based approach termed CRISPiTope.

In the recent years, there has been a tremendous progress in the development and improvement of personalised cancer immunotherapies. Different therapeutic strategies such as cancer vaccines or the transfer of T cells, which target tumours in an epitope-specific manner, are currently evaluated in clinical studies (Chandran et al., 2015; Chodon et al., 2014; Nowicki et al., 2018; Ott et al., 2017; Sahin et al., 2017; Schumacher et al., 2014). Adoptive cell transfer therapy targeting shared melanocyte differentiation antigens has emerged as a powerful treatment option especially in patients with metastatic melanoma as these tumour-associated antigens are shared between patients making it widely applicable. More specifically, with better techniques to describe mutational landscapes of tumours, better understanding of tumour biology, and the results from previous clinical studies, neoantigens that arise from somatic mutations have now emerged as promising targets for successful treatment of patients with ACT immunotherapy or vaccination approaches.

A major challenge to these therapy approaches is the selection of appropriate target epitope(s). These epitopes can be derived from mutated or non-mutated tumour antigens (Blankenstein et al., 2015; Hinrichs and Restifo, 2013). Improved computational prediction algorithms have facilitated target epitope choice (Bulik-Sullivan et al., 2019; Jurtz et al., 2017; O'Donnell et al., 2018). These prediction algorithms largely focus on antigen expression levels and epitope binding affinities to MHC molecules as these are known predictors of ACT efficacy in experimental models (Engels et al., 2013). However, our knowledge on how the regulation and function of epitope-encoding gene products (antigens) influence T cell therapies and how antigen selection contributes to resistance mechanisms remains limited.

The CRISPiTope approach was employed to generate melanoma cell lines that express hgp100 epitope under the control of different endogenous gene

products. These cell lines were used in syngeneic mouse melanoma model that were treated pmel-1 CD8⁺ TCRtg T cells. We targeted melanosomal TYRP1 or oncogenic CDK4^{R24C} as these two proteins represent two major types of melanoma antigens with distinct function and regulation that have been targeted in clinical studies (Chandran et al., 2015; Chodon et al., 2014; Ott et al., 2017; Sahin et al., 2017; Wang et al., 1995; Wolfel et al., 1995). Earlier studies in mice investigated ACT immunotherapy directed against different melanosomal or oncogenic gene products (Anders et al., 2011; Leisegang et al., 2016; Overwijk et al., 1998). However, these studies only demonstrated efficacy against either melanosomal or oncogenic gene products but never compared efficacy against both groups of antigens. So far, no study could compare therapy efficacy against different target proteins on the endogenous expression level context. CRISPiTope circumvents this limitation and demonstrates unique strength. It is difficult to investigate antigen-specific immunotherapies targeting different antigen-encoding genes side by side as many variables impact anti-tumoural T cell responses. One major variable that influences T cell activation and function is peptide-MHC binding affinity and therefore confounds direct comparability of T cell responses.

Using our CRISPiTope approach, we identified different resistance mechanisms depending on whether a melanosomal or oncogenic gene product was targeted by ACT.

Adaptive phenotype switching, also called melanoma cell dedifferentiation, was more pronounced when the melanosomal protein TYRP1 was targeted by pmel-1 TCRtg T cells during the ACT approach. Melanoma cell dedifferentiation, detected by an enrichment in the Verfaillie 'invasive' signature was detected during RNA-seq analysis only in melanomas that underwent reversible inflammation-induced dedifferentiation. The Verfaillie 'invasive' signature is a cellular programme opposing the Verfaillie 'proliferative' signature (Verfaillie et al., 2015). Melanoma cell dedifferentiation is partly driven by pro-inflammatory cytokines such as TNF α which are produced by activated T cells infiltrating the tumour microenvironment. Pro-inflammatory cytokines lead to the downregulating of MITF which controls the melanocytic lineage including

melanosomal proteins (Landsberg et al., 2012; Mehta et al., 2018; Riesenberget al., 2015). Melanoma cells that dedifferentiate have a survival benefit as the melanosomal protein TYRP1 is downregulated and thereby the target of the T cells is lost. Metha and colleagues recently reported that for the first time inflammation induced differentiation was observed in a patient's melanoma as a resistance mechanism to ACT targeting the MDA MART-1. The tumour initially responded to ACT and regressed. But the patient relapsed from therapy and the tumour lacked MDAs including MART-1 which was targeted by the ACT approach and expressed NGFR, an inflammation-induced neural crest marker (Mehta et al., 2018). Although it is known that patients have endogenous T cell responses against melanocyte derived antigens, which can be enhanced or reinvigorated by checkpoint immunotherapy, only limited data is available on phenotypic co-evolution of T cells and the melanoma cells they target (Brichard et al., 1993; Kawakami et al., 1994b; Wang et al., 1995).

However, our approach did not only identify reversible inflammation-induced dedifferentiation as important resistance mechanism during MDA-directed T cell therapy but also genetic and epigenetic resistance mechanisms of antigen loss after ACT immunotherapy. Different mechanisms of antigen loss caused immune evasion of the melanoma cells and thereby therapy failure as tumours can no longer be recognised by specific T cells and efficiently killed. Genetic resistance mechanisms include the lack of the C-terminal hgp100 epitope tag and single base point mutation leading to a premature stop codon which prevents epitope translation. Melanoma cells lacking the C-terminal epitope tag did likely arise from melanoma cells that were not successfully targeted by the CRISPEpitope approach in the first place and thereby had a selective growth advantage. The CRISPEpitope-engineered cell lines that were used for the *in vivo* experiment originate from a polyclonal tagged cell culture and not from a monoclonal culture. This could lead to not all cells being tagged and expressing the antigen recognised by the TCRtg T cells used for ACT. An alternative could be to perform the experiments with a monoclonal cell line which would ensure that the melanoma cells used for the *in vivo* studies all have the same genomic modification.

Verdegaal and colleagues analysed changes in neoantigen expression and

recognition by tumour-specific T cells in two patients with advanced melanoma. In one of the patients, a non-synonymous mutation in the gene RPL28 (60S ribosomal protein L28) was detected. Both alleles (wildtype and mutant) were present in early tumour tissue, whereas in tumour tissue that was harvested later the mutated allele was lost indicating a clonal outgrowth of a tumour subclone with a loss of heterozygosity at this specific locus. Over time, absence of the mutant RPL28 allele that encoded the neoantigen coincided with the absence of RPL28^{mut}-specific T cells (Verdegaal et al., 2016).

In addition to the genetic resistance mechanisms, we also identified a melanoma that showed selective transcriptional silencing of only the epitope-tagged allele but not the wildtype allele. This shows us that epigenetic modifications and epigenetic regulation can have an important impact on antigen expression. A recent longitudinal study demonstrated that the T cell-recognised neoantigen repertoire is not constant during ACT immunotherapy (Verdegaal et al., 2016). This work showed that T cell-recognised neoantigens can be selectively lost during therapy either by the loss of the mutant allele as described above or downregulation of gene expression of the mutated gene. They showed that in one of the patients with advanced melanoma described in this study, DNA sequencing showed that a non-synonymous mutation in the CAD (Carbamoyl-Phosphate Synthetase 2) gene was still present in the genome, however, RNA expression showed a tenfold decrease compared to an earlier tumour sample. Our RNAseq data showed that recurrent melanomas that had lost the antigen, either by a genetic or epigenetic mechanism, were characterised by a non-inflamed tumour microenvironment as defined by the absence of an IFN gene signature. The melanomas with antigen loss recurred after complete regression to ACT immunotherapy suggesting a clonal origin. The absence of the antigen might have led to the reduced activation of the tumour-specific T lymphocytes and consequently reduced cytokine and chemokine release. This in turn, could lead to a reduction in recruitment of other immune cells to the TME. As these melanomas had only limited amounts of infiltrated immune cells they are referred to as 'cold' tumours. They would be unresponsive to salvage immune checkpoint as this therapy approach only invigorates already present tumour-reactive T

lymphocytes (Ayers et al., n.d.; Cristescu et al., 2018; Gajewski et al., 2017). Current research focuses in turning 'cold' tumours 'hot'. Amongst others, researchers use genetically-engineered oncolytic viruses that selectively infect and replicate in human cancer cells. These viruses can produce cytokines/chemokines to attract and mature APCs into the TME and thereby induced an anti-tumour T cell response (Ribas et al., 2017). Moreover, small-molecule IDO1 inhibitors are being tested to re-program inflammatory processes and restoring tumour immunosurveillance (Prendergast et al., 2018).

Recurrent CDK4^{R24C}-NFhp100 melanomas largely presented with persistent antigen expression and showed higher expression levels of IFN response genes, T cell marker genes but also negative immune checkpoint genes such as PD-1 and CTLA-4. Our data shows that the CDK4^{R24C}-NFhgp100 melanomas have a lower target antigen expression compared to TYRP1-NFhgp100 melanomas. We therefore propose that the lower antigen expression increases melanoma escape by the upregulation of negative immune checkpoint molecules in the tumour microenvironment. Benci and colleagues showed that chronic interferon signalling promotes transcriptomic and epigenomic features of resistant tumours and additionally drives PD-L1 independent resistance mechanisms. An interferon-driven multigenic resistance programme and the upregulation of negative immune checkpoint molecules generates the opportunity to treat these tumours with salvage immune checkpoint therapy such as anti-PD-L1 or anti-CTLA-4 (Benci *et al.*, 2016; Cristescu *et al.*, 2018; Ayers *et al.*, 2017).

When the ACT recurrent CDK4^{R24C}-NFhgp100 melanomas were treated with anti-PD-L1 salvage immune checkpoint therapy, we identified additional resistance mechanisms. For instance, we observed a melanoma escape anti-PD-L1 salvage therapy due to an antigen presentation defect identified by lower MHC class I expression upon IFN γ stimulation. B2M loss which leads to the abrogation of MHC class I antigen presentation and therefore loss of antigen recognition by immune cells has recently reported in human melanomas (Rodig et al., 2018; Zaretsky et al., 2016b; Zhao et al., 2016).

Although our model is a powerful experimental tool to explore therapy resistance

mechanisms in a controlled setting, there are still limitations/challenges to this model as it was presented in this chapter. While a larger cohort of HC.PmelKO.TYRP1-NFhgp100 and HC.PmelKO.CDK4^{R24C}-NFhgp100 mice were treated with ACT immunotherapy and relapse tumours were analysed, more patient-relevant resistance mechanisms could possibly be detected if more mice were analysed. Additionally, an experimental setup with different TCRtg T cells might help gain new insights into resistance mechanisms as pmel-1 TCRtg T cells are per se not naïve as they are constantly exposed to their cognate antigen. Nevertheless, research showed that pmel-1 T cells can escape peripheral and central tolerance. These TCRtg T cells are not completely refractory to stimulation by self-antigen (Overwijk et al., 2003). Moreover, other melanosomal or oncogenic targets could help to delineate whether the resistance mechanisms observed are just specific to the individual proteins we targeted, TYRP1 and CDK4^{R24C}, or whether the results also hold true for other targets that belong to the same class of proteins. Furthermore, a larger cohort of mice treated with salvage immunotherapy would be of advantage to investigate further resistance mechanisms. The RNA-seq analyses presented in this chapter only focussed on the melanoma phenotype, T cells and negative immune checkpoints, however, the data also offer the opportunity to gain more insights into other important aspects of the resistance mechanisms such as the composition of the TME.

We conclude that our novel CRISPEpitope approach, in combination with epitope-standardised ACT immunotherapy, recapitulates dynamic changes of the immune landscape in the tumour microenvironment that is also observed in patients. Our study showed that not only the presence of antigen but also the level of antigen expression determines the immune contexture of recurrent tumours and subsequently leads to different escape mechanisms to ACT immunotherapy.

Chapter 5:
Investigating the requirement of
antigen persistence on tumour
surveillance by T_{RM} cells

Chapter 5: Investigating the requirement of antigen persistence on tumour surveillance by T_{RM} cells

5.1. Introduction

Melanoma arises from the malignant transformation of melanocytes. Melanocytes are pigment producing cells that have a neural crest origin (Lin and Fisher, 2007). In humans, melanocytes are predominantly located in the uppermost layer of the skin, the epidermis, where they have a UV-protective function. They provide melanin to neighbouring keratinocytes (Costin and Hearing, 2007). Melanin scatters and absorbs UV radiation and it protects the keratinocytes' nuclei from UV-radiation induced DNA damage (Kaidbey et al., 1979).

Melanocytes can also be found in hair follicle bulbs, inner ear, eyes, central nervous system and mucous membranes (Dupin and Douarin, 2003). The majority of melanoma develops in the skin but may also occur at other sites. Different histopathology, genetic characteristics and etiology of melanomas make it a highly heterogeneous and complex disease. Clinically, melanomas are classified according to their anatomical site, growth pattern and pigmentation status. Cutaneous melanoma is the most frequent type in patients (Bastian, 2014).

Although treatment of melanoma has improved during the past few years, through the advent of targeted therapies and immunotherapeutic approaches, many patients do not respond to therapy or relapse. To tackle these problems, we require an in depth understanding of the tumour biology and the immune cells that mediate anti-tumour immunity. The use of *in vivo* models simulating true melanoma behaviour help to decipher the reciprocal interaction between the tumour and the tumour microenvironment including immune cells, vasculature and extracellular matrix. *In vivo* models must not only recreate these tumours and TME features but also model natural tumour progression. Better modelling of these melanoma characteristics will advance clinical translation and better treatment for melanoma patients.

Modelling of the disease is required to investigate the heterogeneity and high

complexity that we observe in human melanomas to analyse the essential contributors to this disease. The ideal melanoma model should be comparable to human melanoma with regard to pathology, epidemiology and genetic characteristics.

Although melanocyte development during embryogenesis is a conserved mechanism between species, human and mouse skin differ in their functional and anatomical features. These differences may influence melanoma initiation, progression and metastasis. The mammalian skin is consisting of the epidermis, which is formed by several layers of keratinocytes and the dermis, which is formed of connective tissue, sweat glands, hair follicles, nerves and vasculature. Compared to mouse, human skin is generally thicker. Human melanocytes are located at the dermo-epidermal junction and in the hair follicles and they divide more infrequently than in mice (Jimbow et al., 1975). Mouse skin is thinner as the epidermis only contains two to three layers of keratinocytes. Murine melanocytes are primarily found in the bulb regions of the hair follicles. Melanomas generated in genetically engineered mouse models mainly develop in the dermis of the mouse skin and only share limited histological similarities with human melanomas which primarily develop in the basal layer of the epidermis (Pérez- Guijarro et al., 2017).

One of the *in vivo* murine melanoma models is the syngeneic transplantation model that dates back to the 1950s (Teicher, 2010). These models have the benefit that syngeneic tumour cell lines are transplanted in immunocompetent mice which allows the interaction of tumour cells with the host's immune system. One popular syngeneic melanoma model uses the B16 melanoma cells that spontaneously formed after chemical induction of melanoma in C57BL/6 mice. When transplanted subcutaneously or intracutaneously, B16 variants have fast tumour growth kinetics and mice have to be sacrificed within two or three weeks after transplantation (Glodde et al., 2017; Herlyn and Fukunaga-Kalabis, 2010; Park et al., 2019). Recently, a novel orthotopic model of epicutaneous melanoma transplantation has been developed. Mice are inoculated with B16 melanoma cells by abrading the epidermis and placing melanoma cells embedded in matrigel onto the abraded skin, tumour growth kinetics are slower. Approximately

60% of the mice develop tumours within three weeks following epicutaneous inoculation. Due to the slower tumor growth kinetics mice often do not need to be sacrificed until several weeks following inoculation. Moreover, 40 % of the mice do not develop macroscopic tumours (Park et al., 2019; Wylie et al., 2015). The epicutaneous inoculation method mimics melanoma formation in human patients as human melanomas develop in the epidermis. By slower growth kinetics the immune system stands a chance to mount an adaptive immune response before the mice have to be sacrificed due to large tumours.

In the past few years, several studies have shown that T_{RM} cells are directly involved in controlling tumour outgrowth in experimental mouse models (Enamorado et al., 2017; Malik et al., 2017; Nizard et al., 2017; Park et al., 2019). In the epicutaneous melanoma model, it was shown that 40% of tumour-inoculated mice do not develop progressively growing melanoma due to T_{RM} cells at the tumour inoculation site. These so-called non-developer mice do not have macroscopic tumours, however, if analysed using intravital imaging, we observed a few residual tumour cells that are surrounded by tumour-reactive T cells that have adopted a more dendritic-like cell morphology as opposed to their circulating counterparts. This dendritic-like cell morphology is a characteristic of T_{RM} cells. We observed that the $CD8^+ CD103^+$ T_{RM} cells dynamically control the melanoma cells in the skin. T_{RM} cells are sufficient to control melanoma outgrowth independently of circulatory tumour-reactive T cells and when depleted the mice succumb to significantly more tumours (Park et al., 2019). However, the underlying mechanism of T_{RM} cells in melanoma control is not fully understood. The aim of this project was to investigate whether tumour cells need to present antigen constantly to T_{RM} cells in the skin for long term tumour control or whether this control is partially mediated by bystander cells in an antigen-independent manner in an epicutaneous melanoma model. Putative bystander cells include NK cells and T cells activated in an antigen-independent manner. For this purpose, we developed a CRISPR/Cas9-based approach that relies on the CRISPRitope technique presented in Chapter 3. The CRISPR/Cas9-based approach used here, termed SWITCHitope, enables us to abrogate antigen expression of melanoma cells *in vivo* using a Tamoxifen-inducible system.

5.2. Results

5.2.1. Histological characterisation of epicutaneous melanoma model

For this study we used a transplantable model of skin-contained melanoma development. This model is called epicutaneous melanoma model. The melanoma in this model arises in the skin but grows subcutaneously and metastasises as it develops. This model involves transplanting melanoma cells into the epidermis, the outermost layer of the skin (Wylie et al., 2015). We inoculated C57BL/6 mice epicutaneously with B16.gB melanoma cells. B16.gB melanoma cells express the model antigen gB which can be recognised by TCRtg gBT-I T cells. We observed that the epicutaneous B16.gB melanomas show the expected growth kinetics as reported by Park and colleagues (Park et al., 2019). We observed two distinct growth patterns: early and late developers. The earliest melanomas arose around day ten whereas the later ones started growing around day 21 post-inoculation (Figure 5.1). We analysed the tumours histologically and performed H&E (haematoxylin and eosin) stain and immunohistochemistry (IHC) for the melanocytic protein gp100. The H&E stain was used to reveal general skin tissue features whereas the IHC for gp100 was used to identify melanoma cells. We analysed the tumour margin and different areas of the tumour centre. When looking at the tumour margin, we saw a thickening of the epidermis in the H&E stain which co-localised with a positive gp100 stain, largely contained within the epidermis (Figure 5.2). The further we cut into the tissue, the larger the tumour became and the more the skin tissue architecture was disrupted. The melanoma cells grew through the basement membrane and penetrated into the dermal and subcutaneous layers of the skin (Figure 5.2C and D). Additionally, we observed a slough within the tumour (Figure 5.2A and B).

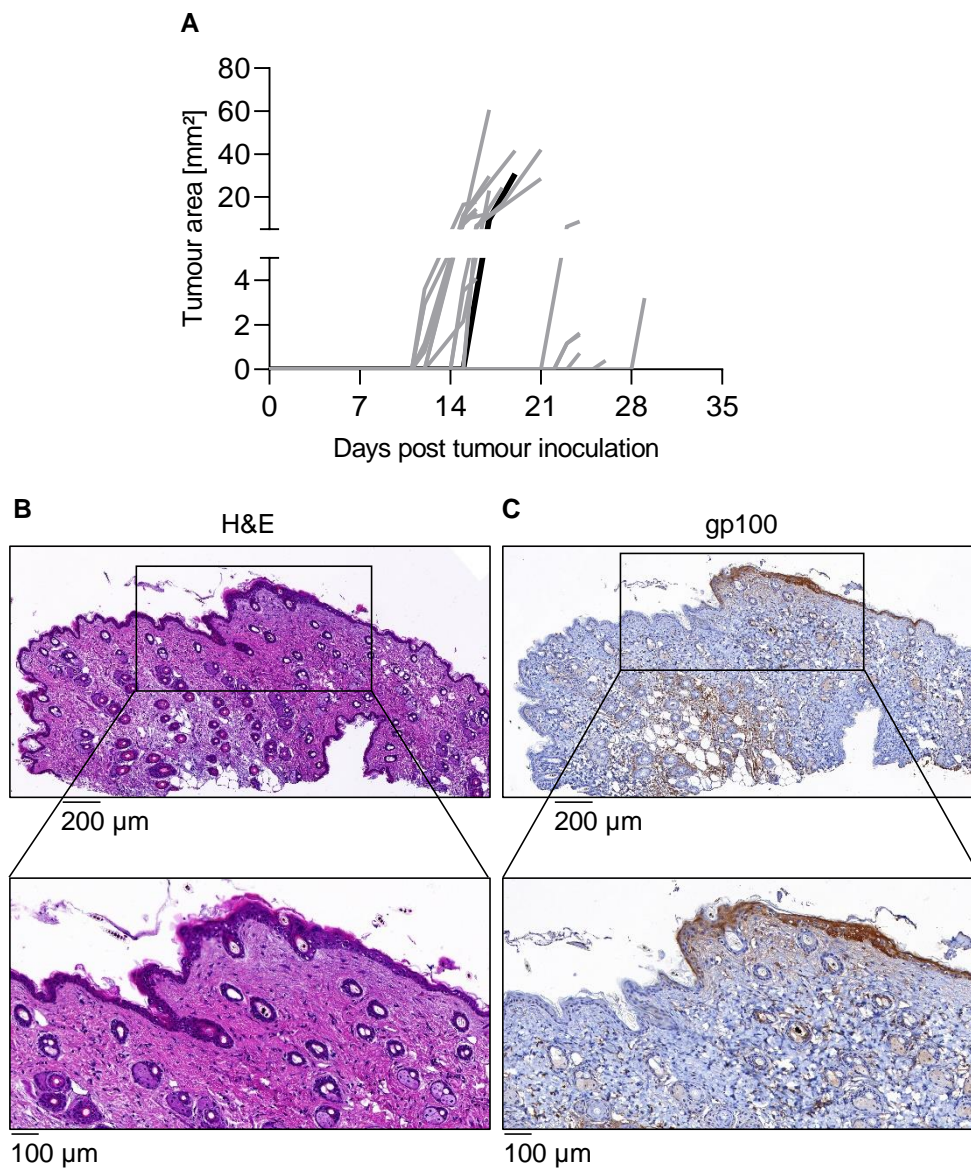


Figure 5.1: Histological analysis of epicutaneous B16.gB melanoma in C57BL/6 mice (tumour margin)

(A) Growth curves of cohort of mice (n = 20) inoculated with B16.gB melanoma. Black line represents mouse 3-4. (B) Representative H&E slides and (C) gp100 IHC slides of tumour of mouse 3-4. Images depict the tumour margin. Magnification: top panels – 20x, bottom panels – 40x. Slides were prepared by the Biomedical Histology Facility – University of Melbourne.

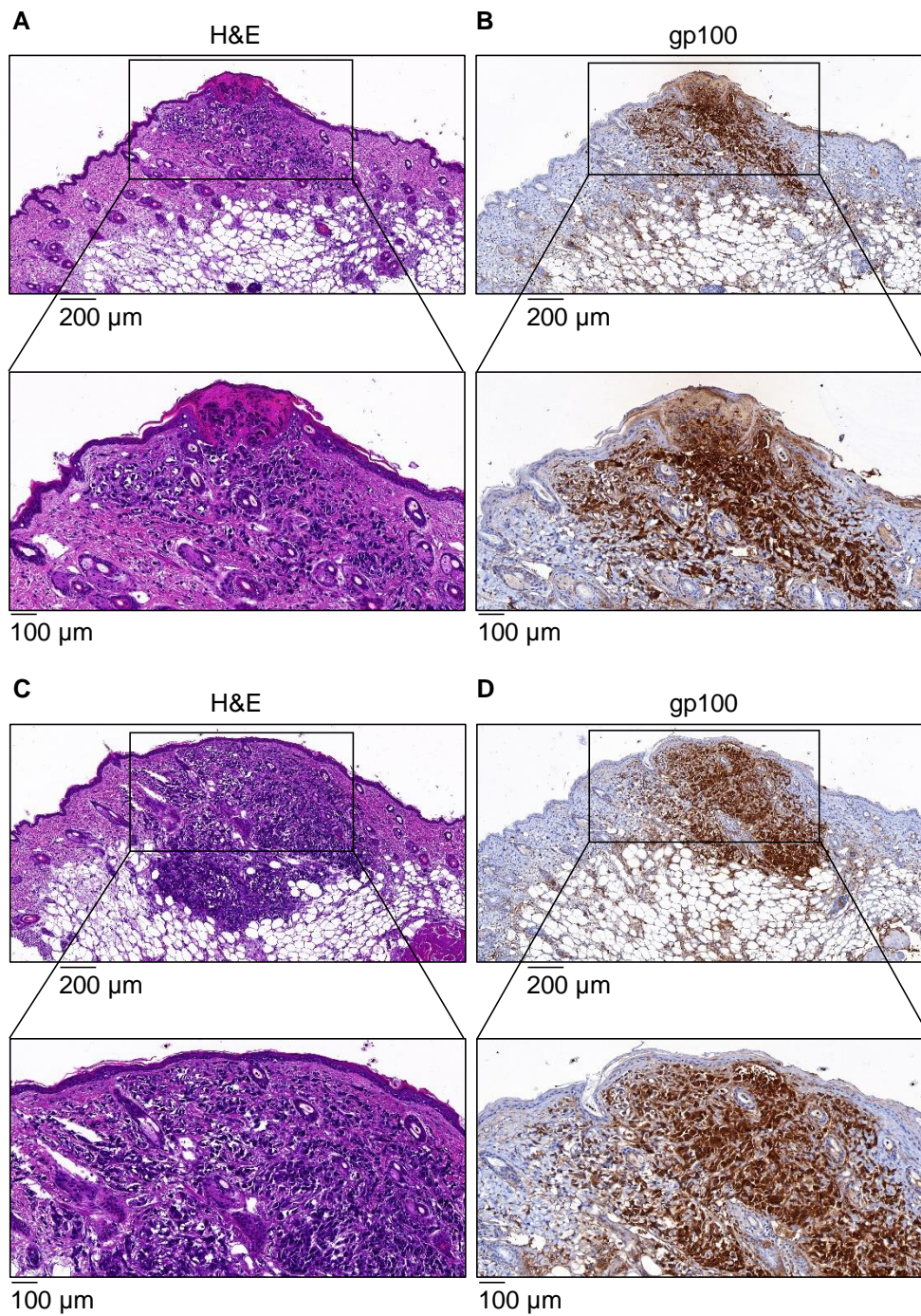


Figure 5.2: Histological analysis of epicutaneous B16.gB melanoma in C57BL/6 mice (tumour centre)

(A, C) Representative H&E slides and (B,D) gp100 IHC slides of tumour of mouse 3-4. Images depict different areas of the tumour centre. Magnification: top panels – 20x, bottom panels – 40x. Slides were prepared by the Biomedical Histology Facility – University of Melbourne.

One feature of the epicutaneous melanoma model is that spontaneously metastasis into the skin-draining brachial lymph node can occur. We analysed brachial lymph nodes of melanoma inoculated mice that had macroscopically visible metastases. On the microscopic level we saw that in the area where the lymphatic vessels enter the lymph node, there was an accumulation of cells that had larger nuclei than the majority of the cells within the lymph node and that these cells were gp100⁺ indicating that the melanoma cells have infiltrated the lymph node (Figure 5.3).

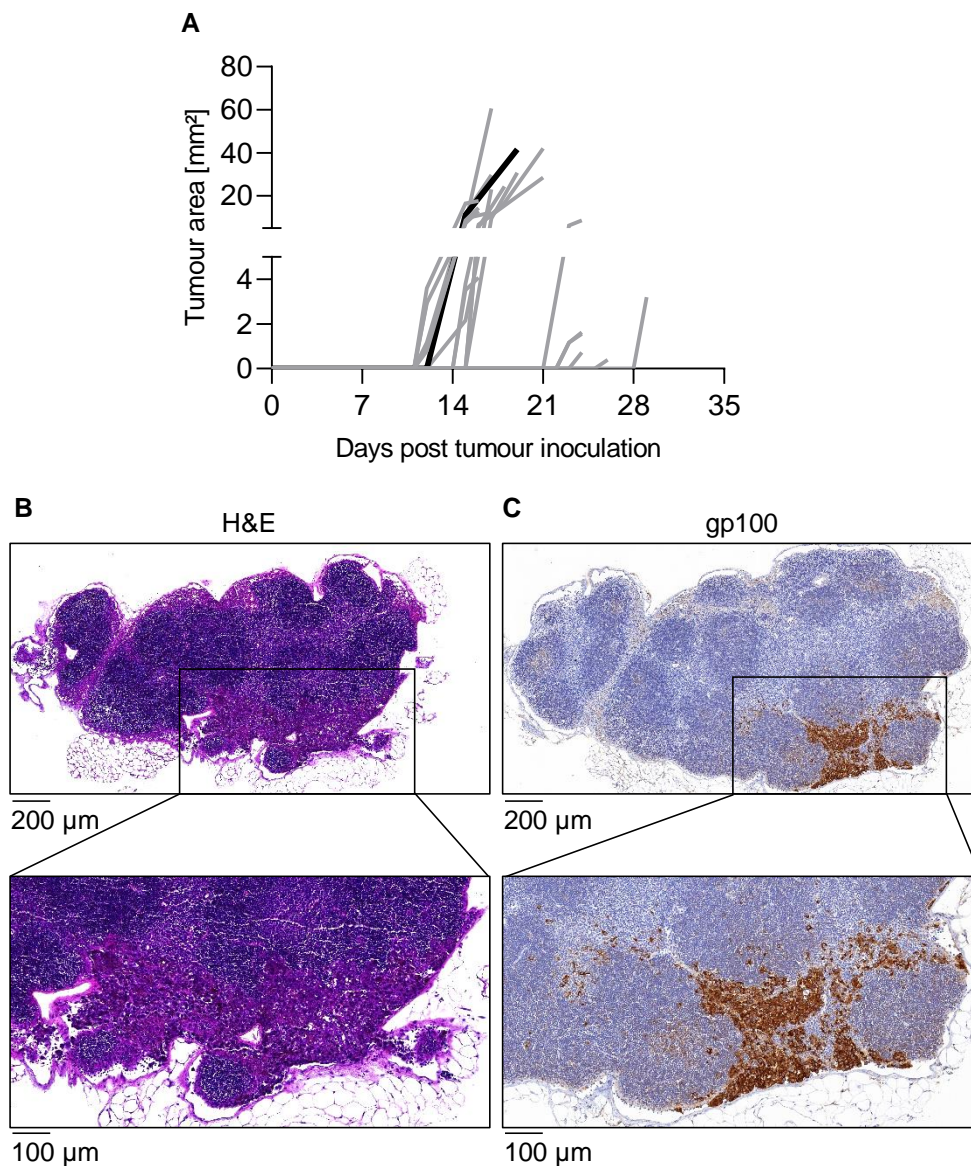


Figure 5.3: Histological analysis of skin-draining brachial lymph node metastasis of epicutaneous B16.gB melanoma in C57BL/6 mice

(A) Growth curves of cohort of mice (n = 20) inoculated with B16.gB melanoma. Black line represents mouse 1-1. (B) Representative H&E slides and (C) gp100 IHC slides of skin-draining brachial lymph node of mouse 1-1. Magnification: top panels – 15x, bottom panels – 30x. Slides were prepared by the Biomedical Histology Facility – University of Melbourne.

5.2.2. Generation of SWITCHitope tagging plasmid

As described in the previous chapters, we developed an easy and efficient polyclonal approach to tag any desired protein with a fluorescent protein and a CD8+ T cell epitope by modifying the CRISPaint approach published by Schmid-Burgk and colleagues (Schmid-Burgk et al., 2016). We further modified the previously described CRISPaint approach by changing the universal donor (UD) plasmids and combining it with a tamoxifen-inducible Cre recombinase. This approach was termed SWITCHitope because the expression of the epitope can be switched off and monitored by a colour change due to switching on a second fluorescent marker of the engineered melanoma cells.

The SWITCHitope approach also relies on the three-plasmid system described in Chapter 3. Plasmid #1 is the target selector and plasmid #2 is the frame selector. Plasmid three is the UD. The UD encodes the following components: mScarlet fluorescent protein – FLAG – loxP - epitope – T2A – Blasticidin resistance – loxP – T2A – mNeon. The UD is integrated into the mammalian genome via non-homologous end-joining (NHEJ) at the DSB induced by the target selector (Figure 5.4).

The UD was generated by digesting the pCRISPaint-mScarlet-F-hgp100-BlastR with the enzyme AvrII and DraIII and cloning a de novo synthesised DNA fragment coding for loxP - epitope – T2A – Blasticidin resistance – loxP – T2A – mNeon into this plasmid backbone. This plasmid was called pCRISPaint-SWITCHgB.

When melanoma cells are engineered using the SWITCHitope approach, the target protein has an extended modified C-terminus. The melanoma cells express mScarlet, a FLAG-tag, the HSV-1 gB epitope and a Blasticidin resistance cassette. When the Cre recombinase that is present in the melanoma cells translocates from the cytosol to the nucleus and thereby becomes active, the loxP sites that are part of the UD plasmid are targeted. By this the DNA that resides within the two loxP sites becomes excised. Thereby the melanoma cell becomes mScarlet and mNeon positive but epitope negative (Figure 5.5).

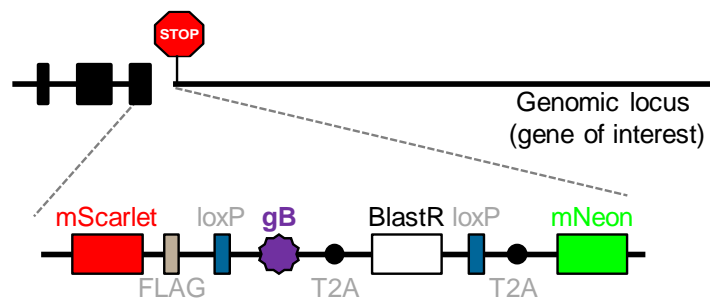


Figure 5.4: SWITCHitope universal donor plasmid to fuse a floxed model CD8⁺ T cell epitope to endogenous gene products

Graphical depiction of the universal donor plasmid that integrates into the genome at a designated DNA double-strand break generated by Cas9.

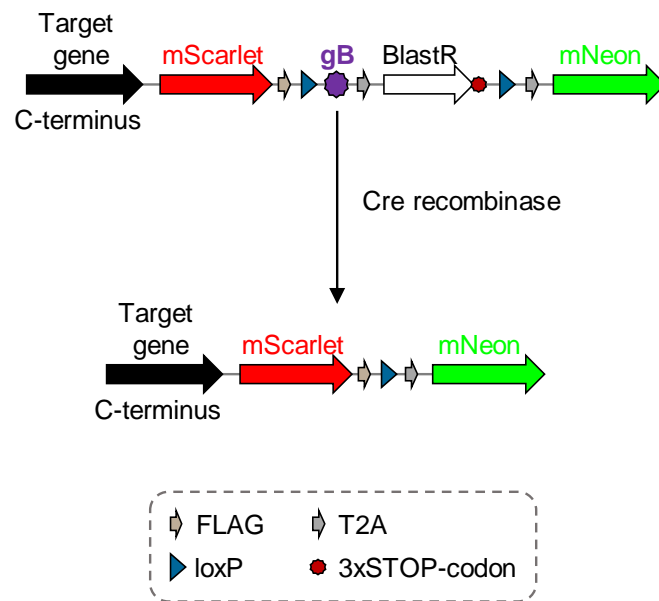


Figure 5.5: Cre-recombinase excises floxed HSV-1 gB epitope which can be monitored by a colour switch

Graphical depiction of C-terminus of target genes after genome engineering using SWITCHitope plasmids before and after Cre-recombinase activity.

5.2.3. Generation of B16 melanoma cells with inducible antigen depletion

For this study, we used the B16 murine melanoma cell line. Firstly, we knocked out the protein Tyrosinase (Tyr) which is responsible for pigment production using a CRISPR/Cas9 knockout plasmid that targeted exon 1 as in the future intravital imaging is planned and pigment of the melanoma cells complicates imaging. (Figure 5.6A). The following experiments were performed by Debby van den Boorn-Konijnenberg, a former member of the Hölzel laboratory. B16 melanoma cells were transfected with a plasmid expressing a Cas9, a sgRNA targeting the first exon of the Tyrosinase gene and GFP. Forty-eight hours after transfection, GFP-positive cells were sorted and plated as monoclonal cells. After establishing monoclonal cultures, cells were analysed using NGS. The data was analysed using the Outknocker 1.2 web tool showing a homozygous knockout of the Tyrosinase gene when aligned against the wildtype sequence in exon 1 in one of the monoclonal cultures (Figure 5.6B). Of note, the B16 cell line is triallelic in many loci (Schmid-Burgk et al., 2014). We performed additional validation of the knockout cells by treating wildtype B16 and B16.TyrKO melanoma cells with Trametinib (1000 nM, 3 days), which inhibited ERK also known as mitogen-activated protein kinase 1, and induced pigment production in melanoma cells. The B16.TyrKO melanoma cells could no longer produce pigment as compared to wildtype B16 cells (Figure 5.6C). The B16.TyrKO cell line established in this experiment was the basis for the following experiments.

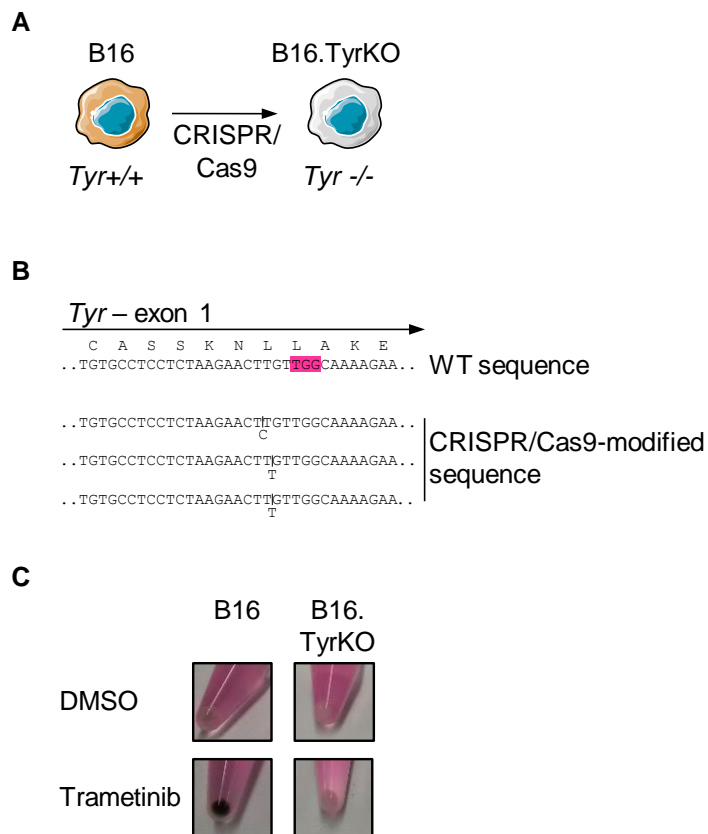


Figure 5.6: Generation of B16.TyrKO melanoma cells using CRISPR/Cas9

(A) Graphical depiction of the generation of Tyrosinase (*Tyr*)-deficient B16 cells (B16.TyrKO). (B) Genomic validation of B16.TyrKO. cells; pink: PAM. (C) Cell pellets of wildtype B16 and B16.TyrKO. cells after Trametinib treatment (1000nM, 3 days). DMSO was used as mock treatment. This experiment was performed by Debby van den Boorn-Konijnenberg.

Next, we generated B16.TyrKO melanoma cells that express tamoxifen-inducible Cre recombinase (Cre-ERT2) by retroviral transduction. We used either the plasmid #22776 (MSCV Cre-ERT2 puro) or #59701 (pRetroQ-Cre-ERT2) for the transduction. After successful selection with puromycin (1 μ g/ml, 3 days), we analysed whether the melanoma cells expressed the Cre-ERT2 on gDNA and mRNA (cDNA) level (Figure 5.7). Both plasmids were successfully integrated into the genomic DNA of the B16.TyrKO melanoma cells and were expressed at the mRNA level.

Then, after generating melanoma cells that stably expressed Cre-ERT2, we transfected these cells with our SWITCHitope plasmids. We chose the housekeeping genes β -Actin (Actb) and γ -Actin (Actg1) as target for the C-terminal fusions as these genes have high and stable expression levels (Figure 5.8).

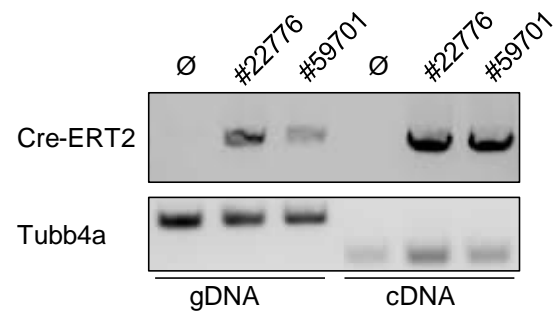


Figure 5.7: B16.TyrKO melanoma cells express Cre-ERT2 after retroviral transduction

PCR analysis of Cre-ERT2 expression on genomic DNA (gDNA) and complementary DNA (cDNA) level of B16.TyrKO melanoma cells transduced with retroviral particles coding for either the plasmid #22776 or #59701. Tubb4a was used as loading control.

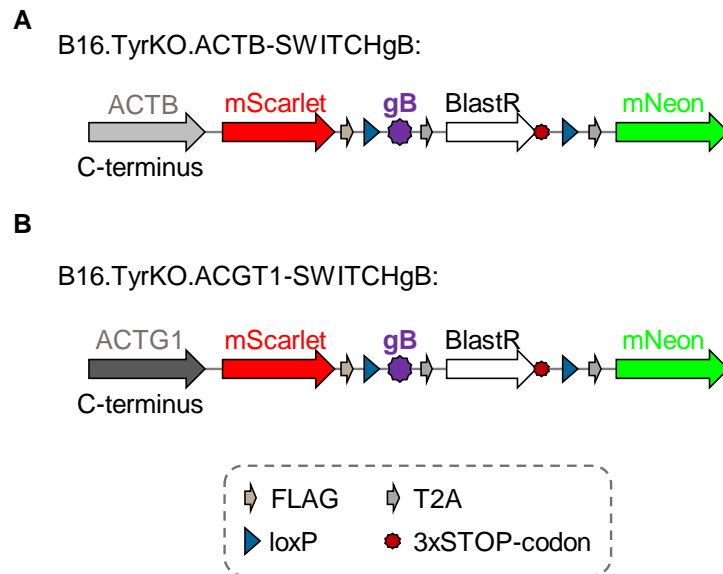


Figure 5.8: The housekeeping proteins β -Actin and γ -Actin were targeted by the SWITCHitope approach

Graphical depiction of the housekeeping proteins (A) β -Actin (ACTB) and (B) γ -Actin (ACTG1) targeted by the SWITCHitope approach in B16.TyrKO melanoma cells expressing Cre-ERT2.

5.2.4. Cre-ERT2 plasmid #22776 has less spontaneous activity than #59701

Before generating monoclonal cell lines for T cell activation and *in vivo* experiments, we analysed spontaneous translocation of Cre-ERT2 into the nucleus and resulting colour switch (leakiness of the construct) in the polyclonal cultures. If the Cre-ERT2 spontaneously translocates from the cytosol to the nucleus, it excises the DNA that resides within the two loxP sites which leads to the expression of mNeon. We analysed the melanoma cells that were transduced with the #22776 plasmid and transfected with the SWITCHitope plasmids by flow cytometry. All successfully transfected melanoma cells should be mScarlet⁺ but if the Cre-ERT2 construct was leaky we would observe mNeon⁺ cells. Cre-ERT2 plasmid #22776 had very little leakiness as only 0.19 % or 0 % of the ACTB- or ACTG1- targeted mScarlet⁺ melanoma cells were also mNeon⁺, respectively (Figure 5.9). Next, we performed the same experiment for the melanoma cells transduced with the Cre-ERT2 plasmid #59701. This plasmid had higher leakiness compared to #22776 and 0.18 % or 4.22 % of the ACTB- or ACTG1- targeted mScarlet⁺ melanoma cells were also mNeon⁺, respectively (Figure 5.10).

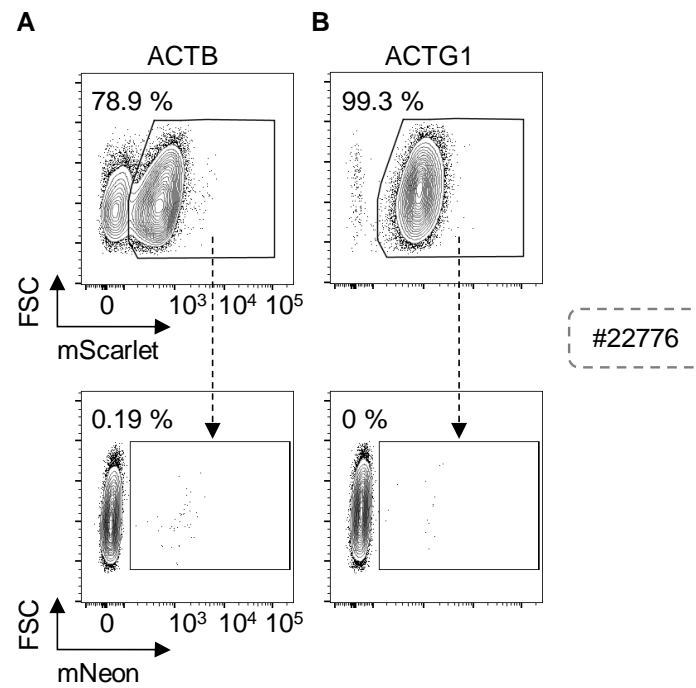


Figure 5.9: Plasmid #22776 shows little spontaneous Cre-ERT2 activity

Flow cytometry analysis of baseline mScarlet and mNeon expression of B16.TyrKO cells that were transduced with the Cre-ERT2 plasmid #22776; either ACTB (A) or ACTG1 (B) were targeted by the SWITCHitope approach.

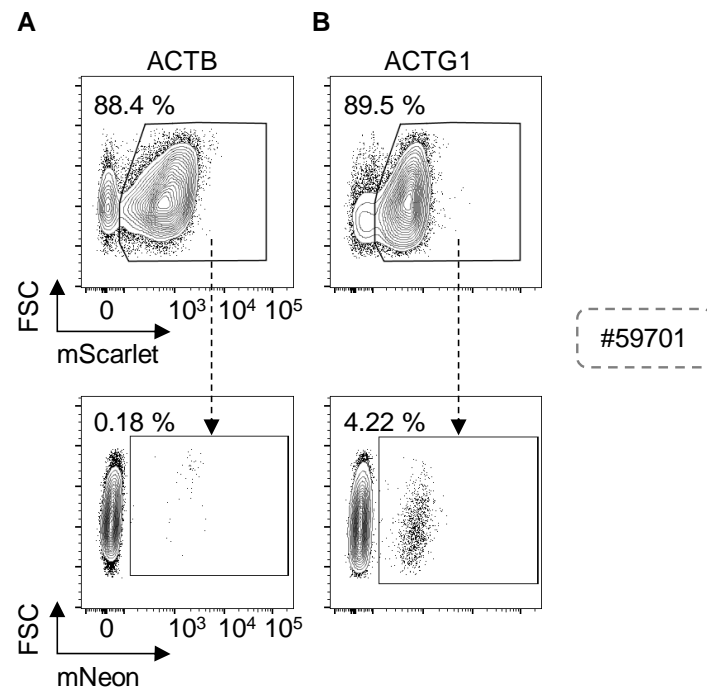


Figure 5.10: Plasmid #59701 has higher spontaneous Cre-ERT2 activity than plasmid #22776

Flow cytometry analysis of baseline mScarlet and mNeon expression of B16.TyrKO cells that were transduced with the Cre-ERT2 plasmid #59701; either ACTB (A) or ACTG1 (B) were targeted by the SWITCHitope approach.

Next, we wanted to compare two different Cre-ERT2 plasmids regarding antigen depletion by monitoring the induction of mNeon expression upon tamoxifen treatment. We titrated time and dose of 4-Hydroxytamoxifen (4-OHT), the active metabolite of tamoxifen, using B16.TyrKO.ACTB-SWITCHgB transduced with either #22776 or #59701. We treated the melanoma cells for 24 h, 48 h or 72 h with increasing concentrations of 4-OHT (0, 100, 250, 500 and 1000 nM) and analysed the cells by flow cytometry immediately after the end of the treatment or 48 h or 96 h afterwards. We saw a better response 48 h after the end of the treatment than immediately after but no increase in the response when we waited for 96 h after the treatment (data not shown). Therefore, only results that were analysed 48 h after the end of the treatment are shown. We observed a time and dose effect of 4-OHT on the mNeon induction in B16.TyrKO.ACTB-SWITCHgB expressing either of the two Cre-ERT2 plasmids (Figures 5.11A and 5.12A). Additionally, we observed that the mean fluorescence intensity (MFI) of mScarlet increased when the cells were treated with 4-OHT (Figures 5.11B and 5.12B). When the melanoma cells were treated with 1000 nM of 4-OHT for 72 h and analysed 48 h after the end of the treatment, we observed 87.8 % mNeon⁺ cells using the Cre-ERT2 construct #22776 compared to 60 % using the construct #59701 (Figures 5.11C and 5.12C). We observed that when the melanoma cells were treated with 4-OHT the cells do not only become mNeon positive but they also show two distinct mScarlet populations (mScarlet^{low} vs. mScarlet^{high}). For the following experiments only the B16.TyrKO melanoma cells that were transduced with #22776 were used as they have less leakiness of the Cre-ERT2 construct and better induction of mNeon compared to #59701.

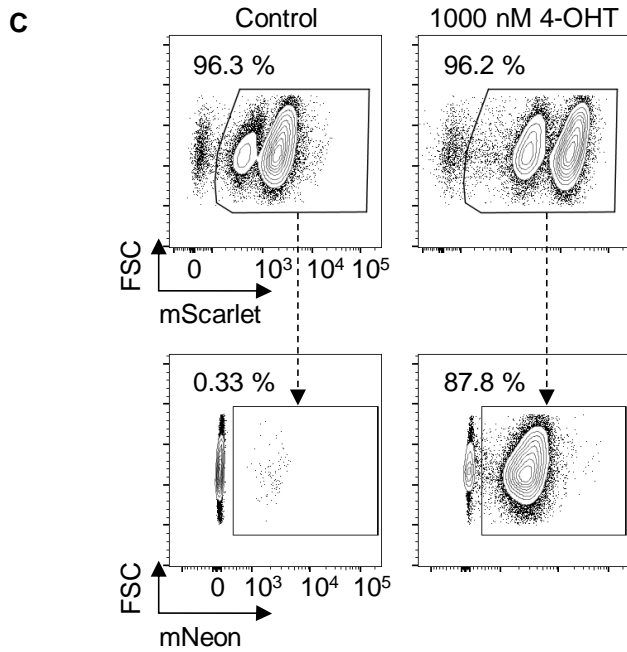
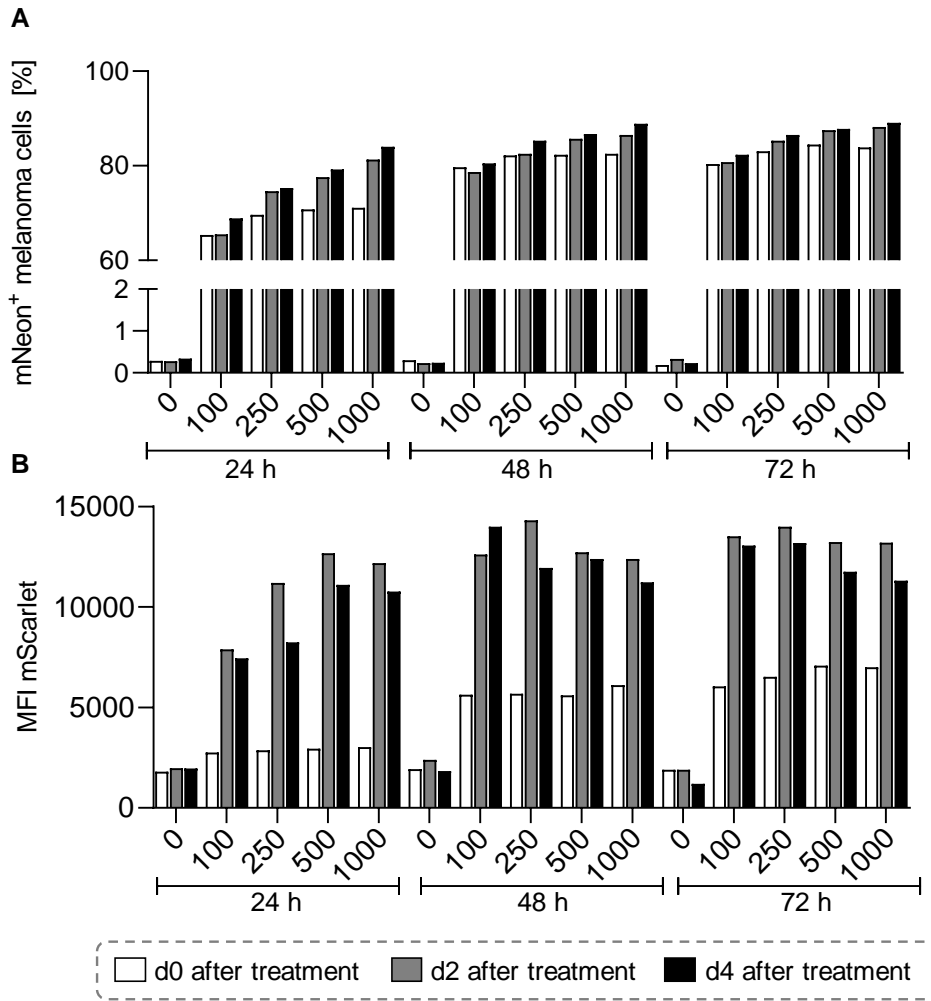


Figure 5.11: 4-OHT induces mNeon expression in B16.TyrKO.ACTB-SWITCHgB-#22776

Flow cytometry analysis of (A) mNeon⁺ cells and the (B) mean fluorescence intensity (MFI) of mScarlet in B16.TyrKO.ACTB-SWITCHgB-#22776 treated with 0-1000 nM 4-Hydroxytamoxifen (4-OHT) for 24-72 h hours (n = 1). (C) Representative contour plots comparing mScarlet and mNeon expression in the melanoma cells treated with 1000 nM 4-OHT for 72 h.

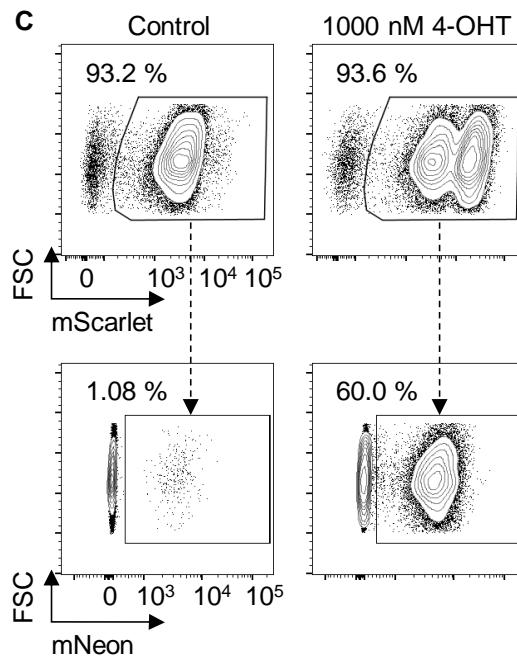
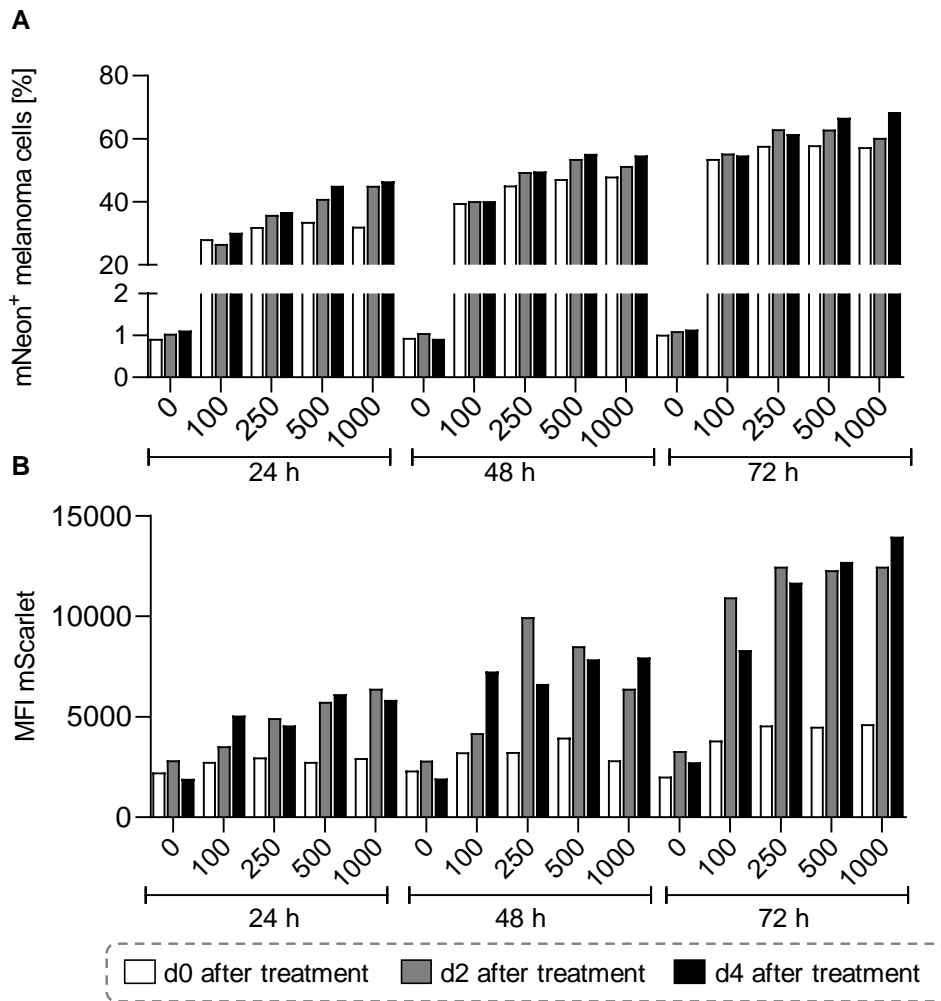


Figure 5.12: 4-OHT induces mNeon expression in B16.TyrKO.ACTB-SWITCHgB-#59701

Flow cytometry analysis of (A) mNeon⁺ cells and the (B) mean fluorescence intensity (MFI) of mScarlet in B16.TyrKO. ACTB-SWITCHgB-#59701 treated with 0-1000 nM 4-Hydroxytamoxifen (4-OHT) for 24-72 h hours (n = 1). (C) Representative contour plots comparing mScarlet and mNeon expression in the melanoma cells treated with 1000 nM 4-OHT for 72 h.

5.2.5. The target γ -actin shows a more robust switch upon 4-hydroxytamoxifen treatment than the target β -actin

After we had chosen the Cre-ERT2 construct to be used for all further experiments, we next evaluated the target gene. We compared B16.TyrKO.ACTB-SWITCHgB and B16.TyrKO.ACTG1-SWITCHgB after 96 h and 120 h of 4-OHT treatment by flow cytometry. The B16.TyrKO.ACTB-SWITCHgB melanoma cells were 95.2 % mNeon⁺ after 120 h of 4-OHT treatment whereas the B16.TyrKO.ACTG1-SWITCHgB cells were 99 % mNeon⁺ (Figures 5.13 and 5.14). Therefore, we chose the cell line B16.TyrKO.ACTG1-SWITCHgB for cell sorting. We sorted for mScarlet^{high} melanoma cells and single cells were cultured.

We screened 20 monoclonal cell lines and chose three, 1G9, 1H9 and 2C3, as these had the most desirable characteristics; similar growth kinetics to the polyclonal culture and parental B16 cell line and had the most reliable switch upon 4-OHT treatment. Clone 1G9 had the lowest background mNeon expression but the weakest mNeon induction upon 4-OHT treatment (Figure 5.15A). Clone 1H9 had higher mNeon background expression compared to 1G9 but also better induction of mNeon expression upon 4-OHT treatment (Figure 5.15B). Clone 2C3 had the best mNeon induction upon 4-OHT treatment after only 24 h of treatment but also had the highest background expression of mNeon of the three chosen clones (Figure 5.15C).

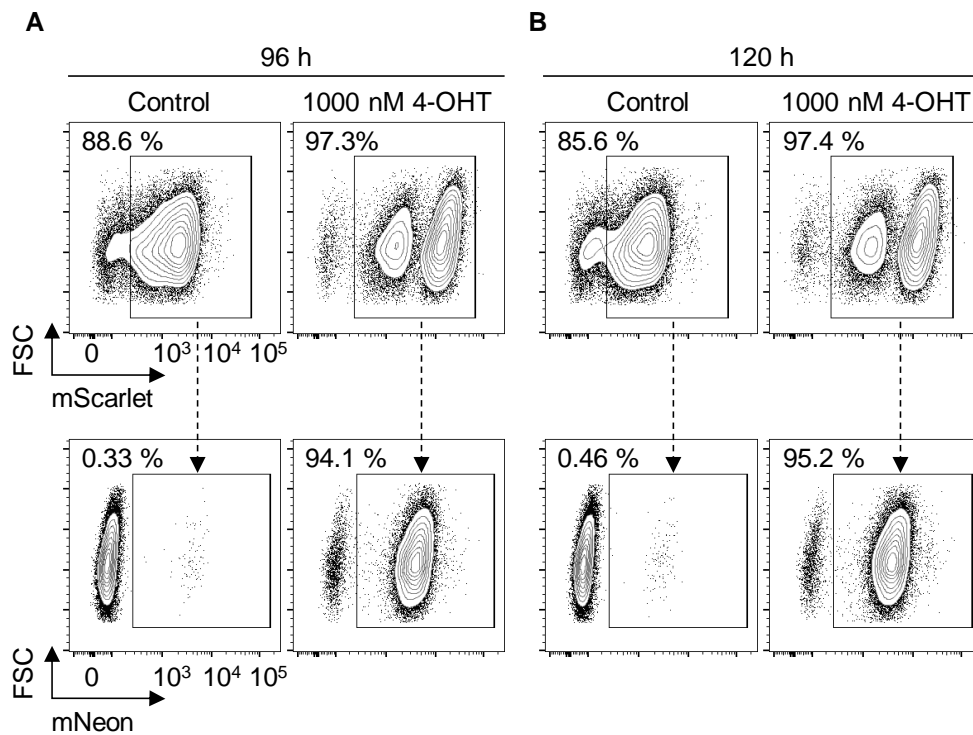


Figure 5.13: Extended treatment with 4-OHT induces robust mNeon expression in B16.TyrKO.ACTB-SWITCHgB-#22776

Flow cytometry analysis of mScarlet and mNeon expression in B16.TyrKO.ACTB-SWITCHgB-#22776 cells after (A) 96 h or (B) 120 h treatment with 1000 nM 4-OHT.

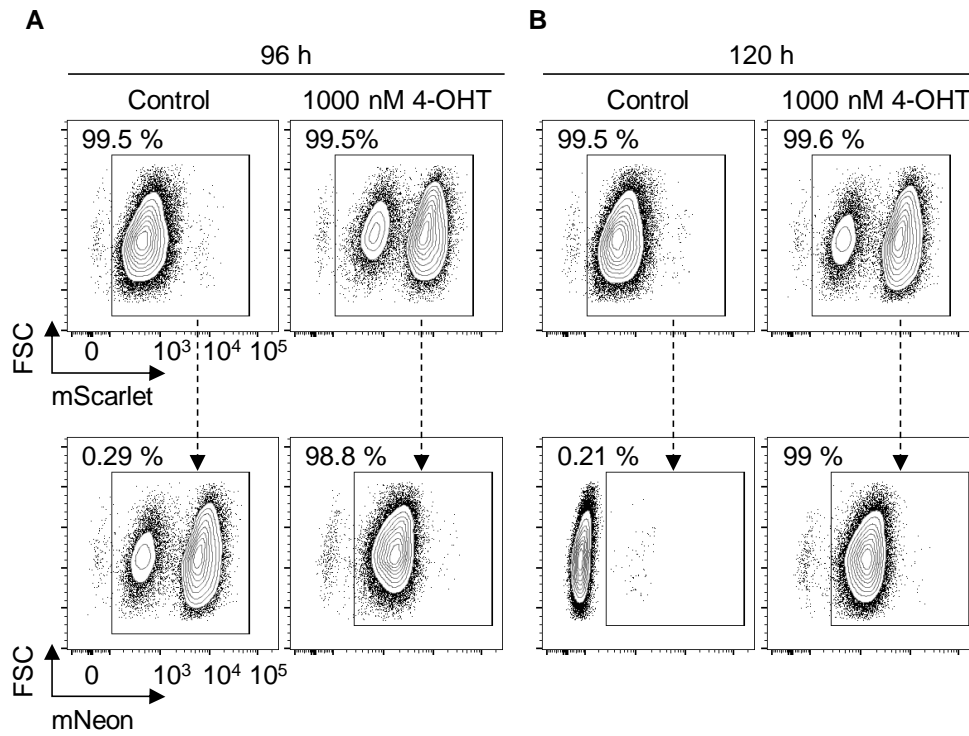


Figure 5.14: SWITCHitope-targeted ACGT1 induces a more robust mNeon expression upon 4-OHT treatment than ACTB

Flow cytometry analysis of mScarlet and mNeon expression in B16.TyrKO.ACTG1-SWITCHgB-#22776 cells after (A) 96 h or (B) 120 h treatment with 1000 nM 4-OHT.

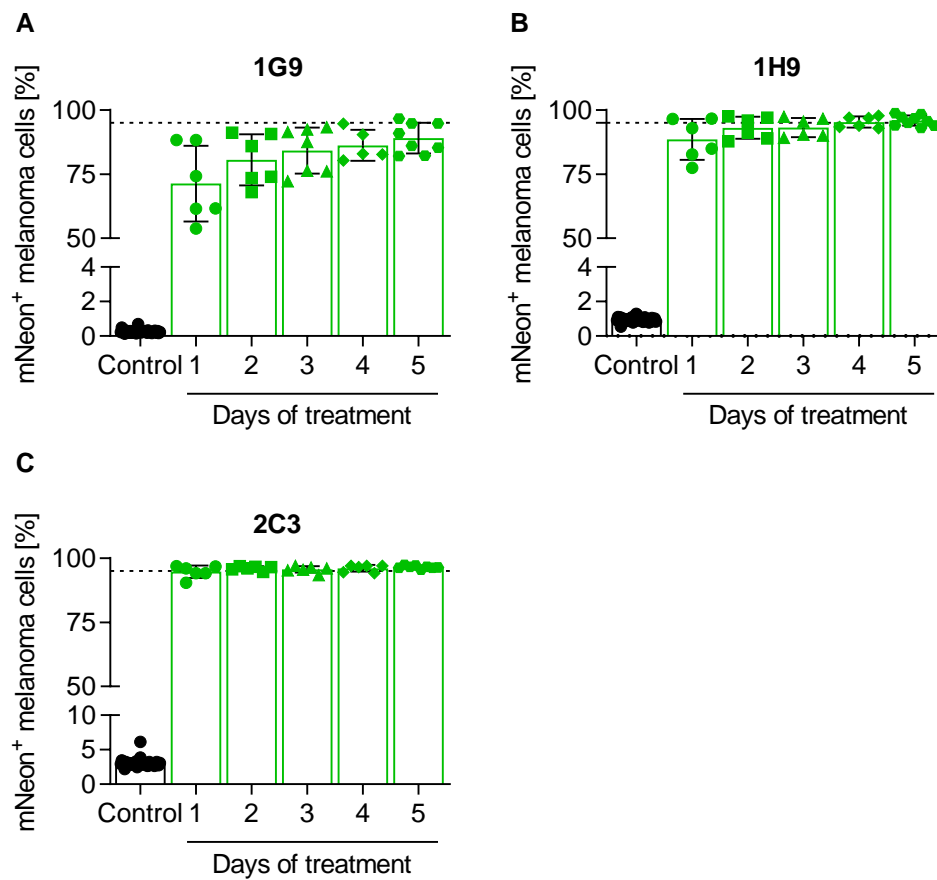


Figure 5.15: Monoclonal B16.TyrKO.ACTG1-SWITCHgB cell lines robustly induce mNeon expression upon 4-OHT treatment

Quantification of mNeon expression after treatment of monoclonal melanoma cells with 1000 nM 4-OHT for 1 to 5 days. Monoclonal cell lines are called (A) 1G9, (B) 1H9 and (C) 2C3. ($n \geq 5 \pm SD$).

5.2.6. SWITCHitope-engineered melanoma cells can activate T cells

Next, we wanted to analyse whether our SWITCHitope-engineered melanoma cells could activate T cells and whether T cell activation was abrogated upon induced antigen loss.

Firstly, we analysed the capacity of the three monoclones to upregulate MHC class I (H2-Kb) expression upon IFN γ stimulation as this is a prerequisite for antigen presentation and therefore T cell activation. All three monoclonal cell lines were treated \pm 4-OHT (1000 nM, 120 h) and \pm IFN γ (0.1 ng/ml, 18 h). All cell lines upregulated MHC class I upon IFN γ stimulation independently of 4-OHT treatment and were therefore equally suited to activate T cells (Figure 5.16).

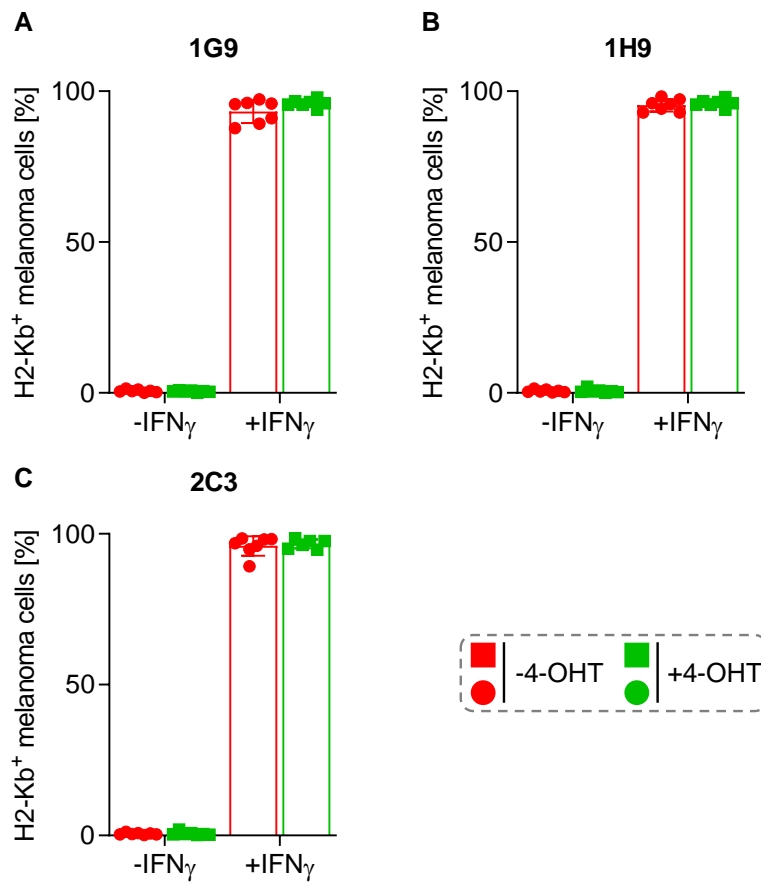


Figure 5.16: Monoclonal B16.TyrKO.ACTG1-SWITCHgB cell lines upregulate H2-Kb expression upon IFN_γ stimulation

Quantification of H2-Kb expression after stimulation with IFN_γ (0.1 ng/ml, 18 h) in combination with 4-OHT treatment in the monoclonal cell lines (A) 1G9, (B) 1H9 and (C) 2C3. (n ≥ 6, mean ± SD).

Following validating that the SWITCHitope-engineered melanoma cells can actually switch-off antigen expression upon 4-OHT treatment and upregulate MHC class I, we wanted to confirm that these cells could activate T cells, and moreover whether 4-OHT treatment leads to abrogation of T cell activation. We treated the monoclonal melanoma cells with 4-OHT (120 h, 1000 nM) and started the T cell activation assay two days after the end of the treatment. Prior to the co-culture of the melanoma cells with gBT-I TCRtg T cells that recognise the HSV-1 gB epitope, we stimulated the melanoma cells with IFN γ (0.1 ng/ml, 18 h). We co-cultured the melanoma cells and the *in vitro* activated gBT-I T cells in a 1:0.5 ratio for 5 h in Brefeldin A-containing media. After the co-culture, we analysed the gBT-I T cells for intracellular IFN γ and TNF α expression by flow cytometry. All three monoclonal melanoma cell lines induced IFN γ and TNF α expression in gBT-I T cells and treatment of the melanoma cells with 4-OHT led to significantly reduced T cell activation. Nevertheless, the 4-OHT-treated melanoma cell lines still induced T cell activation above the background level and we did not observe complete abrogation of T cell activation (Figures 5.17A, 5.17B, 5.17C and 5.18A, 5.18B, 5.18C and 5.19A, 5.19B, 5.19C). As expected, T cell activation was dependent on IFN γ pre-stimulation of the melanoma cells (Figures 5.17A, 5.17B and 5.18A, 5.18B and 5.19A, 5.19B).

As a control, we performed the same co-culture experiment with the SWITCHitope melanoma cells and OT-I TCRtg T cells to validate that T cell activation was antigen-specific. When we co-cultured all three monoclonal melanoma cells with pre-activated OT-I T cells, we did not observe expression of IFN γ and TNF α in the OT-I T cells (Figures 5.17D, 5.17E and 5.18D, 5.18E and 5.19D, 5.19E).

When we compared the fold change of IFN γ ⁺ and TNF α ⁺ gBT-I T cells, we observed the most significant decrease in IFN γ ⁺ gBT-I T cells when co-cultured with 1G9 and the most significant decrease in TNF α ⁺ gBT-I T cells when co-cultured with 1H9 (Figure 5.20). Based on the results from these *in vitro* experiments, we decided to use the monoclonal melanoma cell line B16.TyrKO.ACTG1-SWITCHgB 1H9 for *in vivo* experiments.

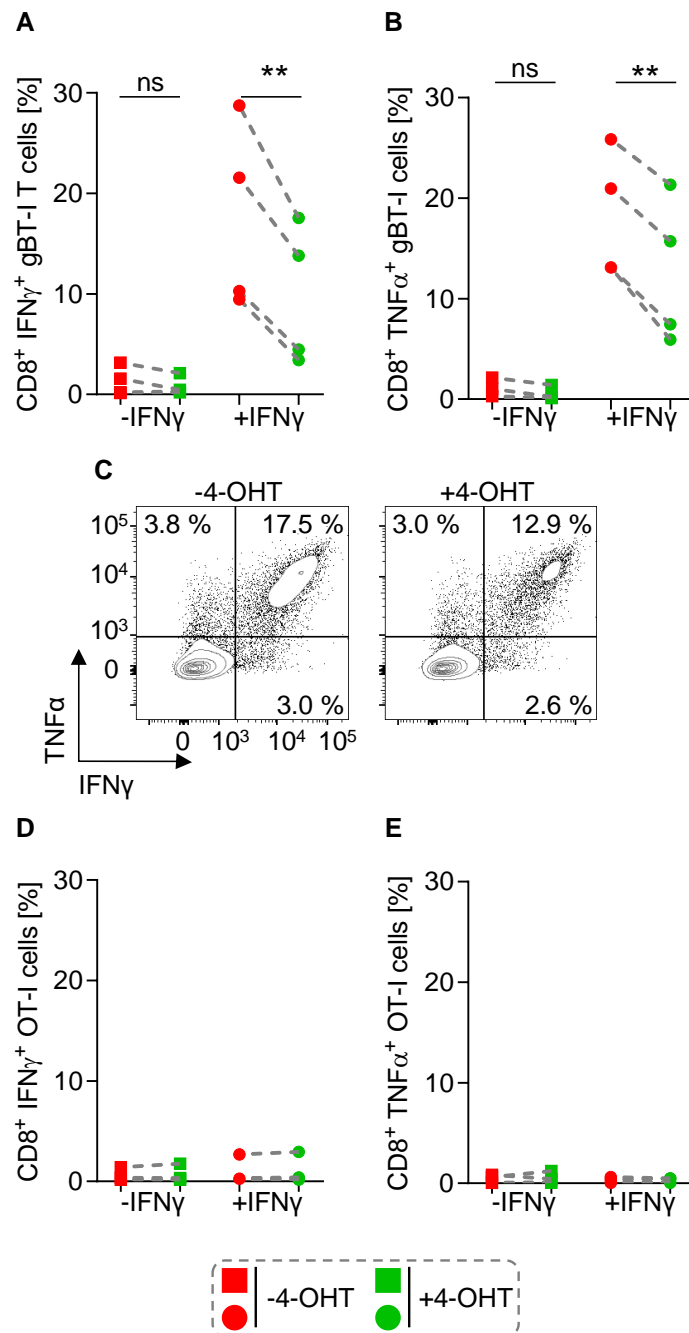


Figure 5.17: 4-OHT treatment of monoclonal 1G9 reduces gBT-I T cell activation

(A and B) Quantification of intracellular (A) IFN γ and (B) TNF α producing gBT-I T cells after co-culture with 4-OHT treated (1000 nM, 5 days) and IFN γ (0.1 ng/ml, 18 h) pre-stimulated B16.TyrKO.ACTG1-SWITCHgB 1G9 cells. (C) Representative contour plot of IFN γ and TNF α producing gBT-I T cells after co-culture with 1G9 cells. (D and E) Quantification of intracellular (D) IFN γ and (E) TNF α producing OT-I T cells after co-culture with 4-OHT treated (1000 nM, 5 days) and IFN γ (0.1 ng/ml, 18 h) pre-stimulated B16.TyrKO.ACTG1-SWITCHgB 1G9 cells. (n = 4). Statistics: ** p<0.01, ns-not significant, paired t-test.

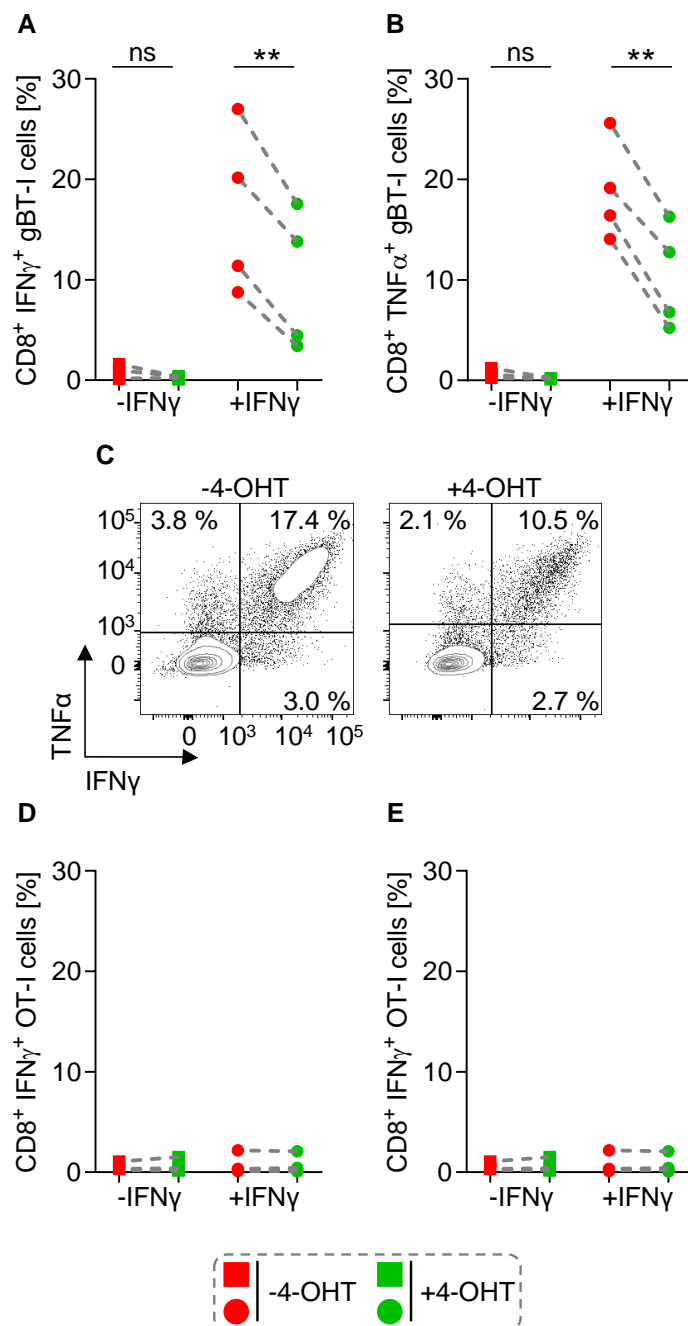


Figure 5.18: 4-OHT treatment of monoclonal 1H9 reduces gBT-I T cell activation

(A and B) Quantification of intracellular (A) IFN γ and (B) TNF α producing gBT-I T cells after co-culture with 4-OHT treated (1000 nM, 5 days) and IFN γ (0.1 ng/ml, 18 h) pre-stimulated B16.TyrKO.ACTG1-SWITCHgB 1H9 cells. (C) Representative contour plot of IFN γ and TNF α producing gBT-I T cells after co-culture with 1G9 cells. (D and E) Quantification of intracellular (D) IFN γ and (E) TNF α producing OT-I T cells after co-culture with 4-OHT treated (1000 nM, 5 days) and IFN γ (0.1 ng/ml, 18 h) pre-stimulated B16.TyrKO.ACTG1-SWITCHgB 1H9 cells. (n = 4). Statistics: ** p<0.01, ns-not significant, paired t-test.

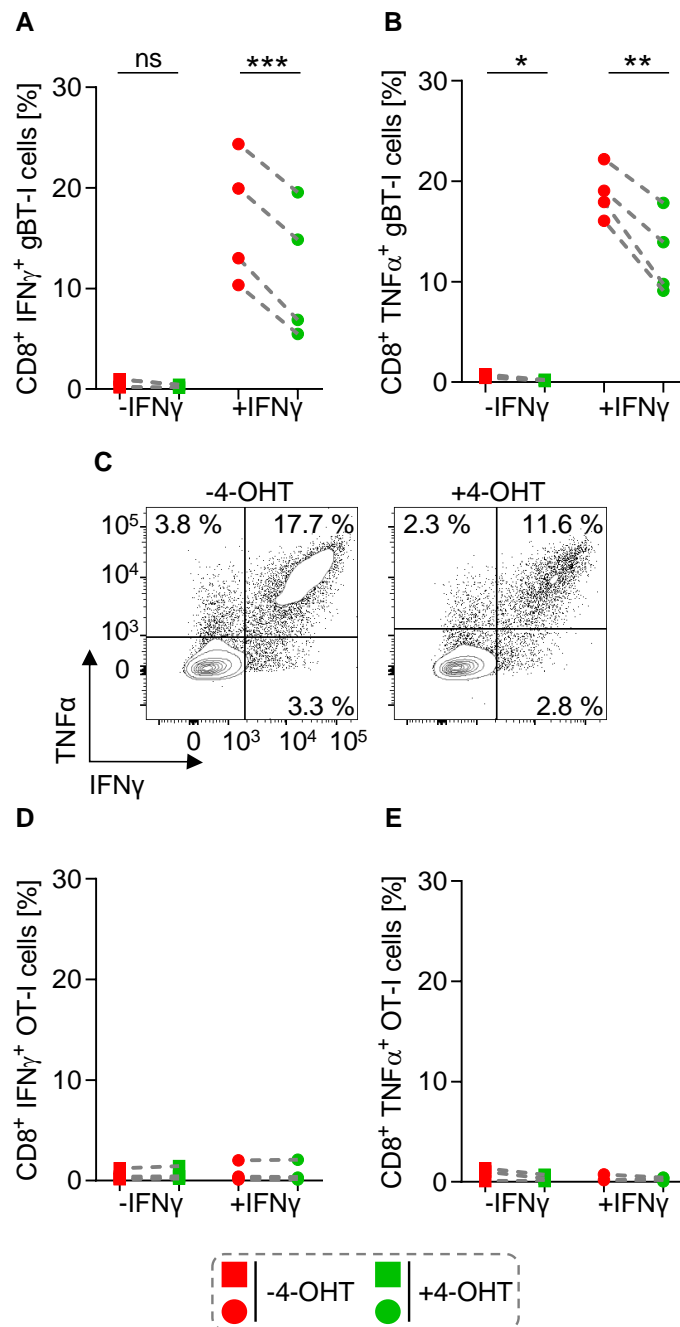


Figure 5.19: 4-OHT treatment of monocline 2C3 reduces gBT-I T cell activation

(A and B) Quantification of intracellular (A) IFN γ and (B) TNF α producing gBT-I T cells after co-culture with 4-OHT treated (1000 nM, 5 days) and IFN γ (0.1 ng/ml, 18 h) pre-stimulated B16.TyrKO.ACTG1-SWITCHgB 2C3 cells. (C) Representative contour plot of IFN γ and TNF α producing gBT-I T cells after co-culture with 1G9 cells. (D and E) Quantification of intracellular (D) IFN γ and (E) TNF α producing OT-I T cells after co-culture with 4-OHT treated (1000 nM, 5 days) and IFN γ (0.1 ng/ml, 18 h) pre-stimulated B16.TyrKO.ACTG1-SWITCHgB 2C3 cells. (n = 4). Statistics: * p<0.05, ** p<0.01, ns-not significant, paired t-test.

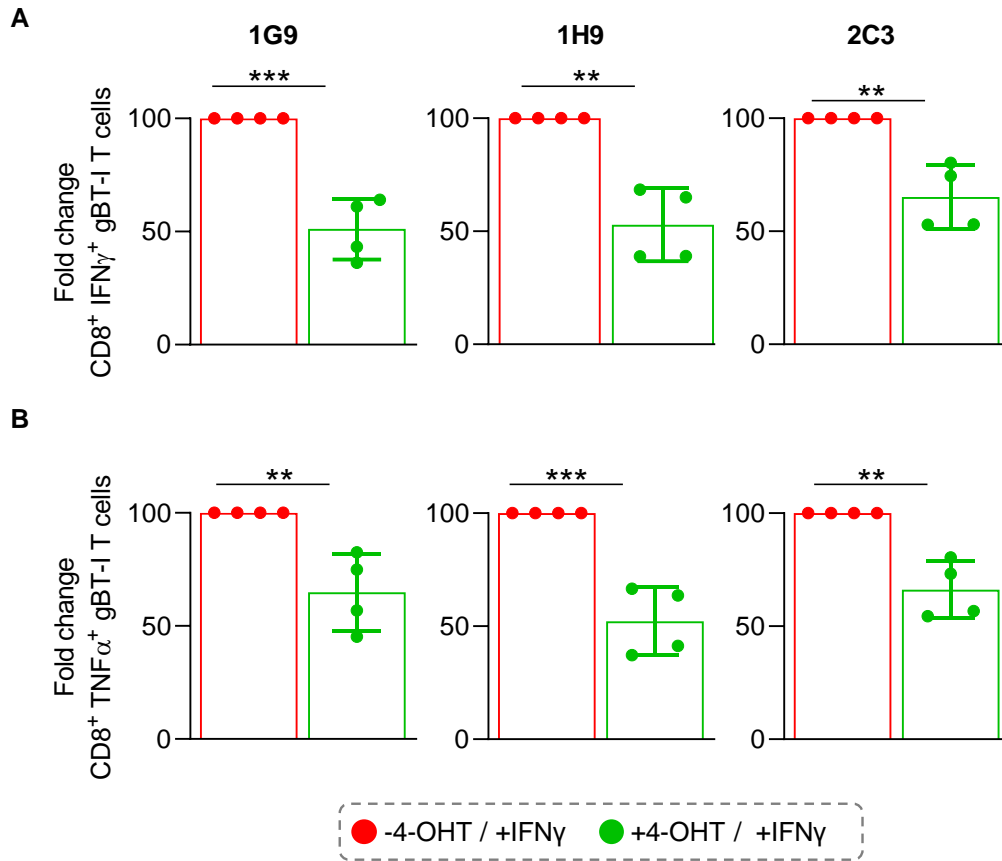


Figure 5.20: gBT-I T cells co-cultured with B16.TyrKO.ACTG1-SWITCHgB 1H9 treated with 4-OHT have the most reduced fold change in intracellular cytokine production

Quantification of intracellular (A) IFN γ and (B) TNF α expression in gBT-I T cells co-cultured with IFN γ pre-stimulated indicated melanoma cells. (n = 4, mean \pm SD) Statistics: **p<0.01, ***p<0.001, unpaired t-test.

5.2.7. Generation of gBT-I tissue-resident memory T cells *in vivo*

We generated T_{RM} gBT-I T cells by locally depositing *in vitro* activated gBT-I T cells via an epicutaneous route as previously established by Park and colleagues (Park et al., 2019). We activated splenocytes from naïve gBT-I mice *in vitro* using gB peptide, LPS and IL-2 for five days. Then, we harvested the cells, resuspended them in Matrigel and inoculated four small abraded skin areas within 1cm² with 1x10⁶ gBT-I T cells on the left flank of a mouse (total amount of gBT-I T cells: 4x10⁶) (Figure 5.21A). Within two to three weeks the gBT-I T cells formed T_{RM} cells in the skin, characterised by the expression of the surface markers CD69 and CD103. Two weeks after the inoculation, we harvested the spleen and skin (1 cm²) of the mice and analysed the circulating and tissue-resident gBT-I T cells.

We observed gBT-I T cells characterised by the expression of CD45.1 and Vα2 in the skin but not in the spleen. The CD45.1⁺ Vα2⁺ T cells in the skin show expression of CD69 and CD103 and therefore the characteristic phenotype of T_{RM} cells in skin (Figure 5.21B). In total, we generated between 0.1 – 0.6x10³ gBT-I T cells in the skin similar to what was described by Park and colleagues (Figure 5.21C) (Park et al., 2019). Using this technique, we could specifically generate gBT-I T_{RM} cells in the skin without generating circulating memory gBT-I T cells.

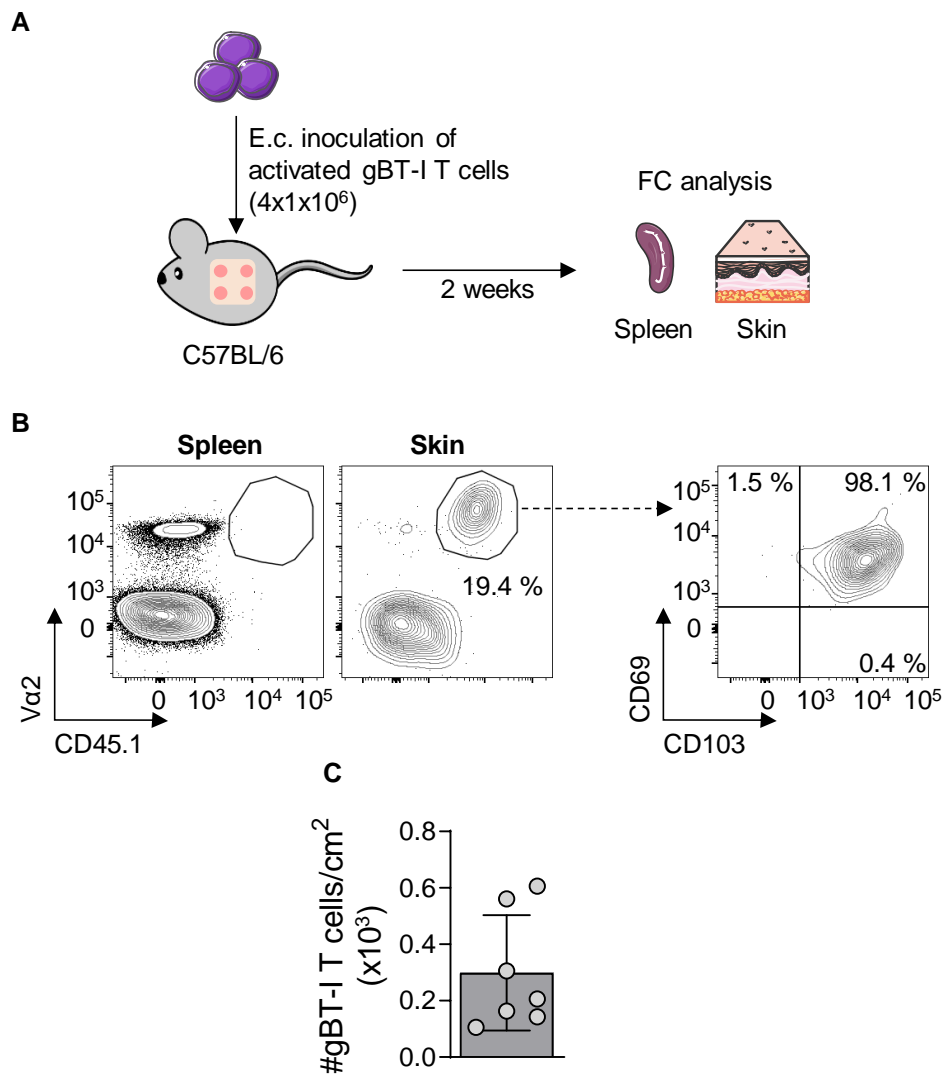


Figure 5.21: Generation of tissue-resident memory gBT-I T cells in the skin
 (A) Graphical depiction of experimental setup. (B) Representative flow cytometry plot of CD45.1⁺ Va2⁺ gBT-I T cells in spleen and skin (left) and CD69⁺ CD103⁺ gBT-I T cells in the skin (right). (C) Quantification of gBT-I T cells per cm² skin. ($n = 7 \pm \text{SD}$)

5.2.8. SWITCHitope-engineered melanoma cells have lower tumour incidence than wildtype B16 melanoma cells

We wanted to test whether our SWITCHitope-engineered melanoma cell line grew *in vivo* and whether the cells retained the expression of the mScarlet fluorescent protein. We intravenously injected 1×10^5 naïve gBT-I T cells into C57BL/6 mice and on the following day we inoculated either 1×10^5 or 1×10^6 melanoma cells epicutaneously (e.c) as previously described or inoculated 1×10^5 melanoma cells subcutaneously (s.c.) (Figure 5.22A). In the group that was inoculated with 1×10^5 cells e.c., only a fraction of mice developed a tumour (two out of five) (Figure 5.22B and 5.22E). In the group that was inoculated with 1×10^6 cells e.c., only one out of five mice developed a tumour (Figures 5.22C and 5.22E). In the group that was inoculated with 1×10^5 cells s.c., all mice developed a tumour; however, two of these tumours spontaneously regressed (Figures 5.22D and 5.22E). We generated *ex vivo* cell lines from the isolated tumour tissue to assess the retention of the mScarlet fluorescent protein *in vivo* and the switch rate induced by spontaneous translocation of the Cre-ERT2 from the cytosol into the nucleus. Flow cytometry analysis showed that 1.8 % and 0.7 % of the cells were mScarlet⁺ mNeon⁺ in the epicutaneous and subcutaneous model, respectively (Figure 5.22F). The frequency of mScarlet⁺ mNeon⁺ cells was comparable to what we observed in clone 1H9 before *in vivo* inoculation (Figure 5.15B)

Next, we wanted to test how the melanoma cells 1H9 grew *in vivo* without the addition of gBT-I T cells and whether the depletion of the antigen by tamoxifen changes the growth kinetics of the tumour. We inoculated C57BL/6 mice with 1×10^5 cells e.c. and started with tamoxifen or control (oil) treatment on the same day. Mice were intraperitoneally (i.p.) injected with 1 mg tamoxifen for five consecutive days (Figure 5.23A). In total, only one out of 10 mice developed a tumour (Figures 5.23B and 5.23C).

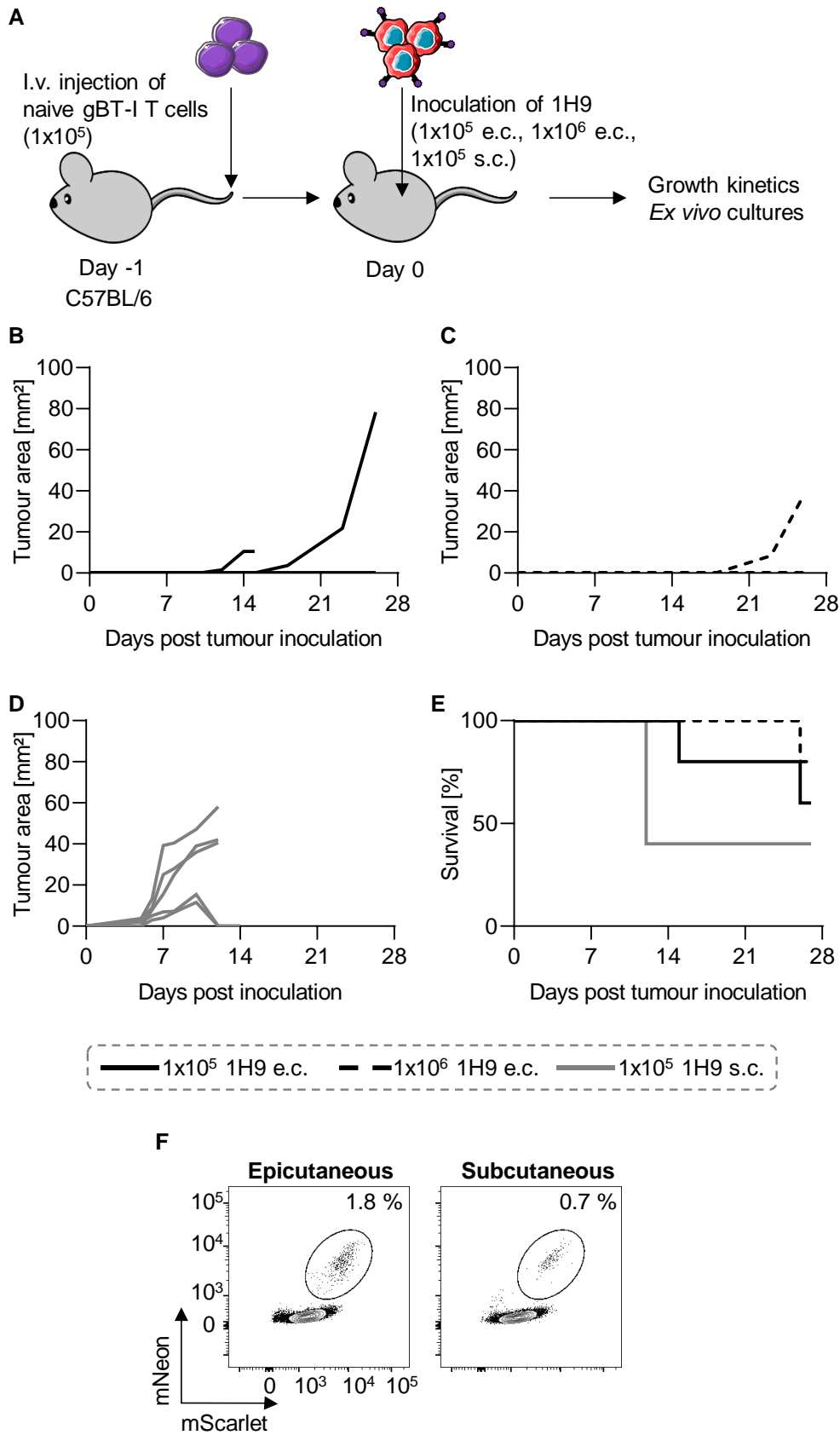


Figure 5. 22: 1H9 melanoma cells have low penetrance in C57BL/6 mice

(A) Graphical depiction of experimental setup. (B – D) Tumour growth curves of mice inoculated with (B) 1×10^5 1H9 cells epicutaneously (e.c.) ($n = 5$), 1×10^6 1H9 cells e.c. ($n = 5$) and (D) 1×10^5 1H9 cells subcutaneously (s.c.) ($n = 5$) shown in tumour area [mm^2]. (E) Kaplan-Meier survival curves of mice inoculated with the indicated melanoma cells. (F) Representative flow cytometry plots of mScarlet and mNeon expression of epicutaneously or subcutaneously isolated melanoma cells.

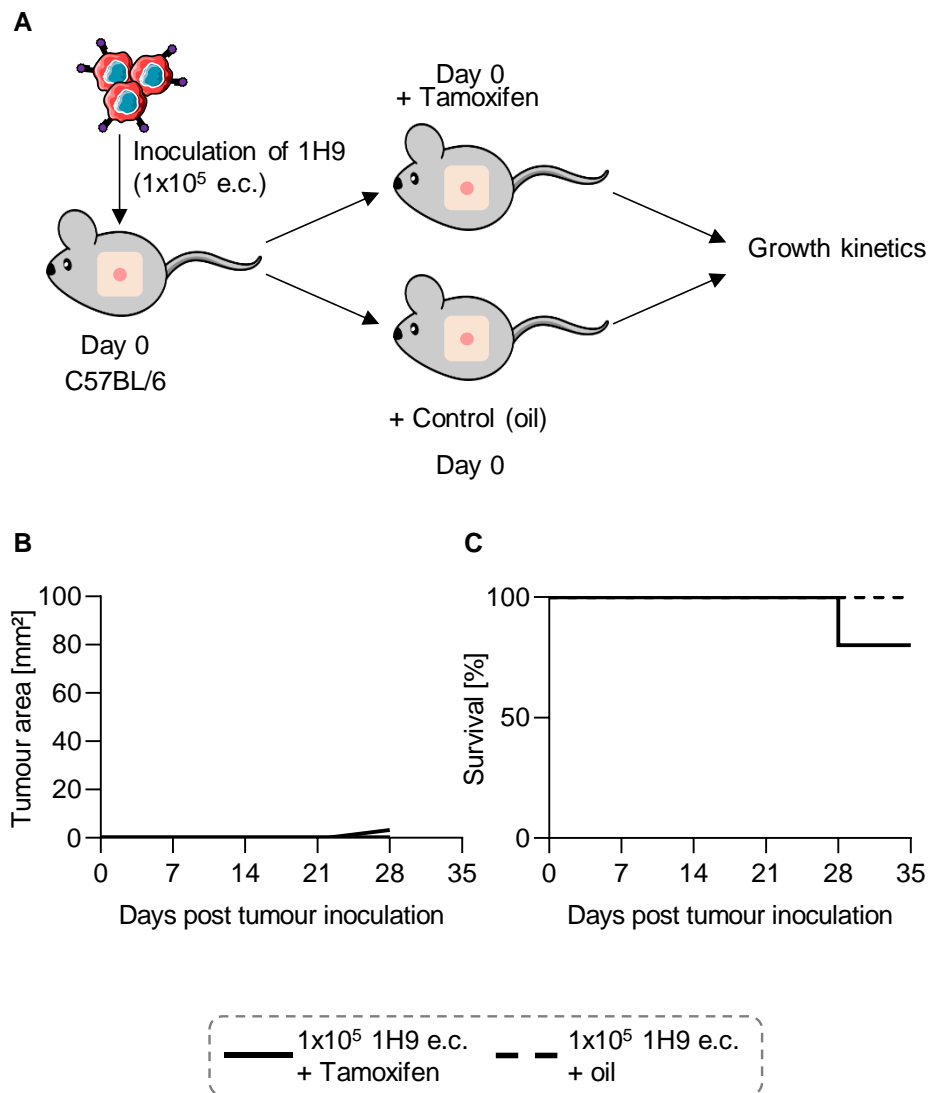


Figure 5. 23: Influence of *in vivo* Tamoxifen treatment on tumour penetrance and growth kinetics

(A) Graphical depiction of experimental setup. (B) Tumour growth curves of mice inoculated with 1×10^5 1H9 cells epicutaneously (e.c.) and either treated with Tamoxifen (1 mg for 5 consecutive days) or with oil ($n = 5$ per group). (C) Kaplan-Meier survival curves of mice inoculated with the indicated melanoma cells.

5.2.9. SWITCHitope-engineered melanoma cells prime naïve gBT-I T cells and recruit them into the skin

Next, we asked whether our SWITCHitope-engineered melanoma cell line 1H9 could prime naïve gBT-I T cells and recruit them to the skin. Additionally, we wanted to test whether the switch worked *in vivo*. We i.v. injected mice with naïve gBT-I T cells and on the following day we e.c. inoculated 1H9 melanoma cells. Twenty-eight days after tumour inoculation, we treated the mice with tamoxifen. We performed flow cytometry analysis of the tumour cells and skin, draining lymph node (brachial; brLN) and spleen when tumours reached the volumetric endpoint (Figure 5.24A). Two out of 15 mice (mouse 3-1 and 3-4) developed a tumour before tamoxifen treatment and no additional mouse developed a tumour after tamoxifen treatment (Figure 5.24B and 5.24C). We analysed the tumour tissue and observed that mouse 3-1 had a mScarlet⁺ tumour whereas mouse 3-4 had a mScarlet⁻ and therefore gB⁻ tumour (Figure 5.25A). Both mice had gBT-I T cells in the peritumoural skin and in the tumour (Figure 5.25B and 5.25C; top panels). In both mice we observed that the majority of gBT-I T cells were CD69⁺ CD103⁺. In mouse 3-1 there were no CD69⁺ CD103⁺ gBT-I T cells in the tumours whereas 21.8% of the gBT-I T cells in peritumoural skin were CD69⁺ CD103⁺ (Figure 5.25B and 5.25C; bottom panels).

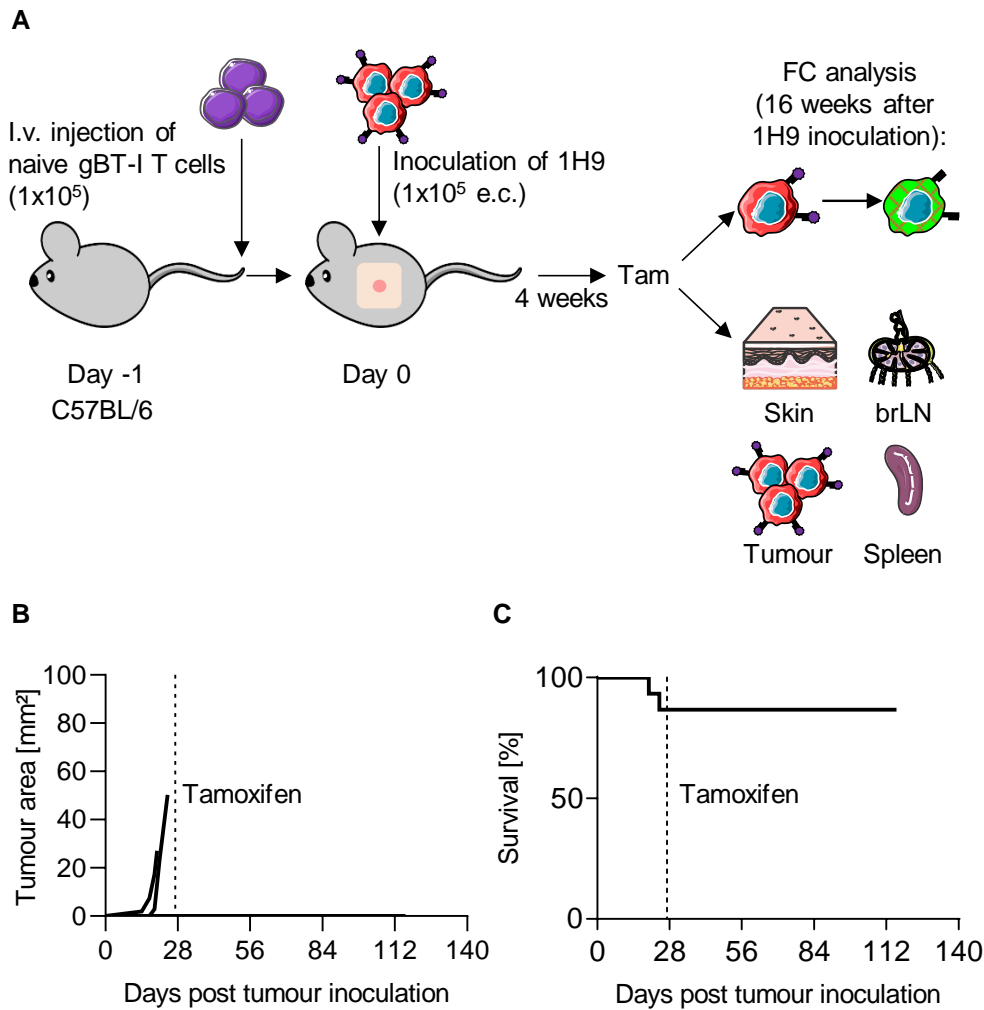


Figure 5.24: Tumour penetrance does not increase when melanoma cells lose antigen in the presence of gBT-I T cells in C57BL/6 mice

(A) Graphical depiction of experimental setup. (B) Tumour growth curves of mice intravenously (i.v.) injected with 1×10^5 naive gBT-I T cells and inoculated with 1×10^5 1H9 cells e.c. ($n = 15$) (C) Kaplan-Meier survival curves of mice inoculated with the melanoma cells.

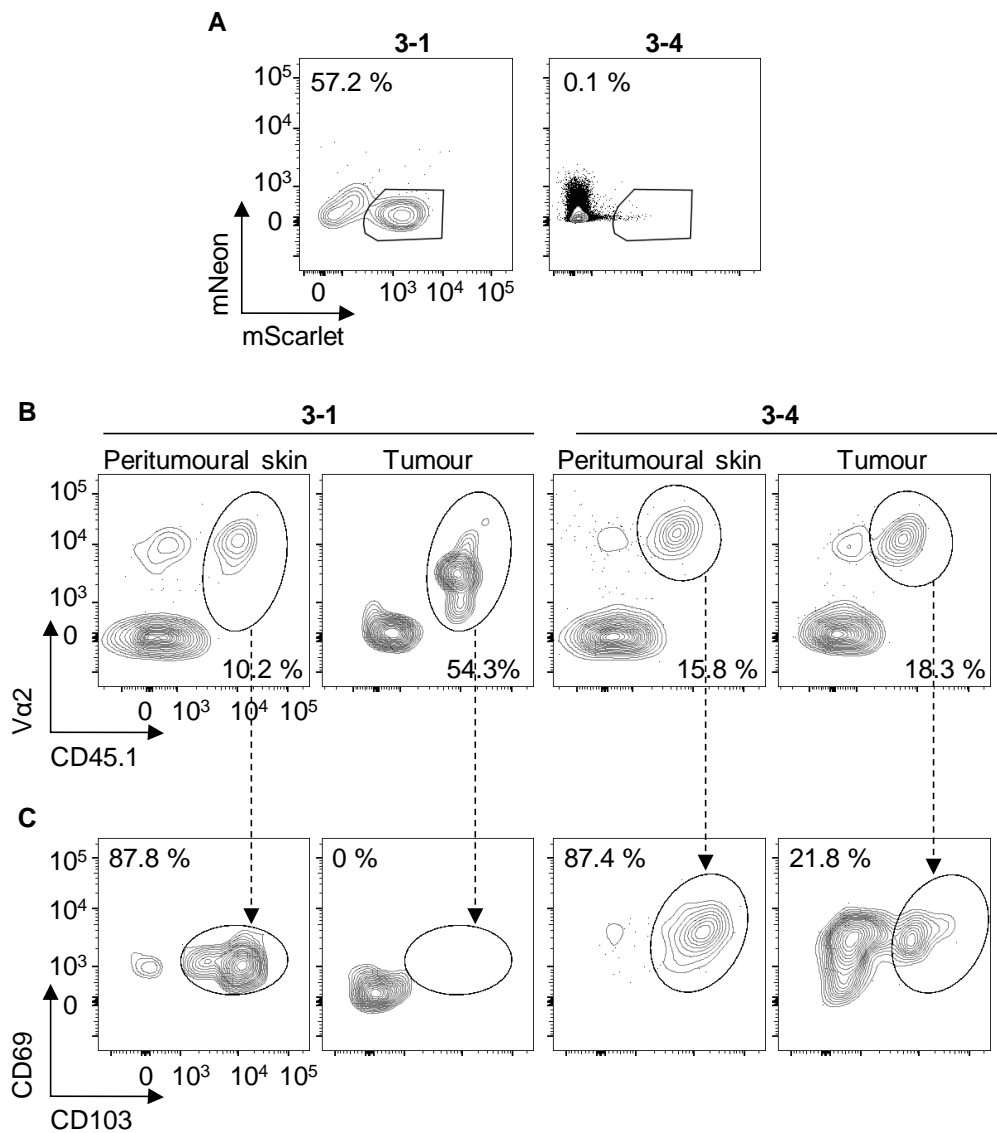


Figure 5.25: SWITCHitope-engineered melanoma cells that are not mScarlet⁺ might form tumours

(A) Flow cytometry analysis of mScarlet and mNeon of the two developer mice, 3-1 and 3-4. (B) Flow cytometry plots of CD45.1⁺ Vα2⁺ gBT-I T cells (of all live CD45.2⁺ CD8⁺ TCRβ⁺ cells) in the peritumoural skin and in the tumour in the mice 3-1 and 3-4. (C) Flow cytometry plots of CD69⁺ CD103⁺ gBT-I T cells in the peritumoural skin and in the tumour in the mice 3-1 and 3-4.

We generated *ex vivo* cell lines from the tumour tissue and analysed these cell lines by flow cytometry. The *ex vivo* data confirmed what we observed *in vivo*. Cell line 3-1 was mScarlet⁺ mNeon⁻ whereas cell line 3-4 was mScarlet⁻ mNeon⁻ (Figure 5.26A). We wanted to test whether these cell lines were still capable of activating gBT-I T cells *in vitro*. Therefore, we performed an *in vitro* co-culture assay as previously described. In addition to the two *ex vivo* cell lines, we used the cell line B16.TyrKO.ACTG1-Scarlet (negative control) and B16.TyrKO.ACTG1-Scarlet-gB (positive control) as controls. We stimulated all melanoma cell lines with IFN γ and measured H2-Kb upregulation on the melanoma cells. All cell lines upregulated H2-Kb however, the two *ex vivo* cell lines 3-1 and 3-4 have a higher MFI (Figure 5.26B). After the co-culture, we analysed intracellular IFN γ and TNF α of the gBT-I T cells. As expected, cell line 3-1 could induce T cell activation whereas cell line 3-4 failed to do so. Cell line 3-1 could even induce production of IFN γ and TNF α without IFN γ pre-stimulation of the melanoma cells (Figures 5.26C and 5.26D).

Lastly, we compared gBT-I T cells and gBT-I T_{RM} cells between developers (2/15) and non-developers (13/15). In the peritumoural skin, we observed gBT-I T cells in both non-developers and developers. The majority of gBT-I T cells were also CD69⁺ and CD103⁺ (Figure 5.27A). In the tumour tissue of mouse 3-1 and 3-4, we found gBT-I T cells but the majority of these T cells did not display the T_{RM} phenotype (Figure 5.27B). In the brLN, we identified more gBT-I T cells in the developers than in the non-developers however this trend was not observed in the spleens of these mice (Figures 5.27C and 5.27D).

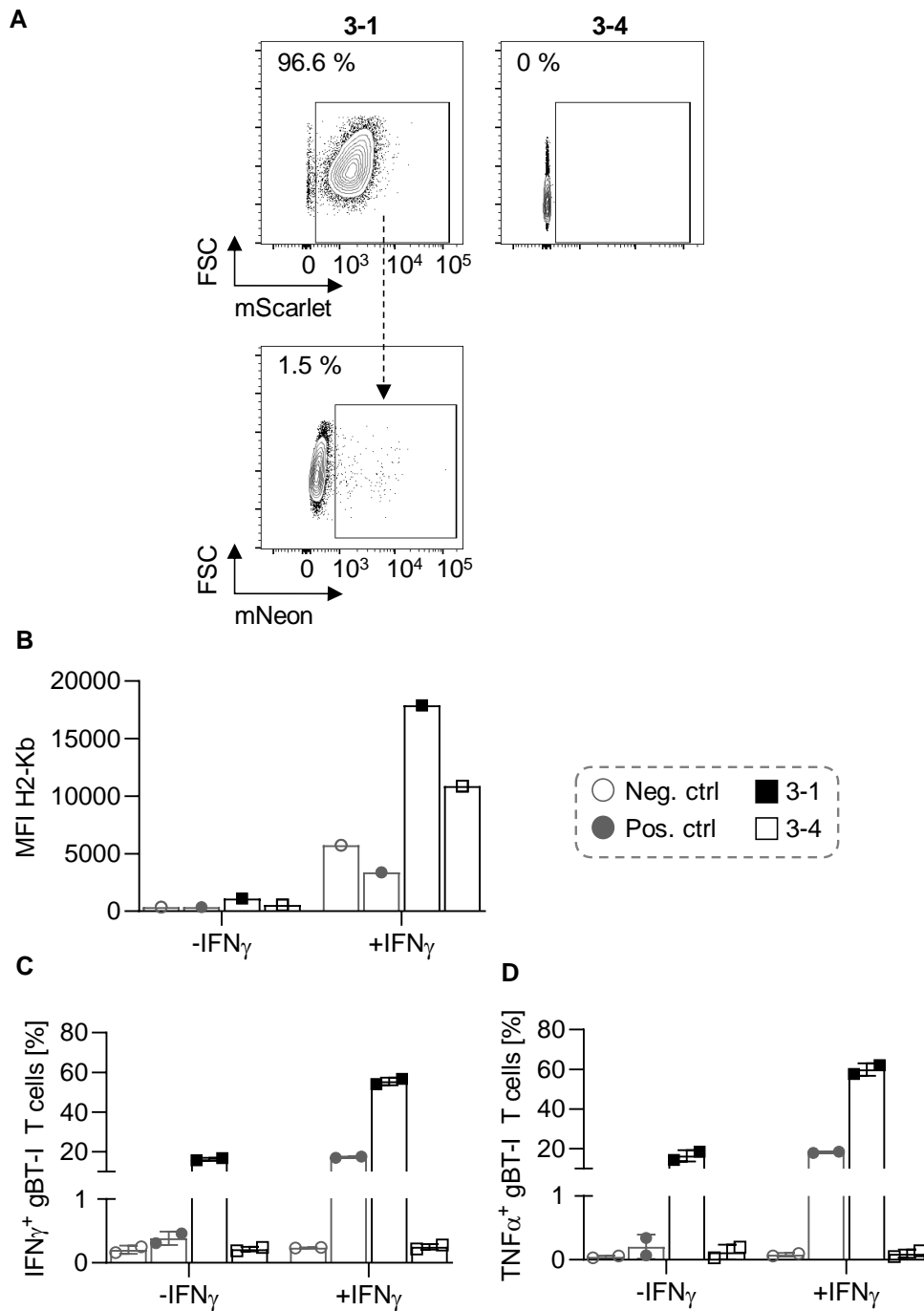


Figure 5.26: *Ex vivo* 1H9 cells that lost mScarlet expression cannot induce gBT-I T cell activation

(A) Flow cytometry analysis of mScarlet and mNeon expression of *ex vivo* generated melanoma cell lines isolated from the mice 3-1 and 3-4. (B) Mean fluorescence intensity of H2-Kb expression of indicated melanoma cells after IFN γ stimulation (0.1 ng/ml, 18 h). (C and D) Intracellular (C) IFN γ and (D) TNF α cytokine expression of *in vitro* activated gBT-I T cells co-cultured with indicated melanoma cell lines for 5 h. (n = 2, mean \pm SD)

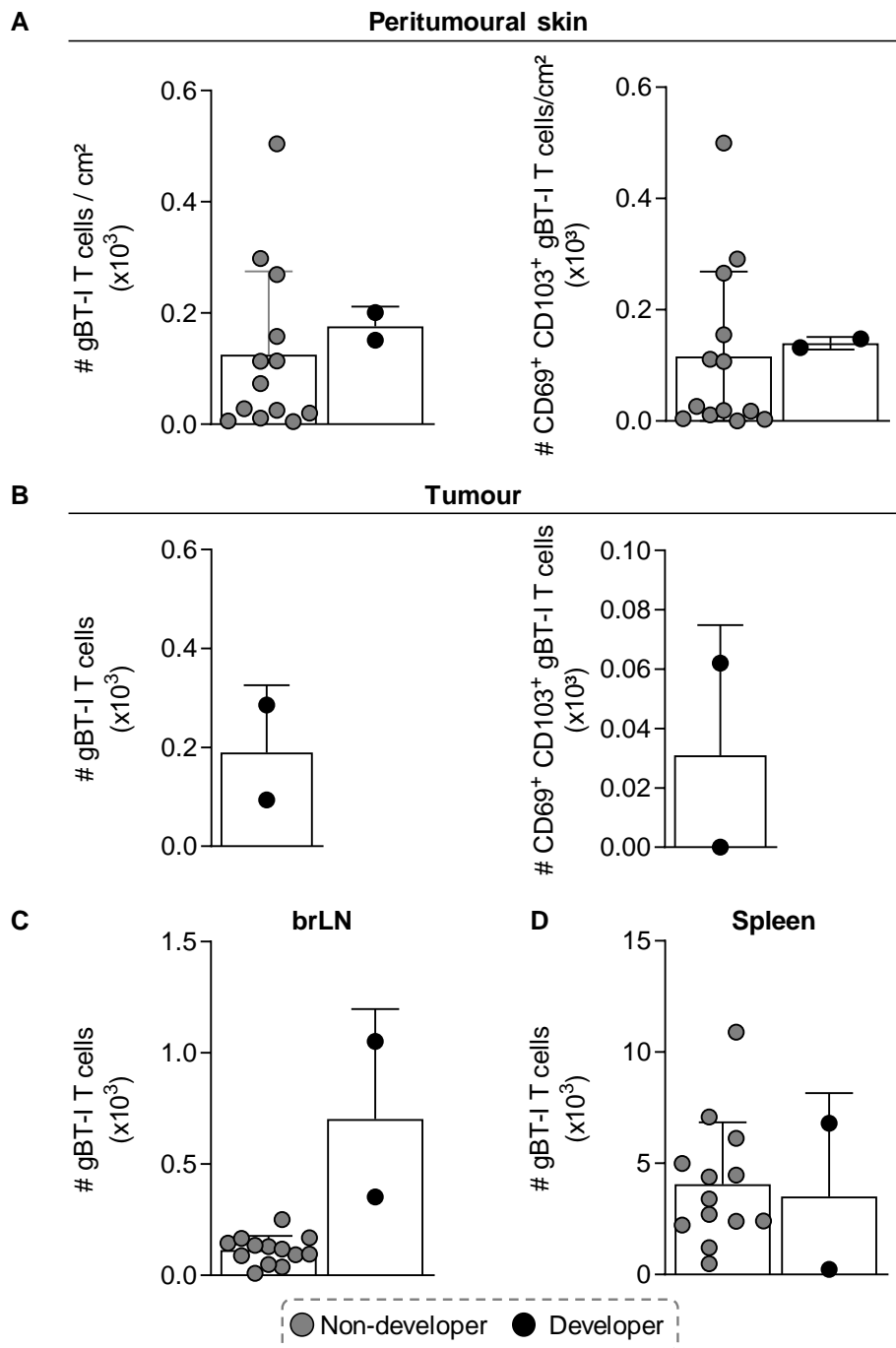


Figure 5.27: SWITCHitope-engineered melanoma cells can prime naïve gBT-I T cells and recruit them into the skin

(A and B) Quantification of gBT-I T cells (left) and CD69⁺ CD103⁺ gBT-I T cells (right) in the (A) peritumoural skin and (B) tumour. (C and D) Quantification of gBT-I T cells in the (C) brLN and (D) spleen. (Non-developer: $n = 13 \pm \text{SD}$; developer: $n = 2$, mean $\pm \text{SD}$)

5.2.10. HSV-1 gB antigen can be depleted in a tamoxifen-inducible fashion

The next experiment we performed, was to test whether the melanoma cells can escape T_{RM} control *in vivo* upon tamoxifen treatment. We know from previous experiments that melanoma cells can reside within the skin under the control of T_{RM} cells without ever forming a macroscopic tumour (Park et al., 2019). We inoculated *in vitro* activated gBT-I T cells e.c. and three weeks later we inoculated melanoma cells e.c. in the same area of the skin. We divided the mice into three groups. Group A was treated with tamoxifen immediately following tumour inoculation to simulate normal growth that would occur without the control of the T_{RM} cells as the antigen is depleted immediately. Mice in group B and C were treated with tamoxifen or oil three to four weeks after tumour inoculation, respectively. We expected tumour outgrowth in Group B and protection in Group C (Figure 5.28A). In Group A, two out of 12 mice (mouse 1-2 and 1-5) developed a tumour (Figures 5.28B and 5.28D). Before we started tamoxifen treatment in Group B/C, one out of 28 mice (mouse 3-4) developed a tumour (Figures 5.28C and 5.28E).

When we analysed the tumour tissue by flow cytometry for mScarlet and mNeon expression, we observed that mouse 1-2 and 1-5 had double positive tumours as expected (Figure 5.29; left and middle panel). However, the tumour of mouse 3-4 was double negative which also meant that it did not express the HSV-1 gB epitope anymore (Figure 5.29; right panel). We analysed peritumoural skin, tumour, brLN and spleen in the developer mice. Mouse 1-2 had gBT-I T cells in the skin and in the tumour. In the skin the majority of these cells had a T_{RM} phenotype; in the tumour over 50% of the gBT-I T cells were also CD69⁺ and CD103⁺ (Figure 5.30A). In mouse 1-5 there were only very few gBT-I cells in the skin and tumour and in mouse 3-4 we detected no gBT-I T cells in the skin or the tumour (Figures 5.30B and 5.30C).

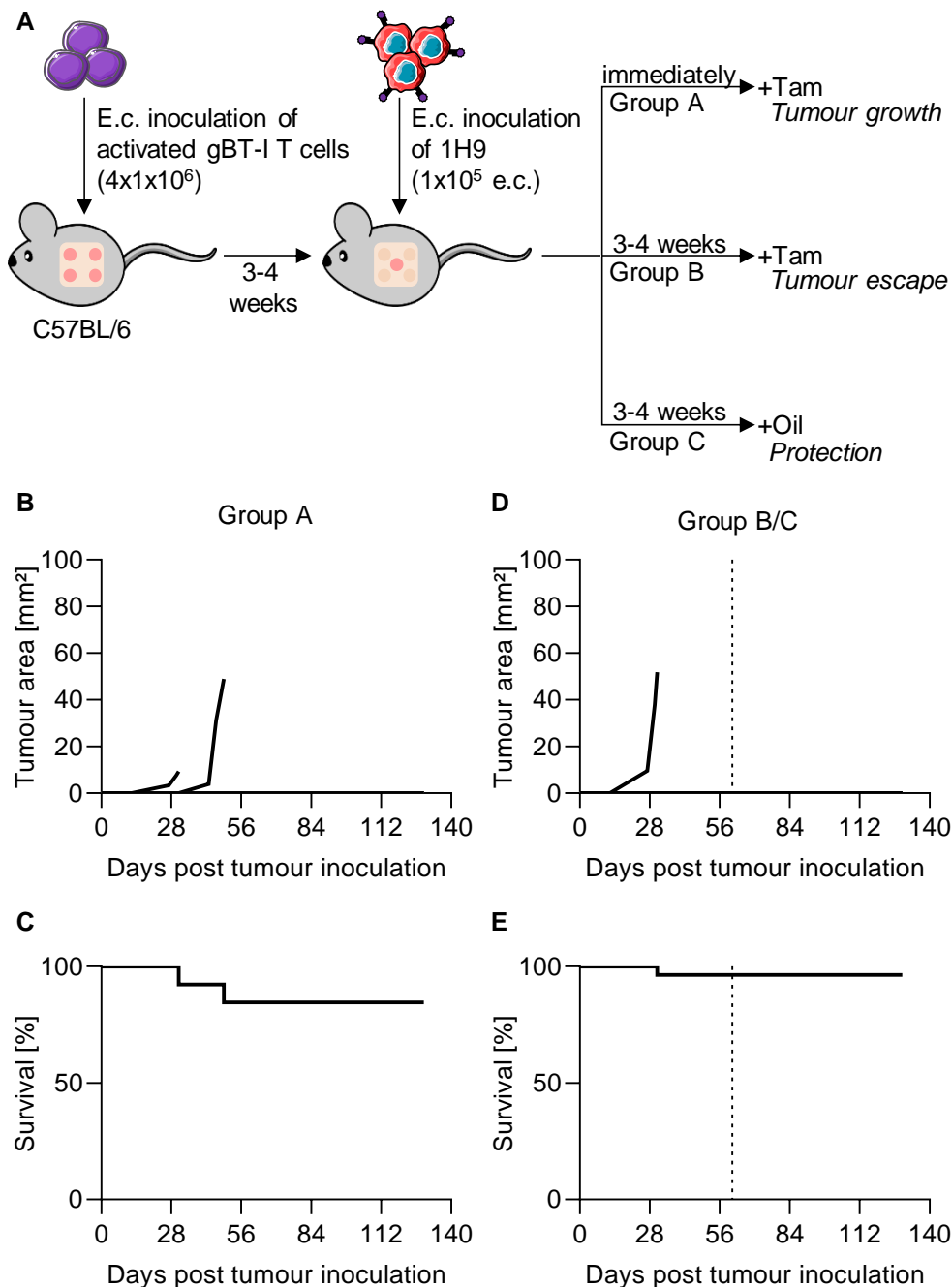


Figure 5.28: Tamoxifen treatment of C57BL/6 mice with gBT-I T_{RM} cells in the skin does not lead to tumour growth

(A) Graphical depiction of experimental setup. (B) Tumour growth curves and (C) Kaplan-Meier survival curves of mice e.c. inoculated with activated gBT-I T cells and e.c. inoculated with 1×10^5 1H9 cells and treated with Tamoxifen immediately after tumour cell inoculation (Group A). (D) Tumour growth curves and (E) Kaplan-Meier survival curves of mice e.c. inoculated with activated gBT-I T cells and e.c. inoculated with 1×10^5 1H9 cells and treated with Tamoxifen or oil three to four weeks post tumour inoculation (Group B and C). (Group A: $n = 12$, Group B: $n = 14$, Group C: $n = 14$).

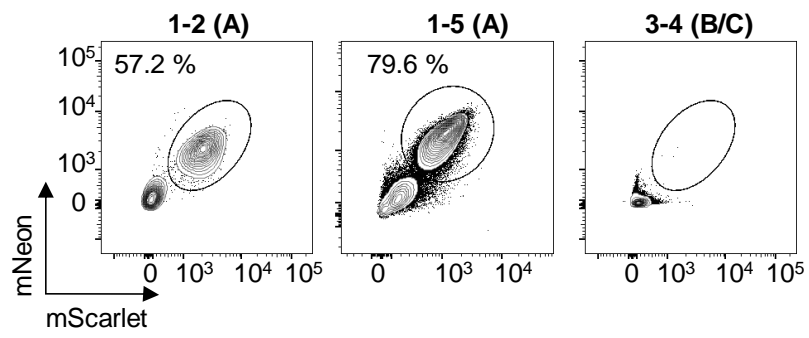


Figure 5.29: *In vivo* Tamoxifen treatment induces a colour switch

(A) Flow cytometry analysis of mScarlet and mNeon of the two developer mice of Group A (mice 1-2 and 1-5), and the one developer mouse of Group B/C (mouse 3-4).

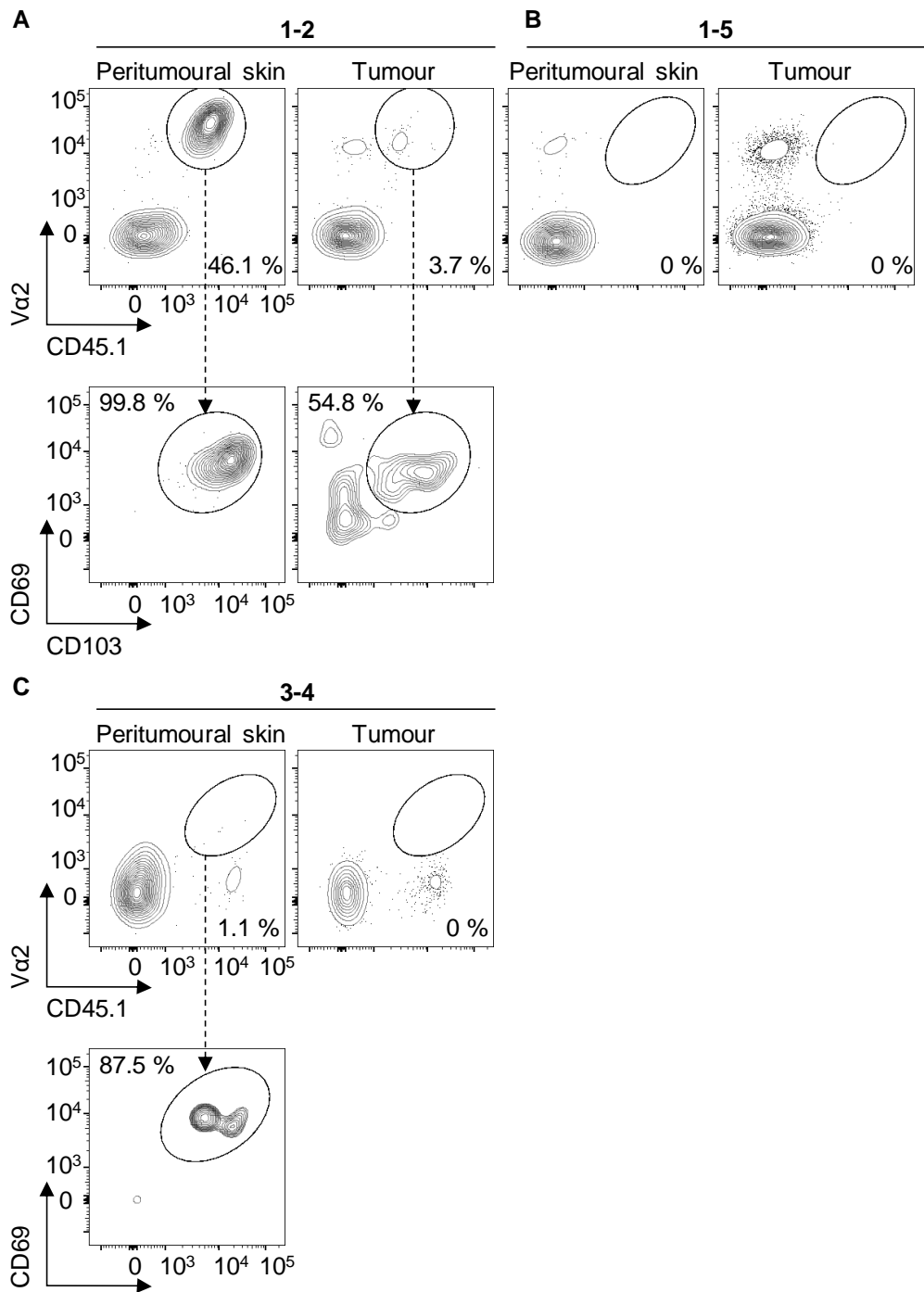


Figure 5.30: gBT-I T_{RM} cells do not correlate with melanoma cell epitope status

Flow cytometry plots of CD45.1⁺ V α 2⁺ gBT-I T cells (of all live CD45.2⁺ CD8⁺ TCR β ⁺ cells) and CD69⁺ CD103⁺ gBT-I T cells in the peritumoural skin and in the tumour in the mice 1-2, 1-5 and 3-4.

We generated *ex vivo* cell lines from the tumour tissue and analysed these cell lines by flow cytometry. The *ex vivo* data confirmed what we observed *in vivo*. Cell lines 1-2 and 1-5 were mScarlet⁺ mNeon⁺ whereas cell line 3-4 was mScarlet⁻ mNeon⁻ (Figure 5.31A). We wanted to analyse whether the cell lines were still capable of activating gBT-I T cells *in vitro*. Therefore, we performed an *in vitro* co-culture assay as previously described. In addition to the three *ex vivo* cell lines, we used the cell line B16.TyrKO.ACTG1-Scarlet (negative control) and B16.TyrKO.ACTG1-Scarlet-gB (positive control) as controls. We stimulated all melanoma cell lines with IFN γ and measured H2-Kb upregulation on the melanoma cells. All cell lines upregulated H2-Kb however, the three *ex vivo* cell lines 1-2, 1-5 and 3-4 had a higher MFI (Figure 5.31B). After the co-culture, we analysed intracellular IFN γ and TNF α of the gBT-I T cells. Cell lines 1-2 and 1-5 could not activate T cells which indicated that the switch worked *in vivo* and that tamoxifen treatment of mice led to the depletion of the HSV-1 gB epitope. Interestingly, cell line 3-4 was capable of stimulating the gBT-I cells despite being mScarlet⁻. The reason for this remains elusive. (Figures 5.31C and 5.31D)

Finally, we assessed frequency and numbers of gBT-I T cells and gBT-I T_{RM} cells between the different groups and between non-developers and developers. In the non-developers there was no significant difference between the Groups A, B and C in frequency and number of gBT-I cells in the skin, brLN and spleen nor in the number of T_{RM} gBT-I T cells in the skin (Figures 5.32A, 5.32B and 5.32C).

In the developers, there was one mouse (1-2) that has gBT-I and T_{RM} gBT-I cells in the skin and in the tumour. The other two mice (1-5 and 3-4) did not have skin nor tumour gBT-I T cells. But all three mice had a few circulatory gBT-I T cells in the brLN and spleen (Figure 5.33A-C).

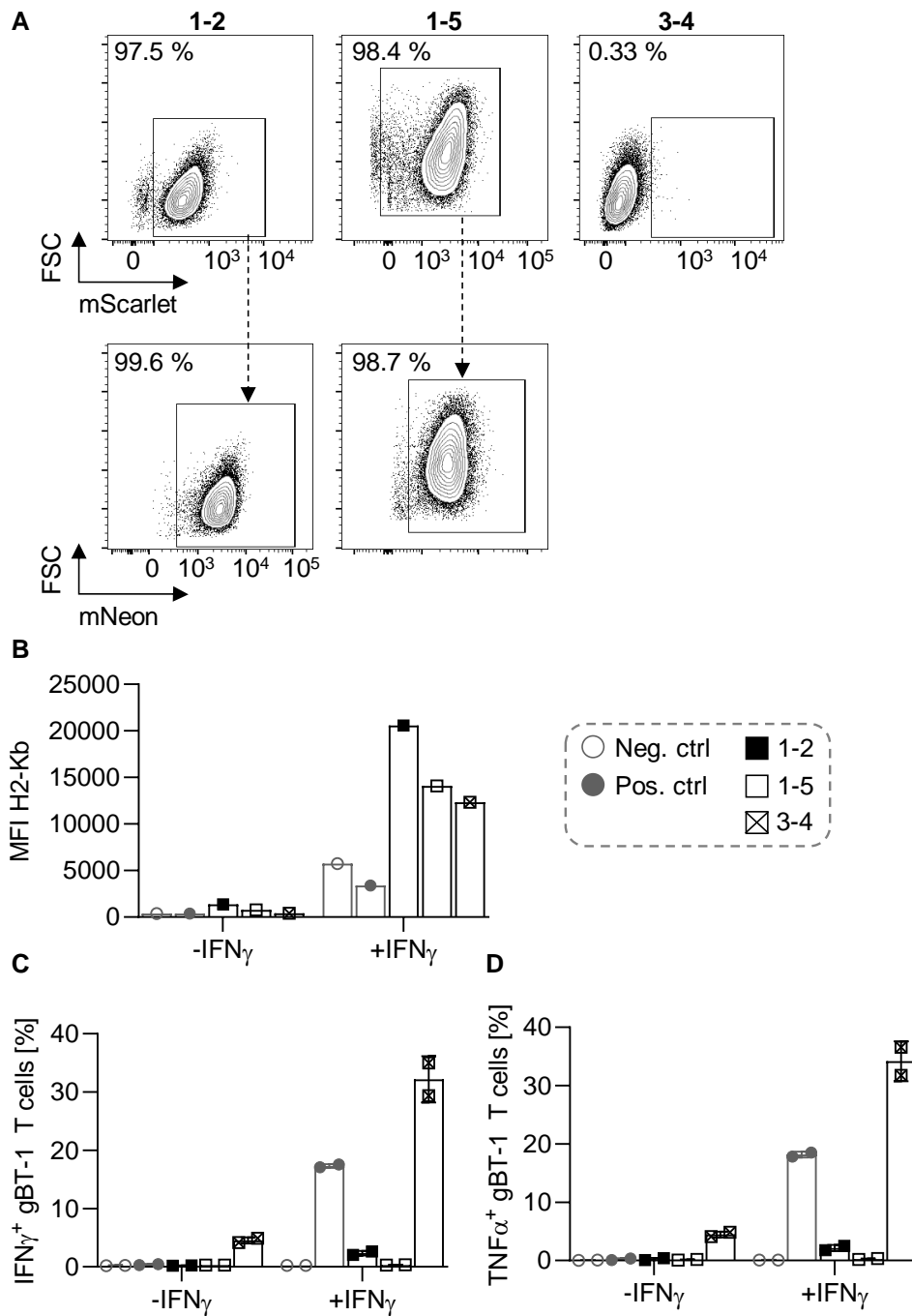


Figure 5.31: *In vivo* switched cells can no longer activate gBT-I T cell *in vitro*

(A) Flow cytometry analysis of mScarlet and mNeon expression of *ex vivo* generated melanoma cell lines isolated from the mice 1-2, 1-5 and 3-4. (B) Mean fluorescence intensity of H2-Kb expression of indicated melanoma cells after IFN γ stimulation (0.1 ng/ml, 18 h). (C and D) Intracellular (C) IFN γ and (D) TNF α cytokine expression of *in vitro* activated gBT-I T cells co-cultured with indicated melanoma cell lines for 5 h. (n = 2, mean \pm SD)

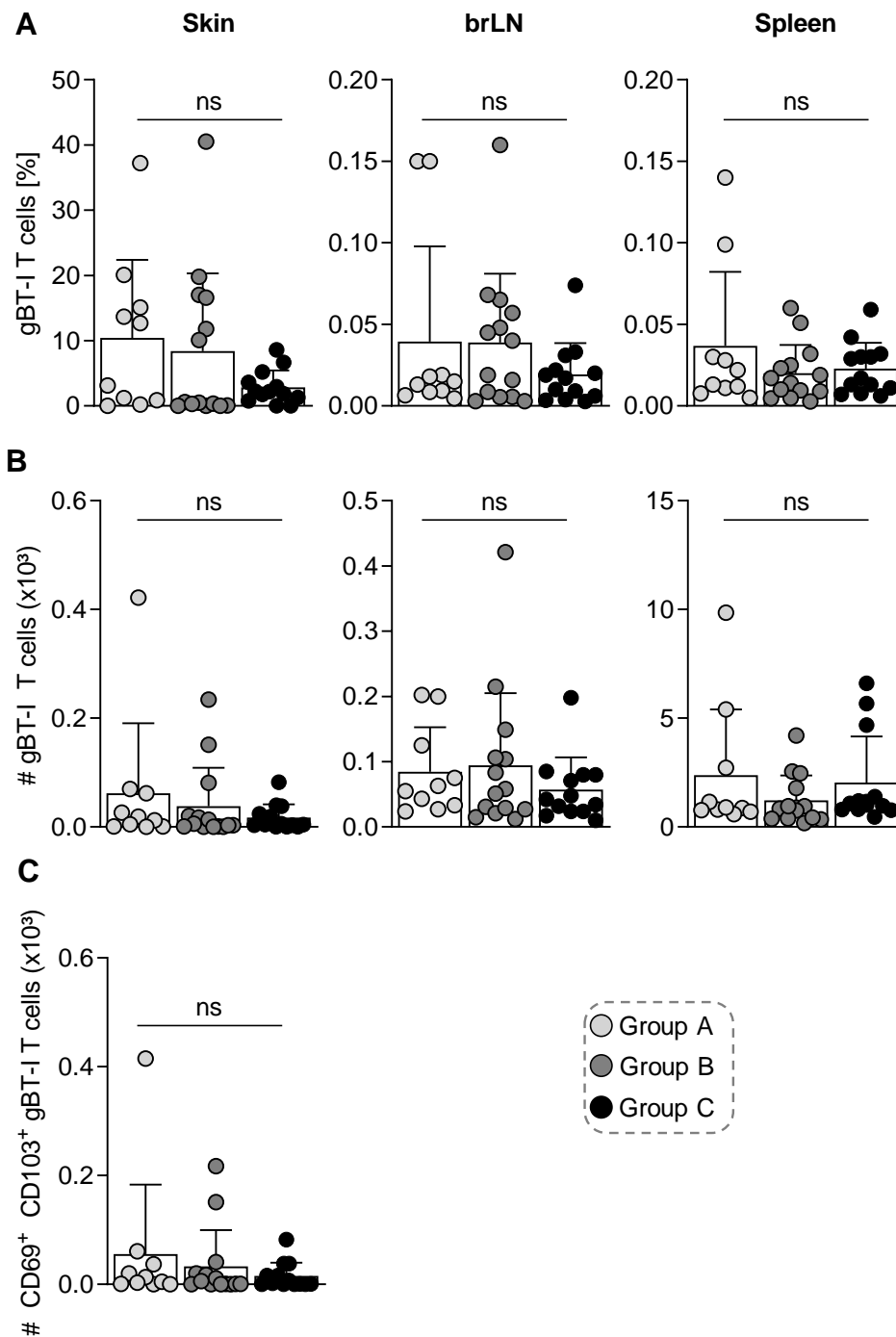


Figure 5.32: Different time points in Tamoxifen treatment does not induce significant differences in frequency and number of gBT-I T cells in different organs

Quantification of (A) frequencies and (B) numbers of gBT-I T cells in skin, brLN and spleen in non-developer mice of the different treatment groups. (C) Quantification of numbers of CD69⁺ CD103⁺ gBT-I T cells in the skin. (Group A: n = 12, Group B: n = 14, Group C: n = 14) Statistics: ns-not significant, Mann-Whitney-U test

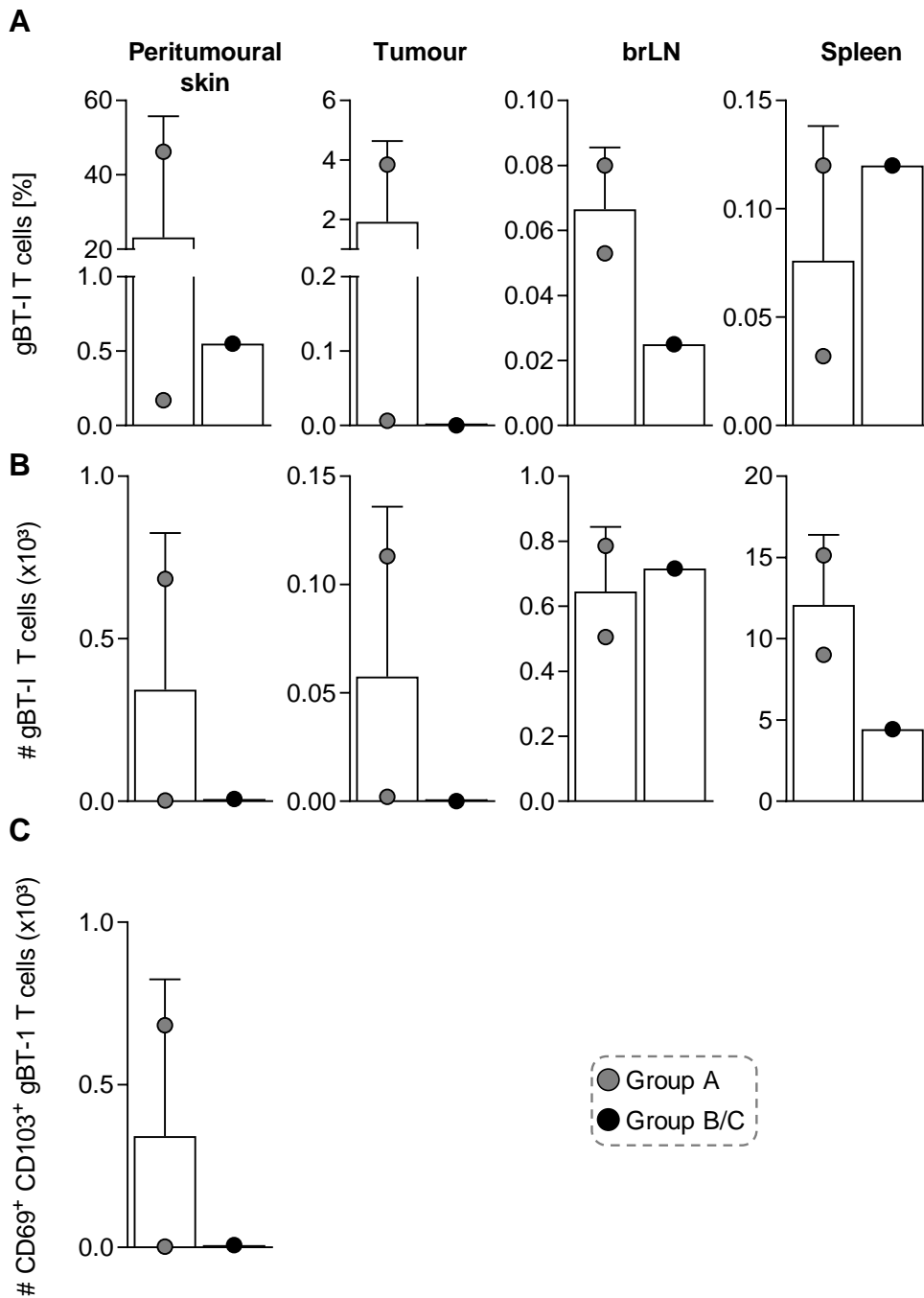


Figure 5.33: gBT-I T cells in the different organs do not correlate with HSV-1 gB epitope status

Quantification of (A) frequencies and (B) numbers of gBT-I T cells in peritumoural skin, tumour, brLN and spleen in developer mice of the different treatment groups. (C) Quantification of numbers of CD69⁺ CD103⁺ gBT-I T cells in the skin. (Group A: n = 2, mean ± SD; Group B/C: n=1)

5.2.11. SWITCHitope-engineered melanoma cells have higher penetrance in immunodeficient mice

As we wanted to analyse the control of the melanoma cells by gBT-I T_{RM} cells independently of the endogenous CD8⁺ T cells, we performed the following experiments in immunocompromised mice. We used Rag1^{-/-} mice which lack B and T cells and Rag2^{-/-}; IL2rg^{-/-} which lack B, T and NK cells. The following experiment was performed by Teagan Wagner, a member of the Gebhardt laboratory. We inoculated either Rag1^{-/-} or Rag2^{-/-}; IL2rg^{-/-} mice with the SWITCHitope-engineered melanoma cell line 1H9 and observed the growth kinetics (Figure 5.34A). In Rag1^{-/-} mice, 67 % of the animals developed melanoma, whereas 100 % of the Rag2^{-/-}; IL2rg^{-/-} mice developed melanoma (Figure 5.34B-D).

Next, we inoculated Rag1^{-/-} mice with activated gBT-I T cells e.c. to generate T_{RM} cells as previously described. Then three weeks later, we inoculated the mice with the cell line 1H9 e.c. and treated non-developer mice 27 days post tumour inoculation with either tamoxifen or oil (Figure 5.35A). We did not observe tumour growth in any group (Figure 5.35B). We analysed the skin, brLN and spleen by flow cytometry for gBT-I T cells. There was no significant difference between the frequency and number of gBT-I T cells and gBT-I T_{RM} cells in the skin. There was also no difference in the frequency and numbers of gBT-I T cells in the brLN and spleen in between the two different treatment groups (Figure 5.36).

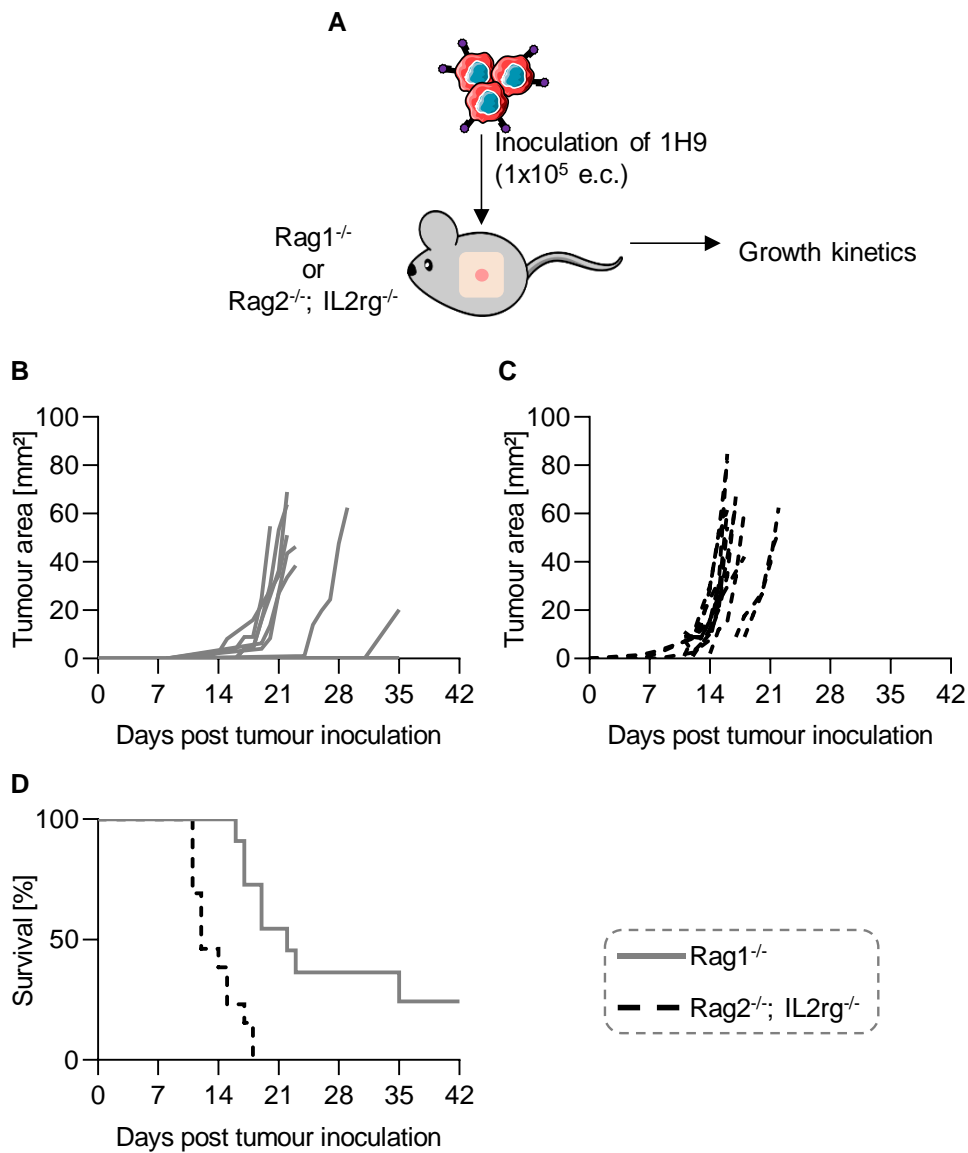


Figure 5.34: 1H9 melanoma cells have higher penetrance in immunodeficient mice

(A) Graphical depiction of experimental setup. (B and C) Tumour growth curves of (B) Rag1^{-/-} or (C) Rag2^{-/-}; IL2rg^{-/-} mice inoculated with 1×10^5 1H9 cells e.c. (D) Kaplan-Meier survival curves of mice inoculated with the melanoma cells. (Rag1^{-/-}: n = 11; Rag2^{-/-}; IL2rg^{-/-}: n = 13). These experiments were jointly performed by Teagan Wagner.

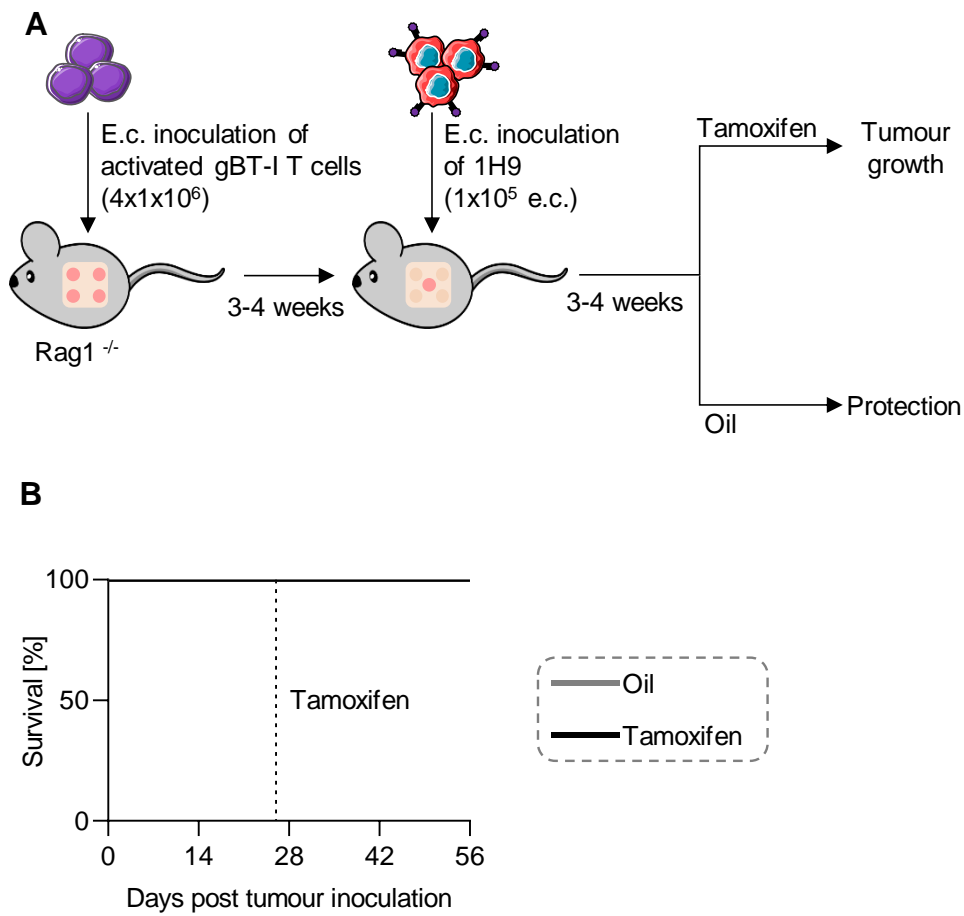


Figure 5.35: *In vivo* treatment of Rag1^{-/-} mice with Tamoxifen does not lead to tumour escape from T_{RM} control

(A) Graphical depiction of experimental setup. (B) Kaplan-Meier survival plot of indicated groups of mice (Oil: n = 5; Tamoxifen: n = 6). These experiments were jointly performed with Emma Bawden and Teagan Wagner.

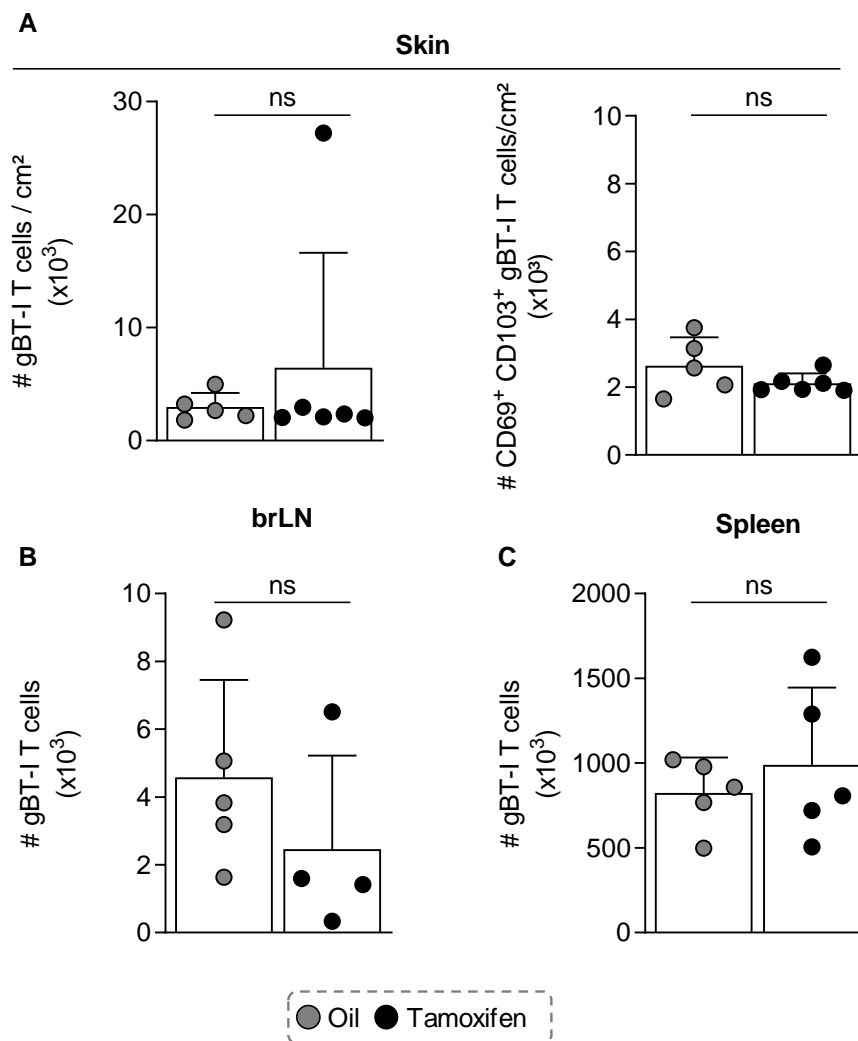


Figure 5.36: Tamoxifen treatment of Rag1^{-/-} mice that were e.c. inoculated with activated gBT-I and 1H9 cells does not lead to significant differences of gBT-I T cells in different organs

(A) Quantification of gBT-I T cells and CD69⁺ CD103⁺ gBT-I T cells in skin. brLN and spleen in non-developer mice of the different treatment groups. (B and C) Quantification of gBT-I T cells in the (B) brLN and (C) spleen of non-developer mice of the different treatment groups. (Oil: n = 5, mean ± SD; Tamoxifen: n = 6; mean ± SD). Statistics: ns-not significant, Mann-Whitney-U test. These experiments were jointly performed with Emma Bawden and Teagan Wagner.

5.3. Discussion

Treatment of melanoma has improved during the past few years especially from the advent of immunotherapies. The development of new therapeutic approaches was made possible by the use of mouse melanoma models that helped to understand tumour biology and immune cells that mediate anti-tumour-immunity. *In vivo* mouse models should reliably recapitulate tumour and TME features found in human melanoma to advance clinical translation.

Primary models such as the *HgfxCdk4^{R24C}* mouse melanoma model offer the opportunities to investigate the role of immune responses during the natural progression of the tumour in an immunocompetent host. In this melanoma model mice spontaneously develop primary melanomas during the first year of life. Additionally, the melanoma cells migrate to the draining lymph nodes and form metastases (Landsberg et al., 2010). However, spontaneous formation of primary melanomas can take up to a year. The epicutaneous melanomas presented in this chapter are localised in the epidermis, dermis or subcutis. Additionally, it forms metastases in the draining lymph nodes and offers an alternative to time consuming primary melanoma models. The epicutaneous melanoma inoculation model has slightly slower growth kinetics compared to other transplantable models and is a more elaborate process but it gives us the opportunity to investigate melanomas that initially arise in the epidermis as opposed to melanomas that initially arise in the dermis or subcutis found in other transplantable models.

Tissue-resident memory T cells have been known to control viral infections such as HSV-1 in non-lymphoid organs. However, only recently it was shown that CD8⁺ T_{RM} cells can also control tumour growth in mouse models although correlative associations between enhanced patient survival and T_{RM} cells have been made before. So far, it is not fully understood how T_{RM} cells in the skin control melanoma outgrowth. We were interested in whether the process of tumour control by T_{RM} cells occurs in an antigen-dependent or antigen-independent manner.

In order to investigate this, we needed a model cell line that allowed inducible antigen loss *in vivo*. To this end, we modified the CRISPiTope approach established in Chapter 3 and Chapter 4. We generated a cell line that expressed

the Cre-recombinase under the control of ERT2. Additionally, we modified the cell line using the SWITCHitope approach by targeting the cytoskeletal housekeeping proteins β -Actin or γ -Actin. The two cytoplasmic actins, β -Actin and γ -Actin, are essential proteins that are highly conserved and ubiquitously high expressed in all cell types. Generating a fusion protein with either β -Actin or γ -Actin and the model antigen gB leads to a ubiquitously high antigen expression in the melanoma cells. Retroviral overexpression of Cre-ERT2 and SWITCHitope-engineering generated a cell line which upon Tamoxifen treatment loses antigen expression and changes colour. The two cytoplasmic actins, β -Actin and γ -Actin, are essential proteins that are highly conserved and ubiquitously high expression in all cell types. Generating a fusion protein with either β -Actin or γ -Actin and the model antigen gB leads to a ubiquitously high antigen expression in the melanoma cells. Retroviral overexpression of Cre-ERT2 and SWITCHitope-engineering generated a cell line which upon Tamoxifen treatment loses antigen expression and changes colour.

We could show that the depletion of the antigen works in vitro in polyclonal cultures in which we targeted the cytoskeletal proteins β -Actin or γ -Actin using 4-Hydroxytamoxifen, the active metabolite of Tamoxifen. We observed that when the melanoma cells were treated with 4-OHT the cells do not only become mNeon positive but they also show two distinct mScarlet populations (mScarlet^{low} vs. mScarlet^{high}). Melanoma cells that have switched colour and lost a big part of the integrated universal donor plasmid upon 4-OHT treatment are mScarlet^{high} whereas cells that have not switched are mScarlet^{low}. We reasoned that nonsense mediated mRNA decay (NMD) might be responsible for the mScarlet^{low} cell population. Although NMD it is often described as a process that controls degradation of mRNAs containing premature translation termination codons it can also target physiological transcripts that do not harbour a premature translation termination codon (Nicholson et al., 2010). The SWITCHitope targeting approach leads to the insertion of approximately 5 kb of DNA immediately upstream of the stop codon potentially generating a scenario in which NMD might play a role.

We decided to use a monoclonal cell line as opposed to polyclonal cell lines to

ensure homogenous expression of Cre-ERT2 and eliminate cells that might not have been targeted by the SWITCHitope approach. All monoclonal cell lines analysed during this study showed successful colour switching and similar expression levels of MHC class I molecule H2-Kb which is essential for the presentation of the gB epitope to gBT-I T cells (Mueller et al., 2002). We found that depletion of the gB epitope by 4-OHT treatment lead to significantly reduced T cell activation using all melanoma cell lines tested. Nevertheless, we did not observe complete abrogation of gBT-I T cell activation. Actin has a relatively long half-life of at least 48 hours (Antecol et al., 1986). This could lead to actin filaments that have not yet been targeted by the Cre-recombinase and therefore residual gB antigen that is still present in the melanoma cells. Longer treatment of the cells with 4-OHT to allow complete turnover of the cytoskeletal proteins or the combination treatment with a compound that enhances general protein turnover could possibly lead to complete abrogation of T cell activation.

The cell line that was selected for the planned in vivo studies showed only a low frequency of mNeon positive cells in steady state condition indicating that only in a few cells the Cre-ERT2 translocates into the nucleus and induces the switch spontaneously (Feil et al., 1997; Indra et al., 1999; Ruzankina et al., 2007). Additionally, this monoclonal cell line showed a robust switch upon 4-OHT treatment and the best fold change in T cell activation compared to the other available cell lines. Although the fusion of the mutated estrogen receptor, ERT2, and the Cre-recombinase was engineered to be more specific and efficient than the original Cre-ERT, spontaneous Cre activity was still observed (Kristianto et al., 2017). Unintended Cre-recombinase activity can be a confounding factor. Therefore, it is critical to consider Cre-activity when designing an experiment.

We observed that inoculation with the melanoma cell line 1H9 resulted in very low tumour incidence in vivo compared to the parental cell line. Park and colleagues showed 60 % of epicutaneously inoculated mice develop melanomas whereas we only observed an incidence of 10-20 % (Park et al., 2019). Actin has a high expression level and therefore expression of the fluorescent protein mScarlet is equally high. Previous studies have reported that expression of fluorescent proteins such as GFP can have a cytotoxic effect on the expressing

cells or induce an immune response *in vivo* (Ansari et al., 2016). This could explain the low tumour incidence observed in our experiments. Of note, we observed lower tumour incidence during intracutaneous injections with other melanoma cell lines in which we targeted β - or γ - Actin using the CRISPRitope approach. For future studies, a protein target that is essential but has lower expression levels might be a better choice and could result in higher incidence rates.

Although tumour incidence is low, we observed that the 1H9 melanoma cells could recruit *in vivo* expanded naïve gBT-I T cells to the skin which then differentiated into T_{RM} cells characterised by the surface markers CD69 and CD103. We analysed peritumoural skin from one tumour that was mScarlet, and therefore also gB antigen negative, and found gBT-I T cells with a T_{RM} phenotype. This indicates that either the tumour was originally mScarlet and gB antigen positive but lost antigen expression due to immune pressure or that the gB antigen was randomly integrated into the genome and still activates, and thereby recruits, antigen-specific T cells. From the tumours that we harvested we generated *ex vivo* cell lines and tested whether these cell lines still have the potential to activate T cells in an *in vitro* assay. The melanoma cell lines that are mScarlet positive, but not the ones that are mScarlet negative, could activate gBT-I T cells indicating that antigen was likely lost due to immune pressure by gBT-I T cells in the peritumoural skin. Although tumour incidence was low we observed gBT-I T cells with a T_{RM} phenotype in the skin in almost all mice independent of tumour growth. gBT-I T_{RM} cells were rare in the brachial lymph node and the spleen.

In order to demonstrate whether T_{RM} cells control melanomas in an antigen-dependent manner, we set up a tripartite experiment. Mice were inoculated with gBT-I T cells in the skin to generate T_{RM} cells to control tumour growth. The idea was to demonstrate that the mice that were inoculated with the 1H9 melanoma cells and immediately treated with Tamoxifen show normal growth kinetics as shown by Park and colleagues. The gB antigen would be depleted and the melanoma cells therefore not recognised by the previously inoculated gBT-I T cells. Additionally, we wanted to demonstrate that mice that were left untreated

only develop tumours after Tamoxifen treatment after several weeks of tumour control. However, as tumour incidence is very low the data is inconclusive. Nevertheless, we analysed the skin, brachial lymph node and spleen of the mice and did not find any significant difference between the different treatment groups. Independent of the fact that tumour growth proved challenging in immunocompetent C57BL/6 mice, we wanted to investigate whether T_{RM} cells control melanoma cells in an antigen-dependent manner, independent of the endogenous T cell repertoire in immunocompromised mice. In Rag1^{-/-} mice which lack B and T cells we observed tumour growth in 50 % of mice whereas we observed 100 % tumour growth in Rag2^{-/-}; IL2rg^{-/-} mice which lack B, T and NK cells (Mazurier et al., 1999; Mombaerts et al., 1992). As only limited amounts of these mouse strains were available results are preliminary. As previously described, we wanted to demonstrate that Rag1^{-/-} mice that were epicutaneously inoculated with activated gBT-I T cells and subsequently inoculated with 1H9 melanomas cells can control tumour growth. Upon Tamoxifen treatment, we expected the treated mice to develop a tumour. However, we did not observe any tumour incidences in Rag1^{-/-} mice. We analysed the skin, brachial lymph node and spleen of control-treated and Tamoxifen-treated mice and did not observe a significant difference in numbers of gBT-I T cells in the different organs between the different treatment groups. As previously mentioned, we only observed 50 % of tumour incidence in a very small cohort of Rag1^{-/-} mice compared to a 100 % tumour incidence in Rag2^{-/-}; IL2rg^{-/-} mice. Experiments need to be repeated to fully address whether the 1H9 cells are controlled in an antigen-dependent manner in Rag2^{-/-}; IL2rg^{-/-} mice. Additionally, one needs to consider targeting a different protein using the SWITCHitope approach as the high expression levels of actin might contribute to the low tumour incidence.

Chapter 6:

Concluding remarks

Chapter 6: Concluding remarks

6.1. General discussion

Malignant melanoma is a highly aggressive form of skin cancer that arises from neoplasms of the melanocytic lineage. In the recent years, therapy outcome of patients suffering from melanoma has significantly increased due to the development of new treatment approaches such as ACT or checkpoint immunotherapy (Chodon et al., 2014; Goff et al., 2016; Hodi et al., 2016; Larkin et al., 2015; Rosenberg and Restifo, 2015; Schachter et al., 2017). Adoptive cell therapy is a highly personalised treatment approach for patients suffering from advanced melanoma. In the past, it has been shown that tumour-reactive T cells can mediate durable and complete tumour regression with limited toxicities. These responses are achieved by T lymphocytes that target public tumour antigens or individual somatic mutations. However, selection of optimal target epitopes and how they impact resistance mechanisms still remains an unresolved challenge (Stranzl et al., 2010). It is largely unknown how the biology and the endogenous regulation of the epitope-encoding gene product (antigen) influences resistance mechanisms of ACT immunotherapy.

Work presented in this thesis therefore aimed to create a platform that enables us to investigate how the biology of an epitope-encoding gene product impacts on resistance mechanisms in the context of ACT immunotherapy. As a proof-of-principle experiment, we aimed to compare resistance mechanisms of melanomas when either a differentiation tumour antigen, such as a melanocyte-derived antigen, or a somatic mutation, such as an oncogene, is targeted by epitope-standardised ACT immunotherapy.

In addition, this thesis aimed at understanding whether CD8⁺ T_{RM} cells control melanomas in an antigen-dependent manner. By adapting the CRISPR/Cas9-based technique developed for the first part of this thesis, we developed a melanoma cell line model in which we can deplete an antigen recognised by TCR_{tg} cells. Combining the antigen depletion model with an epicutaneous TCR_{tg} T cell inoculation, to generate T_{RM} cells in the skin, and an epicutaneous melanoma cell inoculation, we developed a tool to interrogate whether T_{RM} cells

control melanoma outgrowth in an antigen-dependent manner.

6.2. Key findings of the study

6.2.1. Chapter 3

The aim of this chapter was to develop an experimental CRISPR/Cas9-based approach to investigate the diversity of melanoma resistance and immune evasion mechanisms. We generated a highly flexible and modular CRISPR/Cas9-based technique that allows us to generate C-terminal endogenous fusion proteins with a fluorescent protein, a FLAG-tag, an immunological epitope tag and a selection marker. By targeting different proteins using this approach we can model tumour antigens that can be recognised by a single TCRtg T cells species. This gives us the advantage that the immunological epitope tag that is fused to the target protein is recognised by the same T cell species. Thereby we eliminate the confounding factor that different epitopes have different MHC class I affinity and that T cells with different TCRs might vary in their potential to recognise different epitopes. The approach we present in this chapter is efficient and generates polyclonal cell lines. The CRISPEpitope approach allows us to investigate the expression, presentation and recognition of tumour antigens.

6.2.2. Chapter 4

Using a syngeneic mouse melanoma model and the CRISPEpitope approach we investigated how ACT immunotherapy targeting either melanosomal TYRP1 or oncogenic CDK4^{R24C} influences melanoma responses and resistance mechanisms. In the patient setting, a major challenge of ACT immunotherapy is the selection of the right target epitope which can be derived from non-mutated or mutated tumour antigens (Blankenstein et al., 2015; Hinrichs and Restifo, 2013). However, our knowledge on how the function and regulation of epitope-encoding gene products influence ACT and resistance mechanisms remains limited. We identified different resistance mechanisms depending on whether we targeted melanosomal TYRP1 or oncogenic CDK4^{R24C}. Adaptive phenotype switching, which involves the downregulation of melanosomal proteins by pro-

inflammatory cytokines, was more pronounced when TYRP1 was targeted (Landsberg et al., 2012; Riesenberger et al., 2015). Melanoma cells that underwent inflammation induced dedifferentiation had a survival benefit as the melanosomal protein TYRP1 was downregulated and thus the target of the T cells was lost. In addition to the adaptive phenotype switching, we identified genetic and epigenetic resistance mechanism of antigen loss after ACT immunotherapy. Genetic mechanisms included the lack of the C-terminal hgp100 epitope or a single base pair mutation that lead to a premature stop codon and therefore to abrogated epitope translation. We also identified a recurrent melanoma that showed selective transcriptional silencing of only the epitope-encoding allele. Recurrent TYRP1-NFhgp100 melanomas that had lost the epitope by either genetic or epigenetic mechanisms were characterised by a non-inflamed TME. The majority of recurrent CDK4^{R24C}-NFhgp100 melanomas presented with antigen persistence and higher expression levels of IFN response genes, T cell marker genes and negative immune checkpoint genes such as CTLA-4 and PD-1. Although these melanomas were infiltrated with T cells their functionality would be impaired by negative immune checkpoint molecules. In conclusion our study shows that the antigen status determines the immune contexture of recurrent melanomas. Our novel CRISPEpitope approach in combination with ACT immunotherapy can portray changes in the immune landscape in the TME that is also observed in patients.

6.2.3. Chapter 5

Mouse melanoma models help to understand tumour biology and anti-tumour immune responses. These models should recapitulate tumour and TME features found in human melanoma to make findings as translational as possible. The epicutaneous melanoma described in this chapter represents an alternative to time-consuming primary models and has similar tumour features as human melanoma. In the epicutaneous melanoma model, melanoma cells are transplanted onto in the epidermis and spontaneously metastasise into the draining lymph node. The process of how T_{RM} cells control melanoma outgrowth is not fully understood. This chapter aimed at investigating whether epicutaneous

melanomas are controlled in an antigen-dependent manner. We generated a model melanoma cell line using a CRISPR/Cas9-based method termed SWITCHitope. This technique allowed us to deplete the gB model antigen in vitro and in vivo using Tamoxifen and to monitor the antigen depletion by a colour switch. We showed that the antigen depletion could be monitored by a colour switch and that depletion of the antigen lead to reduced T cell activation. However, we did not observe complete abrogation of T cell activation. As tumour incidence was low in C57BL/6 mice, the majority of the results from this chapter are preliminary. Nevertheless, we observed that our SWITCHitope-engineered melanoma cells can recruit naïve gBT-I T cells to the skin where they differentiate into T_{RM} cells. Tumour inoculation experiments performed in immunodeficient Rag1^{-/-} and Rag2^{-/-}; IL2rg^{-/-} mice showed higher incidence compared to C57BL/6 mice. Rag1^{-/-} mice were epicutaneously inoculated with activated gBT-I T cells to form T_{RM} cells and subsequently with the SWITCHitope-engineered melanoma cells. We observed that melanomas did not grow when gBT-I T cells were inoculated in the skin. However, we did not observe tumour growth after the mice had been treated with Tamoxifen and the antigen was depleted. This may indicate that NK cells play a role in melanoma control in this setting or that T_{RM} cells that were shown to secrete pro-inflammatory cytokines such as IFN γ and TNF α and cytotoxic effector proteins such as granzyme B upon local activation have eliminated the melanoma cells (Djenidi et al., 2015; Ganesan et al., 2017; Hombrink et al., 2016; Masopust et al., 2001; Webb et al., 2015). Moreover, it could indicate that tumour incidence was initially low and that tumours would not have grown in the first place even in the absence of antigen-specific T_{RM} cells.

6.3. Relevance

The further improvement of ACT and other immunotherapeutic treatment approaches, such as cancer vaccines or checkpoint blockade, is vastly dependent on the identification and deep understanding of the biology. This involves knowledge about suitable immunogenic target epitopes and the insight into the function of our immune system.

Mutations that are involved in oncogenesis and are shared not only among patients but also across different tumour entities would be excellent targets for ACT using conventional $\alpha\beta$ -TCRs. Next-generation sequencing enables us to analyse the diverse landscape of genetic alterations that can be found in cancer and thereby facilitate precision medicine. The current advances in NGS, computational tools and the access to large-scale human genome databases has created an immense opportunity to implement personalised medicine on a regular basis.

In current therapy concepts, T lymphocytes recognising neo-antigens are used to drive cancer regression (McGranahan et al., 2016; Naiyer A. Rizvi et al., 2015b; Snyder et al., 2014b; Tran et al., 2016; Van Allen et al., 2015). Efficacy of cancer immunotherapy is limited to tumours with high mutational burden, as only a very limited fraction of mutations can elicit a spontaneous immune response (Linnemann et al., 2015; Matsushita et al., 2012; Tran et al., 2015). Moreover, tumour mutations are often restricted to individual patients making personalised cancer therapy highly necessary. Very recently, Sahin *et al.* and Ott *et al.* presented their results of phase I clinical trials with personalised vaccine-based therapy approaches in patients with skin cancer (Ott et al., 2017; Sahin et al., 2017). The treatment strategy presented by Sahin and colleagues is a personalised RNA mutanome vaccine that mobilises poly-specific therapeutic immunity. This approach included identification of individual mutations of tumours, computational predictions of neo-antigens and the design and manufacturing of a vaccine for individual patients. After vaccination, tumours were infiltrated with T cells specific for neo-antigens of the tumour leading to sustained progression-free survival (Sahin et al., 2017). The approach of Ott and colleagues was to use an immunogenic, personalised neo-antigen vaccine that targeted up to 20 individual predicted tumour neo-antigens. This vaccination protocol induced poly-functional CD8⁺ and CD4⁺ T cell responses and 66% of the patients had no tumour recurrence at more than 2 years after vaccination. The other 33% of patients who had tumour recurrence were subsequently treated with α -PD-1 mAB therapy and experienced complete tumour regression (Ott et al., 2017).

Melanoma is the prime example when it comes to immunotherapy and had the greatest success rate with immunotherapy. But a study from 2014 showed that mutated immunogenic epitopes from a metastatic cholangiocarcinoma could be recognised by TILs that led to anti-tumour immune response (Tran et al., 2014). This shows that other epithelial cancers are also treatable with ACT as long as a mutation that produces an immunogenic epitope is identified.

ACT and personalised vaccine approaches are indisputably complex, expensive and labour-intensive approaches to treat cancer compared to immunotherapeutic approaches such as checkpoint blockade. It imposes challenges to cancer centres and pharmaceutical companies that would prefer solutions suitable for more than one individual patient. But new biotechnology companies specialise in the expansion of patient-derived lymphocytes and often larger medical centres have facilities for detailed genetic analyses of tumours. In the end, the effectiveness of the treatment will dictate the broader application of a personalised cancer immunotherapy approach such as ACT. Studies presented by Sahin *et al.* and Ott *et al.* show that individual unique cancer mutations can be exploited for personalised immunotherapy, either as monotherapy or in combination with other immunotherapies (Ott et al., 2017; Sahin et al., 2017).

Failure of TIL or ACT therapy can be caused by the upregulation of negative checkpoint molecules, such as PD-1 or CTLA-4, on the T lymphocytes, and PD-L1 on tumour cells or other immune cells present in the tumour microenvironment. Clinical trials investigating combination therapy of TIL ACT plus α -PD-1 antibody are currently ongoing (NCT01993719, NCT02652455). TIL ACT may also be used in combination with other antibodies that block inhibitory signalling in immune cells such as α -CTLA-4, currently only performed in mice (Mahvi et al., 2015). In addition to ACT plus immune checkpoint combination therapy, clinical trials are currently investigating the effect of CRISPR/Cas9-mediated knockout of the endogenous TCR and PD-1 in engineered T cells and engineered CAR T cells in patients with various types of solid tumours such as melanoma or sarcoma (NCT03545815, NCT03399448).

We present a pre-clinical platform to guide the selection of possible target antigens for individual cancer immunotherapies as advances in NGS technology

make antigen-directed personalised therapeutic approaches possible. This approach provides novel insights into the diversity and context dependent melanoma immune evasion mechanisms. As this approach is highly flexible and modular it can be easily adapted to other syngeneic mouse cancer models making it an attractive methodology to other laboratories.

For a long time, the main focus in cancer immunology was on circulating tumour-reactive CD8⁺ T cells. However, during the past decade, studies showed that lymphocytes can also establish residency in non-lymphoid tissues such as the skin. T_{RM} cells have largely been defined and characterised in the context of immunity to infection but research now shows that they are also a critical component in the host immune response to cancer.

Correlative studies have shown that tissue-resident CD8⁺ T cells identified by the markers CD103 or VLA-1 are associated with improved survival in breast cancer, ovarian cancer and melanoma (Bösmüller et al., 2016; Edwards et al., 2018; Egelston et al., 2017; Murray et al., 2016; Webb et al., 2015). The impact of T_{RM} cells on survival is independent on general infiltration of CD8⁺ T cells (Edwards et al., 2018; Ganesan et al., 2017; Komdeur et al., 2017; Nizard et al., 2017).

Recently, a direct contribution of T_{RM} cells to tumour control in experimental mouse models was established. Among others, Park and colleagues could show that CD8⁺ T_{RM} cells can suppress melanoma progression and promote melanoma-immune equilibrium in skin (Park et al., 2019).

T_{RM} cells have properties that explain their functional role in a tumour context. Firstly, studies have shown that T_{RM} cells respond faster to their cognate antigen upon re-exposure compared to their circulating counterparts (Ariotti et al., 2014; Schenkel et al., 2014). Secondly, they express high levels of cytotoxic molecules. Studies in healthy tissue but also in various cancerous tissues have shown that T_{RM} cells express high levels of cytotoxic molecules such as granzyme B, IFN γ and TNF α (Cheuk et al., 2017; Hombrink et al., 2016; Pallett et al., 2017; Webb et al., 2014). And thirdly, CD103⁺ TILs preferentially localise to epithelial regions of tumours. E-cadherin, the natural ligand of CD103, is expressed by epithelial tumour cells and potentially explains why CD103⁺ TILs are found in close contact

with tumour cells rather than with stroma cells (Z.-Q. Wang et al., 2016; Webb et al., 2014).

Studies investigating negative immune checkpoint molecules on CD8⁺ T cells and T_{RM} cells have suggested that T_{RM} cells are the main target cell population of immune checkpoint blockade. T_{RM} cells from healthy tissue or tumour tissue express higher levels of inhibitory receptors such as PD-1, TIM-3 and CTLA-4 compared to CD8⁺ CD103⁻ TILs or peripheral memory CD8⁺ T cells (Boddupalli et al., n.d.; Ganesan et al., 2017; Hombrink et al., 2016; Kumar et al., 2017; Mackay et al., 2013). The profile of immune checkpoint molecules on T_{RM} cells varies depending on tumour localisation. T_{RM} cells derived from melanoma or non-small cell lung cancer do not express CTLA-4 (Djenidi et al., 2015; Edwards et al., 2018). PD-1⁺ T_{RM} cells derived from ovarian cancer have weak expression of CTLA-4, LAG-3 and TIM-3 (Webb et al., 2015). TCGA (The Cancer Genome Atlas) data analysis showed that the marker CD103 is not only correlated with CD8 but also with PD-1, PD-L1, CTLA-4 and CD137 in cervical cancer (Komdeur et al., 2017). In a preclinical model, combination therapy of T_{CM} transfer and of α-PD-1 antibody lead to increased TILs with a T_{RM} phenotype and inhibited tumour growth (Enamorado et al., 2017). In melanoma patients, CD8⁺ T_{RM} cells significantly expanded early during α-PD-1 checkpoint therapy as presented by Edwards and colleagues. Their study shows that CD103⁺ tumour-resident CD8⁺ T cells are not only important for tumour control but may also be important in predicting responses to α-PD-1 checkpoint therapy or other immune checkpoint therapies as the CD69⁺ CD103⁺ CD8⁺ T cell subset expresses high levels of PD-1 and LAG-3 (Edwards et al., 2018).

A recent study has shown that human CD4⁺ CD103⁺ cutaneous resident memory T cells can recirculate in healthy individuals. Using tissue explant cultures, Klicznik and colleagues identified CD4⁺ CD69⁺ CD103⁺ T_{RM} cells in human skin that can downregulate CD69 and egress from the tissue. Additionally, they identified a CD4⁺ CD69⁻ CD103⁺ cell population that is transcriptionally, clonally and functionally related to the T_{RM} population originating in the skin in human blood and lymph (Klicznik et al., 2019). Beura and colleagues showed that CD8⁺ T_{RM} cells can emigrate from skin and form secondary-lymphoid organ (SLO) T_{RM}

cells in the draining lymph node. These SLO T_{RM} cells partly share phenotypic and transcriptional signatures found in skin T_{RM} cells (Beura et al., 2018). Studies suggest that T_{RM} cells are a main target of checkpoint therapy. Taken together with the data that showed that T_{RM} cells can exit non-lymphoid tissues and recirculate into the draining lymph node might explain why some patients with metastatic tumours respond really well to checkpoint immunotherapy.

Milner and colleagues showed that transcription factor, Runx3, is required to establish T_{RM} cells in different tissue environments. A mouse melanoma model of ACT showed that Runx3-deficient CD8⁺ TILs do not infiltrate in the tumour which results in increased tumour growth and mortality. Overexpression of Runx3 enhanced accumulation of CD8⁺ TILs which led to delayed tumour growth and prolonged survival (Milner et al., 2017). This knowledge is important to eventually enhance vaccine efficacy or ACT strategies to target cancer.

It is evident that T_{RM} cells are involved in the efficacy of different cancer immunotherapy approaches but in order to develop strategies that specifically induce and amplify T_{RM} cells a deep understanding of their biology is critical. We need to understand how T_{RM} cells control tumour cells and whether constant antigen presentation by the tumour cells is critical for this control. Evidently, we are only beginning to understand T_{RM} biology but the potential implications for immuno-oncology are substantial.

6.4. Limitations of the study

Although we could show that different ACT target antigens induce different melanoma escape mechanisms in Chapter 4 some aspects implicated in these processes remain unresolved. Firstly, the expression of TYRP1-NFhgp100 was higher than CDK4^{R24C}-NFhgp100. As such, we do not know whether the expression level influenced the observed differences in resistance mechanisms or whether the different immune escape mechanisms truly reflected distinct differences in tumour antigen biology (melanosomal vs. oncogene product). To address this question, collaborators treated cohorts of C57BL/6 mice inoculated with either HC.PmelKO-TYRP1-NFhgp100 or HC.PmelKO.CDK4^{R24C}-NFhgp100 with the ACT approach presented in Chapter 4 without the *in vivo* activation of

the pmel-1 TCRtg T cells by the adenovirus coding for human gp100 (Ad-hgp100). They observed that mice inoculated with HC.PmelKO.CDK4^{R24C}-NFhgp100 melanoma cells only responded marginally to ACT without Ad-hgp100. None of the mice experienced complete tumour regression and had escaped therapy by 33 days after tumour inoculation at the latest. Mice inoculated with HC.PmelKO.TYRP1-NFhgp100 melanoma cells responded better to ACT without Ad-hgp100 but more mice escaped from therapy than in the ACT approach presented in Chapter 4. The Ad-hgp100 induces a strong T cell activation *in vivo* which gives us the opportunity to solely focus on the biology of the antigen-encoding gene product independent of antigen expression levels. Another option to address whether expression levels influence the observed resistance mechanisms is a repetition of the experiments for a different gene product that is either a lowly expressed differentiation antigen or a highly expressed mutated oncogene. Possible targets for lowly expressed differentiation antigens would be GPNMB which is a transmembrane glycoprotein or Rab38 (Ras-related protein Rab 38) which is involved in pigmentation. Both proteins are regulated by the transcription factor MITF similar to TYRP1 but with expression levels similar to CDK4^{R24C}.

Preliminary results showed that tumours without antigen loss but with an IFN-driven inflamed TME could be controlled by immune modulatory monoclonal antibodies such as α -PD-L1. However, to fully address this aspect of the resistance mechanism, established CDK4^{R24C} melanomas that are characterised by antigen persistence should be treated with immune checkpoint therapy shortly after ACT.

Given the fact that we performed bulk 3' mRNA-Seq, we cannot differentiate between different cell types in the TME that express negative immune checkpoint molecules. Tumour cells can express PD-L1 which can be induced by IFN γ or driven by oncogene expression (Taube *et al.*, 2012; Rodić *et al.*, 2015; Benci *et al.*, 2016). But we also know from previous studies that other immune cells such as neutrophils can acquire an immunosuppressive phenotype characterised by the expression of the negative immune checkpoint molecules PD-L1 (Glodde *et al.*, 2017). Phenotyping of recruited bystander cells and tumour cells by flow

cytometry could elucidate which cells in the TME express PD-L1 or other negative checkpoints and thereby limit the functionality of T cells and efficacy of ACT immunotherapy.

Antigen-presenting cells can capture tumour-associated antigens by various mechanisms and present them to other immune cells. Among the sources for antigens are necrotic or apoptotic tumour cells, fragments of the plasma membrane, soluble proteins, heat-shock protein complexes or vesicles secreted by tumour cells (Albert et al., 1998; Basu et al., 2001; Harshyne et al., 2001; Norbury et al., 2004; Wolfers et al., 2001). This study only addressed resistance mechanisms of two tumour-associated antigens from two different subcellular compartments. However, a minigenes screening approach that analysed TILs from 21 melanoma patients identified a total of 45 mutated proteins. Each mutation was from a different expressed protein originating from different subcellular localisations and not shared among melanomas from other patients. A screen investigating the potential of antigens originating from different subcellular compartments to activate T cells could help elucidate the impact of the localisation of an antigen-producing protein on the efficacy of ACT immunotherapy. Genetic engineering of human melanoma cells by the CRISPiTope approach would enable us to specifically investigate human antigen biology and validate the translational potential of our findings in mouse models. Immunodominant CD8⁺ epitopes derived from different viruses such as cytomegalovirus (CMV) or influenza virus (Flu) are alternatives to what was presented in this study. The majority of people possess, for example, CMV- or Flu-specific CD8⁺ T cells that could be used instead of CD8⁺ TCRtg T cells from mice.

Although we successfully established the SWITCHitope melanoma model in Chapter 5 there are still aspects that need to be addressed in future investigations.

The switch of the melanoma cells is reliable. Nevertheless, we do not see complete abrogation of T cell activation when co-cultured with Tamoxifen-treated antigen-deficient SWITCHitope-engineered melanoma cells. Choosing a different

target that is also essential but has a lower expression level, higher protein turnover or shorter protein half-life could possibly resolve this issue.

Additionally, to the topic discussed above the SWITCHitope-engineered melanoma cells have low tumour incidence in C57BL/6 mice. One reason might be the extensive genetic manipulations of the parental melanoma cell line. The cell line used in this study was modified by CRISPR/Cas9 to ablate Tyrosinase expression, transduced with a retrovirus encoding Cre-ERT2 and modified by the SWITCHitope approach. During the extensive genetic manipulation, cells were transfected, FACS sorted, transduced, antibiotic selected and plated as monoclonal cell lines more than once. In the past we have observed that monoclonal cell lines can differ from the parental cell line with regard to mRNA and protein expression profiles, growth characteristics and morphology. Extensive in vitro engineering of melanoma cells could possibly generate unknown vulnerabilities which are poorly defined.

In this study, the housekeeping gene γ -Actin was targeted by the SWITCHitope approach generating a fusion protein with the fluorescent protein mScarlet and when treated with Tamoxifen additionally with mNeon. γ -Actin has very high protein expression levels and therefore expression of the fluorescent protein is equally high. Previous studies have shown that fluorescent proteins can have a cytotoxic effect on the expressing cells or induce an immune response in the in vivo context (Ansari et al., 2016). As already suggested above, an alternative target protein with lower expression levels could possibly resolve this problem.

Another alternative could be to inoculate the melanoma cells intra- or subcutaneously and generate a new cell line from the resulting tumour. In past experiments, serial transplantation of *ex vivo* cell lines has resolved issues with low tumour incidence. Generally, optimisation of the engineering pipeline and serial transplantation in vivo could help optimise tumour incidence.

We aimed to investigate whether T_{RM} cells control melanoma cells in an antigen-dependent manner independent of the endogenous T cell repertoire and therefore chose immunocompromised Rag1^{-/-} mice. Firstly, we wanted to demonstrate that Rag1^{-/-} mice that were epicutaneously inoculated with activated gBT-I T cells, and subsequently inoculated with SWITCHitope-engineered

melanoma cells, can control tumour growth. Upon Tamoxifen treatment, we predicted that the treated mice may develop tumours due to loss of antigen. However, we did not observe any tumour outgrowth in Tamoxifen-treated Rag1^{-/-} mice. This experiment needs to be performed in Rag2^{-/-}; IL2rg^{-/-} mice that not only lack B and T cells but additionally NK cells. When we inoculated naïve Rag1^{-/-} mice, we only observed 67 % tumour incidence whereas we observed 100 % tumour incidence in Rag2^{-/-}; IL2rg^{-/-} mice suggesting that NK cells are involved in melanoma control in this experimental setting. NK cells could mediate melanoma control in an antigen-independent manner in these experiments.

Bibliography

- Abdel-Malek, Z., Suzuki, I., Tada, A., Im, S., Akcali, C., 1999. The melanocortin-1 receptor and human pigmentation. *Ann. N. Y. Acad. Sci.* 885, 117–133.
- Abdel-Malek, Z., Swope, V.B., Suzuki, I., Akcali, C., Harriger, M.D., Boyce, S.T., Urabe, K., Hearing, V.J., 1995. Mitogenic and melanogenic stimulation of normal human melanocytes by melanotropic peptides. *Proc. Natl. Acad. Sci. U. S. A.* 92, 1789–1793.
- Akbay, E.A., Koyama, S., Carretero, J., Altabef, A., Tchaicha, J.H., Christensen, C.L., Mikse, O.R., Cherniack, A.D., Beauchamp, E.M., Pugh, T.J., Wilkerson, M.D., Fecci, P.E., Butaney, M., Reibel, J.B., Soucheray, M., Cohoon, T.J., Janne, P.A., Meyerson, M., Hayes, D.N., Shapiro, G.I., Shimamura, T., Sholl, L.M., Rodig, S.J., Freeman, G.J., Hammerman, P.S., Dranoff, G., Wong, K.-K., 2013. Activation of the PD-1 pathway contributes to immune escape in EGFR-driven lung tumors. *Cancer Discov.* 3. <https://doi.org/10.1158/2159-8290.CD-13-0310>
- Albert, M.L., Pearce, S.F.A., Francisco, L.M., Sauter, B., Roy, P., Silverstein, R.L., Bhardwaj, N., 1998. Immature Dendritic Cells Phagocytose Apoptotic Cells via $\alpha\beta 5$ and CD36, and Cross-present Antigens to Cytotoxic T Lymphocytes. *J. Exp. Med.* 188, 1359–1368.
- Alsaieedi, A., Holler, A., Velica, P., Bendle, G., Stauss, H.J., 2019. Safety and efficacy of Tet-regulated IL-12 expression in cancer-specific T cells. *Oncoimmunology* 8, 1542917. <https://doi.org/10.1080/2162402X.2018.1542917>
- Anders, K., Buschow, C., Herrmann, A., Milojkovic, A., Loddenkemper, C., Kammertoens, T., Daniel, P., Yu, H., Charo, J., Blankenstein, T., 2011. Oncogene-Targeting T Cells Reject Large Tumors while Oncogene Inactivation Selects Escape Variants in Mouse Models of Cancer. *Cancer Cell* 20, 755–767. <https://doi.org/10.1016/j.ccr.2011.10.019>
- Angell, T.E., Lechner, M.G., Jang, J.K., LoPresti, J.S., Epstein, A.L., 2014. MHC Class I Loss is a Frequent Mechanism of Immune Escape in Papillary Thyroid Cancer that is Reversed by Interferon and Selumetinib Treatment in vitro. *Clin. Cancer Res. Off. J. Am. Assoc. Cancer Res.* 20, 6034–6044. <https://doi.org/10.1158/1078-0432.CCR-14-0879>
- Anichini, A., Maccalli, C., Mortarini, R., Salvi, S., Mazzocchi, A., Squarcina, P., Herlyn, M., Parmiani, G., 1993. Melanoma cells and normal melanocytes share antigens recognized by HLA-A2-restricted cytotoxic T cell clones from melanoma patients. *J. Exp. Med.* 177, 989–998. <https://doi.org/10.1084/jem.177.4.989>
- Ansari, A.M., Ahmed, A.K., Matsangos, A.E., Lay, F., Born, L.J., Marti, G., Harmon, J.W., Sun, Z., 2016. Cellular GFP Toxicity and Immunogenicity: Potential Confounders in in Vivo Cell Tracking Experiments. *Stem Cell Rev.* 12, 553–559. <https://doi.org/10.1007/s12015-016-9670-8>
- Antecol, M.H., Darveau, A., Sonenberg, N., Mukherjee, B.B., 1986. Altered Biochemical Properties of Actin in Normal Skin Fibroblasts from Individuals Predisposed to Dominantly Inherited Cancers. *Cancer Res.* 46, 1867–1873.

- Apalla, Z., Nashan, D., Weller, R.B., Castellsagué, X., 2017. Skin Cancer: Epidemiology, Disease Burden, Pathophysiology, Diagnosis, and Therapeutic Approaches. *Dermatol. Ther.* 7, 5–19. <https://doi.org/10.1007/s13555-016-0165-y>
- Ariotti, S., Beltman, J.B., Chodaczek, G., Hoekstra, M.E., Beek, A.E. van, Gomez-Eerland, R., Ritsma, L., Rheenen, J. van, Marée, A.F.M., Zal, T., Boer, R.J. de, Haanen, J.B.A.G., Schumacher, T.N., 2012a. Tissue-resident memory CD8+ T cells continuously patrol skin epithelia to quickly recognize local antigen. *Proc. Natl. Acad. Sci.* 109, 19739–19744. <https://doi.org/10.1073/pnas.1208927109>
- Ariotti, S., Haanen, J.B., Schumacher, T.N., 2012b. Chapter 8 - Behavior and Function of Tissue-Resident Memory T cells, in: Melief, C.J.M. (Ed.), *Advances in Immunology, Synthetic Vaccines*. Academic Press, pp. 203–216. <https://doi.org/10.1016/B978-0-12-396548-6.00008-1>
- Ariotti, S., Hogenbirk, M.A., Dijkgraaf, F.E., Visser, L.L., Hoekstra, M.E., Song, J.-Y., Jacobs, H., Haanen, J.B., Schumacher, T.N., 2014. Skin-resident memory CD8+ T cells trigger a state of tissue-wide pathogen alert. *Science* 346, 101–105. <https://doi.org/10.1126/science.1254803>
- Artis, D., Spits, H., 2015. The biology of innate lymphoid cells. *Nature* 517, 293–301. <https://doi.org/10.1038/nature14189>
- Atkins, D., Ferrone, S., Schmahl, G.E., Störkel, S., Seliger, B., 2004. Down-regulation of HLA class I antigen processing molecules: an immune escape mechanism of renal cell carcinoma? *J. Urol.* 171, 885–889. <https://doi.org/10.1097/01.ju.0000094807.95420.fe>
- Ayers, M., Lunceford, J., Nebozhyn, M., Murphy, E., Loboda, A., Kaufman, D.R., Albright, A., Cheng, J.D., Kang, S.P., Shankaran, V., Piha-Paul, S.A., Yearley, J., Seiwert, T.Y., Ribas, A., McClanahan, T.K., n.d. IFN- γ -related mRNA profile predicts clinical response to PD-1 blockade. *J. Clin. Invest.* 127, 2930–2940. <https://doi.org/10.1172/JCI91190>
- Bachmann, M.F., Barner, M., Viola, A., Kopf, M., 1999. Distinct kinetics of cytokine production and cytolysis in effector and memory T cells after viral infection. *Eur. J. Immunol.* 29, 291–299. [https://doi.org/10.1002/\(SICI\)1521-4141\(199901\)29:01<291::AID-IMMU291>3.0.CO;2-K](https://doi.org/10.1002/(SICI)1521-4141(199901)29:01<291::AID-IMMU291>3.0.CO;2-K)
- Bachmann, M.F., Wolint, P., Schwarz, K., Oxenius, A., 2005. Recall Proliferation Potential of Memory CD8+ T Cells and Antiviral Protection. *J. Immunol.* 175, 4677–4685. <https://doi.org/10.4049/jimmunol.175.7.4677>
- Bald, T., Quast, T., Landsberg, J., Rogava, M., Glodde, N., Lopez-Ramos, D., Kohlmeyer, J., Riesenberger, S., van den Boorn-Konijnenberg, D., Hömig-Hölzel, C., Reuten, R., Schadow, B., Weighardt, H., Wenzel, D., Helfrich, I., Schadendorf, D., Bloch, W., Bianchi, M.E., Lugassy, C., Barnhill, R.L., Koch, M., Fleischmann, B.K., Förster, I., Kastenmüller, W., Kolanus, W., Hölzel, M., Gaffal, E., Tüting, T., 2014. Ultraviolet-radiation-induced inflammation promotes angiogenesis and metastasis in melanoma. *Nature* 507, 109–113. <https://doi.org/10.1038/nature13111>
- Ballantine, K.R., Watson, H., Macfarlane, S., Winstanley, M., Corbett, R.P., Spearing, R., Stevanovic, V., Yi, M., Sullivan, M.J., 2017. Small Numbers, Big Challenges: Adolescent and Young Adult Cancer Incidence and

- Survival in New Zealand. *J. Adolesc. Young Adult Oncol.* 6, 277–285. <https://doi.org/10.1089/jayao.2016.0074>
- Banerjee, A., Gordon, S.M., Intlekofer, A.M., Paley, M.A., Mooney, E.C., Lindsten, T., Wherry, E.J., Reiner, S.L., 2010. Cutting Edge: The Transcription Factor Eomesodermin Enables CD8+ T Cells To Compete for the Memory Cell Niche. *J. Immunol.* 185, 4988–4992. <https://doi.org/10.4049/jimmunol.1002042>
- Bankovich, A.J., Shiow, L.R., Cyster, J.G., 2010. CD69 Suppresses Sphingosine 1-Phosphate Receptor-1 (S1P1) Function through Interaction with Membrane Helix 4. *J. Biol. Chem.* 285, 22328–22337. <https://doi.org/10.1074/jbc.M110.123299>
- Bassani-Sternberg, M., Bräunlein, E., Klar, R., Engleitner, T., Sinitcyn, P., Audehm, S., Straub, M., Weber, J., Slotta-Huspenina, J., Specht, K., Martignoni, M.E., Werner, A., Hein, R., H. Busch, D., Peschel, C., Rad, R., Cox, J., Mann, M., Krackhardt, A.M., 2016. Direct identification of clinically relevant neopeptides presented on native human melanoma tissue by mass spectrometry. *Nat. Commun.* 7. <https://doi.org/10.1038/ncomms13404>
- Bastian, B.C., 2014. The Molecular Pathology of Melanoma: An Integrated Taxonomy of Melanocytic Neoplasia. *Annu. Rev. Pathol. Mech. Dis.* 9, 239–271. <https://doi.org/10.1146/annurev-pathol-012513-104658>
- Basu, S., Binder, R.J., Ramalingam, T., Srivastava, P.K., 2001. CD91 is a common receptor for heat shock proteins gp96, hsp90, hsp70, and calreticulin. *Immunity* 14, 303–313.
- Becker, T.C., Wherry, E.J., Boone, D., Murali-Krishna, K., Antia, R., Ma, A., Ahmed, R., 2002. Interleukin 15 Is Required for Proliferative Renewal of Virus-specific Memory CD8 T Cells. *J. Exp. Med.* 195, 1541–1548. <https://doi.org/10.1084/jem.20020369>
- Benci, J.L., Xu, B., Qiu, Y., Wu, T., Dada, H., Victor, C.T.-S., Cucolo, L., Lee, D.S.M., Pauken, K.E., Huang, A.C., Gangadhar, T.C., Amaravadi, R.K., Schuchter, L.M., Feldman, M.D., Ishwaran, H., Vonderheide, R.H., Maity, A., Wherry, E.J., Minn, A.J., 2016a. Tumor Interferon Signaling Regulates a Multigenic Resistance Program to Immune Checkpoint Blockade. *Cell* 167, 1540-1554.e12. <https://doi.org/10.1016/j.cell.2016.11.022>
- Benci, J.L., Xu, B., Qiu, Y., Wu, T.J., Dada, H., Twyman-Saint Victor, C., Cucolo, L., Lee, D.S.M., Pauken, K.E., Huang, A.C., Gangadhar, T.C., Amaravadi, R.K., Schuchter, L.M., Feldman, M.D., Ishwaran, H., Vonderheide, R.H., Maity, A., Wherry, E.J., Minn, A.J., 2016b. Tumor Interferon Signaling Regulates a Multigenic Resistance Program to Immune Checkpoint Blockade. *Cell* 167, 1540-1554.e12. <https://doi.org/10.1016/j.cell.2016.11.022>
- Benlalam, H., Vignard, V., Khammari, A., Bonnin, A., Godet, Y., Pandolfino, M.-C., Jotereau, F., Dreno, B., Labarrière, N., 2007. Infusion of Melan-A/Mart-1 specific tumor-infiltrating lymphocytes enhanced relapse-free survival of melanoma patients. *Cancer Immunol. Immunother.* 56, 515–526. <https://doi.org/10.1007/s00262-006-0204-0>
- Berger, C., Jensen, M.C., Lansdorp, P.M., Gough, M., Elliott, C., Riddell, S.R., 2008. Adoptive transfer of effector CD8+ T cells derived from central

- memory cells establishes persistent T cell memory in primates. *J. Clin. Invest.* 118, 294–305. <https://doi.org/10.1172/JCI32103>
- Besser, M.J., Shapira-Frommer, R., Itzhaki, O., Treves, A.J., Zippel, D.B., Levy, D., Kubi, A., Shoshani, N., Zikich, D., Ohayon, Y., Ohayon, D., Shalmon, B., Markel, G., Yerushalmi, R., Apter, S., Ben-Nun, A., Ben-Ami, E., Shimoni, A., Nagler, A., Schachter, J., 2013. Adoptive transfer of tumor-infiltrating lymphocytes in patients with metastatic melanoma: intent-to-treat analysis and efficacy after failure to prior immunotherapies. *Clin. Cancer Res. Off. J. Am. Assoc. Cancer Res.* 19, 4792–4800. <https://doi.org/10.1158/1078-0432.CCR-13-0380>
- Beura, L.K., Wijeyesinghe, S., Thompson, E.A., Macchietto, M.G., Rosato, P.C., Pierson, M.J., Schenkel, J.M., Mitchell, J.S., Vezys, V., Fife, B.T., Shen, S., Masopust, D., 2018. T Cells in Nonlymphoid Tissues Give Rise to Lymph-Node-Resident Memory T Cells. *Immunity* 48, 327–338.e5. <https://doi.org/10.1016/j.immuni.2018.01.015>
- Bevan, M.J., 2011. Memory T cells as an occupying force. *Eur. J. Immunol.* 41, 1192–1195. <https://doi.org/10.1002/eji.201041377>
- Bindels, D.S., Haarbosch, L., van Weeren, L., Postma, M., Wiese, K.E., Mastop, M., Aumonier, S., Gotthard, G., Royant, A., Hink, M.A., Gadella, T.W.J., 2017. mScarlet: a bright monomeric red fluorescent protein for cellular imaging. *Nat. Methods* 14, 53–56. <https://doi.org/10.1038/nmeth.4074>
- Biswas, S.K., Mantovani, A., 2010. Macrophage plasticity and interaction with lymphocyte subsets: cancer as a paradigm. *Nat. Immunol.* 11, 889–896. <https://doi.org/10.1038/ni.1937>
- Blankenstein, T., Leisegang, M., Uckert, W., Schreiber, H., 2015. Targeting cancer-specific mutations by T cell receptor gene therapy. *Curr. Opin. Immunol.* 33, 112–119. <https://doi.org/10.1016/j.coi.2015.02.005>
- Boddupalli, C.S., Bar, N., Kadaveru, K., Krauthammer, M., Pornputtpong, N., Mai, Z., Ariyan, S., Narayan, D., Kluger, H., Deng, Y., Verma, R., Das, R., Bacchiocchi, A., Halaban, R., Sznol, M., Dhodapkar, M.V., Dhodapkar, K.M., n.d. Interlesional diversity of T cell receptors in melanoma with immune checkpoints enriched in tissue-resident memory T cells. *JCI Insight* 1. <https://doi.org/10.1172/jci.insight.88955>
- Borg, Å., Sandberg, T., Nilsson, K., Johannsson, O., Klinker, M., Måsbäck, A., Westerdahl, J., Olsson, H., Ingvar, C., 2000. High Frequency of Multiple Melanomas and Breast and Pancreas Carcinomas in CDKN2A Mutation-Positive Melanoma Families. *JNCI J. Natl. Cancer Inst.* 92, 1260–1266. <https://doi.org/10.1093/jnci/92.15.1260>
- Bösmüller, H.-C., Wagner, P., Peper, J.K., Schuster, H., Pham, D.L., Greif, K., Beschorner, C., Rammensee, H.-G., Stevanović, S., Fend, F., Staebler, A., 2016. Combined Immunoscore of CD103 and CD3 Identifies Long-Term Survivors in High-Grade Serous Ovarian Cancer. *Int. J. Gynecol. Cancer* 26, 671–679. <https://doi.org/10.1097/IGC.0000000000000672>
- Brenner, M., Hearing, V.J., 2008. The Protective Role of Melanin Against UV Damage in Human Skin. *Photochem. Photobiol.* 84, 539–549. <https://doi.org/10.1111/j.1751-1097.2007.00226.x>
- Brichard, V., Pel, A.V., Wölfel, T., Wölfel, C., Plaen, E.D., Lethé, B., Coulie, P., Boon, T., 1993. The tyrosinase gene codes for an antigen recognized by

- autologous cytolytic T lymphocytes on HLA-A2 melanomas. *J. Exp. Med.* 178, 489–495. <https://doi.org/10.1084/jem.178.2.489>
- Broad Institute, Inc., 2018. Gene set enrichment analysis (GSEA).
- Bronte, V., Wang, M., Overwijk, W.W., Surman, D.R., Pericle, F., Rosenberg, S.A., Restifo, N.P., 1998. Apoptotic Death of CD8+ T Lymphocytes After Immunization: Induction of a Suppressive Population of Mac-1+/Gr-1+ Cells. *J. Immunol. Baltim. Md* 1950 161, 5313–5320.
- Brown, Furness, Speight, Thomas, Li, Thornhill, Farthing, 1999. Mechanisms of binding of cutaneous lymphocyte-associated antigen-positive and $\alpha\beta$ 7-positive lymphocytes to oral and skin keratinocytes. *Immunology* 98, 9–15. <https://doi.org/10.1046/j.1365-2567.1999.00855.x>
- Brown, S.D., Warren, R.L., Gibb, E.A., Martin, S.D., Spinelli, J.J., Nelson, B.H., Holt, R.A., 2014. Neo-antigens predicted by tumor genome meta-analysis correlate with increased patient survival. *Genome Res.* 24, 743–750. <https://doi.org/10.1101/gr.165985.113>
- Bruggen, P. van der, Traversari, C., Chomez, P., Lurquin, C., Plaen, E.D., Eynde, B.V. den, Knuth, A., Boon, T., 1991. A gene encoding an antigen recognized by cytolytic T lymphocytes on a human melanoma. *Science* 254, 1643–1647. <https://doi.org/10.1126/science.1840703>
- Buchholz, V.R., Flossdorf, M., Hensel, I., Kretschmer, L., Weissbrich, B., Gräf, P., Verschoor, A., Schiemann, M., Höfer, T., Busch, D.H., 2013. Disparate Individual Fates Compose Robust CD8+ T Cell Immunity. *Science* 340, 630–635. <https://doi.org/10.1126/science.1235454>
- Budd, R.C., Cerottini, J.C., MacDonald, H.R., 1987. Phenotypic identification of memory cytolytic T lymphocytes in a subset of Lyt-2+ cells. *J. Immunol.* 138, 1009–1013.
- Bukur, J., Jasinski, S., Seliger, B., 2012. The role of classical and non-classical HLA class I antigens in human tumors. *Semin. Cancer Biol., Immunosuppression in the Tumor Microenvironment* 22, 350–358. <https://doi.org/10.1016/j.semcancer.2012.03.003>
- Bulik-Sullivan, B., Busby, J., Palmer, C.D., Davis, M.J., Murphy, T., Clark, A., Busby, M., Duke, F., Yang, A., Young, L., Ojo, N.C., Caldwell, K., Abhyankar, J., Boucher, T., Hart, M.G., Makarov, V., De Montpreville, V.T., Mercier, O., Chan, T.A., Scagliotti, G., Bironzo, P., Novello, S., Karachaliou, N., Rosell, R., Anderson, I., Gabrail, N., Hrom, J., Limvarapuss, C., Choquette, K., Spira, A., Rousseau, R., Voong, C., Rizvi, N.A., Fadel, E., Frattini, M., Jooss, K., Skoberne, M., Francis, J., Yelensky, R., 2019. Deep learning using tumor HLA peptide mass spectrometry datasets improves neoantigen identification. *Nat. Biotechnol.* 37, 55–63. <https://doi.org/10.1038/nbt.4313>
- Cabrera, C. m., Jiménez, P., Cabrera, T., Esparza, C., Ruiz-Cabello, F., Garrido, F., 2003. Total loss of MHC class I in colorectal tumors can be explained by two molecular pathways: β 2-microglobulin inactivation in MSI-positive tumors and LMP7/TAP2 downregulation in MSI-negative tumors. *Tissue Antigens* 61, 211–219. <https://doi.org/10.1034/j.1399-0039.2003.00020.x>
- Califano, J., Nance, M., 2009. Malignant Melanoma. *Facial Plast. Surg. Clin. N. Am., Skin Cancer* 17, 337–348. <https://doi.org/10.1016/j.fsc.2009.05.002>
- Casey, K.A., Fraser, K.A., Schenkel, J.M., Moran, A., Abt, M.C., Beura, L.K.,

- Lucas, P.J., Artis, D., Wherry, E.J., Hogquist, K., Vezys, V., Masopust, D., 2012. Antigen-Independent Differentiation and Maintenance of Effector-like Resident Memory T Cells in Tissues. *J. Immunol.* 188, 4866–4875. <https://doi.org/10.4049/jimmunol.1200402>
- Casey, S.C., Tong, L., Li, Y., Do, R., Walz, S., Fitzgerald, K.N., Gouw, A., Baylot, V., Gutgemann, I., Eilers, M., Felsher, D.W., 2016. MYC Regulates the Anti-Tumor Immune Response through CD47 and PD-L1. *Science* 352, 227–231. <https://doi.org/10.1126/science.aac9935>
- Chandran, S.S., Paria, B.C., Srivastava, A.K., Rothermel, L.D., Stephens, D.J., Dudley, M.E., Somerville, R., Wunderlich, J.R., Sherry, R.M., Yang, J.C., Rosenberg, S.A., Kammula, U.S., 2015. Persistence of CTL clones targeting melanocyte differentiation antigens was insufficient to mediate significant melanoma regression in humans. *Clin. Cancer Res. Off. J. Am. Assoc. Cancer Res.* 21, 534–543. <https://doi.org/10.1158/1078-0432.CCR-14-2208>
- Chang, J.T., Wherry, E.J., Goldrath, A.W., 2014. Molecular regulation of effector and memory T cell differentiation. *Nat. Immunol.* 15, 1104–1115. <https://doi.org/10.1038/ni.3031>
- Chanmee, T., Ontong, P., Konno, K., Itano, N., 2014. Tumor-Associated Macrophages as Major Players in the Tumor Microenvironment. *Cancers* 6, 1670–1690. <https://doi.org/10.3390/cancers6031670>
- Chao, L.X., Patterson, S.S.L., Rademaker, A.W., Liu, D., Kundu, R.V., 2017. Melanoma Perception in People of Color: A Targeted Educational Intervention. *Am. J. Clin. Dermatol.* 18, 419–427. <https://doi.org/10.1007/s40257-016-0244-y>
- Chawla, R., Procknow, J.A., Tantravahi, R.V., Khurana, J.S., Litvin, J., Reddy, E.P., 2010. Cooperativity of Cdk4R24C and Ras in melanoma development. *Cell Cycle Georget. Tex* 9, 3305–3314. <https://doi.org/10.4161/cc.9.16.12632>
- Cheli, Y., Giuliano, S., Fenouille, N., Allegra, M., Hofman, V., Hofman, P., Bahadoran, P., Lacour, J.-P., Tartare-Deckert, S., Bertolotto, C., Ballotti, R., 2012. Hypoxia and MITF control metastatic behaviour in mouse and human melanoma cells. *Oncogene* 31, 2461–2470. <https://doi.org/10.1038/onc.2011.425>
- Chen, L., 2004. Co-inhibitory molecules of the B7–CD28 family in the control of T-cell immunity. *Nat. Rev. Immunol.* 4, 336. <https://doi.org/10.1038/nri1349>
- Cheng, P.F., Shakhova, O., Widmer, D.S., Eichhoff, O.M., Zingg, D., Frommel, S.C., Belloni, B., Raaijmakers, M.I., Goldinger, S.M., Santoro, R., Hemmi, S., Sommer, L., Dummer, R., Levesque, M.P., 2015. Methylation-dependent SOX9 expression mediates invasion in human melanoma cells and is a negative prognostic factor in advanced melanoma. *Genome Biol.* 16. <https://doi.org/10.1186/s13059-015-0594-4>
- Cheuk, S., Schlums, H., Gallais S  rezal, I., Martini, E., Chiang, S.C., Marquardt, N., Gibbs, A., Detlofsson, E., Introini, A., Forkel, M., H  g, C., Tjernlund, A., Micha  lsson, J., Folkersen, L., Mj  sberg, J., Blomqvist, L., Ehrstr  m, M., St  hle, M., Bryceson, Y.T., Eidsmo, L., 2017. CD49a Expression Defines Tissue-Resident CD8+ T Cells Poised for Cytotoxic Function in

- Human Skin. Immunity 46, 287–300.
<https://doi.org/10.1016/j.immuni.2017.01.009>
- Chmielewski, M., Kopecky, C., Hombach, A.A., Abken, H., 2011. IL-12 release by engineered T cells expressing chimeric antigen receptors can effectively Muster an antigen-independent macrophage response on tumor cells that have shut down tumor antigen expression. *Cancer Res.* 71, 5697–5706. <https://doi.org/10.1158/0008-5472.CAN-11-0103>
- Cho, E., Rosner, B.A., Colditz, G.A., 2005. Risk factors for melanoma by body site. *Cancer Epidemiol. Biomark. Prev. Publ. Am. Assoc. Cancer Res. Cosponsored Am. Soc. Prev. Oncol.* 14, 1241–1244. <https://doi.org/10.1158/1055-9965.EPI-04-0632>
- Chodon, T., Comin-Anduix, B., Chmielowski, B., Koya, R.C., Wu, Z., Auerbach, M., Ng, C., Avramis, E., Seja, E., Villanueva, A., McCannel, T.A., Ishiyama, A., Czernin, J., Radu, C.G., Wang, X., Gjertson, D.W., Cochran, A.J., Cornetta, K., Wong, D.J.L., Kaplan-Lefko, P., Hamid, O., Samlowski, W., Cohen, P.A., Daniels, G.A., Mukherji, B., Yang, L., Zack, J.A., Kohn, D.B., Heath, J.R., Glaspy, J.A., Witte, O.N., Baltimore, D., Economou, J.S., Ribas, A., 2014. Adoptive transfer of MART-1 T-cell receptor transgenic lymphocytes and dendritic cell vaccination in patients with metastatic melanoma. *Clin. Cancer Res. Off. J. Am. Assoc. Cancer Res.* 20, 2457–2465. <https://doi.org/10.1158/1078-0432.CCR-13-3017>
- Choi, W., Miyamura, Y., Wolber, R., Smuda, C., Reinhold, W., Liu, H., Kolbe, L., Hearing, V.J., 2010. Regulation of Human Skin Pigmentation in situ by Repetitive UV Exposure: Molecular Characterization of Responses to UVA and/or UVB. *J. Invest. Dermatol.* 130, 1685–1696. <https://doi.org/10.1038/jid.2010.5>
- Chung, H., Cho, H., Perry, C., Song, J., Ylaya, K., Lee, H., Kim, J.-H., 2013. Downregulation of ERp57 expression is associated with poor prognosis in early-stage cervical cancer. *Biomarkers* 18, 573–579. <https://doi.org/10.3109/1354750X.2013.827742>
- Clark, R.A., 2015. Resident memory T cells in human health and disease. *Sci. Transl. Med.* 7, 269rv1–269rv1. <https://doi.org/10.1126/scitranslmed.3010641>
- Clark, W.H., Elder, D.E., Guerry, D., Braitman, L.E., Trock, B.J., Schultz, D., Synnestvedt, M., Halpern, A.C., 1989. Model Predicting Survival in Stage I Melanoma Based on Tumor Progression. *JNCI J. Natl. Cancer Inst.* 81, 1893–1904. <https://doi.org/10.1093/jnci/81.24.1893>
- Cohen, C.J., Gartner, J.J., Horovitz-Fried, M., Shamalov, K., Trebska-McGowan, K., Bliskovsky, V.V., Parkhurst, M.R., Ankri, C., Prickett, Todd.D., Crystal, J.S., Li, Y.F., El-Gamil, M., Rosenberg, S.A., Robbins, P.F., 2015. Isolation of neoantigen-specific T cells from tumor and peripheral lymphocytes. *J. Clin. Invest.* 125, 3981–3991. <https://doi.org/10.1172/JCI82416>
- Coley, W.B., 1893. The treatment of malignant tumors by repeated inoculations of erysipelas. With a report of ten original cases. 1893. *Clin. Orthop.* 3–11.
- Cong, L., Ran, F.A., Cox, D., Lin, S., Barretto, R., Habib, N., Hsu, P.D., Wu, X., Jiang, W., Marraffini, L.A., Zhang, F., 2013. Multiplex Genome Engineering Using CRISPR/Cas Systems. *Science* 339, 819–823. <https://doi.org/10.1126/science.1231143>

- Coory, M., Baade, P., Aitken, J., Smithers, M., McLeod, G.R.C., Ring, I., 2006. Trends for in situ and Invasive Melanoma in Queensland, Australia, 1982–2002. *Cancer Causes Control* 17, 21–27. <https://doi.org/10.1007/s10552-005-3637-4>
- Costin, G.-E., Hearing, V.J., 2007. Human skin pigmentation: melanocytes modulate skin color in response to stress. *FASEB J.* 21, 976–994. <https://doi.org/10.1096/fj.06-6649rev>
- Coussens, L.M., Tinkle, C.L., Hanahan, D., Werb, Z., 2000. MMP-9 Supplied by Bone Marrow–Derived Cells Contributes to Skin Carcinogenesis. *Cell* 103, 481–490.
- Cristescu, R., Mogg, R., Ayers, M., Albright, A., Murphy, E., Yearley, J., Sher, X., Liu, X.Q., Lu, H., Nebozhyn, M., Zhang, C., Lunceford, J.K., Joe, A., Cheng, J., Webber, A.L., Ibrahim, N., Plimack, E.R., Ott, P.A., Seiwert, T.Y., Ribas, A., McClanahan, T.K., Tomassini, J.E., Loboda, A., Kaufman, D., 2018. Pan-tumor genomic biomarkers for PD-1 checkpoint blockade–based immunotherapy. *Science* 362, eaar3593. <https://doi.org/10.1126/science.aar3593>
- Cromme, F.V., Airey, J., Heemels, M.T., Ploegh, H.L., Keating, P.J., Stern, P.L., Meijer, C.J., Walboomers, J.M., 1994. Loss of transporter protein, encoded by the TAP-1 gene, is highly correlated with loss of HLA expression in cervical carcinomas. *J. Exp. Med.* 179, 335–340. <https://doi.org/10.1084/jem.179.1.335>
- Crompton, J.G., Sukumar, M., Roychoudhuri, R., Clever, D., Gros, A., Eil, R., Tran, E., Hanada, K., Yu, Z., Palmer, D.C., Kerkar, S.P., Michalek, R.D., Upham, T., Leonardi, A., Aquavella, N., Wang, E., Marincola, F.M., Gattinoni, L., Muranski, P., Sundrud, M.S., Klebanoff, C.A., Rosenberg, S.A., Fearon, D.T., Restifo, N.P., 2015. Akt inhibition enhances expansion of potent tumor-specific lymphocytes with memory cell characteristics. *Cancer Res.* 75, 296–305. <https://doi.org/10.1158/0008-5472.CAN-14-2277>
- Cruz-Guilloty, F., Pipkin, M.E., Djuretic, I.M., Levanon, D., Lotem, J., Lichtenheld, M.G., Groner, Y., Rao, A., 2009. Runx3 and T-box proteins cooperate to establish the transcriptional program of effector CTLs. *J. Exp. Med.* 206, 51–59. <https://doi.org/10.1084/jem.20081242>
- Cui, W., Kaech, S.M., 2010. Generation of effector CD8+ T cells and their conversion to memory T cells. *Immunol. Rev.* 236, 151–166. <https://doi.org/10.1111/j.1600-065X.2010.00926.x>
- Dahle, J., Brunborg, G., Svendsrud, D.H., Stokke, T., Kvam, E., 2008. Overexpression of human OGG1 in mammalian cells decreases ultraviolet A induced mutagenesis. *Cancer Lett.* 267, 18–25. <https://doi.org/10.1016/j.canlet.2008.03.002>
- Darnell, J.E., Kerr, I.M., Stark, G.R., 1994. Jak-STAT pathways and transcriptional activation in response to IFNs and other extracellular signaling proteins. *Science* 264, 1415–1421. <https://doi.org/10.1126/science.8197455>
- Darrow, T.L., Abdel-Wahab, Z., Quinn-Allen, M.A., Seigler, H.F., 1996. Recognition and Lysis of Human Melanoma by a CD3+, CD4+, CD8–T-Cell Clone Restricted by HLA-A2. *Cell. Immunol.* 172, 52–59.

- <https://doi.org/10.1006/cimm.1996.0214>
- de Gruijl, F.R., 2002. Photocarcinogenesis: UVA vs. UVB radiation. *Skin Pharmacol. Appl. Skin Physiol.* 15, 316–320. <https://doi.org/10.1159/000064535>
- De Henau, O., Rausch, M., Winkler, D., Campesato, L.F., Liu, C., Cymerman, D.H., Budhu, S., Ghosh, A., Pink, M., Tchaicha, J., Douglas, M., Tibbitts, T., Sharma, S., Proctor, J., Kosmider, N., White, K., Stern, H., Soglia, J., Adams, J., Palombella, V.J., McGovern, K., Kutok, J.L., Wolchok, J.D., Merghoub, T., 2016. Overcoming resistance to checkpoint blockade therapy by targeting PI3K γ in myeloid cells. *Nature* 539, 443–447. <https://doi.org/10.1038/nature20554>
- De Palma, M., Venneri, M.A., Galli, R., Sergi, L.S., Politi, L.S., Sampaolesi, M., Naldini, L., 2005. Tie2 identifies a hematopoietic lineage of proangiogenic monocytes required for tumor vessel formation and a mesenchymal population of pericyte progenitors. *Cancer Cell* 8, 211–226. <https://doi.org/10.1016/j.ccr.2005.08.002>
- Dębniak, T., 2004. Familial Malignant Melanoma - Overview. *Hered. Cancer Clin. Pract.* 2, 123–129. <https://doi.org/10.1186/1897-4287-2-3-123>
- Delom, F., Fessart, D., Chevet, E., 2007. Regulation of calnexin sub-cellular localization modulates endoplasmic reticulum stress-induced apoptosis in MCF-7 cells. *Apoptosis* 12, 293–305. <https://doi.org/10.1007/s10495-006-0625-4>
- Delp, K., Momburg, F., Hilmes, C., Huber, C., Seliger, B., 2000. Functional deficiencies of components of the MHC class I antigen pathway in human tumors of epithelial origin. *Bone Marrow Transplant.* 25 Suppl 2, S88-95.
- Djenidi, F., Adam, J., Goubar, A., Durgeau, A., Meurice, G., Montpréville, V. de, Validire, P., Besse, B., Mami-Chouaib, F., 2015. CD8+CD103+ Tumor-Infiltrating Lymphocytes Are Tumor-Specific Tissue-Resident Memory T Cells and a Prognostic Factor for Survival in Lung Cancer Patients. *J. Immunol.* 194, 3475–3486. <https://doi.org/10.4049/jimmunol.1402711>
- Dong, H., Strome, S.E., Salomao, D.R., Tamura, H., Hirano, F., Flies, D.B., Roche, P.C., Lu, J., Zhu, G., Tamada, K., Lennon, V.A., Celis, E., Chen, L., 2002. Tumor-associated B7-H1 promotes T-cell apoptosis: A potential mechanism of immune evasion. *Nat. Med.* 8, 793. <https://doi.org/10.1038/nm730>
- Dong, Y., Richards, J.-A., Gupta, R., Aung, P.P., Emley, A., Kluger, Y., Dogra, S.K., Mahalingam, M., Wajapeyee, N., 2014. PTEN functions as a melanoma tumor suppressor by promoting host immune response. *Oncogene* 33, 4632–4642. <https://doi.org/10.1038/onc.2013.409>
- Donohue, J.H., Rosenstein, M., Chang, A.E., Lotze, M.T., Robb, R.J., Rosenberg, S.A., 1984. The systemic administration of purified interleukin 2 enhances the ability of sensitized murine lymphocytes to cure a disseminated syngeneic lymphoma. *J. Immunol.* 132, 2123–2128.
- Dorand, R.D., Nthale, J., Myers, J.T., Barkauskas, D.S., Avril, S., Chirieleison, S.M., Pareek, T.K., Abbott, D.W., Stearns, D.S., Letterio, J.J., Huang, A.Y., Petrosiute, A., 2016. Cdk5 disruption attenuates tumor PD-L1 expression and promotes antitumor immunity. *Science* 353, 399–403. <https://doi.org/10.1126/science.aae0477>

- D'Souza, W.N., Schluns, K.S., Masopust, D., Lefrançois, L., 2002. Essential Role for IL-2 in the Regulation of Antiviral Extralymphoid CD8 T Cell Responses. *J. Immunol.* 168, 5566–5572. <https://doi.org/10.4049/jimmunol.168.11.5566>
- Dudley, M.E., Wunderlich, J.R., Robbins, P.F., Yang, J.C., Hwu, P., Schwartzentruber, D.J., Topalian, S.L., Sherry, R., Restifo, N.P., Hubicki, A.M., Robinson, M.R., Raffeld, M., Duray, P., Seipp, C.A., Rogers-Freezer, L., Morton, K.E., Mavroukakis, S.A., White, D.E., Rosenberg, S.A., 2002. Cancer Regression and Autoimmunity in Patients After Clonal Repopulation with Antitumor Lymphocytes. *Science* 298, 850–854. <https://doi.org/10.1126/science.1076514>
- Dudley, M.E., Yang, J.C., Sherry, R., Hughes, M.S., Royal, R., Kammula, U., Robbins, P.F., Huang, J., Citrin, D.E., Leitman, S.F., Wunderlich, J., Restifo, N.P., Thomasian, A., Downey, S.G., Smith, F.O., Klapper, J., Morton, K., Laurencot, C., White, D.E., Rosenberg, S.A., 2008. Adoptive Cell Therapy for Patients With Metastatic Melanoma: Evaluation of Intensive Myeloablative Chemoradiation Preparative Regimens. *J. Clin. Oncol.* 26, 5233–5239. <https://doi.org/10.1200/JCO.2008.16.5449>
- Dunn, G.P., Bruce, A.T., Sheehan, K.C.F., Shankaran, V., Uppaluri, R., Bui, J.D., Diamond, M.S., Koebel, C.M., Arthur, C., White, J.M., Schreiber, R.D., 2005. A critical function for type I interferons in cancer immunoediting. *Nat. Immunol.* 6, 722. <https://doi.org/10.1038/ni1213>
- Dupin, E., Douarin, N.M.L., 2003. Development of melanocyte precursors from the vertebrate neural crest. *Oncogene* 22, 3016. <https://doi.org/10.1038/sj.onc.1206460>
- D'Urso, C.M., Wang, Z.G., Cao, Y., Tataka, R., Zeff, R.A., Ferrone, S., 1991. Lack of HLA class I antigen expression by cultured melanoma cells FO-1 due to a defect in B2m gene expression. *J. Clin. Invest.* 87, 284–292.
- Eberlein, T.J., Rosenstein, M., Rosenberg, S.A., 1982. Regression of a disseminated syngeneic solid tumor by systemic transfer of lymphoid cells expanded in interleukin 2. *J. Exp. Med.* 156, 385–397. <https://doi.org/10.1084/jem.156.2.385>
- Echchakir, H., Vergnon, I., Dorothée, G., Grunenwald, D., Chouaib, S., Mami-Chouaib, F., 2000. Evidence for in situ expansion of diverse antitumor-specific cytotoxic T lymphocyte clones in a human large cell carcinoma of the lung. *Int. Immunol.* 12, 537–546. <https://doi.org/10.1093/intimm/12.4.537>
- Edwards, J., Wilmott, J.S., Madore, J., Gide, T.N., Quek, C., Tasker, A., Ferguson, A., Chen, J., Hewavisenti, R., Hersey, P., Gebhardt, T., Weninger, W., Britton, W.J., Saw, R.P.M., Thompson, J.F., Menzies, A.M., Long, G.V., Scolyer, R.A., Palendira, U., 2018. CD103+ Tumor-Resident CD8+ T Cells Are Associated with Improved Survival in Immunotherapy-Naïve Melanoma Patients and Expand Significantly During Anti-PD-1 Treatment. *Clin. Cancer Res.* 24, 3036–3045. <https://doi.org/10.1158/1078-0432.CCR-17-2257>
- Egelston, C., Srinivasan, G., Avalos, C., Huang, Y., Rosario, A., Wang, R., Jimenez, G., Simons, D.L., Yost, S., Yuan, Y., Lee, P.P., 2017. CD8+ tissue resident memory T cells are associated with good prognosis in

- breast cancer patients. *J. Immunol.* 198, 196.11-196.11.
- Eichhoff, O.M., Weeraratna, A., Zipser, M.C., Denat, L., Widmer, D.S., Xu, M., Kriegl, L., Kirchner, T., Larue, L., Dummer, R., Hoek, K.S., 2011. Differential LEF1 and TCF4 expression is involved in melanoma cell phenotype switching. *Pigment Cell Melanoma Res.* 24, 631–642. <https://doi.org/10.1111/j.1755-148X.2011.00871.x>
- Ellerhorst, J.A., Greene, V.R., Ekmekcioglu, S., Warneke, C.L., Johnson, M.M., Cooke, C.P., Wang, L.-E., Prieto, V.G., Gershenwald, J.E., Wei, Q., Grimm, E.A., 2011. Clinical Correlates of NRAS and BRAF Mutations in Primary Human Melanoma. *Clin. Cancer Res. Off. J. Am. Assoc. Cancer Res.* 17, 229–235. <https://doi.org/10.1158/1078-0432.CCR-10-2276>
- Elwood, J.M., Lee, J. a. H., Walter, S.D., Mo, T., Green, A.E.S., 1974. Relationship of Melanoma and other Skin Cancer Mortality to Latitude and Ultraviolet Radiation in the United States and Canada. *Int. J. Epidemiol.* 3, 325–332. <https://doi.org/10.1093/ije/3.4.325>
- Enamorado, M., Iborra, S., Priego, E., Cueto, F.J., Quintana, J.A., Martínez-Cano, S., Mejías-Pérez, E., Esteban, M., Melero, I., Hidalgo, A., Sancho, D., 2017. Enhanced anti-tumour immunity requires the interplay between resident and circulating memory CD8⁺ T cells. *Nat. Commun.* 8, 16073. <https://doi.org/10.1038/ncomms16073>
- Engels, B., Engelhard, V.H., Sidney, J., Sette, A., Binder, D.C., Liu, R.B., Kranz, D.M., Meredith, S.C., Rowley, D.A., Schreiber, H., 2013. Relapse or Eradication of Cancer Is Predicted by Peptide-Major Histocompatibility Complex Affinity. *Cancer Cell* 23, 516–526. <https://doi.org/10.1016/j.ccr.2013.03.018>
- Erdei, E., Torres, S.M., 2010. A new understanding in the epidemiology of melanoma. *Expert Rev. Anticancer Ther.* 10, 1811–1823. <https://doi.org/10.1586/era.10.170>
- Erdmann, F., Lortet-Tieulent, J., Schüz, J., Zeeb, H., Greinert, R., Breitbart, E.W., Bray, F., 2013. International trends in the incidence of malignant melanoma 1953–2008—are recent generations at higher or lower risk? *Int. J. Cancer* 132, 385–400. <https://doi.org/10.1002/ijc.27616>
- Evnouchidou, I., Weimershaus, M., Saveanu, L., Endert, P. van, 2014. ERAP1–ERAP2 Dimerization Increases Peptide-Trimming Efficiency. *J. Immunol.* 193, 901–908. <https://doi.org/10.4049/jimmunol.1302855>
- Fan, X., Rudensky, A.Y., 2016. Hallmarks of Tissue-Resident Lymphocytes. *Cell* 164, 1198–1211. <https://doi.org/10.1016/j.cell.2016.02.048>
- Feige, E., Yokoyama, S., Levy, C., Khaled, M., Igras, V., Lin, R.J., Lee, S., Widlund, H.R., Granter, S.R., Kung, A.L., Fisher, D.E., 2011. Hypoxia-induced transcriptional repression of the melanoma-associated oncogene MITF. *Proc. Natl. Acad. Sci.* 108, E924–E933. <https://doi.org/10.1073/pnas.1106351108>
- Feil, R., Wagner, J., Metzger, D., Chambon, P., 1997. Regulation of Cre Recombinase Activity by Mutated Estrogen Receptor Ligand-Binding Domains. *Biochem. Biophys. Res. Commun.* 237, 752–757. <https://doi.org/10.1006/bbrc.1997.7124>
- Ferrer, I., Zugazagoitia, J., Herbertz, S., John, W., Paz-Ares, L., Schmid-Bindert, G., 2018. KRAS-Mutant non-small cell lung cancer: From biology to

- therapy. *Lung Cancer* 124, 53–64.
<https://doi.org/10.1016/j.lungcan.2018.07.013>
- Filippi, A.R., Fava, P., Badellino, S., Astrua, C., Ricardi, U., Quaglino, P., 2016. Radiotherapy and immune checkpoints inhibitors for advanced melanoma. *Radiother. Oncol.* 120, 1–12. <https://doi.org/10.1016/j.radonc.2016.06.003>
- Floc'h, A.L., Jalil, A., Vergnon, I., Chansac, B.L.M., Lazar, V., Bismuth, G., Chouaib, S., Mami-Chouaib, F., 2007. $\alpha E\beta 7$ integrin interaction with E-cadherin promotes antitumor CTL activity by triggering lytic granule polarization and exocytosis. *J. Exp. Med.* 204, 559–570. <https://doi.org/10.1084/jem.20061524>
- Franciszkiewicz, K., Floc'h, A.L., Boutet, M., Vergnon, I., Schmitt, A., Mami-Chouaib, F., 2013. CD103 or LFA-1 Engagement at the Immune Synapse between Cytotoxic T Cells and Tumor Cells Promotes Maturation and Regulates T-cell Effector Functions. *Cancer Res.* 73, 617–628. <https://doi.org/10.1158/0008-5472.CAN-12-2569>
- Franciszkiewicz, K., Floc'h, A.L., Jalil, A., Vigant, F., Robert, T., Vergnon, I., Mackiewicz, A., Benihoud, K., Validire, P., Chouaib, S., Combadière, C., Mami-Chouaib, F., 2009. Intratumoral Induction of CD103 Triggers Tumor-Specific CTL Function and CCR5-Dependent T-Cell Retention. *Cancer Res.* 69, 6249–6255. <https://doi.org/10.1158/0008-5472.CAN-08-3571>
- Fuge, O., Vasdev, N., Allchorne, P., Green, J.S., 2015. Immunotherapy for bladder cancer. *Res. Rep. Urol.* 7, 65–79. <https://doi.org/10.2147/RRU.S63447>
- Gajewski, T.F., Corrales, L., Williams, J., Horton, B., Sivan, A., Spranger, S., 2017. Cancer Immunotherapy Targets Based on Understanding the T Cell-Inflamed Versus Non-T Cell-Inflamed Tumor Microenvironment, in: Kalinski, P. (Ed.), *Tumor Immune Microenvironment in Cancer Progression and Cancer Therapy*, Advances in Experimental Medicine and Biology. Springer International Publishing, Cham, pp. 19–31. https://doi.org/10.1007/978-3-319-67577-0_2
- Gajewski, T.F., Schreiber, H., Fu, Y.-X., 2013. Innate and adaptive immune cells in the tumor microenvironment. *Nat. Immunol.* 14, 1014–1022. <https://doi.org/10.1038/ni.2703>
- Ganesan, A.-P., Clarke, J., Wood, O., Garrido-Martin, E.M., Chee, S.J., Mellows, T., Samaniego-Castruita, D., Singh, D., Seumois, G., Alzetani, A., Woo, E., Friedmann, P.S., King, E.V., Thomas, G.J., Sanchez-Elsner, T., Vijayanand, P., Ottensmeier, C.H., 2017. Tissue-resident memory features are linked to the magnitude of cytotoxic T cell responses in human lung cancer. *Nat. Immunol.* 18, 940–950. <https://doi.org/10.1038/ni.3775>
- Gao, J., Shi, L.Z., Zhao, H., Chen, J., Xiong, L., He, Q., Chen, T., Roszik, J., Bernatchez, C., Woodman, S.E., Chen, P.-L., Hwu, P., Allison, J.P., Futreal, A., Wargo, J.A., Sharma, P., 2016. Loss of IFN- γ pathway genes in tumor cells as a mechanism of resistance to anti-CTLA-4 therapy. *Cell* 167, 397–404.e9. <https://doi.org/10.1016/j.cell.2016.08.069>
- Garbe, C., Leiter, U., 2009. Melanoma epidemiology and trends. *Clin. Dermatol., Melanoma and Pigmented Lesions, Part 1* 27, 3–9. <https://doi.org/10.1016/j.clindermatol.2008.09.001>
- Garraway, L.A., Widlund, H.R., Rubin, M.A., Getz, G., Berger, A.J., Ramaswamy,

- S., Beroukhir, R., Milner, D.A., Granter, S.R., Du, J., Lee, C., Wagner, S.N., Li, C., Golub, T.R., Rimm, D.L., Meyerson, M.L., Fisher, D.E., Sellers, W.R., 2005. Integrative genomic analyses identify MITF as a lineage survival oncogene amplified in malignant melanoma. *Nature* 436, 117. <https://doi.org/10.1038/nature03664>
- Gattinoni, L., Finkelstein, S.E., Klebanoff, C.A., Antony, P.A., Palmer, D.C., Spiess, P.J., Hwang, L.N., Yu, Z., Wrzesinski, C., Heimann, D.M., Surh, C.D., Rosenberg, S.A., Restifo, N.P., 2005a. Removal of homeostatic cytokine sinks by lymphodepletion enhances the efficacy of adoptively transferred tumor-specific CD8⁺ T cells. *J. Exp. Med.* 202, 907–912. <https://doi.org/10.1084/jem.20050732>
- Gattinoni, L., Klebanoff, C.A., Palmer, D.C., Wrzesinski, C., Kerstann, K., Yu, Z., Finkelstein, S.E., Theoret, M.R., Rosenberg, S.A., Restifo, N.P., 2005b. Acquisition of full effector function in vitro paradoxically impairs the in vivo antitumor efficacy of adoptively transferred CD8⁺ T cells. *J. Clin. Invest.* 115, 1616–1626. <https://doi.org/10.1172/JCI24480>
- Gebhardt, T., Wakim, L.M., Eidsmo, L., Reading, P.C., Heath, W.R., Carbone, F.R., 2009. Memory T cells in nonlymphoid tissue that provide enhanced local immunity during infection with herpes simplex virus. *Nat. Immunol.* 10, 524–530. <https://doi.org/10.1038/ni.1718>
- Gebhardt, T., Whitney, P.G., Zaid, A., Mackay, L.K., Brooks, A.G., Heath, W.R., Carbone, F.R., Mueller, S.N., 2011. Different patterns of peripheral migration by memory CD4⁺ and CD8⁺ T cells. *Nature* 477, 216–219. <https://doi.org/10.1038/nature10339>
- Gerlach, C., Rohr, J.C., Perié, L., Rooij, N. van, Heijst, J.W.J. van, Velds, A., Urbanus, J., Naik, S.H., Jacobs, H., Beltman, J.B., Boer, R.J. de, Schumacher, T.N.M., 2013. Heterogeneous Differentiation Patterns of Individual CD8⁺ T Cells. *Science* 340, 635–639. <https://doi.org/10.1126/science.1235487>
- Gerner, M.Y., Mescher, M.F., 2009. Antigen Processing and MHC-II Presentation by Dermal and Tumor-Infiltrating Dendritic Cells. *J. Immunol.* 182, 2726–2737. <https://doi.org/10.4049/jimmunol.0803479>
- Gilchrist, B.A., 2011. Molecular Aspects of Tanning. *J. Invest. Dermatol.* 131, E14–E17. <https://doi.org/10.1038/skinbio.2011.6>
- Giuliano, S., Cheli, Y., Ohanna, M., Bonet, C., Beuret, L., Bille, K., Loubat, A., Hofman, V., Hofman, P., Ponzio, G., Bahadoran, P., Ballotti, R., Bertolotto, C., 2010. Microphthalmia-Associated Transcription Factor Controls the DNA Damage Response and a Lineage-Specific Senescence Program in Melanomas. *Cancer Res.* 70, 3813–3822. <https://doi.org/10.1158/0008-5472.CAN-09-2913>
- Glennie, N.D., Yeramilli, V.A., Beiting, D.P., Volk, S.W., Weaver, C.T., Scott, P., 2015. Skin-resident memory CD4⁺ T cells enhance protection against *Leishmania major* infection. *J. Exp. Med.* 212, 1405–1414. <https://doi.org/10.1084/jem.20142101>
- Glodde, N., Bald, T., Boorn-Konijnenberg, D. van den, Nakamura, K., O'Donnell, J.S., Szczepanski, S., Brandes, M., Eickhoff, S., Das, I., Shridhar, N., Hinze, D., Rogava, M., Sluis, T.C. van der, Ruotsalainen, J.J., Gaffal, E., Landsberg, J., Ludwig, K.U., Wilhelm, C., Riek-Burchardt, M., Müller, A.J.,

- Gebhardt, C., Scolyer, R.A., Long, G.V., Janzen, V., Teng, M.W.L., Kastenmüller, W., Mazzone, M., Smyth, M.J., Tüting, T., Hölzel, M., 2017. Reactive Neutrophil Responses Dependent on the Receptor Tyrosine Kinase c-MET Limit Cancer Immunotherapy. *Immunity* 47, 789-802.e9. <https://doi.org/10.1016/j.immuni.2017.09.012>
- Glynne, R., Powis, S.H., Beck, S., Kelly, A., Kerr, L.-A., Trowsdale, J., 1991. A proteasome-related gene between the two ABC transporter loci in the class II region of the human MHC. *Nature* 353, 357. <https://doi.org/10.1038/353357a0>
- Godfrey, D.I., Uldrich, A.P., McCluskey, J., Rossjohn, J., Moody, D.B., 2015. The burgeoning family of unconventional T cells. *Nat. Immunol.* 16, 1114–1123. <https://doi.org/10.1038/ni.3298>
- Goff, S.L., Dudley, M.E., Citrin, D.E., Somerville, R.P., Wunderlich, J.R., Danforth, D.N., Zlott, D.A., Yang, J.C., Sherry, R.M., Kammula, U.S., Klebanoff, C.A., Hughes, M.S., Restifo, N.P., Langhan, M.M., Shelton, T.E., Lu, L., Kwong, M.L.M., Ilyas, S., Klemen, N.D., Payabyab, E.C., Morton, K.E., Toomey, M.A., Steinberg, S.M., White, D.E., Rosenberg, S.A., 2016. Randomized, Prospective Evaluation Comparing Intensity of Lymphodepletion Before Adoptive Transfer of Tumor-Infiltrating Lymphocytes for Patients With Metastatic Melanoma. *J. Clin. Oncol.* 34, 2389–2397. <https://doi.org/10.1200/JCO.2016.66.7220>
- Goldberg, A.L., Cascio, P., Saric, T., Rock, K.L., 2002. The importance of the proteasome and subsequent proteolytic steps in the generation of antigenic peptides. *Mol. Immunol., Generating Peptide Ligands for MHC Class I Molecules* 39, 147–164. [https://doi.org/10.1016/S0161-5890\(02\)00098-6](https://doi.org/10.1016/S0161-5890(02)00098-6)
- Goldrath, A.W., Sivakumar, P.V., Glaccum, M., Kennedy, M.K., Bevan, M.J., Benoist, C., Mathis, D., Butz, E.A., 2002. Cytokine Requirements for Acute and Basal Homeostatic Proliferation of Naive and Memory CD8+ T Cells. *J. Exp. Med.* 195, 1515–1522. <https://doi.org/10.1084/jem.20020033>
- Gong, D., Malek, T.R., 2007. Cytokine-Dependent Blimp-1 Expression in Activated T Cells Inhibits IL-2 Production. *J. Immunol.* 178, 242–252. <https://doi.org/10.4049/jimmunol.178.1.242>
- Goodson, A.G., Grossman, D., 2009. Strategies for early melanoma detection: approaches to the patient with nevi. *J. Am. Acad. Dermatol.* 60, 719–738. <https://doi.org/10.1016/j.jaad.2008.10.065>
- Gray, S.M., Kaech, S.M., Staron, M.M., 2014. The interface between transcriptional and epigenetic control of effector and memory CD8+ T-cell differentiation. *Immunol. Rev.* 261, 157–168. <https://doi.org/10.1111/imr.12205>
- Gray-Owen, S.D., Blumberg, R.S., 2006. CEACAM1: contact-dependent control of immunity. *Nat. Rev. Immunol.* 6, 433. <https://doi.org/10.1038/nri1864>
- Green, A., Maclennan, R., And, P.Y., Martin, N., 1993. Site distribution of cutaneous melanoma in queensland. *Int. J. Cancer* 53, 232–236. <https://doi.org/10.1002/ijc.2910530210>
- Gros, A., Parkhurst, M.R., Tran, E., Pasetto, A., Robbins, P.F., Ilyas, S., Prickett, T.D., Gartner, J.J., Crystal, J.S., Roberts, I.M., Trebska-McGowan, K., Wunderlich, J.R., Yang, J.C., Rosenberg, S.A., 2016. Prospective

- identification of neoantigen-specific lymphocytes in the peripheral blood of melanoma patients. *Nat. Med.* 22, 433–438. <https://doi.org/10.1038/nm.4051>
- Gros, A., Robbins, P.F., Yao, X., Li, Y.F., Turcotte, S., Tran, E., Wunderlich, J.R., Mixon, A., Farid, S., Dudley, M.E., Hanada, K., Almeida, J.R., Darko, S., Douek, D.C., Yang, J.C., Rosenberg, S.A., 2014. PD-1 identifies the patient-specific CD8+ tumor-reactive repertoire infiltrating human tumors. *J. Clin. Invest.* 124, 2246–2259. <https://doi.org/10.1172/JCI73639>
- Gross, G., Waks, T., Eshhar, Z., 1989. Expression of immunoglobulin-T-cell receptor chimeric molecules as functional receptors with antibody-type specificity. *Proc. Natl. Acad. Sci. U. S. A.* 86, 10024–10028.
- Gubin, M.M., Artyomov, M.N., Mardis, E.R., Schreiber, R.D., 2015. Tumor neoantigens: building a framework for personalized cancer immunotherapy. *J. Clin. Invest.* 125, 3413–3421. <https://doi.org/10.1172/JCI80008>
- Gubin, M.M., Zhang, X., Schuster, H., Caron, E., Ward, J.P., Noguchi, T., Ivanova, Y., Hundal, J., Arthur, C.D., Krebber, W.-J., Mulder, G.E., Toebes, M., Vesely, M.D., Lam, S.S.K., Korman, A.J., Allison, J.P., Freeman, G.J., Sharpe, A.H., Pearce, E.L., Schumacher, T.N., Aebbersold, R., Rammensee, H.-G., Melief, C.J.M., Mardis, E.R., Gillanders, W.E., Artyomov, M.N., Schreiber, R.D., 2014. Checkpoint Blockade Cancer Immunotherapy Targets Tumour-Specific Mutant Antigens. *Nature* 515, 577–581. <https://doi.org/10.1038/nature13988>
- Guy, G.P., Thomas, C.C., Thompson, T., Watson, M., Massetti, G.M., Richardson, L.C., 2015. Vital Signs: Melanoma Incidence and Mortality Trends and Projections — United States, 1982–2030. *MMWR Morb. Mortal. Wkly. Rep.* 64, 591–596.
- Hamann, A., Klugewitz, K., Austrup, F., Jablonski-Westrich, D., 2000. Activation induces rapid and profound alterations in the trafficking of T cells. *Eur. J. Immunol.* 30, 3207–3218. [https://doi.org/10.1002/1521-4141\(200011\)30:11<3207::AID-IMMU3207>3.0.CO;2-L](https://doi.org/10.1002/1521-4141(200011)30:11<3207::AID-IMMU3207>3.0.CO;2-L)
- Hammer, G.E., Gonzalez, F., Champsaur, M., Cado, D., Shastri, N., 2006. The aminopeptidase ERAAP shapes the peptide repertoire displayed by major histocompatibility complex class I molecules. *Nat. Immunol.* 7, 103. <https://doi.org/10.1038/ni1286>
- Hammer, G.E., Gonzalez, F., James, E., Nolla, H., Shastri, N., 2007. In the absence of aminopeptidase ERAAP, MHC class I molecules present many unstable and highly immunogenic peptides. *Nat. Immunol.* 8, 101–108. <https://doi.org/10.1038/ni1409>
- Harshyne, L.A., Watkins, S.C., Gambotto, A., Barratt-Boyes, S.M., 2001. Dendritic cells acquire antigens from live cells for cross-presentation to CTL. *J. Immunol. Baltim. Md 1950* 166, 3717–3723.
- Hasim, A., Abudula, M., Aimiduo, R., Ma, J.-Q., Jiao, Z., Akula, G., Wang, T., Abudula, A., 2012. Post-Transcriptional and Epigenetic Regulation of Antigen Processing Machinery (APM) Components and HLA-I in Cervical Cancers from Uighur Women. *PLOS ONE* 7, e44952. <https://doi.org/10.1371/journal.pone.0044952>
- Hateren, A.V., James, E., Bailey, A., Phillips, A., Dalchau, N., Elliott, T., 2010.

- The cell biology of major histocompatibility complex class I assembly: towards a molecular understanding. *Tissue Antigens* 76, 259–275. <https://doi.org/10.1111/j.1399-0039.2010.01550.x>
- Hawke, S., Stevenson, P.G., Freeman, S., Bangham, C.R.M., 1998. Long-Term Persistence of Activated Cytotoxic T Lymphocytes after Viral Infection of the Central Nervous System. *J. Exp. Med.* 187, 1575–1582. <https://doi.org/10.1084/jem.187.10.1575>
- Herlyn, M., Fukunaga-Kalabis, M., 2010. What Is a Good Model for Melanoma? *J. Invest. Dermatol.* 130, 911–912. <https://doi.org/10.1038/jid.2009.441>
- Higgins, J.M.G., Mandlebrot, D.A., Shaw, S.K., Russell, G.J., Murphy, E.A., Chen, Y.-T., Nelson, W.J., Parker, C.M., Brenner, M.B., 1998. Direct and Regulated Interaction of Integrin $\alpha\beta 7$ with E-Cadherin. *J. Cell Biol.* 140, 197–210.
- Hinrichs, C.S., Restifo, N.P., 2013. Reassessing target antigens for adoptive T cell therapy. *Nat. Biotechnol.* 31, 999–1008. <https://doi.org/10.1038/nbt.2725>
- Hla, T., Venkataraman, K., Michaud, J., 2008. The vascular S1P gradient— Cellular sources and biological significance. *Biochim. Biophys. Acta BBA - Mol. Cell Biol. Lipids, Lysophospholipids* 1781, 477–482. <https://doi.org/10.1016/j.bbali.2008.07.003>
- Hodi, F.S., Chesney, J., Pavlick, A.C., Robert, C., Grossmann, K.F., McDermott, D.F., Linette, G.P., Meyer, N., Giguere, J.K., Agarwala, S.S., Shaheen, M., Ernstoff, M.S., Minor, D.R., Salama, A.K., Taylor, M.H., Ott, P.A., Horak, C., Gagnier, P., Jiang, J., Wolchok, J.D., Postow, M.A., 2016. Combined nivolumab and ipilimumab versus ipilimumab alone in patients with advanced melanoma: 2-year overall survival outcomes in a multicentre, randomised, controlled, phase 2 trial. *Lancet Oncol.* 17, 1558–1568. [https://doi.org/10.1016/S1470-2045\(16\)30366-7](https://doi.org/10.1016/S1470-2045(16)30366-7)
- Hodis, E., Watson, I.R., Kryukov, G.V., Arold, S.T., Imielinski, M., Theurillat, J.-P., Nickerson, E., Auclair, D., Li, L., Place, C., DiCara, D., Ramos, A.H., Lawrence, M.S., Cibulskis, K., Sivachenko, A., Voet, D., Saksena, G., Stransky, N., Onofrio, R.C., Winckler, W., Ardlie, K., Wagle, N., Wargo, J., Chong, K., Morton, D.L., Stemke-Hale, K., Chen, G., Noble, M., Meyerson, M., Ladbury, J.E., Davies, M.A., Gershenwald, J.E., Wagner, S.N., Hoon, D.S.B., Schadendorf, D., Lander, E.S., Gabriel, S.B., Getz, G., Garraway, L.A., Chin, L., 2012. A Landscape of Driver Mutations in Melanoma. *Cell* 150, 251–263. <https://doi.org/10.1016/j.cell.2012.06.024>
- Hoek, K.S., Eichhoff, O.M., Schlegel, N.C., Döbbeling, U., Kobert, N., Schaerer, L., Hemmi, S., Dummer, R., 2008. In vivo Switching of Human Melanoma Cells between Proliferative and Invasive States. *Cancer Res.* 68, 650–656. <https://doi.org/10.1158/0008-5472.CAN-07-2491>
- Hoek, K.S., Goding, C.R., 2010. Cancer stem cells versus phenotype-switching in melanoma. *Pigment Cell Melanoma Res.* 23, 746–759. <https://doi.org/10.1111/j.1755-148X.2010.00757.x>
- Hofmann, M., Oschowitz, A., Kurzhals, S.R., Krüger, C.C., Pircher, H., 2013. Thymus-resident memory CD8+ T cells mediate local immunity. *Eur. J. Immunol.* 43, 2295–2304. <https://doi.org/10.1002/eji.201343519>
- Hofmann, M., Pircher, H., 2011. E-cadherin promotes accumulation of a unique

- memory CD8 T-cell population in murine salivary glands. *Proc. Natl. Acad. Sci.* 108, 16741–16746. <https://doi.org/10.1073/pnas.1107200108>
- Hogquist, K.A., Jameson, S.C., Heath, W.R., Howard, J.L., Bevan, M.J., Carbone, F.R., 1994. T cell receptor antagonist peptides induce positive selection. *Cell* 76, 17–27. [https://doi.org/10.1016/0092-8674\(94\)90169-4](https://doi.org/10.1016/0092-8674(94)90169-4)
- Hölzel, M., Rohrmoser, M., Schlee, M., Grimm, T., Harasim, T., Malamoussi, A., Gruber-Eber, A., Kremmer, E., Hiddemann, W., Bornkamm, G.W., Eick, D., 2005. Mammalian WDR12 is a novel member of the Pes1–Bop1 complex and is required for ribosome biogenesis and cell proliferation. *J. Cell Biol.* 170, 367–378. <https://doi.org/10.1083/jcb.200501141>
- Hombrink, P., Helbig, C., Backer, R.A., Piet, B., Oja, A.E., Stark, R., Brassler, G., Jongejan, A., Jonkers, R.E., Nota, B., Basak, O., Clevers, H.C., Moerland, P.D., Amsen, D., van Lier, R.A.W., 2016. Programs for the persistence, vigilance and control of human CD8⁺ lung-resident memory T cells. *Nat. Immunol.* 17, 1467–1478. <https://doi.org/10.1038/ni.3589>
- Hsiao, J.J., Fisher, D.E., 2014. The roles of microphthalmia-associated transcription factor and pigmentation in melanoma. *Arch. Biochem. Biophys.*, *Advances in Melanocyte and Melanoma Biology* 563, 28–34. <https://doi.org/10.1016/j.abb.2014.07.019>
- Hu, W., Li, X., Zhang, C., Yang, Y., Jiang, J., Wu, C., 2016. Tumor-associated macrophages in cancers. *Clin. Transl. Oncol.* 18, 251–258. <https://doi.org/10.1007/s12094-015-1373-0>
- Huang, J., El-Gamil, M., Dudley, M.E., Li, Y.F., Rosenberg, S.A., Robbins, P.F., 2004. T Cells Associated with Tumor Regression Recognize Frameshifted Products of the CDKN2A Tumor Suppressor Gene Locus and a Mutated HLA Class I Gene Product. *J. Immunol. Baltim. Md 1950* 172, 6057–6064.
- Hugo, W., Zaretsky, J.M., Sun, L., Song, C., Moreno, B.H., Hu-Lieskovan, S., Berent-Maoz, B., Pang, J., Chmielowski, B., Cherry, G., Seja, E., Lomeli, S., Kong, X., Kelley, M.C., Sosman, J.A., Johnson, D.B., Ribas, A., Lo, R.S., 2016. Genomic and Transcriptomic Features of Response to Anti-PD-1 Therapy in Metastatic Melanoma. *Cell* 165, 35–44. <https://doi.org/10.1016/j.cell.2016.02.065>
- IARC Cancer Base, 2013. GLOBOCAN 2012 v1.0, Cancer Incidence and Mortality Worldwide.
- Indra, A.K., Warot, X., Brocard, J., Bornert, J.M., Xiao, J.H., Chambon, P., Metzger, D., 1999. Temporally-controlled site-specific mutagenesis in the basal layer of the epidermis: comparison of the recombinase activity of the tamoxifen-inducible Cre-ER(T) and Cre-ER(T2) recombinases. *Nucleic Acids Res.* 27, 4324–4327.
- Intlekofer, A.M., Banerjee, A., Takemoto, N., Gordon, S.M., DeJong, C.S., Shin, H., Hunter, C.A., Wherry, E.J., Lindsten, T., Reiner, S.L., 2008. Anomalous Type 17 Response to Viral Infection by CD8⁺ T Cells Lacking T-bet and Eomesodermin. *Science* 321, 408–411. <https://doi.org/10.1126/science.1159806>
- Intlekofer, A.M., Takemoto, N., Wherry, E.J., Longworth, S.A., Northrup, J.T., Palanivel, V.R., Mullen, A.C., Gasink, C.R., Kaeck, S.M., Miller, J.D., Gapin, L., Ryan, K., Russ, A.P., Lindsten, T., Orange, J.S., Goldrath, A.W., Ahmed, R., Reiner, S.L., 2005. Effector and memory CD8 + T cell fate

- coupled by T-bet and eomesodermin. *Nat. Immunol.* 6, 1236. <https://doi.org/10.1038/ni1268>
- Jameson, S.C., Masopust, D., 2009. Diversity in T Cell Memory: An Embarrassment of Riches. *Immunity* 31, 859–871. <https://doi.org/10.1016/j.immuni.2009.11.007>
- Javelaud, D., Alexaki, V.-I., Pierrat, M.-J., Hoek, K.S., Dennler, S., Van Kempen, L., Bertolotto, C., Ballotti, R., Saule, S., Delmas, V., Mauviel, A., 2011. GLI2 and M-MITF transcription factors control exclusive gene expression programs and inversely regulate invasion in human melanoma cells. *Pigment Cell Melanoma Res.* 24, 932–943. <https://doi.org/10.1111/j.1755-148X.2011.00893.x>
- Jemal, A., Devesa, S.S., Hartge, P., Tucker, M.A., 2001. Recent Trends in Cutaneous Melanoma Incidence Among Whites in the United States. *JNCI J. Natl. Cancer Inst.* 93, 678–683. <https://doi.org/10.1093/jnci/93.9.678>
- Jenkinson, S.E., Whawell, S.A., Swales, B.M., Corps, E.M., Kilshaw, P.J., Farthing, P.M., 2011. The α E(CD103) β 7 integrin interacts with oral and skin keratinocytes in an E-cadherin-independent manner*. *Immunology* 132, 188–196. <https://doi.org/10.1111/j.1365-2567.2010.03352.x>
- Jiang, X., Clark, R.A., Liu, L., Wagers, A.J., Fuhlbrigge, R.C., Kupper, T.S., 2012. Skin infection generates non-migratory memory CD8⁺ T_{RM} cells providing global skin immunity. *Nature* 483, 227–231. <https://doi.org/10.1038/nature10851>
- Jimbow, K., Roth, S.I., Fitzpatrick, T.B., Szabo, G., 1975. Mitotic activity in non-neoplastic melanocytes in vivo as determined by histochemical, autoradiographic, and electron microscope studies. *J. Cell Biol.* 66, 663–670. <https://doi.org/10.1083/jcb.66.3.663>
- Jo, P., König, A., Schirmer, M., Kitz, J., Conradi, L.-C., Azizian, A., Bernhardt, M., Wolff, H.A., Grade, M., Ghadimi, M., Ströbel, P., Schildhaus, H.-U., Gaedcke, J., 2016. Heterogeneity of KRAS Mutation Status in Rectal Cancer. *PLoS ONE* 11. <https://doi.org/10.1371/journal.pone.0153278>
- Johnson, L.A., Morgan, R.A., Dudley, M.E., Cassard, L., Yang, J.C., Hughes, M.S., Kammula, U.S., Royal, R.E., Sherry, R.M., Wunderlich, J.R., Lee, C.-C.R., Restifo, N.P., Schwarz, S.L., Cogdill, A.P., Bishop, R.J., Kim, H., Brewer, C.C., Rudy, S.F., VanWaes, C., Davis, J.L., Mathur, A., Ripley, R.T., Nathan, D.A., Laurencot, C.M., Rosenberg, S.A., 2009. Gene therapy with human and mouse T-cell receptors mediates cancer regression and targets normal tissues expressing cognate antigen. *Blood* 114, 535–546. <https://doi.org/10.1182/blood-2009-03-211714>
- Joshi, N.S., Cui, W., Chandele, A., Lee, H.K., Urso, D.R., Hagman, J., Gapin, L., Kaech, S.M., 2007. Inflammation Directs Memory Precursor and Short-Lived Effector CD8⁺ T Cell Fates via the Graded Expression of T-bet Transcription Factor. *Immunity* 27, 281–295. <https://doi.org/10.1016/j.immuni.2007.07.010>
- Joshi, N.S., Cui, W., Dominguez, C.X., Chen, J.H., Hand, T.W., Kaech, S.M., 2011. Increased Numbers of Preexisting Memory CD8 T Cells and Decreased T-bet Expression Can Restrain Terminal Differentiation of Secondary Effector and Memory CD8 T Cells. *J. Immunol.* 187, 4068–4076. <https://doi.org/10.4049/jimmunol.1002145>

- Judge, A.D., Zhang, X., Fujii, H., Surh, C.D., Sprent, J., 2002. Interleukin 15 Controls both Proliferation and Survival of a Subset of Memory-Phenotype CD8⁺ T Cells. *J. Exp. Med.* 196, 935–946. <https://doi.org/10.1084/jem.20020772>
- June, C.H., 2016. Drugging the Undruggable Ras — Immunotherapy to the Rescue? *N. Engl. J. Med.* 375, 2286–2289. <https://doi.org/10.1056/NEJMe1612215>
- Jurtz, V., Paul, S., Andreatta, M., Marcatili, P., Peters, B., Nielsen, M., 2017. NetMHCpan 4.0: Improved peptide-MHC class I interaction predictions integrating eluted ligand and peptide binding affinity data. *J. Immunol. Baltim. Md* 1950 199, 3360–3368. <https://doi.org/10.4049/jimmunol.1700893>
- Kaech, S.M., Cui, W., 2012. Transcriptional control of effector and memory CD8⁺ T cell differentiation. *Nat. Rev. Immunol.* 12, 749–761. <https://doi.org/10.1038/nri3307>
- Kaech, S.M., Tan, J.T., Wherry, E.J., Konieczny, B.T., Surh, C.D., Ahmed, R., 2003. Selective expression of the interleukin 7 receptor identifies effector CD8 T cells that give rise to long-lived memory cells. *Nat. Immunol.* 4, 1191. <https://doi.org/10.1038/ni1009>
- Kaidbey, K.H., Agin, P.P., Sayre, R.M., Kligman, A.M., 1979. Photoprotection by melanin—a comparison of black and Caucasian skin. *J. Am. Acad. Dermatol.* 1, 249–260. [https://doi.org/10.1016/S0190-9622\(79\)70018-1](https://doi.org/10.1016/S0190-9622(79)70018-1)
- Kaklamani, L., Townsend, A., Doussis-Anagnostopoulou, I.A., Mortensen, N., Harris, A.L., Gatter, K.C., 1994. Loss of major histocompatibility complex-encoded transporter associated with antigen presentation (TAP) in colorectal cancer. *Am. J. Pathol.* 145, 505–509.
- Kalaora, S., Barnea, E., Merhavi-Shoham, E., Qutob, N., Teer, J.K., Shimony, N., Schachter, J., Rosenberg, S.A., Besser, M.J., Admon, A., Samuels, Y., 2016. Use of HLA peptidomics and whole exome sequencing to identify human immunogenic neo-antigens. *Oncotarget* 7, 5110–5117. <https://doi.org/10.18632/oncotarget.6960>
- Kallies, A., Xin, A., Belz, G.T., Nutt, S.L., 2009. Blimp-1 Transcription Factor Is Required for the Differentiation of Effector CD8⁺ T Cells and Memory Responses. *Immunity* 31, 283–295. <https://doi.org/10.1016/j.immuni.2009.06.021>
- Kamphausen, E., Kellert, C., Abbas, T., Akkad, N., Tenzer, S., Pawelec, G., Schild, H., van Endert, P., Seliger, B., 2010. Distinct molecular mechanisms leading to deficient expression of ER-resident aminopeptidases in melanoma. *Cancer Immunol. Immunother.* 59, 1273–1284. <https://doi.org/10.1007/s00262-010-0856-7>
- Kaneda, M.M., Messer, K.S., Ralainirina, N., Li, H., Leem, C.J., Gorjestani, S., Woo, G., Nguyen, A.V., Figueiredo, C.C., Foubert, P., Schmid, M.C., Pink, M., Winkler, D.G., Rausch, M., Palombella, V.J., Kutok, J., McGovern, K., Frazer, K.A., Wu, X., Karin, M., Sasik, R., Cohen, E.E.W., Varner, J.A., 2016. PI3K γ is a molecular switch that controls immune suppression. *Nature* 539, 437–442. <https://doi.org/10.1038/nature19834>
- Kaneko, K., Ishigami, S., Kijima, Y., Funasako, Y., Hirata, M., Okumura, H., Shinchi, H., Koriyama, C., Ueno, S., Yoshinaka, H., Natsugoe, S., 2011.

- Clinical implication of HLA class I expression in breast cancer. *BMC Cancer* 11, 454. <https://doi.org/10.1186/1471-2407-11-454>
- Kaplan, M.H., Wurster, A.L., Grusby, M.J., 1998. A Signal Transducer and Activator of Transcription (Stat)4-independent Pathway for the Development of T Helper Type 1 Cells. *J. Exp. Med.* 188, 1191–1196.
- Kataoka, K., Shiraishi, Y., Takeda, Y., Sakata, S., Matsumoto, M., Nagano, S., Maeda, T., Nagata, Y., Kitanaka, A., Mizuno, S., Tanaka, H., Chiba, K., Ito, S., Watatani, Y., Kakiuchi, N., Suzuki, H., Yoshizato, T., Yoshida, K., Sanada, M., Itonaga, H., Imaizumi, Y., Totoki, Y., Munakata, W., Nakamura, H., Hama, N., Shide, K., Kubuki, Y., Hidaka, T., Kameda, T., Masuda, K., Minato, N., Kashiwase, K., Izutsu, K., Takaori-Kondo, A., Miyazaki, Y., Takahashi, S., Shibata, T., Kawamoto, H., Akatsuka, Y., Shimoda, K., Takeuchi, K., Seya, T., Miyano, S., Ogawa, S., 2016. Aberrant *PD-L1* expression through 3'-UTR disruption in multiple cancers. *Nature* 534, 402–406. <https://doi.org/10.1038/nature18294>
- Kawakami, Y., Eliyahu, S., Delgado, C.H., Robbins, P.F., Rivoltini, L., Topalian, S.L., Miki, T., Rosenberg, S.A., 1994a. Cloning of the gene coding for a shared human melanoma antigen recognized by autologous T cells infiltrating into tumor. *Proc. Natl. Acad. Sci. U. S. A.* 91, 3515–3519.
- Kawakami, Y., Eliyahu, S., Delgado, C.H., Robbins, P.F., Sakaguchi, K., Appella, E., Yannelli, J.R., Adema, G.J., Miki, T., Rosenberg, S.A., 1994b. Identification of a human melanoma antigen recognized by tumor-infiltrating lymphocytes associated with in vivo tumor rejection. *Proc. Natl. Acad. Sci. U. S. A.* 91, 6458–6462.
- Kelly, A., Powis, S.H., Glynn, R., Radley, E., Beck, S., Trowsdale, J., 1991. Second proteasome-related gene in the human MHC class II region. *Nature* 353, 667. <https://doi.org/10.1038/353667a0>
- Kerkar, S.P., Goldszmid, R.S., Muranski, P., Chinnasamy, D., Yu, Z., Reger, R.N., Leonardi, A.J., Morgan, R.A., Wang, E., Marincola, F.M., Trinchieri, G., Rosenberg, S.A., Restifo, N.P., 2011. IL-12 triggers a programmatic change in dysfunctional myeloid-derived cells within mouse tumors. *J. Clin. Invest.* 121, 4746–4757. <https://doi.org/10.1172/JCI58814>
- Klebanoff, C.A., Acquavella, N., Yu, Z., Restifo, N.P., 2011. Therapeutic cancer vaccines: are we there yet? *Immunol. Rev.* 239, 27–44. <https://doi.org/10.1111/j.1600-065X.2010.00979.x>
- Klebanoff, C.A., Gattinoni, L., Torabi-Parizi, P., Kerstann, K., Cardones, A.R., Finkelstein, S.E., Palmer, D.C., Antony, P.A., Hwang, S.T., Rosenberg, S.A., Waldmann, T.A., Restifo, N.P., 2005. Central memory self/tumor-reactive CD8+ T cells confer superior antitumor immunity compared with effector memory T cells. *Proc. Natl. Acad. Sci. U. S. A.* 102, 9571–9576. <https://doi.org/10.1073/pnas.0503726102>
- Klicznik, M.M., Morawski, P.A., Höllbacher, B., Varkhande, S.R., Motley, S.J., Kuri-Cervantes, L., Goodwin, E., Rosenblum, M.D., Long, S.A., Bracht, G., Duhon, T., Betts, M.R., Campbell, D.J., Gratz, I.K., 2019. Human CD4+CD103+ cutaneous resident memory T cells are found in the circulation of healthy individuals. *Sci. Immunol.* 4, eaav8995. <https://doi.org/10.1126/sciimmunol.aav8995>
- Kochenderfer, J.N., Wilson, W.H., Janik, J.E., Dudley, M.E., Stetler-Stevenson,

- M., Feldman, S.A., Maric, I., Raffeld, M., Nathan, D.-A.N., Lanier, B.J., Morgan, R.A., Rosenberg, S.A., 2010. Eradication of B-lineage cells and regression of lymphoma in a patient treated with autologous T cells genetically engineered to recognize CD19. *Blood* 116, 4099–4102. <https://doi.org/10.1182/blood-2010-04-281931>
- Kodumudi, K.N., Weber, A., Sarnaik, A.A., Pilon-Thomas, S., 2012. Blockade of Myeloid-Derived Suppressor Cells after Induction of Lymphopenia Improves Adoptive T Cell Therapy in a Murine Model of Melanoma. *J. Immunol.* 189, 5147–5154. <https://doi.org/10.4049/jimmunol.1200274>
- Koh, H.K., Geller, A.C., Miller, D.R., Grossbart, T.A., Lew, R.A., 1996. Prevention and Early Detection Strategies for Melanoma and Skin Cancer: Current Status. *Arch. Dermatol.* 132, 436–443. <https://doi.org/10.1001/archderm.1996.03890280098014>
- Kohlmeyer, J., Cron, M., Landsberg, J., Bald, T., Renn, M., Mikus, S., Bondong, S., Wikasari, D., Gaffal, E., Hartmann, G., Tüting, T., 2009. Complete Regression of Advanced Primary and Metastatic Mouse Melanomas following Combination Chemoimmunotherapy. *Cancer Res.* 69, 6265–6274. <https://doi.org/10.1158/0008-5472.CAN-09-0579>
- Komdeur, F.L., Prins, T.M., Wall, S. van de, Plat, A., Wisman, G.B.A., Hollema, H., Daemen, T., Church, D.N., Bruyn, M. de, Nijman, H.W., 2017. CD103+ tumor-infiltrating lymphocytes are tumor-reactive intraepithelial CD8+ T cells associated with prognostic benefit and therapy response in cervical cancer. *Oncolmmunology* 6, e1338230. <https://doi.org/10.1080/2162402X.2017.1338230>
- Konieczkowski, D.J., Johannessen, C.M., Abudayyeh, O., Kim, J.W., Cooper, Z.A., Piris, A., Frederick, D.T., Barzily-Rokni, M., Straussman, R., Haq, R., Fisher, D.E., Mesirov, J.P., Hahn, W.C., Flaherty, K.T., Wargo, J.A., Tamayo, P., Garraway, L.A., 2014. A Melanoma Cell State Distinction Influences Sensitivity to MAPK Pathway Inhibitors. *Cancer Discov.* 4, 816–827. <https://doi.org/10.1158/2159-8290.CD-13-0424>
- Kosary, C.L., Altekruse, S.F., Ruhl, J., Lee, R., Dickie, L., 2014. Clinical and prognostic factors for melanoma of the skin using SEER registries: collaborative stage data collection system, version 1 and version 2. *Cancer* 120 Suppl 23, 3807–3814. <https://doi.org/10.1002/cncr.29050>
- Kristianto, J., Johnson, M.G., Zastrow, R.K., Radcliff, A.B., Blank, R.D., 2017. Spontaneous recombinase activity of Cre–ERT2 in vivo. *Transgenic Res.* 26, 411–417. <https://doi.org/10.1007/s11248-017-0018-1>
- Kryczek, I., Zou, L., Rodriguez, P., Zhu, G., Wei, S., Mottram, P., Brumlik, M., Cheng, P., Curiel, T., Myers, L., Lackner, A., Alvarez, X., Ochoa, A., Chen, L., Zou, W., 2006. B7-H4 expression identifies a novel suppressive macrophage population in human ovarian carcinoma. *J. Exp. Med.* 203, 871–881. <https://doi.org/10.1084/jem.20050930>
- Kuang, D.-M., Zhao, Q., Peng, C., Xu, J., Zhang, J.-P., Wu, C., Zheng, L., 2009. Activated monocytes in peritumoral stroma of hepatocellular carcinoma foster immune privilege and disease progression through PD-L1. *J. Exp. Med.* 206, 1327–1337. <https://doi.org/10.1084/jem.20082173>
- Kumar, B.V., Ma, W., Miron, M., Granot, T., Guyer, R.S., Carpenter, D.J., Senda, T., Sun, X., Ho, S.-H., Lerner, H., Friedman, A.L., Shen, Y., Farber, D.L.,

2017. Human Tissue-Resident Memory T Cells Are Defined by Core Transcriptional and Functional Signatures in Lymphoid and Mucosal Sites. *Cell Rep.* 20, 2921–2934. <https://doi.org/10.1016/j.celrep.2017.08.078>
- Laborde, R.R., Lin, Y., Gustafson, M.P., Bulur, P.A., Dietz, A.B., 2014. Cancer Vaccines in the World of Immune Suppressive Monocytes (CD14+HLA-DRlo/neg Cells): The Gateway to Improved Responses. *Front. Immunol.* 5. <https://doi.org/10.3389/fimmu.2014.00147>
- Lamers, C.H., Sleijfer, S., van Steenbergen, S., van Elzakker, P., van Krimpen, B., Groot, C., Vulto, A., den Bakker, M., Oosterwijk, E., Debets, R., Gratama, J.W., 2013. Treatment of Metastatic Renal Cell Carcinoma With CAIX CAR-engineered T cells: Clinical Evaluation and Management of On-target Toxicity. *Mol. Ther.* 21, 904–912. <https://doi.org/10.1038/mt.2013.17>
- Lancaster, H.O., 1956. Some geographical aspects of the mortality from melanoma in Europeans. *Med. J. Aust.* 43, 1082–1087.
- Landsberg, J., Gaffal, E., Cron, M., Kohlmeyer, J., Renn, M., Tüting, T., 2010. Autochthonous primary and metastatic melanomas in Hgf-Cdk4 R24C mice evade T-cell-mediated immune surveillance. *Pigment Cell Melanoma Res.* 23, 649–660. <https://doi.org/10.1111/j.1755-148X.2010.00744.x>
- Landsberg, J., Kohlmeyer, J., Renn, M., Bald, T., Rogava, M., Cron, M., Fatho, M., Lennerz, V., Wölfel, T., Hölzel, M., Tüting, T., 2012. Melanomas resist T-cell therapy through inflammation-induced reversible dedifferentiation. *Nature* 490, 412–416. <https://doi.org/10.1038/nature11538>
- Lanfredini, S., Thapa, A., O'Neill, E., 2019. RAS in pancreatic cancer. *Biochem. Soc. Trans.* BST20170521. <https://doi.org/10.1042/BST20170521>
- Larkin, J., Chiarion-Sileni, V., Gonzalez, R., Grob, J.J., Cowey, C.L., Lao, C.D., Schadendorf, D., Dummer, R., Smylie, M., Rutkowski, P., Ferrucci, P.F., Hill, A., Wagstaff, J., Carlino, M.S., Haanen, J.B., Maio, M., Marquez-Rodas, I., McArthur, G.A., Ascierto, P.A., Long, G.V., Callahan, M.K., Postow, M.A., Grossmann, K., Sznol, M., Dreno, B., Bastholt, L., Yang, A., Rollin, L.M., Horak, C., Hodi, F.S., Wolchok, J.D., 2015. Combined Nivolumab and Ipilimumab or Monotherapy in Untreated Melanoma [WWW Document]. <https://doi.org/10.1056/NEJMoa1504030>. <https://doi.org/10.1056/NEJMoa1504030>
- Lasithiotakis, K.G., Leiter, U., Gorkiewicz, R., Eigentler, T., Breuninger, H., Metzler, G., Strobel, W., Garbe, C., 2006. The incidence and mortality of cutaneous melanoma in southern Germany. *Cancer* 107, 1331–1339. <https://doi.org/10.1002/cncr.22126>
- Lastwika, K.J., Wilson, W., Li, Q.K., Norris, J., Xu, H., Ghazarian, S.R., Kitagawa, H., Kawabata, S., Taube, J.M., Yao, S., Liu, L.N., Gills, J.J., Dennis, P.A., 2016. Control of PD-L1 Expression by Oncogenic Activation of the AKT–mTOR Pathway in Non–Small Cell Lung Cancer. *Cancer Res.* 76, 227–238. <https://doi.org/10.1158/0008-5472.CAN-14-3362>
- Lauder, I., Aherne, W., 1972. The Significance of Lymphocytic Infiltration in Neuroblastoma. *Br. J. Cancer* 26, 321–330.
- Law, C.W., Chen, Y., Shi, W., Smyth, G.K., 2014. voom: precision weights unlock linear model analysis tools for RNA-seq read counts. *Genome Biol.* 15, R29. <https://doi.org/10.1186/gb-2014-15-2-r29>

- Lawrence, M.S., Stojanov, P., Polak, P., Kryukov, G.V., Cibulskis, K., Sivachenko, A., Carter, S.L., Stewart, C., Mermel, C.H., Roberts, S.A., Kiezun, A., Hammerman, P.S., McKenna, A., Drier, Y., Zou, L., Ramos, A.H., Pugh, T.J., Stransky, N., Helman, E., Kim, J., Sougnez, C., Ambrogio, L., Nickerson, E., Shefler, E., Cortés, M.L., Auclair, D., Saksena, G., Voet, D., Noble, M., DiCara, D., Lin, P., Lichtenstein, L., Heiman, D.I., Fennell, T., Imielinski, M., Hernandez, B., Hodis, E., Baca, S., Dulak, A.M., Lohr, J., Landau, D.-A., Wu, C.J., Melendez-Zajgla, J., Hidalgo-Miranda, A., Koren, A., McCarroll, S.A., Mora, J., Crompton, B., Onofrio, R., Parkin, M., Winckler, W., Ardlie, K., Gabriel, S.B., Roberts, C.W.M., Biegel, J.A., Stegmaier, K., Bass, A.J., Garraway, L.A., Meyerson, M., Golub, T.R., Gordenin, D.A., Sunyaev, S., Lander, E.S., Getz, G., 2013. Mutational heterogeneity in cancer and the search for new cancer genes. *Nature* 499, 214–218. <https://doi.org/10.1038/nature12213>
- Le, D.T., Uram, J.N., Wang, H., Bartlett, B.R., Kemberling, H., Eyring, A.D., Skora, A.D., Luber, B.S., Azad, N.S., Laheru, D., Biedrzycki, B., Donehower, R.C., Zaheer, A., Fisher, G.A., Crocenzi, T.S., Lee, J.J., Duffy, S.M., Goldberg, R.M., de la Chapelle, A., Koshiji, M., Bhajee, F., Huebner, T., Hruban, R.H., Wood, L.D., Cuka, N., Pardoll, D.M., Papadopoulos, N., Kinzler, K.W., Zhou, S., Cornish, T.C., Taube, J.M., Anders, R.A., Eshleman, J.R., Vogelstein, B., Diaz, L.A., 2015. PD-1 Blockade in Tumors with Mismatch-Repair Deficiency. *N. Engl. J. Med.* 372, 2509–2520. <https://doi.org/10.1056/NEJMoa1500596>
- Lebrun, J.-J., 2012. The Dual Role of TGF β in Human Cancer: From Tumor Suppression to Cancer Metastasis. *ISRN Mol. Biol.* 2012. <https://doi.org/10.5402/2012/381428>
- Lefrançois, L., Parker, C.M., Olson, S., Muller, W., Wagner, N., Puddington, L., 1999. The Role of β 7 Integrins in CD8 T Cell Trafficking During an Antiviral Immune Response. *J. Exp. Med.* 189, 1631–1638. <https://doi.org/10.1084/jem.189.10.1631>
- Leisegang, M., Engels, B., Schreiber, K., Yew, P.Y., Kiyotani, K., Idel, C., Arina, A., Duraiswamy, J., Weichselbaum, R.R., Uckert, W., Nakamura, Y., Schreiber, H., 2016. Eradication of Large Solid Tumors by Gene Therapy with a T-Cell Receptor Targeting a Single Cancer-Specific Point Mutation. *Clin. Cancer Res.* 22, 2734–2743. <https://doi.org/10.1158/1078-0432.CCR-15-2361>
- Leone, P., Shin, E.-C., Perosa, F., Vacca, A., Dammacco, F., Racanelli, V., 2013. MHC Class I Antigen Processing and Presenting Machinery: Organization, Function, and Defects in Tumor Cells. *JNCI J. Natl. Cancer Inst.* 105, 1172–1187. <https://doi.org/10.1093/jnci/djt184>
- Lerner, A.B., Mcguire, J.S., 1964. MELANOCYTE-STIMULATING HORMONE AND ADRENOCORTICOTROPHIC HORMONE. THEIR RELATION TO PIGMENTATION. *N. Engl. J. Med.* 270, 539–546. <https://doi.org/10.1056/NEJM196403122701101>
- Levy, C., Khaled, M., Fisher, D.E., 2006. MITF: master regulator of melanocyte development and melanoma oncogene. *Trends Mol. Med.* 12, 406–414. <https://doi.org/10.1016/j.molmed.2006.07.008>
- Leys, C.M., Nomura, S., LaFleur, B.J., Ferrone, S., Kaminishi, M., Montgomery,

- E., Goldenring, J.R., 2007. Expression and prognostic significance of prothymosin- α and ERp57 in human gastric cancer. *Surgery* 141, 41–50. <https://doi.org/10.1016/j.surg.2006.05.009>
- Li, W.-Q., Cho, E., Weinstock, M.A., Mashfiq, H., Qureshi, A.A., 2016. Epidemiological Assessments of Skin Outcomes in the Nurses' Health Studies. *Am. J. Public Health* 106, 1677–1683. <https://doi.org/10.2105/AJPH.2016.303315>
- Li, Y., Bleakley, M., Yee, C., 2005. IL-21 Influences the Frequency, Phenotype, and Affinity of the Antigen-Specific CD8 T Cell Response. *J. Immunol.* 175, 2261–2269. <https://doi.org/10.4049/jimmunol.175.4.2261>
- Liao, Y., Smyth, G.K., Shi, W., 2013. The Subread aligner: fast, accurate and scalable read mapping by seed-and-vote. *Nucleic Acids Res.* 41, e108. <https://doi.org/10.1093/nar/gkt214>
- Liberzon, A., Birger, C., Thorvaldsdóttir, H., Ghandi, M., Mesirov, J.P., Tamayo, P., 2015a. The Molecular Signatures Database Hallmark Gene Set Collection. *Cell Syst.* 1, 417–425. <https://doi.org/10.1016/j.cels.2015.12.004>
- Liberzon, A., Birger, C., Thorvaldsdóttir, H., Ghandi, M., Mesirov, J.P., Tamayo, P., 2015b. The Molecular Signatures Database (MSigDB) hallmark gene set collection. *Cell Syst.* 1, 417–425. <https://doi.org/10.1016/j.cels.2015.12.004>
- Lin, E.Y., Nguyen, A.V., Russell, R.G., Pollard, J.W., 2001. Colony-Stimulating Factor 1 Promotes Progression of Mammary Tumors to Malignancy. *J. Exp. Med.* 193, 727–740.
- Lin, J.Y., Fisher, D.E., 2007. Melanocyte biology and skin pigmentation. *Nature* 445, 843–850. <https://doi.org/10.1038/nature05660>
- Lin, R.-L., Zhao, L.-J., 2015. Mechanistic basis and clinical relevance of the role of transforming growth factor- β in cancer. *Cancer Biol. Med.* 12, 385–393. <https://doi.org/10.7497/j.issn.2095-3941.2015.0015>
- Linette, G.P., Stadtmauer, E.A., Maus, M.V., Rapoport, A.P., Levine, B.L., Emery, L., Litzky, L., Bagg, A., Carreno, B.M., Cimino, P.J., Binder-Scholl, G.K., Smethurst, D.P., Gerry, A.B., Pumphrey, N.J., Bennett, A.D., Brewer, J.E., Dukes, J., Harper, J., Tayton-Martin, H.K., Jakobsen, B.K., Hassan, N.J., Kalos, M., June, C.H., 2013. Cardiovascular toxicity and titin cross-reactivity of affinity-enhanced T cells in myeloma and melanoma. *Blood* 122, 863–871. <https://doi.org/10.1182/blood-2013-03-490565>
- Linnemann, C., van Buuren, M.M., Bies, L., Verdegaal, E.M.E., Schotte, R., Calis, J.J.A., Behjati, S., Velds, A., Hilkmann, H., Atmioui, D. el, Visser, M., Stratton, M.R., Haanen, J.B.A.G., Spits, H., van der Burg, S.H., Schumacher, T.N.M., 2015. High-throughput epitope discovery reveals frequent recognition of neo-antigens by CD4⁺ T cells in human melanoma. *Nat. Med.* 21, 81–85. <https://doi.org/10.1038/nm.3773>
- Linos, E., Swetter, S.M., Cockburn, M.G., Colditz, G.A., Clarke, C.A., 2009. Increasing burden of melanoma in the United States. *J. Invest. Dermatol.* 129, 1666–1674. <https://doi.org/10.1038/jid.2008.423>
- Lipsker, D., Engel, F., Cribier, B., Velten, M., Hedelin, G., 2007. Trends in melanoma epidemiology suggest three different types of melanoma. *Br. J. Dermatol.* 157, 338–343. <https://doi.org/10.1111/j.1365->

- 2133.2007.08029.x
- Liu, C., Peng, W., Xu, C., Lou, Y., Zhang, M., Wargo, J.A., Chen, J.Q., Li, H.S., Watowich, S.S., Yang, Y., Frederick, D.T., Cooper, Z.A., Mbofung, R.M., Whittington, M., Flaherty, K.T., Woodman, S.E., Davies, M.A., Radvanyi, L.G., Overwijk, W.W., Lizée, G., Hwu, P., 2013. BRAF Inhibition Increases Tumor Infiltration by T cells and Enhances the Anti-tumor Activity of Adoptive Immunotherapy in Mice. *Clin. Cancer Res. Off. J. Am. Assoc. Cancer Res.* 19, 393–403. <https://doi.org/10.1158/1078-0432.CCR-12-1626>
- Lu, Y.-C., Weng, W.-C., Lee, H., 2015. Functional Roles of Calreticulin in Cancer Biology. *BioMed Res. Int.* 2015. <https://doi.org/10.1155/2015/526524>
- Lu, Y.-C., Yao, X., Crystal, J.S., Li, Y.F., El-Gamil, M., Gross, C., Davis, L., Dudley, M.E., Yang, J.C., Samuels, Y., Rosenberg, S.A., Robbins, P.F., 2014. Efficient identification of mutated cancer antigens recognized by T cells associated with durable tumor regressions. *Clin. Cancer Res. Off. J. Am. Assoc. Cancer Res.* 20, 3401–3410. <https://doi.org/10.1158/1078-0432.CCR-14-0433>
- Lu, Y.-C., Yao, X., Li, Y.F., El-Gamil, M., Dudley, M.E., Yang, J.C., Almeida, J.R., Douek, D.C., Samuels, Y., Rosenberg, S.A., Robbins, P.F., 2013. Mutated PPP1R3B is recognized by T cells used to treat a melanoma patient who experienced a durable complete tumor regression. *J. Immunol. Baltim. Md 1950* 190, 6034–6042. <https://doi.org/10.4049/jimmunol.1202830>
- Łuksza, M., Riaz, N., Makarov, V., Balachandran, V.P., Hellmann, M.D., Solovyov, A., Rizvi, N.A., Merghoub, T., Levine, A.J., Chan, T.A., Wolchok, J.D., Greenbaum, B.D., 2017. A neoantigen fitness model predicts tumour response to checkpoint blockade immunotherapy. *Nature* 551, 517–520. <https://doi.org/10.1038/nature24473>
- Ma, C., Cheung, A.F., Chodon, T., Koya, R.C., Wu, Z., Ng, C., Avramis, E., Cochran, A.J., Witte, O.N., Baltimore, D., Chmielowski, B., Economou, J.S., Comin-Anduix, B., Ribas, A., Heath, J.R., 2013. Multifunctional T-cell Analyses to Study Response and Progression in Adoptive Cell Transfer Immunotherapy. *Cancer Discov.* 3, 418–429. <https://doi.org/10.1158/2159-8290.CD-12-0383>
- Ma, C., Fan, R., Ahmad, H., Shi, Q., Comin-Anduix, B., Chodon, T., Koya, R.C., Liu, C.-C., Kwong, G.A., Radu, C.G., Ribas, A., Heath, J.R., 2011. A clinical microchip for evaluation of single immune cells reveals high functional heterogeneity in phenotypically similar T cells. *Nat. Med.* 17, 738–743. <https://doi.org/10.1038/nm.2375>
- Ma, Y., Shurin, G.V., Peiyuan, Z., Shurin, M.R., 2012. Dendritic Cells in the Cancer Microenvironment. *J. Cancer* 4, 36–44. <https://doi.org/10.7150/jca.5046>
- Mackay, L.K., Minnich, M., Kragten, N.A.M., Liao, Y., Nota, B., Seillet, C., Zaid, A., Man, K., Preston, S., Freestone, D., Braun, A., Wynne-Jones, E., Behr, F.M., Stark, R., Pellicci, D.G., Godfrey, D.I., Belz, G.T., Pellegrini, M., Gebhardt, T., Busslinger, M., Shi, W., Carbone, F.R., Lier, R.A.W. van, Kallies, A., Gisbergen, K.P.J.M. van, 2016. Hobit and Blimp1 instruct a universal transcriptional program of tissue residency in lymphocytes. *Science* 352, 459–463. <https://doi.org/10.1126/science.aad2035>

- Mackay, L.K., Rahimpour, A., Ma, J.Z., Collins, N., Stock, A.T., Hafon, M.-L., Vega-Ramos, J., Lauzurica, P., Mueller, S.N., Stefanovic, T., Tschärke, D.C., Heath, W.R., Inouye, M., Carbone, F.R., Gebhardt, T., 2013. The developmental pathway for CD103⁺CD8⁺ tissue-resident memory T cells of skin. *Nat. Immunol.* 14, 1294–1301. <https://doi.org/10.1038/ni.2744>
- Mackay, L.K., Stock, A.T., Ma, J.Z., Jones, C.M., Kent, S.J., Mueller, S.N., Heath, W.R., Carbone, F.R., Gebhardt, T., 2012. Long-lived epithelial immunity by tissue-resident memory T (TRM) cells in the absence of persisting local antigen presentation. *Proc. Natl. Acad. Sci.* 109, 7037–7042. <https://doi.org/10.1073/pnas.1202288109>
- Mackay, L.K., Wynne-Jones, E., Freestone, D., Pellicci, D.G., Mielke, L.A., Newman, D.M., Braun, A., Masson, F., Kallies, A., Belz, G.T., Carbone, F.R., 2015. T-box Transcription Factors Combine with the Cytokines TGF- β and IL-15 to Control Tissue-Resident Memory T Cell Fate. *Immunity* 43, 1101–1111. <https://doi.org/10.1016/j.immuni.2015.11.008>
- Mackie, R.M., Bray, C.A., Hole, D.J., Morris, A., Nicolson, M., Evans, A., Doherty, V., Vestey, J., 2002. Incidence of and survival from malignant melanoma in Scotland: an epidemiological study. *The Lancet* 360, 587–591. [https://doi.org/10.1016/S0140-6736\(02\)09779-9](https://doi.org/10.1016/S0140-6736(02)09779-9)
- Maher, J., Brentjens, R.J., Gunset, G., Rivière, I., Sadelain, M., 2002. Human T-lymphocyte cytotoxicity and proliferation directed by a single chimeric TCR ζ /CD28 receptor. *Nat. Biotechnol.* 20, 70. <https://doi.org/10.1038/nbt0102-70>
- Mahvi, D.A., Meyers, J.V., Tatar, A.J., Contreras, A., Suresh, M., Levenson, G.E., Sen, S., Cho, C.S., 2015. CTLA-4 blockade plus adoptive T cell transfer promotes optimal melanoma immunity in mice. *J. Immunother. Hagerstown Md* 1997 38, 54–61. <https://doi.org/10.1097/CJI.0000000000000064>
- Malik, B.T., Byrne, K.T., Vella, J.L., Zhang, P., Shabaneh, T.B., Steinberg, S.M., Molodtsov, A.K., Bowers, J.S., Angeles, C.V., Paulos, C.M., Huang, Y.H., Turk, M.J., 2017. Resident memory T cells in the skin mediate durable immunity to melanoma. *Sci. Immunol.* 2, eaam6346. <https://doi.org/10.1126/sciimmunol.aam6346>
- Mami-Chouaib, F., Blanc, C., Cognac, S., Hans, S., Malenica, I., Granier, C., Tihy, I., Tartour, E., 2018. Resident memory T cells, critical components in tumor immunology. *J. Immunother. Cancer* 6, 87. <https://doi.org/10.1186/s40425-018-0399-6>
- Mandic, R., Lieder, A., Sadowski, M., Peldszus, R., Werner, J.A., 2004. Comparison of Surface HLA Class I Levels in Squamous Cell Carcinoma Cell Lines of the Head and Neck. *Anticancer Res.* 24, 973–980.
- Marincola, F.M., Jaffee, E.M., Hicklin, D.J., Ferrone, S., 2000. Escape of human solid tumors from T-cell recognition: molecular mechanisms and functional significance. *Adv. Immunol.* 74, 181–273.
- Marrett, L.D., Nguyen, H.L., Armstrong, B.K., 2001. Trends in the incidence of cutaneous malignant melanoma in New South Wales, 1983–1996. *Int. J. Cancer* 92, 457–462. <https://doi.org/10.1002/ijc.1203>
- Martins, G.A., Cimmino, L., Liao, J., Magnusdottir, E., Calame, K., 2008. Blimp-1 directly represses Il2 and the Il2 activator Fos, attenuating T cell

- proliferation and survival. *J. Exp. Med.* 205, 1959–1965. <https://doi.org/10.1084/jem.20080526>
- Masopust, D., Vezys, V., Marzo, A.L., Lefrançois, L., 2001. Preferential Localization of Effector Memory Cells in Nonlymphoid Tissue. *Science* 291, 2413–2417. <https://doi.org/10.1126/science.1058867>
- Masopust, D., Vezys, V., Usherwood, E.J., Cauley, L.S., Olson, S., Marzo, A.L., Ward, R.L., Woodland, D.L., Lefrançois, L., 2004. Activated Primary and Memory CD8 T Cells Migrate to Nonlymphoid Tissues Regardless of Site of Activation or Tissue of Origin. *J. Immunol.* 172, 4875–4882. <https://doi.org/10.4049/jimmunol.172.8.4875>
- Masopust, D., Vezys, V., Wherry, E.J., Barber, D.L., Ahmed, R., 2006. Cutting Edge: Gut Microenvironment Promotes Differentiation of a Unique Memory CD8 T Cell Population. *J. Immunol.* 176, 2079–2083. <https://doi.org/10.4049/jimmunol.176.4.2079>
- Massagué, J., 2008. TGF β in Cancer. *Cell* 134, 215–230. <https://doi.org/10.1016/j.cell.2008.07.001>
- Matsushita, H., Vesely, M.D., Koboldt, D.C., Rickert, C.G., Uppaluri, R., Magrini, V.J., Arthur, C.D., White, J.M., Chen, Y.-S., Shea, L.K., Hundal, J., Wendl, M.C., Demeter, R., Wylie, T., Allison, J.P., Smyth, M.J., Old, L.J., Mardis, E.R., Schreiber, R.D., 2012. Cancer exome analysis reveals a T-cell-dependent mechanism of cancer immunoediting. *Nature* 482, 400–404. <https://doi.org/10.1038/nature10755>
- Mazurier, F., Fontanellas, A., Salesse, S., Taine, L., Landriau, S., Moreau-Gaudry, F., Reiffers, J., Peault, B., Santo, J.P.D., Verneuil, H.D., 1999. A Novel Immunodeficient Mouse Model-RAG2 gamma Cytokine Receptor Chain Double Mutants-Requiring Exogenous Cytokine Administration for Human Hematopoietic Stem Cell Engraftment Common. *J. Interferon Cytokine Res.* 19, 533–541. <https://doi.org/10.1089/107999099313983>
- McGranahan, N., Furness, A.J.S., Rosenthal, R., Ramskov, S., Lyngaa, R., Saini, S.K., Jamal-Hanjani, M., Wilson, G.A., Birkbak, N.J., Hiley, C.T., Watkins, T.B.K., Shafi, S., Murugaesu, N., Mitter, R., Akarca, A.U., Linares, J., Marafioti, T., Henry, J.Y., Van Allen, E.M., Miao, D., Schilling, B., Schadendorf, D., Garraway, L.A., Makarov, V., Rizvi, N.A., Snyder, A., Hellmann, M.D., Merghoub, T., Wolchok, J.D., Shukla, S.A., Wu, C.J., Peggs, K.S., Chan, T.A., Hadrup, S.R., Quezada, S.A., Swanton, C., 2016. Clonal neoantigens elicit T cell immunoreactivity and sensitivity to immune checkpoint blockade. *Science* 351, 1463–1469. <https://doi.org/10.1126/science.aaf1490>
- Mehta, A., Kim, Y.J., Robert, L., Tsoi, J., Comin-Anduix, B., Berent-Maoz, B., Cochran, A.J., Economou, J.S., Tumei, P.C., Puig-Saus, C., Ribas, A., 2018. Immunotherapy Resistance by Inflammation-Induced Dedifferentiation. *Cancer Discov.* 8, 935–943. <https://doi.org/10.1158/2159-8290.CD-17-1178>
- Mehta, A.M., Jordanova, E.S., Corver, W.E., Wezel, T. van, Uh, H.-W., Kenter, G.G., Fleuren, G.J., 2009. Single nucleotide polymorphisms in antigen processing machinery component ERAP1 significantly associate with clinical outcome in cervical carcinoma. *Genes Chromosomes Cancer* 48, 410–418. <https://doi.org/10.1002/gcc.20648>

- Mehta, A.M., Jordanova, E.S., Kenter, G.G., Ferrone, S., Fleuren, G.-J., 2008. Association of antigen processing machinery and HLA class I defects with clinicopathological outcome in cervical carcinoma. *Cancer Immunol. Immunother.* 57, 197–206. <https://doi.org/10.1007/s00262-007-0362-8>
- Mehta, A.M., Jordanova, E.S., Wezel, T. van, Uh, H.-W., Corver, W.E., Kwappenberg, K.M.C., Verduijn, W., Kenter, G.G., Burg, S.H. van der, Fleuren, G.J., 2007. Genetic variation of antigen processing machinery components and association with cervical carcinoma. *Genes. Chromosomes Cancer* 46, 577–586. <https://doi.org/10.1002/gcc.20441>
- Meissner, M., Reichert, T.E., Kunkel, M., Gooding, W., Whiteside, T.L., Ferrone, S., Seliger, B., 2005. Defects in the Human Leukocyte Antigen Class I Antigen Processing Machinery in Head and Neck Squamous Cell Carcinoma: Association with Clinical Outcome. *Clin. Cancer Res.* 11, 2552–2560. <https://doi.org/10.1158/1078-0432.CCR-04-2146>
- Melamed, R.D., Aydin, I.T., Rajan, G.S., Phelps, R., Silvers, D.N., Emmett, K.J., Brunner, G., Rabadan, R., Celebi, J.T., 2017. Genomic Characterization of Dysplastic Nevi Unveils Implications for Diagnosis of Melanoma. *J. Invest. Dermatol.* 137, 905–909. <https://doi.org/10.1016/j.jid.2016.11.017>
- Meyer, C., Cagnon, L., Costa-Nunes, C.M., Baumgaertner, P., Montandon, N., Leyvraz, L., Michielin, O., Romano, E., Speiser, D.E., 2014. Frequencies of circulating MDSC correlate with clinical outcome of melanoma patients treated with ipilimumab. *Cancer Immunol. Immunother.* 63, 247–257. <https://doi.org/10.1007/s00262-013-1508-5>
- Michaloglou, C., Vredeveld, L.C.W., Soengas, M.S., Denoyelle, C., Kuilman, T., Horst, C.M.A.M. van der, Majoor, D.M., Shay, J.W., Mooi, W.J., Peeper, D.S., 2005. BRAF E600 -associated senescence-like cell cycle arrest of human naevi. *Nature* 436, 720. <https://doi.org/10.1038/nature03890>
- Milner, J.J., Toma, C., Yu, B., Zhang, K., Omilusik, K., Phan, A.T., Wang, D., Getzler, A.J., Nguyen, T., Crotty, S., Wang, W., Pipkin, M.E., Goldrath, A.W., 2017. Runx3 programs CD8⁺ T cell residency in non-lymphoid tissues and tumours. *Nature* 552, 253–257. <https://doi.org/10.1038/nature24993>
- Moan, J., Grigalavicius, M., Baturaite, Z., Dahlback, A., Juzeniene, A., 2015. The relationship between UV exposure and incidence of skin cancer. *Photodermatol. Photoimmunol. Photomed.* 31, 26–35. <https://doi.org/10.1111/phpp.12139>
- Mokrani, M., Klibi, J., Bluteau, D., Bismuth, G., Mami-Chouaib, F., 2014. Smad and NFAT Pathways Cooperate To Induce CD103 Expression in Human CD8 T Lymphocytes. *J. Immunol.* 192, 2471–2479. <https://doi.org/10.4049/jimmunol.1302192>
- Mombaerts, P., Iacomini, J., Johnson, R.S., Herrup, K., Tonegawa, S., Papaioannou, V.E., 1992. RAG-1-deficient mice have no mature B and T lymphocytes. *Cell* 68, 869–877. [https://doi.org/10.1016/0092-8674\(92\)90030-G](https://doi.org/10.1016/0092-8674(92)90030-G)
- Morales, A., Eiding, D., Bruce, A.W., 1976. Intracavitary Bacillus Calmette-Guerin in the treatment of superficial bladder tumors. *J. Urol.* 116, 180–183. [https://doi.org/10.1016/s0022-5347\(17\)58737-6](https://doi.org/10.1016/s0022-5347(17)58737-6)
- Morgan, R.A., Chinnasamy, N., Abate-Daga, D.D., Gros, A., Robbins, P.F.,

- Zheng, Z., Feldman, S.A., Yang, J.C., Sherry, R.M., Phan, G.Q., Hughes, M.S., Kammula, U.S., Miller, A.D., Hessman, C.J., Stewart, A.A., Restifo, N.P., Quezado, M.M., Alimchandani, M., Rosenberg, A.Z., Nath, A., Wang, T., Bielekova, B., Wuest, S.C., Nirmala, A., McMahon, F.J., Wilde, S., Mosetter, B., Schendel, D.J., Laurencot, C.M., Rosenberg, S.A., 2013. Cancer regression and neurologic toxicity following anti-MAGE-A3 TCR gene therapy. *J. Immunother. Hagerstown Md* 1997 36, 133–151. <https://doi.org/10.1097/CJI.0b013e3182829903>
- Morgan, R.A., Dudley, M.E., Wunderlich, J.R., Hughes, M.S., Yang, J.C., Sherry, R.M., Royal, R.E., Topalian, S.L., Kammula, U.S., Restifo, N.P., Zheng, Z., Nahvi, A., de Vries, C.R., Rogers-Freezer, L.J., Mavroukakis, S.A., Rosenberg, S.A., 2006. Cancer Regression in Patients After Transfer of Genetically Engineered Lymphocytes. *Science* 314, 126–129. <https://doi.org/10.1126/science.1129003>
- Mueller, S.N., Heath, W.R., McLain, J.D., Carbone, F.R., Jones, C.M., 2002. Characterization of two TCR transgenic mouse lines specific for herpes simplex virus. *Immunol. Cell Biol.* 80, 156–163. <https://doi.org/10.1046/j.1440-1711.2002.01071.x>
- Mueller, S.N., Mackay, L.K., 2016. Tissue-resident memory T cells: local specialists in immune defence. *Nat. Rev. Immunol.* 16, 79–89. <https://doi.org/10.1038/nri.2015.3>
- Müller, J., Krijgsman, O., Tsoi, J., Robert, L., Hugo, W., Song, C., Kong, X., Possik, P.A., Cornelissen-Steijger, P.D.M., Foppen, M.H.G., Kemper, K., Goding, C.R., McDermott, U., Blank, C., Haanen, J., Graeber, T.G., Ribas, A., Lo, R.S., Peeper, D.S., 2014. Low MITF/AXL ratio predicts early resistance to multiple targeted drugs in melanoma. *Nat. Commun.* 5, 5712. <https://doi.org/10.1038/ncomms6712>
- Murray, T., Fuertes Marraco, S.A., Baumgaertner, P., Bordry, N., Cagnon, L., Donda, A., Romero, P., Verdeil, G., Speiser, D.E., 2016. Very Late Antigen-1 Marks Functional Tumor-Resident CD8 T Cells and Correlates with Survival of Melanoma Patients. *Front. Immunol.* 7. <https://doi.org/10.3389/fimmu.2016.00573>
- Muul, L.M., Spiess, P.J., Director, E.P., Rosenberg, S.A., 1987. Identification of specific cytolytic immune responses against autologous tumor in humans bearing malignant melanoma. *J. Immunol.* 138, 989–995.
- Nasti, T.H., Timares, L., 2015. MC1R, Eumelanin and Pheomelanin: Their Role in Determining the Susceptibility to Skin Cancer. *Photochem. Photobiol.* 91, 188–200. <https://doi.org/10.1111/php.12335>
- Neefjes, J.J., Momburg, F., Hammerling, G.J., 1993. Selective and ATP-dependent translocation of peptides by the MHC-encoded transporter. *Science* 261, 769–771. <https://doi.org/10.1126/science.8342042>
- Nicholson, P., Yepiskoposyan, H., Metze, S., Zamudio Orozco, R., Kleinschmidt, N., Mühlemann, O., 2010. Nonsense-mediated mRNA decay in human cells: mechanistic insights, functions beyond quality control and the double-life of NMD factors. *Cell. Mol. Life Sci.* 67, 677–700. <https://doi.org/10.1007/s00018-009-0177-1>
- Nikolaou, V., Stratigos, A.J., 2014. Emerging trends in the epidemiology of melanoma. *Br. J. Dermatol.* 170, 11–19. <https://doi.org/10.1111/bjd.12492>

- Nizard, M., Roussel, H., Diniz, M.O., Karaki, S., Tran, T., Voron, T., Dransart, E., Sandoval, F., Riquet, M., Rance, B., Marcheteau, E., Fabre, E., Mandavit, M., Terme, M., Blanc, C., Escudie, J.-B., Gibault, L., Barthes, F.L.P., Granier, C., Ferreira, L.C.S., Badoual, C., Johannes, L., Tartour, E., 2017. Induction of resident memory T cells enhances the efficacy of cancer vaccine. *Nat. Commun.* 8, 15221. <https://doi.org/10.1038/ncomms15221>
- Nonaka, D., Chiriboga, L., Rubin, B., 2008. Sox10: A Pan-Schwannian and Melanocytic Marker. *Am. J. Surg. Pathol.* 32, 1291–1298. <https://doi.org/10.1097/PAS.0b013e3181658c14>
- Norbury, C.C., Basta, S., Donohue, K.B., Tschärke, D.C., Princiotta, M.F., Berglund, P., Gibbs, J., Bennink, J.R., Yewdell, J.W., 2004. CD8+ T cell cross-priming via transfer of proteasome substrates. *Science* 304, 1318–1321. <https://doi.org/10.1126/science.1096378>
- Nowicki, T.S., Berent-Maoz, B., Cheung-Lau, G., Huang, R.R., Wang, X., Tsoi, J., Kaplan-Lefko, P., Cabrera, P., Tran, J., Pang, J., Macabali, M., Garcilazo, I.P., Carretero, I.B., Kalbasi, A., Cochran, A.J., Grasso, C.S., Hu-Lieskovan, S., Chmielowski, B., Comin-Anduix, B., Singh, A., Ribas, A., 2018. A Pilot Trial of the Combination of Transgenic NY-ESO-1–reactive Adoptive Cellular Therapy with Dendritic Cell Vaccination with or without Ipilimumab. *Clin. Cancer Res.* <https://doi.org/10.1158/1078-0432.CCR-18-3496>
- O'Connell, M.P., Marchbank, K., Webster, M.R., Valiga, A.A., Kaur, A., Vultur, A., Li, L., Herlyn, M., Villanueva, J., Liu, Q., Yin, X., Widura, S., Nelson, J., Ruiz, N., Camilli, T.C., Indig, F.E., Flaherty, K.T., Wargo, J.A., Frederick, D.T., Cooper, Z.A., Nair, S., Amaravadi, R.K., Schuchter, L.M., Karakousis, G.C., Xu, W., Xu, X., Weeraratna, A.T., 2013. Hypoxia Induces Phenotypic Plasticity and Therapy Resistance in Melanoma via the Tyrosine Kinase Receptors ROR1 and ROR2. *Cancer Discov.* 3, 1378–1393. <https://doi.org/10.1158/2159-8290.CD-13-0005>
- O'Donnell, T.J., Rubinsteyn, A., Bonsack, M., Riemer, A.B., Laserson, U., Hammerbacher, J., 2018. MHCflurry: Open-Source Class I MHC Binding Affinity Prediction. *Cell Syst.* 7, 129-132.e4. <https://doi.org/10.1016/j.cels.2018.05.014>
- Ogino, T., Shigyo, H., Ishii, H., Katayama, A., Miyokawa, N., Harabuchi, Y., Ferrone, S., 2006. HLA Class I Antigen Down-regulation in Primary Laryngeal Squamous Cell Carcinoma Lesions as a Poor Prognostic Marker. *Cancer Res.* 66, 9281–9289. <https://doi.org/10.1158/0008-5472.CAN-06-0488>
- Olsen, C.M., Neale, R.E., Green, A.C., Webb, P.M., Study, the Qs., Study, the E., Whiteman, D.C., 2015. Independent Validation of Six Melanoma Risk Prediction Models. *J. Invest. Dermatol.* 135, 1377–1384. <https://doi.org/10.1038/jid.2014.533>
- Ortenberg, R., Sapir, Y., Raz, L., Hershkovitz, L., Arav, A.B., Sapoznik, S., Barshack, I., Avivi, C., Berkun, Y., Besser, M.J., Ben-Moshe, T., Schachter, J., Markel, G., 2012. Novel Immunotherapy for Malignant Melanoma with a Monoclonal Antibody That Blocks CEACAM1 Homophilic Interactions. *Mol. Cancer Ther.* 11, 1300–1310. <https://doi.org/10.1158/1535-7163.MCT-11-0526>

- Ortiz-Navarrete, V., Seelig, A., Gernold, M., Frentzel, S., Kloetzel, P.M., Hämmerling, G.J., 1991. Subunit of the “20S” proteasome (multicatalytic proteinase) encoded by the major histocompatibility complex. *Nature* 353, 662. <https://doi.org/10.1038/353662a0>
- Ott, P.A., Hu, Z., Keskin, D.B., Shukla, S.A., Sun, J., Bozym, D.J., Zhang, W., Luoma, A., Giobbie-Hurder, A., Peter, L., Chen, C., Olive, O., Carter, T.A., Li, S., Lieb, D.J., Eisenhaure, T., Gjini, E., Stevens, J., Lane, W.J., Javeri, I., Nellaiappan, K., Salazar, A.M., Daley, H., Seaman, M., Buchbinder, E.I., Yoon, C.H., Harden, M., Lennon, N., Gabriel, S., Rodig, S.J., Barouch, D.H., Aster, J.C., Getz, G., Wucherpfennig, K., Neuberg, D., Ritz, J., Lander, E.S., Fritsch, E.F., Hacohen, N., Wu, C.J., 2017. An immunogenic personal neoantigen vaccine for patients with melanoma. *Nature* 547, 217–221. <https://doi.org/10.1038/nature22991>
- Overwijk, W.W., Theoret, M.R., Finkelstein, S.E., Surman, D.R., de Jong, L.A., Vyth-Dreese, F.A., DelleMijn, T.A., Antony, P.A., Spiess, P.J., Palmer, D.C., Heimann, D.M., Klebanoff, C.A., Yu, Z., Hwang, L.N., Feigenbaum, L., Kruisbeek, A.M., Rosenberg, S.A., Restifo, N.P., 2003. Tumor Regression and Autoimmunity after Reversal of a Functionally Tolerant State of Self-reactive CD8+ T Cells. *J. Exp. Med.* 198, 569–580. <https://doi.org/10.1084/jem.20030590>
- Overwijk, W.W., Tsung, A., Irvine, K.R., Parkhurst, M.R., Goletz, T.J., Tsung, K., Carroll, M.W., Liu, C., Moss, B., Rosenberg, S.A., Restifo, N.P., 1998. gp100/pmel 17 Is a Murine Tumor Rejection Antigen: Induction of “Self”-reactive, Tumoricidal T Cells Using High-affinity, Altered Peptide Ligand. *J. Exp. Med.* 188, 277–286.
- Padovese, V., Franco, G., Valenzano, M., Pecoraro, L., Cammilli, M., Petrelli, A., 2018. Skin cancer risk assessment in dark skinned immigrants: the role of social determinants and ethnicity. *Ethn. Health* 23, 649–658. <https://doi.org/10.1080/13557858.2017.1294657>
- Pagano, M., Tam, S.W., Theodoras, A.M., Beer-Romero, P., Sal, G.D., Chau, V., Yew, P.R., Draetta, G.F., Rolfe, M., 1995. Role of the ubiquitin-proteasome pathway in regulating abundance of the cyclin-dependent kinase inhibitor p27. *Science* 269, 682–685. <https://doi.org/10.1126/science.7624798>
- Pagès, F., Berger, A., Camus, M., Sanchez-Cabo, F., Costes, A., Molitor, R., Mlecnik, B., Kirilovsky, A., Nilsson, M., Damotte, D., Meatchi, T., Bruneval, P., Cugnenc, P.-H., Trajanoski, Z., Fridman, W.-H., Galon, J., 2009. Effector Memory T Cells, Early Metastasis, and Survival in Colorectal Cancer [WWW Document]. <http://dx.doi.org/10.1056/NEJMoa051424>. <https://doi.org/10.1056/NEJMoa051424>
- Pallett, L.J., Davies, J., Colbeck, E.J., Robertson, F., Hansi, N., Easom, N.J.W., Burton, A.R., Stegmann, K.A., Schurich, A., Swadling, L., Gill, U.S., Male, V., Luong, T., Gander, A., Davidson, B.R., Kennedy, P.T.F., Maini, M.K., 2017. IL-2high tissue-resident T cells in the human liver: Sentinels for hepatotropic infection. *J. Exp. Med.* 214, 1567–1580. <https://doi.org/10.1084/jem.20162115>
- Palma, L., Lorenzo, N.D., Guidetti, B., 1978. Lymphocytic infiltrates in primary glioblastomas and recidivous gliomas: Incidence, fate, and relevance to prognosis in 228 operated cases. *J. Neurosurg.* 49, 854–861.

- <https://doi.org/10.3171/jns.1978.49.6.0854>
- Palmer, D.C., Chan, C.-C., Gattinoni, L., Wrzesinski, C., Paulos, C.M., Hinrichs, C.S., Powell, D.J., Klebanoff, C.A., Finkelstein, S.E., Fariss, R.N., Yu, Z., Nussenblatt, R.B., Rosenberg, S.A., Restifo, N.P., 2008. Effective tumor treatment targeting a melanoma/melanocyte-associated antigen triggers severe ocular autoimmunity. *Proc. Natl. Acad. Sci. U. S. A.* 105, 8061–8066. <https://doi.org/10.1073/pnas.0710929105>
- Pardoll, D.M., 2012. The blockade of immune checkpoints in cancer immunotherapy. *Nat. Rev. Cancer* 12, 252–264. <https://doi.org/10.1038/nrc3239>
- Park, S.L., Buzzai, A., Rautela, J., Hor, J.L., Hochheiser, K., Efferm, M., McBain, N., Wagner, T., Edwards, J., McConville, R., Wilmott, J.S., Scolyer, R.A., Tüting, T., Palendira, U., Gyorki, D., Mueller, S.N., Huntington, N.D., Bedoui, S., Hölzel, M., Mackay, L.K., Waithman, J., Gebhardt, T., 2019. Tissue-resident memory CD8 + T cells promote melanoma–immune equilibrium in skin. *Nature* 565, 366. <https://doi.org/10.1038/s41586-018-0812-9>
- Park, S.L., Zaid, A., Hor, J.L., Christo, S.N., Prier, J.E., Davies, B., Alexandre, Y.O., Gregory, J.L., Russell, T.A., Gebhardt, T., Carbone, F.R., Tschärke, D.C., Heath, W.R., Mueller, S.N., Mackay, L.K., 2018. Local proliferation maintains a stable pool of tissue-resident memory T cells after antiviral recall responses. *Nat. Immunol.* 19, 183. <https://doi.org/10.1038/s41590-017-0027-5>
- Parkhurst, M., Gros, A., Pasetto, A., Prickett, T., Crystal, J.S., Robbins, P., Rosenberg, S.A., 2017. Isolation of T-Cell Receptors Specifically Reactive with Mutated Tumor-Associated Antigens from Tumor-Infiltrating Lymphocytes Based on CD137 Expression. *Clin. Cancer Res.* 23, 2491–2505. <https://doi.org/10.1158/1078-0432.CCR-16-2680>
- Parkhurst, M.R., Yang, J.C., Langan, R.C., Dudley, M.E., Nathan, D.-A.N., Feldman, S.A., Davis, J.L., Morgan, R.A., Merino, M.J., Sherry, R.M., Hughes, M.S., Kammula, U.S., Phan, G.Q., Lim, R.M., Wank, S.A., Restifo, N.P., Robbins, P.F., Laurencot, C.M., Rosenberg, S.A., 2011. T Cells Targeting Carcinoembryonic Antigen Can Mediate Regression of Metastatic Colorectal Cancer but Induce Severe Transient Colitis. *Mol. Ther.* 19, 620–626. <https://doi.org/10.1038/mt.2010.272>
- Parsa, A.T., Waldron, J.S., Panner, A., Crane, C.A., Parney, I.F., Barry, J.J., Cachola, K.E., Murray, J.C., Tihan, T., Jensen, M.C., Mischel, P.S., Stokoe, D., Pieper, R.O., 2007. Loss of tumor suppressor PTEN function increases B7-H1 expression and immunoresistance in glioma. *Nat. Med.* 13, 84–88. <https://doi.org/10.1038/nm1517>
- Paulos, C.M., Wrzesinski, C., Kaiser, A., Hinrichs, C.S., Chieppa, M., Cassard, L., Palmer, D.C., Boni, A., Muranski, P., Yu, Z., Gattinoni, L., Antony, P.A., Rosenberg, S.A., Restifo, N.P., 2007. Microbial translocation augments the function of adoptively transferred self/tumor-specific CD8+ T cells via TLR4 signaling. *J. Clin. Invest.* 117, 2197–2204. <https://doi.org/10.1172/JCI32205>
- Pearce, E.L., Mullen, A.C., Martins, G.A., Krawczyk, C.M., Hutchins, A.S., Zediak, V.P., Banica, M., DiCioccio, C.B., Gross, D.A., Mao, C., Shen, H., Cereb,

- N., Yang, S.Y., Lindsten, T., Rossant, J., Hunter, C.A., Reiner, S.L., 2003. Control of Effector CD8+ T Cell Function by the Transcription Factor Eomesodermin. *Science* 302, 1041–1043. <https://doi.org/10.1126/science.1090148>
- Pearl, R., 1929. CANCER AND TUBERCULOSIS. *Am. J. Epidemiol.* 9, 97–159. <https://doi.org/10.1093/oxfordjournals.aje.a121646>
- Peng, W., Chen, J.Q., Liu, C., Malu, S., Creasy, C., Tetzlaff, M.T., Xu, C., McKenzie, J.A., Zhang, C., Liang, X., Williams, L.J., Deng, W., Chen, G., Mbofung, R., Lazar, A.J., Torres-Cabala, C.A., Cooper, Z.A., Chen, P.-L., Tieu, T.N., Spranger, S., Yu, X., Bernatchez, C., Forget, M.-A., Haymaker, C., Amaria, R., McQuade, J.L., Glitza, I.C., Cascone, T., Li, H.S., Kwong, L.N., Heffernan, T.P., Hu, J., Bassett, R.L., Bosenberg, M.W., Woodman, S.E., Overwijk, W.W., Lizée, G., Roszik, J., Gajewski, T.F., Wargo, J.A., Gershenwald, J.E., Radvanyi, L., Davies, M.A., Hwu, P., 2016. Loss of PTEN promotes resistance to T cell-mediated immunotherapy. *Cancer Discov.* 6, 202–216. <https://doi.org/10.1158/2159-8290.CD-15-0283>
- Pérez-Guijarro, E., Day, C.-P., Merlino, G., Zaidi, M.R., 2017. Genetically engineered mouse models of melanoma. *Cancer* 123, 2089–2103. <https://doi.org/10.1002/cncr.30684>
- Pilon-Thomas, S., Kuhn, L., Ellwanger, S., Janssen, W., Royster, E., Marzban, S., Kudchadkar, R., Zager, J., Gibney, G., Sondak, V.K., Weber, J., Mulé, J.J., Sarnaik, A.A., 2012. Brief Communication: Efficacy of Adoptive Cell Transfer of Tumor Infiltrating Lymphocytes after Lymphopenia Induction for Metastatic Melanoma. *J. Immunother. Hagerstown Md* 1997 35, 615–620. <https://doi.org/10.1097/CJI.0b013e31826e8f5f>
- Pipkin, M.E., Sacks, J.A., Cruz-Guilloty, F., Lichtenheld, M.G., Bevan, M.J., Rao, A., 2010. Interleukin-2 and Inflammation Induce Distinct Transcriptional Programs that Promote the Differentiation of Effector Cytolytic T Cells. *Immunity* 32, 79–90. <https://doi.org/10.1016/j.immuni.2009.11.012>
- Platanias, L.C., 2005. Mechanisms of type-I- and type-II-interferon-mediated signalling. *Nat. Rev. Immunol.* 5, 375. <https://doi.org/10.1038/nri1604>
- Posavad, C.M., Zhao, L., Dong, L., Jin, L., Stevens, C.E., Magaret, A.S., Johnston, C., Wald, A., Zhu, J., Corey, L., Koelle, D.M., 2017. Enrichment of herpes simplex virus type 2 (HSV-2) reactive mucosal T cells in the human female genital tract. *Mucosal Immunol.* 10, 1259–1269. <https://doi.org/10.1038/mi.2016.118>
- Powles, T., Eder, J.P., Fine, G.D., Braiteh, F.S., Loria, Y., Cruz, C., Bellmunt, J., Burris, H.A., Petrylak, D.P., Teng, S., Shen, X., Boyd, Z., Hegde, P.S., Chen, D.S., Vogelzang, N.J., 2014. MPDL3280A (anti-PD-L1) treatment leads to clinical activity in metastatic bladder cancer. *Nature* 515, 558–562. <https://doi.org/10.1038/nature13904>
- Prendergast, G.C., Mondal, A., Dey, S., Laury-Kleintop, L.D., Muller, A.J., 2018. Inflammatory Reprogramming with IDO1 Inhibitors: Turning Immunologically Unresponsive ‘Cold’ Tumors ‘Hot.’ *Trends Cancer* 4, 38–58. <https://doi.org/10.1016/j.trecan.2017.11.005>
- Purcell, A.W., Ramarathnam, S.H., Ternette, N., 2019. Mass spectrometry-based identification of MHC-bound peptides for immunopeptidomics. *Nat. Protoc.* 1. <https://doi.org/10.1038/s41596-019-0133-y>

- Quatromoni, J.G., Eruslanov, E., 2012. Tumor-associated macrophages: function, phenotype, and link to prognosis in human lung cancer. *Am. J. Transl. Res.* 4, 376–389.
- Radvanyi, L.G., Bernatchez, C., Zhang, M., Fox, P.S., Miller, P., Chacon, J., Wu, R., Lizee, G., Mahoney, S., Alvarado, G., Glass, M., Johnson, V.E., McMannis, J.D., Shpall, E., Prieto, V., Papadopoulos, N., Kim, K., Homsí, J., Bedikian, A., Hwu, W.-J., Patel, S., Ross, M.I., Lee, J.E., Gershenwald, J.E., Lucci, A., Royal, R., Cormier, J.N., Davies, M.A., Mansaray, R., Fulbright, O.J., Toth, C., Ramachandran, R., Wardell, S., Gonzalez, A., Hwu, P., 2012. Specific lymphocyte subsets predict response to adoptive cell therapy using expanded autologous tumor-infiltrating lymphocytes in metastatic melanoma patients. *Clin. Cancer Res. Off. J. Am. Assoc. Cancer Res.* 18, 6758–6770. <https://doi.org/10.1158/1078-0432.CCR-12-1177>
- Raimondi, S., Sera, F., Gandini, S., Iodice, S., Caini, S., Maisonneuve, P., Fagnoli, M.C., 2008. MC1R variants, melanoma and red hair color phenotype: A meta-analysis. *Int. J. Cancer* 122, 2753–2760. <https://doi.org/10.1002/ijc.23396>
- Rao, R.R., Li, Q., Odunsi, K., Shrikant, P.A., 2010. The mTOR Kinase Determines Effector versus Memory CD8+ T Cell Fate by Regulating the Expression of Transcription Factors T-bet and Eomesodermin. *Immunity* 32, 67–78. <https://doi.org/10.1016/j.immuni.2009.10.010>
- Rapoport, A.P., Stadtmauer, E.A., Binder-Scholl, G.K., Goloubeva, O., Vogl, D.T., Lacey, S.F., Badros, A.Z., Garfall, A., Weiss, B., Finklestein, J., Kulikovskaya, I., Sinha, S.K., Kronsberg, S., Gupta, M., Bond, S., Melchiori, L., Brewer, J.E., Bennett, A.D., Gerry, A.B., Pumphrey, N.J., Williams, D., Tayton- Martin, H.K., Ribeiro, L., Holdich, T., Yanovich, S., Hardy, N., Yared, J., Kerr, N., Philip, S., Westphal, S., Siegel, D.L., Levine, B.L., Jakobsen, B.K., Kalos, M., June, C.H., 2015. NY-ESO-1-specific TCR-engineered T cells mediate sustained antigen-specific antitumor effects in myeloma. *Nat. Med.* 21, 914–921. <https://doi.org/10.1038/nm.3910>
- Reeves, E., Colebatch-Bourn, A., Elliott, T., Edwards, C.J., James, E., 2014. Functionally distinct ERAP1 allotype combinations distinguish individuals with Ankylosing Spondylitis. *Proc. Natl. Acad. Sci. U. S. A.* 111, 17594–17599. <https://doi.org/10.1073/pnas.1408882111>
- Reinhardt, J., Landsberg, J., Schmid-Burgk, J.L., Ramis, B.B., Bald, T., Glodde, N., Lopez-Ramos, D., Young, A., Ngiow, S.F., Nettersheim, D., Schorle, H., Quast, T., Kolanus, W., Schadendorf, D., Long, G.V., Madore, J., Scolyer, R.A., Ribas, A., Smyth, M.J., Tumei, P.C., Tüting, T., Hölzel, M., 2017. MAPK Signaling and Inflammation Link Melanoma Phenotype Switching to Induction of CD73 during Immunotherapy. *Cancer Res.* 77, 4697–4709. <https://doi.org/10.1158/0008-5472.CAN-17-0395>
- Restifo, N.P., Marincola, F.M., Kawakami, Y., Taubenberger, J., Yannelli, J.R., Rosenberg, S.A., 1996. Loss of Functional Beta 2 -Microglobulin in Metastatic Melanomas From Five Patients Receiving Immunotherapy. *JNCI J. Natl. Cancer Inst.* 88, 100–108. <https://doi.org/10.1093/jnci/88.2.100>

- Ribas, A., 2015. Adaptive immune resistance: How cancer protects from immune attack. *Cancer Discov.* 5, 915–919. <https://doi.org/10.1158/2159-8290.CD-15-0563>
- Ribas, A., Dummer, R., Puzanov, I., VanderWalde, A., Andtbacka, R.H.I., Michielin, O., Olszanski, A.J., Malvehy, J., Cebon, J., Fernandez, E., Kirkwood, J.M., Gajewski, T.F., Chen, L., Gorski, K.S., Anderson, A.A., Diede, S.J., Lassman, M.E., Gansert, J., Hodi, F.S., Long, G.V., 2017. Oncolytic Virotherapy Promotes Intratumoral T Cell Infiltration and Improves Anti-PD-1 Immunotherapy. *Cell* 170, 1109-1119.e10. <https://doi.org/10.1016/j.cell.2017.08.027>
- Richter, M.V., Topham, D.J., 2007. The $\alpha 1\beta 1$ Integrin and TNF Receptor II Protect Airway CD8+ Effector T Cells from Apoptosis during Influenza Infection. *J. Immunol.* 179, 5054–5063. <https://doi.org/10.4049/jimmunol.179.8.5054>
- Riesenberg, S., Groetchen, A., Siddaway, R., Bald, T., Reinhardt, J., Smorra, D., Kohlmeyer, J., Renn, M., Phung, B., Aymans, P., Schmidt, T., Hornung, V., Davidson, I., Goding, C.R., Jönsson, G., Landsberg, J., Tüting, T., Hölzel, M., 2015. MITF and c-Jun antagonism interconnects melanoma dedifferentiation with pro-inflammatory cytokine responsiveness and myeloid cell recruitment. *Nat. Commun.* 6, 8755. <https://doi.org/10.1038/ncomms9755>
- Rigel, D.S., Carucci, J.A., 2000. Malignant melanoma: prevention, early detection, and treatment in the 21st century. *CA. Cancer J. Clin.* 50, 215–236; quiz 237–240.
- Rizvi, Naiyer A., Hellmann, M.D., Snyder, A., Kvistborg, P., Makarov, V., Havel, J.J., Lee, W., Yuan, J., Wong, P., Ho, T.S., Miller, M.L., Rekhtman, N., Moreira, A.L., Ibrahim, F., Bruggeman, C., Gasmı, B., Zappasodi, R., Maeda, Y., Sander, C., Garon, E.B., Merghoub, T., Wolchok, J.D., Schumacher, T.N., Chan, T.A., 2015a. Mutational landscape determines sensitivity to PD-1 blockade in non–small cell lung cancer. *Science* 348, 124–128. <https://doi.org/10.1126/science.aaa1348>
- Rizvi, Naiyer A., Hellmann, M.D., Snyder, A., Kvistborg, P., Makarov, V., Havel, J.J., Lee, W., Yuan, J., Wong, P., Ho, T.S., Miller, M.L., Rekhtman, N., Moreira, A.L., Ibrahim, F., Bruggeman, C., Gasmı, B., Zappasodi, R., Maeda, Y., Sander, C., Garon, E.B., Merghoub, T., Wolchok, J.D., Schumacher, T.N., Chan, T.A., 2015b. Cancer immunology. Mutational landscape determines sensitivity to PD-1 blockade in non-small cell lung cancer. *Science* 348, 124–128. <https://doi.org/10.1126/science.aaa1348>
- Rizvi, Naiyer A., Mazières, J., Planchard, D., Stinchcombe, T.E., Dy, G.K., Antonia, S.J., Horn, L., Lena, H., Minenza, E., Mennequier, B., Otterson, G.A., Campos, L.T., Gandara, D.R., Levy, B.P., Nair, S.G., Zalcman, G., Wolf, J., Souquet, P.-J., Baldini, E., Cappuzzo, F., Chouaid, C., Dowlati, A., Sanborn, R., Lopez-Chavez, A., Grohe, C., Huber, R.M., Harbison, C.T., Baudelet, C., Lestini, B.J., Ramalingam, S.S., 2015. Activity and safety of nivolumab, an anti-PD-1 immune checkpoint inhibitor, for patients with advanced, refractory squamous non-small-cell lung cancer (CheckMate 063): a phase 2, single-arm trial. *Lancet Oncol.* 16, 257–265. [https://doi.org/10.1016/S1470-2045\(15\)70054-9](https://doi.org/10.1016/S1470-2045(15)70054-9)

- Robbins, P.F., Kassim, S.H., Tran, T.L.N., Crystal, J.S., Morgan, R.A., Feldman, S.A., Yang, J.C., Dudley, M.E., Wunderlich, J.R., Sherry, R.M., Kammula, U.S., Hughes, M.S., Restifo, N.P., Raffeld, M., Lee, C.-C.R., Li, Y.F., El-Gamil, M., Rosenberg, S.A., 2015. A Pilot Trial Using Lymphocytes Genetically Engineered with an NY-ESO-1–Reactive T-cell Receptor: Long-term Follow-up and Correlates with Response. *Clin. Cancer Res.* 21, 1019–1027. <https://doi.org/10.1158/1078-0432.CCR-14-2708>
- Robbins, P.F., Lu, Y.-C., El-Gamil, M., Li, Y.F., Gross, C., Gartner, J., Lin, J.C., Teer, J.K., Cliften, P., Tycksen, E., Samuels, Y., Rosenberg, S.A., 2013. Mining Exomic Sequencing Data to Identify Mutated Antigens Recognized by Adoptively Transferred Tumor-reactive T cells. *Nat. Med.* 19, 747–752. <https://doi.org/10.1038/nm.3161>
- Robinson, M.D., McCarthy, D.J., Smyth, G.K., 2010. edgeR: a Bioconductor package for differential expression analysis of digital gene expression data. *Bioinformatics* 26, 139–140. <https://doi.org/10.1093/bioinformatics/btp616>
- Rock, K.L., Gramm, C., Rothstein, L., Clark, K., Stein, R., Dick, L., Hwang, D., Goldberg, A.L., 1994. Inhibitors of the proteasome block the degradation of most cell proteins and the generation of peptides presented on MHC class I molecules. *Cell* 78, 761–771. [https://doi.org/10.1016/S0092-8674\(94\)90462-6](https://doi.org/10.1016/S0092-8674(94)90462-6)
- Rodić, N., Anders, R.A., Eshleman, J.R., Lin, M.-T., Xu, H., Kim, J.H., Beierl, K., Chen, S., Lubber, B.S., Wang, H., Topalian, S.L., Pardoll, D.M., Taube, J.M., 2015. PD-L1 Expression in Melanocytic Lesions Does Not Correlate with the BRAF V600E Mutation. *Cancer Immunol. Res.* 3, 110–115. <https://doi.org/10.1158/2326-6066.CIR-14-0145>
- Rodig, S.J., Gusenleitner, D., Jackson, D.G., Gjini, E., Giobbie-Hurder, A., Jin, C., Chang, H., Lovitch, S.B., Horak, C., Weber, J.S., Weirather, J.L., Wolchok, J.D., Postow, M.A., Pavlick, A.C., Chesney, J., Hodi, F.S., 2018. MHC proteins confer differential sensitivity to CTLA-4 and PD-1 blockade in untreated metastatic melanoma. *Sci. Transl. Med.* 10, eaar3342. <https://doi.org/10.1126/scitranslmed.aar3342>
- Rolland, P., Deen, S., Scott, I., Durrant, L., Spendlove, I., 2007. Human Leukocyte Antigen Class I Antigen Expression Is an Independent Prognostic Factor in Ovarian Cancer. *Clin. Cancer Res.* 13, 3591–3596. <https://doi.org/10.1158/1078-0432.CCR-06-2087>
- Rosato, P.C., Beura, L.K., Masopust, D., 2017. Tissue resident memory T cells and viral immunity. *Curr. Opin. Virol., Emerging viruses: intraspecies transmission • Viral immunology* 22, 44–50. <https://doi.org/10.1016/j.coviro.2016.11.011>
- Rosenberg, S.A., Lotze, M.T., Muul, L.M., Leitman, S., Chang, A.E., Ettinghausen, S.E., Matory, Y.L., Skibber, J.M., Shiloni, E., Vetto, J.T., Seipp, C.A., Simpson, C., Reichert, C.M., 1985. Observations on the Systemic Administration of Autologous Lymphokine-Activated Killer Cells and Recombinant Interleukin-2 to Patients with Metastatic Cancer. *N. Engl. J. Med.* 313, 1485–1492. <https://doi.org/10.1056/NEJM198512053132327>
- Rosenberg, S.A., Packard, B.S., Aebbersold, P.M., Solomon, D., Topalian, S.L.,

- Toy, S.T., Simon, P., Lotze, M.T., Yang, J.C., Seipp, C.A., Simpson, C., Carter, C., Bock, S., Schwartzentruber, D., Wei, J.P., White, D.E., 1988. Use of Tumor-Infiltrating Lymphocytes and Interleukin-2 in the Immunotherapy of Patients with Metastatic Melanoma. *N. Engl. J. Med.* 319, 1676–1680. <https://doi.org/10.1056/NEJM198812223192527>
- Rosenberg, S.A., Restifo, N.P., 2015. Adoptive cell transfer as personalized immunotherapy for human cancer. *Science* 348, 62–68. <https://doi.org/10.1126/science.aaa4967>
- Rosenberg, S.A., Spiess, P., Lafreniere, R., 1986. A new approach to the adoptive immunotherapy of cancer with tumor-infiltrating lymphocytes. *Science* 233, 1318–1321. <https://doi.org/10.1126/science.3489291>
- Rosenberg, S.A., Yang, J.C., Restifo, N.P., 2004. Cancer immunotherapy: moving beyond current vaccines. *Nat. Med.* 10, 909–915. <https://doi.org/10.1038/nm1100>
- Rosenberg, S.A., Yang, J.C., Sherry, R.M., Kammula, U.S., Hughes, M.S., Phan, G.Q., Citrin, D.E., Restifo, N.P., Robbins, P.F., Wunderlich, J.R., Morton, K.E., Laurencot, C.M., Steinberg, S.M., White, D.E., Dudley, M.E., 2011. Durable Complete Responses in Heavily Pretreated Patients with Metastatic Melanoma Using T Cell Transfer Immunotherapy. *Clin. Cancer Res. Off. J. Am. Assoc. Cancer Res.* 17, 4550–4557. <https://doi.org/10.1158/1078-0432.CCR-11-0116>
- Rutishauser, R.L., Martins, G.A., Kalachikov, S., Chandele, A., Parish, I.A., Meffre, E., Jacob, J., Calame, K., Kaech, S.M., 2009. Transcriptional Repressor Blimp-1 Promotes CD8+ T Cell Terminal Differentiation and Represses the Acquisition of Central Memory T Cell Properties. *Immunity* 31, 296–308. <https://doi.org/10.1016/j.immuni.2009.05.014>
- Ruzankina, Y., Pinzon-Guzman, C., Asare, A., Ong, T., Pontano, L., Cotsarelis, G., Zediak, V.P., Velez, M., Bhandoola, A., Brown, E.J., 2007. Deletion of the Developmentally Essential Gene ATR in Adult Mice Leads to Age-Related Phenotypes and Stem Cell Loss. *Cell Stem Cell* 1, 113–126. <https://doi.org/10.1016/j.stem.2007.03.002>
- Sahin, U., Derhovanessian, E., Miller, M., Kloke, B.-P., Simon, P., Löwer, M., Bukur, V., Tadmor, A.D., Luxemburger, U., Schrörs, B., Omokoko, T., Vormehr, M., Albrecht, C., Paruzynski, A., Kuhn, A.N., Buck, J., Heesch, S., Schreeb, K.H., Müller, F., Ortseifer, I., Vogler, I., Godehardt, E., Attig, S., Rae, R., Breikreuz, A., Tolliver, C., Suchan, M., Martic, G., Hohberger, A., Sorn, P., Diekmann, J., Ciesla, J., Waksman, O., Brück, A.-K., Witt, M., Zillgen, M., Rothermel, A., Kasemann, B., Langer, D., Bolte, S., Diken, M., Kreiter, S., Nemecek, R., Gebhardt, C., Grabbe, S., Höller, C., Utikal, J., Huber, C., Loquai, C., Türeci, Ö., 2017. Personalized RNA mutanome vaccines mobilize poly-specific therapeutic immunity against cancer. *Nature* 547, 222–226. <https://doi.org/10.1038/nature23003>
- Sallusto, F., Geginat, J., Lanzavecchia, A., 2004. Central Memory and Effector Memory T Cell Subsets: Function, Generation, and Maintenance. *Annu. Rev. Immunol.* 22, 745–763. <https://doi.org/10.1146/annurev.immunol.22.012703.104702>
- Sallusto, F., Lenig, D., Förster, R., Lipp, M., Lanzavecchia, A., 1999. Two subsets of memory T lymphocytes with distinct homing potentials and effector

- functions. *Nature* 401, 708. <https://doi.org/10.1038/44385>
- Saric, T., Chang, S.-C., Hattori, A., York, I.A., Markant, S., Rock, K.L., Tsujimoto, M., Goldberg, A.L., 2002. An IFN- γ -induced aminopeptidase in the ER, ERAP1, trims precursors to MHC class I-presented peptides. *Nat. Immunol.* 3, 1169. <https://doi.org/10.1038/ni859>
- Sathaliyawala, T., Kubota, M., Yudanin, N., Turner, D., Camp, P., Thome, J.J.C., Bickham, K.L., Lerner, H., Goldstein, M., Sykes, M., Kato, T., Farber, D.L., 2013. Distribution and Compartmentalization of Human Circulating and Tissue-Resident Memory T Cell Subsets. *Immunity* 38, 187–197. <https://doi.org/10.1016/j.immuni.2012.09.020>
- Schachter, J., Ribas, A., Long, G.V., Arance, A., Grob, J.-J., Mortier, L., Daud, A., Carlino, M.S., McNeil, C., Lotem, M., Larkin, J., Lorigan, P., Neyns, B., Blank, C., Petrella, T.M., Hamid, O., Zhou, H., Ebbinghaus, S., Ibrahim, N., Robert, C., 2017. Pembrolizumab versus ipilimumab for advanced melanoma: final overall survival results of a multicentre, randomised, open-label phase 3 study (KEYNOTE-006). *The Lancet* 390, 1853–1862. [https://doi.org/10.1016/S0140-6736\(17\)31601-X](https://doi.org/10.1016/S0140-6736(17)31601-X)
- Schenkel, J.M., Fraser, K.A., Beura, L.K., Pauken, K.E., Vezys, V., Masopust, D., 2014. Resident memory CD8 T cells trigger protective innate and adaptive immune responses. *Science* 346, 98–101. <https://doi.org/10.1126/science.1254536>
- Schenkel, J.M., Fraser, K.A., Vezys, V., Masopust, D., 2013. Sensing and alarm function of resident memory CD8⁺ T cells. *Nat. Immunol.* 14, 509–513. <https://doi.org/10.1038/ni.2568>
- Schenkel, J.M., Masopust, D., 2014. Tissue-Resident Memory T Cells. *Immunity* 41, 886–897. <https://doi.org/10.1016/j.immuni.2014.12.007>
- Schluns, K.S., Kieper, W.C., Jameson, S.C., Lefrançois, L., 2000. Interleukin-7 mediates the homeostasis of naïve and memory CD8 T cells in vivo. *Nat. Immunol.* 1, 426. <https://doi.org/10.1038/80868>
- Schmid-Burgk, J.L., Höning, K., Ebert, T.S., Hornung, V., 2016. CRISPaint allows modular base-specific gene tagging using a ligase-4-dependent mechanism. *Nat. Commun.* 7, 12338. <https://doi.org/10.1038/ncomms12338>
- Schmid-Burgk, J.L., Schmidt, T., Gaidt, M.M., Pelka, K., Latz, E., Ebert, T.S., Hornung, V., 2014. OutKnocker: a web tool for rapid and simple genotyping of designer nuclease edited cell lines. *Genome Res.* 24, 1719–1723. <https://doi.org/10.1101/gr.176701.114>
- Schön, M.P., Arya, A., Murphy, E.A., Adams, C.M., Strauch, U.G., Agace, W.W., Marsal, J., Donohue, J.P., Her, H., Beier, D.R., Olson, S., Lefrançois, L., Brenner, M.B., Grusby, M.J., Parker, C.M., 1999. Mucosal T Lymphocyte Numbers Are Selectively Reduced in Integrin α E (CD103)-Deficient Mice. *J. Immunol.* 162, 6641–6649.
- Schumacher, T., Bunse, L., Pusch, S., Sahm, F., Wiestler, B., Quandt, J., Menn, O., Osswald, M., Oezen, I., Ott, M., Keil, M., Balß, J., Rauschenbach, K., Grabowska, A.K., Vogler, I., Diekmann, J., Trautwein, N., Eichmüller, S.B., Okun, J., Stevanović, S., Riemer, A.B., Sahin, U., Friese, M.A., Beckhove, P., von Deimling, A., Wick, W., Platten, M., 2014. A vaccine targeting mutant IDH1 induces antitumour immunity. *Nature* 512, 324–327.

- <https://doi.org/10.1038/nature13387>
- Schumacher, T.N., Schreiber, R.D., 2015. Neoantigens in cancer immunotherapy. *Science* 348, 69–74. <https://doi.org/10.1126/science.aaa4971>
- Schwarz, K., Giuli, R. de, Schmidtke, G., Kostka, S., Broek, M. van den, Kim, K.B., Crews, C.M., Kraft, R., Groettrup, M., 2000. The Selective Proteasome Inhibitors Lactacystin and Epoxomicin Can Be Used to Either Up- or Down-Regulate Antigen Presentation at Nontoxic Doses. *J. Immunol.* 164, 6147–6157. <https://doi.org/10.4049/jimmunol.164.12.6147>
- Seebode, C., Lehmann, J., Emmert, S., 2016. Photocarcinogenesis and Skin Cancer Prevention Strategies. *Anticancer Res.* 36, 1371–1378.
- Seliger, B., Höhne, A., Jung, D., Kallfelz, M., Knuth, A., Jaeger, E., Bernhard, H., Momburg, F., Tampé, R., Huber, C., 1997. Expression and function of the peptide transporters in escape variants of human renal cell carcinomas. *Exp. Hematol.* 25, 608–614.
- Seliger, Barbara, Ritz, U., Abele, R., Bock, M., Tampé, R., Sutter, G., Drexler, I., Huber, C., Ferrone, S., 2001. Immune Escape of Melanoma: First Evidence of Structural Alterations in Two Distinct Components of the MHC Class I Antigen Processing Pathway. *Cancer Res.* 61, 8647–8650.
- Seliger, B., Schreiber, K., Delp, K., Meissner, M., Hammers, S., Reichert, T., Pawlischko, K., Tampé, R., Huber, C., 2001. Downregulation of the constitutive tapasin expression in human tumor cells of distinct origin and its transcriptional upregulation by cytokines. *Tissue Antigens* 57, 39–45. <https://doi.org/10.1034/j.1399-0039.2001.057001039.x>
- Seliger, B., Stoehr, R., Handke, D., Mueller, A., Ferrone, S., Wullich, B., Tannapfel, A., Hofstaedter, F., Hartmann, A., 2010. Association of HLA class I antigen abnormalities with disease progression and early recurrence in prostate cancer. *Cancer Immunol. Immunother.* CII 59, 529–540. <https://doi.org/10.1007/s00262-009-0769-5>
- Shah, P., He, Y.-Y., 2015. Molecular Regulation of UV-Induced DNA Repair. *Photochem. Photobiol.* 91, 254–264. <https://doi.org/10.1111/php.12406>
- Shaner, N.C., Lambert, G.G., Chammass, A., Ni, Y., Cranfill, P.J., Baird, M.A., Sell, B.R., Allen, J.R., Day, R.N., Israelsson, M., Davidson, M.W., Wang, J., 2013. A bright monomeric green fluorescent protein derived from *Branchiostoma lanceolatum*. *Nat. Methods* 10, 407–409. <https://doi.org/10.1038/nmeth.2413>
- Shankaran, V., Ikeda, H., Bruce, A.T., White, J.M., Swanson, P.E., Old, L.J., Schreiber, R.D., 2001. IFN γ and lymphocytes prevent primary tumour development and shape tumour immunogenicity. *Nature* 410, 1107–1111. <https://doi.org/10.1038/35074122>
- Sharma, N., Benechet, A.P., Lefrançois, L., Khanna, K.M., 2015. CD8 T Cells Enter the Splenic T Cell Zones Independently of CCR7, but the Subsequent Expansion and Trafficking Patterns of Effector T Cells after Infection Are Dysregulated in the Absence of CCR7 Migratory Cues. *J. Immunol.* 195, 5227–5236. <https://doi.org/10.4049/jimmunol.1500993>
- Sheridan, B.S., Lefrançois, L., 2011. Regional and mucosal memory T cells. *Nat. Immunol.* 12, 485–491.
- Shin, D.S., Zaretsky, J.M., Escuin-Ordinas, H., Garcia-Diaz, A., Hu-Lieskovan,

- S., Kalbasi, A., Grasso, C.S., Hugo, W., Sandoval, S., Torrejon, D.Y., Palaskas, N., Rodriguez, G.A., Parisi, G., Azhdam, A., Chmielowski, B., Cherry, G., Seja, E., Berent-Maoz, B., Shintaku, I.P., Le, D.T., Pardoll, D.M., Diaz, L.A., Tumei, P.C., Graeber, T.G., Lo, R.S., Comin-Anduix, B., Ribas, A., 2017. Primary resistance to PD-1 blockade mediated by JAK1/2 mutations. *Cancer Discov.* 7, 188–201. <https://doi.org/10.1158/2159-8290.CD-16-1223>
- Shin, H., Iwasaki, A., 2012. A vaccine strategy that protects against genital herpes by establishing local memory T cells. *Nature* 491, 463–467. <https://doi.org/10.1038/nature11522>
- Skon, C.N., Lee, J.-Y., Anderson, K.G., Masopust, D., Hogquist, K.A., Jameson, S.C., 2013. Transcriptional downregulation of *S1pr1* is required for the establishment of resident memory CD8⁺ T cells. *Nat. Immunol.* 14, 1285–1293. <https://doi.org/10.1038/ni.2745>
- Smith, C.J., Caldeira-Dantas, S., Turula, H., Snyder, C.M., 2015. Murine CMV Infection Induces the Continuous Production of Mucosal Resident T Cells. *Cell Rep.* 13, 1137–1148. <https://doi.org/10.1016/j.celrep.2015.09.076>
- Smyth, M.J., Crowe, N.Y., Godfrey, D.I., 2001. NK cells and NKT cells collaborate in host protection from methylcholanthrene-induced fibrosarcoma. *Int. Immunol.* 13, 459–463. <https://doi.org/10.1093/intimm/13.4.459>
- Smyth, M.J., Thia, K.Y.T., Street, S.E.A., MacGregor, D., Godfrey, D.I., Trapani, J.A., 2000. Perforin-Mediated Cytotoxicity Is Critical for Surveillance of Spontaneous Lymphoma. *J. Exp. Med.* 192, 755–760.
- Sneyd, M.J., Cox, B., 2013. A comparison of trends in melanoma mortality in New Zealand and Australia: the two countries with the highest melanoma incidence and mortality in the world. *BMC Cancer* 13, 372. <https://doi.org/10.1186/1471-2407-13-372>
- Snyder, A., Makarov, V., Merghoub, T., Yuan, J., Zaretsky, J.M., Desrichard, A., Walsh, L.A., Postow, M.A., Wong, P., Ho, T.S., Hollmann, T.J., Bruggeman, C., Kannan, K., Li, Y., Elipenahli, C., Liu, C., Harbison, C.T., Wang, L., Ribas, A., Wolchok, J.D., Chan, T.A., 2014a. Genetic Basis for Clinical Response to CTLA-4 Blockade in Melanoma. *N. Engl. J. Med.* 371, 2189–2199. <https://doi.org/10.1056/NEJMoa1406498>
- Snyder, A., Makarov, V., Merghoub, T., Yuan, J., Zaretsky, J.M., Desrichard, A., Walsh, L.A., Postow, M.A., Wong, P., Ho, T.S., Hollmann, T.J., Bruggeman, C., Kannan, K., Li, Y., Elipenahli, C., Liu, C., Harbison, C.T., Wang, L., Ribas, A., Wolchok, J.D., Chan, T.A., 2014b. Genetic Basis for Clinical Response to CTLA-4 Blockade in Melanoma. *N. Engl. J. Med.* 371, 2189–2199. <https://doi.org/10.1056/NEJMoa1406498>
- Solito, S., Falisi, E., Diaz-Montero, C.M., Doni, A., Pinton, L., Rosato, A., Francescato, S., Basso, G., Zanovello, P., Onicescu, G., Garrett-Mayer, E., Montero, A.J., Bronte, V., Mandruzzato, S., 2011. A human promyelocytic-like population is responsible for the immune suppression mediated by myeloid-derived suppressor cells. *Blood* 118, 2254–2265. <https://doi.org/10.1182/blood-2010-12-325753>
- Song, D.-G., Ye, Q., Carpenito, C., Poussin, M., Wang, L.-P., Ji, C., Figini, M., June, C.H., Coukos, G., Powell, D.J., 2011. In vivo persistence, tumor localization and anti-tumor activity of CAR engineered T cells is enhanced

- by costimulatory signaling through CD137 (4-1BB). *Cancer Res.* 71, 4617–4627. <https://doi.org/10.1158/0008-5472.CAN-11-0422>
- Soufir, N., Avril, M.-F., Chompret, A., Demenais, F., Bombléd, J., Spatz, A., Stoppa-Lyonnet, D., Bénard, J., Bressac-de Paillerets, B., 1998. Prevalence of p16 and CDK4 Germline Mutations in 48 Melanoma-Prone Families in France. *Hum. Mol. Genet.* 7, 209–216. <https://doi.org/10.1093/hmg/7.2.209>
- Spranger, S., Bao, R., Gajewski, T.F., 2015. Melanoma-intrinsic β -catenin signalling prevents anti-tumour immunity. *Nature* 523, 231–235. <https://doi.org/10.1038/nature14404>
- Spranger, S., Dai, D., Horton, B., Gajewski, T.F., 2017. Tumor-Residing Batf3 Dendritic Cells Are Required for Effector T Cell Trafficking and Adoptive T Cell Therapy. *Cancer Cell* 31, 711–723.e4. <https://doi.org/10.1016/j.ccell.2017.04.003>
- Stagg, J., Divisekera, U., McLaughlin, N., Sharkey, J., Pommey, S., Denoyer, D., Dwyer, K.M., Smyth, M.J., 2010. Anti-CD73 antibody therapy inhibits breast tumor growth and metastasis. *Proc. Natl. Acad. Sci. U. S. A.* 107, 1547–1552. <https://doi.org/10.1073/pnas.0908801107>
- Stang, A., Pukkala, E., Sankila, R., Söderman, B., Hakulinen, T., 2006. Time trend analysis of the skin melanoma incidence of Finland from 1953 through 2003 including 16,414 cases. *Int. J. Cancer* 119, 380–384. <https://doi.org/10.1002/ijc.21836>
- Stierner, U., Augustsson, A., Rosdahl, I., Suurküla, M., 1992. Regional distribution of common and dysplastic naevi in relation to melanoma site and sun exposure. A case-control study. *Melanoma Res.* 1, 367–375.
- Stranzl, T., Larsen, M.V., Lundegaard, C., Nielsen, M., 2010. NetCTLpan: pan-specific MHC class I pathway epitope predictions. *Immunogenetics* 62, 357–368. <https://doi.org/10.1007/s00251-010-0441-4>
- Strub, T., Giuliano, S., Ye, T., Bonet, C., Keime, C., Kobi, D., Le Gras, S., Cormont, M., Ballotti, R., Bertolotto, C., Davidson, I., 2011. Essential role of microphthalmia transcription factor for DNA replication, mitosis and genomic stability in melanoma. *Oncogene* 30, 2319–2332. <https://doi.org/10.1038/onc.2010.612>
- Subramanian, A., Tamayo, P., Mootha, V.K., Mukherjee, S., Ebert, B.L., Gillette, M.A., Paulovich, A., Pomeroy, S.L., Golub, T.R., Lander, E.S., Mesirov, J.P., 2005. Gene set enrichment analysis: A knowledge-based approach for interpreting genome-wide expression profiles. *Proc. Natl. Acad. Sci. U. S. A.* 102, 15545–15550. <https://doi.org/10.1073/pnas.0506580102>
- Sucker, A., Zhao, F., Real, B., Heeke, C., Bielefeld, N., Maßen, S., Horn, S., Moll, I., Maltaner, R., Horn, P.A., Schilling, B., Sabbatino, F., Lennerz, V., Kloor, M., Ferrone, S., Schadendorf, D., Falk, C.S., Griewank, K., Paschen, A., 2014. Genetic Evolution of T-cell Resistance in the Course of Melanoma Progression. *Clin. Cancer Res.* 20, 6593–6604. <https://doi.org/10.1158/1078-0432.CCR-14-0567>
- Szymczak, A.L., Vignali, D.A.A., 2005. Development of 2A peptide-based strategies in the design of multicistronic vectors. *Expert Opin. Biol. Ther.* 5, 627–638. <https://doi.org/10.1517/14712598.5.5.627>
- Takamura, S., Yagi, H., Hakata, Y., Motozono, C., McMaster, S.R., Masumoto,

- T., Fujisawa, M., Chikaishi, T., Komeda, J., Itoh, J., Umemura, M., Kyusai, A., Tomura, M., Nakayama, T., Woodland, D.L., Kohlmeier, J.E., Miyazawa, M., 2016. Specific niches for lung-resident memory CD8+ T cells at the site of tissue regeneration enable CD69-independent maintenance. *J. Exp. Med.* 213, 3057–3073. <https://doi.org/10.1084/jem.20160938>
- Tan, J.T., Ernst, B., Kieper, W.C., LeRoy, E., Sprent, J., Surh, C.D., 2002. Interleukin (IL)-15 and IL-7 Jointly Regulate Homeostatic Proliferation of Memory Phenotype CD8+ Cells but Are Not Required for Memory Phenotype CD4+ Cells. *J. Exp. Med.* 195, 1523–1532. <https://doi.org/10.1084/jem.20020066>
- Taube, J.M., Anders, R.A., Young, G.D., Xu, H., Sharma, R., McMiller, T.L., Chen, S., Klein, A.P., Pardoll, D.M., Topalian, S.L., Chen, L., 2012. Colocalization of Inflammatory Response with B7-H1 Expression in Human Melanocytic Lesions Supports an Adaptive Resistance Mechanism of Immune Escape. *Sci. Transl. Med.* 4, 127ra37-127ra37. <https://doi.org/10.1126/scitranslmed.3003689>
- Teicher, B.A., 2010. *Tumor Models in Cancer Research*. Springer Science & Business Media.
- Teijaro, J.R., Turner, D., Pham, Q., Wherry, E.J., Lefrançois, L., Farber, D.L., 2011. Cutting Edge: Tissue-Retentive Lung Memory CD4 T Cells Mediate Optimal Protection to Respiratory Virus Infection. *J. Immunol.* 187, 5510–5514. <https://doi.org/10.4049/jimmunol.1102243>
- Thom, J.T., Weber, T.C., Walton, S.M., Torti, N., Oxenius, A., 2015. The Salivary Gland Acts as a Sink for Tissue-Resident Memory CD8+ T Cells, Facilitating Protection from Local Cytomegalovirus Infection. *Cell Rep.* 13, 1125–1136. <https://doi.org/10.1016/j.celrep.2015.09.082>
- Topalian, S.L., Hodi, F.S., Brahmer, J.R., Gettinger, S.N., Smith, D.C., McDermott, D.F., Powderly, J.D., Carvajal, R.D., Sosman, J.A., Atkins, M.B., Leming, P.D., Spigel, D.R., Antonia, S.J., Horn, L., Drake, C.G., Pardoll, D.M., Chen, L., Sharfman, W.H., Anders, R.A., Taube, J.M., McMiller, T.L., Xu, H., Korman, A.J., Jure-Kunkel, M., Agrawal, S., McDonald, D., Kollia, G.D., Gupta, A., Wigginton, J.M., Sznol, M., 2012a. Safety, Activity, and Immune Correlates of Anti-PD-1 Antibody in Cancer [WWW Document]. <http://dx.doi.org/10.1056/NEJMoa1200690>. <https://doi.org/10.1056/NEJMoa1200690>
- Topalian, S.L., Hodi, F.S., Brahmer, J.R., Gettinger, S.N., Smith, D.C., McDermott, D.F., Powderly, J.D., Carvajal, R.D., Sosman, J.A., Atkins, M.B., Leming, P.D., Spigel, D.R., Antonia, S.J., Horn, L., Drake, C.G., Pardoll, D.M., Chen, L., Sharfman, W.H., Anders, R.A., Taube, J.M., McMiller, T.L., Xu, H., Korman, A.J., Jure-Kunkel, M., Agrawal, S., McDonald, D., Kollia, G.D., Gupta, A., Wigginton, J.M., Sznol, M., 2012b. Safety, Activity, and Immune Correlates of Anti-PD-1 Antibody in Cancer. *N. Engl. J. Med.* 366, 2443–2454. <https://doi.org/10.1056/NEJMoa1200690>
- Tormo, D., Ferrer, A., Bosch, P., Gaffal, E., Basner-Tschakarjan, E., Wenzel, J., Tüting, T., 2006a. Therapeutic efficacy of antigen-specific vaccination and toll-like receptor stimulation against established transplanted and

- autochthonous melanoma in mice. *Cancer Res.* 66, 5427–5435. <https://doi.org/10.1158/0008-5472.CAN-06-0399>
- Tormo, D., Ferrer, A., Gaffal, E., Wenzel, J., Basner-Tschakarjan, E., Steitz, J., Heukamp, L.C., Gütgemann, I., Buettner, R., Malumbres, M., Barbacid, M., Merlino, G., Tüting, T., 2006b. Rapid growth of invasive metastatic melanoma in carcinogen-treated hepatocyte growth factor/scatter factor-transgenic mice carrying an oncogenic CDK4 mutation. *Am. J. Pathol.* 169, 665–672. <https://doi.org/10.2353/ajpath.2006.060017>
- Tran, E., Ahmadzadeh, M., Lu, Y.-C., Gros, A., Turcotte, S., Robbins, P.F., Gartner, J.J., Zheng, Z., Li, Y.F., Ray, S., Wunderlich, J.R., Somerville, R.P., Rosenberg, S.A., 2015. Immunogenicity of somatic mutations in human gastrointestinal cancers. *Science* 350, 1387–1390. <https://doi.org/10.1126/science.aad1253>
- Tran, E., Robbins, P.F., Lu, Y.-C., Prickett, T.D., Gartner, J.J., Jia, L., Pasetto, A., Zheng, Z., Ray, S., Groh, E.M., Kriley, I.R., Rosenberg, S.A., 2016. T-Cell Transfer Therapy Targeting Mutant KRAS in Cancer. *N. Engl. J. Med.* 375, 2255–2262. <https://doi.org/10.1056/NEJMoa1609279>
- Tran, E., Turcotte, S., Gros, A., Robbins, P.F., Lu, Y.-C., Dudley, M.E., Wunderlich, J.R., Somerville, R.P., Hogan, K., Hinrichs, C.S., Parkhurst, M.R., Yang, J.C., Rosenberg, S.A., 2014. Cancer Immunotherapy Based on Mutation-Specific CD4+ T Cells in a Patient with Epithelial Cancer. *Science* 344, 641–645. <https://doi.org/10.1126/science.1251102>
- Tsatmali, M., Ancans, J., Thody, A.J., 2002. Melanocyte function and its control by melanocortin peptides. *J. Histochem. Cytochem. Off. J. Histochem. Soc.* 50, 125–133. <https://doi.org/10.1177/002215540205000201>
- Tudrej, K.B., Czepielewska, E., Kozłowska-Wojciechowska, M., 2017. SOX10-MITF pathway activity in melanoma cells. *Arch. Med. Sci. AMS* 13, 1493–1503. <https://doi.org/10.5114/aoms.2016.60655>
- Turk, M.J., Guevara-Patiño, J.A., Rizzuto, G.A., Engelhorn, M.E., Houghton, A.N., 2004. Concomitant Tumor Immunity to a Poorly Immunogenic Melanoma Is Prevented by Regulatory T Cells. *J. Exp. Med.* 200, 771–782. <https://doi.org/10.1084/jem.20041130>
- Van Allen, E.M., Miao, D., Schilling, B., Shukla, S.A., Blank, C., Zimmer, L., Sucker, A., Hillen, U., Foppen, M.H.G., Goldinger, S.M., Utikal, J., Hassel, J.C., Weide, B., Kaehler, K.C., Loquai, C., Mohr, P., Gutzmer, R., Dummer, R., Gabriel, S., Wu, C.J., Schadendorf, D., Garraway, L.A., 2015. Genomic correlates of response to CTLA-4 blockade in metastatic melanoma. *Science* 350, 207–211. <https://doi.org/10.1126/science.aad0095>
- van den Berg, J.H., Gomez-Eerland, R., van de Wiel, B., Hulshoff, L., van den Broek, D., Bins, A., Tan, H.L., Harper, J.V., Hassan, N.J., Jakobsen, B.K., Jorritsma, A., Blank, C.U., Schumacher, T.N.M., Haanen, J.B.A.G., 2015. Case Report of a Fatal Serious Adverse Event Upon Administration of T Cells Transduced With a MART-1-specific T-cell Receptor. *Mol. Ther.* 23, 1541–1550. <https://doi.org/10.1038/mt.2015.60>
- Van den Eynde, B.J., van der Bruggen, P., 1997. T cell defined tumor antigens. *Curr. Opin. Immunol.* 9, 684–693. [https://doi.org/10.1016/S0952-7915\(97\)80050-7](https://doi.org/10.1016/S0952-7915(97)80050-7)

- van Herpen, C.M.L., van der Laak, J.A.W.M., de Vries, I.J.M., van Krieken, J.H., de Wilde, P.C., Balvers, M.G.J., Adema, G.J., De Mulder, P.H.M., 2005. Intratumoral recombinant human interleukin-12 administration in head and neck squamous cell carcinoma patients modifies locoregional lymph node architecture and induces natural killer cell infiltration in the primary tumor. *Clin. Cancer Res. Off. J. Am. Assoc. Cancer Res.* 11, 1899–1909. <https://doi.org/10.1158/1078-0432.CCR-04-1524>
- van Rooij, N., van Buuren, M.M., Philips, D., Velds, A., Toebes, M., Heemskerk, B., van Dijk, L.J.A., Behjati, S., Hilkmann, H., el Atmioui, D., Nieuwland, M., Stratton, M.R., Kerkhoven, R.M., Kesmir, C., Haanen, J.B., Kvistborg, P., Schumacher, T.N., 2013. Tumor Exome Analysis Reveals Neoantigen-Specific T-Cell Reactivity in an Ipilimumab-Responsive Melanoma. *J. Clin. Oncol. Off. J. Am. Soc. Clin. Oncol.* 31. <https://doi.org/10.1200/JCO.2012.47.7521>
- Vasquez, J.C., Huttner, A., Zhang, L., Marks, A., Chan, A., Baehring, J.M., Kahle, K.T., Dhodapkar, K.M., 2017. SOX2 immunity and tissue resident memory in children and young adults with glioma. *J. Neurooncol.* 134, 41–53. <https://doi.org/10.1007/s11060-017-2515-8>
- Verdegaal, E.M.E., de Miranda, N.F.C.C., Visser, M., Harryvan, T., van Buuren, M.M., Andersen, R.S., Hadrup, S.R., van der Minne, C.E., Schotte, R., Spits, H., Haanen, J.B.A.G., Kapiteijn, E.H.W., Schumacher, T.N., van der Burg, S.H., 2016. Neoantigen landscape dynamics during human melanoma–T cell interactions. *Nature* 536, 91–95. <https://doi.org/10.1038/nature18945>
- Verfaillie, A., Imrichova, H., Atak, Z.K., Dewaele, M., Rambow, F., Hulselmans, G., Christiaens, V., Svetlichnyy, D., Luciani, F., Van den Mooter, L., Claerhout, S., Fiers, M., Journe, F., Ghanem, G.-E., Herrmann, C., Halder, G., Marine, J.-C., Aerts, S., 2015. Decoding the regulatory landscape of melanoma reveals TEADS as regulators of the invasive cell state. *Nat. Commun.* 6, 6683. <https://doi.org/10.1038/ncomms7683>
- Vesely, M.D., Schreiber, R.D., 2013. Cancer immunoediting: antigens, mechanisms, and implications to cancer immunotherapy. *Ann. N. Y. Acad. Sci.* 1284, 1–5. <https://doi.org/10.1111/nyas.12105>
- Viros, A., Sanchez-Laorden, B., Pedersen, M., Furney, S.J., Rae, J., Hogan, K., Ejima, S., Girotti, M.R., Cook, M., Dhomen, N., Marais, R., 2014. Ultraviolet radiation accelerates BRAF-driven melanomagenesis by targeting TP53. *Nature* 511, 478–482. <https://doi.org/10.1038/nature13298>
- Vo, D.D., Prins, R.M., Begley, J.L., Donahue, T.R., Morris, L.F., Bruhn, K.W., de la Rocha, P., Yang, M.-Y., Mok, S., Garban, H.J., Craft, N., Economou, J.S., Marincola, F.M., Wang, E., Ribas, A., 2009. Enhanced anti-tumor activity induced by adoptive T cell transfer and the adjunctive use of the HDAC Inhibitor LAQ824. *Cancer Res.* 69, 8693–8699. <https://doi.org/10.1158/0008-5472.CAN-09-1456>
- Vries, E. de, Bray, F.I., Coebergh, J.W.W., Parkin, D.M., 2003. Changing epidemiology of malignant cutaneous melanoma in Europe 1953–1997: Rising trends in incidence and mortality but recent stabilizations in Western Europe and decreases in Scandinavia. *Int. J. Cancer* 107, 119–

126. <https://doi.org/10.1002/ijc.11360>
- Wakim, L.M., Gebhardt, T., Heath, W.R., Carbone, F.R., 2008. Cutting Edge: Local Recall Responses by Memory T Cells Newly Recruited to Peripheral Nonlymphoid Tissues. *J. Immunol.* 181, 5837–5841. <https://doi.org/10.4049/jimmunol.181.9.5837>
- Wakim, L.M., Woodward-Davis, A., Bevan, M.J., 2010. Memory T cells persisting within the brain after local infection show functional adaptations to their tissue of residence. *Proc. Natl. Acad. Sci.* 107, 17872–17879. <https://doi.org/10.1073/pnas.1010201107>
- Wang Bo, Wu Shaoxu, Zeng Hong, Liu Zhuowei, Dong Wen, He Wang, Chen Xu, Dong Xiaoliang, Zheng Limin, Lin Tianxin, Huang Jian, 2015. CD103+ Tumor Infiltrating Lymphocytes Predict a Favorable Prognosis in Urothelial Cell Carcinoma of the Bladder. *J. Urol.* 194, 556–562. <https://doi.org/10.1016/j.juro.2015.02.2941>
- Wang, J., Maldonado, M.A., 2006. The Ubiquitin-Proteasome System and Its Role in Inflammatory and Autoimmune Diseases. *Mol. Immunol.* 3, 7.
- Wang, Q.J., Yu, Z., Griffith, K., Hanada, K., Restifo, N.P., Yang, J.C., 2016. Identification of T-cell Receptors Targeting KRAS-mutated Human Tumors. *Cancer Immunol. Res.* 4, 204–214. <https://doi.org/10.1158/2326-6066.CIR-15-0188>
- Wang, R.F., Robbins, P.F., Kawakami, Y., Kang, X.Q., Rosenberg, S.A., 1995. Identification of a gene encoding a melanoma tumor antigen recognized by HLA-A31-restricted tumor-infiltrating lymphocytes. *J. Exp. Med.* 181, 799–804. <https://doi.org/10.1084/jem.181.2.799>
- Wang, Z.-Q., Milne, K., Derocher, H., Webb, J.R., Nelson, B.H., Watson, P.H., 2016. CD103 and Intratumoral Immune Response in Breast Cancer. *Clin. Cancer Res.* 22, 6290–6297. <https://doi.org/10.1158/1078-0432.CCR-16-0732>
- Ward, M.J., Thirdborough, S.M., Mellows, T., Riley, C., Harris, S., Suchak, K., Webb, A., Hampton, C., Patel, N.N., Randall, C.J., Cox, H.J., Jogai, S., Primrose, J., Piper, K., Ottensmeier, C.H., King, E.V., Thomas, G.J., 2014. Tumour-infiltrating lymphocytes predict for outcome in HPV-positive oropharyngeal cancer. *Br. J. Cancer* 110, 489–500. <https://doi.org/10.1038/bjc.2013.639>
- Watson, M., Geller, A.C., Tucker, M.A., Guy, G.P., Weinstock, M.A., 2016. Melanoma burden and recent trends among non-Hispanic whites aged 15–49 years, United States. *Prev. Med.* 91, 294–298. <https://doi.org/10.1016/j.ypmed.2016.08.032>
- Webb, J.R., Milne, K., Nelson, B.H., 2015. PD-1 and CD103 Are Widely Coexpressed on Prognostically Favorable Intraepithelial CD8 T Cells in Human Ovarian Cancer. *Cancer Immunol. Res.* 3, 926–935. <https://doi.org/10.1158/2326-6066.CIR-14-0239>
- Webb, J.R., Milne, K., Watson, P., deLeeuw, R.J., Nelson, B.H., 2014. Tumor-Infiltrating Lymphocytes Expressing the Tissue Resident Memory Marker CD103 Are Associated with Increased Survival in High-Grade Serous Ovarian Cancer. *Clin. Cancer Res.* 20, 434–444. <https://doi.org/10.1158/1078-0432.CCR-13-1877>
- Webster, M.R., Xu, M., Kinzler, K.A., Kaur, A., Appleton, J., O’Connell, M.P.,

- Marchbank, K., Valiga, A., Dang, V.M., Perego, M., Zhang, G., Slipicevic, A., Keeney, F., Lehrmann, E., Wood III, W., Becker, K.G., Kossenkov, A.V., Frederick, D.T., Flaherty, K.T., Xu, X., Herlyn, M., Murphy, M.E., Weeraratna, A.T., 2015. Wnt5A promotes an adaptive, senescent-like stress response, while continuing to drive invasion in melanoma cells. *Pigment Cell Melanoma Res.* 28, 184–195. <https://doi.org/10.1111/pcmr.12330>
- Weinstein, I.B., Joe, A., 2008. Oncogene Addiction. *Cancer Res.* 68, 3077–3080. <https://doi.org/10.1158/0008-5472.CAN-07-3293>
- Weir, H.K., Marrett, L.D., Cokkinides, V., Barnholtz-Sloan, J., Patel, P., Tai, E., Jemal, A., Li, J., Kim, J., Ekwueme, D.U., 2011. Melanoma in adolescents and young adults (ages 15-39 years): United States, 1999-2006. *J. Am. Acad. Dermatol.* 65, S38–S49. <https://doi.org/10.1016/j.jaad.2011.04.038>
- Westergaard, M.C.W., Andersen, R., Chong, C., Kjeldsen, J.W., Pedersen, M., Friese, C., Hasselager, T., Lajer, H., Coukos, G., Bassani-Sternberg, M., Donia, M., Svane, I.M., 2019. Tumour-reactive T cell subsets in the microenvironment of ovarian cancer. *Br. J. Cancer* 120, 424. <https://doi.org/10.1038/s41416-019-0384-y>
- Wherry, E.J., Teichgräber, V., Becker, T.C., Masopust, D., Kaech, S.M., Antia, R., Andrian, U.H. von, Ahmed, R., 2003. Lineage relationship and protective immunity of memory CD8 T cell subsets. *Nat. Immunol.* 4, 225. <https://doi.org/10.1038/ni889>
- Whiteman, D.C., Green, A.C., Olsen, C.M., 2016. The Growing Burden of Invasive Melanoma: Projections of Incidence Rates and Numbers of New Cases in Six Susceptible Populations through 2031. *J. Invest. Dermatol.* 136, 1161–1171. <https://doi.org/10.1016/j.jid.2016.01.035>
- Widmer, D.S., Hoek, K.S., Cheng, P.F., Eichhoff, O.M., Biedermann, T., Raaijmakers, M.I.G., Hemmi, S., Dummer, R., Levesque, M.P., 2013. Hypoxia Contributes to Melanoma Heterogeneity by Triggering HIF1 α -Dependent Phenotype Switching. *J. Invest. Dermatol.* 133, 2436–2443. <https://doi.org/10.1038/jid.2013.115>
- Williams, A.P., Peh, C.A., Purcell, A.W., McCluskey, J., Elliott, T., 2002. Optimization of the MHC Class I Peptide Cargo Is Dependent on Tapasin. *Immunity* 16, 509–520. [https://doi.org/10.1016/S1074-7613\(02\)00304-7](https://doi.org/10.1016/S1074-7613(02)00304-7)
- Wolchok, J.D., Chiarion-Sileni, V., Gonzalez, R., Rutkowski, P., Grob, J.-J., Cowey, C.L., Lao, C.D., Wagstaff, J., Schadendorf, D., Ferrucci, P.F., Smylie, M., Dummer, R., Hill, A., Hogg, D., Haanen, J., Carlino, M.S., Bechter, O., Maio, M., Marquez-Rodas, I., Guidoboni, M., McArthur, G., Lebbé, C., Ascierto, P.A., Long, G.V., Cebon, J., Sosman, J., Postow, M.A., Callahan, M.K., Walker, D., Rollin, L., Bhore, R., Hodi, F.S., Larkin, J., 2017. Overall Survival with Combined Nivolumab and Ipilimumab in Advanced Melanoma. *N. Engl. J. Med.* 377, 1345–1356. <https://doi.org/10.1056/NEJMoa1709684>
- Wölfel, T., Hauer, M., Schneider, J., Serrano, M., Wölfel, C., Klehmann-Hieb, E., De Plaen, E., Hankeln, T., Meyer zum Büschenfelde, K.H., Beach, D., 1995. A p16INK4a-insensitive CDK4 mutant targeted by cytolytic T lymphocytes in a human melanoma. *Science* 269, 1281–1284.
- Wolfel, T., Hauer, M., Schneider, J., Serrano, M., Wolfel, C., Klehmann-Hieb, E.,

- Plaen, E.D., Hankeln, T., Buschenfelde, K.M. zum, Beach, D., 1995. A p16INK4a-insensitive CDK4 mutant targeted by cytolytic T lymphocytes in a human melanoma. *Science* 269, 1281–1284. <https://doi.org/10.1126/science.7652577>
- Wolfers, J., Lozier, A., Raposo, G., Regnault, A., Théry, C., Masurier, C., Flament, C., Pouzieux, S., Faure, F., Tursz, T., Angevin, E., Amigorena, S., Zitvogel, L., 2001. Tumor-derived exosomes are a source of shared tumor rejection antigens for CTL cross-priming. *Nat. Med.* 7, 297–303. <https://doi.org/10.1038/85438>
- Woodberry, T., Suscovich, T.J., Henry, L.M., August, M., Waring, M.T., Kaur, A., Hess, C., Kutok, J.L., Aster, J.C., Wang, F., Scadden, D.T., Brander, C., 2005. α E β 7 (CD103) Expression Identifies a Highly Active, Tonsil-Resident Effector-Memory CTL Population. *J. Immunol.* 175, 4355–4362. <https://doi.org/10.4049/jimmunol.175.7.4355>
- Workel, H.H., Komdeur, F.L., Wouters, M.C.A., Plat, A., Klip, H.G., Eggink, F.A., Wisman, G.B.A., Arts, H.J.G., Oonk, M.H.M., Mourits, M.J.E., Yigit, R., Versluis, M., Duiker, E.W., Hollema, H., de Bruyn, M., Nijman, H.W., 2016. CD103 defines intraepithelial CD8+ PD1+ tumour-infiltrating lymphocytes of prognostic significance in endometrial adenocarcinoma. *Eur. J. Cancer* 60, 1–11. <https://doi.org/10.1016/j.ejca.2016.02.026>
- Wu, S., Han, J., Laden, F., Qureshi, A.A., 2014. Long-term ultraviolet flux, other potential risk factors, and skin cancer risk: a cohort study. *Cancer Epidemiol. Biomark. Prev. Publ. Am. Assoc. Cancer Res. Cosponsored Am. Soc. Prev. Oncol.* 23, 1080–1089. <https://doi.org/10.1158/1055-9965.EPI-13-0821>
- Wu, T., Hu, Y., Lee, Y.-T., Bouchard, K.R., Benechet, A., Khanna, K., Cauley, L.S., 2014. Lung-resident memory CD8 T cells (TRM) are indispensable for optimal cross-protection against pulmonary virus infection. *J. Leukoc. Biol.* 95, 215–224. <https://doi.org/10.1189/jlb.0313180>
- Wylie, B., Seppanen, E., Xiao, K., Zemek, R., Zanker, D., Prato, S., Foley, B., Hart, P.H., Kroczeck, R.A., Chen, W., Waithman, J., 2015. Cross-presentation of cutaneous melanoma antigen by migratory XCR1+CD103- and XCR1+CD103+ dendritic cells. *Oncoimmunology* 4. <https://doi.org/10.1080/2162402X.2015.1019198>
- Xia, J., Jia, P., Hutchinson, K.E., Dahlman, K.B., Johnson, D., Sosman, J., Pao, W., Zhao, Z., 2014. A Meta-analysis of Somatic Mutations from Next Generation Sequencing of 241 Melanomas: A Road Map for the Study of Genes with Potential Clinical Relevance. *Mol. Cancer Ther.* 13, 1918–1928. <https://doi.org/10.1158/1535-7163.MCT-13-0804>
- Yamaguchi, Y., Hearing, V.J., 2009. Physiological factors that regulate skin pigmentation. *BioFactors Oxf. Engl.* 35, 193–199. <https://doi.org/10.1002/biof.29>
- Yang, L., DeBusk, L.M., Fukuda, K., Fingleton, B., Green-Jarvis, B., Shyr, Y., Matrisian, L.M., Carbone, D.P., Lin, P.C., 2004. Expansion of myeloid immune suppressor Gr+CD11b+ cells in tumor-bearing host directly promotes tumor angiogenesis. *Cancer Cell* 6, 409–421. <https://doi.org/10.1016/j.ccr.2004.08.031>
- Yang, L., Huang, J., Ren, X., Gorska, A.E., Chytil, A., Aakre, M., Carbone, D.P.,

- Matrisian, L.M., Richmond, A., Lin, P.C., Moses, H.L., 2008. Abrogation of TGF β Signaling in Mammary Carcinomas Recruits Gr-1+CD11b+ Myeloid Cells that Promote Metastasis. *Cancer Cell* 13, 23–35. <https://doi.org/10.1016/j.ccr.2007.12.004>
- Yao, X., Ahmadzadeh, M., Lu, Y.-C., Liewehr, D.J., Dudley, M.E., Liu, F., Schrumpp, D.S., Steinberg, S.M., Rosenberg, S.A., Robbins, P.F., 2012. Levels of peripheral CD4+FoxP3+ regulatory T cells are negatively associated with clinical response to adoptive immunotherapy of human cancer. *Blood* 119, 5688–5696. <https://doi.org/10.1182/blood-2011-10-386482>
- York, I.A., Brehm, M.A., Zendzian, S., Towne, C.F., Rock, K.L., 2006. Endoplasmic reticulum aminopeptidase 1 (ERAP1) trims MHC class I-presented peptides in vivo and plays an important role in immunodominance. *Proc. Natl. Acad. Sci. U. S. A.* 103, 9202–9207. <https://doi.org/10.1073/pnas.0603095103>
- York, I.A., Chang, S.-C., Saric, T., Keys, J.A., Favreau, J.M., Goldberg, A.L., Rock, K.L., 2002. The ER aminopeptidase ERAP1 enhances or limits antigen presentation by trimming epitopes to 8–9 residues. *Nat. Immunol.* 3, 1177. <https://doi.org/10.1038/ni860>
- Young, A., Ngiow, S.F., Madore, J., Reinhardt, J., Landsberg, J., Chitsazan, A., Rautela, J., Bald, T., Barkauskas, D.S., Ahern, E., Huntington, N.D., Schadendorf, D., Long, G.V., Boyle, G.M., Hölzel, M., Scolyer, R.A., Smyth, M.J., 2017. Targeting Adenosine in BRAF-Mutant Melanoma Reduces Tumor Growth and Metastasis. *Cancer Res.* 77, 4684–4696. <https://doi.org/10.1158/0008-5472.CAN-17-0393>
- Zaretsky, J.M., Garcia-Diaz, A., Shin, D.S., Escuin-Ordinas, H., Hugo, W., Hu-Lieskovan, S., Torrejon, D.Y., Abril-Rodriguez, G., Sandoval, S., Barthly, L., Saco, J., Homet Moreno, B., Mezzadra, R., Chmielowski, B., Ruchalski, K., Shintaku, I.P., Sanchez, P.J., Puig-Saus, C., Cherry, G., Seja, E., Kong, X., Pang, J., Berent-Maoz, B., Comin-Anduix, B., Graeber, T.G., Tumei, P.C., Schumacher, T.N.M., Lo, R.S., Ribas, A., 2016a. Mutations Associated with Acquired Resistance to PD-1 Blockade in Melanoma [WWW Document]. <https://doi.org/10.1056/NEJMoa1604958>
- Zaretsky, J.M., Garcia-Diaz, A., Shin, D.S., Escuin-Ordinas, H., Hugo, W., Hu-Lieskovan, S., Torrejon, D.Y., Abril-Rodriguez, G., Sandoval, S., Barthly, L., Saco, J., Moreno, B.H., Mezzadra, R., Chmielowski, B., Ruchalski, K., Shintaku, I.P., Sanchez, P.J., Puig-Saus, C., Cherry, G., Seja, E., Kong, X., Pang, J., Berent-Maoz, B., Comin-Anduix, B., Graeber, T.G., Tumei, P.C., Schumacher, T.N.M., Lo, R.S., Ribas, A., 2016b. Mutations Associated with Acquired Resistance to PD-1 Blockade in Melanoma. *N. Engl. J. Med.* 375, 819–829. <https://doi.org/10.1056/NEJMoa1604958>
- Zeelenberg, I.S., van Maren, W.W.C., Boissonnas, A., Van Hout-Kuijer, M.A., Den Brok, M.H.M.G.M., Wagenaars, J.A.L., van der Schaaf, A., Jansen, E.J.R., Amigorena, S., Théry, C., Figdor, C.G., Adema, G.J., 2011. Antigen localization controls T cell-mediated tumor immunity. *J. Immunol. Baltim. Md* 1950 187, 1281–1288. <https://doi.org/10.4049/jimmunol.1003905>
- Zens, K.D., Chen, J.K., Farber, D.L., 2016. Vaccine-generated lung tissue–

- resident memory T cells provide heterosubtypic protection to influenza infection. *JCI Insight* 1. <https://doi.org/10.1172/jci.insight.85832>
- Zhang, H., Conrad, D.M., Butler, J.J., Zhao, C., Blay, J., Hoskin, D.W., 2004. Adenosine Acts through A2 Receptors to Inhibit IL-2-Induced Tyrosine Phosphorylation of STAT5 in T Lymphocytes: Role of Cyclic Adenosine 3',5'-Monophosphate and Phosphatases. *J. Immunol.* 173, 932–944. <https://doi.org/10.4049/jimmunol.173.2.932>
- Zhao, F., Sucker, A., Horn, S., Heeke, C., Bielefeld, N., Schrörs, B., Bicker, A., Lindemann, M., Roesch, A., Gaudernack, G., Stiller, M., Becker, J.C., Lennerz, V., Wölfel, T., Schadendorf, D., Griewank, K., Paschen, A., 2016. Melanoma Lesions Independently Acquire T-cell Resistance during Metastatic Latency. *Cancer Res.* 76, 4347–4358. <https://doi.org/10.1158/0008-5472.CAN-16-0008>
- Zhou, J., Dudley, M.E., Rosenberg, S.A., Robbins, P.F., 2005. Persistence of Multiple Tumor-Specific T-Cell Clones Is Associated with Complete Tumor Regression in a Melanoma Patient Receiving Adoptive Cell Transfer Therapy. *J. Immunother. Hagerstown Md* 28, 53–62.
- Zhou, X., Yu, S., Zhao, D.-M., Harty, J.T., Badovinac, V.P., Xue, H.-H., 2010. Differentiation and Persistence of Memory CD8+ T Cells Depend on T Cell Factor 1. *Immunity* 33, 229–240. <https://doi.org/10.1016/j.immuni.2010.08.002>
- Zuo, L., Weger, J., Yang, Q., Goldstein, A.M., Tucker, M.A., Walker, G.J., Hayward, N., Dracopoli, N.C., 1996. Germline mutations in the p16INK4a binding domain of CDK4 in familial melanoma. *Nat. Genet.* 12, 97. <https://doi.org/10.1038/ng0196-97>

Curriculum vitae

Education

- 2015 – present **Doctor of Philosophy**
 Experimental Medicine
Jointly awarded by The Rheinische Friedrich-Wilhelms-Universität Bonn and The University of Melbourne
- 2012 – 2014 **Master of Science**
 Molecular Medicine
Friedrich-Alexander-Universität Erlangen-Nürnberg
- 2011 – 2012 **Bachelor of Science (Honours)**
 Molecular Genetics
University of Dundee
- 2009 – 2012 **Bachelor of Science**
 Applied Biology
Hochschule Bonn-Rhein-Sieg

Conference participations

Oral presentations

- 2019 Cluster Science Days 2019 – Bonn, Germany
- 2018 47th Annual Meeting of the Australasian Society for Immunology – Perth, Australia
- 2018 Victoria Infection and Immunity Network Young Investigator Symposium – Melbourne, Australia
- 2018 Melbourne Immunotherapy Network Winter Retreat – Melbourne, Australia
- 2018 Victoria Comprehensive Cancer Centre Student Symposium – Melbourne, Australia
- 2016 Cluster Science Days 2016 – Bonn, Germany

Poster presentations

2019	Cluster Science Days 2019 – Bonn, Germany
2018	Biomed Link 2018 – Melbourne, Australia
2018	4 th MDHS ECR Network Symposium – Melbourne, Australia
2017	Bonn Immunoscience Days 2017 – Bonn, Germany
2017	14 th International Congress of the Society for Melanoma – Brisbane, Australia

PhD program participations

2018 - present	Member of the Victorian Comprehensive Cancer PhD Program
2016 - present	Member of the International Research and Training Group 2168
2016 - present	Member of the Peter Doherty PhD Program
2015 - present	Member of the International Training Program Bonn within the Excellence Cluster 1023

Engagement

2019	Invited chair at the Immunology Theme Meeting seminar series at the Peter Doherty Institute for Infection and Immunity – Melbourne, Australia
2019	Scientific Communicator of the International Research and Training Group 2168
2018	Invited chair and judge at the 4 th Annual MDHS ECR Network Symposium, University of Melbourne – Melbourne, Australia
2018	Invited Chair at the Immunology Theme Meeting seminar series at the Peter Doherty Institute for Infection and Immunity – Melbourne, Australia

Scholarships, prizes and awards

- 2019 2019 Seqirus PhD Oration Award at the Peter Doherty
Institute of Infection and Immunity – Melbourne, Australia
- 2019 Best Poster Awards at the Cluster Science Days 2019 –
Bonn, Germany
- 2018 Travel grant awarded by the German Academic Exchange
Service to attend the 47th Annual Meeting of the Australasian
Society for Immunology in Perth
- 2018 Best Poster Award at the 4th Annual MDHS ECR Network
Symposium, University of Melbourne – Melbourne, Australia
- 2016 Melbourne Research Scholarship awarded by the University
of Melbourne

Memberships

- 2019 – present Member of the Australasian Society for Immunology Inc.
- 2019 – present Member of the German Society for Immunology

Appendix

Appendix 1: Heatmap annotation for Figure 4.11

List of differentially regulated genes shown in the heatmap *Melanoma invasive genes* of Figure 4.11. Gene # 1-149 correspond to the signature in the heatmap (top to bottom).

#	Gene ID	Gene symbol
1	240725	Sulf1
2	19335	Rab23
3	26921	Map4k4
4	17082	Il1r1
5	12832	Col5a2
6	329152	Hecw2
7	11761	Aox1
8	77300	Raph1
9	93691	Klf7
10	22779	Ikzf2
11	320982	Arl4c
12	240913	Adamts4
13	21808	Tgfb2
14	212898	Dse
15	66686	Dcbld1
16	13713	Elk3
17	67972	Atp2b1
18	17904	Myl6
19	68585	Rtn4
20	94176	Dock2
21	11492	Adam19
22	16362	Irf1
23	57783	Tnip1
24	171212	Galnt10
25	216799	Nlrp3
26	20304	Ccl5
27	12842	Col1a1
28	53859	Map3k14
29	66313	Smurf2
30	18035	Nfkbia
31	16997	Ltbp2
32	21928	Tnfaip2
33	16323	Inhba
34	13610	S1pr3
35	192657	Eil2
36	218397	Rasa1

#	Gene ID	Gene symbol
37	13003	Vcan
38	16195	Il6st
39	16475	Ajuba
40	68813	Dock5
41	20855	Stc1
42	94352	Loxl2
43	223272	Itgbl1
44	16197	Il7r
45	70350	Basp1
46	22402	Wisp1
47	17886	Myh9
48	67760	Slc38a2
49	16012	Igfbp6
50	16402	Itga5
51	246154	Vasn
52	77446	Heg1
53	107589	Mylk
54	57875	Angptl4
55	21354	Tap1
56	14962	Cfb
57	268977	Ltbp1
58	50766	Crim1
59	225020	Fez2
60	193813	Mcf2
61	240185	9430020K01Rik
62	75739	Mpp7
63	16774	Lama3
64	15200	Hbegf
65	14815	Nr3c1
66	16948	Lox
67	14119	Fbn2
68	54670	Atp8b1
69	21413	Tcf4
70	70445	Cd248
71	104252	Cdc42ep2
72	18797	Plcb3

#	Gene ID	Gene symbol
73	65221	Slc15a3
74	21888	Tle4
75	60533	Cd274
76	54519	Apbb1ip
77	12831	Col5a1
78	30934	Tor1b
79	20448	St6galnac4
80	14828	Hspa5
81	74194	Rnd3
82	21825	Thbs1
83	14118	Fbn1
84	16176	Il1b
85	21817	Tgm2
86	20971	Sdc4
87	20482	Skil
88	19288	Ptx3
89	20198	S100a4
90	20501	Slc16a1
91	80281	Ctnnbp2nl
92	22329	Vcam1
93	69608	Sec24d
94	211550	Tifa
95	56376	Pdlim5
96	55932	Gbp3
97	99899	Ifi44
98	65973	Asph
99	14745	Lpar1
100	77739	Adamts1
101	16476	Jun
102	230738	Zc3h12a
103	16792	Laptm5
104	27984	Efhd2
105	74155	Errfi1
106	21942	Tnfrsf9
107	74511	Lrrc17
108	20657	Sod3
109	20310	Cxcl2
110	231633	Tmem119
111	68420	Ankrd13a
112	231655	Oasl1
113	246728	Oas2
114	18787	Serpine1
115	231842	Amz1
116	209086	Samd9l

#	Gene ID	Gene symbol
117	12843	Col1a2
118	214642	Cped1
119	67138	Herc6
120	14115	Fbln2
121	108960	Irak2
122	19698	Relb
123	12051	Bcl3
124	18987	Pou2f2
125	26362	Axl
126	29861	Dpf1
127	20130	Rras
128	11819	Nr2f2
129	11501	Adam8
130	66853	Pnpla2
131	13642	Efnb2
132	59009	Sh3rf1
133	74256	Cyld
134	74347	Tlhc1
135	16412	Itgb1
136	235041	Kank2
137	235283	Gramd1b
138	71566	Clmp
139	21345	Tagln
140	18113	Nnmt
141	16949	Loxl1
142	12816	Col12a1
143	26432	Plod2
144	235587	Parp3
145	208869	Dock3
146	14678	Gnai2
147	66940	Shisa5
148	108737	Oxsr1
149	209446	Tfe3